Lymph Node Metastasis in Gastrointestinal Cancer

Shoji Natsugoe
Editor

Springer

Lymph Node Metastasis in Gastrointestinal Cancer

Shoji Natsugoe
Editor

Lymph Node Metastasis in Gastrointestinal Cancer

Springer

Editor
Shoji Natsugoe
Department of Digestive Surgery, Breast and Thyroid Surgery
Kagoshima
Japan

ISBN 978-981-10-4698-8 ISBN 978-981-10-4699-5 (eBook)
https://doi.org/10.1007/978-981-10-4699-5

Library of Congress Control Number: 2018965728

This Springer imprint is published by the registered company Springer Nature Singapore Pte Ltd.
The registered company address is: 152 Beach Road, #21-01/04 Gateway East, Singapore 189721, Singapore

Preface

There is a famous sentence: “The doctor who controls metastasis controls cancer”. One of the characteristics of a malignant tumor is the ability to metastasize. If a tumor has high malignant potential, metastasis is often seen in wide areas. Thus, lymph node metastasis is one of the most important prognostic factors in various carcinomas, including gastrointestinal (GI) cancer. There are several biological and morphological pathways by which lymph node metastasis can arise: invasion into a deeper layer, detachment of tumor cells from the primary tumor, infiltration into intramural lymphatics, flow to extramural lymphatics, arrival to afferent lymphatics of a marginal sinus, movement to the lymph node cortex, and implantation of tumor cells into the node and formation of metastasis.

When surgeons and oncologists treat cancer patients, it is necessary to have sufficient understanding of both the basic and clinical aspects of nodal metastasis. In the basic aspect, knowledge of the anatomy and physiology of lymphatics and lymph nodes is essential when performing surgical treatment. The molecular mechanism in lymph node metastasis and immunology for lymph nodes is also important when doing chemo and/or chemo radiotherapy, molecular target treatment, and immunotherapy. The theory of basic imaging diagnosis and in vivo imaging is useful in the planning of cancer treatment.

In the clinical aspect, lymph node metastasis and metastatic sites should be analyzed in detail, because such data are important to plan the treatment strategy, especially in surgical lymph node dissection and radiation therapy. Usually, histological examination for lymph node metastasis is performed using representative sections from the removed nodes. Even if complete lymph node dissection is performed in patients with early cancer, recurrent disease is sometimes encountered. The development of sensitive immunohistochemical techniques and reverse transcription–polymerase chain reaction (RT-PCR) and other methods has led to the detection of lymph node micrometastasis (LNM) that could not be found in routine histological examination. Although overt lymph node metastasis is thought to be related to prognosis, what is the relationship between LNM and prognosis? Clinical evaluation of LNM is somewhat difficult, but in this book we review the clinical significance of LNM in each type of GI cancer.

Currently, minimally invasive treatments such as endoscopic submucosal dissection and laparoscopic surgery with individualized lymphadenectomy are increasingly being performed. Accurate diagnosis of LNM can clarify issues of curability

and safety when performing such treatments. Sentinel node navigation surgery (SNNS), especially, has recently been introduced in treatment of GI cancer. When SNNS with individualized lymphadenectomy in early cancer is performed, it is important to consider the balance between postsurgical quality of life and curability. Increasingly, SNNS will become firmly established as a beneficial procedure for patients with early cancer.

This book summarizes the current knowledge of lymph node metastasis in GI cancer from the perspectives of both molecular and biological characteristics, and from clinical aspects. The book will be helpful as an overview of the current understanding of lymph node metastasis and areas requiring further investigation.

Kagoshima, Japan Shoji Natsugoe

Contents

Physiology of the Gastrointestinal Lymphatics

1

Toshio Ohhashi and Yoshiko Kawai

Abstract

In this chapter, we focus on the physiology of gastrointestinal lymphatic system and then demonstrate with current inspired studies that (1) functional properties of the intestinal microcirculation are summarized as higher permeability of plasma protein, especially albumin through the venule walls, which contribute to the oncotic pressure-mediated much absorption of interstitial fluid into lymphatic capillaries, (2) the larger amount of lymph formation in the intestinal villi may be related to the presence of lacteal vessels in the tissues, (3) the mesenteric collecting lymphatics demonstrate marked heart-like spontaneous contractions working as transport of the larger amount of lymph to chylous cyst, (4) the sentinel lymph node (SLN) may be defined as the node subjected to higher lymph flow from physiological point of view, and (5) the higher lymph flow may be, in part, related to develop the suitable microenvironment of the SLN for metastasis of carcinoma cells, which is produced by the cell surface F_1/F_0 ATP synthase-dependent overexpression of intercellular adhesion molecule-1 on the marginal endothelial-like cells of SLN.

T. Ohhashi (✉)
Department of Innovation of Medical and Health Sciences Research, School of Medicine, Shinshu University, Matsumoto, Japan
e-mail: ohhashi@shinshu-u.ac.jp

Y. Kawai
Faculty of Medicine, Division of Physiology, Tohoku Medical and Pharmaceutical University, Sendai, Japan

S. Natsugoe (ed.), *Lymph Node Metastasis in Gastrointestinal Cancer*,
https://doi.org/10.1007/978-981-10-4699-5_1

Keywords
Albumin · Starling's law · Spontaneous contraction · Lipid absorption · Lacteal vessel

1.1 Introduction

As one of the lymphatic functions, it is well known that transport and drainage of hydrophilic substances including plasma protein through the lymphatic system play pivotal roles in maintaining the homeostasis of the internal environment between the cells in collaboration with the exchange of substances through blood capillaries and venules [1–3].

Another important function of the lymphatic system is concerned with the immune system. The lymphatic system provides the anatomical structures which contain the cellular elements involved in this system and provides the circulatory pathways for interaction between these cells and other tissues [4]. Thus, there is a large population of resident lymphocytes within the lymph node. These lymphocytes moved from the node into efferent lymph travel to other lymph nodes or to the blood via the thoracic duct. Similarly, lymphocytes leave the vascular compartment at high endothelium venules within the node to enter the lymphatic compartment [5]. These processes are physiologically balanced since lymph nodes do not change in size with time. Under normal circumstances there is only a low rate of division of lymphocytes within the node [6].

The two main roles of the lymphatic system should not be considered in isolation since it is likely that the system has evolved to optimally suite for both functions. Therefore, we have proposed a new lymphology combined with current knowledge of lymphatic physiology included with microcirculation, innate immunology, and oncology from a defense mechanisms point of view [7].

In addition, the functional and anatomical properties of lymphatic system have also a marked heterogeneity between gut and limbs. Thus, the intestinal lymphatic system works as the transport of absorbed lipids with long-chain, and macromolecules such as plasma protein, especially albumin [8]. Figure 1.1 demonstrates a representative photomicrograph showing murine mesenteric lymphatics contained with white-colored lymph after lipid absorption. In this chapter, in collaboration with the title of this book, we would like to demonstrate the gastrointestinal lymphatic physiology included with the specialized property of higher permeability of albumin through the venular walls in the intestinal microcirculation, the modified concept of Starling's law applicable for the microcirculation, physiological roles of heart-like spontaneous contraction of the lymphatic smooth muscles and the effects of shear stress stimulation produced by lymph flow on the lymphatic endothelial cells and sentinel lymph node (SLN).

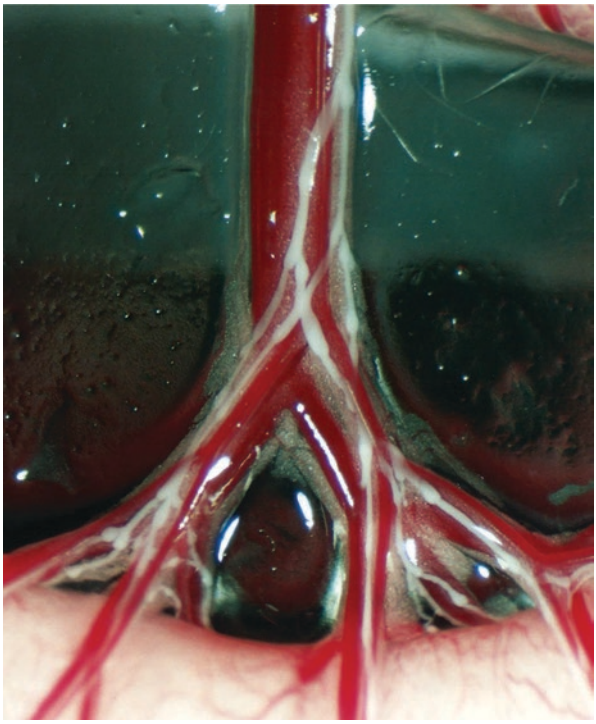

Fig. 1.1 A representative microphotograph shows murine mesenteric lymphatics contained with white-colored lymph after lipid absorption. The opal-colored tube at the bottom is the small intestine. The red-colored blood vessels are portal veins. The bubble-like pink-colored tissues around the lymphatics are adipose tissues

1.2 Characteristics of Lymph Formation in the Gastrointestinal Lymphatic System

1.2.1 Recirculation of Plasma Protein Through the Lymphatic System

Figure 1.2 [9] shows schematically the volumes of these several "circulations" in terms of exchanges in 24 h. With a cardiac output of 5.0~6.0 L/min, the first circulation amounts to about 8400 L per 24 h. From this volume, filtration in the capillary bed removes a minimum of 20 L per 24 h, a "filtration fraction" of 0.25%. This capillary filtrate begins the second circulation, that of interstitial fluid with capillary absorption, during rest, of 80–90% or 16 to 18 L/24 h, of the originally capillary filtrate. The remaining 2 to 4 L/24 h, including the unabsorbed protein of the original capillary filtrate, then produces the third circulation, that of protein in lymph. The potential magnitude of this protein circulation can be estimated from the observation of Wasserman & Mayerson [10] on the rates at which intravenously injected labeled albumin and globulin disappeared from plasma and appeared in thoracic

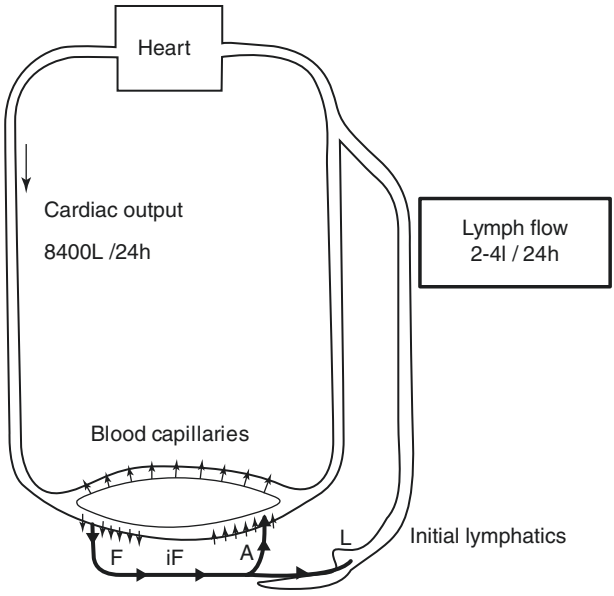

F : Filtration A: Reabsorption

iF : interstitial fluid

	Filtration	Reabsorption	Lymph flow
Water	20 l	– 16~18 l	= 2 ~ 4 l
Plasma protein	80 ~ 200 g	– 5 (?) g	= 75 ~ 195 g

Fig. 1.2 Schematic diagram of the "several circulations" with approximate magnitudes of each. For explanation of figures relating to filtration, absorption, and lymph flow see text of this section. Data from [9] Landis and Poppenheimer, with permission

duct lymph. The faster component of these two-phase disappearance curves indicated a steady disappearance of plasma albumin from plasma, and corresponding appearance in lymph, at the rate of approximately 0.1% of the total circulating plasma protein per minute. This includes passage from more permeable hepatic and intestinal capillaries as well as the less permeable limb capillaries.

In addition, lymph nodes [11, 12] and small lymph vessel walls [13] have a condensing mechanism of albumin in lymph. A significant amount of albumin in lymph may accompany the migration of lymphocytes across the high endothelium venules within the lymph nodes, and the mechanisms of protein transfer in the lymph nodes may explain the higher concentration of albumin observed in the efferent lymph of the regional node compared with that in the afferent lymph [14, 15].

However, the detailed physiological meaning of such increases in the albumin concentration of lymph through lymph nodes and small lymph vessel walls is still unknown. One possibility is that the protein concentration of afferent lymph may be an important regulator of innate immunity. Thus, the excretion of nonselective T- and B-cell lymphocytes into the efferent lymph vessels was confirmed to be positively correlated with the protein concentration of lymph in the afferent lymph vessels [16]. No study has, however, investigated the effects of albumin on the activation or migration of the lymphocytes or its related cells within gut-associated lymphoid tissue (GALT).

1.2.2 Higher Permeability of Albumin Through the Venules in Intestinal Microcirculation

It is well known that intestinal lymph flow and lymphatic protein flux increase and lymph protein decreases following fluid ingestion [17]. Granger and Taylor et al. [18, 19] also have demonstrated that the magnitude of intestinal venular protein leakage during lipid absorption is far greater than that predicted using lymphatic protein flux changes. The massive movement of plasma proteins into and out of the mucosal interstitium during food absorption may be advantageous for the removal of albumin-bound nutrients into the lacteal vessels. In fact, the contraction of rat venular endothelial cells has contributed to increase the permeability of albumin in the intestinal interstitium, resulting in higher tissue osmotic pressure in the venular site [20, 21].

1.2.3 Modified Staring's Law-Dependent Higher Lymph Formation in Intestinal Microcirculation

Taking into consideration the abovementioned characteristics of intestinal microcirculation, Taylor and Townsley [22] have proposed the modified Starling's law explaining for higher lymph formation in the intestinal microcirculation. Figure 1.3a shows a schematic model of how fluid likely filters across average capillary walls for the intestinal microcirculation. The lower portion of Fig. 1.3a shows the capillary pressure (P_c) drop form the arterial to the venous end of the capillary and the colloid osmotic pressure (π_p) within the plasma. The numbers shown by the arrows indicate that the capillary forces are positive in the arterial end (arrow pointing out), zero at capillary midpoint, and negative in the venous end (arrow pointing inward), i.e., this is the classical Landis model of capillary filtration.

On the other hand, in the intestinal microcirculation, we now know that the colloid osmotic pressure of tissues (π_p) will be lower in the vicinity of the arterial portion because the capillary is less permeable there and tissue pressure will be more positive because the tissues should be more hydrated. At the venous end of the capillary, the π_T will be increased because the venule is more leaky to plasma protein, albumin, and tissue pressures (P_T) will be more negative because the tendency for fluid to filter across this portion of the capillary is less.

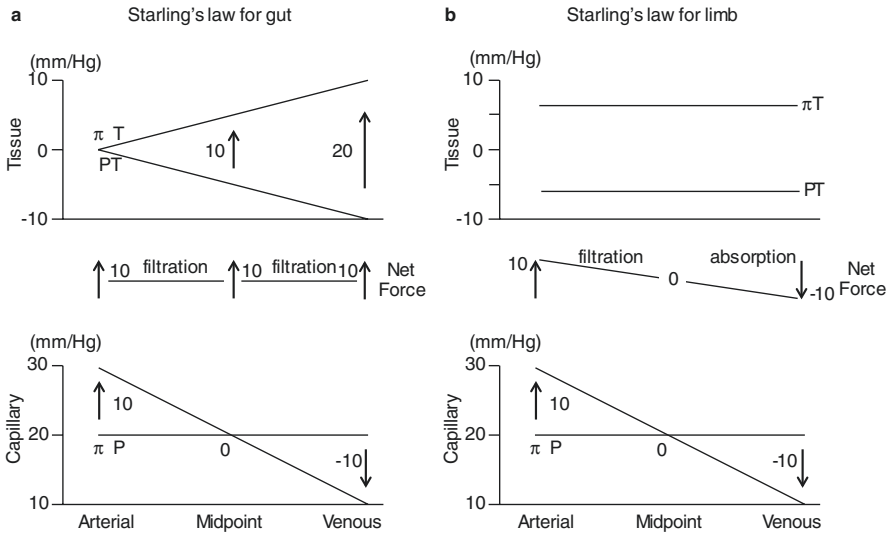

Fig. 1.3 Representative diagrams of vascular and tissue forces acting on the capillary in gut (**a**) and limbs (**b**) microcirculation. Each middle value show net force acting along the capillary is shown between tissue and capillary diagrams. Thus, net force = $(P_c - P_T) - (\pi_P - \pi_T)$. The P_c and P_T are capillary and tissue hydrostatic pressure, respectively. The π_P and π_T are plasma and tissue colloid osmotic pressure, respectively. The upward-pointing and downward-pointing arrows show the vascular tendency to filter and absorb, respectively. Data from partial modification of [22] Taylor and Townsky, with permission

The Starling forces in the interstitium are always providing a tendency for the capillaries to filter such that net filtration in the model shown in Fig. 1.3a is always 10. It is now well established that π_T and P_T are functions of capillary pressure and that different tissue forces must exist along the length of the capillary. A reabsorbable model must incorporate with the intestinal microcirculation. Thus, larger amount of lymph formation has appeared in the intestinal microcirculation, comparing with that obtained in the limb microcirculation. The higher lymph formation may be also collaborated with the existence of lacteal vessels in the villi of small intestine.

Figure 1.3b shows the classical model of Starling's law applicable for the limb microcirculation.

1.3 Characteristics of Lymph Transport in the Gastrointestinal Lymphatic System

1.3.1 Heart-Like Spontaneous Contraction-Dependent Lymph Transport in Mesenteric Lymphatics

It is well known that the lymph flow from thoracic duct is passively influenced by respiratory movement and pulsation of blood vessels [23]. On the other hand, the lymph transport of mesenteric lymphatics in human beings, sheep, cattle, rat, and

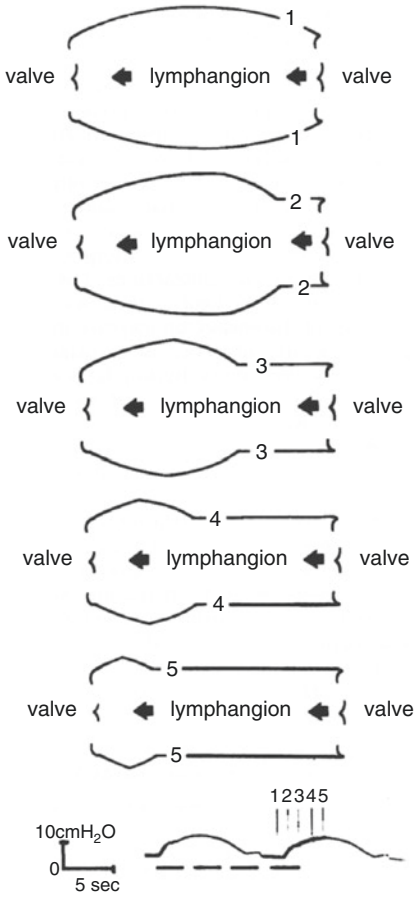

Fig. 1.4 Schematic diagram of propagation of heart-like spontaneous contraction in a one-lymphangion of bovine mesenteric lymphatic. Each of the schemes was drawn from the photograph taken at the moment indicated by a number on the intraluminal pressure curve shown in the lower most panel. Broken line is zero-pressure level. Data from [26] Ohhashi, Azuma, Sakaguchi, with permission

mice is mainly dependent upon the heart-like contractions of lymphatic smooth muscles in the walls [24–26], which may be related to the evidence that the lymph flow originated from gut is the maximum in all kinds of organ-produced lymph flow. The rhythmic activity of mesenteric collecting lymphatics combined with the presence of valves inside these vessels can create pumping pressures as great as 20–30 mmHg [27]. Therefore, the lymphatic system is, in effect, a sump pump for the tissues, always attempting to propel excess free fluid away from tissue spaces. The frequency of heart-like contractions seems to be determined mainly by the amount of lymph in the lymphatics. Thus, when a segment of the vessel immediately below a valve becomes distended, it contracts, and the fluid is pushed forward beyond the valve (Fig. 1.4). The excess filling on the upstream side causes the next segment of the lymphatic to contract, thus propelling the lymph forward to still another segment. In other words, each segment of lymphatic operates as a separate individual pump and is responsive to the amount of lymph that fills its chamber. Thus, the lymphatic pump activity in mesenteric collecting lymphatics is defined as

an active propulsion mechanism of lymph mediated by heart-like spontaneous contractions of lymphatic smooth muscles.

1.3.2 Electrical Characteristics of the Heart-Like Contractions in Mesenteric Collecting Lymphatics

We studied the electrical activity corresponding to the spontaneous contractions of lymphatic smooth muscles by using the sucrose gap [28] and intracellular microelectrode techniques [29, 30]. The mean resting membrane potential of the lymphatic smooth muscle cells is about −50 mV. The resting membrane potential sometimes shows rhythmic fluctuations or slow waves that resemble those in visceral smooth muscles [31]. The minimum depolarization necessary for inducing the spontaneous contraction is about 6 mV in the lymphatic smooth muscle cells [30]. In potassium-free solution, the resting membrane potential is depolarized by about 9 mV, and then the lymphatic smooth muscles demonstrate a sustained contraction. Ouabain at 10^{-5} M also causes a depolarization of the membrane potential with a tetanic contraction in isolated bovine mesenteric lymphatics. The findings suggest that changes in membrane potential seem to play a significant role in the activation of contractile proteins in lymphatic smooth muscles and that an electrogenic sodium pump exists on the plasma membrane of the smooth muscle cells. The depolarization and tension development in the potassium-free solution may be due to decreased activity of the electrogenic sodium pump in the lymphatic smooth muscle cells.

1.3.3 Aminergic Nerve Fibers-Mediated Changes in Physiological Roles of the Heart-Like Spontaneous Contractions: From Lymph Transport to Lymph Formation

1.3.3.1 Presence of Vasa Vasorum in the Mesenteric Collecting Lymphatic Walls for Keeping the Spontaneous Contractions

It is noteworthy that vasa vasorum exists within the media of mesenteric collecting lymphatics with spontaneous contractions [32], which may be essential for maintaining the vigorous spontaneous contractions because of lower oxygen tension in lymph [33]. Thus, large numbers of smooth muscle layers are well developed in the collecting mesenteric lymphatic vessel walls. Quite large numbers of mitochondria are seen on both sides of the nucleus of the smooth muscle cells. Numerous glycogen granules are also found among and around the mitochondria. These structural features might be a morphological manifestation of the high metabolic activity required for the spontaneous contractions of the lymphatic smooth muscles [32].

1.3.3.2 Aminergic Nerve Fibers Are Innervated Densely in the Walls of Mesenteric Collecting Lymphatics

We demonstrated clearly, using the glyoxylic acid method, that the aminergic nerve fibers are distributed densely in the media as well as in the adventitia of bovine

mesenteric collecting lymphatics [34]. The greenish fluorescence of the glyoxylic acid-treated nerves was confirmed to be due to the presence of norepinephrine, which might be neurotransmitter. In addition, non-myelinated nerve fibers, with the small, dense granular vesicles in their varicosities, which are characteristic features of adrenergic cells, penetrated into the smooth muscle layers within the media. Thus, aminergic nerve fibers in bovine mesenteric collecting lymphatics are distributed throughout the entire thickness of the media.

1.3.3.3 Excitation of Aminergic Nerve Fibers-Mediated Changes in the Pacemaker Sites of Spontaneous Contractions on Lymphatic Smooth Muscle Cells

Next, we evaluated the reasons for excitation of aminergic nerve fibers-mediated changes in contraction types of the spontaneous contractions in the isolated bovine mesenteric lymphatics. As shown in Fig. 1.5, we demonstrated very clearly that an activation of aminergic nerve fibers innervated in the lymphatic vessel walls caused a clear movement of the pacemaker site of the regular spontaneous contractions, peristaltic movement type, resulting in the development of irregular spontaneous contractions, of pendulum movement type [35]. Thus, the collecting lymphatics were dissected from fresh bovine mesentery, cannulated at both ends, and set up in the Krebs-bicarbonate solution in a horizontal organ bath. The outflow pressure and outer diameter of the lymph vessel at the pacemaker site of the spontaneous

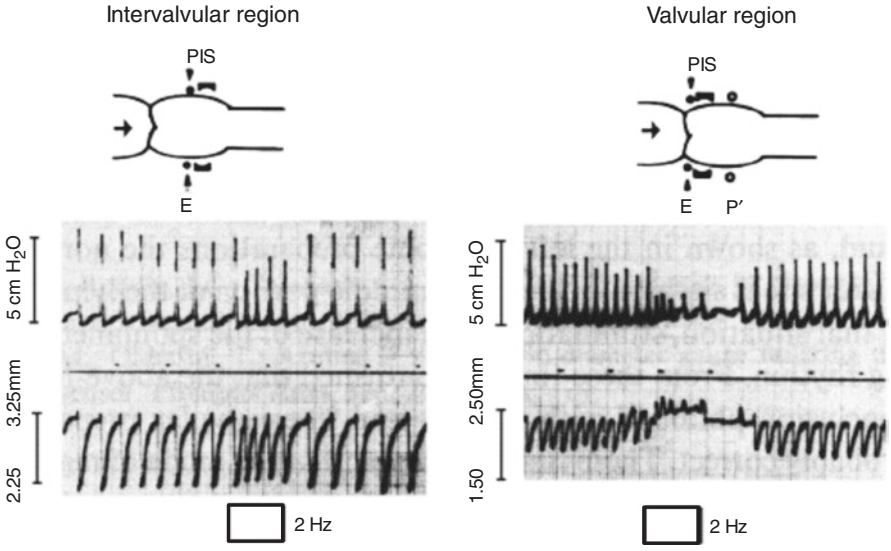

Fig. 1.5 Representative responses of two kinds of pumping preparations in bovine mesenteric collecting lymphatics to electrical stimulatory, which are rectangular pulses of 50 V, 0.5 ms induration at 2 Hz. The pacemaker sites are situated in valvular (right panel) and intervalvular (left panel) region, respectively. *p* Pacemaker position of the rhythmic spontaneous contraction in each preparation, *p′* new pacemaker position of the contraction, *IS* recording position of outer diameter of the lymphatics in each preparation. Data from [35] Ohhashi, with permission

contractions were simultaneously measured by a pressure transducer and a handmade diameter gauge with an image sensor [36]. The platinum electrode was adjusted at the pacemaker site to stimulate, selectively, aminergic nerve fibers innervated into the lymphatic walls. Figure 1.5 shows the responses of two kinds of spontaneous contractions to the electrical stimulation. As shown in the right panel, the electrical stimulation of the pacemaker site, which was located in the wall of the immediate vicinity of the inlet valve, made it to move to the intervalvular region of the lymphatics (p′ in the panel). Spontaneous contractions with the new pacemaker site resulting in the contractions of the pendulum movement type produced passive distension of the outer diameter at the valvular region. About 1 min after an interruption of the stimulation, the pacemaker site returned to the previous site, the valvular region. On the other hand, as shown in the left panel of Fig. 1.5, in some preparations with increasing the organ-bath temperature (~38 °C) the pacemaker site of the spontaneous contractions is observed at the middle portion of the lymphangion. In this case, the electrical stimulation caused an increase of the frequency of the contractions only, but did not change the pacemaker site. These findings suggest that the regulatory effects of aminergic nerve fibers on the lymphatic pump activity may depend upon the position of pacemaker site of the spontaneous contractions, resulting in the change of type of contractions, from peristaltic movement to pendulum movement. The physiological meaning of the aminergic nerve fibers-dependent changes of the type of contractions may be related to the modifications from the spontaneous contraction-mediated active lymph transport to the tentative increase of lymph formation, since the pendulum-type spontaneous contractions may accelerate the absorption of tissue fluid and albumin through the lymph capillaries in the intestinal microcirculation.

1.4 Physiological Insights of Sentinel Lymph Node (SLN)

1.4.1 The SLN May Be Defined as It Is Constantly Subjected to Higher Lymph Flow from Physiological Point of View

The clinical impact of the SLN concept has become one of the most important current topics in surgical oncology in patients with breast cancer and melanoma [37]. Recently, gastric cancer has also been identified as a target for SN navigation surgery [38]. We attempted to evaluate the usefulness of the contrast-enhanced ultrasonography (CEUS)-guided method with Sonazoid for imaging of the lymphatic channels and the SLN of stomach in a porcine model [39]. Contrast imaging using the intragastric or transcutaneous CEUS-guided method with Sonazoid enabled us to produce clear images of the afferent lymph vessel and SLN of the stomach within 2 h after the injection of Sonazoid (Fig. 1.6). Intranodal flow of the microbubble agent would be also clearly observed using tissue linear harmonic images of the SLN. With the CEUS-guided study, we reached the conclusion that the SLN may be

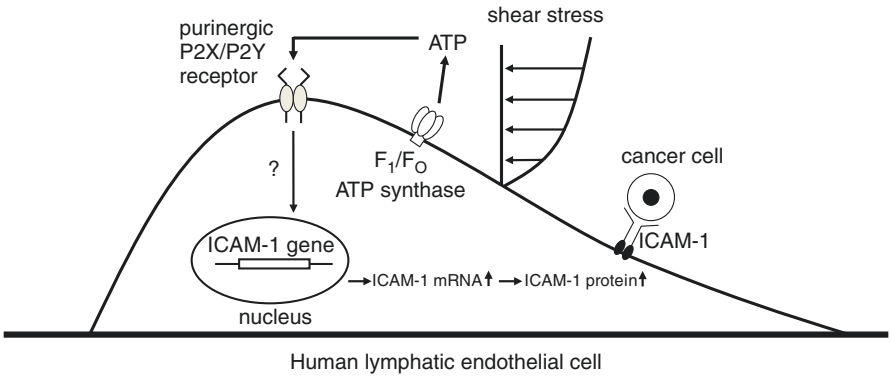

Fig. 1.6 Schematic diagram outlining shear stress stimulation inducing ATP release by activating cell surface F_1/F_0 ATP synthase, which results in the overexpression on human lymphatic endothelial cells. Data from [41] Kawai et al., with permission

physiologically defined as the SLN to be constantly subjected to higher lymph flow comparing with these within the regional lymph nodes.

1.4.2 Higher Lymph Flow-Induced ATP-Mediated Intercellular Adhesion Molecule (ICAM)-1-Dependent Micrometastasis of Carcinoma Cells in SLN

The SLN are the most common and earliest site of malignant tumor metastasis. The clinical success of sentinel node navigation surgery suggests that the SLN are an effective mechanical barrier against migrating cancer cells. It is known that primary tumors influence the microenvironments of distant organs during the development of metastasis [40]. However, it is unclear which molecules in premetastatic SLN produce a suitable environment for micrometastasis within the node. The SLN also contain marginal endothelial cells, which might be constantly loaded with higher shear stress. Thus, we examined the hypothesis that the higher shear stress generated by increased lymph flow through the SLN contributes to the development of premetastatic environment that is suitable for carcinoma micrometastases within the node.

Therefore, we attempted to investigate (1) the effects of shear stress stimulation on the expression of adhesion molecules on cultured human lymphatic endothelial cell (LEC) isolated from the afferent lymph vessels nearest to SLN and (2) on the release of ATP from human LEC, and (3) to study whether shear stress-mediated increases in adhesion molecule expression accelerate the attachment of carcinoma cells to cultured human LEC. Finally, in *in vivo* rat experiments we (4) evaluated whether the ATP released from lymphatic endothelial cells in response to shear stress stimulation facilitates the expression of carcinoma cell-ligated adhesion molecules within rat SLN.

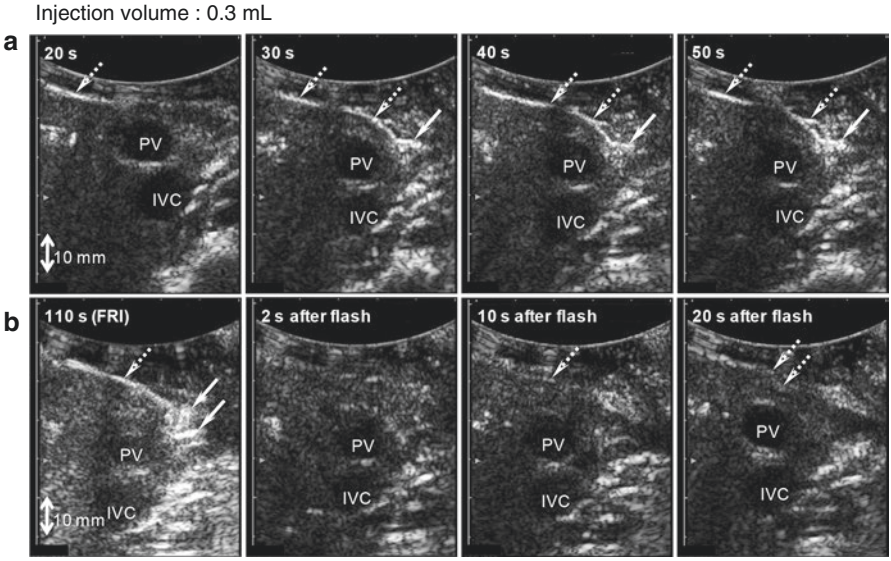

Fig. 1.7 (**a**) Representative tracings of contrast images of the afferent lymph vessels and sentinel lymph node (SLN) of the porcine stomach obtained using the CEUS-guided method with the intra- and sub-mucosal injection of 0.3 mL Sonazoid. (**b**) Representative tracings of flash replenishment images (FRI) and contrast harmonic FRI images obtained at 2, 10, and 20 s after stimulation in the same animal. The dotted arrows show the afferent lymph vessels. The solid arrows are SLN of the stomach. The PV and IVC show the portal vein and inferior caval vein, respectively. Data from [39] Kawai et al., with permission

In conclusion, shear stress stimulation induced ATP release by activating cell surface F_1/F_0 ATP synthase, which resulted in the overexpression of ICAM-1 on human LEC, and hence facilitated the ICAM-1-mediated attachment of carcinoma cells to human LEC in the afferent lymph vessels of SLN from breast cancer patients [41] (Fig. 1.7).

In fact, we confirmed the overexpression of ICAM-1 on the SLN tissues with metastasis of carcinoma cells in the patients with breast cancer [42]. Figure 1.8 demonstrates representative microphotographs of immunohistochemical expression of E-selectin and ICAM-1 on the fresh-frozen SLN tissues isolated from breast cancer patients. As shown in Fig. 1.8f, h, the immunohistochemical expressions of ICAM-1 are strongly observed on the SLN tissues with metastasis of carcinoma cells. In contrast, the expression of ICAM-1 is weakly found on the SLN tissue without metastasis of carcinoma cells isolated from the same patient with breast cancer (Fig. 1.8e, g).

On the other hand, no or little expression of E-selectin is confirmed on the SLN tissues with and without metastasis of carcinoma cells (Fig. 1.8c, d).

Representative hematoxylin-eosin stained microphotographs of the SLN tissues with and without metastasis of carcinoma cells was shown (Fig. 1.8a, b).

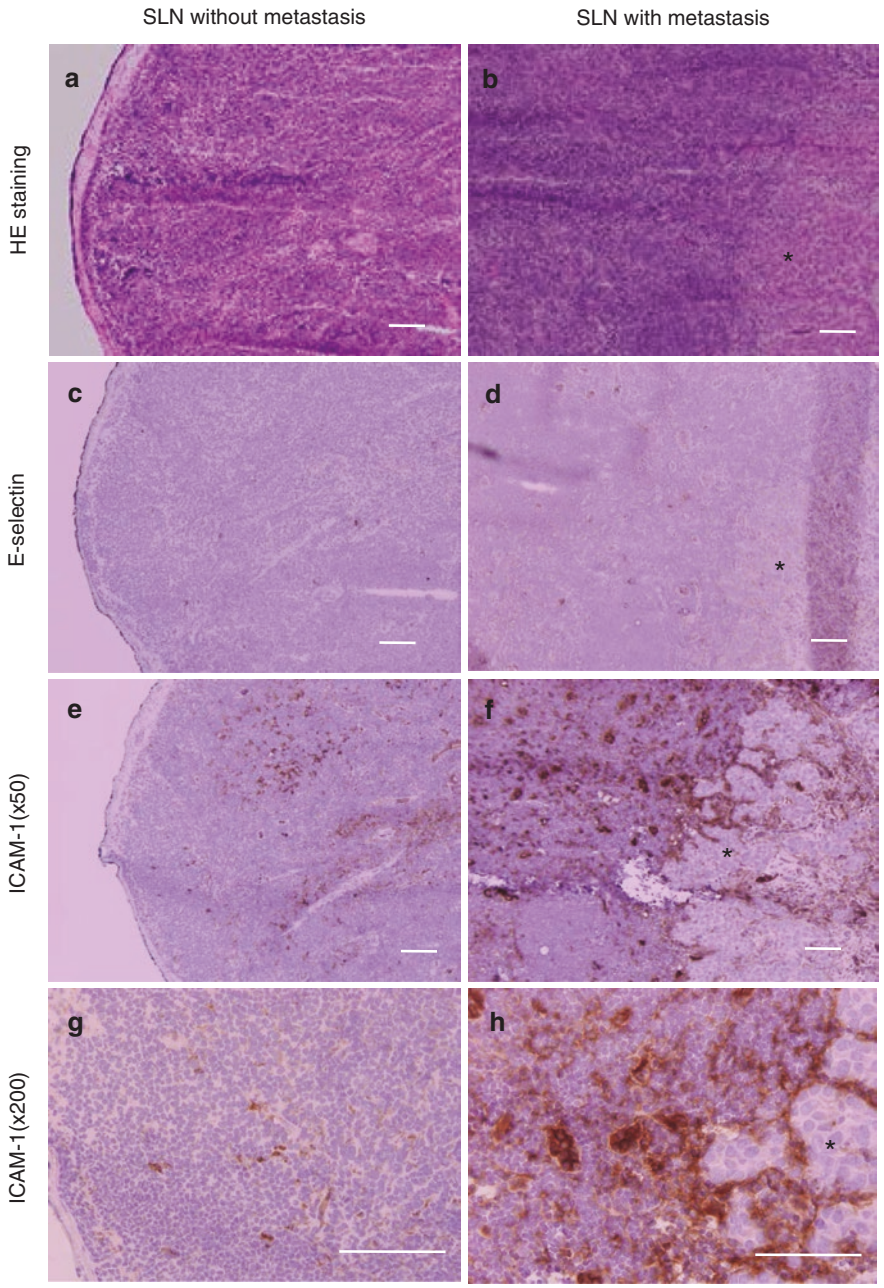

Fig. 1.8 Representative photomicrographs of immunohistochemical expression of E-selectin (**c**, and **d**) and ICAM-1 (**e**, **f**, **g**, and **h**) on the fresh-frozen SLNs tissues with or without carcinoma cells isolated from a patient with breast cancer. The panels of (**a**) and (**b**) show the hematoxylin-eosin stained SLNs tissues. *, metastatic region of carcinoma cells in the SLN. Each bar is 100 μm. Data from [42] Kawai et al., with permission

1.5 Summary

In this chapter, the characteristic properties of lymph formation and transport in the gastrointestinal lymphatic system are shown. The pivotal roles of the intestinal lymphatic system may be summarized as the transported route of absorbed lipids with long-chain and albumin-binded hydrophilic substances, and of lymphocytes and immune-related cells released from the GALT of intestinal villi.

Thus, the higher permeability of plasma protein, especially albumin through the venules in the intestinal microcirculation, may contribute to the maximal lymph formation and large amount of lymph flow in the gastrointestinal lymphatic system compared with those produced in the other organs. The presence of lacteal vessels in the villi in the intestine mucosa is compatible with the higher lymph flow in intestinal lymphatic system. In addition, the unique property of heart-like spontaneous contraction of the lymphatic smooth muscles in mesenteric collecting lymphatics may develop the functional properties of intestinal lymphatic system. The spontaneous contractions in the mesenteric lymphatics are observed in almost all kinds of animals including human beings. Therefore, higher shear stress originated by the large amount of lymph flow and the spontaneous contractions demonstrates important physiological or pathophysiological roles in the gastrointestinal lymphatic system as well. Thus, the shear stress stimulation may be collaborated with development of suitable microenvironment for micrometastasis of carcinoma cells with the SLN.

In future, new lymphology will be established by the combination of these physiological properties in the gastrointerstinal lymphatic system with gut immunology, we have expected.

References

1. Yoffey JM, Courtice FC. Lymphatics, lymph and the lymph myeloid complex. London: Academic Press; 1970.
2. Guyton AC, Taylor AE, Granger HJ. Circulatory physiology II, dynamics and control of body fluids. Philadelphia: Saunders; 1975. p. 125–60.
3. Ohhashi T, Mizuno R, Ikomi F, Kawai Y. Current topics of physiology and pharmacology. Pharmacol Ther. 2005;105:165–88.
4. Roitt I. Essential immunology. Oxford: Blackwell Scientific Publication; 1980.
5. Gowans JL, Knight EJ. The route of re-circulation of lymphocytes in the rat. Proc R Soc Lond B Biol Sci. 1964;159:257–82.
6. Hall JG, Morris B. The origin of the cells in the efferent lymph from a single lymph node. J Exp Med. 1965;121:901–10.
7. Ohhashi T, Kawai Y. Proposed new lymphology combined with lymphatic physiology, innate immunology, and oncology. J Physiol Sci. 2015;65:51–66.
8. Hargens AR, Zweifach BW. Transport between blood and peripheral lymph in intestine. Microvasc Res. 1976;11:89–101.
9. Landis EM, Pappenhimer JR. Exchange of substances through the capillary walls. In: Hamilton WF, Dow P, editors. Circulation, Handbook of physiology, vol. II. Washington, DC: American Physiological Society; 1963. p. 961–1034.
10. Wasserman K, Mayerson HS. Exchange of albumin between plasma and lymph. Am J Phys. 1951;165:15–26.

11. Brace RA, Taylor AE, Guyton AC. Time course of lymph protein concentration in the dog. Microvasc Res. 1977;14:243–9.
12. Adair TH, Moffatt DS, Paulsen A. Quantitation of changes in lymph protein concentration during lymph node transit. Am J Phys. 1982;243:H351–9.
13. Ono N, Mizuno R, Ohhashi T. Effective permeability of hydrophilic substances through walls of lymph vessels: roles of endothelial barrier. Am J Phys. 2005;289:H1676–82.
14. Adair TH, Guyton AC. Modification of lymph by lymph nodes. III. Effect of increased lymph hydrostatic pressure. Am J Phys. 1985;249:H777–82.
15. Quin JW, Shannon AD. The influence of the lymph node on the protein concentration of efferent lymph leaving the node. J Physiol Lond. 1977;264:307–21.
16. Knox P, Pflug JJ. The effect of the canine popliteal node on the composition of lymph. J Physiol Lond. 1983;345:1–14.
17. Borgstrom B, Lau Rell CB. Studies on lymph and lymph-protein during absorption of fat and saline. Acta Physiol Scand. 1953;29:264–80.
18. Granger DN, Taylor AE. Effects of solute-coupled transport on lymph flow and oncotic pressures in cat ileum. Am J Phys. 1978;235:E429–36.
19. Granger DN, Perry MA, Kvietys PR, Taylor AE. Interstitium-to-blood movement of macromolecules in the absorbing small intestine. Am J Phys. 1981;241:G31–6.
20. Adamson RH, Zeng M, Adamson GN, Lenz JF, Curry FE. PAF- and bradykinin-induced hyperpermeability of rat venules is independent of actin-myosin contraction. Am J Phys. 2003;285:H406–17.
21. Moy AB, Van Engelenhoven J, Bodmer J, Kamath J, Keese C, et al. Histamine and thrombin modulate endothelial focal adhesion through centripetal and centrifugal forces. J Clin Invest. 1996;97:1020–7.
22. Taylor AE, Townsley MI. Evaluating of the Starling fluid flux equation. NIPS. 1987;2:48–52.
23. Webb RC Jr, Starzl TE. The effect of blood vessel pulsations on lymph pressure in large lymphatics. Bull Johns Hopkins Hosp. 1953;93:401–7.
24. Kinmonth JB, Taylor GW. Spontaneous rhythmic contractility in human lymphatics. J Physiol Lond. 1956;133:3P.
25. Mawhinney HJ, Roddie IC. Spontaneous activity in isolated bovine mesenteric lymphatics. J Physiol Lond. 1973;229:339–48.
26. Ohhashi T, Azuma T, Sakaguchi M. Active and passive mechanical characteristics of bovine mesenteric lymphatics. Am J Phys. 1980;239:H88–95.
27. Hall JG, Morris B, Woolley G. Intrinsic rhythmic propulsion of lymph in the unanaesthetized sheep. J Physiol Lond. 1965;180:336–49.
28. Azuma T, Ohhashi T, Sakaguchi M. Electrical activity of lymphatic smooth muscles. Proc Soc Exp Biol Med. 1977;155:270–3.
29. Ohhashi T, Azuma T, Sakaguchi M. Transmembrane potentials in bovine lymphatic smooth muscle. Proc Soc Exp Biol Med. 1978;159:350–2.
30. Ohhashi T, Azuma T. Effect of potassium on membrane potential and tension development in bovine mesenteric lymphatics. Microvasc Res. 1982;23:93–8.
31. Speden RN. Electrical activity of single smooth muscle cells of the mesenteric artery produced by splanchnic nerve stimulation in the Guinea pig. Nature. 1964;202:193–4.
32. Ohhashi T, Fukushima S, Azuma T. Vasa vasorum within the media of bovine mesenteric lymphatics. Proc Soc Exp Biol Med. 1977;154:582–6.
33. Ikomi F, Mizuno R, Nakaya K, Ohhashi T. Effects of vasoactive substances on oxygen tension in thoracic duct lymph. Jpn J Physiol. 2000;50(Suppl):S74.
34. Ohhashi T, Kobayashi S, Tsukahara S, Azuma T. Innervation of bovine mesenteric lymphatics: from histochemical point of view. Microvasc Res. 1982;24:377–85.
35. Ohhashi T. Regulation of motility of small collecting lymphatics. In: Staub NC, Hargens AR, editors. Interstitial-lymphatic liquid and solute movement. Basel: Karger; 1987. p. 171–83.
36. Sakaguchi M, Ohhashi T, Azuma T. A photoelectric diameter gauge utilizing the image sensor. Pflügers Arch. 1979;378:263–8.

37. Morton DL, Wen DR, Wang JH, et al. Technical details of intraoperative lymphatic mapping for early stage melanoma. Arch Surg. 1992;127:392–9.
38. Kitagawa Y, Kitajima M. Gastrointestinal cancer and sentinel node navigation surgery. J Surg Oncol. 2002;79:188–93.
39. Kawai Y, Ajima K, Nagai T, Kaidoh M, Ohhashi T. Real-time imaging of the lymphatic channels and sentinel lymph nodes of the stomach using contrast-enhanced ultrasonography with Sonazoid in a porcine model. Cancer Sci. 2011;102:2073–81.
40. Hiratsuka S, Watanabe A, Aburatani H, et al. Tumor-mediated upregulation of chemoattractants and recruitment of myeloid cells predetermines lung metastasis. Nat Cell Biol. 2006;8:1369–75.
41. Kawai Y, Yokoyama Y, Kaidoh M, Ohhashi T. Pivotal roles of shear stress in the microenvironmental changes that occur within sentinel lymph nodes. Cancer Sci. 2012;103:1245–52.
42. Kawai Y, Kaidoh M, Yokoyama Y, Sano K, Ohhashi T. Chemokine CCL2 facilitates ICAM-1-mediated interactions of cancer cells and lymphatic endothelial cells in sentinel lymph nodes. Cancer Sci. 2009;100:419–28.

Anatomy of Lymphatics

2

Tatsuo Sato

Abstract

To facilitate a clearer understanding of the topographical arrangement of lymphatics, pictorial demonstrations based on actual cadaveric dissections of four segments of the digestive tract (esophagus, stomach, colon, and rectum) are provided.

1. The lymphatics of the esophagus: Due to the pressure of the aortic arch from the left, asymmetrical development of the ascending lymphatics along the trachea and esophagus is observed. The typical right ascending lymphatic chain reaches the lower neck and follows upstream along the inferior thyroid artery to reach the right venous angle. Several branches are given off from this chain at various levels to finally reach the venous angle. As the left ascending chain is generally poorly developed, most of the lymphatics of the left tracheobronchial nodes move rightward to join the right chain. The left chain is located close to and anterior to the left recurrent laryngeal nerve. The lymphatic chain of the lower thoracic esophagus connects with the lymph vessels of the left gastric nodes via the superior diaphragmatic nodes close to the esophagus.
2. The lymphatics of the stomach: In general, lymphatics accompany the typical arteries and finally connect to the coeliac nodes at the origin of the coeliac trunk. However, in the case of the right gastroepiploic artery, lymph vessels do not accompany the artery, but rather they run along the vein and drain into the superior mesenteric nodes. Furthermore, atypical lymphatics are observed: (a) those which descend along the posterior gastric artery to join the splenic lymphatics, and (b) those which run along the cardioesophageal branch of the left inferior phrenic artery, and then descend along this artery, to finally drain into the lateral aortic nodes.

T. Sato (✉)
Tokyo Medical and Dental University, Tokyo, Japan
e-mail: tsato@ikadoso-tmdu.jp

S. Natsugoe (ed.), *Lymph Node Metastasis in Gastrointestinal Cancer*,
https://doi.org/10.1007/978-981-10-4699-5_2

3. The lymphatics of the colon: The lymphatics of the right hemicolon accompany the colic branches of the superior mesenteric artery and then gather around this artery. Before reaching the superior mesenteric artery, lymph vessels cross the superior mesenteric vein. The lymphatics of the left hemicolon also run along the inferior mesenteric artery and gather at the lateroaortic nodes. Some lymph vessels cross in front of the abdominal aorta and reach the interaorticocaval nodes.
4. The lymphatics of the rectum: In addition to the classically recognized superior group, the lateral (middle) group of the lymphatics are demonstrated. In order to reach the subaortic nodes, lymphatics from the rectum first reach the nodes of the interiliac area with or without accompanying the middle rectal artery. The iliac lymph vessels surround and run alongside the iliac blood vessels. Before reaching the interiliac area, the lymphatics cross over or under the cord of the umbilical artery. Some lymph vessels from the posterior wall of the rectum run backwards and pierce the fascial membrane between the right and left hypogastric nerves before reaching the subaortic nodes. The subaortic nodes are of great importance as they perform the role of a terminal station of the pelvic lymphatics as well as the starting station of the para-aortic lymphatics.
5. The para-aortic nodes (lumbar nodes): Para-aortic nodes surround not only the abdominal aorta, but also the inferior vena cava. The para-aortic lymphatics originate from the subaortic nodes and from the lateral aortic and lateral caval nodes at the level of the lower ends of the aorta and inferior vena cava. These lymphatics are also well developed behind the two great blood vessels. Up to the level of the renal blood vessels, the lymphatics surrounding the inferior vena cava gather around the interaorticocaval nodes. The lymph vessels from the uppermost interaorticocaval and lateral aortic nodes converge behind the aorta to form the thoracic duct.

Keywords
Esophageal lymphatics · Gastric lymphatics · Lymphatics of the large intestine
Para-aortic lymph nodes · Topographical anatomy

Abbreviations

aa Arch of aorta
ac Ascending colon
acc Accessory nerve
ai Angular incisure
alg Accessory left gastric artery
an Anterior group node of deep lateral cervical nodes
ap Appendix vermiformis
apa Appendicular artery
av Anterior vagus trunk
az Azygos vein

aza Arch of azygos vein
bc Brachiocephalic trunk
bca Brachiocephalic angle node
bd Common bile duct
bt Bifurcation of trachea
cae Caecum
cc Common carotid artery
cd Cardia
ceb Cardioesophageal branch
ch Common hepatic artery
ci Common iliac artery
civ Common iliac vein
co Coeliac node
cp Caudate process
ct Coeliac trunk
di Diaphragm
du Duodenum
eb Esophageal branch
ec External carotid artery
ei External iliac artery
eiv External iliac vein
epc Epicolic node
es Esophagus
gb Gallbladder
gct Gastrocolic trunk
gd Gastrodudenal artery
hb Hepatic branch (anterior vagus)
hp Hepatic artery proper
ica Ileocolic artery
iil Interiliac node
ii Internal iliac artery
ij Internal jejunal vein
ile Ileum
im Intermediate node
ima Inferior mesenteric artery
imv Inferior mesenteric vein
ipv Left inferior phrenic vein
ita Internal thoracic artery
itb Inferior tracheobronchial node
ith Inferior thyroid artery
ivc Inferior vena cava
jd Jugulodigastric node
jo Jugulo-omohyoid node
la Lateral aortic node
lb Left bronchus
lbc Left brachiocephalic vein

lc Lateral caval node
lca Left colic artery
lg Left gastric artery
lga Ligamentum arteriosum
lgo Left gastro-omental artery
lgv Left gastric vein
li Liver
lia Ligamentum arteriosum
lip Left inferior phrenic artery
lk Left kidney
ll Left lung
ln Lateral group node of deep lateral cervical nodes
lrv Left renal vein
lt Lumbar trunk
lv Left vagus nerve
lva Levator ani
mca Middle colic artery
mra Middle rectal artery
of Omental foramen node
ov Ovarian vein
pa Pre-aortic
pb Pubic bone
pc Paracolic node
pd Pancreaticoduodenal node
pe Peritoneum
pg Posterior gastric artery
ph Phrenic nerve
pl Pleura
poc Postcaval node
pr Principal node
prm Promontorium
ps Pelvic splanchnic nerve
pso Psoas major
pu Pubis
pua Pulmonary artery
pv Portal vein
py Pylorus
rb Right bronchus
rbc Right brachiocephalic vein
rc Recurrent laryngeal nerve
rca Right colic artery
rg Right gastric artery
rgo Right gastro-omental artery
rgov Right gastro-omental vein
rk Right kidney
rl Right lung

rrv Right renal vein
S1 First sacral vertebra
Sa Subaortic node
sc Subclavian artery
scv Subclavian vein
sg Short gastric artery
sh Superior hypogastric plexus
si Sigmoid colon
sia Sigmoid artery
sl Superior laryngeal nerve
sm Submandibular gland
sp Spleen
spa Splenic artery
spv Splenic vein
sr Suprarenal gland
sra Superior rectal artery
srpd Superior retropancreaticoduodenal node (Rouvière)
srv Suprarenal vein
st Stomach
sth Superior thyroid artery
sva Superior vesical artery
svc Superior vena cava
syt Sympathetic trunk
ta Testicular artery
tc Thyroid cartilage
td Thoracic duct
th Thyroid gland
tr Trachea
tv Testicular vein
ua Uterine artery
ub Urinary bladder
ur Ureter
ut Uterus
utt Uterine tube
va Venous angle
vc Vertebral column
vg Vagus nerve
vgn Vagina

2.1 Introduction

In routine dissections students have little chance to observe the lymphatics which are very complicated and difficult to dissect. Yet the lymphatics are crucial structures, not to be overlooked, because for cancer surgery, precise knowledge of the lymphatics of an affected organ is of utmost importance. The gastrointestinal tract

is long and extends over many regions. Each organ has a very specific relationship with the lymphatics. In addition to common problems, there are many specific difficulties based on topographic anatomical relationships. In cancer surgery, in particular, the precise and detailed anatomy of the lymphatics of the affected organ(s) and their topographic relationships is of utmost importance. In this chapter, the basic anatomy of the lymphatics of the esophagus, stomach, colon, and rectum is described. To facilitate understanding, a pictorial demonstration of actual dissections of the lymphatics surrounding each organ is included. For orientation, schemes based upon actual dissection findings are shown. In anatomy and particularly in lymphatics, terminology can be a hurdle; therefore, an attempt was made to provide a range of terms including basic terminology from Rouvière [1], the terminology used in cancer guidelines in Japan [2–4], and Terminologia Anatomica (1998 [5]) from the Federative Committee on Anatomical Terminology (FCAT) of the International Federation of Anatomists (IFAA).

2.1.1 Lymphatics of the Esophagus

The esophagus is situated within three regions: cervical, thoracic, and abdominal regions. Here, the cervical and thoracic lymphatics will be discussed.

2.1.1.1 Lateral Cervical Nodes (Internal Jugular Chain)

Lymphatics of the cervical part of the esophagus drain into the deep lateral cervical nodes. The prominent lateral cervical nodes are located along the internal jugular vein and have been termed the internal jugular chain (Rouvière [1], Feind in Haagensen [6]) (Fig. 2.1) [7]. According to the positional relationship to this vein, this chain is subdivided into anterior and lateral groups which are connected by numerous transverse lymph vessels; these vessels run both over and behind the jugular vein. The well-developed lateral group descends and drains into the venous angle, while the anterior group gradually becomes less developed, descends behind the omohyoid muscle, then traverses over and under the jugular vein and joins the lateral group to finally drain into the venous angle. In addition to these deep cervical lymphatics, a superficial lymph vessel runs on the thyroid gland and crosses over the lower part of the internal jugular vein to join the jugulo-omohyoid node.

The deep anterior cervical nodes are sometimes called the juxtavisceral nodes based on their location and nodal associations (Rouvière [1], Feind in Haagensen [6]). In this specimen a paratracheal node close to the lower end of the right lobe of the thyroid gland sends a vessel to the large nodes located in front of the junction of brachiocephalic veins (Fig. 2.2) [7]. From these brachiocephalic angle nodes two vessels ascend in front of the right brachiocephalic vein and drain into the right venous angle. Between the left tracheal wall and the left brachiocephalic vein well-developed lymph chains are detected. Some deep nodes of these paratracheal chains receive lymph from the esophagus.

A typical accompanying lymph vessel along the inferior thyroid artery is shown in Fig. 2.3. From a lymph node mass close to the lower end of the right thyroid lobe and near the right groove between the trachea and esophagus, a lymph vessel

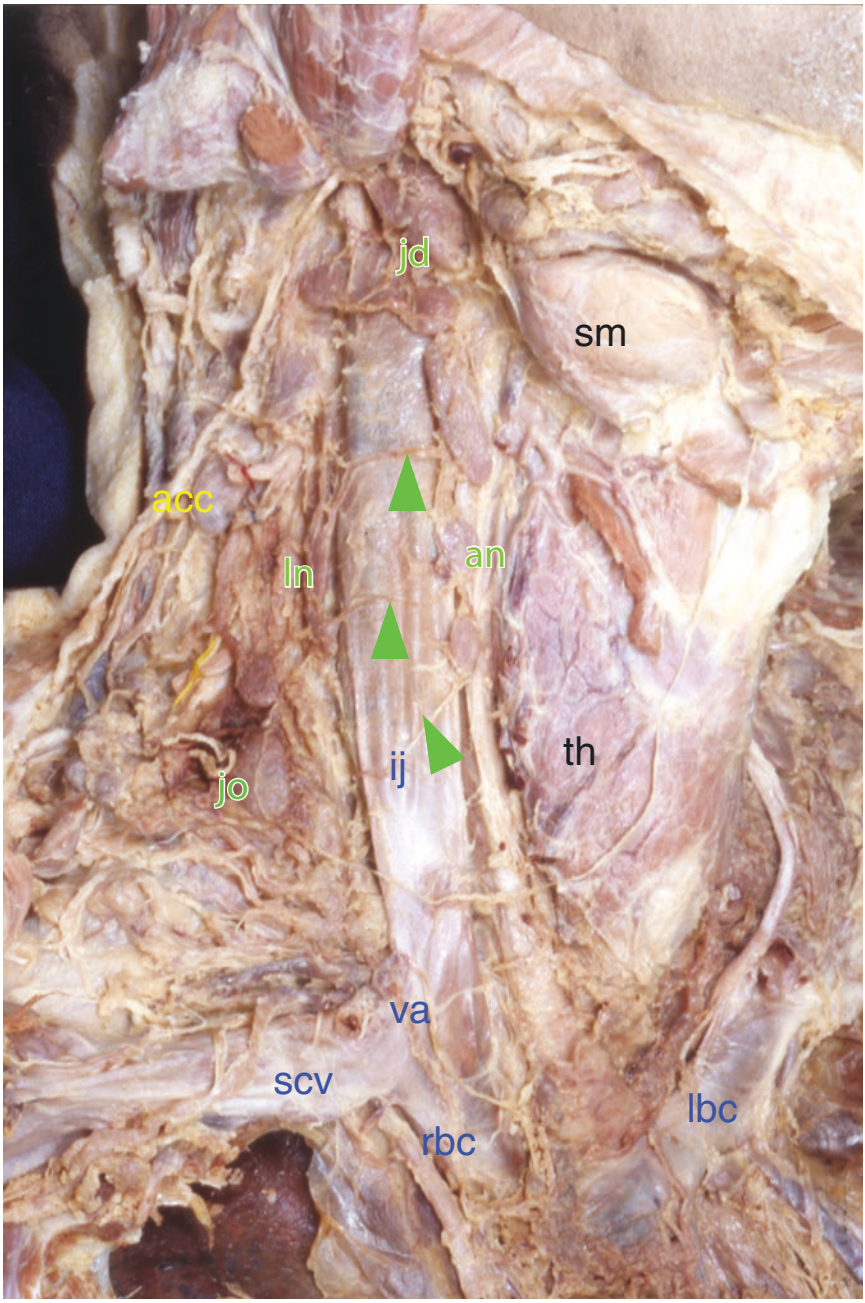

Fig. 2.1 Lateral deep cervical lymphatic chains. Anteromedial and posterolateral to the right internal jugular vein, the lymphatic chains, which are connected by numerous transverse slender lymph vessels (green arrowheads), finally drain into the venous angle (Specimen 1, male)

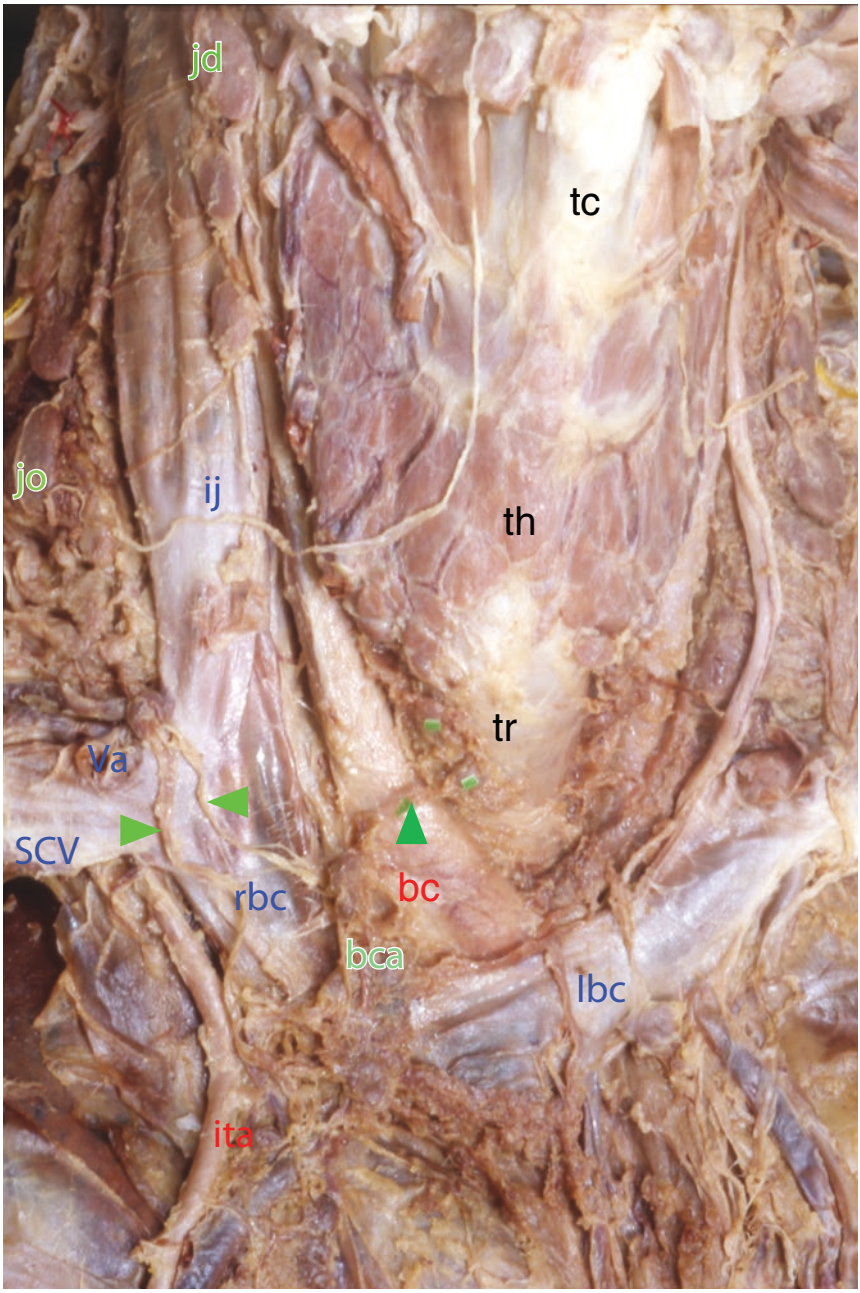

Fig. 2.2 Brachiocephalic angle nodes. From the right paratracheal nodes, close to the lower end of the right thyroid lobe, a lymph vessel (dark green arrowhead) drains into the nodes at the confluence of the brachiocephalic veins (brachiocephalic angle nodes). From these nodes, two thick lymph vessels (light green arrowheads) obliquely ascend to drain into the venous angle (Specimen 1, male)

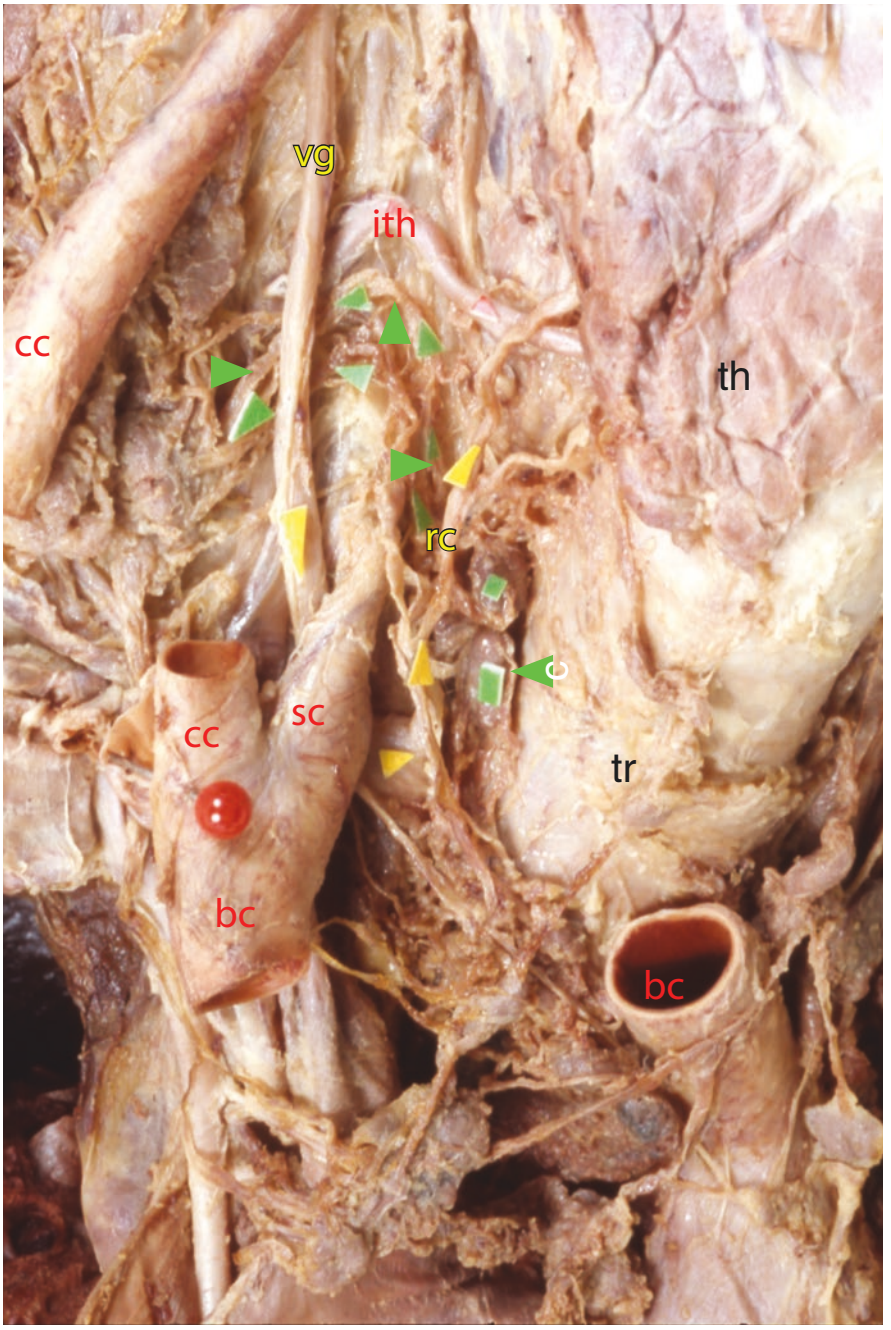

Fig. 2.3 A lymph vessel along the inferior thyroid artery. The brachiocephalic and right common carotid arteries have been cut. A lymph vessel (green arrowheads) originates from the right paratracheal chain and runs parallel to and caudal to the inferior thyroid artery to reach the venous angle area (Specimen 1, male)

originates, runs parallel and caudal to the inferior thyroid artery, and then continues to the node mass near the origin of this artery. During its course, it first crosses the recurrent laryngeal nerve and then the vagus nerve (yellow arrowheads) before reaching the venous angle area.

A lymph vessel from the left paratracheal node group, which drains into the left venous angle, is shown in Fig. 2.4. From the upper end of the left cervical paratracheal node mass, which is situated in front of the left margin of the esophagus, a lymph vessel originates; it follows an arched course in front of the recurrent laryngeal nerve to reach the venous angle.

A special dissection of the lymphatics and autonomic nerves from behind is demonstrated (Fig. 2.5, Saito et al.) [8]. After the en masse removal of the tongue, pharynx, esophagus, and sympathetic trunks, dissection was performed from behind. Note the well-developed internal jugular lymphatic chains and also the slender lymph vessels along the carotid arteries. In the upper part of the pharynx and in the transitional area of the pharynx and esophagus, also in the area of the cervical esophagus, dense networks of lymphatics can be seen. Behind the pharynx and along its lateral margin, lymphatics connect to the abovementioned networks.

The lymphatics of the thoracic esophagus are closely related to the tracheobronchial lymphatics. First, the tracheobronchial ascending lymphatics are shown (Fig. 2.6) [9]. In general there are four main ascending pathways: right and left superficial pathways, which run along the great blood vessels, and right and left deep pathways, which run along the trachea and esophagus. Here, the right and left deep pathways will be explained.

A typical right deep pathway is seen in Fig. 2.7. From the right tracheobronchial nodes, a lymphatic chain ascends along the right margin of the trachea, reaches the lower neck and then changes direction to run obliquely along the inferior thyroid artery and finally drains into the venous angle. From the vertical ascending course, shown in Fig. 2.8, several lymphatic vessels originate at various levels and then run obliquely to reach the venous angle [10].

In a rather rare example, interestingly, a lymphatic vessel from the right tracheobronchial node can be very lengthy, yet still take a direct course to the venous angle (Fig. 2.9) [11]. Although the frequency of such a lengthy and non-interrupted lymphatic vessel remains to be clarified, for esophageal and lung cancer this is a particularly critical pathway, due to its direct course.

It is also important to note here that there are lymphatic pathways which run directly from the esophagus. In an important example (Fig. 2.10) [11], after reflection of the vagus, it was noted that lymph vessels ascend to reach the venous angle, not only from the tracheobronchial nodes, but also from the esophagus and primarily from the vertebral column.

In addition to the discussion of the abovementioned lymphatic pathways, significant node groups should be carefully considered based on their critical location. In the space between the arch of the azygos and the subclavian artery (Baréty's space [12]), there are no large structures to compress the right side of the trachea and esophagus, thereby allowing the development of lymph nodes and vessels (Fig. 2.11) [13]. The nodes in front of the right vagus are more closely related to the trachea,

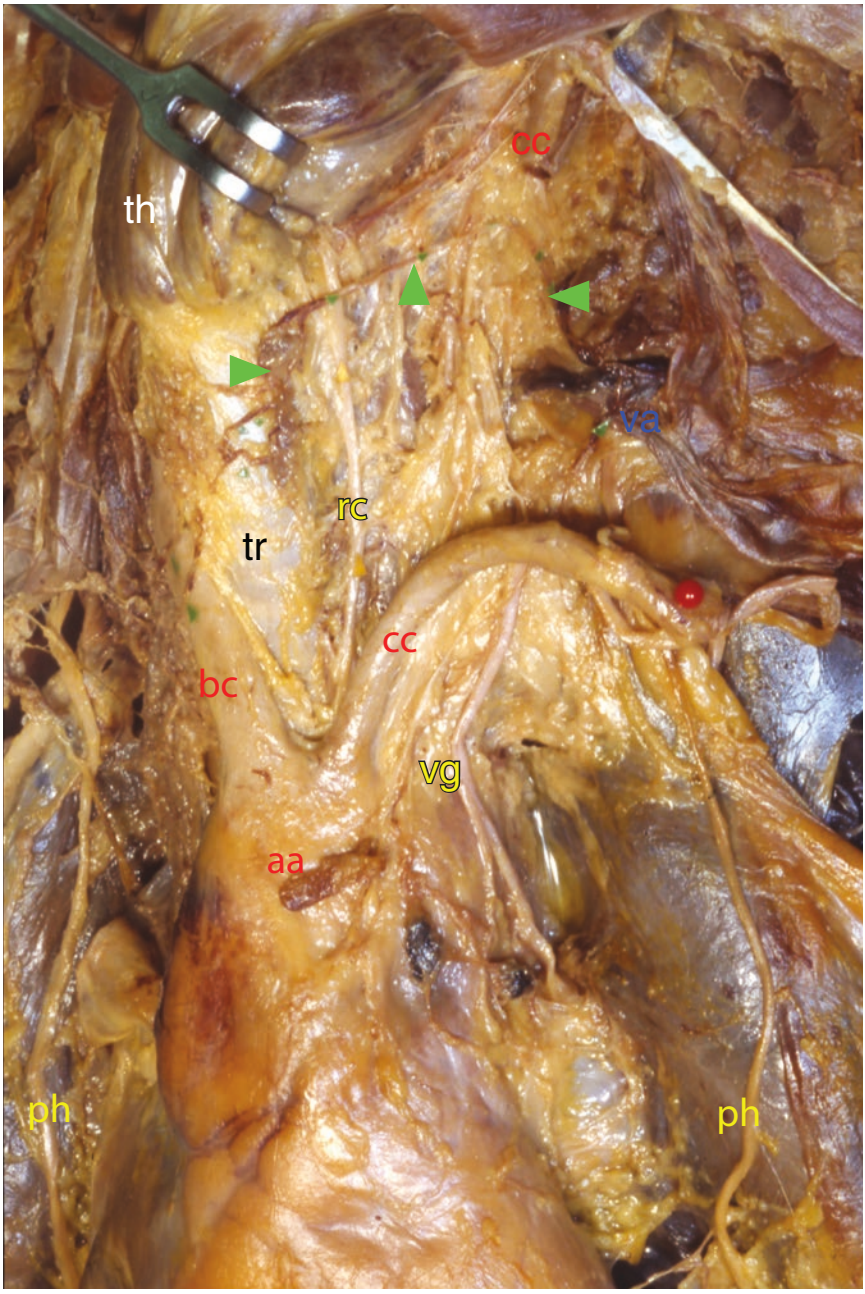

Fig. 2.4 A lymph vessel from the left paratracheal chain to the left venous angle. The left common carotid artery has been cut at the level of the thyroid gland and its proximal segment is pulled inferiorly (red pin). A lymph vessel (green arrowheads), from the nodes slightly below the thyroid, runs laterally to reach the venous angle (Specimen 2, male)

Fig. 2.5 Posterior dissection of the pharynx and upper esophagus as viewed from behind. Although the difference between the lymphatics (reddish) and nerves (whitish) is barely distinguishable in this picture, it is obvious that the lymphatics from the hypopharynx and upper esophagus run laterally to converge at the venous angle area (taken from Fig. 2.8 of Saito et al. [8])

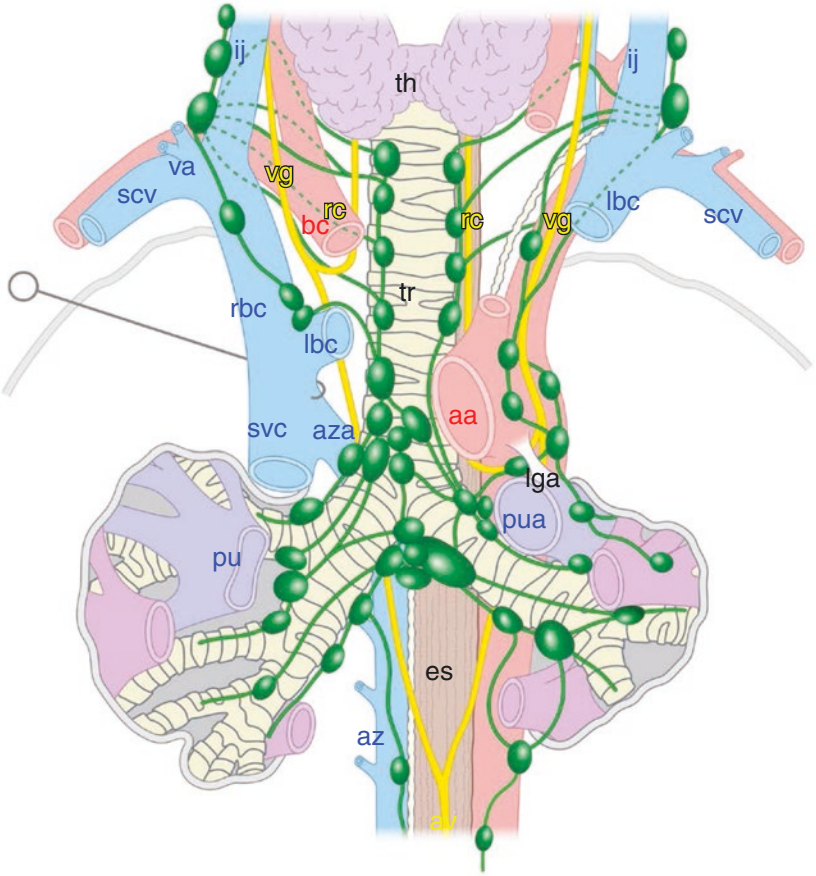

Fig. 2.6 Diagram of the ascending mediastinal lymphatics from the lungs and esophagus. After removal of the heart and pericardium, the left brachiocephalic vein was cut, and the superior vena cava was pulled to the right to reveal the lymphatic arrangement along the bronchi, trachea and esophagus

while those behind the nerve are more closely related to the esophagus. The nodes adjacent to the subclavian artery, sometimes noted as the "highest mediastinal nodes," are thought to hold a significant position.

The left deep pathways are classified into two types of pathways: (1) A well-developed lymphatic pathway which ascends in front of and adjacent to the left recurrent laryngeal nerve (Fig. 2.12a) [11]. Interestingly, behind the left recurrent laryngeal nerve, numerous segmental branches are distributed to the esophagus (Fig. 2.12b) [11]. (2) A lesser developed pathway, which follows the same route as the above pathway, is poorly developed, due to the pressure of the aortic arch against the left margin of the trachea (Fig. 2.13). Some lymph vessels from the left tracheobronchial nodes obliquely cross the trachea and ascend as a right pathway.

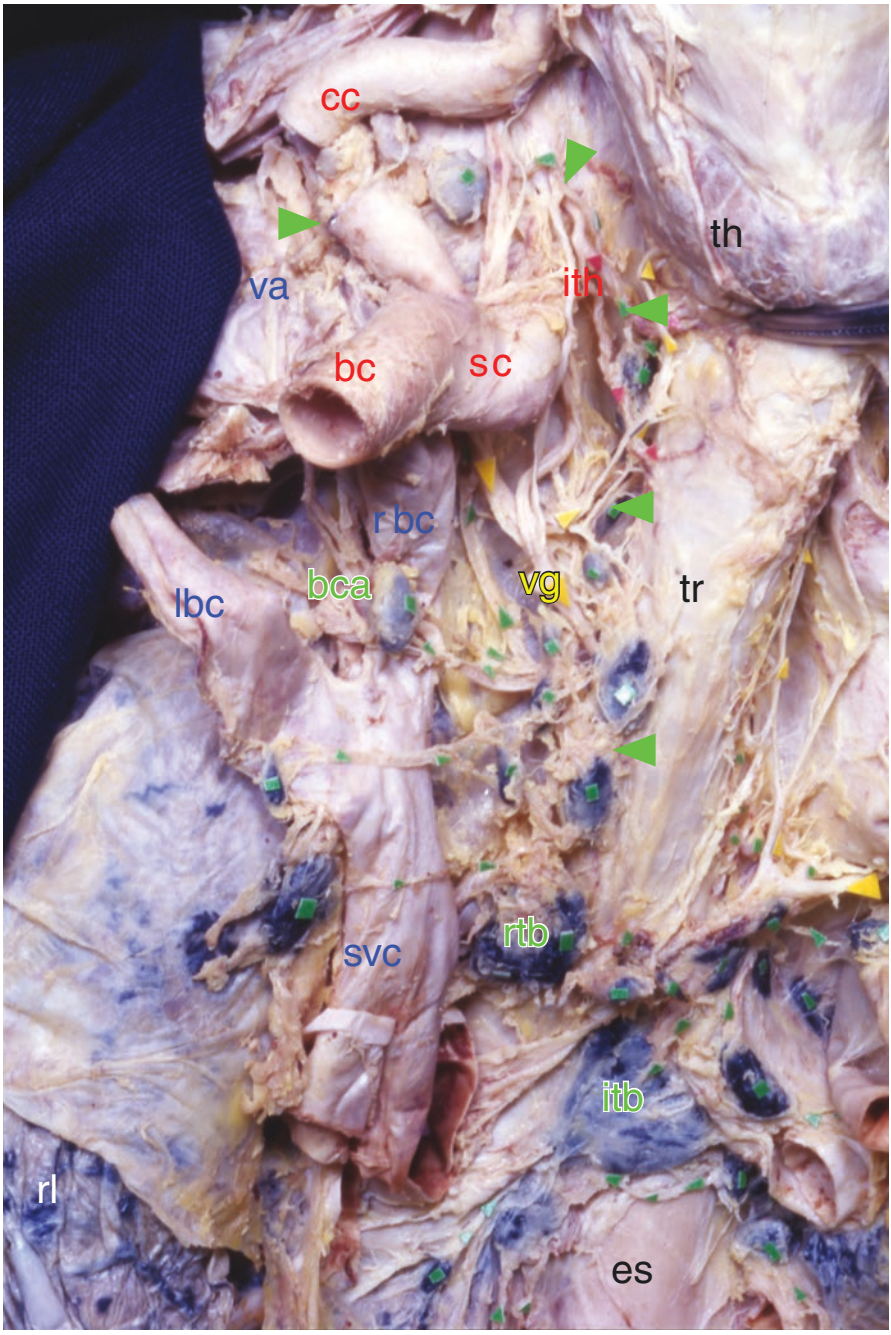

Fig. 2.7 Typical right paratracheal lymphatic chain. The brachiocephalic trunk and veins have been cut and shifted to reveal the course of the lymphatics. The right paratracheal lymphatic chain (green arrowheads), ascends to the lower neck and runs lateralward along the inferior thyroid artery to reach the right venous angle (Specimen 3, male)

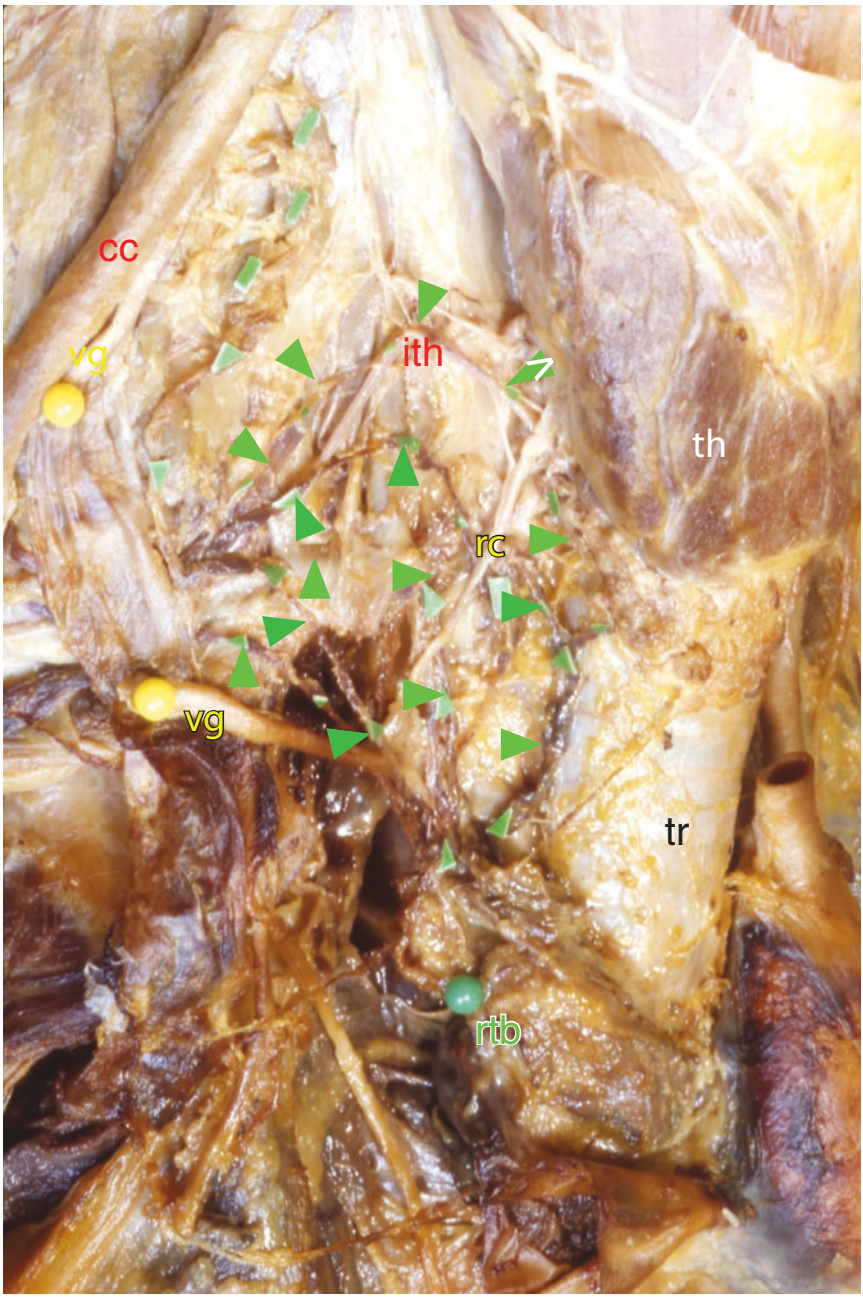

Fig. 2.8 Numerous oblique lymphatic branches to the venous angle. As indicated by the two alternating shades of green arrowheads, these five lymphatic branches originate at various levels from the ascending right paratracheal lymph chain (Specimen 4, male)

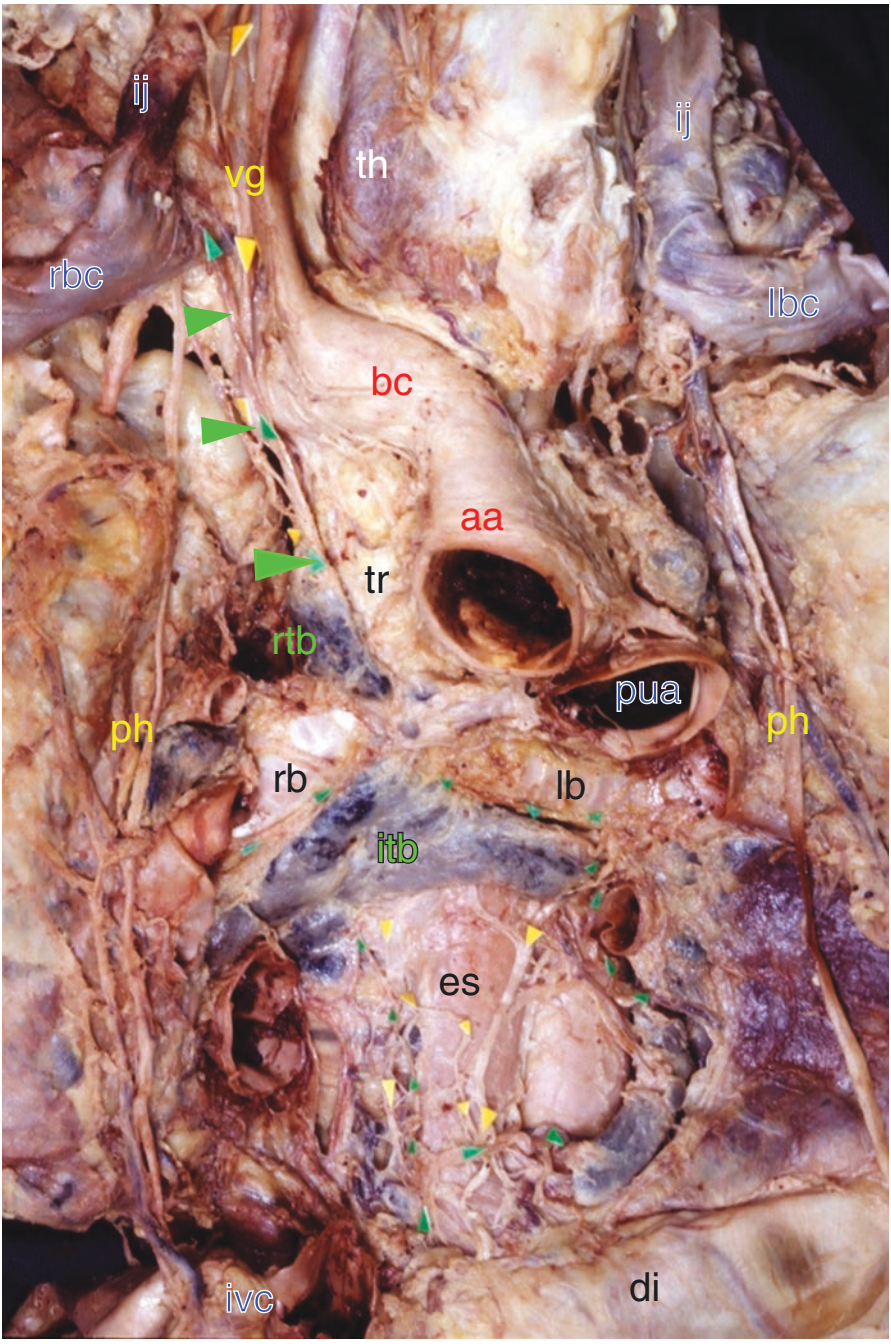

Fig. 2.9 Rare direct lymph vessel to the venous angle. A lengthy lymph vessel (green arrowheads), which originates from the right tracheobronchial node, ascends slightly rightwards to directly drain into the right venous angle (Specimen 5, male)

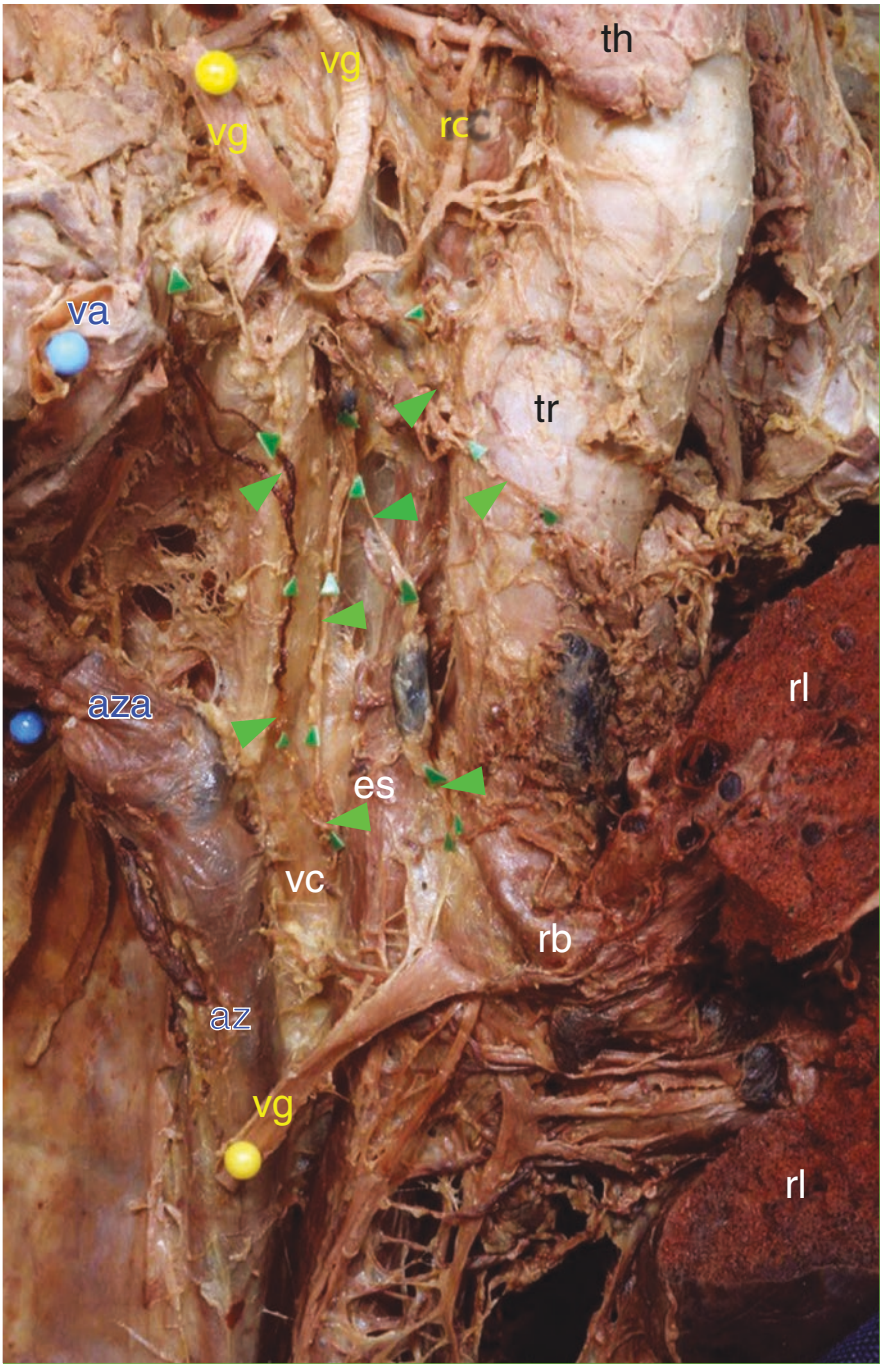

Fig. 2.10 Unique lymph vessels from three structures (trachea, esophagus and vertebral column). After cutting the vagus (yellow pin), the right side of the trachea and esophagus were dissected. As seen from a slightly oblique view, four direct vessels, which converge to the right venous angle, are shown by the green arrowheads (Specimen 1, male)

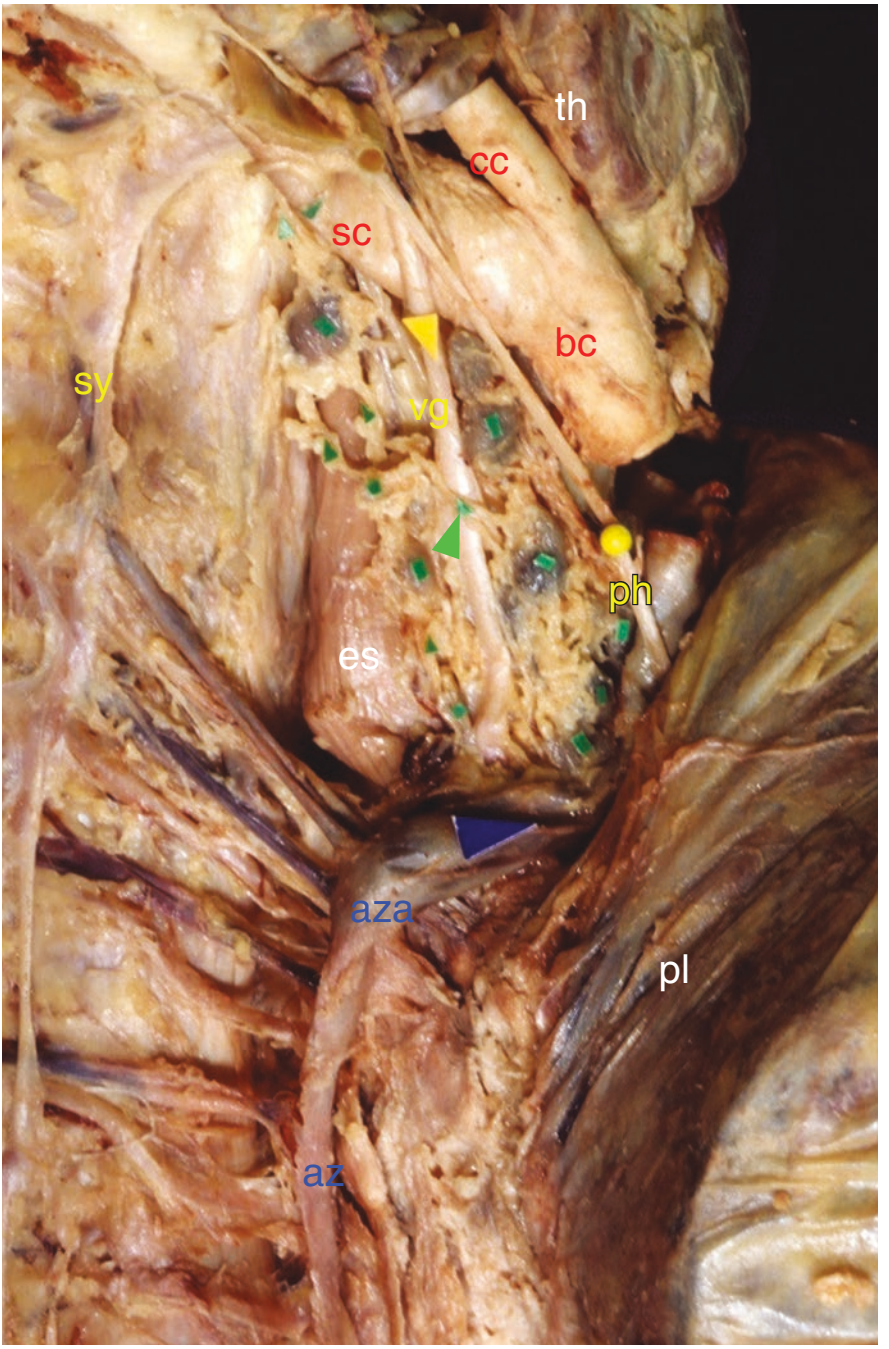

Fig. 2.11 Lymphatics within Baréty's space. The right tracheoesophageal lymphatics are well developed in the space (Baréty's space) between the subclavian artery and the arch of the azygos vein (blue arrowhead). Some communications among these nodes and their relationships to the vagus nerve are seen. Some connections are hidden behind the vagus nerve. Green arrowhead: communicating lymph vessel; yellow pin: phrenic nerve; yellow arrowhead: vagus nerve (Specimen 6, male)

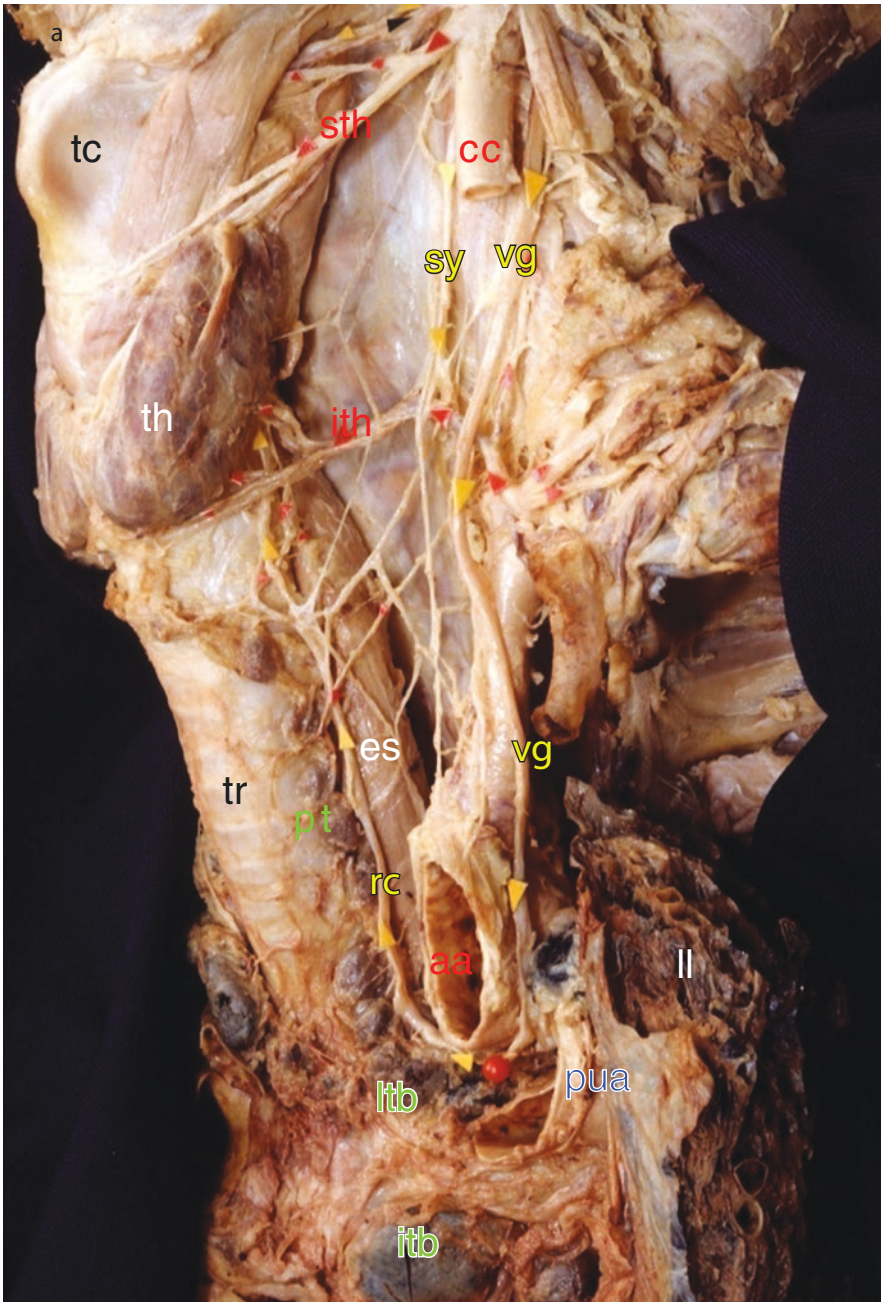

Fig. 2.12 Relationship between the left paratracheal lymph chain and the recurrent laryngeal nerve. (**a**) A well-developed left paratracheal lymph chain, as seen from the left. The lymph chain ascends immediately anterior to and medial to the left recurrent laryngeal nerve. [The original position of the ligamentum arteriosum is shown by the red pin.] (**b**) After the thyroid cartilage was median sectioned and reflected posteriorly, the left recurrent laryngeal nerve was pulled anteriorly, to reveal numerous segmental branches to the esophagus (Specimen 7, male). Yellow arrowheads: vagus and recurrent laryngeal nerves

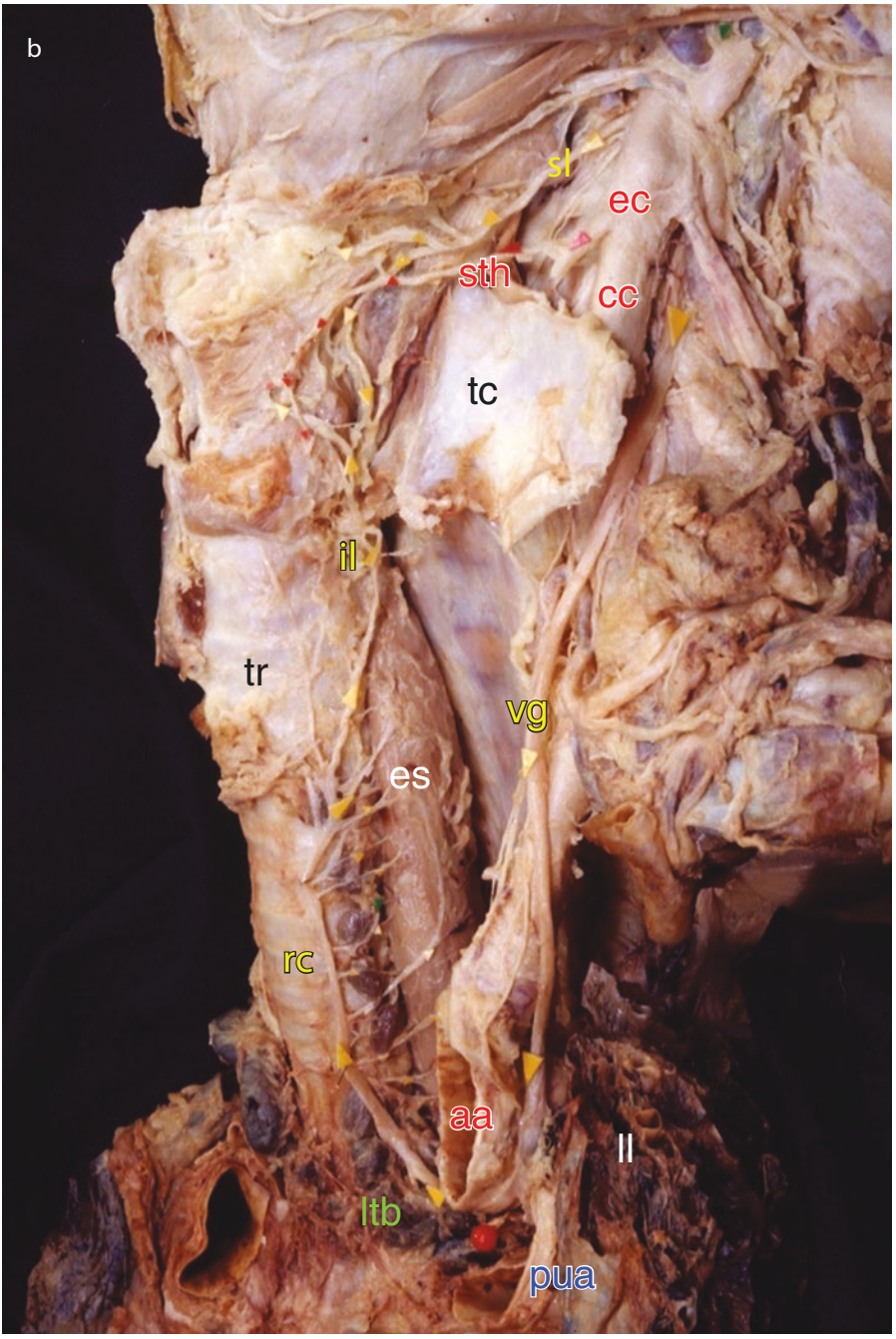

Fig. 2.12 (continued)

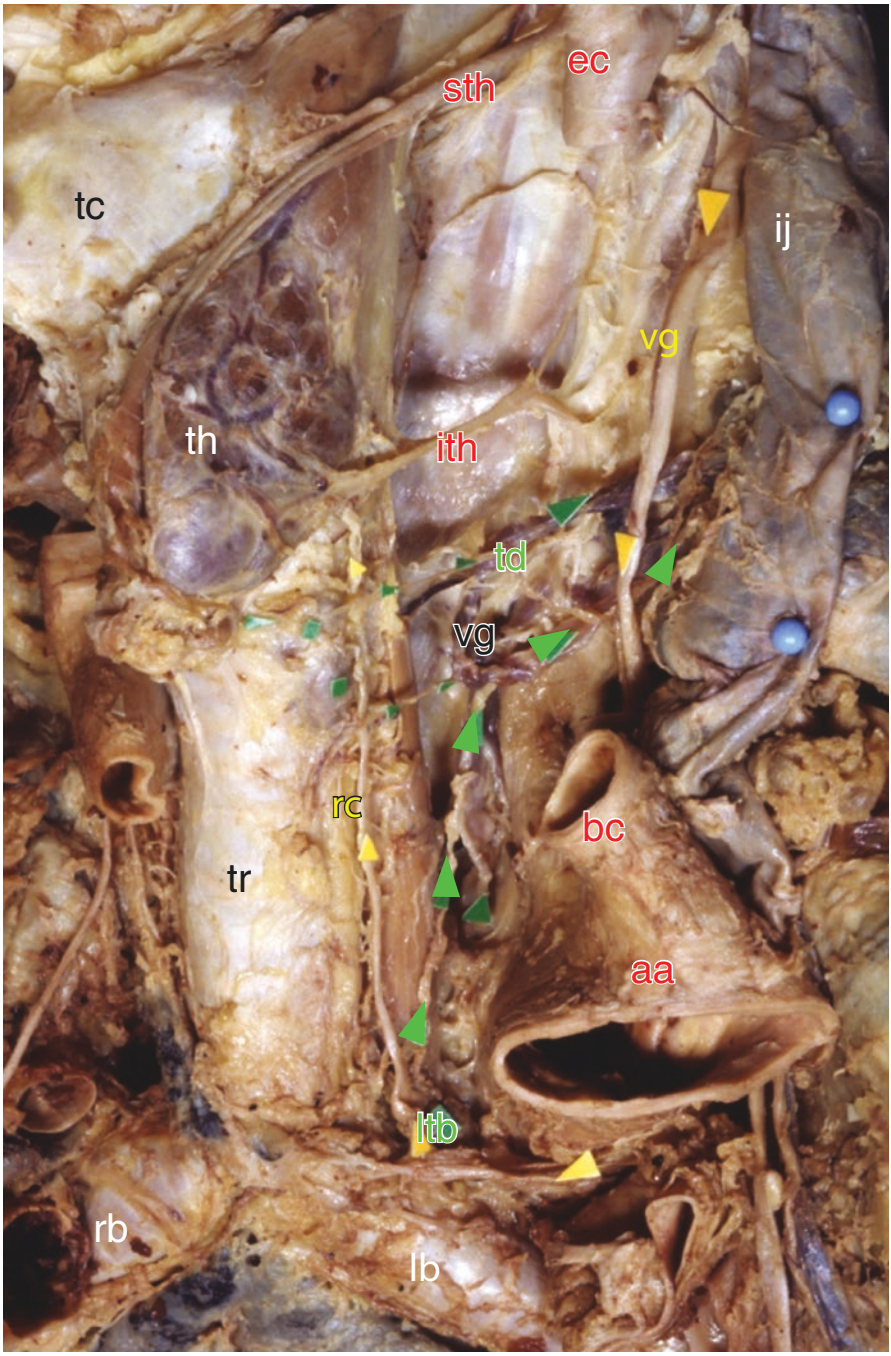

Fig. 2.13 Lymph vessel draining into the thoracic duct. The left paratracheoesophageal area was dissected after removal of the great vessels. The left paratracheal lymph chain is poorly developed. A lymph vessel (green arrowheads), which originates from the left tracheobronchial node, ascends almost vertically and drains into the terminal portion of the thoracic duct (Specimen 8, male). Yellow arrowheads: vagus and recurrent laryngeal nerves

Interestingly, there is also a third pathway from the left tracheobronchial nodes which runs slightly obliquely and drains into the terminal portion of the thoracic duct (Fig. 2.13). In addition to the abovementioned typical paratracheal lymphatics of the esophagus, there are also atypical lymph vessels which drain into the thoracic duct on both the left and right sides.

There is a recess close to the esophageal hiatus of the diaphragm between the thoracic surface of the diaphragm and the esophagus. Lymph nodes at the lower end of the thoracic esophagus are sometimes situated within this recess. In Fig. 2.14 [11] a large node is located within the recess adjacent to the left margin of the esophagus. In addition to the connections with the esophageal lymphatics, this node has a transverse communication with the nodes between the esophagus and inferior vena cava on the upper surface of the diaphragm. An even more critical communication is seen between this node and the left gastric lymphatics (Fig. 2.14). These findings indicate that the lymph nodes adjacent to the left margin of the esophagus at the level of the hiatus serve as a relay station from the lymphatics of the lower mediastinum to those of the upper abdomen.

2.1.2 Lymphatics of the Stomach

Rouvière divided the stomach lymphatics into four territories according to the four gastric branches of the coeliac trunk, as shown (Fig. 2.15) in his classic scheme [Rouvière's Fig. 83; 1]: left gastric, right gastric, right gastroepiploic, and left gastroepiploic territories. The lymphatics from these four territories run along their accompanying artery to the coeliac nodes. The left and right lymphatics of the lesser curvature can be typically seen as in Fig. 2.16 [14]. In this figure additional lymphatic chains are seen along the accessory left gastric artery and the proper hepatic artery; interestingly, they form a figure 8-like shape between the liver and the lesser curvature.

From the right gastroepiploic territories, the right gastroepiploic vein follows an oblique descending route on the anterior surface of the pancreas head and drains into the superior mesenteric vein (Fig. 2.17) [15]. The question is what do the lymphatics of the greater curvature do? Do they ascend to the coeliac nodes or descend to the superior mesenteric nodes? Minute dissection reveals that lymph vessels of the right gastroepiploic territory do not follow the right gastroepiploic artery to reach the coeliac nodes, but rather they accompany the right gastroepiploic vein to reach the superior mesenteric nodes (Fig. 2.18) [16].

Although the lymphatics along the right gastric artery typically follow the hepatic artery and drain into the coeliac nodes, they are also connected to the cystic lymphatics. Some cystic lymphatics drain into a node which is located within the middle level at the free margin of the lesser omentum (Fig. 2.19) [17, 18]. This node was already noted as the "ganglion de l'hiatus" by Rouvière (1932) [1], and was recognized as the "nodus foraminus" or the "node of anterior border of omental foramen" in Terminologia Anatomica (1998 [5]). As this node is located at the free margin of the lesser omentum, it can serve as a relay station between the anterior

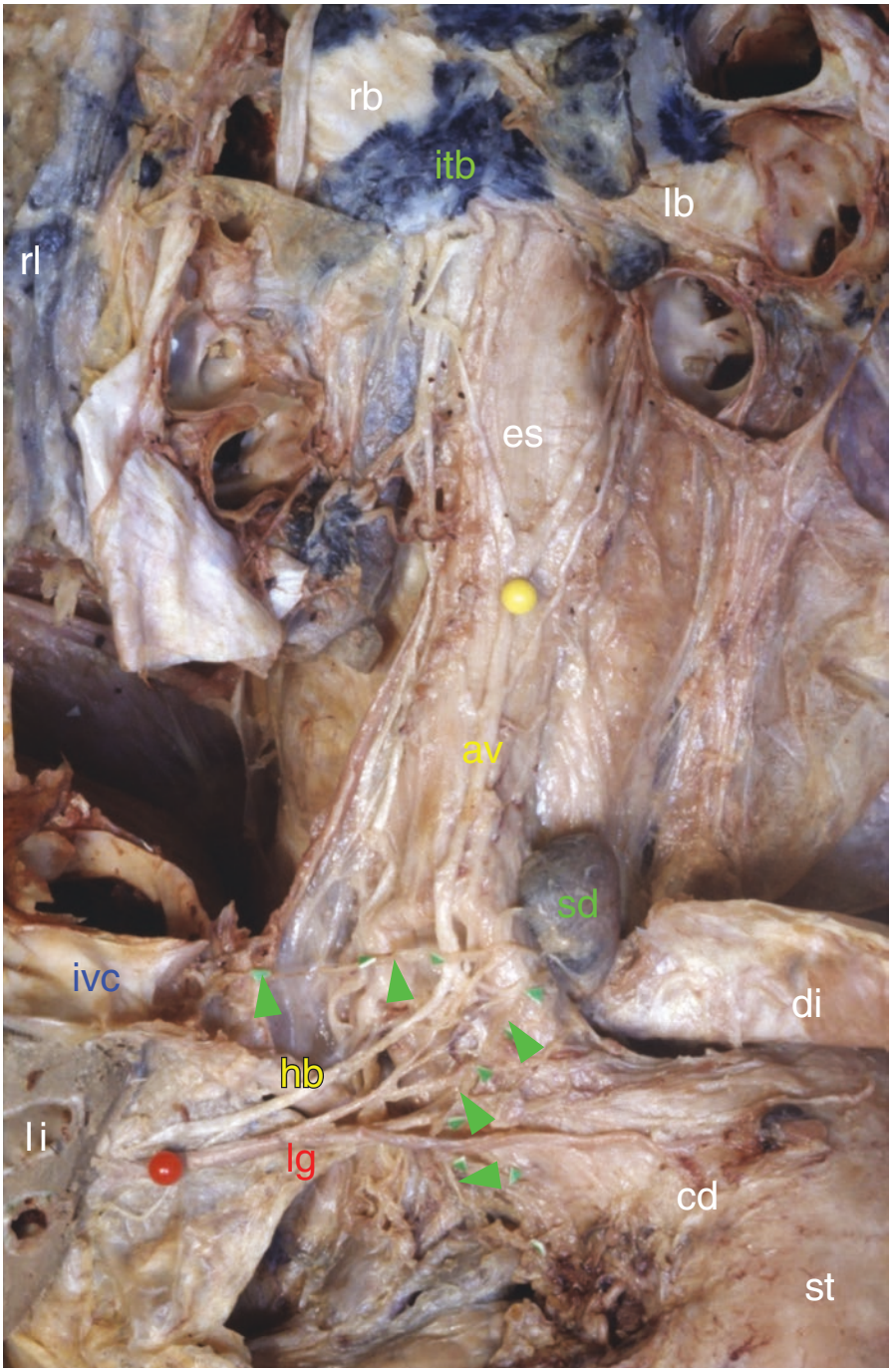

Fig. 2.14 Huge superior diaphragmatic node close to the left esophageal margin. With the diaphragm cut and opened, the continuation of the esophagus from the mediastinum to the abdominal cavity can be seen. Note the unusually large node (superior diaphragmatic node) in the recess between the left margin of the esophagus and the diaphragm. From this node, numerous connections with a variety of nodes are seen. Particularly noteworthy are those connections to the coeliac lymphatics via gastric lymphatics (lower green arrowheads) (Specimen 9, male)

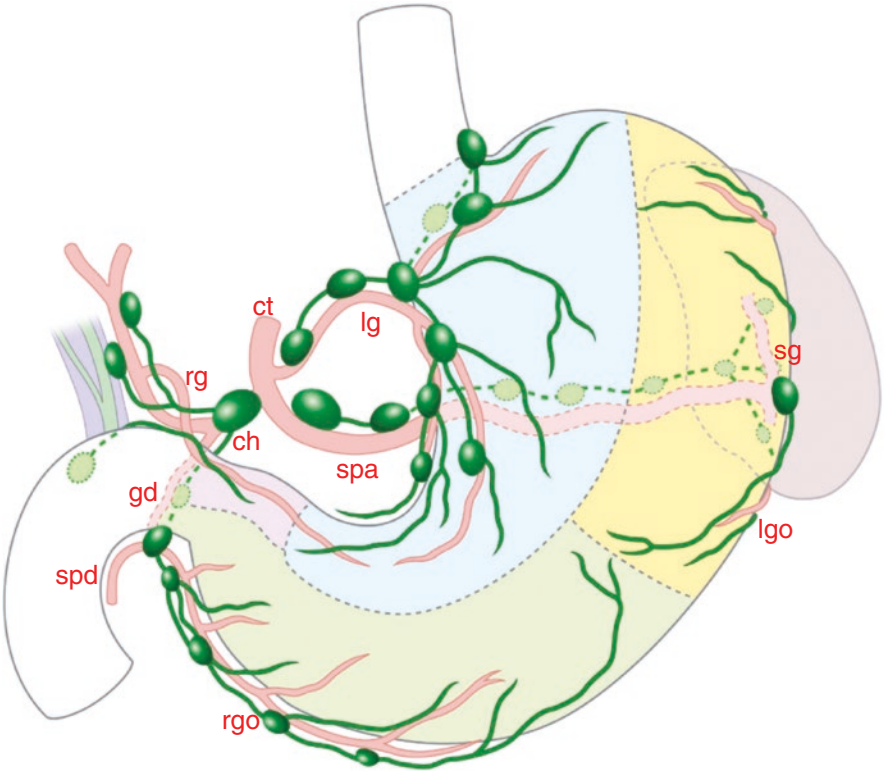

Fig. 2.15 Classical scheme of gastric lymphatics by Rouvière. Rouvière (taken from Fig. 83; 1932 [1]) divided the gastric lymphatics into four lymphatic territories with reference to the distribution of arterial branches of the coeliac trunk

and posterior lymphatics within the lesser omentum. In the same specimen as Fig. 2.19 lymph vessels from the nodus foraminus are connected with those of the posterior pancreas head and drain finally into the interaorticocaval nodes (Fig. 2.20) [17, 18]. These two illustrations suggest that some lymphatics of the lesser curvature may be relayed via the nodus foraminus and the nodes of the posterior pancreas head and drain into the interaorticocaval nodes.

Regarding atypical pathways in relation to variant arteries, the following lymphatic connections will be noted. On the posterior wall of the fundus of the stomach the posterior gastric artery, which originates from the splenic artery, is often observed (62%, Suzuki et al.) [19]. Along this atypical artery, lymphatics descend and drain into the splenic lymphatic chain (Fig. 2.21).

The left inferior phrenic artery often gives off a branch to the cardiac notch of the stomach (about 50%, Sato et al. [20]) (Fig. 2.22) [21]. Some lymph vessels from the cardioesophageal area run along the branch and the stem of the left inferior phrenic artery and then descend along the stem to finally drain into the coeliac nodes, superior mesenteric nodes, or into the nodes along the upper margin of the left renal vein (Fig. 2.23) [15].

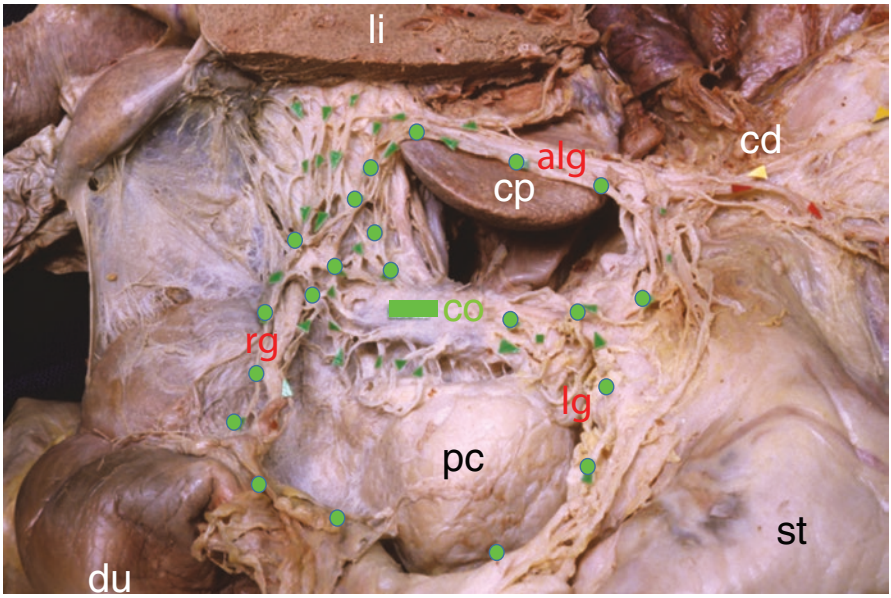

Fig. 2.16 Lymphatics along the coeliac arterial branches. The arterial branches of the coeliac trunk between the lesser curvature and the liver form a figure 8-like shape. Lymphatics along these vessels are shown with green markers. The coeliac node is indicated by the green rectangle (Specimen 10, male)

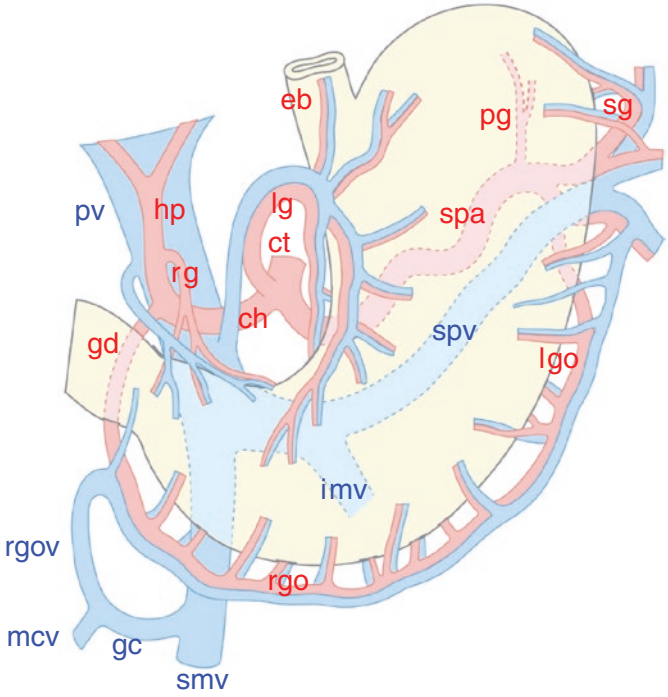

Fig. 2.17 The veins of the stomach and their relation to the arteries. Note the difference in the course between the right gastro-omental artery and vein

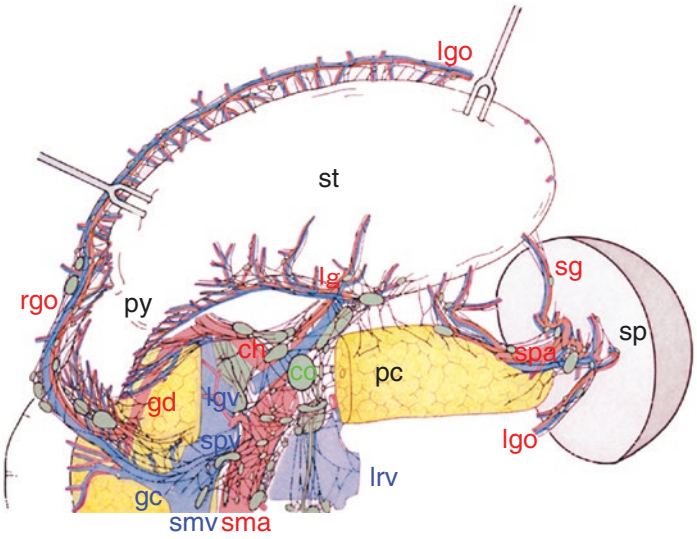

Fig. 2.18 Dissection of the stomach and pancreas. The stomach was reflected and the neck of the pancreas was cut, then the lymph vessels of the stomach were traced to the origins of the coeliac and superior mesenteric arteries. Lymphatic vessels along the right greater curvature run along the superior mesenteric vein to reach the superior mesenteric nodes (taken from Fig. 6 of Deki [16])

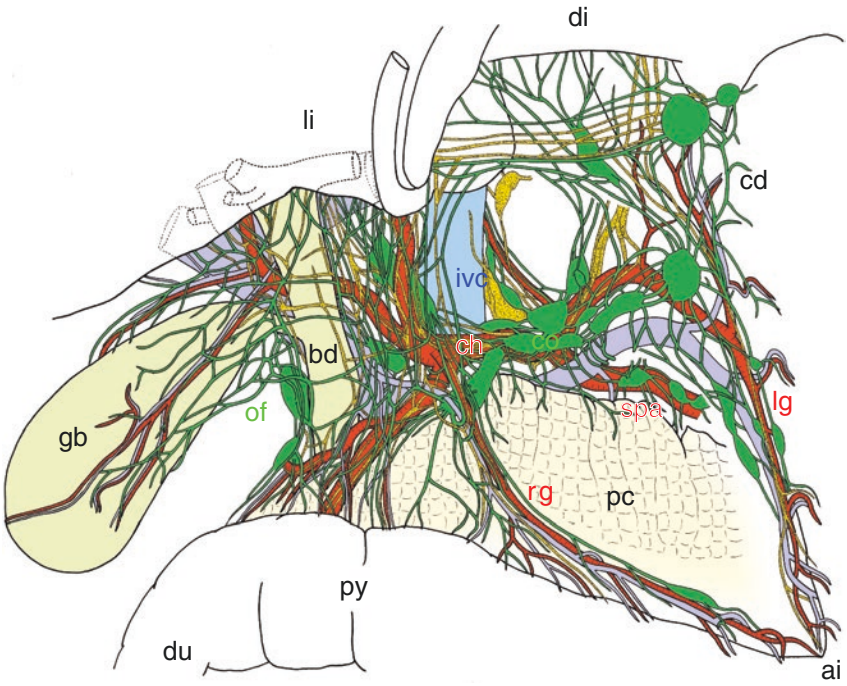

Fig. 2.19 Lymphatics of the lesser curvature, liver and gallbladder. Connections of the lymphatics of the stomach and the hepatic pedicle are shown. Note the omental foramen node (node of the anterior border of the omental foramen [5]) (taken from Fig. 1 of Ito et al. [17])

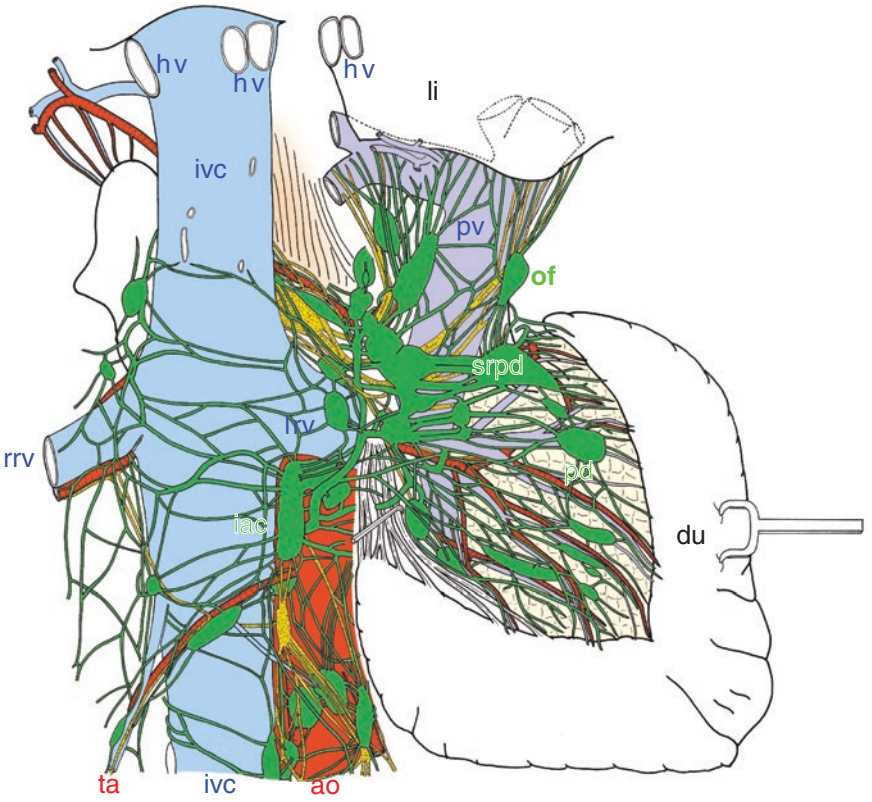

Fig. 2.20 Lymphatics of the pancreas head. The pancreas has been reflected to the left (same specimen as in Fig. 2.19). Dissection showing the omental foramen node connecting with the lymphatics behind the pancreas head and then with the para-aortic nodes (taken from Fig. 2 of Ito et al. [17])

In the lymphatic arrangement of the stomach, two points should be made: (1) Although the general emphasis is placed on the lymphatics that reach the coeliac nodes, it is important to note that in addition to those well-known lymphatic chains, there are also atypical chains which run to the superior mesenteric lymphatics. (2) Also noteworthy are those lymphatics that run along the atypical arteries, such as the posterior gastric artery and the left inferior phrenic artery.

2.1.3 Lymphatics of the Colon

The lymphatics of the colon generally follow the colic arteries; thus, a comprehensive understanding of the arterial arrangement is crucial. There are two major arteries supplying the colon, the superior and inferior mesenteric arteries (Fig. 2.24) [22]. From the superior mesenteric artery, the ileocolic, right colic, and middle colic arteries originate and these supply the caecum, ascending colon, and transverse

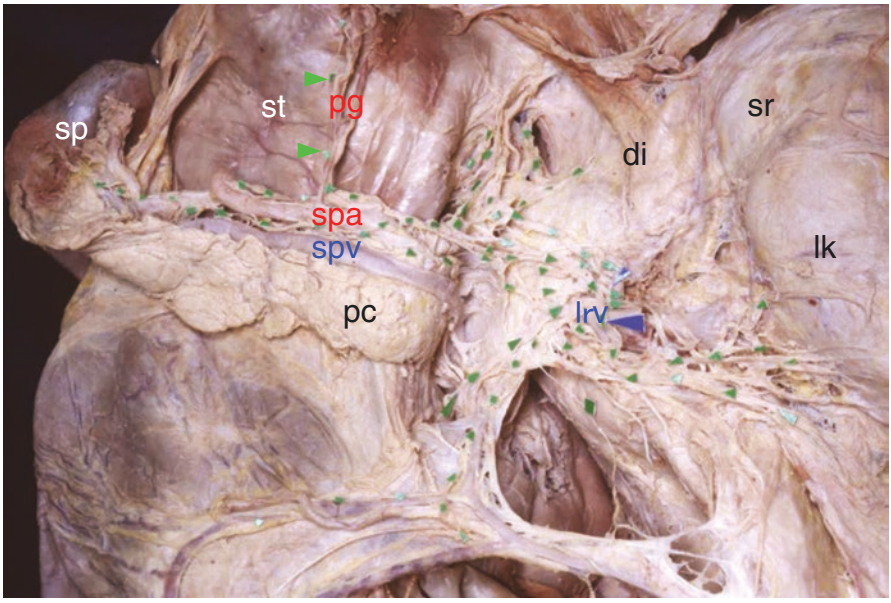

Fig. 2.21 Lymphatics along the posterior gastric artery. The stomach, spleen, and pancreas body and tail have been reflected to the right to reveal the lymphatics along the posterior gastric artery (green arrowheads) which drain into nodes of the splenic artery (Specimen 11, male)

colon, respectively. From the inferior mesenteric artery, the left colic, sigmoid, and the superior rectal arteries originate.

The colic arteries of the superior and inferior mesenteric arteries bifurcate close to the colon and form an arterial arcade, termed the marginal artery. From the marginal artery numerous vasa recta originate and supply the colic wall. Many lymph nodes lie alongside the vasa recta and marginal artery. These are paracolic lymph nodes. Along the colic arteries lie intermediate nodes. These are termed according to the name of the accompanying colic artery. The principal lymph nodes near the origin of the mesenteric arteries are termed the superior and inferior mesenteric nodes (Fig. 2.24).

A typical lymphatic arrangement of the right hemicolon is shown in Fig. 2.25 [taken from Fig. 8 of Sato and Sato, 23]. In this figure three points should be noted: (1) As the superior mesenteric vein is located alongside and to the right of the superior mesenteric artery, lymph vessels of the right hemicolon first cross the superior mesenteric vein and then move to the arterial side. (2) In this specimen, the right colic artery is well developed and forms a common stem with the artery of the right colic flexure (hepatic flexure). In general however, the presence of the right colic artery is somewhat unpredictable. A distinct right colic artery is

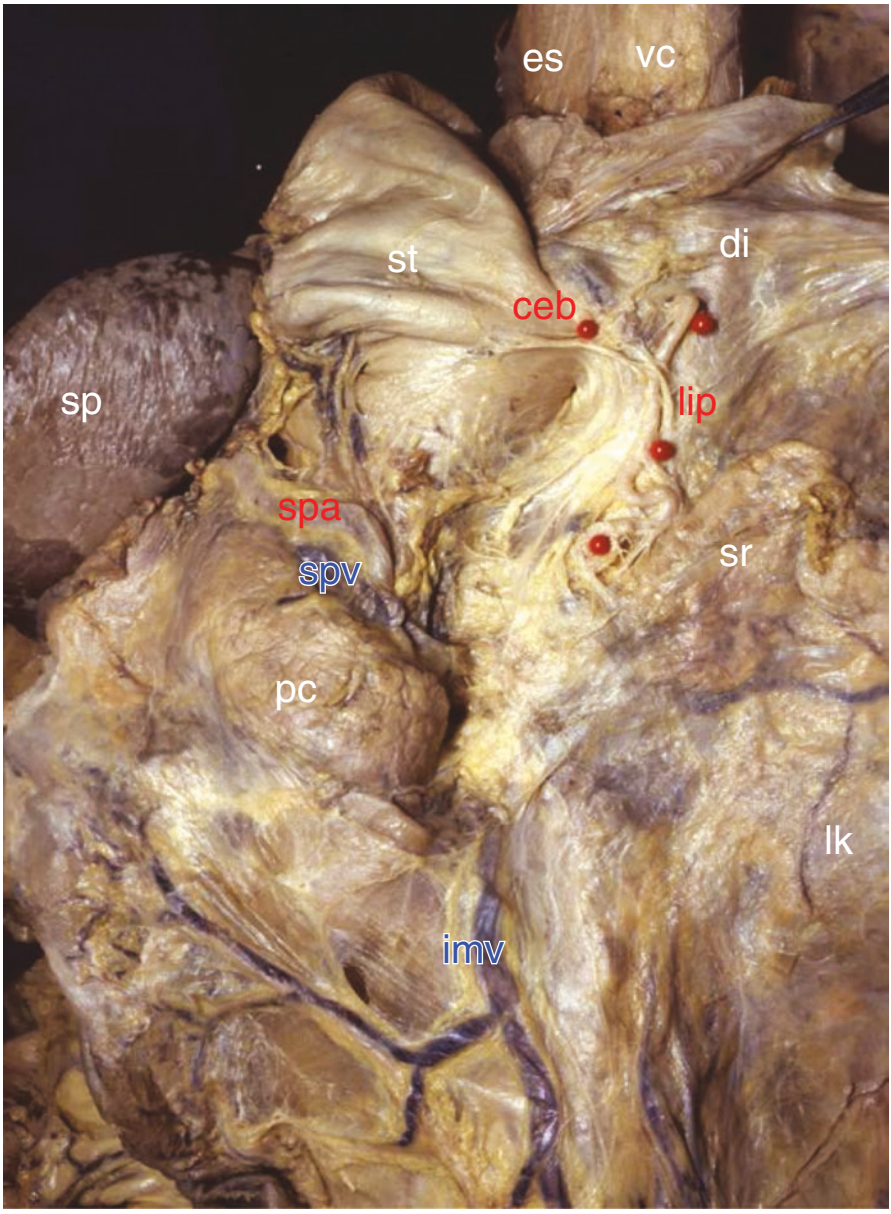

Fig. 2.22 Left inferior phrenic artery and its cardioesophageal branch. The stomach, spleen, and pancreas body and tail have been reflected to the right to reveal the left inferior phrenic artery and its cardioesophageal branch (red pins) (Specimen 12, male)

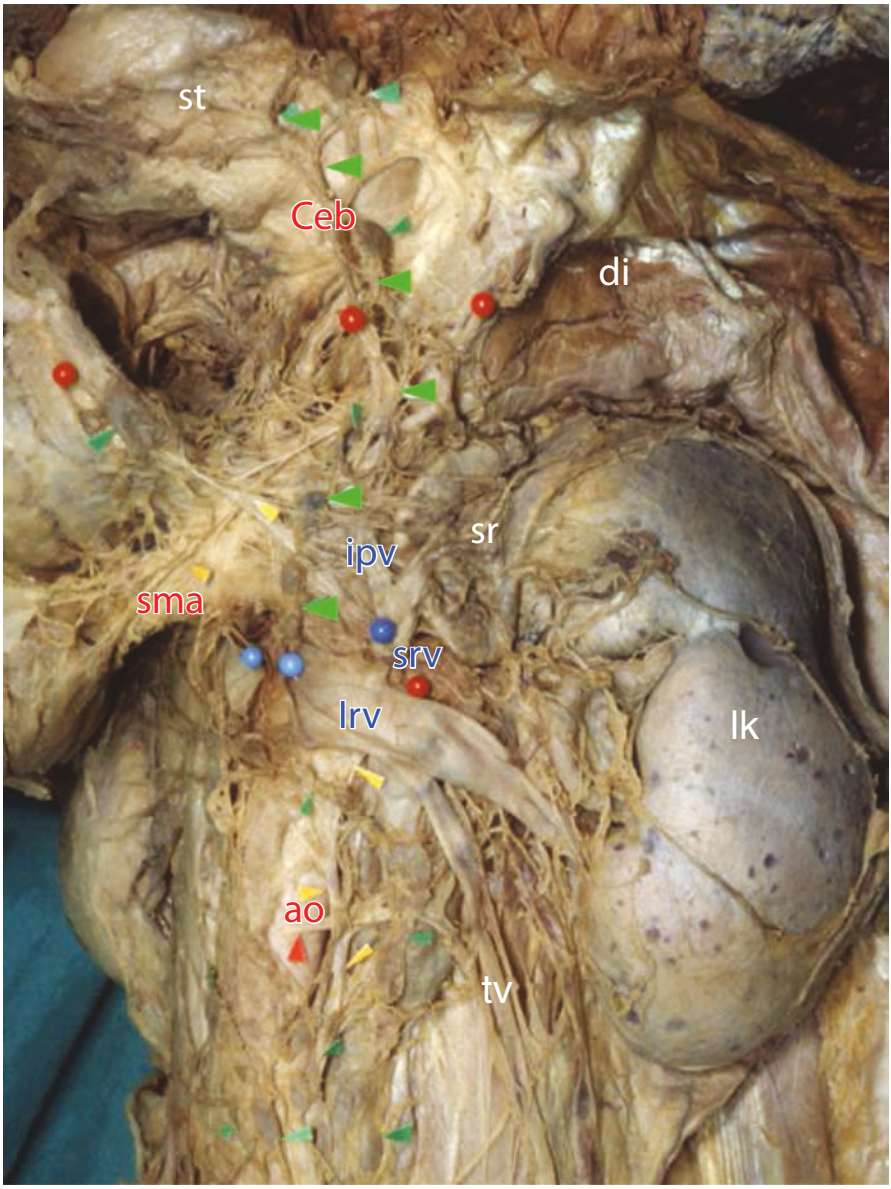

Fig. 2.23 Lymphatics along the left inferior phrenic artery. A lymph vessel (green arrowheads) from the cardia runs along the cardio-esophageal branch of the left inferior phrenic artery and descends along this artery, then finally drains into the superior mesenteric nodes (Specimen 13, male)

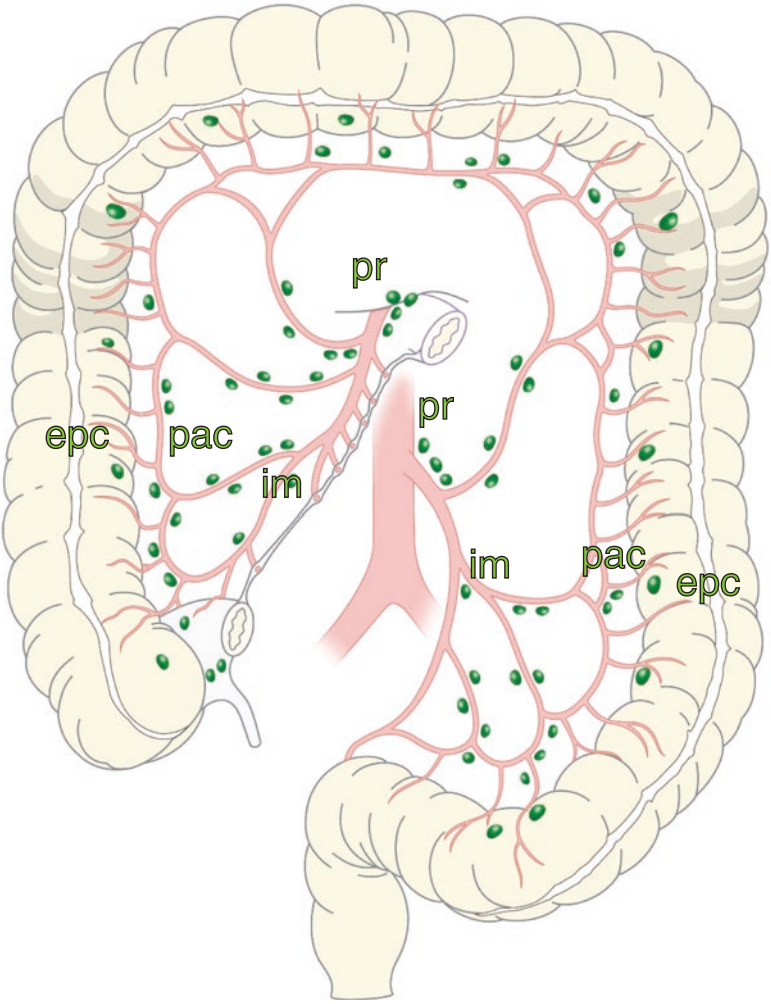

Fig. 2.24 Manner of lymph node distribution of the large intestine. This scheme shows the lymph node distribution in relation to the superior and inferior mesenteric arteries and their colic branches (taken from Fig. 11-4 of Slanetz and Herter [22])

observed in only about one-third of specimens [24], and therefore the ascending colon is often supplied via the marginal artery from the ileocolic and middle colic arteries. Based on this arterial arrangement, numerous lymphatics of the right colon tend to gather to the ileocolic and middle colic nodes. The anterior and posterior ileocolic nodes are shown in Fig. 2.26a, b [25]. (3) Arteries of the

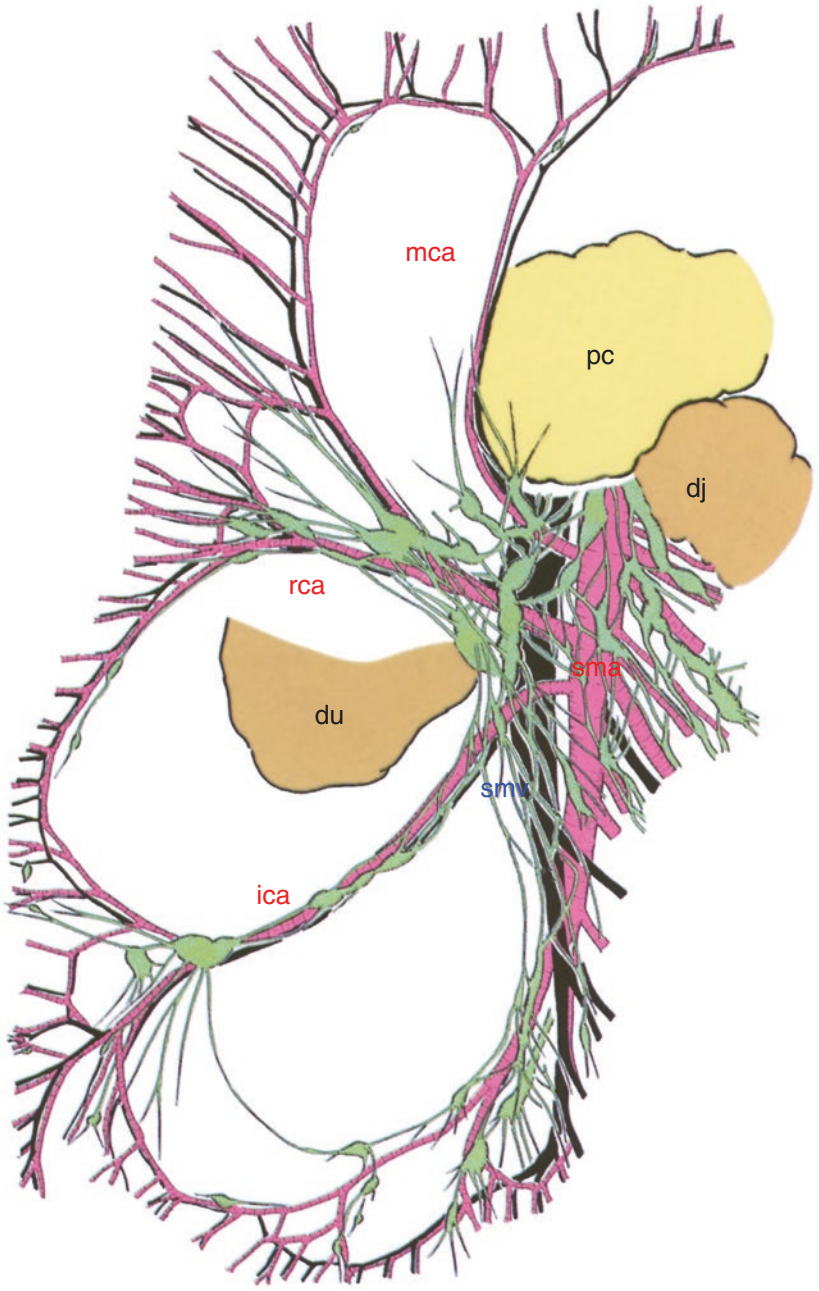

Fig. 2.25 Lymphatics along the superior mesenteric vessels. Note the complex lymphatic arrangement adjacent to the superior mesenteric artery and vein (taken from Fig. 8 of Sato and Sato [23])

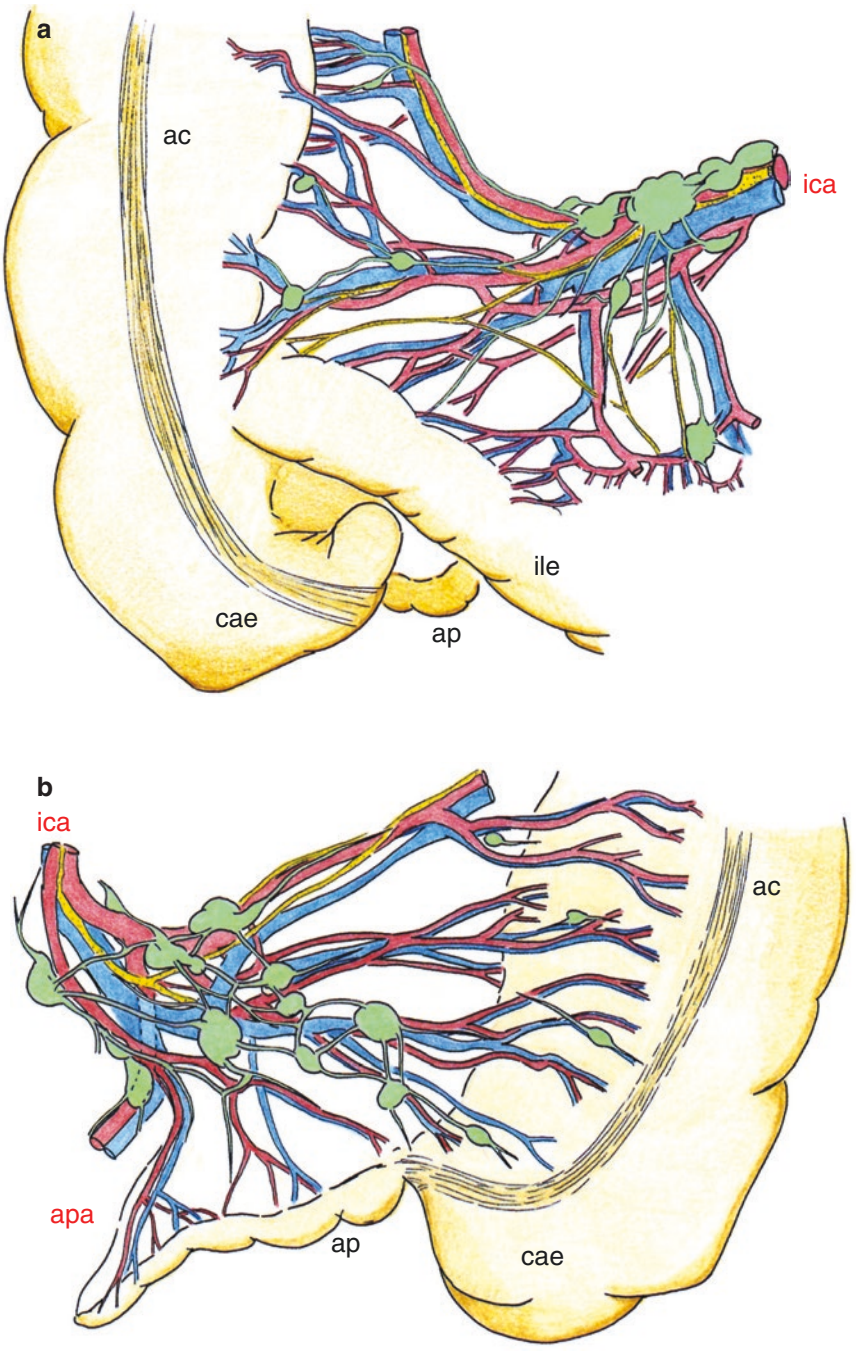

Fig. 2.26 Lymphatics of the caecum. (**a**) Anterior view; (**b**) Posterior view (taken from Figs. 5 and 6 of K. Sato [25])

transverse colon are complex. In French textbooks of anatomy, the arteries of the transverse colon are classified into three types [26]: (a) artery of the right colic flexure, (b) artery of the transverse colon, and (c) artery of the left colic flexure. In the specimen of Fig. 2.25, the middle colic artery reached the middle part of the transverse colon; unfortunately however during dissection, the paracolic branch was not traced to the left colic flexure.

Regarding the typical left colic flexure, from the inferior mesenteric artery, the upper left colic artery reaches the marginal artery which joins that from the superior mesenteric artery. This segment of the marginal artery is termed Riolan's anastomosis. The major stem of the inferior mesenteric artery sends numerous sigmoid arteries before continuing as the superior rectal artery (Fig. 2.27) [taken from Fig. 2.10 of Sato and Sato, 23]. Well-developed lymphatics along the sigmoid arteries ascend along the stem of the inferior mesenteric artery to reach the lymphatics surrounding the abdominal aorta. These lymphatics gather at the origin of the inferior mesenteric artery and reach not only the lateral aortic lymph nodes, but also the interaorticocaval lymph nodes. Lymphatics of the colon tend to gather at the lymph nodes surrounding the abdominal aorta below the left renal vein.

2.1.4 Lymphatics of the Rectum

Lymphatic pathways of the rectum are roughly classified into superior, lateral, and inferior pathways (Fig. 2.28) [27]. The latter, the inferior pathway, which originates from the anal canal and runs subcutaneously to reach the superficial inguinal nodes, will not be demonstrated in this chapter.

The superior pathway ascends along the superior rectal artery (Fig. 2.29). Regarding the manner of drainage into the para-aortic nodes, the ascending lymph vessels from the rectum not only concentrate around the origin of the inferior mesenteric artery but also these vessels are vertically scattered between the level of the left renal vein and the bifurcation of the aorta (Fig. 2.30) [28]. In addition, also within this region, numerous horizontal communications are noted.

The lateral pathway typically runs along the middle rectal artery. The typical middle rectal artery is shown in Fig. 2.31 [29]. This artery, however, is often absent, and thus it is only rather rarely observed (22%, Sato and Sato) [30]; without this guiding artery, it is difficult to trace lymph vessels from the rectum. However, in a rather rare dissection in the absence of the middle rectal artery, we were able to trace a lymph vessel of the rectum (Fig. 2.32) [31].

The lateral lymph vessels do not always run along the organ-supplying branches to reach the stem of the internal iliac artery, but rather they tend to run lateralward to drain into the interiliac nodes near the obturator nerve (Fig. 2.32) [31]. To reach

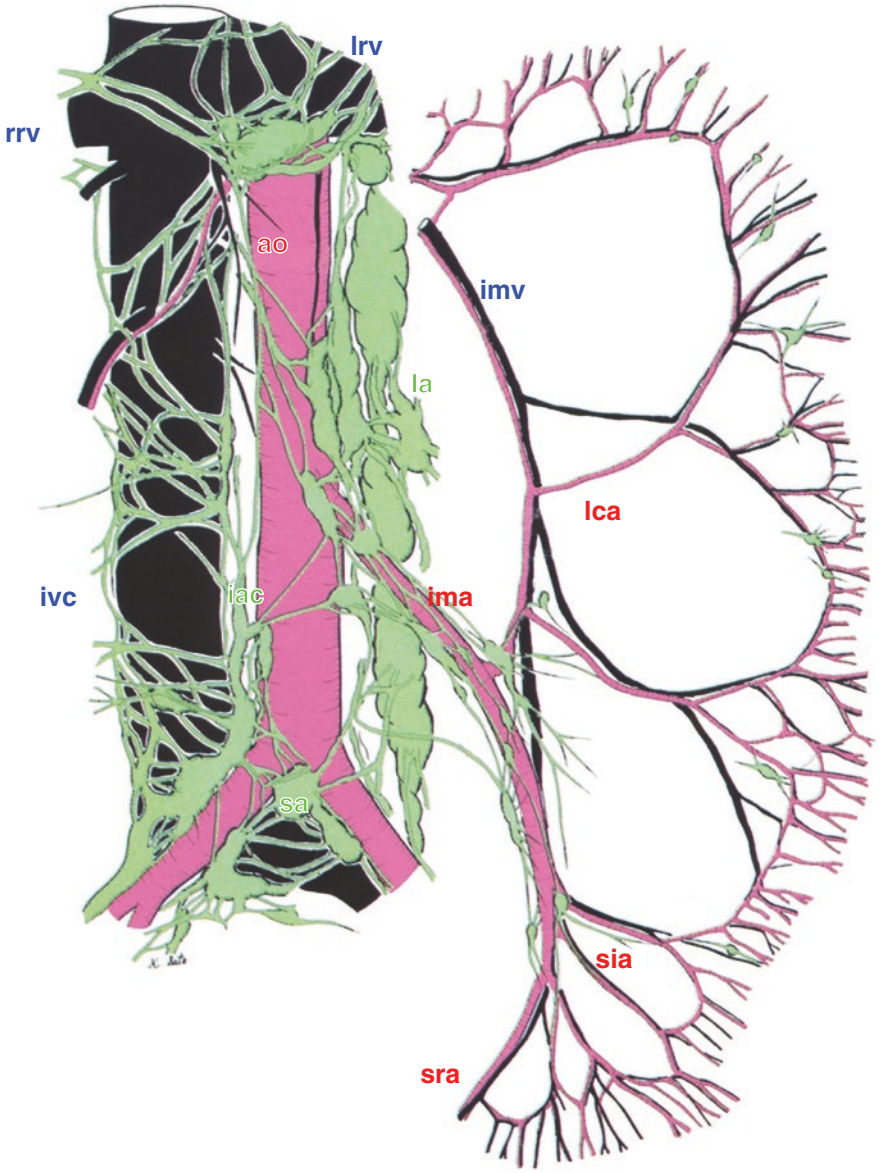

Fig. 2.27 Lymphatics along the inferior mesenteric vessels. Note the intimate relationship between these lymphatics and the para-aortic nodes (taken from Fig. 10 of Sato and Sato [23])

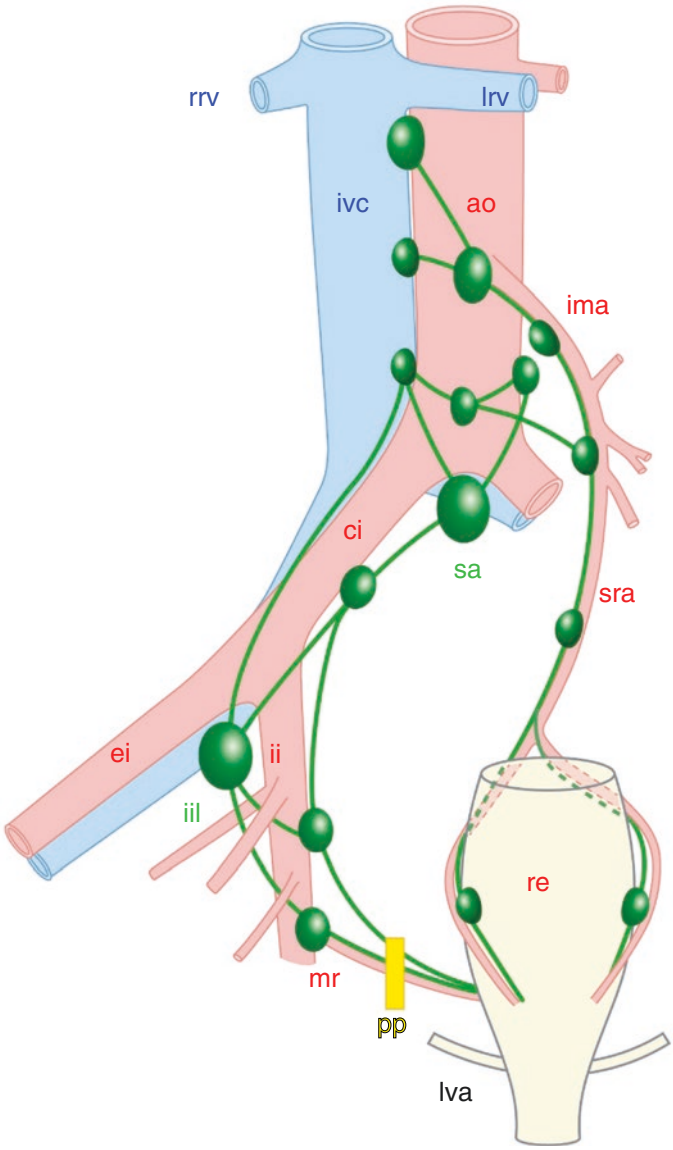

Fig. 2.28 Lymphatic pathways of the rectum. The scheme of the relationship of the superior and lateral lymphatic pathways of the rectum to the surrounding structures (K Sato [25])

the interiliac nodes, the lymph vessels must cross the cord of umbilical artery, which originates from the internal iliac artery, run alongside the urinary bladder, and ascend on the posterior wall of the rectus abdominis muscle to reach the navel. Lymph vessels originating from the upper region of the pelvic organs pass over the cord of umbilical artery, while those from the lower region pass under the cord

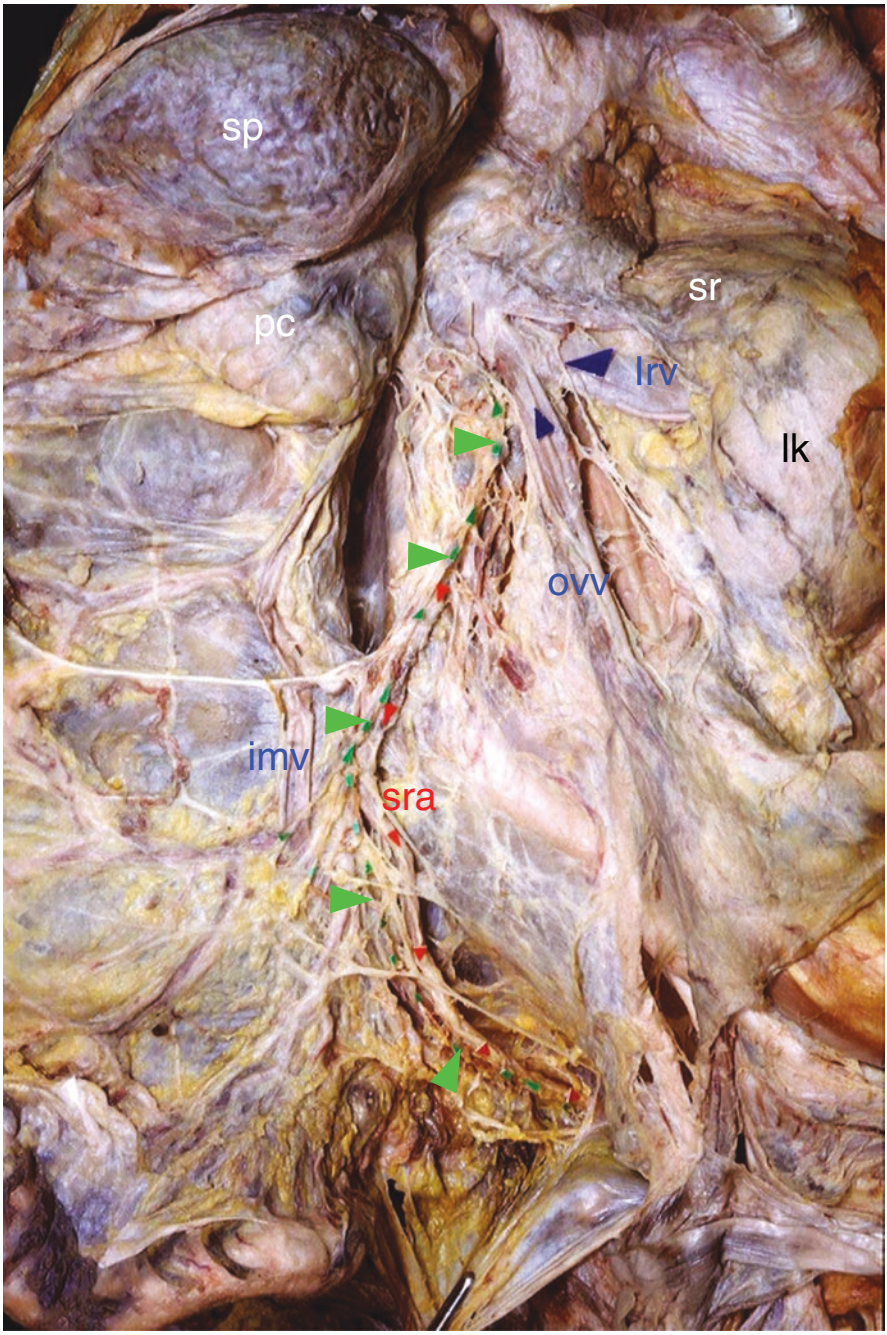

Fig. 2.29 Ascending lymph vessel from a female rectum. As viewed from the front, the stomach, spleen, pancreas body and tail, and the descending and sigmoid colon have been reflected to the right, showing an ascending lymph vessel (green arrowheads) along the superior rectal artery/inferior mesenteric artery (Specimen 14, female)

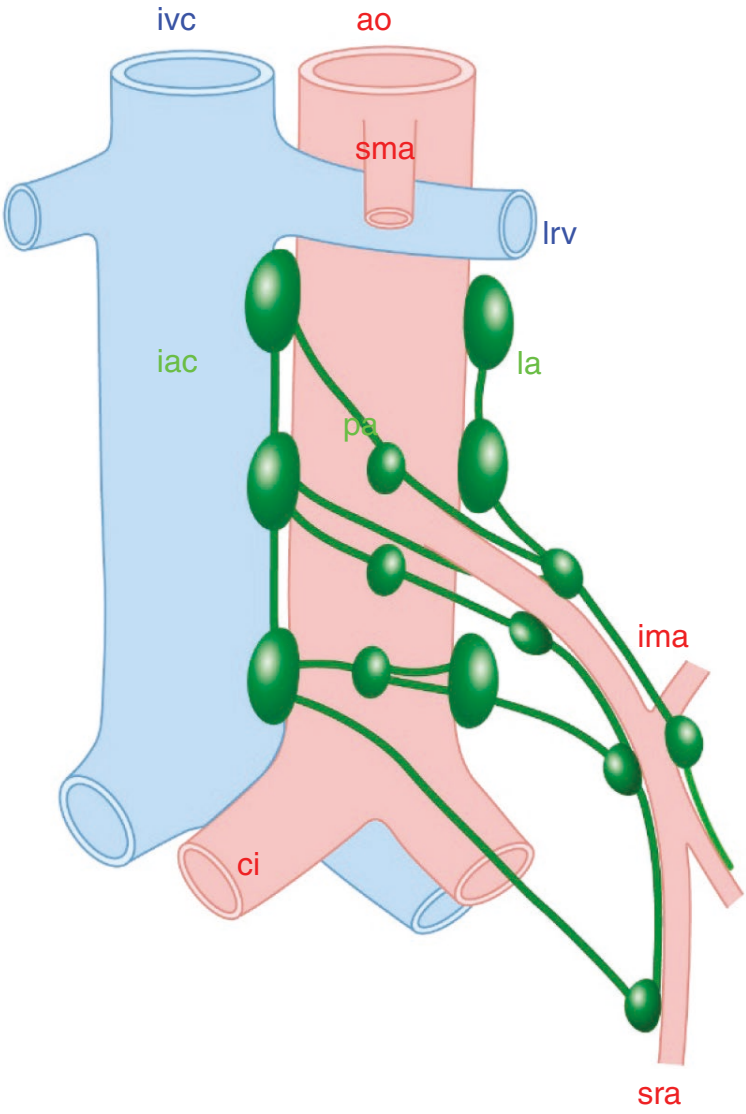

Fig. 2.30 Ascending rectal lymphatics to the abdominal aorta. The distribution manner of the ascending lymph vessels along the superior rectal artery and the inferior mesenteric artery to the abdominal aorta is shown (K Sato [25])

(Fig. 2.33) [29]. Another critical relationship of the lateral pathway is the positional relationship to the pelvic plexus. Many lymph vessels from the upper portion of the rectum cross over the pelvic plexus as shown in Fig. 2.34 [32]. However, as shown in Fig. 2.31, the middle rectal artery pierces the pelvic plexus which indicates that some lymph vessels of the lower rectum also pass through the pelvic plexus.

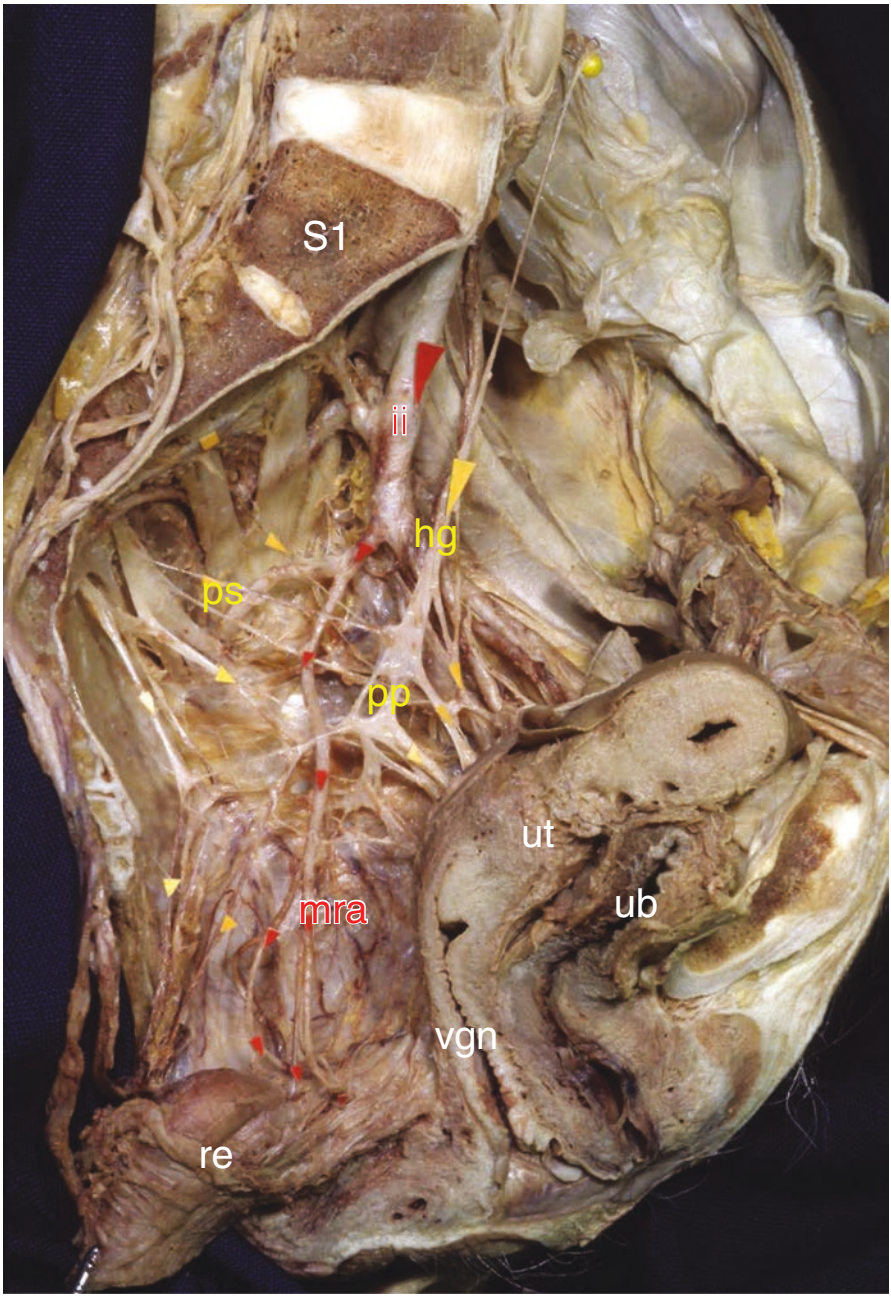

Fig. 2.31 Female middle rectal artery course. The left half of the median-sectioned female pelvis is seen from the right. The rectum has been pulled posteriorly. The typical middle rectal artery originates from the initial part of the internal pudendal artery which is a branch of the internal iliac artery. This middle rectal artery pierces the pelvic plexus and reaches the rectum (Specimen 15, female)

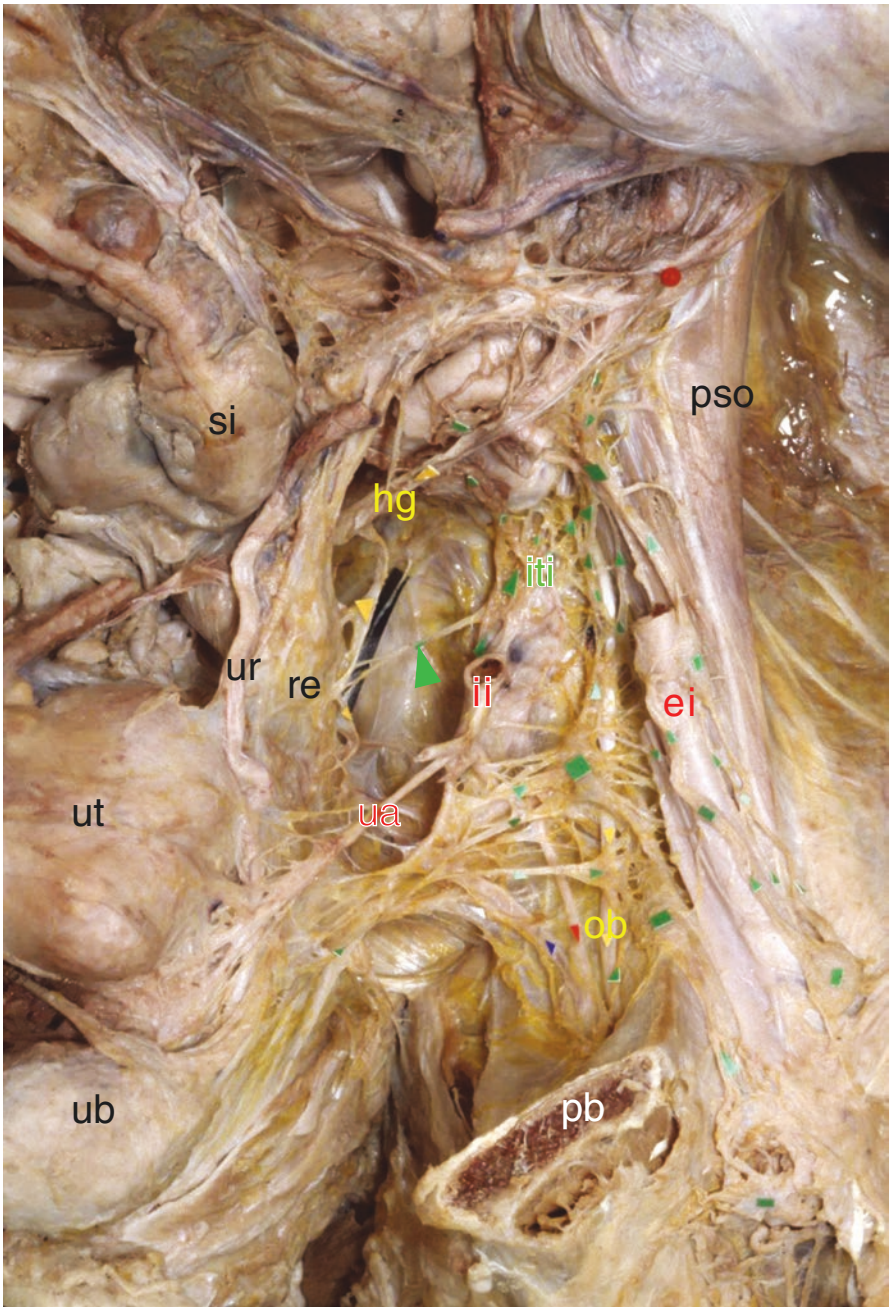

Fig. 2.32 Rectal lymphatics reaching the interiliac lymphatics. Transitional portions of the left common, external and internal iliac arteries have been removed. Although in this specimen the middle rectal artery was not present, a lymph vessel (green arrowheads) from the rectum to the interiliac lymphatics was dissected (Specimen 16, female)

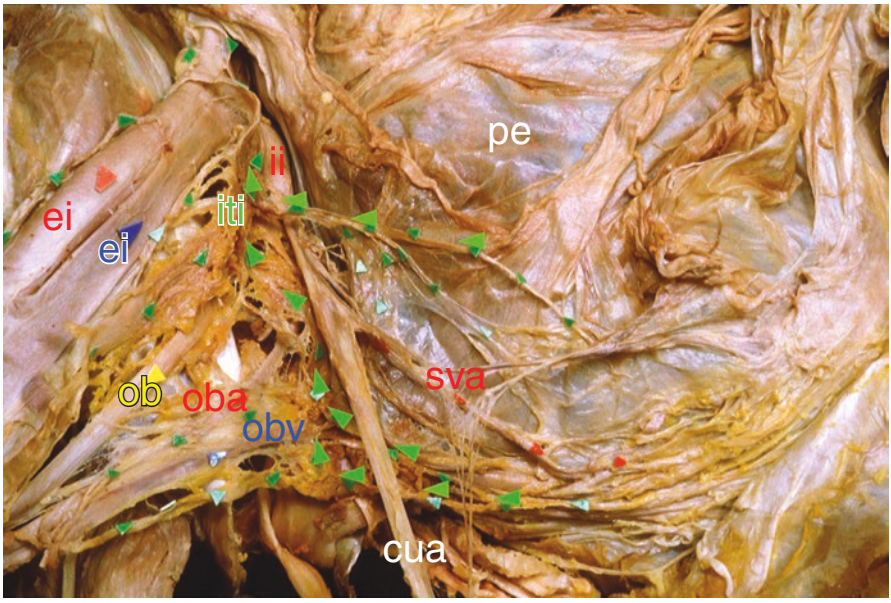

Fig. 2.33 Relationship of the pelvic lymphatics and the umbilical artery. After removal of the hip bone, the right half of a female pelvis was dissected from the outside. The external iliac artery and the cord of the umbilical artery were shifted slightly lateralward. Note that the lymph vessels of higher origin (light green arrowheads) cross over the cord of the umbilical artery, while those of lower origin (dark green arrowheads) cross under the cord (Specimen 17, female)

In addition to the lateral pathway, some lymph vessels run posteriorly and drain into the lymphatics along the lateral sacral artery to reach the lymphatics along the common iliac nodes (Fig. 2.35) [32]. This figure shows that the lymph vessel pierces the fascial membrane which unites the right and left hypogastric nerves (interhypogastric fascia).

The iliac lymphatics are typically observed medial to, lateral to, and anterior to the iliac arteries and veins. In addition to these lymphatics, minute dissection after cutting the united portions of the three iliac arteries revealed that many lymph vessels (light green arrowheads) wind around and behind the arteries to connect with the iliac lymphatics (Figs. 2.35 and 2.36 [32]). This clarifies that the iliac lymphatics are not simply single layer lymphatics, but rather they are lymphatics which surround the iliac vessels.

2.1.5 Lymphatics Surrounding the Abdominal Aorta (Ganglions Abdomino-Aortiques, Rouvière)

The medial groups of the right and left common iliac lymph chains converge at the subaortic nodes. As shown in Fig. 2.36, the subaortic node receives the right and left medial groups of the common iliac chains on the one hand, but on

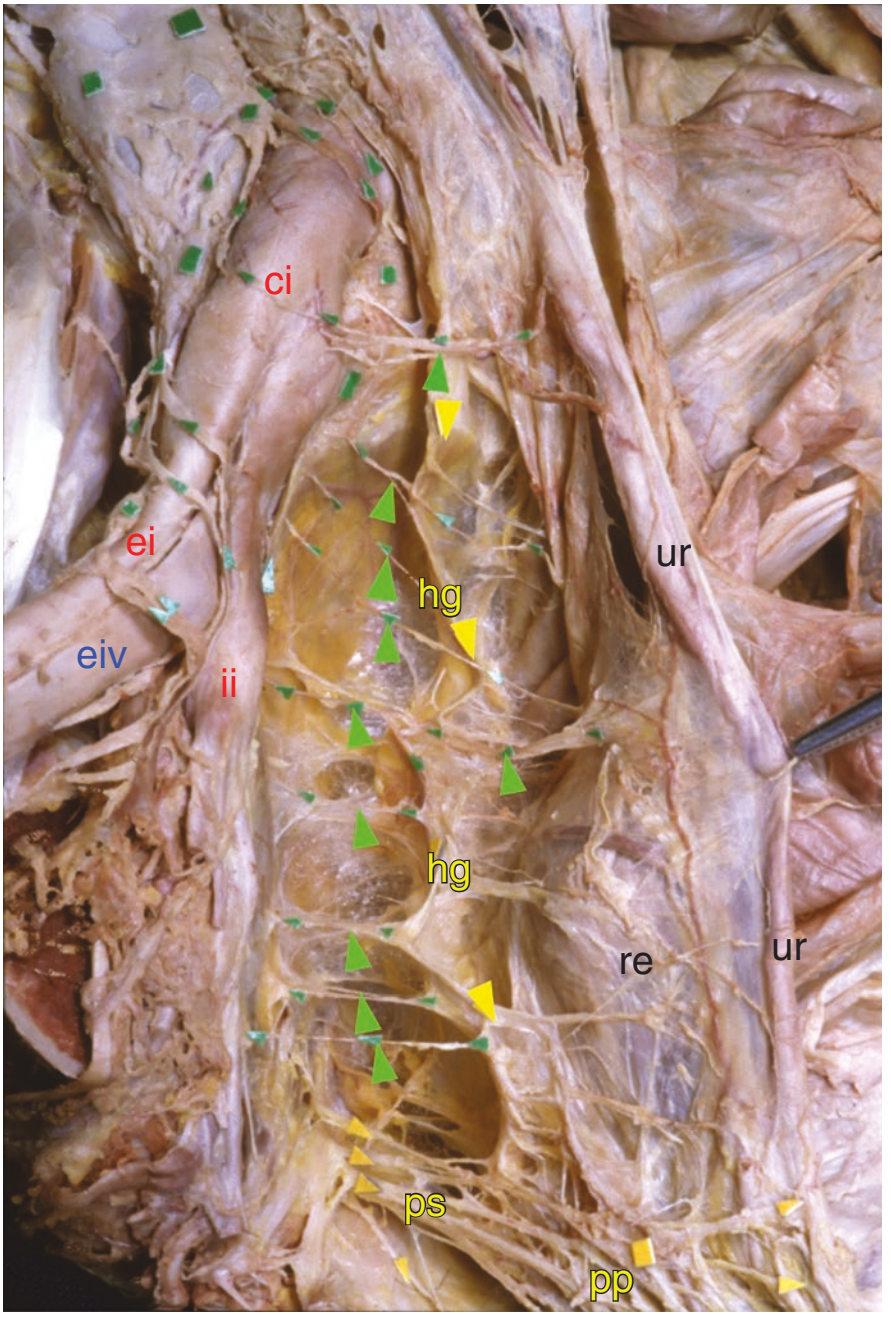

Fig. 2.34 Relationship between the lymphatics and nerves in a female pelvis. In a female pelvis, the rectum and the right ureter have been shifted to the left. The right hypogastric nerve and pelvic plexus are wrapped by fascial structures, and several lymph vessels (green arrowheads) cross over them (dissection video photograph: Specimen 18, female)

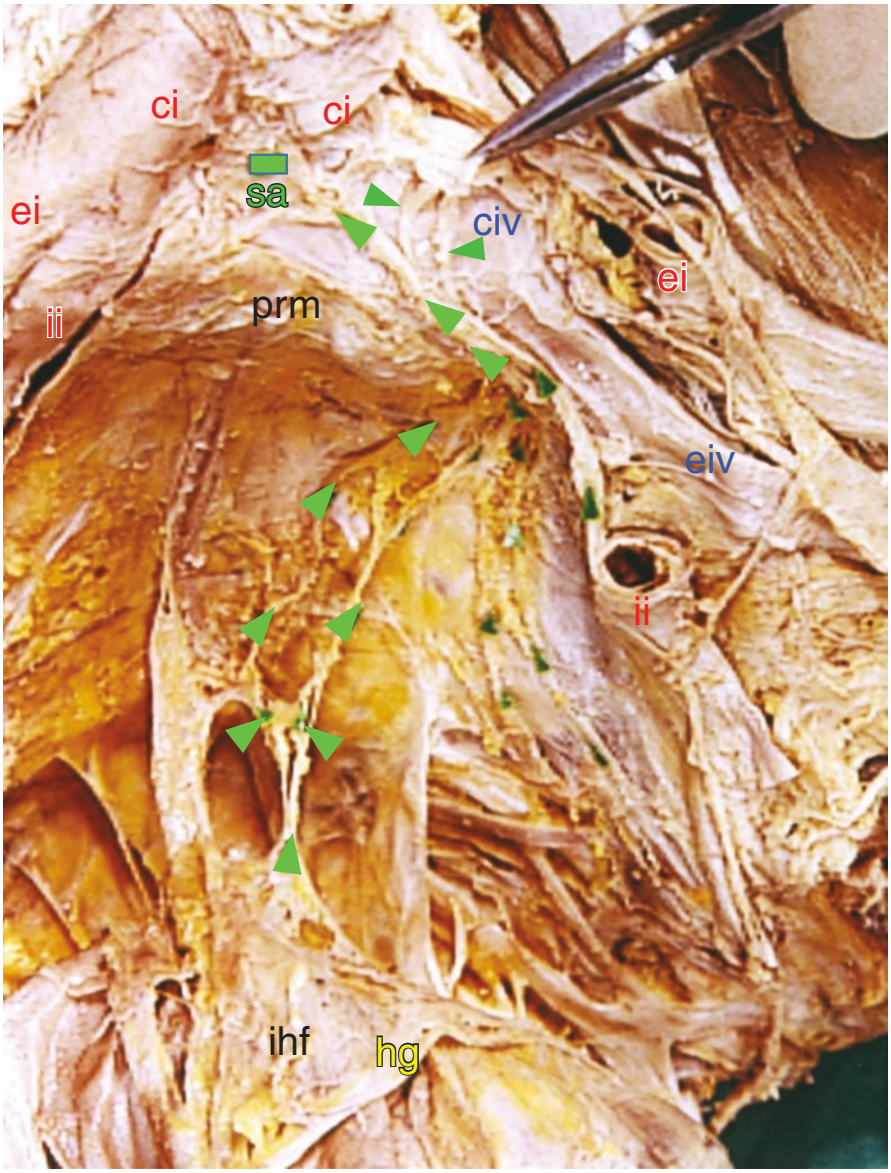

Fig. 2.35 Female pelvic lymphatics (seen from above). The rectum and fascia which unite the right and left hypogastric nerves, are shifted anteriorly. A lymph vessel (green arrowheads) from the rectum pierces the fascia to reach the anterior surface of the sacrum and finally, via the left common iliac lymphatics (light green arrowheads), it drains into the subaortic node (dissection video photograph: Specimen 18, female)

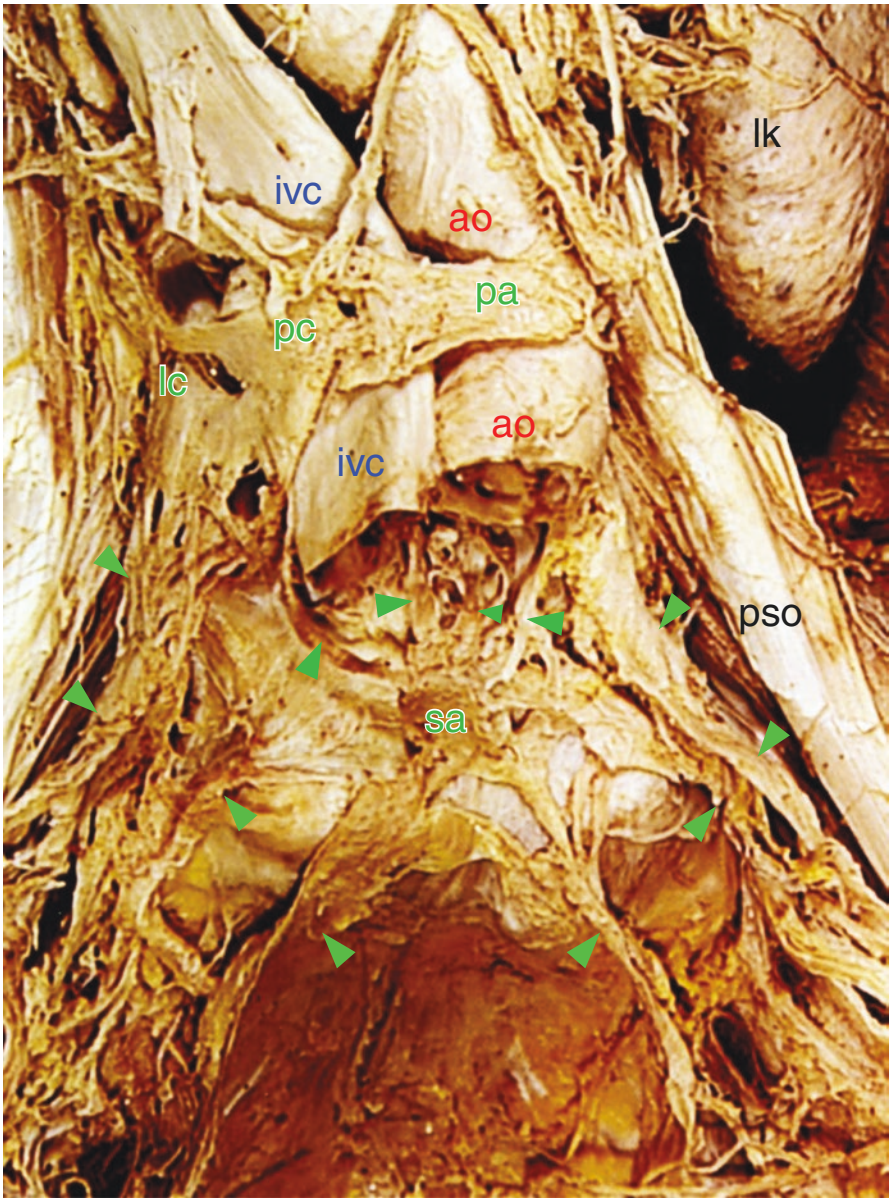

Fig. 2.36 Para-aortic lymphatic chains. Bilateral iliac arteries and veins and also the lower ends of the aorta and inferior vena cava have been removed. The subaortic node receives the right and left medial iliac chains (light green arrowheads) and sends three thick vessels of the major chains of the para-aortic lymphatics (lateral aortic, interaorticocaval, and lateral caval chains) (dark green arrowheads) (dissection video photograph: Specimen 18, female)

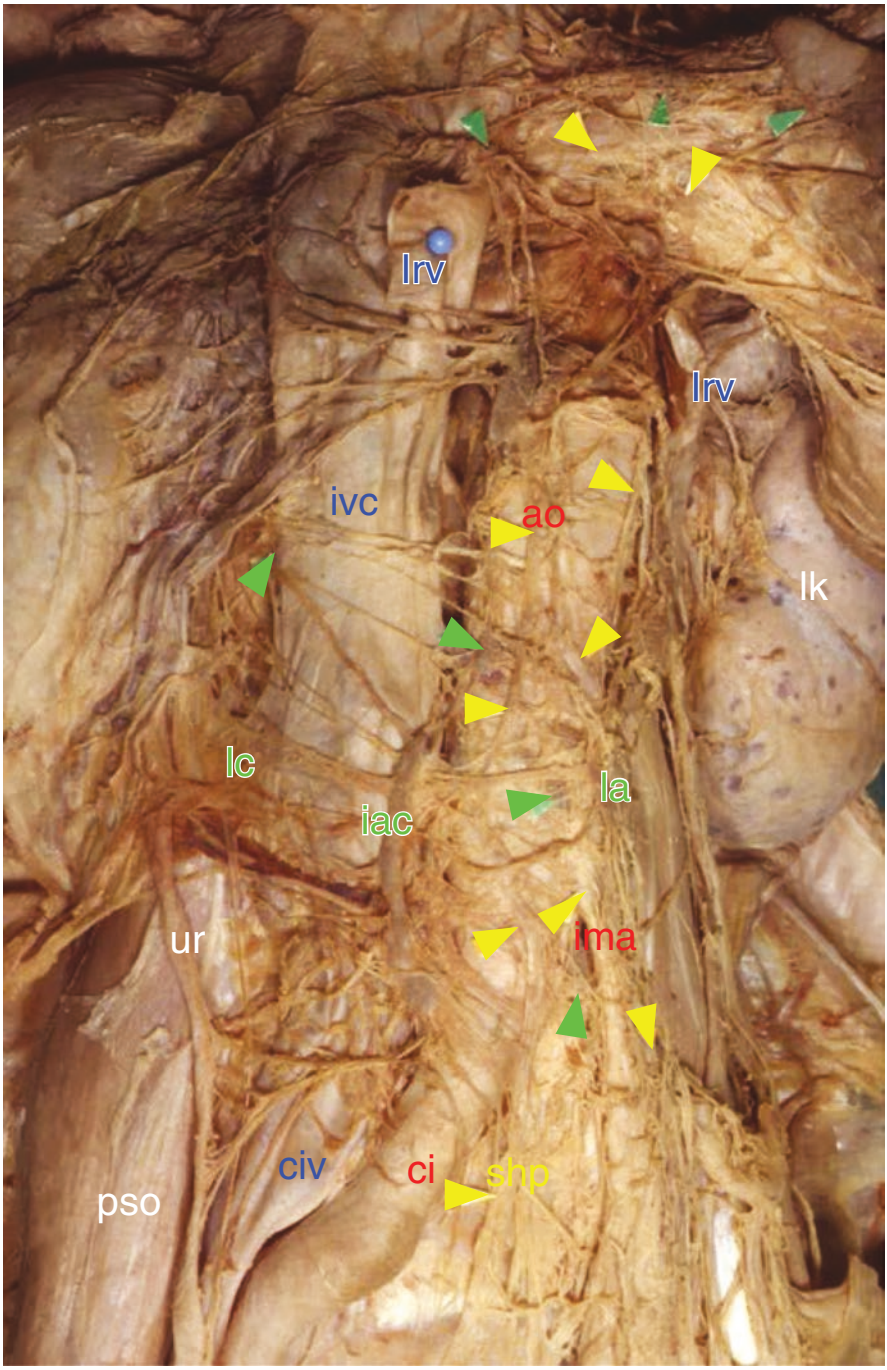

Fig. 2.37 Well-developed lymphatics around the aorta and the inferior vena cava. These lymphatics (green arrowheads) intermingle with the autonomic nerves (yellow arrowheads) (Specimen 19, male)

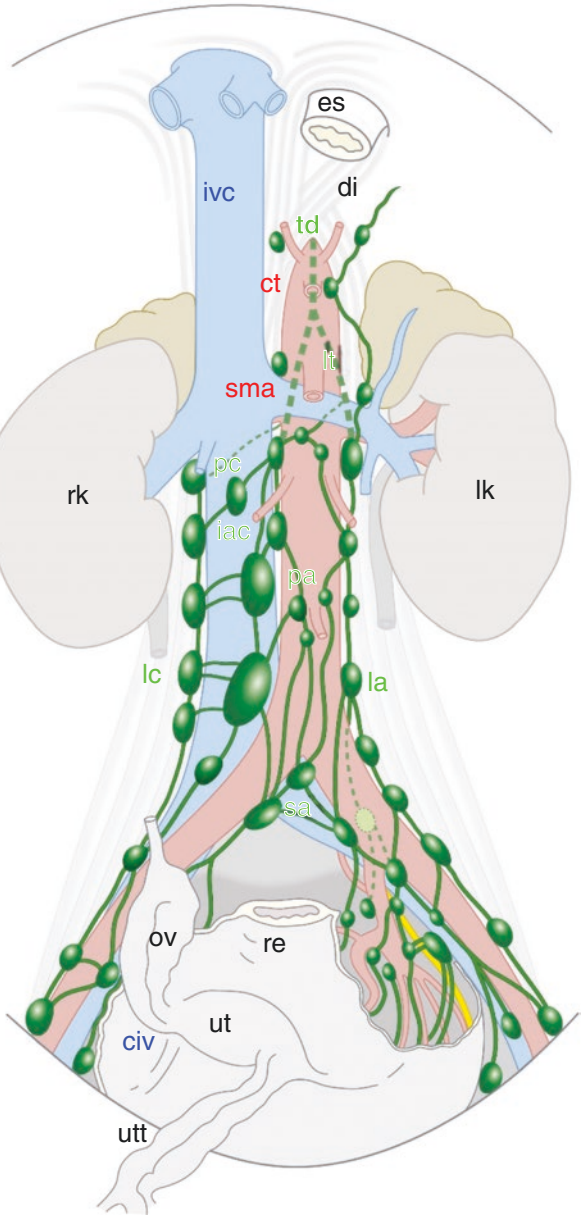

Fig. 2.38 Para-aortic lymphatics. This excellent scheme is taken from a textbook of anatomy of the lymphatic system (Rouvière) [1]

the other hand it sends three thick lymph vessels to the lateral aortic, interaorticocaval, and lateral caval lymph chains. In other words, the subaortic node is not only the ending point of the iliac chains but also the beginning point of the para-aortic chains. The left lateral common iliac chain continues to the lateral

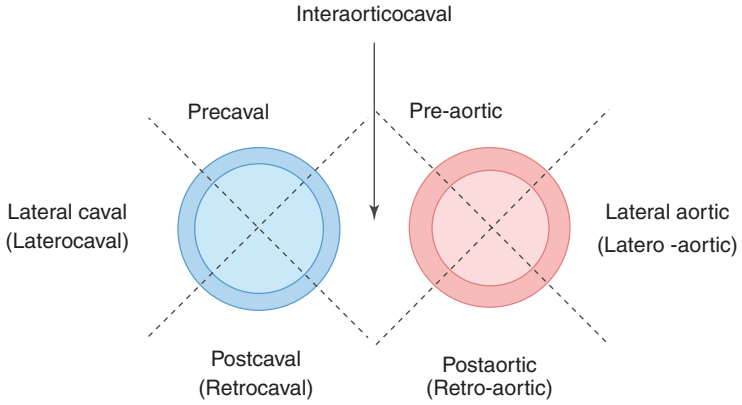

Fig. 2.39 Para-aortic node classification. Scheme showing a cross-section classification of the para-aortic nodes (Japanese Classification of Gastric Cancer [3]). Terms within parentheses are taken from Rouvière [1]

aortic chain, while the right corresponding chain is connected to the lateral caval chain (Fig. 2.36). The three lymph chains are connected to each other in front of as well as behind the two great vessels, and many nodes are detected in this communication network (Figs. 2.36 and 2.37 [33]). Therefore, the abdominal aortic nodes can be schematically subdivided into seven nodes: lateral aortic (latero-aortic), preaortic, retroaortic (postaortic), interaorticocaval, precaval, retrocaval (postcaval), and lateral caval (laterocaval) nodes (Fig. 2.38) [1], (Fig. 2.39) [3].

Accordingly, the abdominal aortic nodes are not simple para-aortic nodes, rather they are actually para-aorticocaval nodes. However, the paracaval chain gradually joins the para-aortic chain near the level of the left renal vein, and shifts posteriorly to eventually drain into the thoracic duct (Fig. 2.38). After removal of the abdominal aorta, the retroaortic lymphatics can be seen (Fig. 2.40 [32]). At about the level of the renal blood vessels, the para-aortic lymphatics gather to form two major lymphatic trunks, the lateroaortic trunk and the interaorticocaval trunk. These two trunks form the left and right lumbar trunks which unite to form the thoracic duct (Figs. 2.38 and 2.40). It has been described in textbooks that at the gathering point of the two trunks, in other words, the origin of the thoracic duct, the duct appears dilated (cisterna chili). However, in our dissections, this dilatation formation is rather rare, as seen in Fig. 2.40.

Another critical problem is the relationship of the para-aortic and inferior mesenteric chains to the autonomic nerve plexus (Fig. 2.37). Descending nerves from the coeliac plexus mainly join the inferior mesenteric plexus. Below the origin of the inferior mesenteric artery, the right and left lumbar splanchnic nerves, which originate from the lumbar parts of the sympathetic trunks, unite to form the superior hypogastric plexus. This plexus divides again into the right and left hypogastric nerves which join the pelvic plexuses. The para-aortic lymphatics are closely related to these nerve networks surrounding

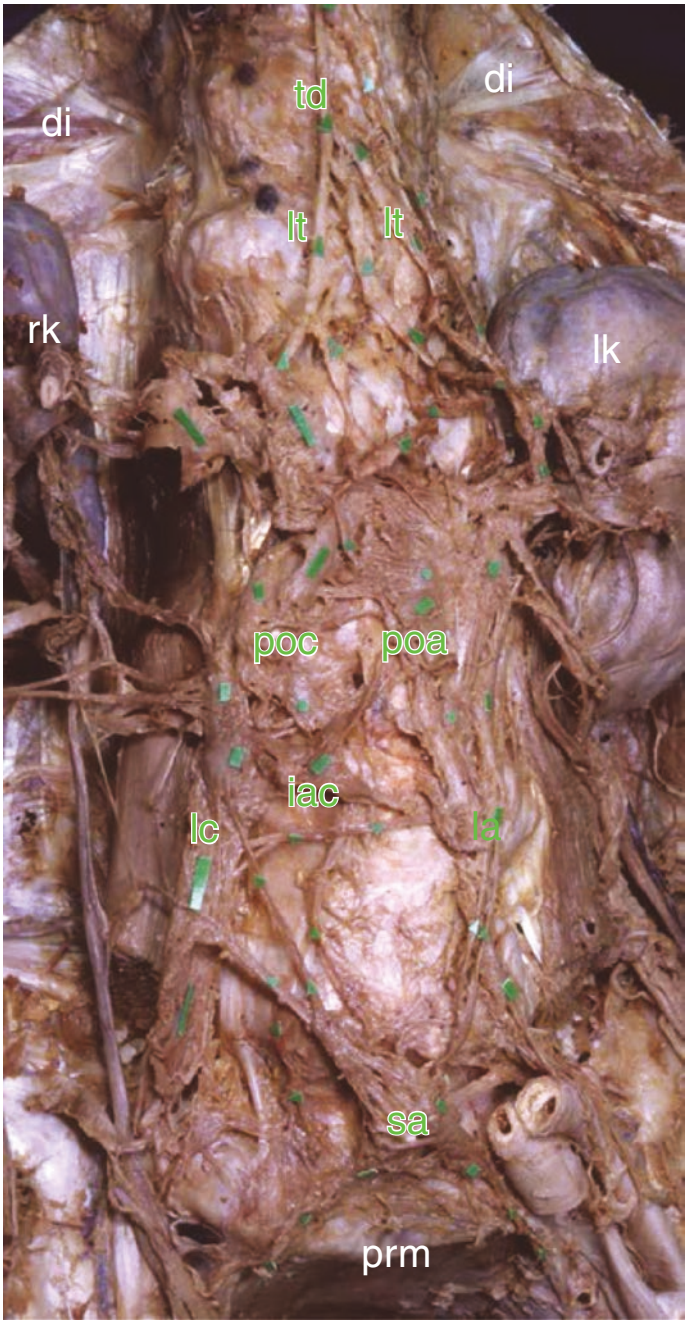

Fig. 2.40 Para-aortic lymphatics and the formation of the thoracic duct. After the removal of the abdominal aorta, the postaortic nodes and their communications with other lymphatics can be seen. As the aortic hiatus of the diaphragm has been opened, the formation of the thoracic duct is seen slightly superior to the kidneys (Specimen 20, male)

the lower abdominal aorta (Fig. 2.37). The intimate relationship of these nerves and lymphatics is very critical in rectal cancer surgery from the viewpoint of urinary and sexual functions.

2.2 Conclusion

In this chapter a pictorial demonstration of actual dissection findings of the lymphatics of the esophagus, stomach, colon, and rectum were described. In those descriptions, the following regional features of the arrangement of the lymphatics were included.

Regarding the lymphatics of the esophagus, the right ascending chain is generally more well developed than the left chain which runs anterior to and close to the left recurrent laryngeal nerve. Some esophageal lymph vessels may drain into the thoracic duct. Lymphatics of the lower thoracic esophagus continue to the gastric lymphatics via the superior diaphragmatic nodes close to the esophagus.

The lymphatics of the stomach typically run along the branches of the coeliac trunk to reach the coeliac nodes. The lymph vessels run along the right gastroepiploic blood vessels; however, they do not accompany the gastroepiploic artery, rather they run along the corresponding vein to reach the superior mesenteric nodes.

The lymphatics of the colon are divided into two pathways: that from the right hemicolon drains into the superior mesenteric nodes, whereas that from the left hemicolon reaches the inferior mesenteric nodes.

Regarding the lymphatics of the rectum, in addition to the superior (ascending) lymphatics along the superior rectal artery, the lateral (middle) lymphatics are critical. The lateral lymphatics first drain into the iliac nodes and/or presacral nodes and finally reach the subaortic nodes.

Drawings and photographs of actual dissections have been included to facilitate ease of understanding to achieve overall comprehension and to contribute to the precise knowledge of lymphatics. It is hoped that these additions will substantially contribute to the wide-encompassing significance of the lymphatics—a key to optimal surgical performance.

Acknowledgments I'm deeply indebted to all of my colleagues, and, in particular, Prof. K. Sato, Prof. H. Sakamoto, Dr. H. Deki, and Dr. M. Ito, for their expert dissection skills to make such remarkable figures possible. I also wish to thank Mr. M. Kohga for his excellent artistic skills to create meaningful precise schemes.

References

1. Rouvière H. Anatomie des lymphatiques de l'homme. Paris: Masson; 1932. p. 168–85, 283–350, 424–437 (in French).
2. Japan Esophageal Society. Japanese classification of esophageal cancer. 11th edition. Part 1. Esophagus. 2017;14:1–36.
3. Japanese Gastric Cancer Association. Japanese classification of gastric cancer: 3rd English edition. Gastric Cancer. 2011;14:101–12.

4. Japanese Society for Cancer of the Colon and Rectum. Japanese classification of colorectal carcinoma. 2nd English edition. Tokyo: Kanehara Shuppan; 2009. p. 100.
5. Federative Committee on Anatomical Terminology. Terminologia anatomica: International anatomical terminology. Stuttgart: Thieme; 1998. p. 100–3.
6. Feind CR. The head and neck. In: Haagensen CD, et al., editors. The lymphatics in cancer. Philadelphia: WB Saunders Co.; 1972. p. 59–230.
7. Sato T, Sakamoto H. Regional anatomy of the head and neck (10) lymphatic system of the neck. Otolaryngol Head Neck Surg. 1993;65:967–73. (in Japanese)
8. Saito H, Sato T, Yamashita Y, Amagasa T. Topographical analysis of lymphatic pathways from the meso- and hypopharynx based on minute cadaveric dissection: possible application to neck dissection in pharyngeal cancer surgery. Surg Radiol Anat. 2002;25:38–49.
9. Sato T, Sakamoto H. Illustrations and photographs of surgical esophageal anatomy specially prepared for lymph node dissection. In: Sato T, Iizuka T, editors. Color atlas of surgical anatomy for esophageal cancer. Tokyo: Springer-Verlag; 1992. p. 25–90.
10. Sato T, Sakamoto H. Regional anatomy of the lymphatics along the trachea. J Jpn Soc Bronchol. 1997;19:591–6. (in Japanese)
11. Sato T. Color photo-atlas of lymphatic anatomy: part 1. Lymphatics of the mediastinum. Operation. 2003;57:1203–10. (in Japanese)
12. Perlemuter L, Waligora J. Cahiers d'anatomie. In: Thorax, vol. 6. 3rd ed. Paris: Masson; 1976. p. 6. (in French).
13. Sato T, Takiguchi T, Sakamoto H. Anatomical features of the esophagus. Nippon Rinsho. 2011;69(Suppl. 6):17–27. (in Japanese)
14. Sato T, Sakamoto H. Color photo-atlas of lymphatic anatomy: part 2. Lymphatics of the abdomen. Operation. 2003;57:1371–8. (in Japanese)
15. Sato T. Macroscopic anatomy of the lymphatics of the upper abdominal organs with special emphasis on those of the stomach. Ochanomizu Igaku Zassi (Tokyo). 2013;61:1–16. in Japanese with English abstract
16. Deki H. Lymphatics of the stomach. In: Sato T, editor. Color atlas of topographic anatomy of the lymphatic system. Tokyo: Nankodo; 1997. p. 1–17. (in Japanese).
17. Ito M, Mishima Y, Sato T. An anatomical study of the lymphatic drainage of the gall bladder. Surg Radiol Anat. 1991;13:89–104.
18. Sato T, Ito M, Sakamoto H. Pictorial dissection review of the lymphatic pathways from the gallbladder to the abdominal para-aortic lymph nodes and their relationships to the surrounding structures. Sur Radiol Anat. 2013;35:615–21.
19. Suzuki K, Prates JC, DiDio LJA. Incidence and surgical importance of the posterior gastric artery. Ann Surg. 1978;187:134–6.
20. Sato K, Deki H, Sato T. Topographic relationship between the left cardiac nodes and the left inferior phrenic artery. Lymphology. 1987;10:177–90. (Japanese with English abstract)
21. Sato T. Topographic anatomy of the digestive organs—esophagus and stomach. Tokyo: Kanehara Shuppan; 1993. p. 239. (in Japanese)
22. Slanetz CA Jr, Herter FP. The large intestine. In: Haagensen CD, et al., editors. The lymphatics in cancer. Philadelphia: WB Saunders Co; 1972. p. 494.
23. Sato K, Sato T. Lymphatic pathways of the colon. Shujutsu (Operation). 1991;45:1341–51. (in Japanese)
24. Michels NA, Siddharth P, Kornblith P, Parke WW. The variant blood supply to the small intestines: its import in regional resections. J Intern Coll Surg. 1963;39:127–70.
25. Sato K. Lymphatics of the caecum and right hemicolon. In: Sato T, editor. Color atlas of topographic anatomy of the lymphatic system. Tokyo: Nankodo; 1997. p. 85–94. (in Japanese).
26. Perlemuter L, Waligora J. Cahiers d'anatomie. In: Abdomen 2, vol. 3. 4th ed. Paris: Masson; 1976. p. 6. (in French).
27. Sato K. Lymphatics of the rectum. In: Sato T, editor. Color atlas of topographic anatomy of the lymphatic system. Tokyo: Nankodo; 1997. p. 105–20. (in Japanese).
28. Sato K. Lymphatics of the left hemicolon. In: Sato T, editor. Color atlas of topographic anatomy of the lymphatic system. Tokyo: Nankodo; 1997. p. 95–104. (in Japanese).

29. Sato T. An introduction to the pelvic surgical anatomy. Jpn J Endourol. 2012;25:2–10. (in Japanese)
30. Sato K, Sato T. The vascular and neuronal composition of the lateral ligament of the rectum and the rectosacral fascia. Surg Radiol Anat. 1991;13:17–22.
31. Sato T. Normal anatomy of the female pelvis. In: Takeda Y, editor. Anatomy for obstetric and gynecologic surgery. Tokyo: Medical View Co.; 1999. p. 10–29. (in Japanese).
32. Sato T, Sakamoto H. Color photo-atlas of lymphatic anatomy: part 3. Lymphatics in the pelvis. Operation. 2003;57:1499–507. (in Japanese)
33. Sato T. Regional anatomy for operative surgery of genito-urinary organs. 36 Juxta-aortic lymph nodes. Clin Urol (Tokyo). 1992;46:385–91. (in Japanese)

Molecular Mechanisms of Lymph Node Metastasis

3

Naohide Oue, Yasuhiko Kitadai, and Wataru Yasui

Abstract

Despite improvements in diagnostic and therapeutic modalities, the prognosis of advanced cancer with extensive invasion and metastasis remains poor. The severity of a clinical prognosis depends on whether lymph node metastasis has occurred. For metastasis to occur, tumor cells must undergo a multistep process through a series of sequential and selective events. The metastatic process consists of detachment, local invasion, motility, lymphangiogenesis, lymphatic vessel invasion, survival in the circulation, adhesion to endothelial cells, extravasation, and regrowth in lymph nodes. Among them, the most important process is lymphangiogenesis, which is regulated by members of the vascular endothelial growth factor (VEGF) family and their receptors. In addition to lymphangiogenesis, it is well accepted that cancer stem cells play a significant role in metastasis. Although several types of metastasis-associated molecules have been identified, the expression of these molecules differs among esophageal, gastric, and colorectal cancer. This chapter will review the cellular and molecular mechanisms of lymph node metastasis including lymphangiogenesis and cancer stem cells in these human cancer types.

Keywords

VEGF · PDGF · Migration · Cancer stem cell

N. Oue · Y. Kitadai · W. Yasui (✉)
Department of Molecular Pathology, Hiroshima University Institute of Biomedical and Health Sciences, Hiroshima, Japan
e-mail: wyasui@hiroshima-u.ac.jp

S. Natsugoe (ed.), *Lymph Node Metastasis in Gastrointestinal Cancer*,
https://doi.org/10.1007/978-981-10-4699-5_3

3.1 Lymphangiogenesis

In the multistep process of lymph node metastasis, the most important step is lymphangiogenesis, which plays an important role in both tumor growth and metastasis [1, 2]. Beasley et al. [3] analyzed human head and neck cancers by immunohistochemical staining for the lymphatic endothelial markers LYVE-1 and CD34, and the proliferation marker Ki-67. They observed Ki-67 nuclear staining in a proportion of small intratumoral lymphatic endothelial cells, suggesting that the intratumoral lymphatics do indeed generate new vessels. Furthermore, they found that a high intratumoral lymphatic vessel density is associated with lymph node metastases and an infiltrating margin of tumor invasion. Their study provided evidence that lymphatic growth can occur in human cancers and may in some cases contribute to lymph node metastasis. It has been also reported that tumor lymphangiogenesis correlates with lymphatic metastasis in esophageal squamous cell carcinoma [4], gastric cancer [5, 6], and colorectal cancer [7].

Lymphangiogenesis is regulated by members of the VEGF family and their receptors. The VEGF family includes VEGF-A, -B, -C, -D, -E, and -F and placental growth factor (PlGF) [8]. Among them, VEGF-C and VEGF-D are essential for lymphangiogenesis. Both VEGF-C and VEGF-D are ligands for VEGF receptor (VEGFR)2 and VEGFR3 [9]. Activation of VEGFR3 induces lymphangiogenesis, whereas activation of VEGFR2 is thought to drive angiogenesis. In addition to these molecules, platelet-derived growth factors (PDGFs) and PDGF receptors (PDGFRs) not only promote angiogenesis but are also important players in lymphangiogenesis. These molecules are summarized in Fig. 3.1.

He et al. [10] investigated how tumor cells gain access to lymphatic vessels and at what stage tumor cells initiate metastasis. They showed that VEGF-C produced by tumor cells induces extensive lymphatic sprouting towards the tumor cells as well as dilation of the draining lymphatic vessels in a mouse model. In this model, a significant increase in lymphatic vessel growth occurs between 2 and 3 weeks after tumor xenotransplantation, and lymph node metastasis occurs at the same stage. Lymphatic vessel growth can be blocked by inhibition of VEGFR3 signaling by systemic delivery of a soluble VEGFR3 immunoglobulin. However, VEGFR3 immunoglobulin cannot suppress lymph node metastasis when the treatment is started at a later stage after the tumor cells have already spread. Therefore, tumor cell entry into lymphatic vessels is a critical step during tumor dissemination.

3.1.1 VEGF-C

VEGF-C is an essential chemotactic and survival factor during lymphangiogenesis and is required for the sprouting of the first lymphatic vessels from embryonic veins [11]. Skobe et al. [12] reported that VEGF-C can selectively induce hyperplasia of the lymphatic vasculature in breast cancer in a mouse model. In gastrointestinal cancers, a correlation between VEGF-C expression and lymph node metastasis has been reported. Moreover, expression of VEGF-C protein is observed in cancer cells

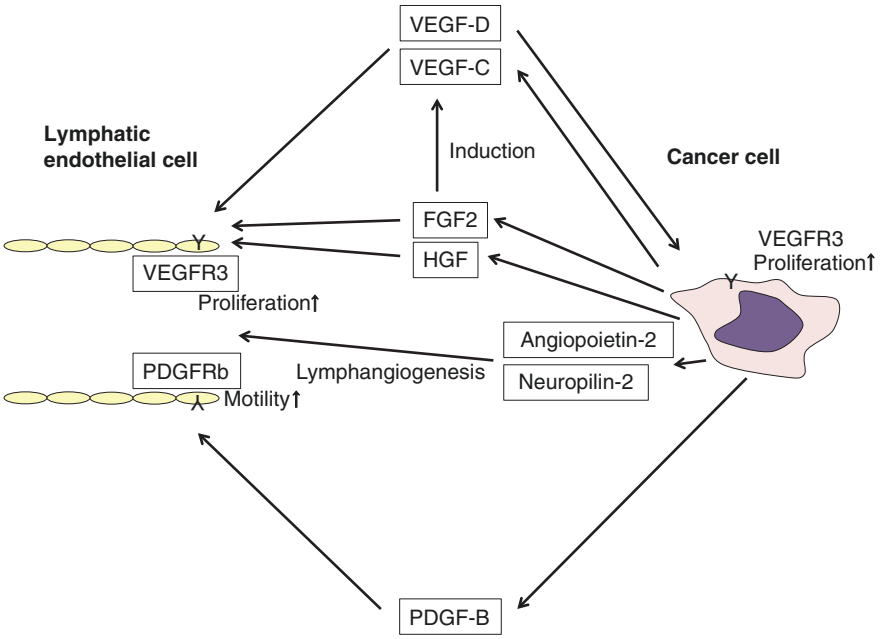

Fig. 3.1 Lymphangiogenesis-associated molecules. Lymphangiogenesis is regulated by members of the VEGF and PDGF families and their receptors

by immunohistochemical analysis. Kitadai et al. [13] examined the expression of VEGF-C in 48 specimens of human esophageal carcinoma tissues by immunohistochemistry. They reported that VEGF-C expression was correlated with depth of tumor invasion, tumor stage, venous invasion, lymphatic invasion, and lymph node metastasis in esophageal squamous cell carcinoma. Matsumoto et al. [14] examined VEGF-C expression in esophageal squamous cell carcinoma and analyzed the relationships between VEGF-C expression and clinicopathological findings such as lymph node metastasis. They demonstrated that VEGF-C overexpression was significantly correlated with depth of tumor invasion, lymphatic invasion, and lymph node metastasis in esophageal squamous cell carcinoma. Moreover, Yonemura et al. [5] studied the expression of VEGF-C in 32 gastric cancer tissue samples by immunohistochemistry. They showed that VEGF-C expression was correlated with lymph node status, lymphatic invasion, venous invasion, and tumor infiltrating patterns in gastric cancer. Furthermore, Amioka et al. [6] analyzed VEGF-C expression in 139 gastric cancer cases. They found that VEGF-C immunoreactivity was associated with a greater depth of tumor invasion, lymphatic invasion, and lymph node metastases in gastric cancers invading the submucosa. Onogawa et al. [15] analyzed the expression of VEGF-C and VEGF-D protein by immunohistochemistry in 139 surgical specimens of human colorectal cancer. They found VEGF-C expression in 46.8% of colorectal cancer cases, which was correlated with the depth of tumor invasion, lymphatic involvement, venous involvement, lymph node metastasis, and

liver metastasis. These reports demonstrate that VEGF-C plays an important role in lymph node metastasis in gastrointestinal cancers.

Tumor-associated lymphatic vessel density is correlated with metastasis to draining lymph nodes and poor prognosis. In gastrointestinal cancers, a correlation between VEGF-C expression and lymphatic vessel density has been reported. Hachisuka et al. [16] investigated VEGF-C expression and lymphatic vessel density in gastric cancer. They found that the expression of VEGF-C was correlated with high lymphatic vessel density. Li et al. [17] evaluated the expression of VEGF-C and VEGFR3 in 147 colon cancer cases. They reported that VEGF-C expression was positively correlated with lymphatic vessel density. These results demonstrate that VEGF-C promotes lymph node metastasis through lymphangiogenesis.

Although overexpression of VEGF-C has been reported, the mechanism that underlies this overexpression in cancers remains unclear. Matsumura et al. [18] investigated DNA methylation and expression of the VEGF-C gene (*VEGFC*) in gastric cancer. Bisulfite DNA sequencing analysis revealed that *VEGFC* was not methylated in nine of 31 gastric cancer samples, while demethylation was not observed in the corresponding non-neoplastic mucosa samples. Overexpression of VEGF-C was frequently found in gastric cancer cases with *VEGFC* demethylation. Thus, these results suggest that demethylation and activation of *VEGFC* is likely involved in lymphangiogenesis in gastric cancer.

3.1.2 VEGF-D

In addition to VEGF-C, VEGF-D also promotes tumor metastasis through lymphangiogenesis [19]. The mature form of VEGF-D shares 61% amino acid sequence identity with VEGF-C, and binds to both VEGFR2 and VEGFR3 [9]. In mice, Vegfd binds only to Vegfr3, indicating that Vegfd might have a somewhat different function in mice and humans [20]. It has been reported that VEGF-D also modulates prostaglandin levels to regulate lymphatic vessel dilation [21]. Expression of VEGF-D protein can be detected in cancer cells by immunohistochemical analysis, and a correlation between VEGF-D expression and lymph node metastasis has been reported in gastrointestinal cancers. Kozlowski et al. [22] reported that VEGF-D expression was significantly correlated with tumor location, tumor size, histological grade, depth of invasion, and lymph node metastasis in esophageal squamous cell carcinoma. Onogawa et al. [23] examined VEGF-C and VEGF-D expression by immunohistochemistry in 140 surgical specimens of submucosally invasive gastric cancer. VEGF-C expression was associated with lymphatic invasion and lymph node metastasis; however, there was no association between VEGF-D expression and clinicopathological features. Arigami et al. [24] analyzed VEGF-C and VEGF-D expression in 80 early-stage gastric cancers. VEGF-C and VEGF-D was detected in 27.5 and 21.3% cases, respectively, and their expression was closely related to lymph node micrometastasis. Furthermore, Onogawa et al. [15] analyzed VEGF-C and VEGF-D protein expression by immunohistochemistry in 139 surgical

specimens of human colorectal cancer. They observed VEGF-D expression in 29.5% of colorectal cancer cases, which was correlated with the depth of tumor invasion, lymph node metastasis, and liver metastasis. These results indicate that in addition to VEGF-C, VEGF-D also plays an important role in lymph node metastasis in gastrointestinal cancers.

Besides VEGF-C, a correlation between VEGF-D expression and lymphatic vessel density has been reported. Wang et al. [25] examined the expression of VEGF-D in 123 patients with gastric cancer. They reported that peritumoral-lymphatic vessel density was significantly associated with lymph node metastasis, lymphatic vessel invasion, VEGF-C expression, and VEGF-D expression. Su et al. [26] analyzed the expression of VEGF-D, SMAD4, and SMAD7 in 251 colon cancer samples. They found that positive expression of VEGF-D was significantly correlated with lymph node metastasis and high lymphatic vessel density. Therefore, VEGF-D also promotes lymph node metastasis through lymphangiogenesis.

3.1.3 VEGFR3

VEGFR3 is a tyrosine kinase receptor that is expressed predominantly in the endothelium of lymphatic vessels [27]. VEGFR3 stimulation alone protects the lymphatic endothelial cells from serum deprivation-induced apoptosis and induces their proliferation and migration. At least some of these signals are transduced via protein kinase C-dependent activation of the ERK1/ERK2 MAPK signaling cascade and via a wortmannin-sensitive induction of AKT phosphorylation. These results demonstrate a critical role of VEGF-C/VEGFR3 signaling in the proliferation and survival of lymphatic endothelial cells [28]. VEGFR3 was originally thought to be expressed specifically in the lymphatic endothelium; however, VEGFR3 is also expressed in a small subset of blood vessels in normal tissues and can be reexpressed in angiogenic blood vessels in certain pathological conditions [29]. Furthermore, VEGFR3 has also been detected in cancer cells, including lung adenocarcinoma [30] and gastric cancer cells. Su et al. [30] reported that the VEGF-C/VEGFR3 axis enhances cancer cell mobility and invasiveness, and contributes to the promotion of cancer cell metastasis through upregulation of the neural cell adhesion molecule contactin-1. Immunohistochemical analyses in lung cancer and colorectal cancer revealed that high levels of VEGFR3 and VEGF-C expression correlated closely with clinical metastasis and patient survival. Kodama et al. [31] found that VEGFR3-specific immunoreactivity was detected on gastric cancer cells. Furthermore, in vitro treatment of a gastric cancer cell line with VEGF-C stimulated cell proliferation and increased expression of cyclin D1, PlGF, and autocrine motility factor. In a mice xenograft model, the tumor growth of VEGF-C-transfected cells was greatly accelerated in comparison with that of control cells. Greater angiogenesis and lymphangiogenesis were also detected in VEGF-C-transfected tumors than in control tumors. Therefore, the VEGF-C/VEGFR3 axis plays a role in the progressive growth of human gastric cancer through both autocrine and paracrine

mechanisms. Tanaka et al. [32] examined the expression and function of the VEGF-D/VEGFR3 axis in human gastric cancer. They found that 34% of gastric cancer cases expressed both VEGF-D and VEGFR3. In vitro treatment of a gastric cancer cell line with VEGF-D increased the expression of cyclin D1 and BCL-2 and stimulated cell proliferation. Therefore, in addition to VEGF-C, VEGF-D is likely to participate in the progression of gastric cancer by acting via autocrine and paracrine mechanisms.

3.1.4 PDGF-B

Members of the PDGF family are often expressed at high levels in many cancers [33]. The PDGF family consists of five isoforms, -AA, -AB, -BB, -CC, and -DD, usually referred to as PDGF-A (AA), PDGF-B (AB and BB), PDGF-C (CC), and PDGF-D (DD) [34]. Their biological activities are mediated by the tyrosine kinase receptors PDGF receptor (PDGFR)a and PDGFRb. PDGFRa binds all possible forms of PDGF except PDGF-DD, whereas PDGFRb preferentially binds PDGF-BB. PDGFs induce tumor growth and stimulate angiogenesis [35]. In addition, Cao et al. [36] showed that PDGF-BB stimulates MAP kinase activity and cell motility of isolated lymphatic endothelial cells. Expression of PDGF-BB in murine fibrosarcoma cells induces tumor lymphangiogenesis, leading to enhanced metastasis in lymph nodes. Matsumoto et al. [37] examined the expression of PDGF-BB and VEGF-C by immunohistochemistry in esophageal squamous cell carcinoma, and found that expression of PDGF-BB and VEGF-C was correlated with lymph node metastasis and lymphatic invasion. Furthermore, they found that lymphangiogenesis in PDGF-BB- or VEGF-C-positive tumors was higher than in negative tumors. Kodama et al. [38] examined the expression of PDGF-BB and PDGFRb in 38 surgical specimens of gastric cancer. They showed that PDGF-B and PDGFRb mRNA expression was significantly higher in patients with lymph node metastasis than in those without, and was also significantly higher in diffuse-type carcinoma than in intestinal-type carcinoma. Expression of PDGF-B was detected in gastric cancer cells, whereas PDGFRb was expressed predominantly in stromal cells. In orthotopic TMK-1 gastric cancer cell line tumors, the cancer cells expressed PDGF-B but not PDGFRb. PDGFRb was expressed by stromal cells, including lymphatic endothelial cells. These data demonstrate that secretion of PDGF-B by cancer cells and expression of PDGFRb by tumor-associated stromal cells are associated with lymphatic metastasis.

3.1.5 Angiopoietin-2

The angiopoietin family growth factors have been identified as ligands for Tie-2. Angiopoietin-1 activates Tie-2, leading to receptor autophosphorylation upon binding, and it simulates endothelial cell migration in vitro, contributing to blood vessel stabilization by recruitment of pericytes [39]. In contrast, angiopoietin-2 is crucial for establishing the lymphatic vasculature. VEGF-C/VEGFR3 signaling is a critical

primary proliferation pathway for lymphatic vessels, whereas angiopoietin-2 is important in later remodeling stages [40].

Jo et al. [41] measured the serum levels of angiopoietin-2 in patients with gastric cancer by immunoassay; elevated serum angiopoietin-2 levels were associated with positive lymph node involvement. Wang et al. [42] analyzed the expression of angiopoietin-2 by immunohistochemistry in 53 gastric cancer and 23 normal gastric mucosa samples. They found that angiopoietin-2 expression was significantly increased in gastric cancer tissues (74%) and was correlated with lymph node metastasis. However, the importance of angiopoietin-2 for lymphatic metastasis of human esophageal cancer or colorectal cancer is still unknown.

3.1.6 Neuropilin-2

Neuropilin-2 was initially identified as a semaphorin receptor and mediator of axon guidance [43]. However, it has been reported that neuropilin-2 binds to VEGF-C [44]. Homozygous neuropilin-2 mutants show a reduction in small lymphatic vessels and capillaries prenatally [45]. Caunt et al. [46] reported that an antibody against neuropilin-2 disrupts VEGF-C-induced lymphatic endothelial cell migration, but not proliferation. It does not affect established lymphatics in normal adult mice but reduces tumoral lymphangiogenesis and functional lymphatics associated with tumors. It also reduces metastasis to sentinel lymph nodes and distant organs.

In normal tissue, neuropilin-2 staining is detected in blood or lymphatic vessels, while staining of neuropilin-2 is identified not only in the vascular or lymphatic endothelial cells, but also in the cytoplasm of cancer cells. Fung et al. [47] examined the expression of neuropilin-2 in esophageal squamous cell carcinoma by immunohistochemistry. They found that levels of neuropilin-2 expression were significantly upregulated in esophageal squamous cell carcinoma, and were correlated with lymph node metastasis. These results suggest that neuropilin-2 plays an important role in lymphatic endothelial cells, as well as in cancer cells. Nonetheless, the importance of neuropilin-2 for lymphatic metastasis of human gastric cancer or colorectal cancer is still unknown.

3.1.7 MicroRNAs

MicroRNAs are 18- to 25-nucleotide-long noncoding RNA molecules that regulate the translation of many genes [48]. Recent studies have indicated that microRNA expression levels are altered in most types of human cancers, and microRNAs are important gene regulators that play critical roles in biological processes and function as either tumor suppressors or oncogenes.

Yang et al. [49] observed altered expression of miRNAs in human lymphatic endothelial cells cocultured with lymphangiogenesis-inducing VEGF-C-transformed gastric cancer cells, with 47 upregulated and 42 downregulated

miRNAs. Upregulated miRNAs included miR-648, miR-5002-3p, miR-4754, miR-4760-5p, miR-4491, miR-4252, miR-5007-3p, and miR-647; and downregulated miRNAs included miR-3178, miR-593-5p, miR-4485, miR-135a-3p, miR-17, miR-1469, and miR-124-5p.

Hu et al. [50] determined that ectopic miR-128 overexpression inhibited VEGF-C expression and reduced the activity of a luciferase reporter containing the VEGF-C 3′-untranslated region. Furthermore, in vivo restoration of miR-128 significantly suppressed the tumorigenicity of A549 cells in nude mice and inhibited lymphangiogenesis of tumor xenografts.

Liu et al. [51] reported that miR-486-5p was significantly downregulated in colorectal cancer tissues compared with adjacent normal tissue by quantitative real-time polymerase chain reaction. They found that neuropilin-2 is a direct functional target of miR-486-5p in colorectal cancer cells, and upregulation of miR-486-5p in colorectal cancer cells was negatively correlated with neuropilin-2 expression. Furthermore, overexpression of miR-486-5p inhibited tumor growth and lymphangiogenesis in nude mice.

3.1.8 Other Factors

Fibroblast growth factor 2 (FGF2, also known as basic FGF) is another factor that is reported to promote lymphangiogenesis. It stimulates lymphangiogenesis in the mouse cornea and upregulates expression of VEGF-C and VEGF-D in this model; this effect was blocked by VEGFR3 antibodies, indicating that FGF2 promotes lymphangiogenesis via induction of VEGF-C expression and activation of VEGFR3 signaling [52]. Mikami et al. [53] analyzed FGF2 expression in human esophageal carcinoma. They found that FGF2 was associated with tumor invasion, lymph node metastasis, and pathological stages. Furthermore, Ueki et al. [54] examined FGF2 expression in gastric cancer. They observed FGF2 expression in 70% of gastric cancer cases, which was confined to the tumor cells. FGF2 expression was correlated with a higher rate of lymph node metastases. It was also shown that hepatocyte growth factor (HGF) can bind to VEGFR3 and induce lymphangiogenesis [55]. Kammula et al. [56] reported that HGF expression is associated with primary colorectal cancer progression and can be used to predict outcome.

3.2 Cell Migration and Lymph Node Metastasis

In addition to lymphangiogenesis, cell migration is also an important process in lymph node metastasis. Cell migration is a process that involves reorganization of the cytoskeleton, formation of protrusions, establishment of adhesive contacts at the leading edge, and cell contraction and detachment at the trailing edge. In gastrointestinal cancers, several genes were found to promote cell migration, thereby enhancing cancer cell invasion and metastasis (Fig. 3.2).

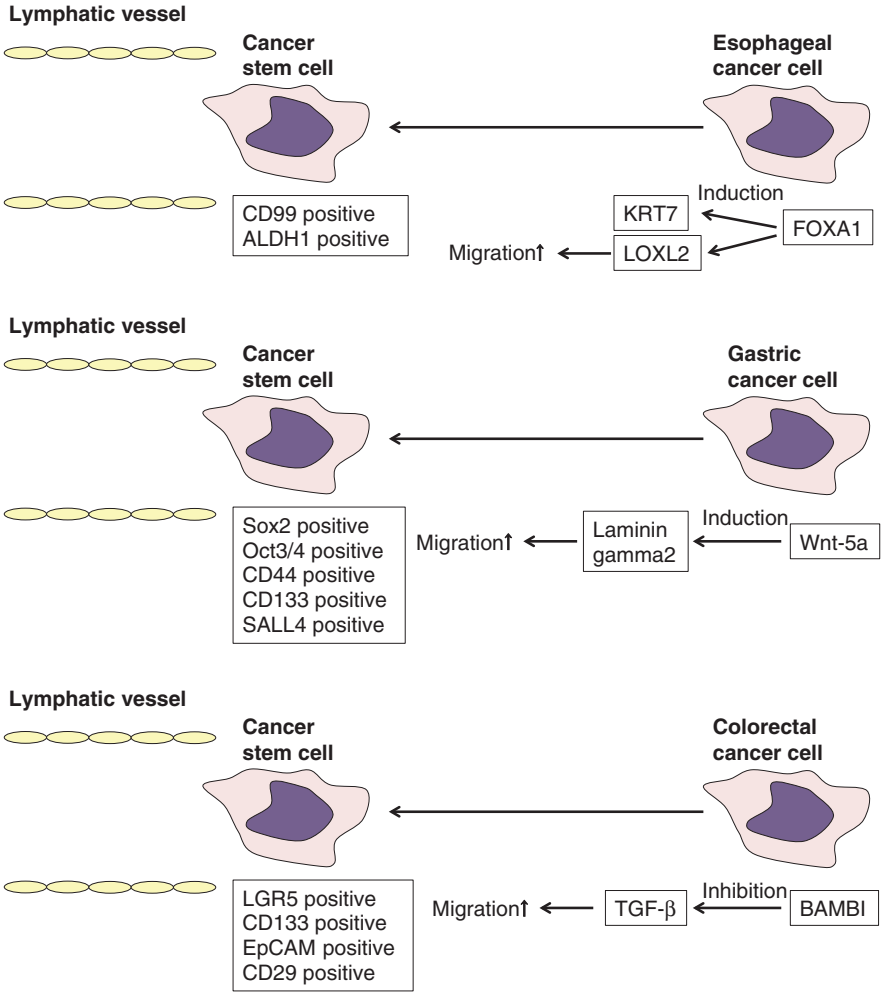

Fig. 3.2 Cell migration-associated molecules in esophageal, gastric, and colorectal cancer. Several markers for cancer stem cells have been reported in esophageal (**a**), gastric (**b**), and colorectal cancer (**c**)

3.2.1 FOXA1 Promotes Lymph Node Metastasis in Esophageal Squamous Cell Carcinoma

Sano et al. [57] compared the gene expression profiles of 24 esophageal squamous cell carcinomas with extensive lymph node metastasis and 11 esophageal squamous cell carcinomas with no metastatic lymph nodes by microarray. They found 209 genes whose expression was associated with lymph node metastasis. Among them, overexpression of *CALB1*, *KRT7*, *MUC1*, and *CEACAM5* in poor prognostic cases with metastatic lymph nodes was confirmed by RT-PCR. They also identified

FOXA1 as a transcriptional factor co-expressed with *KRT7*. FOXA1 is a pioneer factor that possesses the ability to engage with closed chromatin, move nucleosomes, and ultimately allow subsequent binding of other transcription factors [58]. In esophageal squamous cell carcinoma, FOXA1 induces *KRT7* and *LOXL2* expression, both of which are associated with lymph node metastasis.

The *KRT7* gene, which encodes cytokeratin 7, is expressed in several simple ductal epithelia, in mesothelium, and in urothelium. However, cytokeratin 7 is sparsely expressed or absent in gastric foveolar epithelium, intestinal epithelium, hepatocytes, and squamous epithelia [59]. It has been reported that cytokeratin 7 expression is a statistically significant prognostic factor in patients with stage I and II esophageal squamous cell carcinoma [60]. In stage 0–III esophageal squamous cell carcinoma, lymph node metastasis is frequently found in cytokeratin 7-positive cases but not in cytokeratin 7-negative cases [61]. In contrast, a direct association between cytokeratin 7 expression and lymph node metastasis remains unclear. Because cytokeratin 7 expression is regulated by FOXA1, FOXA1 may also regulate several cancer-related genes, such as FOXA1-inducing genes.

The *LOXL2* gene, which encodes lysyl oxidase-like 2 protein, is a member of the LOX family of extracellular matrix-modifying enzymes [62]. Lysyl oxidase-like 2 catalyzes the cross-linking of collagens and elastin [63]. Furthermore, lysyl oxidase-like 2 protein promotes invasion by regulating the expression and activity of the extracellular proteins tissue inhibitor of metalloproteinase-1 (TIMP1) and matrix metalloproteinase-9 (MMP9) [64]. Overexpression of lysyl oxidase-like 2 is observed preferentially in esophageal squamous cell carcinomas with greater than five metastatic lymph nodes [57]. Lysyl oxidase-like 2 overexpression in pancreatic cancer cells enhances the epithelial–mesenchymal transition-like process, and increases migratory and invasive activity [65]. Taken together, these results suggest that FOXA1 plays an important role in lymph node metastasis in esophageal squamous cell carcinoma.

In contrast, Ren et al. [66] reported that expression of FOXA1 was not associated with lymph node metastasis in gastric cancer. Therefore, promotion of lymph node metastasis by FOXA1 may be a specific event in esophageal squamous cell carcinoma.

3.2.2 Wnt-5a Stimulates Cell Migration in Gastric Cancer Cells

Wnt-5a, a member of the Wnt family of proteins, is a representative ligand that activates the β-catenin-independent pathway via mobilization of intracellular Ca^{2+}, and the activation of protein kinase C, resulting in the stimulation of migration of several cultured cell lines, including cancer cells [67]. Kurayoshi et al. [68] analyzed the expression of Wnt-5a in 237 gastric cancer cases. They found that Wnt-5a expression was correlated with the depth of tumor invasion, tumor stage, and lymph node metastasis. They also found that Wnt-5a stimulates cell migration and invasion in gastric cancer cells. Overexpression of Wnt-5a activates focal adhesion kinase, and knockdown of Wnt-5a reduces the turnover of paxillin in focal adhesion.

Yamamoto et al. [69] performed microarray analyses to compare expression patterns between mouse fibroblast L cells that stably express wild-type *Wnt5a* and a mutant form of *Wnt5a*. They found that *Wnt5a* induces the expression of laminin gamma2 through the activation of protein kinase C and c-Jun-N-terminal kinase. The invasive activity of gastric cancer cells depends on laminin gamma2. These results demonstrate that Wnt-5a contributes to gastric cancer metastasis by increasing cell migration activity.

In contrast, Li et al. [70] showed that *WNT5A* is silenced in the highly invasive colon cancer cell line by histone modifications. Dejmek et al. [71] showed that the addition of recombinant Wnt-5a significantly reduces the migratory capacity of SW480 colon cancer cells. Therefore, promotion of lymph node metastasis by Wnt-5a may be a specific event in gastric cancer.

3.2.3 BAMBI Promotes Migration of HCT116 Colon Cancer Cells

Fritzmann et al. [72] compared gene expression patterns between metastatic and nonmetastatic stage-matched human colorectal cancers by microarray analysis. They found that *BAMBI* is highly expressed in approximately half of metastatic primary tumors and metastases but not in nonmetastatic tumors. BAMBI antagonizes the effects of TGF-β superfamily ligands by stably associating with the surface receptors [73], and is directly regulated by β-catenin in colon cancer cells [74]. Fritzmann et al. reported that BAMBI was expressed at a low level in normal colon mucosa and nonmetastatic primary tumors, and was highly expressed in the epithelial compartment of a subset of metastatic primary tumors. Forced expression of BAMBI inhibited TGF-β signaling and increased migration in colon cancer cells. In a mouse model, forced expression of BAMBI caused colon cancer cells to form tumors that metastasized more frequently to the liver and lymph nodes than control cancer cells.

Zhang et al. [75] investigated the expression of BAMBI in 276 gastric cancer tissues by immunohistochemistry. They found that BAMBI expression was significantly correlated with increased depth of invasion, lymphatic invasion, and lymph node metastasis. However, the significance of BAMBI for lymphatic metastasis of human esophageal cancer remains unknown.

3.3 Cancer Stem Cells and Metastasis

In the cancer stem cell model, tumors consist of subsets of cells with functional heterogeneity, and one small subset of cancer cells has the characteristics of stem cells. These cancer stem cells have the capability of both self-renewal and multilineage differentiation into diverse cancer cells, which play a decisive role in maintaining the capacity for malignant proliferation, invasion, metastasis, and tumor recurrence [76, 77]. Cancer stem cells play an important role not only in tumorigenicity but also in cancer metastasis [78]. CD133 is a marker of cancer stem cells or

tumor-initiating cells that can promote human colorectal cancer after being xenografted into immunodeficient mice [79]. A higher percentage of CD133-positive cancer cells is an unfavorable prognostic factor for colorectal cancer patients with locally advanced disease, and CD133-positive cancer cells contribute to tumor progression [80]. Li et al. [81] cultured CD133-positive colorectal cancer cells and analyzed the invasive and metastatic capabilities of CD133-positive single cell-derived progenies in a nude mouse model; all were tumorigenic, and the subcutaneous tumors expanded rapidly, while only one of three CD133-negative single cell progenies developed a minimal tumor in nude mice. They also found that CD133-positive single cell progenies possessed heterogeneity in intestinal wall invasion and lymph node and liver metastases, while CD133-negative single cell progenies did not produce secondary transplanted tumors or intestinal invasion and metastasis. Therefore, the ability of cancer stem cells to initiate new tumors is important for metastatic colonization. Among esophageal, gastric, and colorectal cancers, several markers for cancer stem cells have been reported (Fig. 3.2). It remains unclear which marker is the most important and specific.

3.3.1 Esophageal Cancer Stem Cells

Tang et al. [82] reported that CD90-positive cell populations in esophageal squamous cell carcinoma are endowed with stem cell-like properties and high tumorigenic and metastatic potential. In freshly resected clinical specimens, CD90-positive cells represent a rare cell population, the levels of which correlate with lymph node metastasis.

Aldehyde dehydrogenase 1 (ALDH1) is a detoxifying enzyme responsible for oxidizing a variety of intracellular aldehydes to carboxylic acids. ALDH1 is proposed as a common marker for both normal and malignant stem and progenitor cells. Its activity has been employed successfully as a stem cell marker in breast cancer [83]. Wang et al. [84] investigated the expression of ALDH1 protein in human esophageal squamous cell carcinoma tissues by immunohistochemistry. They found that ALDH1 expression was correlated with lymph node metastasis and late pathologic TNM classification staging.

3.3.2 Gastric Cancer Stem Cells

The stemness factors Sox2, Oct3/4, and Nanog are associated with induced pluripotent stem cells, suggesting a correlation between these stemness factors and cancer stem cells [85]. Matsuoka et al. analyzed the expression of Sox2, Oct3/4, and Nanog in gastric cancer by immunohistochemistry. They found a significant correlation between Sox2-positive or Oct3/4-negative expression and invasion depth, lymph node metastasis, and lymphatic invasion.

In addition to ALDH1 and CD133, CD44 can be used to isolate cancer stem cell populations in colorectal cancer [86]. CD44-positive fractions of gastric cancer could

generate spheroid colonies under non-adherent conditions, and small numbers of these cells could generate tumors in mice [87]. Wakamatsu et al. [88] immunohistochemically examined the expression and distribution of representative cancer stem cell markers ALDH1, CD44, and CD133 in primary tumors and lymph node metastases of gastric cancer. They found that CD44 and CD133 expression was associated with lymph node metastasis, and the expression pattern of cancer stem cell markers in lymph node metastases tended to be the same as that in primary tumors.

SALL4 is a member of the *SALL* gene family and acts as a zinc-finger transcription factor. Previous studies have demonstrated that SALL4 has an essential role in maintaining the self-renewal and pluripotency of embryonic stem cells [89]. Zhang et al. [90] analyzed SALL4 expression in gastric cancer. They found that SALL4 levels were highly correlated with lymph node metastasis, and forced expression of SALL4 enhanced the proliferation and migration of human gastric cancer cells.

3.3.3 Colorectal Cancer Stem Cells

Leucine-rich repeat-containing G protein-coupled receptor 5 (LGR5) is a target of Wnt signaling [91]. LGR5 is a marker for stem cells in the small intestine and colon, and plays a crucial role in the biological function of stem cells [92]. Uchida et al. [93] performed quantitative RT-PCR for *LGR5* expression in 37 colon cancer cell lines. They found that *LGR5* expression was higher in colon cancer cell lines derived from metastatic tumors compared with those from primary tumors. In clinical colorectal cancer specimens, *LGR5* expression was correlated with lymphatic invasion, vascular invasion, tumor depth, lymph node metastasis, and tumor stage.

Silinsky et al. [94] analyzed CD133-positive colorectal cancer cells by fluorescence-activated cell sorting analysis. They found that CD133-positive cancer cells correlated with the presence of lymph node metastasis in colorectal cancer.

Langan et al. [95] examined the expression of non-CD133 colorectal cancer stem cell markers including CD29, CD44, ALDH1A1, ALDH1B1, EpCAM, and CD166 in colorectal cancer tissue samples; of these, EpCAM and CD29 expression was associated with lymph node metastases.

3.4 Biomarkers for Lymph Node Metastasis

A better understanding of the changes in gene expression during invasion and metastasis may lead to new paradigms and possible improvements in the diagnosis and treatment of gastrointestinal cancer. In the past 20 years, numerous genes whose expression is upregulated or downregulated in lymph node metastasis have been reported by microarray analysis. Lymph node metastasis-associated genes identified by microarray analysis are summarized in Table 3.1. Although these genes are useful for the prediction of lymph node metastasis, their functions are largely unknown. Functional analysis of these molecules will further improve our understanding of the basic mechanisms of lymph node metastasis.

Table 3.1 Summary of genetic/epigenetic/gene expression alterations in gastric and intestinal phenotypes of gastric cancer

Cancer	Genes whose expression is upregulated in lymph node metastasis-positive cases	Genes whose expression is upregulated in lymph node metastasis-positive cases	Ref.
Esophagus	CD33, GJB1, ITGA2B, ITGAX, ITGB6, CD2, ERBB4, CSF2RB, MAD1L1, BNIP3, CD38, ARHGDIG, CYP17A1, RVNP2, CRYZ, MMP13	AR, EPHB6, INSR, TLR3, TLR6, CYP24A1, CYP2D6, PDE4A, PDE4C, DFFB, PDCD1, ATR, MDM2, BMP5, CCL1, HSPA4, RXRB, IFNA1	[96]
Esophagus	IL6, DMN, JUND, SDS, PRDX2, PELP1, D8S2298E, PCP4, NDUFA7, ACCN1, GCK, ONECUT1, GPX4, TM7SF2, MAPK8IP1, IDH2, DKFZP434D146	NUP153, DUSP1, PPIC, POT1, LIG4, KIAA1128, MYOG, IFIT4, IL1RAP, PLSCR1, TUBA1, CCNA2, HMGB2, CLCN4, TLR4, MRS2L, GNB5, IFNGR1, KNSL1, FADD, IL1B, GNS, LAMA3, PPFIA1, DAZ, KIAA0562, DDX17, ALOX5, APP, NHLH1, MRS2L, NCYM, CRLF3, ICSBP1, KIAA1128, LOC58525	[97]
Esophagus	NFIL3, SUV39H2, FLJ34941, WNT10B, RIF1, CCNT2, KCNJ14, SCAMP5, SUV39H1, MCM6, NAV2, PCGF6, B2M, EVI1, C7orf26	DUSP22, EHD3, PGS1, SLC26A2, LOC128977, DCTN2, DKFZp564C1964, SYNPO2, RABAC1, GGTL3, AIM2, CXorf40, LRP2, THUMPD1, ATOH1, HPRP8BP	[98]
Esophagus	SPP1, KRT14, TACSTD1, I_1152283, STMN1, COL7A1, COL1A1, BIRC5, H2AFZ, CKS2, CCT5, I_957781, MLF1, CKS1B, STK31, TK1, KIFC1, CTSZ, CENPF, BG1, DEFB105, MCM7, ATP1B3, NM_144668.1, MYNN, ANLN, I_960942, KPNA2, H2AV, HMG4L, SPAG5, LOC152217, LIMS1, ENAH, CDC20, MSH6, I_941570, HSPE1, NDUFB9, SNRPG, RPA3, ATR, MGC10911	MAL, C1orf10, NICE-1, SPINK5, HBB, EMP1, TGM1, SCEL, KRT13, CSTB, IL1RN, I_1110078, RUNX2, CSTA, PPL, SNTA1, CLIC3, LAGY, S100A9, ANXA1, SPRR3, I_955703, HAT, I_958335, RHCG, XRCC5, K5B, SERPINB1, SPRR1A, I_959634, MYO1A, I_966519, BCE-1, I_1002369, FLJ21511, CLCA4, PPP1R3C, LOC84518, TRAPPC1, I_1152130, I_958949, KRT4, PSCA, KIAA0790, CD24, I_928865, IBA2, FLJ20626, MECP2	[99]
Esophagus	CALB1, TFF3, KRT7, SCGB1A1, ITSN2, ADH1A, CLDN10, SETD1B, FOXA1, MAL, NEBL, GDF15, MME, CEACAM5, MUC1, CTBP1, PCP4, FCGR2A, MMP10, CD19, GZMK, BARX2, SELENBP1, RBBP8, CTSD, AQP3, CIB1, FUCA1, CAT, ITPKB, TST, NR1D1, HPCAL1, INDO, MUC1, FBXO7, ASS1	FABP4, LTBR, ENO2, NCAPD2, ZNF384, FTO, KIAA0146, TUSC3	[57]

Stomach	RBP4, OCT2, IGF2, PFN2, KIAA1093, FN1, PCOLCE, FN1	MUC4, LYZ	[100]
Stomach	MMP7, THBS2, FN1, MMP10, TGFB3, IGFBP3, SPARC, COL1A2, MMP1, PDGFRB	–	[101]
Stomach	SCAND1, RGS5, S100A11, RNPC2, APOE, FLJ10815, RNASE1, H3F3B, P24B, CLDN3, MRPL14	BCL2L2, RPLP1, ZYX, RPS17, FLJ11151, CTNND1, CYP20A1, SPC18, LOC339290, ELOVL5	[102]
Stomach	DAG, HMMR, ARL1, CRTAP, EST	–	[103]
Colon	RPS28, SFp32	KRT5, CST4, SAA1	[107]
Colon	RBP1, RPS4Y1, B2M, SERPINA1, PCK1, LRRFIP1, ANXA3, COPS5, TFF3, HIST1H2AE, COL17A1, HRASLS3, BAMBI, RPS12, LSR, SSBP1, APLP2, HSP90B1, NME1, NFIL3, HNRNPA2B1, CFB, RABGGTB, UQCRB, FBL, BTF3, DNAJA1, HNRPM, SUB1, CKS2, HSP90AB1, CD47, ERP29, MDK, EMG1, HERPUD1, GSTP1, DNAJC9, SULT1A3, CCT3, ABP1, TXNDC13, NME1, UBE2E3, TXN, INSIG1, FBL, KANK1, HNRPA3, NACA, TARS, FTH1, PDZK1IP1, PRSS23, COX4I1, STK3, YIPF3, MGST3, RPL31, RPS15A, BSG, SLC25A13, NDUFA1, PPL, BOP1, RPS5, ALDH9A1, COX6C, POLR2H, COX6B1, SLC7A7, LAMB3, HNRNPC, AHNAK2, NDUFS2, MRPL12, RPS12, CALCOCO2, NACA, MSH2, TAF7, SMPD4, PSMD13, C6orf108	SLC25A17, POLD2, RUNX1, BRD3, CRKL, CYB5B, JUND, CASP6, MNT, XRCC5, ATXN2, C5orf21, KLF7, CYP2A13, DKFZP564O0823, RUNX1, FRYL, LAGE3, TMCC1, OGT, ENTPD6, TMEM97, AMOTL2, FOXO3, MYCBP2, CAMTA2, SELENBP1, SAT1, ELISC-1, DDX3X, PTPRD, MGAT5, MAOA	[72]

3.4.1 Esophageal Cancer

Tamoto et al. [96] measured gene expression in 36 esophageal squamous cell carcinoma cases by microarray. They identified 44 genes (including *CD33*, *GJB1*, *ITGA2B*, and *ITGB6*) whose expression was associated with lymph node metastasis. Likewise, Kan et al. [97] analyzed the gene expression profile of 28 esophageal squamous cell carcinoma cases by microarray and found genes whose expression was upregulated in lymph node metastasis-positive cases (including *IL6*, *DMN*, and *JUND*) and genes whose expression is downregulated in lymph node metastasis-positive cases (including *NUP153*, *DUSP1*, and *POT1*). Yamabuki et al. [98] also analyzed the gene expression profile of 19 esophageal squamous cell carcinoma cases by microarray. They found genes whose expression was upregulated in lymph node metastasis-positive cases (including *NFIL3*, *SUV39H2*, and *WNT10B*) and genes whose expression was downregulated in lymph node metastasis-positive cases (including *DUSP22*, *EHD3*, and *PGS1*). Similarly, Uchikado et al. [99] analyzed gene expression in 16 patients with esophageal squamous cell carcinoma using oligomicroarray. They found overexpressed genes correlated with lymph node metastasis (including *SPP1*, *KRT14*, and *TACSTD1*) and suppressed genes correlated with lymph node metastasis (including *MAL*, *SPINK5*, and *HBB*). Sano et al. [57] compared the gene expression profiles of 24 esophageal squamous cell carcinomas with extensive lymph node metastasis and 11 esophageal squamous cell carcinomas with no metastatic lymph nodes. They found overexpression of *CALB1*, *KRT7*, *MUC1,* and *CEACAM5* in cases with metastatic lymph nodes.

3.4.2 Gastric Cancer

Hippo et al. [100] reported that overexpression of *RBP4*, *OCT2*, *IGF2*, *PFN2*, *KIAA1093*, *PCOLCE*, and *FN1* is associated with lymph node metastasis by microarray. Inoue et al. [101] found several genes that were differentially expressed with a significant difference between the two groups with respect to the depth of tumor invasion and lymph node metastasis by cDNA microarray. Upregulation of *MMP7*, *THBS2*, *FN1*, *MMP10*, *TGFB3*, *IGFBP3*, *SPARC*, *COL1A2*, *MMP1*, and *PDGFRB* were associated with lymph node metastasis. Oue et al. [102] performed serial analysis of gene expression (SAGE) on five gastric cancer samples, and reported that upregulation of *FUS* and *APOE* was associated with lymph node metastasis. Marchet A et al. [103] evaluated the gene expression profile in 32 gastric cancer cases. They reported that only three genes (*BIK*, *AURKB*, and *EIF5A2*) could correctly predict lymph node status. Mimori K et al. [104] performed microarray analysis of total RNA from whole bone marrow blood from six cases with metastasis and three cases without metastasis in human gastric cancer. They found that *MT1-MMP*-positive expression in peripheral blood was associated with the incidence of lymph node metastasis. Ueda T et al. [105] analyzed microRNA expression in human gastric cancer. They found 17 microRNAs whose expression was associated with lymph node metastasis. Yamashita et al. [106] examined 242 gastric cancer

patients without or with lymph node metastasis by lectin microarray and found that vicia villosa agglutinin was linked to lymph node metastasis.

3.4.3 Colorectal Cancer

Parle-McDermott et al. [107] performed SAGE on a primary colon cancer cell line (SW480) and an isogenic lymph node metastasis cell line (SW620) and found genes whose expression was upregulated in lymph node metastasis-positive cases (including *KRT5*, *CST4*, and *SAA1*) and genes whose expression was downregulated in lymph node metastasis-positive cases (including *RPS28* and *SFP32*). Bertucci et al. [108] profiled 50 colon cancer tissues using DNA microarray and identified 46 genes as significantly differentially expressed between cancers with and without lymph node metastases. Kwon et al. [109] performed microarray analysis in 12 colorectal cancer cases and found 60 genes possibly associated with lymph node metastasis. Fritzmann et al. [72] compared gene expression patterns between metastatic and nonmetastatic stage-matched human colorectal cancers by microarray analysis. They established a signature of 115 genes that differentiated metastatic from nonmetastatic primary tumors. Among them, *BAMBI* was highly expressed in approximately half of metastatic primary tumors and metastases but not in nonmetastatic tumors. Watanabe et al. [110] analyzed the gene expression profile of 89 colorectal cancer cases. They identified 73 genes whose expression significantly differed between patients with and without lymph node metastasis (including *WSX1*, *GUCY2C*, and *DISPA*).

3.5 Anti-lymphangiogenic Therapies for Gastrointestinal Cancer

Although the efficacy of anti-angiogenic therapy has been extensively studied, the concept of targeting lymphangiogenesis to obtain a therapeutic advantage in cancer is only a recent development. The lymphatic network plays an important role in cancer metastasis, allowing spread to draining lymph nodes. Thus, targeting the induction of tumor lymphangiogenesis and functional alteration of existing lymphatic vessels may help to prevent a route for lymphatic metastasis.

In mice experiments, a neutralizing antibody to VEGFR3 was shown to completely block tumor lymphangiogenesis with no effect on pre-existing vessels [111]. Soluble VEGFR3 fusion proteins as well as monoclonal antibodies targeted to VEGF-C and VEGF-D have been developed, and several preclinical and clinical trials using these agents are currently in progress. Multikinase inhibitors that target VEGFR3 have already been developed and used for the treatment of some solid tumors.

Ang/Tie-2 signaling is another promising target for anti-lymphangiogenesis therapy, and a selective neutralizing antibody against Ang1/2 has been developed. The multikinase inhibitor regorafenib inhibits multiple membrane-bound and intracellular kinases involved in lymphangiogenesis (VEGFR1, 2, and 3, Tie-2), and is used

for the treatment of patients with metastatic colorectal cancer. Takigawa et al. [112] reported that single treatment with regorafenib inhibited tumor growth and metastasis by inhibiting both tumor cells and stromal response in an orthotopic implanted mouse model of colon cancer. Because VEGF-C and PDGF-B expressed by tumor cells are associated with lymphangiogenesis and lymphatic metastasis in gastric cancer, blockage of these factors by regorafenib may be a reasonable approach to the prevention and treatment of lymphatic metastasis. Interestingly, Onoyama et al. [113] examined the effects of PDGFR tyrosine kinase inhibitor (nilotinib) and mTOR inhibitor (everolimus) on tumor stroma in an orthotopic nude mouse model of human gastric cancer. They found that treatment with nilotinib did not suppress tumor growth but significantly decreased stromal reactivity, lymphatic invasion, and lymphatic vessel area. In contrast, treatment with everolimus decreased tumor growth and microvessel density but not stromal reactivity. Nilotinib and everolimus in combination reduced both the growth rate and stromal reaction. These results suggest that targeted molecule-based inhibition of cancer–stromal cell interactions appears promising as an effective antitumor therapy. Further understanding of the cellular and molecular mechanisms that regulate lymphangiogenesis of tumors may facilitate the development of effective anti-lymphangiogenic therapies.

3.6 Conclusion

In this chapter, the cellular and molecular mechanisms of lymph node metastasis in human esophageal, gastric, and colorectal cancers were described. In the multistep development of lymph node metastasis, the most important process is lymphangiogenesis. VEGF-C and PDGF-B expressed by tumor cells plays crucial roles in lymphangiogenesis and lymphatic metastasis. Thus, blockage of the factors inducing lymphangiogenesis could be a reasonable approach to the prevention and treatment of lymphatic metastasis. Interference with the growth of lymphatic endothelial cells via several different signaling pathways should enhance the efficacy of anti-metastatic treatments. In addition to lymphangiogenesis, it is well accepted that cancer stem cells play a significant role in metastasis. A possible therapeutic strategy for eliminating cancer stem cells is to specifically target the signaling pathways and transcription factors that are involved in cancer stem cell maintenance and proliferation. The Wnt, Notch, Hedgehog, and Bmi-1 signaling pathways regulate cancer stem cells. Further understanding of the cellular and molecular mechanisms that regulate lymphangiogenesis and cancer stem cell maintenance and proliferation will facilitate the development of effective anti-metastatic therapies.

References

1. Kumar R, Eue I, Dong Z, Killion JJ, Fidler IJ. Expression of inflammatory cytokines by murine macrophages activated with a new synthetic lipopeptide JT3002. Cancer Biother Radiopharm. 1997;12:333–40.
2. Sundar SS, Ganesan TS. Role of lymphangiogenesis in cancer. J Clin Oncol. 2007;25:4298–307.

3. Beasley NJ, Prevo R, Banerji S, Leek RD, Moore J, van Trappen P, et al. Intratumoral lymphangiogenesis and lymph node metastasis in head and neck cancer. Cancer Res. 2002;62:1315–20.
4. Nakayama Y, Matsumoto K, Nagato M, Inoue Y, Katsuki T, Minagawa N, et al. Significance of lymphangiogenesis as assessed by immunohistochemistry for podoplanin in patients with esophageal carcinoma. Anticancer Res. 2007;27:619–25.
5. Yonemura Y, Endo Y, Fujita H, Fushida S, Ninomiya I, Bandou E, et al. Role of vascular endothelial growth factor C expression in the development of lymph node metastasis in gastric cancer. Clin Cancer Res. 1999;5:1823–9.
6. Amioka T, Kitadai Y, Tanaka S, Haruma K, Yoshihara M, Yasui W, et al. Vascular endothelial growth factor-C expression predicts lymph node metastasis of human gastric carcinomas invading the submucosa. Eur J Cancer. 2002;38:1413–9.
7. Parr C, Jiang WG. Quantitative analysis of lymphangiogenic markers in human colorectal cancer. Int J Oncol. 2003;23:533–9.
8. Kitadai Y. Angiogenesis and lymphangiogenesis of gastric cancer. J Oncol. 2010;2010:468725.
9. Stacker SA, Achen MG, Jussila L, Baldwin ME, Alitalo K. Lymphangiogenesis and cancer metastasis. Nat Rev Cancer. 2002;2:573–83.
10. He Y, Rajantie I, Pajusola K, Jeltsch M, Holopainen T, Yla-Herttuala S, et al. Vascular endothelial cell growth factor receptor 3-mediated activation of lymphatic endothelium is crucial for tumor cell entry and spread via lymphatic vessels. Cancer Res. 2005;65:4739–46.
11. Karkkainen MJ, Haiko P, Sainio K, Partanen J, Taipale J, Petrova TV, et al. Vascular endothelial growth factor C is required for sprouting of the first lymphatic vessels from embryonic veins. Nat Immunol. 2004;5:74–80.
12. Skobe M, Hawighorst T, Jackson DG, Prevo R, Janes L, Velasco P, et al. Induction of tumor lymphangiogenesis by VEGF-C promotes breast cancer metastasis. Nat Med. 2001;7:192–8.
13. Kitadai Y, Amioka T, Haruma K, Tanaka S, Yoshihara M, Sumii K, et al. Clinicopathological significance of vascular endothelial growth factor (VEGF)-C in human esophageal squamous cell carcinomas. Int J Cancer. 2001;93:662–6.
14. Matsumoto M, Natsugoe S, Okumura H, Arima H, Yanagita S, Uchikado Y, et al. Overexpression of vascular endothelial growth factor-C correlates with lymph node micrometastasis in submucosal esophageal cancer. J Gastrointest Surg. 2006;10:1016–22.
15. Onogawa S, Kitadai Y, Tanaka S, Kuwai T, Kimura S, Chayama K. Expression of VEGF-C and VEGF-D at the invasive edge correlates with lymph node metastasis and prognosis of patients with colorectal carcinoma. Cancer Sci. 2004;95:32–9.
16. Hachisuka T, Narikiyo M, Yamada Y, Ishikawa H, Ueno M, Uchida H, et al. High lymphatic vessel density correlates with overexpression of VEGF-C in gastric cancer. Oncol Rep. 2005;13:733–7.
17. Li X, Liu B, Xiao J, Yuan Y, Ma J, Zhang Y. Roles of VEGF-C and Smad4 in the lymphangiogenesis, lymphatic metastasis, and prognosis in colon cancer. J Gastrointest Surg. 2011;15:2001–10.
18. Matsumura S, Oue N, Mitani Y, Kitadai Y, Yasui W. DNA demethylation of vascular endothelial growth factor-C is associated with gene expression and its possible involvement of lymphangiogenesis in gastric cancer. Int J Cancer. 2007;120:1689–95.
19. Stacker SA, Caesar C, Baldwin ME, Thornton GE, Williams RA, Prevo R, et al. VEGF-D promotes the metastatic spread of tumor cells via the lymphatics. Nat Med. 2001;7:186–91.
20. Baldwin ME, Catimel B, Nice EC, Roufail S, Hall NE, Stenvers KL, et al. The specificity of receptor binding by vascular endothelial growth factor-d is different in mouse and man. J Biol Chem. 2001;276:19166–71.
21. Karnezis T, Shayan R, Caesar C, Roufail S, Harris NC, Ardipradja K, et al. VEGF-D promotes tumor metastasis by regulating prostaglandins produced by the collecting lymphatic endothelium. Cancer Cell. 2012;21:181–95.
22. Kozlowski M, Naumnik W, Niklinski J, Milewski R, Dziegielewski P, Laudanski J. Vascular endothelial growth factor C and D expression correlates with lymph node metastasis and poor prognosis in patients with resected esophageal cancer. Neoplasma. 2011;58:311–9.
23. Onogawa S, Kitadai Y, Amioka T, Kodama M, Cho S, Kuroda T, et al. Expression of vascular endothelial growth factor (VEGF)-C and VEGF-D in early gastric carcinoma: correlation with clinicopathological parameters. Cancer Lett. 2005;226:85–90.

24. Arigami T, Natsugoe S, Uenosono Y, Yanagita S, Ehi K, Arima H, et al. Vascular endothelial growth factor-C and -D expression correlates with lymph node micrometastasis in pN0 early gastric cancer. J Surg Oncol. 2009;99:148–53.
25. Wang XL, Fang JP, Tang RY, Chen XM. Different significance between intratumoral and peritumoral lymphatic vessel density in gastric cancer: a retrospective study of 123 cases. BMC Cancer. 2010;10:299.
26. Su F, Li X, You K, Chen M, Xiao J, Zhang Y, et al. Expression of VEGF-D, SMAD4, and SMAD7 and their relationship with lymphangiogenesis and prognosis in colon cancer. J Gastrointest Surg. 2016;20:2074–82.
27. Kaipainen A, Korhonen J, Mustonen T, van Hinsbergh VW, Fang GH, Dumont D, et al. Expression of the fms-like tyrosine kinase 4 gene becomes restricted to lymphatic endothelium during development. Proc Natl Acad Sci U S A. 1995;92:3566–70.
28. Makinen T, Veikkola T, Mustjoki S, Karpanen T, Catimel B, Nice EC, et al. Isolated lymphatic endothelial cells transduce growth, survival and migratory signals via the VEGF-C/D receptor VEGFR-3. EMBO J. 2001;20:4762–73.
29. Valtola R, Salven P, Heikkila P, Taipale J, Joensuu H, Rehn M, et al. VEGFR-3 and its ligand VEGF-C are associated with angiogenesis in breast cancer. Am J Pathol. 1999;154:1381–90.
30. Su JL, Yang PC, Shih JY, Yang CY, Wei LH, Hsieh CY, et al. The VEGF-C/Flt-4 axis promotes invasion and metastasis of cancer cells. Cancer Cell. 2006;9:209–23.
31. Kodama M, Kitadai Y, Tanaka M, Kuwai T, Tanaka S, Oue N, et al. Vascular endothelial growth factor C stimulates progression of human gastric cancer via both autocrine and paracrine mechanisms. Clin Cancer Res. 2008;14:7205–14.
32. Tanaka M, Kitadai Y, Kodama M, Shinagawa K, Sumida T, Tanaka S, et al. Potential role for vascular endothelial growth factor-D as an autocrine factor for human gastric carcinoma cells. Cancer Sci. 2010;101:2121–7.
33. Pietras K, Sjoblom T, Rubin K, Heldin CH, Ostman A. PDGF receptors as cancer drug targets. Cancer Cell. 2003;3:439–43.
34. Heldin CH, Eriksson U, Ostman A. New members of the platelet-derived growth factor family of mitogens. Arch Biochem Biophys. 2002;398:284–90.
35. Uehara H, Kim SJ, Karashima T, Shepherd DL, Fan D, Tsan R, et al. Effects of blocking platelet-derived growth factor-receptor signaling in a mouse model of experimental prostate cancer bone metastases. J Natl Cancer Inst. 2003;95:458–70.
36. Cao R, Bjorndahl MA, Religa P, Clasper S, Garvin S, Galter D, et al. PDGF-BB induces intratumoral lymphangiogenesis and promotes lymphatic metastasis. Cancer Cell. 2004;6:333–45.
37. Matsumoto S, Yamada Y, Narikiyo M, Ueno M, Tamaki H, Miki K, et al. Prognostic significance of platelet-derived growth factor-BB expression in human esophageal squamous cell carcinomas. Anticancer Res. 2007;27:2409–14.
38. Kodama M, Kitadai Y, Sumida T, Ohnishi M, Ohara E, Tanaka M, et al. Expression of platelet-derived growth factor (PDGF)-B and PDGF-receptor beta is associated with lymphatic metastasis in human gastric carcinoma. Cancer Sci. 2010;101:1984–9.
39. Davis S, Aldrich TH, Jones PF, Acheson A, Compton DL, Jain V, et al. Isolation of angiopoietin-1, a ligand for the TIE2 receptor, by secretion-trap expression cloning. Cell. 1996;87:1161–9.
40. Gale NW, Thurston G, Hackett SF, Renard R, Wang Q, McClain J, et al. Angiopoietin-2 is required for postnatal angiogenesis and lymphatic patterning, and only the latter role is rescued by Angiopoietin-1. Dev Cell. 2002;3:411–23.
41. Jo MJ, Lee JH, Nam BH, Kook MC, Ryu KW, Choi IJ, et al. Preoperative serum angiopoietin-2 levels correlate with lymph node status in patients with early gastric cancer. Ann Surg Oncol. 2009;16:2052–7.
42. Wang J, Wu K, Zhang D, Tang H, Xie H, Hong L, et al. Expressions and clinical significances of angiopoietin-1, -2 and Tie2 in human gastric cancer. Biochem Biophys Res Commun. 2005;337:386–93.
43. Chen H, Chedotal A, He Z, Goodman CS, Tessier-Lavigne M. Neuropilin-2, a novel member of the neuropilin family, is a high affinity receptor for the semaphorins Sema E and Sema IV but not Sema III. Neuron. 1997;19:547–59.

44. Favier B, Alam A, Barron P, Bonnin J, Laboudie P, Fons P, et al. Neuropilin-2 interacts with VEGFR-2 and VEGFR-3 and promotes human endothelial cell survival and migration. Blood. 2006;108:1243–50.
45. Yuan L, Moyon D, Pardanaud L, Breant C, Karkkainen MJ, Alitalo K, et al. Abnormal lymphatic vessel development in neuropilin 2 mutant mice. Development. 2002;129:4797–806.
46. Caunt M, Mak J, Liang WC, Stawicki S, Pan Q, Tong RK, et al. Blocking neuropilin-2 function inhibits tumor cell metastasis. Cancer Cell. 2008;13:331–42.
47. Fung TM, Ng KY, Tong M, Chen JN, Chai S, Chan KT, et al. Neuropilin-2 promotes tumourigenicity and metastasis in oesophageal squamous cell carcinoma through ERK-MAPK-ETV4-MMP-E-cadherin deregulation. J Pathol. 2016;239:309–19.
48. Huntzinger E, Izaurralde E. Gene silencing by microRNAs: contributions of translational repression and mRNA decay. Nat Rev Genet. 2011;12:99–110.
49. Yang B, Jing C, Wang J, Guo X, Chen Y, Xu R, et al. Identification of microRNAs associated with lymphangiogenesis in human gastric cancer. Clin Transl Oncol. 2014;16:374–9.
50. Hu J, Cheng Y, Li Y, Jin Z, Pan Y, Liu G, et al. microRNA-128 plays a critical role in human non-small cell lung cancer tumourigenesis, angiogenesis and lymphangiogenesis by directly targeting vascular endothelial growth factor-C. Eur J Cancer. 2014;50:2336–50.
51. Liu C, Li M, Hu Y, Shi N, Yu H, Liu H, et al. miR-486-5p attenuates tumor growth and lymphangiogenesis by targeting neuropilin-2 in colorectal carcinoma. Onco Targets Ther. 2016;9:2865–71.
52. Chang LK, Garcia-Cardena G, Farnebo F, Fannon M, Chen EJ, Butterfield C, et al. Dose-dependent response of FGF-2 for lymphangiogenesis. Proc Natl Acad Sci U S A. 2004;101:11658–63.
53. Mikami S, Ohashi K, Katsube K, Nemoto T, Nakajima M, Okada Y. Coexpression of heparanase, basic fibroblast growth factor and vascular endothelial growth factor in human esophageal carcinomas. Pathol Int. 2004;54:556–63.
54. Ueki T, Koji T, Tamiya S, Nakane PK, Tsuneyoshi M. Expression of basic fibroblast growth factor and fibroblast growth factor receptor in advanced gastric carcinoma. J Pathol. 1995;177:353–61.
55. Cao R, Bjorndahl MA, Gallego MI, Chen S, Religa P, Hansen AJ, et al. Hepatocyte growth factor is a lymphangiogenic factor with an indirect mechanism of action. Blood. 2006;107:3531–6.
56. Kammula US, Kuntz EJ, Francone TD, Zeng Z, Shia J, Landmann RG, et al. Molecular co-expression of the c-Met oncogene and hepatocyte growth factor in primary colon cancer predicts tumor stage and clinical outcome. Cancer Lett. 2007;248:219–28.
57. Sano M, Aoyagi K, Takahashi H, Kawamura T, Mabuchi T, Igaki H, et al. Forkhead box A1 transcriptional pathway in KRT7-expressing esophageal squamous cell carcinomas with extensive lymph node metastasis. Int J Oncol. 2010;36:321–30.
58. Jozwik KM, Carroll JS. Pioneer factors in hormone-dependent cancers. Nat Rev Cancer. 2012;12:381–5.
59. Moll R, Divo M, Langbein L. The human keratins: biology and pathology. Histochem Cell Biol. 2008;129:705–33.
60. Yamada A, Sasaki H, Aoyagi K, Sano M, Fujii S, Daiko H, et al. Expression of cytokeratin 7 predicts survival in stage I/IIA/IIB squamous cell carcinoma of the esophagus. Oncol Rep. 2008;20:1021–7.
61. Oue N, Noguchi T, Anami K, Kitano S, Sakamoto N, Sentani K, et al. Cytokeratin 7 is a predictive marker for survival in patients with esophageal squamous cell carcinoma. Ann Surg Oncol. 2012;19:1902–10.
62. Payne SL, Hendrix MJ, Kirschmann DA. Paradoxical roles for lysyl oxidases in cancer--a prospect. J Cell Biochem. 2007;101:1338–54.
63. Csiszar K. Lysyl oxidases: a novel multifunctional amine oxidase family. Prog Nucleic Acid Res Mol Biol. 2001;70:1–32.
64. Barker HE, Chang J, Cox TR, Lang G, Bird D, Nicolau M, et al. LOXL2-mediated matrix remodeling in metastasis and mammary gland involution. Cancer Res. 2011;71:1561–72.

65. Park JS, Lee JH, Lee YS, Kim JK, Dong SM, Yoon DS. Emerging role of LOXL2 in the promotion of pancreas cancer metastasis. Oncotarget. 2016;7:42539–52.
66. Ren H, Zhang P, Tang Y, Wu M, Zhang W. Forkhead box protein A1 is a prognostic predictor and promotes tumor growth of gastric cancer. Onco Targets Ther. 2015;8:3029–39.
67. Weeraratna AT, Jiang Y, Hostetter G, Rosenblatt K, Duray P, Bittner M, et al. Wnt5a signaling directly affects cell motility and invasion of metastatic melanoma. Cancer Cell. 2002;1:279–88.
68. Kurayoshi M, Oue N, Yamamoto H, Kishida M, Inoue A, Asahara T, et al. Expression of Wnt-5a is correlated with aggressiveness of gastric cancer by stimulating cell migration and invasion. Cancer Res. 2006;66:10439–48.
69. Yamamoto H, Kitadai Y, Yamamoto H, Oue N, Ohdan H, Yasui W, et al. Laminin gamma2 mediates Wnt5a-induced invasion of gastric cancer cells. Gastroenterology. 2009;137:242–52. 52 e1–6
70. Li Q, Chen H. Silencing of Wnt5a during colon cancer metastasis involves histone modifications. Epigenetics. 2012;7:551–8.
71. Dejmek J, Dejmek A, Safholm A, Sjolander A, Andersson T. Wnt-5a protein expression in primary dukes B colon cancers identifies a subgroup of patients with good prognosis. Cancer Res. 2005;65:9142–6.
72. Fritzmann J, Morkel M, Besser D, Budczies J, Kosel F, Brembeck FH, et al. A colorectal cancer expression profile that includes transforming growth factor beta inhibitor BAMBI predicts metastatic potential. Gastroenterology. 2009;137:165–75.
73. Onichtchouk D, Chen YG, Dosch R, Gawantka V, Delius H, Massague J, et al. Silencing of TGF-beta signalling by the pseudoreceptor BAMBI. Nature. 1999;401:480–5.
74. Sekiya T, Adachi S, Kohu K, Yamada T, Higuchi O, Furukawa Y, et al. Identification of BMP and activin membrane-bound inhibitor (BAMBI), an inhibitor of transforming growth factor-beta signaling, as a target of the beta-catenin pathway in colorectal tumor cells. J Biol Chem. 2004;279:6840–6.
75. Zhang Y, Yu Z, Xiao Q, Sun X, Zhu Z, Zhang J, et al. Expression of BAMBI and its combination with Smad7 correlates with tumor invasion and poor prognosis in gastric cancer. Tumour Biol. 2014;35:7047–56.
76. Clarke MF, Fuller M. Stem cells and cancer: two faces of eve. Cell. 2006;124:1111–5.
77. Visvader JE, Lindeman GJ. Cancer stem cells in solid tumours: accumulating evidence and unresolved questions. Nat Rev Cancer. 2008;8:755–68.
78. Brabletz T, Jung A, Spaderna S, Hlubek F, Kirchner T. Opinion: migrating cancer stem cells – an integrated concept of malignant tumour progression. Nat Rev Cancer. 2005;5:744–9.
79. O'Brien CA, Pollett A, Gallinger S, Dick JE. A human colon cancer cell capable of initiating tumour growth in immunodeficient mice. Nature. 2007;445:106–10.
80. Li CY, Li BX, Liang Y, Peng RQ, Ding Y, Xu DZ, et al. Higher percentage of CD133+ cells is associated with poor prognosis in colon carcinoma patients with stage IIIB. J Transl Med. 2009;7:56.
81. Li G, Liu C, Yuan J, Xiao X, Tang N, Hao J, et al. CD133(+) single cell-derived progenies of colorectal cancer cell line SW480 with different invasive and metastatic potential. Clin Exp Metastasis. 2010;27:517–27.
82. Tang KH, Dai YD, Tong M, Chan YP, Kwan PS, Fu L, et al. A CD90(+) tumor-initiating cell population with an aggressive signature and metastatic capacity in esophageal cancer. Cancer Res. 2013;73:2322–32.
83. Ginestier C, Hur MH, Charafe-Jauffret E, Monville F, Dutcher J, Brown M, et al. ALDH1 is a marker of normal and malignant human mammary stem cells and a predictor of poor clinical outcome. Cell Stem Cell. 2007;1:555–67.
84. Wang Y, Zhe H, Gao P, Zhang N, Li G, Qin J. Cancer stem cell marker ALDH1 expression is associated with lymph node metastasis and poor survival in esophageal squamous cell carcinoma: a study from high incidence area of northern China. Dis Esophagus. 2012;25:560–5.
85. Takahashi K, Tanabe K, Ohnuki M, Narita M, Ichisaka T, Tomoda K, et al. Induction of pluripotent stem cells from adult human fibroblasts by defined factors. Cell. 2007;131:861–72.
86. Dalerba P, Dylla SJ, Park IK, Liu R, Wang X, Cho RW, et al. Phenotypic characterization of human colorectal cancer stem cells. Proc Natl Acad Sci U S A. 2007;104:10158–63.

87. Takaishi S, Okumura T, Tu S, Wang SS, Shibata W, Vigneshwaran R, et al. Identification of gastric cancer stem cells using the cell surface marker CD44. Stem Cells. 2009;27: 1006–20.
88. Wakamatsu Y, Sakamoto N, Oo HZ, Naito Y, Uraoka N, Anami K, et al. Expression of cancer stem cell markers ALDH1, CD44 and CD133 in primary tumor and lymph node metastasis of gastric cancer. Pathol Int. 2012;62:112–9.
89. Zhang J, Tam WL, Tong GQ, Wu Q, Chan HY, Soh BS, et al. Sall4 modulates embryonic stem cell pluripotency and early embryonic development by the transcriptional regulation of Pou5f1. Nat Cell Biol. 2006;8:1114–23.
90. Zhang L, Xu Z, Xu X, Zhang B, Wu H, Wang M, et al. SALL4, a novel marker for human gastric carcinogenesis and metastasis. Oncogene. 2014;33:5491–500.
91. Yamamoto Y, Sakamoto M, Fujii G, Tsuiji H, Kenetaka K, Asaka M, et al. Overexpression of orphan G-protein-coupled receptor, Gpr49, in human hepatocellular carcinomas with beta-catenin mutations. Hepatology. 2003;37:528–33.
92. Barker N, van Es JH, Kuipers J, Kujala P, van den Born M, Cozijnsen M, et al. Identification of stem cells in small intestine and colon by marker gene Lgr5. Nature. 2007;449:1003–7.
93. Uchida H, Yamazaki K, Fukuma M, Yamada T, Hayashida T, Hasegawa H, et al. Overexpression of leucine-rich repeat-containing G protein-coupled receptor 5 in colorectal cancer. Cancer Sci. 2010;101:1731–7.
94. Silinsky J, Grimes C, Driscoll T, Green H, Cordova J, Davis NK, et al. CD 133+ and CXCR4+ colon cancer cells as a marker for lymph node metastasis. J Surg Res. 2013;185:113–8.
95. Langan RC, Mullinax JE, Ray S, Raiji MT, Schaub N, Xin HW, et al. A pilot study assessing the potential role of non-CD133 colorectal cancer stem cells as biomarkers. J Cancer. 2012;3:231–40.
96. Tamoto E, Tada M, Murakawa K, Takada M, Shindo G, Teramoto K, et al. Gene-expression profile changes correlated with tumor progression and lymph node metastasis in esophageal cancer. Clin Cancer Res. 2004;10:3629–38.
97. Kan T, Shimada Y, Sato F, Ito T, Kondo K, Watanabe G, et al. Prediction of lymph node metastasis with use of artificial neural networks based on gene expression profiles in esophageal squamous cell carcinoma. Ann Surg Oncol. 2004;11:1070–8.
98. Yamabuki T, Daigo Y, Kato T, Hayama S, Tsunoda T, Miyamoto M, et al. Genome-wide gene expression profile analysis of esophageal squamous cell carcinomas. Int J Oncol. 2006;28:1375–84.
99. Uchikado Y, Inoue H, Haraguchi N, Mimori K, Natsugoe S, Okumura H, et al. Gene expression profiling of lymph node metastasis by oligomicroarray analysis using laser microdissection in esophageal squamous cell carcinoma. Int J Oncol. 2006;29:1337–47.
100. Hippo Y, Taniguchi H, Tsutsumi S, Machida N, Chong JM, Fukayama M, et al. Global gene expression analysis of gastric cancer by oligonucleotide microarrays. Cancer Res. 2002;62:233–40.
101. Inoue H, Matsuyama A, Mimori K, Ueo H, Mori M. Prognostic score of gastric cancer determined by cDNA microarray. Clin Cancer Res. 2002;8:3475–9.
102. Oue N, Hamai Y, Mitani Y, Matsumura S, Oshimo Y, Aung PP, et al. Gene expression profile of gastric carcinoma: identification of genes and tags potentially involved in invasion, metastasis, and carcinogenesis by serial analysis of gene expression. Cancer Res. 2004;64: 2397–405.
103. Marchet A, Mocellin S, Belluco C, Ambrosi A, DeMarchi F, Mammano E, et al. Gene expression profile of primary gastric cancer: towards the prediction of lymph node status. Ann Surg Oncol. 2007;14:1058–64.
104. Mimori K, Fukagawa T, Kosaka Y, Ishikawa K, Iwatsuki M, Yokobori T, et al. A large-scale study of MT1-MMP as a marker for isolated tumor cells in peripheral blood and bone marrow in gastric cancer cases. Ann Surg Oncol. 2008;15:2934–42.
105. Ueda T, Volinia S, Okumura H, Shimizu M, Taccioli C, Rossi S, et al. Relation between microRNA expression and progression and prognosis of gastric cancer: a microRNA expression analysis. Lancet Oncol. 2010;11:136–46.

106. Yamashita K, Kuno A, Matsuda A, Ikehata Y, Katada N, Hirabayashi J, et al. Lectin microarray technology identifies specific lectins related to lymph node metastasis of advanced gastric cancer. Gastric Cancer. 2016;19:531–42.
107. Parle-McDermott A, McWilliam P, Tighe O, Dunican D, Croke DT. Serial analysis of gene expression identifies putative metastasis-associated transcripts in colon tumour cell lines. Br J Cancer. 2000;83:725–8.
108. Bertucci F, Salas S, Eysteries S, Nasser V, Finetti P, Ginestier C, et al. Gene expression profiling of colon cancer by DNA microarrays and correlation with histoclinical parameters. Oncogene. 2004;23:1377–91.
109. Kwon HC, Kim SH, Roh MS, Kim JS, Lee HS, Choi HJ, et al. Gene expression profiling in lymph node-positive and lymph node-negative colorectal cancer. Dis Colon Rectum. 2004;47:141–52.
110. Watanabe T, Kobunai T, Tanaka T, Ishihara S, Matsuda K, Nagawa H. Gene expression signature and the prediction of lymph node metastasis in colorectal cancer by DNA microarray. Dis Colon Rectum. 2009;52:1941–8.
111. Pytowski B, Goldman J, Persaud K, Wu Y, Witte L, Hicklin DJ, et al. Complete and specific inhibition of adult lymphatic regeneration by a novel VEGFR-3 neutralizing antibody. J Natl Cancer Inst. 2005;97:14–21.
112. Takigawa H, Kitadai Y, Shinagawa K, Yuge R, Higashi Y, Tanaka S, et al. Multikinase inhibitor regorafenib inhibits the growth and metastasis of colon cancer with abundant stroma. Cancer Sci. 2016;107:601–8.
113. Onoyama M, Kitadai Y, Tanaka Y, Yuge R, Shinagawa K, Tanaka S, et al. Combining molecular targeted drugs to inhibit both cancer cells and activated stromal cells in gastric cancer. Neoplasia. 2013;15:1391–9.

Part I

Basic Science of the Lymphatic System

Immunology of a Lymph Node

4

Ryota Hokari and Soichiro Miura

Abstract

Lymph nodes are the organs where an acquired immune response takes place rapidly (after infection) under the influence of antigen-presenting cells such as dendritic cells. Because the chance to encounter foreign antigens for each lymphocyte is quite small, lymphocytes keep moving through the whole body until they encounter a matching antigen-presenting cell. Antigens and dendritic cells enter the lymph node through afferent lymphatic vessels and migrate deep into lymph nodes to activate T lymphocytes. Naïve lymphocytes enter lymph nodes from blood through high endothelial venules (HEVs): specialized blood vessels found in secondary lymphoid tissues except for the spleen. Within lymph nodes, stromal cells interact closely with lymphocytes and dendritic cells, providing scaffolds on which these cells migrate. More recently, stromal cells were found to induce tolerance. This review summarizes the present understanding of the mechanisms regulating the movement of lymphocytes and antigen-presenting cells through the lymph node. In addition, lymph nodes are necessary for the induction of tolerance against harmless antigens. The fundamental understanding of how the lymphatic system participates in immune regulation is necessary for elucidation of the lymphatic function in various diseases.

Keywords

High endothelial venules · Tolerance · Antigen-presenting cells

R. Hokari (✉)
Department of Internal Medicine, National Defense Medical College, Tokorozawa, Japan
e-mail: ryota@ndmc.ac.jp

S. Miura
International University of Health and Welfare Graduate School, Tokyo, Japan

S. Natsugoe (ed.), *Lymph Node Metastasis in Gastrointestinal Cancer*,
https://doi.org/10.1007/978-981-10-4699-5_4

4.1 Entry of Lymphocytes from the Vascular Endothelium

Lymph nodes play significant roles in the immune system. This system makes it possible to maximize the exposure of each individual lymphocyte to the largest possible number of antigen-presenting cells. To this end, lymphocytes are continuously recirculating throughout the body patrolling against possible invasion of antigens from outside. The lymphocytes that differentiated from stem cells in the primary lymphoid tissues and obtained the capacity for discrimination between self- and non-self-antigens begin to collect antigen information after they immigrate into secondary lymphoid tissues, such as lymph nodes, the spleen, and Peyer's patches. If they do not encounter the corresponding antigen there, these lymphocytes recirculate though blood vessels or lymphatic vessels. If specific antigens stimulate them, then the activated lymphocytes follow distinct patterns of migration. Antigen-experienced lymphocytes can be further subdivided into subsets based on their expression of characteristic sets of trafficking receptors that favor their accumulation in certain target organs, including the skin and gut [1]. Interaction of lymphocytes with vascular endothelial cells is necessary not only for the organogenesis of secondary lymphoid tissues but also for the maintenance of lymphocyte recirculation. In this process, adhesion molecules and chemokines play significant roles.

Naïve T and B lymphocytes reach lymph nodes from the thymus and bone marrow. At this time, the recruitment of circulating lymphocytes from blood into these secondary lymphoid organs is believed to take place exclusively via specialized postcapillary venules—high endothelial venules (HEVs)—in the interfollicular area. The characteristic structure of HEVs is well developed in lymph nodes and mucosa-associated secondary lymphoid tissues but not in the spleen. HEVs routinely recruit lymphocytes even in the absence of inflammatory signals.

The HEVs in lymph nodes continuously express so-called addressin-like peripheral lymph node addressin (PNAd) and interact with L-selectin on lymphocytes, thereby driving the lymphocyte tethering to (and rolling on) endothelial cells of an HEV. In the intestinal tissue, the tethering–rolling step is mediated by mucosal addressin cell adhesion molecule 1 (MAdCAM-1). Multimolecular adhesion cascades contribute to lymphocyte migration into lymph nodes [2, 3]. Naïve T and B cells strongly express L-selectin and moderately express α4β7 integrin (lymphocytic receptor for MAdCAM-1) and lymphocyte function-associated antigen 1 (LFA-1; CD11a or CD18), which mediate three sequential types of adhesive interactions: (1) an L-selectin-mediated initial contact, (2) α4β7 integrin-mediated slow rolling, and (3) interactions with LFA-1 in conjunction with α4β7 integrin and/or MAdCAM-1 to induce activation-dependent arrest. Thus, naïve lymphocytes migrate into the mesenteric lymph nodes through HEVs using these adhesion molecules just like a key for a lock (Fig. 4.1).

Besides interaction of these adhesion molecules, interaction of a chemokine receptor and chemokine plays an important role in the regulation of lymphocyte trafficking via integrin activation. Chemokines are a group of low-molecular-weight cytokines that can induce chemotaxis in lymphocytes by binding to the G protein-coupled receptors (GPCRs) that possess seven membrane-spanning domains

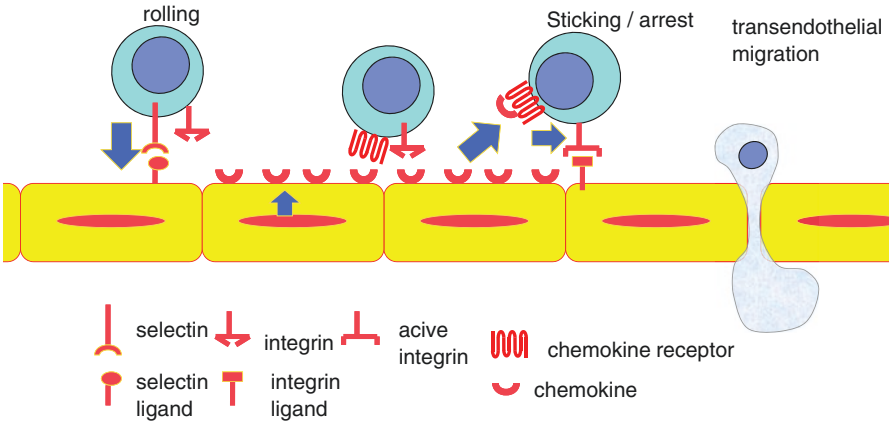

Fig. 4.1 Entry of a lymphocyte via an HEV. Naïve lymphocytes strongly express L-selectin and moderately express α4β7 integrin and lymphocyte function-associated antigen 1 (LFA-1; CD11a or CD18) to mediate three sequential types of adhesive interactions: (1) an L-selectin-mediated initial contact, leading to the release of a chemokine; (2) slow rolling mediated by the active form of α4β7 integrin; and (3) LFA-1 in conjunction with α4β7 integrin and MAdCAM-1 mediate activation-dependent arrest

(transmembrane helices). The representative chemokines that mainly participate in lymphocyte migration to intestinal lymphoid tissues (like Peyer's patches and mesenteric lymph nodes) are CCL19, CCL21, and CXCL13. In case of T cells, both CCL21 and CCL19 molecules are strongly expressed on the surface of the HEV endothelium, and these molecules promote migration of naïve lymphocytes that are expressing CCR7, a specific ligand of CCL21 and CCL19 [4]. In case of B cells, they are less CCR7 dependent and express CXCR5, a ligand for CXCL13; the function of CXCR5 in naïve-B-cell recruitment appears to be quite specific for Peyer's patches [5]. Namely, during the rolling process on the surface of endothelial cells of HEVs, naïve T cells start surface expression of CCR7, and naïve B cells start expressing CXCR5 (through which cell surface integrin molecules are activated) and are then transferred into lymphoid tissues. If antigens are presented to the T cells, their surface expression of CCR7 and L-selectin is decreased, then these T cells will lose their ability to migrate into peripheral lymph nodes.

4.2 The Role of the Autotaxin (ATX)–Lysophosphatidic Acid (LPA) Axis in Lymphocyte Migration

LPA regulates a wide range of cellular processes, including cell motility through GPCRs [6].

LPA can be generated from lysophosphatidylcholine (LPC) via removal of the choline moiety by the enzyme lysophospholipase D (lyso-PLD). LPC circulates in blood at a higher concentration than LPA does [7].

ATX was originally known to be involved in a wide range of cellular processes, including cell motility. Later, the dominant lyso-PLD in serum was found to be ATX. Two independent groups reported that the LPA-producing ectoenzyme ATX is highly expressed by HEVs in lymph nodes, and that ATX controls adhesion and transmigration of lymphocytes [8, 9].

LPA binds to at least six specific LPA receptors (LPA1–LPA6) [6]. In addition, it binds to non-GPCR targets such as RAGE, PPAR-g, and TRPV1 [10–12]. LPA receptors are expressed by T cells and enhance the motility of human and mouse T cells in vitro [8, 13, 14].

Thus, it is possible that ATX secreted from an HEV into the lumen binds to the surface of the cells and hydrolyzes LPC to LPA, leading to activation of LPA receptor on T cells. Nevertheless, it is uncertain whether ATX-generated LPA acts on T cells (Fig. 4.2).

Recently, it was reported that lymph node stromal cells constitutively express ATX. CCL21^{+} stromal cells in the T zone produce and immobilize ATX on their surface. Inhibition of ATX or LPA receptors reduces T-cell migration, and this effect is exacerbated further by LFA-1 or Ga-I inhibition, suggesting that ATX from stromal cells promotes interstitial T-cell movement in an LFA-1-independent manner [15].

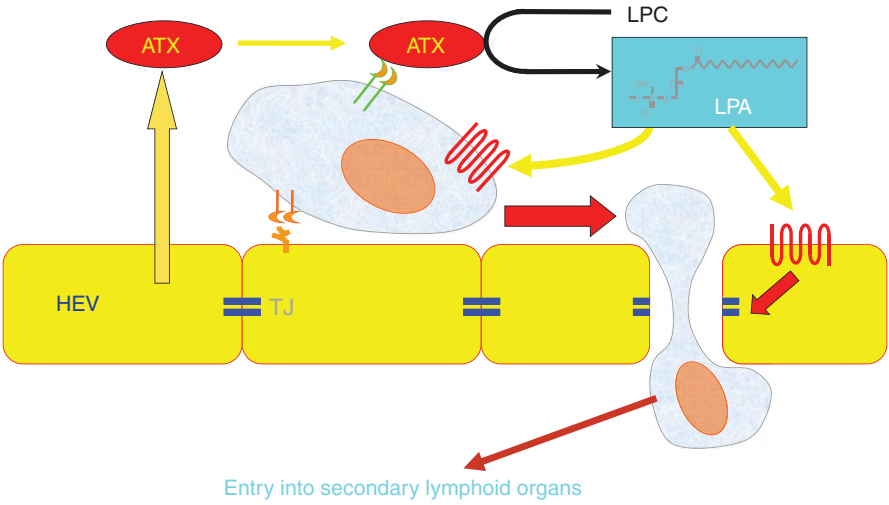

Fig. 4.2 The function of LPA in lymphocyte migration in lymph nodes. Lymphocytes enter lymph nodes from blood by migrating across specialized venules, termed HEVs. LPA in blood is converted into LPC by ATX which has a lysophospholipase D (lyso-PLD) activity. LPA regulates lymphocyte extravasation across the HEV basal lamina. *LPA* lysophosphatidic acid, *ATX* autotaxin, *HEV* high endothelial venule, *FRC* fibroblastic reticular cell

4.3 The Effects of Retinoic Acid (RA) on Lymphocyte Migration

Recently, the important role of RA, a vitamin A metabolite, in intestinal immunity was widely recognized. RA has an ability to enhance the barrier function of the intestinal mucosa and to increase IgA production by inducing differentiation of naïve T cells toward the T helper 2 (Th2) lineage. Moreover, it was recently recognized that RA possesses the ability to force lymphocytes to home specifically to small-intestinal tissues [16]. RA induces not only the effector and memory function but also regulatory-T-cell activity and is intimately involved in oral tolerance and inhibition of inflammation by enhancing differentiation into $FoxP3^+$ regulatory T cells or via suppression of differentiation toward Th17 cells [17].

In intestinal lymphoid cells, the main cells that produce RA from vitamin A and supply it to lymphocytes are DCs. In Peyer's patches and MLNs, there are DCs that express an RA-synthesizing enzyme, retinaldehyde dehydrogenase 2 (RALDH2). These are matured DCs expressing CD103. When these DCs present antigen to naïve T cells in the presence of RA, the specific expression of α4β7 integrin (a ligand for MAdCAM-1) and CCR9 (a ligand for CCL25) is enhanced on the stimulated T cells. These α4β7 integrin-expressing and CCR9-expressing activated T cells can migrate into the intestinal lamina propria of the villus mucosa as CD4 or $CD8ab^+TCR\alpha\beta^+$ effector or memory T cells after their specific interaction with the MAdCAM-1 molecule on the vascular endothelium. Then, some of them can further migrate into the intraepithelial layer to transform into $CD8ab^+TCR\alpha\beta^+$ IEL cells under the influence of CCR9. Similarly, when the RA-producing DCs present antigens to naïve B cells, these activated B cells acquire the capacity for homing to the intestine with increased expression of α4β7 integrin and CCR9 [18]. These DCs can also produce cytokines such as IL-6, which will facilitate the IgA production by plasma cells in concert with RA. For the specific expression of RALDH2 in the intestine, granulocyte macrophage colony-stimulating factor in the intestinal tissue possibly makes a significant contribution. The involvement of other cytokines such as IL-4 and IL-13 in RALDH2 expression has also been postulated. It was reported that if $CD8^+$ T cells of various lymphoid tissues are activated by DCs isolated from Peyer's patches, then these T cells not only increase their expression of α4β7 integrin and CCR9 but also downregulate the E-selectin ligand or P-selectin ligand on their surface, thus obtaining the specific capacity for transformation to suppress the nonintestinal homing.

On the other hand, in the skin, another vitamin is suggested to be involved in organ tropism of lymphocytes. The skin-specific chemokine CCL27 is a chemoattractant for a subset of cutaneous memory T cells that expresses CC chemokine receptor 10 (CCR10).

Vitamin D3 is generated in the skin in response to sun exposure and is converted through an enzymatic cascade to $1,25(OH)_2D3$. The latter induces T-cell expression of CCR10 and T-cell migration toward the epidermal chemokine CCL27. In contrast, $1,25(OH)_2D3$ inhibits the gut-homing receptors α4β7 integrin and CCR9 (Fig. 4.3) [19].

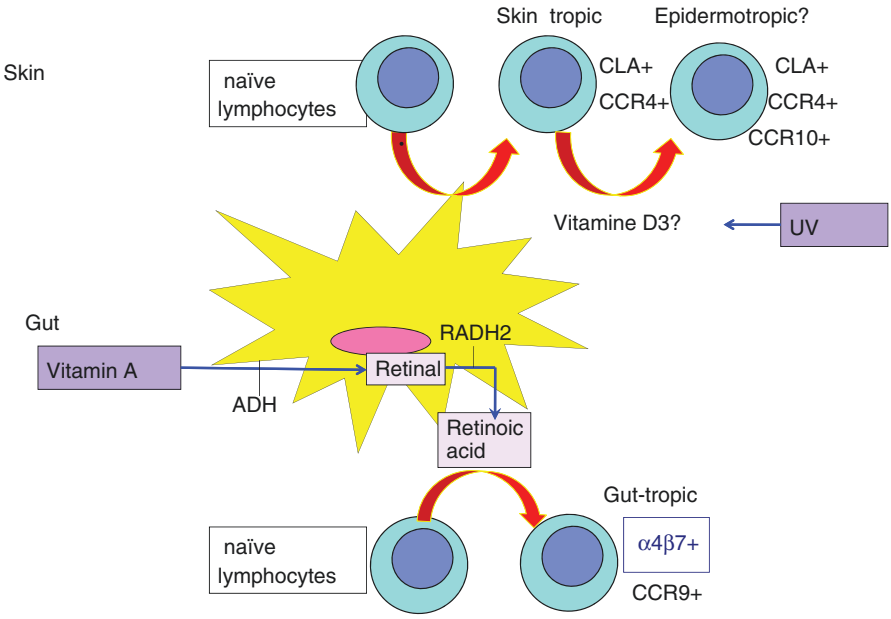

Fig. 4.3 Imprinting of lymphocyte homing by DCs. Activation of naïve lymphocytes by DCs in a lymph node induces tropism of various extralymphoid tissues, such as skin and gut. DCs from GALT induce the expression of α4β7 integrin and CCR9 on naïve T and B cells upon activation. They show strong expression of RALDH2 to produce retinoic acid (RA) from vitamin A and imprint gut-homing specificity on lymphocytes. RA inhibits formation of T cells expressing the skin-homing receptors. On the other hand, $1,25(OH)_2D3$ induces T-cell expression of CCR10 and T-cell migration toward the epidermal chemokine CCL27. RALDH2: retinal dehydrogenase 2

4.4 Transport of Antigens and Immune Cells to a Lymph Node

Lymph nodes are the site where immune reactions or immunosuppression take place. The function of lymph nodes is to filter the lymph from the draining area and to detect antigens in this lymph [20]. Afferent lymphatic vessels are well recognized as the channels through which antigens and immune cells are transported to the draining lymph node for immune responses. Lymph nodes are enclosed in a collagen-rich capsule, which is lined with lymphatic endothelial cells forming subcapsular sinuses. Medullary sinuses are also covered with lymphatic endothelial cells. Afferent lymphatic vessels facilitate the passive entry of tissue-derived antigens, and they are subsequently processed by lymph node-resident antigen-presenting cells [21]. Because initial lymphatic vessels are highly permeable to objects less than 1 μm, bacteria and viruses can enter lymphatic vessels.

Macrophages are present among lymphatic endothelial cells in the subcapsular sinuses and medullary sinuses to sample antigens [22]. In addition, tissue-resident DCs migrate to draining lymph nodes via afferent lymphatics to carry

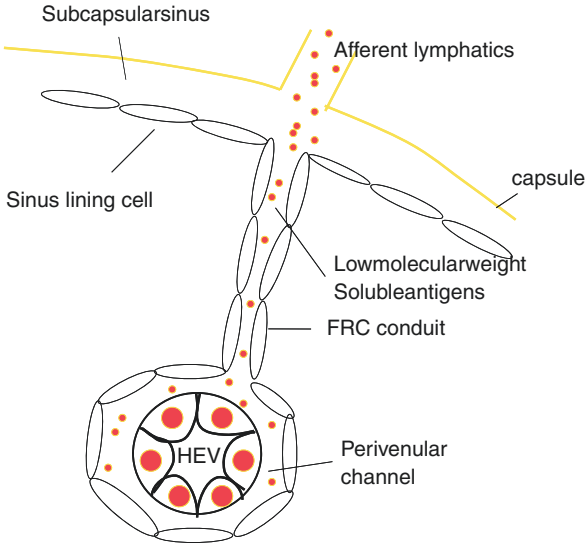

Fig. 4.4 Transport of antigens and regulation of HEV function through afferent lymphatics. Conduits are the spaces enclosed by fibroblastic reticular cells (FRCs). Conduits facilitate transport of low-molecular-weight compounds such as chemokines or cytokines to HEVs

antigens. A DC can enter a lymphatic vessel through gaps in the perilymphatic basement membrane [23].

The magnitude of expression of adhesion molecules on HEVs is closely related to afferent lymphatic vessels. After ligation of afferent lymphatic vessels, expression of adhesion molecules decreases, inhibiting the homing of lymphocytes from HEV into lymph nodes [24].

How is the interaction between afferent lymphatic vessels and HEV regulated? Gretz et al. reported that specialized architectural elements named *conduits* facilitate the transport of low-molecular-weight molecules such as chemokines or cytokines to HEVs [25]. Conduits are the spaces enclosed by fibroblastic reticular cells (FRCs; Fig. 4.4) [26].

DCs also regulate the HEV phenotype and function. After removal of afferent lymph from a peripheral lymph node, HEV-specific genes such as glycam-1 and markers are downregulated, and the function of lymphocyte migration in HEVs disappears [24, 27].

Intravital microscopy analysis of DC-depleted mice revealed decreased interaction between HEVs and lymphocytes [28]. These results suggest that not only low-molecular-weight molecules but also DCs coming through afferent lymphatics to lymph nodes contribute to the regulation of the HEV function.

4.5 Transport of Naïve or Memory Lymphocytes Through Afferent Lymphatics

Effector and memory T cells do not enter lymph nodes from HEV, and the main route of entrance into a lymph node is afferent lymphatics as previously described. In contrast, naïve lymphocytes enter the lymph node via an HEV and exit via

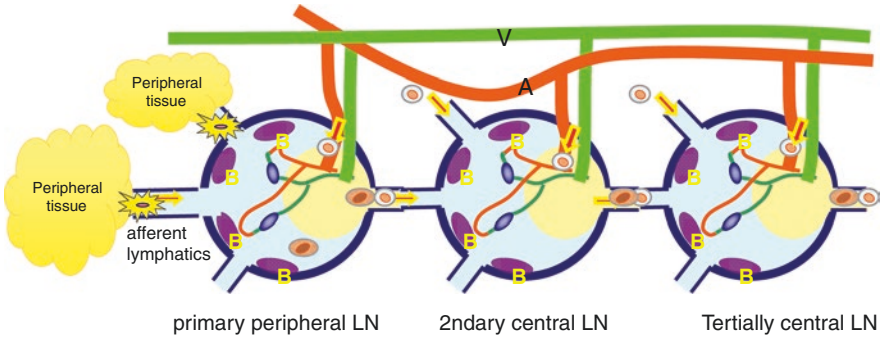

Fig. 4.5 T-cell trafficking routes through a chain of lymph nodes. Primary peripheral lymph nodes (LNs) receive lymph and immune cells directly from the (nonlymphatic) tissue in the respective drainage area. Thus, the vast majority of T cells present in afferent lymph vessels of a secondary central lymph node have an effector or memory phenotype. Nonetheless, due to the constant additional influx of large numbers of recirculating naïve T lymphocytes into all lymph nodes via HEVs, efferent lymph of higher-order central lymph nodes contains predominantly naïve T cells. Naïve T cells migrate to secondary lymph nodes via two routes: HEVs and afferent lymphatics

efferent lymphatics thereafter. Because lymph nodes are organized in chains, these naïve lymphocytes also enter downstream secondary lymph nodes through afferent lymphatics [29, 30]. Thus, naïve T cells migrate to secondary lymph nodes via two routes: HEVs and afferent lymphatics. Evidence that naïve T cells move from one lymph node to another was obtained in vivo by means of mice transgenic for a photoconvertible fluorescent protein called "Kaede" [31] (Fig. 4.5).

4.6 Stromal Cell Interaction with Lymphocytes and DCs

Once naïve lymphocytes enter a lymph node, they move along stromal networks to scan the surface of antigen-presenting cells for cognate antigens. Stromal cells interact with lymphocytes and DCs, provide scaffolds on which these cells migrate, and recruit them into niches by secreting chemokines. Lymph node structure can be subdivided into cortical, paracortical, and medullary areas according to the distribution of specific stromal cells. Lymph node stromal cells are classified into several groups based on the expression of CD31 and podoplanin: FRCs ($CD31^{-}podoplanin^{+}$ phenotype), follicular dendritic cells ($CD31^{-}podoplanin^{\pm}$), blood endothelial cells ($CD31^{+}podoplanin^{-}$), lymphatic endothelial cells (LECs; $CD31^{+}podoplanin^{+}$), and $a7ITG^{+}$ pericytes ($CD31^{-}podoplanin^{-}a7ITG^{+}$) [32, 33].

Recent in vivo live imaging studies showed that stromal cells perform important functions in lymphocytic migration within lymph nodes. Naïve lymphocytes form intimate contacts with FRC networks [34, 35]. After transendothelial migration from HEVs, naive lymphocytes access FRC networks at specific sites and actively crawl along the surface of FRC networks.

Stromal cell subsets show high expression of adhesion molecules such as integrins α1, α5, α7, α8, α9, αv, β1, and β5 [33].

In addition to providing a cellular scaffold to lymphocytes, FRCs secrete chemokines CCL19, CCL21a, and CXCL12 [36, 37]. The intranodal migration and positioning of T cells, B cells, and DCs is regulated by these chemokines.

T cells enter perivascular space transiently after leaving HEVs [38]. After a short period of retention in this area, T cells rapidly migrate along the FRC network [34].

B cells remain near the HEVs for 3–4 h after lymph node entry [39]. Next, B cells crawl on the FRC network in the T-cell area [34]. Finally, B cells enter the follicles depending on the interaction between CXCR5 on T cells and CXCL13 on follicular dendritic cells [40]. The differential positioning of B cells in the outer and central follicles is dependent on EBI2 [41].

Among signaling molecules, CCL21a appears to confer directional cues by binding to the heparin sulfate residues on the surface of FRCs, thus inducing integrin-dependent motility of DCs [42].

Furthermore, podoplanin-rich FRC networks induce DC motility via activation of CLEC2 [43]. A large number of T cells accumulates in the paracortex (T zone), and DCs that have migrated from tissues display foreign antigens to prime T cells in this area. T cells migrate vigorously within the paracortex at high velocity. A recent study revealed that ICAM-1 expressed by DCs but not stromal cells interacts with LFA-1 on T cells, thereby playing a crucial role not only in supporting firm arrest during antigen recognition but also in facilitating the antigen-scanning processes [44].

Thus, multiple molecular mechanisms regulate the movement of lymphocytes and DCs interacting with stromal cells.

4.7 Antigen Presentation by a DC

On the body surface, in contrast to Langerhans cells (LCs), which are located mainly in the skin outside the basement membrane preparing for viral invasion, dendritic cells (DCs) are located inside the basement membrane, preparing for bacteria invading across the basement membrane. DCs act as sentinel cells, catching the information about invading foreign antigens, transferring this information to the immune defense system, and inducing effective memory for the invading antigens. Usually, antigens taken up from outside are presented to $CD4^+$ helper T cells via MHC class II molecules; however, in a particular situation, for example, if DCs were stimulated through a TLR3 molecule, antigens are also cross-presented via MHC class I molecules, resulting in possible induction of cytotoxic T lymphocytes.

In mucosal lymphoid tissues, there are different kinds of DC subsets that express CD11c on the surface. These DCs are classified into several categories according to their expression pattern of CD11b, CD8a, and B220 [45]. DCs derived from Peyer's patches are $b7^-CD103^-$, and they are transported into mesenteric lymph independently of CCR7 signals [46]. In Peyer's patches, DCs are transferred into the

subepithelial dome area via CCR6 stimulation under physiological conditions. The $CD11b^-$ conventional type of DCs has a strong ability to produce IL-12 and performs antigen capture via M-cells in the follicle-associated epithelium or presents the antigen to $CD4^+$ T cells in the interfollicular (parafollicular) area. On the other hand, $CD11b^+$ subsets may commit to the IgA class switching. Especially $CD11b^+$ DCs in the subdome area are producing TGF-β and IL-6, strongly involved in the T-cell-dependent IgA class switching. DCs in GALT constitutively express matrix metalloproteinases (MMPs 2, 3, or 9) or αvβ8 integrin, which are necessary for the induction of TGF-β. The $CD11b^+$ DCs are also supposed to be engaged in IL-10 production and regulatory T-cell induction. In Peyer's patches, there are both CD8a-negative and CD8a-positive subsets of DCs.

There are DCs in the follicular area called follicular DCs. These DCs produce a B-cell-attracting chemokine, CXCL13, and can cause B-cell accumulation in the follicular area. These follicular DCs are known to recruit follicular helper T cells to this area as well.

In MLNs, there are various kinds of DCs, a mixture of those derived from Peyer's patches and intestinal lamina propria, drained from the intestine and reaching the MLNs via intestinal lymphatics. As described above, DCs from Peyer's patches are a $b7^-CD103^-$ population and stay in MLNs in a CCR7-independent manner [46]. In contrast, DCs from intestinal lamina propria, which are strongly positive for b7 and CD103, reach MLNs in a CCR7-dependent manner. Among those DCs, $CD103^+CD11b^{-/low}$ $CD8int^+B220^-$ subsets are expressing enzymes involved in RA production in MLNs. These DCs can induce intestinal homing receptors such as α4β7 integrin and CCR9 on IgA plasma cells. In CCR7-deficient mice, the number of DCs in MLNs is low, and it is hard to induce oral tolerance in these mice. Thus, $CCR7^+$ DCs in MLNs (not in Peyer's patches), which were derived from the lamina propria of the intestine, may be intimately involved in the induction of oral tolerance.

4.8 The Function of Lymph Nodes in Peripheral Tolerance Mediated by LECs and Stromal Cells

It was found that without mLNs, oral tolerance is no longer inducible [47]. Accumulating evidence shows that LECs, stromal cells, $CD103^+$ DCs drained from an induction site, and regulatory T cells are involved in this mechanism.

LECs cover lymph node sinuses. They participate in peripheral tolerance rather than T-cell activation. This property is restricted only to LECs in lymph nodes by LTβR signaling [48].

LECs strongly express peripheral-tissue antigens, which is not the case in tissue lymphatics [49]. LECs express MHC-I and MHC-II (but not costimulatory molecules) and present the antigen on MHC-I via both direct and cross-presentation. Direct presentation of peripheral-tissue antigens to $CD8^+$ T cells results in abortive proliferation and deletion owing to both a lack of costimulation and active PD-L1 engagement.

There is growing appreciation that not only do LNSCs guide antigens to antigen-presenting cells but also themselves present the antigen to educate T cells. LNSCs actively take up exogenous molecules, and some subsets process antigens for cross-presentation and cross-priming of antigen-specific $CD8^+$ T cells [50].

In addition, the presence of DCs and regulatory T cells coming from the draining area plays a significant role in the induction of tolerance after feeding of low doses of an antigen [47]. $CD103^+$ DCs from afferent lymphatics produce IL-10, TGF-β, RA, and indoleamine-2,3-dioxygenase [51–53].

4.9 Regulation of Lymphocyte Emigration from Secondary Lymphoid Tissues and the Effects of Sphingosine-1-Phosphate (S1P)

Naïve lymphocytes that do not encounter their target antigen leave the lymph node through efferent lymphatics. It is now well known that S1P is a key regulatory molecule when lymphocytes emigrate from secondary lymphoid organs such as lymph nodes or Peyer's patches [54] (Fig. 4.6). S1P is one of the lipid mediators and like chemokines S1P can induce chemotaxis in lymphocytes by binding to GPCRs that possess seven membrane-spanning domains (transmembrane helices). S1P is produced by phosphorylation of sphingosine, which is a metabolite of representative cell membrane components: sphingomyelins and ceramides. In blood, S1P is mainly derived from platelets and red blood cells, and its concentration is kept relatively high (several hundred nanomoles per liter). On the other hand, S1P concentration in lymphoid tissues is maintained at a low (nanomolar) level by the action of S1P lyase and dephosphorylation enzymes. This difference causes a concentration gradient of S1P as follows: blood > lymph fluid > lymphoid tissue.

Naïve lymphocytes strongly express the receptor for S1P (S1P-R). After these naïve lymphocytes migrate into secondary lymphoid tissues under the influence of chemokines such as CCL19, CCL21, and CXCL13, if they do not encounter antigens, they will emigrate from the secondary lymphoid tissues into peripheral blood or lymphatics in response to a high concentration of S1P in blood or lymph fluid. In contrast, after antigens have been presented to naïve T lymphocytes, expression of S1P-R on T lymphocytes is reduced. The exit of T lymphocytes from secondary lymphoid follicles is suppressed, and they remain inside the lymphoid tissues. Thereafter, antigen-specific T lymphocytes receive activation signals from antigens, and accessory stimulatory molecules will restore the S1P-R expression on their surface. The T lymphocytes are transported to the periphery again in an S1P-dependent manner. In the case of B cells immediately after antigen stimulation, naïve B cells also show downregulation of S1P-R during their differentiation into IgA-positive B cells with class switch recombination of the immunoglobulin constant region. Nevertheless, with further differentiation into IgA plasmablasts in lymph nodes, the expression of S1P-R recovers, and eventually the IgA plasmablasts emigrate from lymph nodes and enter the periphery.

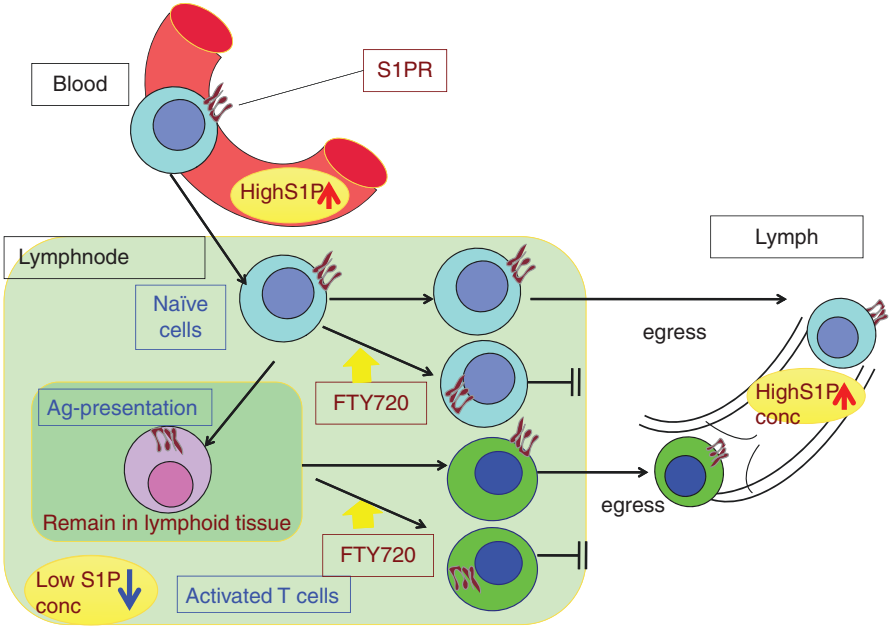

Fig. 4.6 The effect of S1P on lymphocyte emigration. S1P concentration in lymphoid tissues is maintained low by the action of S1P lyase and dephosphorylation enzymes. This difference causes a concentration gradient of S1P as follows: blood > lymph fluid > lymphoid tissue. Naïve lymphocytes strongly express the receptor for S1P (S1P-R). After these naïve lymphocytes have migrated into secondary lymphoid tissues under the influence of chemokines, they will emigrate from the secondary lymphoid tissues into lymphatics in response to a high concentration of S1P in the lymph fluid. After antigens have been presented to naïve T lymphocytes, the exit of T lymphocytes from secondary lymphoid follicles is suppressed by downregulation of S1P-R expression. The activated T lymphocytes recover S1P-R expression under the influence of accessory stimulatory molecules and are transported to the periphery again in an S1P-dependent manner

S1Ps are known to be involved not only in physiological migration of lymphocytes but also in migration of pathological cells. It is thought that S1Ps participate in intestinal food allergies or inflammatory bowel diseases [55]. In this regard, much attention has been given to FTY720, a drug derived from a herb, as an immunomodulator. FTY720 can downregulate S1P-R expression on the lymphocyte surface and can inhibit the abovementioned lymphocyte emigration. Accordingly, administration of FTY720 was reported to ameliorate pathological infiltration of T lymphocytes into the inflamed colonic mucosa in an experimental model of colitis.

S1P secretion is regulated by α9 integrin, and its ligand, tenascin-C, colocalizes with each other on medullary and cortical sinuses of draining lymph nodes, which are a gate for lymphocytes to exit under inflammatory conditions [56]. Blockade of α9 integrin-mediated signaling reduces lymphocyte egress from draining lymph nodes in several experimental models, including experimental autoimmune encephalomyelitis, where this approach improves clinical scores.

Under inflammatory conditions, the flow of lymph increases. Proinflammatory cytokines upregulate adhesion molecules, such as P-selectin and E-selectin on HEVs, facilitating the entry of lymphocytes into lymph nodes [57]. In this situation, lymphocyte egress from a lymph node is also decreased [58]. This decrease is controlled by downregulation of S1P-R1 expression on lymphocytes. Accordingly, accelerated entry and decreased egress of lymphocytes increase accumulation of lymphocytes in lymph nodes. This state of affairs gives lymphocytes a chance to encounter cognate antigens, thereby enhancing immune function.

S1P also helps to maintain integrity of HEVs. How HEVs enable lymphocyte transmigration while maintaining vascular integrity is still unknown. Mice lacking PDPN lose HEV integrity and develop spontaneous bleeding in lymph nodes after immunization. PDPN expressed on FRCs around HEVs functions as an activating ligand for platelet CLEC-2. PDPN–CLEC-2-mediated platelet activation causes a local S1P release from platelets leading to maintenance of vascular integrity of HEVs [59].

References

1. Mora JR, von Andrian UH. T-cell homing specificity and plasticity: new concepts and future challenges. Trends Immunol. 2006;27(5):235–43.
2. Briskin M, Winsor-Hines D, Shyjan A, Cochran N, Bloom S, Wilson J, McEvoy LM, Butcher EC, Kassam N, Mackay CR, Newman W, Ringler DJ. Human mucosal addressin cell adhesion molecule-1 is preferentially expressed in intestinal tract and associated lymphoid tissue. Am J Pathol. 1997;151:97–110.
3. Bargatze RF, Jutila MA, Butcher EC. Distinct roles of L-selectin and integrins alpha 4 beta 7 and LFA-1 in lymphocyte homing to Peyer's patch-HEV in situ: the multistep model confirmed and refined. Immunity. 1995;3:99–108.
4. Warnock RA, Campbell JJ, Dorf ME, Matsuzawa A, McEvoy LM, Butcher EC. The role of chemokines in the microenvironmental control of T versus B cell arrest in Peyer's patch high endothelial venules. J Exp Med. 2000;191:77–88.
5. Okada T, Ngo VN, Ekland EH, Förster R, Lipp M, Littman DR, Cyster JG. Chemokine requirements for B cell entry to lymph nodes and Peyer's patches. J Exp Med. 2002;196:65–75.
6. Choi JW, Herr DR, Noguchi K, Yung YC, Lee CW, Mutoh T, Lin ME, Teo ST, Park KE, Mosley AN, Chun J. LPA receptors: subtypes and biological actions. Annu Rev Pharmacol Toxicol. 2010;50:157–86.
7. Nakamura K, Kishimoto T, Ohkawa R, Okubo S, Tozuka M, Yokota H, Ikeda H, Ohshima N, Mizuno K, Yatomi Y. Suppression of lysophosphatidic acid and lysophosphatidylcholine formation in the plasma in vitro: proposal of a plasma sample preparation method for laboratory testing of these lipids. Anal Biochem. 2007;367(1):20–7.
8. Kanda H, Newton R, Klein R, Morita Y, Gunn MD, Rosen SD. Autotaxin, an ectoenzyme that produces lysophosphatidic acid, promotes the entry of lymphocytes into secondary lymphoid organs. Nat Immunol. 2008;9(4):415–23.
9. Nakasaki T, Tanaka T, Okudaira S, Hirosawa M, Umemoto E, Otani K, Jin S, Bai Z, Hayasaka H, Fukui Y, Aozasa K, Fujita N, Tsuruo T, Ozono K, Aoki J, Miyasaka M. Involvement of the lysophosphatidic acid-generating enzyme autotaxin in lymphocyte-endothelial cell interactions. Am J Pathol. 2008;173(5):1566–76.

10. Rai V, Touré F, Chitayat S, Pei R, Song F, Li Q, Zhang J, Rosario R, Ramasamy R, Chazin WJ, Schmidt AM. Lysophosphatidic acid targets vascular and oncogenic pathways via RAGE signaling. J Exp Med. 2012;209(13):2339–50.
11. Zhang C, Baker DL, Yasuda S, Makarova N, Balazs L, Johnson LR, Marathe GK, McIntyre TM, Xu Y, Prestwich GD, Byun HS, Bittman R, Tigyi G. Lysophosphatidic acid induces neointima formation through PPARgamma activation. J Exp Med. 2004;199(6):763–74.
12. Nieto-Posadas A, Picazo-Juárez G, Llorente I, Jara-Oseguera A, Morales-Lázaro S, Escalante-Alcalde D, Islas LD, Rosenbaum T. Lysophosphatidic acid directly activates TRPV1 through a C-terminal binding site. Nat Chem Biol. 2011;8(1):78–85.
13. Zheng Y, Kong Y, Goetzl EJ. Lysophosphatidic acid receptor-selective effects on Jurkat T cell migration through a Matrigel model basement membrane. J Immunol. 2001;166(4):2317–22.
14. Stam JC, Michiels F, van der Kammen RA, Moolenaar WH, Collard JG. Invasion of T-lymphoma cells: cooperation between Rho family GTPases and lysophospholipid receptor signaling. EMBO J. 1998;17(14):4066–74.
15. Katakai T, Kondo N, Ueda Y, Kinashi T. Autotaxin produced by stromal cells promotes LFA-1-independent and Rho-dependent interstitial T cell motility in the lymph node paracortex. J Immunol. 2014;193(2):617–26.
16. Iwata M, Hirakiyama A, Eshima Y, Kagechika H, Kato C, Song SY. Retinoic acid imprints gut-homing specificity on T cells. Immunity. 2004;21:527–38.
17. Mucida D, Park Y, Kim G, Turovskaya O, Scott I, Kronenberg M, Cheroutre H. Reciprocal TH17 and regulatory T cell differentiation mediated by retinoic acid. Science. 2007;317:256–60.
18. Mora JR, Iwata M, Eksteen B, Song SY, Junt T, Senman B, Otipoby KL, Yokota A, Takeuchi H, Ricciardi-Castagnoli P, Rajewsky K, Adams DH, von Andrian UH. Generation of gut-homing IgA-secreting B cells by intestinal dendritic cells. Science. 2006;314:1157–60.
19. Sigmundsdottir H, Pan J, Debes GF, Alt C, Habtezion A, Soler D, Butcher EC. DCs metabolize sunlight-induced vitamin D3 to 'program' T cell attraction to the epidermal chemokine CCL27. Nat Immunol. 2007;8(3):285–93.
20. Buettner M, Bode U. Lymph node dissection--understanding the immunological function of lymph nodes. Clin Exp Immunol. 2012;169(3):205–12.
21. Roozendaal R, Mebius RE, Kraal G. The conduit system of the lymph node. Int Immunol. 2008;20(12):1483–7.
22. Kuka M, Iannacone M. The role of lymph node sinus macrophages in host defense. Ann N Y Acad Sci. 2014;1319:38–46.
23. Pflicke H, Sixt M. Preformed portals facilitate dendritic cell entry into afferent lymphatic vessels. J Exp Med. 2009;206(13):2925–35.
24. Mebius RE, Streeter PR, Brevé J, Duijvestijn AM, Kraal G. The influence of afferent lymphatic vessel interruption on vascular addressin expression. J cell Biol. 1991;115(1):85–95.
25. Gretz JE, Norbury CC, Anderson AO, Proudfoot AE, Shaw S. Lymph-borne chemokines and other low molecular weight molecules reach high endothelial venules via specialized conduits while a functional barrier limits access to the lymphocyte microenvironments in lymph node cortex. J Exp Med. 2000;192(10):1425–40.
26. Gretz JE, Anderson AO, Shaw S. Cords, channels, corridors and conduits: critical architectural elements facilitating cell interactions in the lymph node cortex. Immunol Rev. 1997;156:11–24.
27. Mebius RE, Dowbenko D, Williams A, Fennie C, Lasky LA, Watson SR. Expression of GlyCAM-1, an endothelial ligand for L-selectin, is affected by afferent lymphatic flow. J Immunol. 1993;151(12):6769–76.
28. Moussion C, Girard JP. Dendritic cells control lymphocyte entry to lymph nodes through high endothelial venules. Nature. 2011;479(7374):542–6.
29. Braun A, Worbs T, Moschovakis GL, Halle S, Hoffmann K, Bölter J, Münk A, Förster RB. Afferent lymph-derived T cells and DCs use different chemokine receptor CCR7-dependent routes for entry into the lymph node and intranodal migration. Nat Immunol. 2011;12(9):879–87.

30. Girard JP, Moussion C, Förster R. HEVs, lymphatics and homeostatic immune cell trafficking in lymph nodes. Nat Rev Immunol. 2012;12(11):762–73.
31. Tomura M, Yoshida N, Tanaka J, Karasawa S, Miwa Y, Miyawaki A, Kanagawa O. Monitoring cellular movement in vivo with photoconvertible fluorescence protein "Kaede" transgenic mice. Proc Natl Acad Sci U S A. 2008;105(31):10871–6.
32. Link A, Vogt TK, Favre S, Britschgi MR, Acha-Orbea H, Hinz B, Cyster JG, Luther SA. Fibroblastic reticular cells in lymph nodes regulate the homeostasis of naive T cells. Nat Immunol. 2007;8(11):1255–65.
33. Malhotra D, Fletcher AL, Astarita J, Lukacs-Kornek V, Tayalia P, Gonzalez SF, Elpek KG, Chang SK, Knoblich K, Hemler ME, Brenner MB, Carroll MC, Mooney DJ, Turley SJ, Immunological Genome Project Consortium. Transcriptional profiling of stroma from inflamed and resting lymph nodes defines immunological hallmarks. Nat Immunol. 2012;13(5):499–510.
34. Bajénoff M, Egen JG, Koo LY, Laugier JP, Brau F, Glaichenhaus N, Germain RN. Stromal cell networks regulate lymphocyte entry, migration, and territoriality in lymph nodes. Immunity. 2006;25(6):989–1001.
35. Bajénoff M, Glaichenhaus N, Germain RN. Fibroblastic reticular cells guide T lymphocyte entry into and migration within the splenic T cell zone. J Immunol. 2008;181(6):3947–54.
36. Luther SA, Tang HL, Hyman PL, Farr AG, Cyster JG. Coexpression of the chemokines ELC and SLC by T zone stromal cells and deletion of the ELC gene in the plt/plt mouse. Proc Natl Acad Sci U S A. 2000;97(23):12694–9.
37. Peduto L, Dulauroy S, Lochner M, Späth GF, Morales MA, Cumano A, Eberl G. Inflammation recapitulates the ontogeny of lymphoid stromal cells. J Immunol. 2009;182(9):5789–99.
38. Boscacci RT, Pfeiffer F, Gollmer K, Sevilla AI, Martin AM, Soriano SF, Natale D, Henrickson S, von Andrian UH, Fukui Y, Mellado M, Deutsch U, Engelhardt B, Stein JV. Comprehensive analysis of lymph node stroma-expressed Ig superfamily members reveals redundant and nonredundant roles for ICAM-1, ICAM-2, and VCAM-1 in lymphocyte homing. Blood. 2010;116(6):915–25.
39. Park C, Hwang IY, Sinha RK, Kamenyeva O, Davis MD, Kehrl JH. Lymph node B lymphocyte trafficking is constrained by anatomy and highly dependent upon chemoattractant desensitization. Blood. 2012;119(4):978–89.
40. Cyster JG. Chemokines, sphingosine-1-phosphate, and cell migration in secondary lymphoid organs. Annu Rev Immunol. 2005;23:127–59.
41. Pereira JP, Kelly LM, Xu Y, Cyster JG. EBI2 mediates B cell segregation between the outer and centre follicle. Nature. 2009;460(7259):1122–6.
42. Schumann K, Lämmermann T, Bruckner M, Legler DF, Polleux J, Spatz JP, Schuler G, Förster R, Lutz MB, Sorokin L, Sixt M. Immobilized chemokine fields and soluble chemokine gradients cooperatively shape migration patterns of dendritic cells. Immunity. 2010;32(5):703–13.
43. Acton SE1, Astarita JL, Malhotra D, Lukacs-Kornek V, Franz B, Hess PR, Jakus Z, Kuligowski M, Fletcher AL, Elpek KG, Bellemare-Pelletier A, Sceats L, Reynoso ED, Gonzalez SF, Graham DB, Chang J, Peters A, Woodruff M, Kim YA, Swat W, Morita T, Kuchroo V, Carroll MC, Kahn ML, Wucherpfennig KW, Turley SJ. Podoplanin-rich stromal networks induce dendritic cell motility via activation of the C-type lectin receptor CLEC-2. Immunity. 2012;37(2):276–89.
44. Katakai T, Habiro K, Katakai KT. Dendritic cells regulate high-speed interstitial T cell migration in the lymph node via LFA-1/ICAM-1. J Immunol. 2013;191(3):1188–99.
45. Iwasaki A. Mucosal dendritic cells. Annu Rev Immunol. 2007;25:381–418.
46. Jang MH, Sougawa N, Tanaka T, Hirata T, Hiroi T, Tohya K, Guo Z, Umemoto E, Ebisuno Y, Yang BG, Seoh JY, Lipp M, Kiyono H, Miyasaka M. CCR7 is critically important for migration of dendritic cells in intestinal lamina propria to mesenteric lymph nodes. J Immunol. 2006;176:803–10.
47. Worbs T, Bode U, Yan S, Hoffmann MW, Hintzen G, Bernhardt G, Förster R, Pabst O. Oral tolerance originates in the intestinal immune system and relies on antigen carriage by dendritic cells. J Exp Med. 2006;203(3):519–27.

48. Cohen JN, Tewalt EF, Rouhani SJ, Buonomo EL, Bruce AN, Xu X, Bekiranov S, Fu YX, Engelhard VH. Tolerogenic properties of lymphatic endothelial cells are controlled by the lymph node microenvironment. PLoS One. 2014;9(2):e87740.
49. Tewalt EF, Cohen JN, Rouhani SJ, Engelhard VH. Lymphatic endothelial cells – key players in regulation of tolerance and immunity. Front Immunol. 2012;3:305.
50. Hirosue S, Dubrot J. Modes of antigen presentation by lymph node stromal cells and their immunological implications. Front Immunol. 2015;446:6.
51. Schulz O, Jaensson E, Persson EK, Liu X, Worbs T, Agace WW, Pabst O. Intestinal CD103+, but not CX3CR1+, antigen sampling cells migrate in lymph and serve classical dendritic cell functions. J Exp Med. 2009;206(13):3101–14.
52. Shiokawa A, Tanabe K, Tsuji NM, Sato R, Hachimura S. IL-10 and IL-27 producing dendritic cells capable of enhancing IL-10 production of T cells are induced in oral tolerance. Immunol Lett. 2009;125(1):7–14.
53. Matteoli G, Mazzini E, Iliev ID, Mileti E, Fallarino F, Puccetti P, Chieppa M, Rescigno M. Gut CD103+ dendritic cells express indoleamine 2,3-dioxygenase which influences T regulatory/T effector cell balance and oral tolerance induction. Gut. 2010;59(5):595–604.
54. Schwab SR, Cyster JG. Finding a way out: lymphocyte egress from lymphoid organs. Nat Immunol. 2007;8:1295–301.
55. Fujii R, Kanai T, Nemoto Y, Makita S, Oshima S, Okamoto R, Tsuchiya K, Totsuka T, Watanabe M. FTY720 suppresses CD4+CD44highCD62L- effector memory T cell-mediated colitis. Am J Physiol Gastrointest Liver Physiol. 2006;291:G267–74.
56. Ito K, Morimoto J, Kihara A, Matsui Y, Kurotaki D, Kanayama M, Simmons S, Ishii M, Sheppard D, Takaoka A, Uede T. Integrin α9 on lymphatic endothelial cells regulates lymphocyte egress. Proc Natl Acad Sci U S A. 2014;111(8):3080–5.
57. Miyasaka M, Miyasaka TT. Lymphocyte trafficking across high endothelial venules: dogmas and enigmas. Nature Rev Immunol. 2004;4(5):360–70.
58. Shiow LR, Rosen DB, Brdicková N, Xu Y, An J, Lanier LL, Cyster JG, Matloubian M. CD69 acts downstream of interferon-alpha/beta to inhibit S1P1 and lymphocyte egress from lymphoid organs. Nature. 2006;440(7083):540–4.
59. Herzog BH, Fu J, Wilson SJ, Hess PR, Sen A, McDaniel JM, Pan Y, Sheng M, Yago T, Silasi-Mansat R, McGee S, May F, Nieswandt B, Morris AJ, Lupu F, Coughlin SR, McEver RP, Chen H, Kahn ML, Xia L. Podoplanin maintains high endothelial venule integrity by interacting with platelet CLEC-2. Nature. 2013;502(7469):105–9.

Lymphoid Tissues Associated with Gastrointestinal (GI) Mucosa

5

Takahiro Nagatake, Jun Kunisawa, and Hiroshi Kiyono

Abstract

GI mucosa covers huge area of internal but outside of the body and encounters tremendous numbers and amounts of food antigens and nonpathogenic microorganisms, and occasionally expose to pathogens. Mucosa-associated lymphoid tissue or gut-associated lymphoid tissue (GALT) is a key organized lymphoid structure for the regulation and induction of antigen-specific immune responses. In

T. Nagatake
Laboratory of Vaccine Materials, Center for Vaccine and Adjuvant Research, and Laboratory of Gut Environmental System, National Institutes of Biomedical Innovation, Health and Nutrition (NIBIOHN), Ibaraki-city, Osaka, Japan

J. Kunisawa
Laboratory of Vaccine Materials, Center for Vaccine and Adjuvant Research, and Laboratory of Gut Environmental System, National Institutes of Biomedical Innovation, Health and Nutrition (NIBIOHN), Ibaraki-city, Osaka, Japan

International Research and Development Center for Mucosal Vaccines, The Institute of Medical Science, The University of Tokyo, Minato-ku, Tokyo, Japan

Department of Microbiology and Immunology, Kobe University Graduate School of Medicine, Kobe-city, Hyogo, Japan

Graduate School of Medicine, Graduate School of Pharmaceutical Sciences, Graduate School of Dentistry, Osaka University, Suita-city, Osaka, Japan

H. Kiyono (✉)
Department of Mucosal Immunology, The University of Tokyo Distinguished Professor Department, Minato-ku, Tokyo, Japan

Department of Immunology, Graduate School of Medicine, Chiba University (CU), Chiba-city, Chiba, Japan

Division of Gastroenterology, Department of Medicine, School of Medicine, University of California San Diego (UCSD) and CU-UCSD Center for Mucosal Immunology, Allergy and Vaccines, UCSD, San Diego, CA, USA
e-mail: kiyono@ims.u-tokyo.ac.jp

S. Natsugoe (ed.), *Lymph Node Metastasis in Gastrointestinal Cancer*,
https://doi.org/10.1007/978-981-10-4699-5_5

this chapter, we describe the structure, function, and development of several types of GALTs, including Peyer's patches, cecum patches, colonic patches, isolated lymphoid follicles, mesenteric lymph nodes, and cryptopatches. Lymphoid tissues associated with small intestine and large intestine are not only anatomically but also immunologically segregated for the induction of necessary immune responses. In addition, the GALT development can be divided into pre- and postnatal organogenesis with similarity and differences existing in the molecular and cellular requirement. Prenatal development of GALT is programed in the ontogeny, while postnatal development of GALT is controlled by external stimuli such as microbial stimulation and dietary materials. Therefore, each GALT shares some common features with unique function and developmental requirement which contribute for the creation of dynamism and homeostasis of gut immune system.

Keywords
Peyer's patches · Cecum patches · Colonic patches · Isolated lymphoid follicles
Mesenteric lymph nodes · Cryptopatches

5.1 Structure and Function of Lymphoid Tissues in GI Mucosa

5.1.1 Secondary Lymphoid Tissues

There are three types of lymphoid tissues in the body: primary, secondary, and tertiary lymphoid tissues [1]. Among them, GI mucosa is equipped with various types of secondary lymphoid tissues such as Peyer's patches, cecum patches, colonic patches, and mesenteric lymph nodes (Fig. 5.1a). Secondary lymphoid tissues provide the optimized immunological environment for the accumulation of and interactive microenvironment for immunocompetent cells such as dendritic cells, T cells, and B cells; therefore, they play a critical role in the induction and regulation of antigen-specific immune responses [2]. Peyer's patches, cecum patches, and colonic patches are representative secondary lymphoid tissues in GI mucosa, which are generally termed as gut-associated lymphoid tissue (GALT), and found in the small intestine, cecum, and large intestine, respectively (Fig. 5.1a). Peyer's patches are always found on the anti-mesentery side of the small intestine; there are 8 to 10 Peyer's patches in mice and hundreds in humans [3]. Cecum patches develop as a single large lymphoid cluster in mouse while they are found as multiple small clusters in the human cecum [4]. Mouse and human have 2 to 5 colonic patches in the large intestine [5, 6]. One Peyer's patch, cecum patch, and colonic patch each possesses several B cell-rich follicle regions, which are surrounded by T cell- and dendritic cell-rich interfollicular regions, as well as dendritic cell-rich subepithelial dome region (Fig. 5.1b) [5, 7]. In addition to them, mice and human possess hundreds of isolated lymphoid follicles as single aggregations of B cells, but lack T cell-rich interfollicular regions in the small and large intestine (Fig. 5.1a, b) [5, 8, 9].

All these lymphoid tissues (i.e., Peyer's patches, cecum patches, colonic patches, and isolated lymphoid follicles) do not contain afferent lymphatics; instead they take

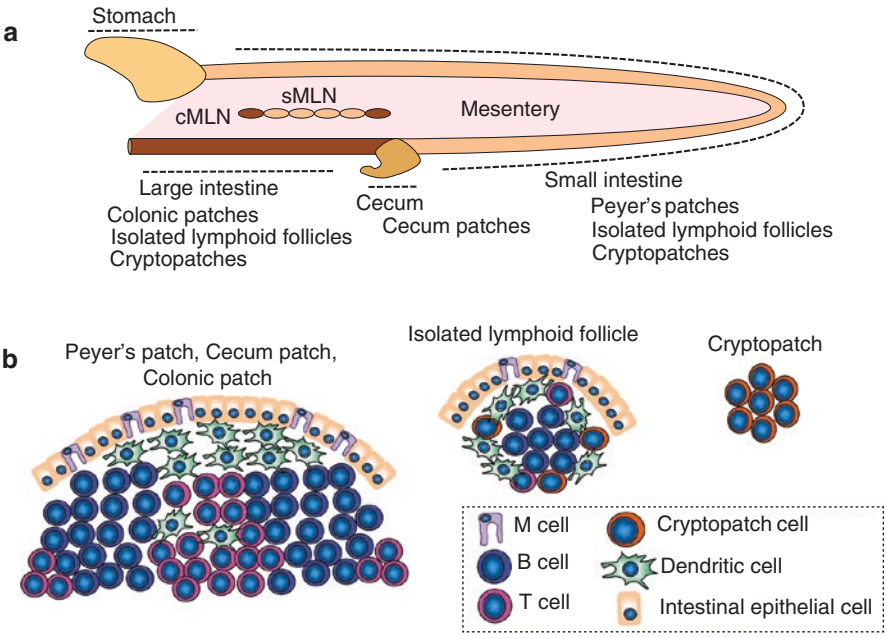

Fig. 5.1 Schematic illustration of lymphoid tissues in GI mucosa. (**a**) GI mucosa is equipped with various types of organized lymphoid tissues. Peyer's patches, cecum patches, and colonic patches are distributed in the small intestine, cecum, and large intestine, respectively. Isolated lymphoid follicles and cryptopatches are found throughout intestine. sMLN and cMLN are draining lymph nodes that drain small and large intestinal mucosa, respectively. (**b**) One Peyer's patch, cecum patch, and colonic patch each possesses several B cell-rich follicle regions, which are surrounded by T cell- and dendritic cell-rich interfollicular regions, as well as dendritic cell-rich subepithelial dome region. Isolated lymphoid follicle is detected as single aggregations of B cells, but lack T cell-rich interfollicular regions. Peyer's patch, cecum patch, colonic patch, and isolated lymphoid follicle have M cells in the follicle-associated epithelium. Cryptopatch is identified as a tiny cell aggregation of $CD3\varepsilon^{-}$c-Kit^{+} cryptopatch cells in the crypt lamina propria

up luminal antigens through follicle-associated epithelium, a single epithelial layer containing antigen-sampling M cells (Fig. 5.1b) [8, 10–13]. M cells have unique morphological characters in that they have irregular and short microvilli, and possess pocket structure enfolding dendritic cells [8], allowing efficient uptake of luminal antigen by M cells and subsequently transported to dendritic cells [11]. Luminal surface of M cells has thus been shown to express antigen-recognition molecules [14]. Glycoprotein 2 and cellular prion protein are glycosylphosphatidylinositol-anchored proteins, and are selectively expressed on luminal surface of M cells [15, 16]. Glycoprotein 2 binds to the FimH component of the type I pili and acts as transcytotic receptor for type-I-piliated bacteria such as *Escherichia coli* and *Salmonella* Typhimurium [17]. Cellular prion protein can interact with heat-shock protein 60 and involves in uptake of bacteria including *Brucella abortus* [18]. Indeed, mice lacking the expression of glycoprotein 2 and cellular prion protein show decreased colony counts of *S.* Typhimurium and *B. abortus* in the Peyer's patches after oral inoculation, indicating that glycoprotein 2 and cellular prion protein function as transcytotic receptors in M cells.

By continuous exposure to tremendous numbers of commensal bacteria in the gut, Peyer's patches, cecum patches, colonic patches and isolated lymphoid follicles spontaneously form germinal center even in the steady state, with expression of activation-induced cytidine deaminase, an essential enzyme for immunoglobulin class-switch recombination and somatic hypermutation [7, 8]. The study using *Tcrβ*$^{-/-}$*Tcrδ*$^{-/-}$ mice that totally lack T cells revealed that Peyer's patches and isolated lymphoid follicles are, respectively, responsible for T-cell-dependent and T cell-independent IgA antibody production [19]. Cecum patches, as like Peyer's patches, are shown to be responsible for T-cell-dependent IgA antibody production, however, it was revealed that cecum patch-derived IgA^{+} B cells migrated to the small and large intestine while Peyer's patch cells preferentially migrated to the small intestine, indicating that cecum patches and Peyer's patches show anatomical and functional differences for their contribution to the gut immune system [7].

As molecular mechanism in the determination of tissue tropism of lymphocytes, C-C chemokine receptor (CCR)9 is reportedly mediates migration to the small intestine but not large intestine [20], while CCR10 is involved in migration to both the small and large intestine [21]. Indeed, dendritic cells reside in the cecum patches induced the expression of CCR9 and CCR10 on B cells including those committed to IgA production, while that in the Peyer's patches induced selective and predominant expression of CCR9 [7]. It was reported that dendritic cells in the Peyer's patches induced CCR9 expression on T and B cells through production of retinoic acid [22, 23]. Given that cecum patch-dendritic cells induce not only CCR9 but also CCR10 [7], cecum patch-dendritic cells might produce not only retinoic acid for the induction of CCR9 but also another factor for CCR10. However, it remains unclear what tissue tropism inducing molecules are involved in the induction of CCR10. G-protein-coupled receptor (GPR)15 is another homing receptor to the large intestine [24]. In contrast to CCR9, the expression of GPR15 is induced by transforming growth factor (TGF)β1, but not retinoic acid [24]. Therefore, it is likely that cecum patch dendritic cells can induce the expression of GPR15 on lymphocytes though production of TGFβ1. Further investigation is needed to reveal the different immunological properties of dendritic cells reside in the cecum patches and Peyer's patches.

Mesenteric lymph nodes (MLNs) are draining lymph nodes of the gut. There are anatomical segregation of lymphatic drainage from the small and large intestine [25–29]. Among the MLN chain, the central nodes of mesenteric lymph nodes are drained from the small intestine (small intestinal MLN; sMLN), whereas the most distal nodes of the mesenteric lymph nodes are drained from the large intestine (colonic MLN; cMLN) [25–29] (Fig. 5.1a). In accordance with the digestive function of the small intestine, fed antigens were absorbed and presented in the sMLN, but not cMLN [28]. As small intestine encounters much amounts of food antigens for digestion and absorption than large intestine [30, 31], immune responses initiated in the sMLN may tend to exert immune tolerance rather than active immune responses to fed antigens which are necessary for the host subsistence. In this context, it is reasonable that dendritic cells from the sMLN possessed higher aldehyde dehydrogenase activity than that from the cMLN [28, 29], as retinoic acid has been

shown to enhance the induction of Foxp3$^+$ T regulatory cells for the control of undesired hyperimmune reaction including inflammation [32, 33]. On the other hand, cMLN may tend to exert active immune responses in infection. It has been shown that mice orally inoculated with *Citrobacter rodentium* showed increased size of cMLN but not sMLN [29]. Indeed, in early phase of infection, plasmacytoid dendritic cells upregulated both CD80 and CD86 costimulatory molecules, followed by induction of IFNγ-producing Th1 cells in cMLN but not sMLN [29]. These findings suggest that differences of the lymph node drainage system between small and large intestines may reflect the necessary anatomical and biological compartmentalization of the immune responses between the two distinct regions of the gut with their respective digestive functions and surrounded microbial environments.

5.1.2 Primary Lymphoid Tissue

Primary lymphoid tissues are site of lymphocyte development, and include thymus and bone marrow in the systemic compartment [1]. In the gut, cryptopatches (also known as lymphocyte-filled villi) are identified as a tiny cell aggregation of CD3ε$^-$c-Kit$^+$ immature lymphocytes that also express interleukin-7 receptor α (IL-7Rα) and retinoic acid receptor-related orphan receptor (ROR)γt in the crypt lamina propria of murine but not human small and large intestine (Fig. 5.1a, b) [9, 34–36]. Generally, ~1500 and ~150 cryptopatches are present in mouse small and large intestine, respectively [34]. Cryptopatch cells have been shown to give rise to thymus-independent T cells but not B cells in the limited compartment of intestinal intraepithelial lymphocytes and MLNs [37, 38]. Indeed, cryptopatch cells showed gene expression of pre-Tα [39] that is expressed in immature lymphocytes before T cell receptor α gene rearrangement but is absent from mature T cells [40, 41]. In addition, gene expressions of rag-2, CD3ε, and T cell receptor gene rearrangements were detected in cryptopatches [39], suggesting the role of cryptopatches as a primary lymphoid tissue in the gut. In addition, recent papers suggested that cryptopatches serve as organizing center of isolated lymphoid follicles in response to microbial stimulations (see below) [36, 42, 43].

5.1.3 Tertiary Lymphoid Tissue

Generally, tertiary lymphoid tissues are defined as the lymphoid organ whose development is inducible in inflammatory conditions, caused by infections and autoimmune diseases [44]. In the gut, it has been shown that tertiary lymphoid tissues developed in the large intestine in response to intestinal inflammation induced by the chemical agent, dextran sodium sulfate in murine experimental system [45, 46]. The induction of tertiary lymphoid tissue development in the large intestine was also shown to be dependent on the presence of intestinal microbiota [46]. Its structure was composed of a well-developed B cell follicle with germinal center formation but lacked T cell-rich interfollicular regions; thus the structure resembled

isolated lymphoid follicles but larger in size [46]. The pathology of intestinal inflammation was ameliorated by inhibition of the development of colonic tertiary lymphoid tissue where hyperactive IgG^+ plasma cells are generated [46]. As the epithelial barrier is destroyed in dextran sodium sulfate-induced intestinal inflammation, it is likely that IgG produced by tertiary lymphoid tissue recognizes microbiota antigens in the intestine, which induces inflammation via Fc receptor-mediated pathways. In contrast to the gut, gastric mucosa generally lacks organized lymphoid tissues; however, it has been shown that infection with *Helicobacter pylori* induced the development of gastric lymphoid follicles in mice [47, 48]. This lymphoid structure in the gastric mucosa showed germinal center formation and contributed to the production of anti-*Helicobacter pylori* antibody response [47]. It is still unclear whether this antibody production regulates pathogenesis and/or protection from *Helicobacter pylori*.

5.2 Development of Lymphoid Tissues Associated with GI Mucosa

5.2.1 Prenatal Development (Peyer's Patches and Mesenteric Lymph Nodes)

Organogenesis of mouse Peyer's patches occurs during the 15 and 19 days of gestation [49] (Fig. 5.2). Human Peyer's patches also develop in the embryogenesis during the 11 and 19 weeks of gestation [50]. Developmental program of Peyer's patches is initiated by the interaction between hematopoietic lymphoid tissue inducer (LTi) cells and stromal lymphoid tissue organizer (LTo) cells which are characterized by $CD3^-CD4^+CD45^+$ and $VCAM\text{-}1^+ICAM\text{-}1^+CD45^-$, respectively (Fig. 5.3) [51]. LTi cells are a member of group 3 innate lymphoid cells, and play an essential role in the initiation of lymphoid tissue developmental programs [52]. LTi cells differentiate from fetal liver $IL\text{-}7R\alpha^+\alpha4\beta7$ $integrin^+$ precursor cells [53, 54] where it depends on the expression of transcriptional regulators, including inhibitor of DNA binding/differentiation (Id)2 [55, 56], RORγt [57, 58] and core binding factor (Cbf)β2 [59]. Cbfβ2 makes a complex with promotor-1-regulated

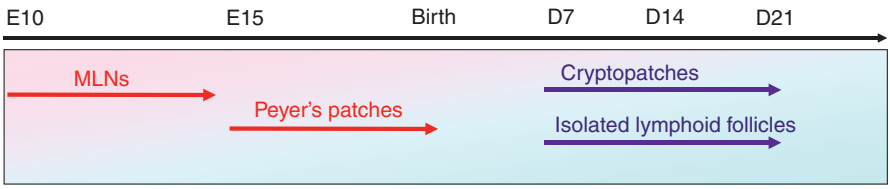

Fig. 5.2 Chronological order of pre- and postnatal development of different GALTs in mice. Each GALT has developmental time window for tissue genesis. Interaction of LTi cells and LTo cells occur in MLNs at embryonic day 10 followed by that in Peyer's patches at embryonic day 15. Cryptopatches and isolated lymphoid follicles are absent during the embryogenesis but develop at neonatal stages during 1 and 3 weeks after birth

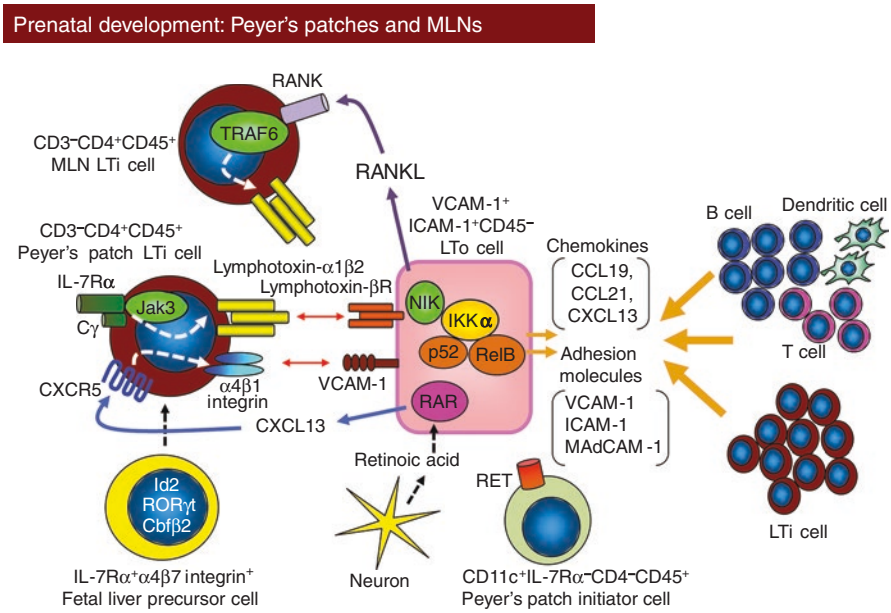

Fig. 5.3 Prenatal development of lymphoid tissues in GI mucosa. Development of Peyer's patches and mesenteric lymph nodes occur during the embryogenesis. Prenatal lymphoid tissue genesis is initiated by the interaction between $CD3^{-}CD4^{+}CD45^{+}$ LTi cells and $VCAM\text{-}1^{+}ICAM\text{-}1^{+}CD45^{-}$ LTo cells via lymphotoxin signals. LTi cells are differentiated at fetal liver in Id2-, RORγt-, and Cbfβ2-dependent manner. Peyer's patch LTi cells are activated by IL-7R-mediated signals while MLN LTi cells are activated by RANK-mediated signals for the production of membrane-bound lymphotoxin-α1β2. Neuron-derived retinoic acid and RET expression on Peyer's patch initiator cells contribute to migration of Peyer's patch LTi cells to the site of tissue genesis through induction of CXCL13 by LTo cells. LTo cells are activated via lymphotoxin-βR-mediated NIK-dependent alternative NF-κB pathway for the production of chemokines and adhesion molecules, which contribute to recruitment of conventional leukocytes as well as LTi cells

Runx1 protein, and induces RORγt transcription for differentiation of LTi cells [59]. Id2 has been shown to bind and suppress E protein transcriptional activity, and induces the differentiation of LTi cells [56]. LTi cells migrate and accumulate at the site of Peyer's patch genesis in the small intestine in a interaction between C-X-C chemokine ligand (CXCL)13 and CXCR5 dependent manner [60]. Indeed, CXCR5-mediated signal was shown to activate α4β1 integrin structure to active form on LTi cells, which ensures their stable cell-cell interaction with $VCAM\text{-}1^{+}$ LTo cells [61]. LTi cells are then activated by IL-7R-mediated signals, leading to the production of membrane-bound lymphotoxin-α1β2 [54, 62, 63], which stimulates LTo cells predominantly via lymphotoxin-βR-NIK-IKKα-dependent alternative NF-κB pathway [64–67]. The ligand(s) of IL-7Rα for the activation of LTi cells in the development of Peyer's patches are unidentified as conventional IL-7Rα ligands of IL-7 and TSLP are likely to be dispensable for the development of Peyer's patches, indicating the existence of the third ligand for IL-7Rα for Peyer's

patch development [68]. Upon activation of LTo cells, they produce abundant amount of lymphoid chemokines (e.g., CXCL13, CCL19, and CCL21) and adhesion molecules (e.g., VCAM-1, ICAM-1, and MAdCAM-1) to recruit leukocytes such as B cells, T cells, and dendritic cells for the creation of lymphoid tissue microenvironment [62, 69]. As these lymphoid chemokines (e.g., CCL19, CCL21, and CXCL13) and adhesion molecules (e.g., VCAM-1, ICAM-1, and MAdCAM-1) are also attractive to LTi cells with their phenotype of $CXCR5^+$, $CCR7^+$ as well as $\alpha4\beta1$ integrin$^+$ and $\alpha4\beta7$ integrin$^+$, the developmental program of Peyer's patches proceeds in a positive feedback manner between the inducer and organizer cells [51]. It was also uncovered the molecular and cellular mechanisms of initial expression of CXCL13 by LTo cells to recruit LTi cells. It was shown that retinoic acid produced by neurons adjacent to the lymph node anlagen stimulated LTo cells to generate initial expression of CXCL13 [70]. In addition, neuron-regulator of receptor tyrosine kinase, RET, was found to be a common key molecules for the development of mammalian enteric nerve system and Peyer's patches [71, 72] (Fig. 5.2). It was indicated that RET expression on $CD11c^+IL\text{-}7R^-CD4^-CD45^+$ Peyer's patch initiator cells might be required in LTi cell accumulation at Peyer's patch anlagen [71, 72]. These findings suggest that nervous system involves in early event of lymphoid tissue organogenesis (Fig. 5.2).

Mesenteric lymph nodes develop earlier than Peyer's patches. In mice, the cell-cell interaction of MLN-LTi cells and LTo cells are found since embryonic day 10, whereas that of Peyer's patch are embryonic day 15 [51] (Fig. 5.2). In human, LTi cells are found at 8 weeks of gestation in MLN anlagen and the tissue becomes discernable from approximately 14 weeks of gestation [73, 74]. Developmental program of MLNs follows the central dogma of Peyer's patch tissue genesis with some differences (Fig. 5.3). Thus, lymphotoxin signals provided by $CD3^-CD4^+CD45^+$ LTi cells are essential for the activation of LTo cells in the MLN anlagen, as like Peyer's patches, and following the development of MLNs [51] (Fig. 5.2). Indeed, mice lack the expression of Id2, RORγt and lymphotoxin βR show impairment of MLN organogenesis [55, 57, 58, 64]. However, it is worth noting that lymphotoxin-β-deficient mice possess MLNs but lack Peyer's patches while lymphotoxin-α-deficient mice lack both MLNs and Peyer's patches [75–78]. In the absence of lymphotoxin-β, LIGHT and TNFR1 are likely to play a compensative role in the development of MLNs [79, 80]. Further, Cbfβ2 and CXCL13/CXCR5, which plays essential role in the development of Peyer's patches, are dispensable for the development of MLNs, suggesting the presence of Cbfβ2-independent LTi cells for MLN genesis whose migration to MLN anlagen is independent of CXCL13/CXCR5 chemokine interaction [59, 60, 81, 82]. In addition, the activation of MLN-LTi cells is mediated by RANKL-RANK-TRAF6 signals [83–86], instead of the IL-7R-Jak3 signals for Peyer's patches [87–89]. Consistent with this difference, LTo cells in the MLN anlagen has been shown to produce higher level of RANKL when compared with that in Peyer's patch anlagen [90].

5.2.2 Postnatal Development (Cryptopatches and Isolated Lymphoid Follicles)

Organogenesis of cryptopatches and isolated lymphoid follicles resembles in that it occurs after birth. Cryptopatches develop during 1 and 3 weeks after birth [8, 34]. In addition, both of the tissue development proceeds in the absence of influence from microbial stimulations [8, 34]. As like Peyer's patches, it has been shown that the expression of RORγt and IL-7R-mediated signal played essential roles in their postnatal tissue genesis [8, 34, 36]. Interestingly, lymphotoxin signals, mediated by NIK-dependent pathway, are required for the development of isolated lymphoid follicles but not cryptopatches [8, 34]. As cryptopatch cells contain RORγt-expressing LTi-like cells, it is interesting to postulate that these LTi-like cells provide NIK-mediated lymphotoxin signals for the development of isolated lymphoid follicles; therefore, it has been suggested that cryptopatches serve as an organizing center of isolated lymphoid follicles [42]. However, isolated lymphoid follicles were located in tandem on the anti-mesenteric wall of the small intestine, whereas cryptopatches were interspersed throughout the mucosa; thus, the anatomical localization is different [8]. Therefore, the mechanism for the formation of isolated lymphoid follicles from selected cryptopatches remains to be elucidated.

Isolated lymphoid follicles develop in the absence of intestinal microbiota; therefore, categorized to secondary lymphoid tissues, germinal center formation is not detected in germ-free mice [8, 43]. Thus, it is suggested that isolated lymphoid follicle possessing germinal center (or mature isolated lymphoid follicles) could be classified into a category of tertiary lymphoid tissues [42]. Organogenesis of these mature isolated lymphoid follicles from immature isolated lymphoid follicles requires both TNFR-I mediated and microbial stimulations [43, 91]. Indeed, several types of receptors and adaptor molecules involved in the recognition of bacteria-derived molecular patterns, including TLR2/4, MyD88, and NOD2, were shown to contribute to the maturation of isolated lymphoid follicles [92]. These innate receptor signals activate NF-κB pathways and induce proinflammatory cytokines such as TNFα which is essential for maturation of isolated lymphoid follicles but not formation of immature isolated lymphoid follicles [43] (Fig. 5.4). NOD1, on the other hand, played an important role in the formation of immature isolated lymphoid follicles [92] (Fig. 5.4). NOD1 was expressed in the small intestinal epithelial cells and its activation induced the secretion of CCL20 and β-defensin 3, both factors are ligands for CCR6 which is essential chemokine receptor for the development of immature isolated lymphoid follicles [92, 93]. CCR6 is preferentially expressed on intestinal B cells and LTi-like cells in the cryptopatches [93–95]. Indeed, B cell expression of CCR6 was shown to be essential for the development of immature isolated lymphoid follicles as B cells were inefficient at localizing to the intestine in the absence of CCR6 [93]. The role of CCR6 expression on LTi-like cells in the development of immature isolated lymphoid follicles remains unclear.

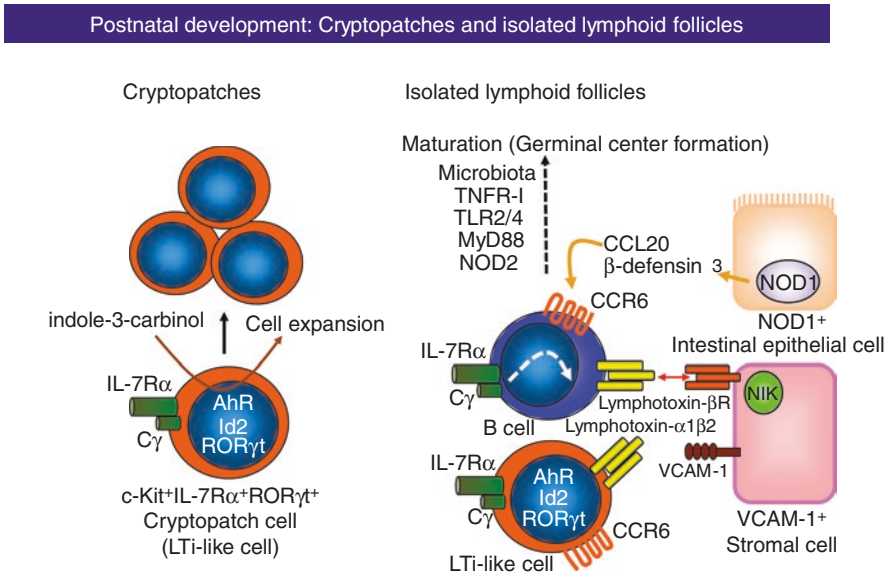

Fig. 5.4 Postnatal development of lymphoid tissues in GI mucosa. Development of cryptopatches and isolated lymphoid follicles occur after birth. In cryptopatches, indole-3-carbinol, a plant-derived ligand for AhR, induces expansion of RORγt+ LTi-like cells for the development of cryptopatches. In isolated lymphoid follicles, RORγt+ LTi-like cells and B cells provide lymphotoxin-α1β2 signals for the development of immature isolated lymphoid follicles. Activation of NOD1 induces the production of CCL20 and β-defensin 3, which recruit CCR6+ B cells. For maturation of isolated lymphoid follicles that contain germinal center formation, microbial stimulation is required through recognition by TLR2/4, MyD88 and NOD2 innate receptors and signaling pathways, which lead to production of TNFα

Organogenesis of cryptopatches and isolated lymphoid follicles are also regulated by dietary materials; signals mediated by aryl hydrocarbon receptor (AhR) (Fig. 5.4). AhR is a ligand-inducible transcription factor, and the ligands include dietary flavonoids and glucosinolates as well as environmental toxins such as dioxin [96]. Mice deficient in AhR or mice fed with phytochemical-free diets lacked the development of cryptopatches and isolated lymphoid follicles but possessed normal Peyer's patches [96, 97]. Indeed, activation of AhR was required for postnatal expansion of LTi-like cells through induction of the expression of Kit [96]. Supplementation of indole-3-carbinol, which is an AhR ligand and hydrolytic product of the glucose glucobrassicin contained in plants of the *Brassicaceae* family (e.g., broccoli and Brussels sprouts) to phytochemical-free diets recovered the organogenesis of cryptopatches and isolated lymphoid follicles through activation of AhR and induction of the expansion of LTi-like cells, suggesting that dietary materials are key factor in the induction and control of postnatal development of intestinal lymphoid tissues [96].

5.3 Concluding Remarks

GI mucosa is equipped with various types of mucosa-associated lymphoid tissues whose function and developmental program show similarity with individual unique features based on their respective anatomical and surrounded environmental characteristics. Accumulating evidences suggest that lymphoid tissues associated with small and large intestines are not only anatomically but also immunologically segregated and possessed their unique biological characteristics in order to execute their distinct role as the gut-associated organized lymphoid tissue. GI mucosa-draining MLNs are classified into sMLN and cMLN which drains small and large intestine, respectively, for the induction of appropriate immune responses. Developmental pathways of prenatal lymphoid tissues (e.g., Peyer's patches and MLNs) and postnatal lymphoid tissues (e.g., cryptopatches and isolated lymphoid follicles) are differently controlled as the development of prenatal lymphoid tissues proceed without outside environmental stimulation whereas that of postnatal lymphoid tissues can be regulated and fine-tuned by various kinds of environmental stimulation such as dietary materials and microbiota. Nonetheless, Id2- and RORγt-dependent prenatal LTi cells and postnatal LTi-like cells play central roles in the induction and regulation of GALTs. Better understanding for organogenesis of GALTs will provide fundamental information for the development of successful mucosal vaccines by induction and/or inhibition of respective GALT genesis.

References

1. Pabst R. Plasticity and heterogeneity of lymphoid organs. What are the criteria to call a lymphoid organ primary, secondary or tertiary? Immunol Lett. 2007;112(1):1–8. https://doi.org/10.1016/j.imlet.2007.06.009.
2. Turley SJ, Fletcher AL, Elpek KG. The stromal and haematopoietic antigen-presenting cells that reside in secondary lymphoid organs. Nat Rev Immunol. 2010;10(12):813–25. https://doi.org/10.1038/nri2886.
3. Kunisawa J, Nochi T, Kiyono H. Immunological commonalities and distinctions between airway and digestive immunity. Trends Immunol. 2008;29(11):505–13. https://doi.org/10.1016/j.it.2008.07.008.
4. Mizoguchi A, Mizoguchi E, Chiba C, Bhan AK. Role of appendix in the development of inflammatory bowel disease in TCR-α mutant mice. J Exp Med. 1996;184(2):707–15.
5. Baptista AP, Olivier BJ, Goverse G, Greuter M, Knippenberg M, Kusser K, et al. Colonic patch and colonic SILT development are independent and differentially regulated events. Mucosal Immunol. 2013;6(3):511–21. https://doi.org/10.1038/mi.2012.90.
6. O'Leary AD, Sweeney EC. Lymphoglandular complexes of the colon: structure and distribution. Histopathology. 1986;10(3):267–83.
7. Masahata K, Umemoto E, Kayama H, Kotani M, Nakamura S, Kurakawa T, et al. Generation of colonic IgA-secreting cells in the caecal patch. Nat Commun. 2014;5:3704. https://doi.org/10.1038/ncomms4704.
8. Hamada H, Hiroi T, Nishiyama Y, Takahashi H, Masunaga Y, Hachimura S, et al. Identification of multiple isolated lymphoid follicles on the antimesenteric wall of the mouse small intestine. J Immunol. 2002;168(1):57–64.

9. Moghaddami M, Cummins A, Mayrhofer G. Lymphocyte-filled villi: comparison with other lymphoid aggregations in the mucosa of the human small intestine. Gastroenterology. 1998;115(6):1414–25.
10. Dohi T, Fujihashi K, Rennert PD, Iwatani K, Kiyono H, McGhee JR. Hapten-induced colitis is associated with colonic patch hypertrophy and T helper cell 2-type responses. J Exp Med. 1999;189(8):1169–80.
11. Owen RL. Sequential uptake of horseradish peroxidase by lymphoid follicle epithelium of Peyer's patches in the normal unobstructed mouse intestine: an ultrastructural study. Gastroenterology. 1977;72(3):440–51.
12. Clark MA, Jepson MA, Simmons NL, Hirst BH. Differential surface characteristics of M cells from mouse intestinal Peyer's and caecal patches. Histochem J. 1994;26(3):271–80.
13. Kweon MN, Yamamoto M, Rennert PD, Park EJ, Lee AY, Chang SY, et al. Prenatal blockage of lymphotoxin β receptor and TNF receptor p55 signaling cascade resulted in the acceleration of tissue genesis for isolated lymphoid follicles in the large intestine. J Immunol. 2005;174(7):4365–72.
14. Mabbott NA, Donaldson DS, Ohno H, Williams IR, Mahajan A. Microfold (M) cells: important immunosurveillance posts in the intestinal epithelium. Mucosal Immunol. 2013;6(4):666–77. https://doi.org/10.1038/mi.2013.30.
15. Terahara K, Yoshida M, Igarashi O, Nochi T, Pontes GS, Hase K, et al. Comprehensive gene expression profiling of Peyer's patch M cells, villous M-like cells, and intestinal epithelial cells. J Immunol. 2008;180(12):7840–6.
16. Nakato G, Fukuda S, Hase K, Goitsuka R, Cooper MD, Ohno H. New approach for m-cell-specific molecules screening by comprehensive transcriptome analysis. DNA Res. 2009;16(4):227–35. https://doi.org/10.1093/dnares/dsp013.
17. Hase K, Kawano K, Nochi T, Pontes GS, Fukuda S, Ebisawa M, et al. Uptake through glycoprotein 2 of FimH(+) bacteria by M cells initiates mucosal immune response. Nature. 2009;462(7270):226–30. https://doi.org/10.1038/nature08529.
18. Nakato G, Hase K, Suzuki M, Kimura M, Ato M, Hanazato M, et al. Cutting Edge: Brucella abortus exploits a cellular prion protein on intestinal M cells as an invasive receptor. J Immunol. 2012;189(4):1540–4. https://doi.org/10.4049/jimmunol.1103332.
19. Tsuji M, Suzuki K, Kitamura H, Maruya M, Kinoshita K, Ivanov II, et al. Requirement for lymphoid tissue-inducer cells in isolated follicle formation and T cell-independent immunoglobulin A generation in the gut. Immunity. 2008;29(2):261–71. https://doi.org/10.1016/j.immuni.2008.05.014.
20. Pabst O, Ohl L, Wendland M, Wurbel MA, Kremmer E, Malissen B, et al. Chemokine receptor CCR9 contributes to the localization of plasma cells to the small intestine. J Exp Med. 2004;199(3):411–6. https://doi.org/10.1084/jem.20030996.
21. Hu S, Yang K, Yang J, Li M, Xiong N. Critical roles of chemokine receptor CCR10 in regulating memory IgA responses in intestines. Proc Natl Acad Sci U S A. 2011;108(45):E1035–44. https://doi.org/10.1073/pnas.1100156108.
22. Iwata M, Hirakiyama A, Eshima Y, Kagechika H, Kato C, Song SY. Retinoic acid imprints gut-homing specificity on T cells. Immunity. 2004;21(4):527–38. https://doi.org/10.1016/j.immuni.2004.08.011.
23. Mora JR, Iwata M, Eksteen B, Song SY, Junt T, Senman B, et al. Generation of gut-homing IgA-secreting B cells by intestinal dendritic cells. Science. 2006;314(5802):1157–60. https://doi.org/10.1126/science.1132742.
24. Kim SV, Xiang WV, Kwak C, Yang Y, Lin XW, Ota M, et al. GPR15-mediated homing controls immune homeostasis in the large intestine mucosa. Science. 2013;340(6139):1456–9. https://doi.org/10.1126/science.1237013.
25. Tilney NL. Patterns of lymphatic drainage in the adult laboratory rat. J Anat. 1971;109(Pt 3):369–83.
26. Carter PB, Collins FM. The route of enteric infection in normal mice. J Exp Med. 1974;139(5):1189–203.

27. Van den Broeck W, Derore A, Simoens P. Anatomy and nomenclature of murine lymph nodes: descriptive study and nomenclatory standardization in BALB/cAnNCrl mice. J Immunol Methods. 2006;312(1–2):12–9. https://doi.org/10.1016/j.jim.2006.01.022.
28. Houston SA, Cerovic V, Thomson C, Brewer J, Mowat AM, Milling S. The lymph nodes draining the small intestine and colon are anatomically separate and immunologically distinct. Mucosal Immunol. 2016;9(2):468–78. https://doi.org/10.1038/mi.2015.77.
29. Toivonen R, Kong L, Rasool O, Lund RJ, Lahesmaa R, Hanninen A. Activation of plasmacytoid dendritic cells in colon-draining lymph nodes during citrobacter rodentium infection involves pathogen-sensing and inflammatory pathways distinct from conventional dendritic cells. J Immunol. 2016;196(11):4750–9. https://doi.org/10.4049/jimmunol.1600235.
30. Spiller RC. Intestinal absorptive function. Gut. 1994;35(1 Suppl):S5–9.
31. Nordgaard I, Mortensen PB. Digestive processes in the human colon. Nutrition. 1995;11(1):37–45.
32. Coombes JL, Siddiqui KR, Arancibia-Carcamo CV, Hall J, Sun CM, Belkaid Y, et al. A functionally specialized population of mucosal CD103$^+$ DCs induces Foxp3$^+$ regulatory T cells via a TGF-β and retinoic acid-dependent mechanism. J Exp Med. 2007;204(8):1757–64. https://doi.org/10.1084/jem.20070590.
33. Sun CM, Hall JA, Blank RB, Bouladoux N, Oukka M, Mora JR, et al. Small intestine lamina propria dendritic cells promote de novo generation of Foxp3 T reg cells via retinoic acid. J Exp Med. 2007;204(8):1775–85. https://doi.org/10.1084/jem.20070602.
34. Kanamori Y, Ishimaru K, Nanno M, Maki K, Ikuta K, Nariuchi H, et al. Identification of novel lymphoid tissues in murine intestinal mucosa where clusters of c-kit$^+$ IL-7R$^+$ Thy1$^+$ lymphohemopoietic progenitors develop. J Exp Med. 1996;184(4):1449–59.
35. Hitotsumatsu O, Hamada H, Naganuma M, Inoue N, Ishii H, Hibi T, et al. Identification and characterization of novel gut-associated lymphoid tissues in rat small intestine. J Gastroenterol. 2005;40(10):956–63. https://doi.org/10.1007/s00535-005-1679-8.
36. Eberl G, Littman DR. Thymic origin of intestinal alphabeta T cells revealed by fate mapping of RORγt$^+$ cells. Science. 2004;305(5681):248–51. https://doi.org/10.1126/science.1096472.
37. Saito H, Kanamori Y, Takemori T, Nariuchi H, Kubota E, Takahashi-Iwanaga H, et al. Generation of intestinal T cells from progenitors residing in gut cryptopatches. Science. 1998;280(5361):275–8.
38. Suzuki K, Oida T, Hamada H, Hitotsumatsu O, Watanabe M, Hibi T, et al. Gut cryptopatches: direct evidence of extrathymic anatomical sites for intestinal T lymphopoiesis. Immunity. 2000;13(5):691–702.
39. Oida T, Suzuki K, Nanno M, Kanamori Y, Saito H, Kubota E, et al. Role of gut cryptopatches in early extrathymic maturation of intestinal intraepithelial T cells. J Immunol. 2000;164(7):3616–26.
40. Bruno L, Rocha B, Rolink A, von Boehmer H, Rodewald HR. Intra- and extra-thymic expression of the pre-T cell receptor alpha gene. Eur J Immunol. 1995;25(7):1877–82. https://doi.org/10.1002/eji.1830250713.
41. Fehling HJ, Krotkova A, Saint-Ruf C, von Boehmer H. Crucial role of the pre-T-cell receptor α gene in development of αβ but not γδT cells. Nature. 1995;375(6534):795–8. https://doi.org/10.1038/375795a0.
42. Eberl G. Inducible lymphoid tissues in the adult gut: recapitulation of a fetal developmental pathway? Nat Rev Immunol. 2005;5(5):413–20. https://doi.org/10.1038/nri1600.
43. Lorenz RG, Chaplin DD, McDonald KG, McDonough JS, Newberry RD. Isolated lymphoid follicle formation is inducible and dependent upon lymphotoxin-sufficient B lymphocytes, lymphotoxin β receptor, and TNF receptor I function. J Immunol. 2003;170(11):5475–82.
44. Aloisi F, Pujol-Borrell R. Lymphoid neogenesis in chronic inflammatory diseases. Nat Rev Immunol. 2006;6(3):205–17. https://doi.org/10.1038/nri1786.
45. Spahn TW, Herbst H, Rennert PD, Lugering N, Maaser C, Kraft M, et al. Induction of colitis in mice deficient of Peyer's patches and mesenteric lymph nodes is associated with increased disease severity and formation of colonic lymphoid patches. Am J Pathol. 2002;161(6):2273–82. https://doi.org/10.1016/s0002-9440(10)64503-8.

46. Lochner M, Ohnmacht C, Presley L, Bruhns P, Si-Tahar M, Sawa S, et al. Microbiota-induced tertiary lymphoid tissues aggravate inflammatory disease in the absence of RORγt and LTi cells. J Exp Med. 2011;208(1):125–34. https://doi.org/10.1084/jem.20100052.
47. Oshima C, Okazaki K, Matsushima Y, Sawada M, Chiba T, Takahashi K, et al. Induction of follicular gastritis following postthymectomy autoimmune gastritis in Helicobacter pylori-infected BALB/c mice. Infect Immun. 2000;68(1):100–6.
48. Shiu J, Piazuelo MB, Ding H, Czinn SJ, Drakes ML, Banerjee A, et al. Gastric LTi cells promote lymphoid follicle formation but are limited by IRAK-M and do not alter microbial growth. Mucosal Immunol. 2015;8(5):1047–59. https://doi.org/10.1038/mi.2014.132.
49. Adachi S, Yoshida H, Kataoka H, Nishikawa S. Three distinctive steps in Peyer's patch formation of murine embryo. Int Immunol. 1997;9(4):507–14.
50. Spencer J, MacDonald TT, Finn T, Isaacson PG. The development of gut associated lymphoid tissue in the terminal ileum of fetal human intestine. Clin Exp Immunol. 1986;64(3):536–43.
51. Mebius RE. Organogenesis of lymphoid tissues. Nat Rev Immunol. 2003;3(4):292–303. https://doi.org/10.1038/nri1054.
52. Bar-Ephraim YE, Mebius RE. Innate lymphoid cells in secondary lymphoid organs. Immunol Rev. 2016;271(1):185–99. https://doi.org/10.1111/imr.12407.
53. Mebius RE, Miyamoto T, Christensen J, Domen J, Cupedo T, Weissman IL, et al. The fetal liver counterpart of adult common lymphoid progenitors gives rise to all lymphoid lineages, $CD45^+CD4^+CD3^-$ cells, as well as macrophages. J Immunol. 2001;166(11):6593–601.
54. Yoshida H, Kawamoto H, Santee SM, Hashi H, Honda K, Nishikawa S, et al. Expression of α4β7 integrin defines a distinct pathway of lymphoid progenitors committed to T cells, fetal intestinal lymphotoxin producer, NK, and dendritic cells. J Immunol. 2001;167(5):2511–21.
55. Yokota Y, Mansouri A, Mori S, Sugawara S, Adachi S, Nishikawa S, et al. Development of peripheral lymphoid organs and natural killer cells depends on the helix-loop-helix inhibitor Id2. Nature. 1999;397(6721):702–6. https://doi.org/10.1038/17812.
56. Boos MD, Yokota Y, Eberl G, Kee BL. Mature natural killer cell and lymphoid tissue-inducing cell development requires Id2-mediated suppression of E protein activity. J Exp Med. 2007;204(5):1119–30. https://doi.org/10.1084/jem.20061959.
57. Sun Z, Unutmaz D, Zou YR, Sunshine MJ, Pierani A, Brenner-Morton S, et al. Requirement for RORγ in thymocyte survival and lymphoid organ development. Science. 2000;288(5475):2369–73.
58. Eberl G, Marmon S, Sunshine MJ, Rennert PD, Choi Y, Littman DR. An essential function for the nuclear receptor RORγt in the generation of fetal lymphoid tissue inducer cells. Nat Immunol. 2004;5(1):64–73. https://doi.org/10.1038/ni1022.
59. Tachibana M, Tenno M, Tezuka C, Sugiyama M, Yoshida H, Taniuchi I. Runx1/Cbfβ2 complexes are required for lymphoid tissue inducer cell differentiation at two developmental stages. J Immunol. 2011;186(3):1450–7. https://doi.org/10.4049/jimmunol.1000162.
60. Fukuyama S, Nagatake T, Kim DY, Takamura K, Park EJ, Kaisho T, et al. Cutting edge: uniqueness of lymphoid chemokine requirement for the initiation and maturation of nasopharynx-associated lymphoid tissue organogenesis. J Immunol. 2006;177(7):4276–80.
61. Finke D, Acha-Orbea H, Mattis A, Lipp M, Kraehenbuhl J. $CD4^+CD3^-$ cells induce Peyer's patch development: role of α4β1 integrin activation by CXCR5. Immunity. 2002;17(3):363–73.
62. Honda K, Nakano H, Yoshida H, Nishikawa S, Rennert P, Ikuta K, et al. Molecular basis for hematopoietic/mesenchymal interaction during initiation of Peyer's patch organogenesis. J Exp Med. 2001;193(5):621–30.
63. Yoshida H, Naito A, Inoue J, Satoh M, Santee-Cooper SM, Ware CF, et al. Different cytokines induce surface lymphotoxin-αβ on IL-7 receptor-α cells that differentially engender lymph nodes and Peyer's patches. Immunity. 2002;17(6):823–33.
64. Futterer A, Mink K, Luz A, Kosco-Vilbois MH, Pfeffer K. The lymphotoxin β receptor controls organogenesis and affinity maturation in peripheral lymphoid tissues. Immunity. 1998;9(1):59–70.

65. Shinkura R, Kitada K, Matsuda F, Tashiro K, Ikuta K, Suzuki M, et al. Alymphoplasia is caused by a point mutation in the mouse gene encoding Nf-κ b-inducing kinase. Nat Genet. 1999;22(1):74–7. https://doi.org/10.1038/8780.
66. Yin L, Wu L, Wesche H, Arthur CD, White JM, Goeddel DV, et al. Defective lymphotoxin-β receptor-induced NF-κB transcriptional activity in NIK-deficient mice. Science. 2001;291(5511):2162–5. https://doi.org/10.1126/science.1058453.
67. Matsushima A, Kaisho T, Rennert PD, Nakano H, Kurosawa K, Uchida D, et al. Essential role of nuclear factor (NF)-κB-inducing kinase and inhibitor of κB (IκB) kinase α in NF-κB activation through lymphotoxin β receptor, but not through tumor necrosis factor receptor I. J Exp Med. 2001;193(5):631–6.
68. Nishikawa S, Honda K, Vieira P, Yoshida H. Organogenesis of peripheral lymphoid organs. Immunol Rev. 2003;195:72–80.
69. Ngo VN, Korner H, Gunn MD, Schmidt KN, Riminton DS, Cooper MD, et al. Lymphotoxin α/β and tumor necrosis factor are required for stromal cell expression of homing chemokines in B and T cell areas of the spleen. J Exp Med. 1999;189(2):403–12.
70. van de Pavert SA, Olivier BJ, Goverse G, Vondenhoff MF, Greuter M, Beke P, et al. Chemokine CXCL13 is essential for lymph node initiation and is induced by retinoic acid and neuronal stimulation. Nat Immunol. 2009;10(11):1193–9. https://doi.org/10.1038/ni.1789.
71. Veiga-Fernandes H, Coles MC, Foster KE, Patel A, Williams A, Natarajan D, et al. Tyrosine kinase receptor RET is a key regulator of Peyer's patch organogenesis. Nature. 2007;446(7135):547–51. https://doi.org/10.1038/nature05597.
72. Fukuyama S, Kiyono H. Neuroregulator RET initiates Peyer's-patch tissue genesis. Immunity. 2007;26(4):393–5. https://doi.org/10.1016/j.immuni.2007.04.004.
73. Kyriazis AA, Esterly JR. Development of lymphoid tissues in the human embryo and early fetus. Arch Pathol. 1970;90(4):348–53.
74. Cupedo T, Crellin NK, Papazian N, Rombouts EJ, Weijer K, Grogan JL, et al. Human fetal lymphoid tissue-inducer cells are interleukin 17-producing precursors to $RORC^{+}$ $CD127^{+}$ natural killer-like cells. Nat Immunol. 2009;10(1):66–74. https://doi.org/10.1038/ni.1668.
75. De Togni P, Goellner J, Ruddle NH, Streeter PR, Fick A, Mariathasan S, et al. Abnormal development of peripheral lymphoid organs in mice deficient in lymphotoxin. Science. 1994;264(5159):703–7.
76. Banks TA, Rouse BT, Kerley MK, Blair PJ, Godfrey VL, Kuklin NA, et al. Lymphotoxin-α-deficient mice. Effects on secondary lymphoid organ development and humoral immune responsiveness. J Immunol. 1995;155(4):1685–93.
77. Koni PA, Sacca R, Lawton P, Browning JL, Ruddle NH, Flavell RA. Distinct roles in lymphoid organogenesis for lymphotoxins α and β revealed in lymphotoxin β-deficient mice. Immunity. 1997;6(4):491–500.
78. Alimzhanov MB, Kuprash DV, Kosco-Vilbois MH, Luz A, Turetskaya RL, Tarakhovsky A, et al. Abnormal development of secondary lymphoid tissues in lymphotoxin β-deficient mice. Proc Natl Acad Sci U S A. 1997;94(17):9302–7.
79. Scheu S, Alferink J, Potzel T, Barchet W, Kalinke U, Pfeffer K. Targeted disruption of LIGHT causes defects in costimulatory T cell activation and reveals cooperation with lymphotoxin β in mesenteric lymph node genesis. J Exp Med. 2002;195(12):1613–24.
80. Koni PA, Flavell RA. A role for tumor necrosis factor receptor type 1 in gut-associated lymphoid tissue development: genetic evidence of synergism with lymphotoxin β. J Exp Med. 1998;187(12):1977–83.
81. Forster R, Mattis AE, Kremmer E, Wolf E, Brem G, Lipp M. A putative chemokine receptor, BLR1, directs B cell migration to defined lymphoid organs and specific anatomic compartments of the spleen. Cell. 1996;87(6):1037–47.
82. Ansel KM, Ngo VN, Hyman PL, Luther SA, Forster R, Sedgwick JD, et al. A chemokine-driven positive feedback loop organizes lymphoid follicles. Nature. 2000;406(6793):309–14. https://doi.org/10.1038/35018581.

83. Kim D, Mebius RE, MacMicking JD, Jung S, Cupedo T, Castellanos Y, et al. Regulation of peripheral lymph node genesis by the tumor necrosis factor family member TRANCE. J Exp Med. 2000;192(10):1467–78.
84. Kong YY, Yoshida H, Sarosi I, Tan HL, Timms E, Capparelli C, et al. OPGL is a key regulator of osteoclastogenesis, lymphocyte development and lymph-node organogenesis. Nature. 1999;397(6717):315–23. https://doi.org/10.1038/16852.
85. Dougall WC, Glaccum M, Charrier K, Rohrbach K, Brasel K, De Smedt T, et al. RANK is essential for osteoclast and lymph node development. Genes Dev. 1999;13(18):2412–24.
86. Naito A, Azuma S, Tanaka S, Miyazaki T, Takaki S, Takatsu K, et al. Severe osteopetrosis, defective interleukin-1 signalling and lymph node organogenesis in TRAF6-deficient mice. Genes Cells. 1999;4(6):353–62.
87. Adachi S, Yoshida H, Honda K, Maki K, Saijo K, Ikuta K, et al. Essential role of IL-7 receptor α in the formation of Peyer's patch anlage. Int Immunol. 1998;10(1):1–6.
88. Cao X, Shores EW, Hu-Li J, Anver MR, Kelsall BL, Russell SM, et al. Defective lymphoid development in mice lacking expression of the common cytokine receptor γ chain. Immunity. 1995;2(3):223–38.
89. Park SY, Saijo K, Takahashi T, Osawa M, Arase H, Hirayama N, et al. Developmental defects of lymphoid cells in Jak3 kinase-deficient mice. Immunity. 1995;3(6):771–82.
90. Okuda M, Togawa A, Wada H, Nishikawa S. Distinct activities of stromal cells involved in the organogenesis of lymph nodes and Peyer's patches. J Immunol. 2007;179(2):804–11.
91. McDonald KG, McDonough JS, Newberry RD. Adaptive immune responses are dispensable for isolated lymphoid follicle formation: antigen-naive, lymphotoxin-sufficient B lymphocytes drive the formation of mature isolated lymphoid follicles. J Immunol. 2005;174(9):5720–8.
92. Bouskra D, Brezillon C, Berard M, Werts C, Varona R, Boneca IG, et al. Lymphoid tissue genesis induced by commensals through NOD1 regulates intestinal homeostasis. Nature. 2008;456(7221):507–10. https://doi.org/10.1038/nature07450.
93. McDonald KG, McDonough JS, Wang C, Kucharzik T, Williams IR, Newberry RD. CC chemokine receptor 6 expression by B lymphocytes is essential for the development of isolated lymphoid follicles. Am J Pathol. 2007;170(4):1229–40. https://doi.org/10.2353/ajpath.2007.060817.
94. Lugering A, Kucharzik T, Soler D, Picarella D, Hudson JT 3rd, Williams IR. Lymphoid precursors in intestinal cryptopatches express CCR6 and undergo dysregulated development in the absence of CCR6. J Immunol. 2003;171(5):2208–15.
95. Lugering A, Ross M, Sieker M, Heidemann J, Williams IR, Domschke W, et al. CCR6 identifies lymphoid tissue inducer cells within cryptopatches. Clin Exp Immunol. 2010;160(3):440–9. https://doi.org/10.1111/j.1365-2249.2010.04103.x.
96. Kiss EA, Vonarbourg C, Kopfmann S, Hobeika E, Finke D, Esser C, et al. Natural aryl hydrocarbon receptor ligands control organogenesis of intestinal lymphoid follicles. Science. 2011;334(6062):1561–5. https://doi.org/10.1126/science.1214914.
97. Lee JS, Cella M, McDonald KG, Garlanda C, Kennedy GD, Nukaya M, et al. AHR drives the development of gut ILC22 cells and postnatal lymphoid tissues via pathways dependent on and independent of Notch. Nat Immunol. 2011;13(2):144–51. https://doi.org/10.1038/ni.2187.

6 Nonclinical Imaging Studies for the Diagnosis of Lymph Node Metastases

Kazunobu Ohnuki and Hirofumi Fujii

Abstract

Nonclinical studies using animal models are essential to elucidate the pathogenesis of lymph node metastases and the application of imaging tests in this research field is very important because these tests can yield reliable results at the sacrifice of minimal number of animals.

Animal models and imaging modalities must be carefully selected to obtain fruitful results. Recently, imaging devices dedicated for small animal tests have been developed for various kinds of imaging modalities including combined scanners and they have contributed to the improvement of the quality of images of metastatic lesions in lymph nodes.

In the imaging study of lymph node metastases, direct detection of metastatic foci in lymph nodes is ideal. But, it is often difficult because early stages of metastatic lesions are too small to depict. Sentinel node mapping is an alternative way to diagnose small metastatic lesions in regional lymph nodes. Since new imaging modalities including optical imaging are recently proposed to identify sentinel nodes, nonclinical animal experiments to investigate these new imaging tests are attracting attentions of researchers.

Another idea to detect small metastatic foci is to observe the change in non-tumor areas of metastatic lymph nodes. As recent animal models can simulate tumor microenvironments in human tumors well, visualization of functional information inside lymph nodes such as immunological response in sentinel nodes is expected.

Keywords

Lymph node metastases · Small animal imaging · Dedicated scanner Sentinel node

K. Ohnuki · H. Fujii (✉)
Division of Functional Imaging, Exploratory Oncology Research and Clinical Trial Center (EPOC), National Cancer Center, Kashiwa, Japan
e-mail: fujii-rad@umin.org

S. Natsugoe (ed.), *Lymph Node Metastasis in Gastrointestinal Cancer*,
https://doi.org/10.1007/978-981-10-4699-5_6

6.1 Introduction

Nonclinical studies using animal models play an important role to elucidate the pathogenesis of various kinds of disease including cancer. As for the investigation of lymph node (LN) metastases of malignant tumors, animal experiments are useful to develop methods to evaluate lymphatic flow from tumor foci and to evaluate metabolic changes inside metastatic nodes. When a good candidate of a new tracer for sentinel node (SN) mapping is successfully developed, preclinical studies to evaluate its biodistribution and toxicity are essential before starting its clinical trial.

An in vivo imaging test can provide biological information in living bodies. It is very important in biological studies because it is doubtful whether the information obtained from conventional postmortem studies can correctly express the activities inside living animals or not. Recent advance in veterinary science such as gene recombination has also enabled researchers to reproduce almost natural environments in animal models. The investigation of immune response is extremely important in researches about metastases of cancer. Now, we can have animal models with human tumor xenografts whose immune system is almost natural [1]. Under such conditions, immunological response in metastatic nodes might be experimentally evaluated.

When animal experiments are performed, it is very important to derive reliable and meaningful results from the least number of animals in the light of animal welfare. Researchers can observe the longitudinal change of same animals by examining them using in vivo imaging tests. As a result, the total number of sacrificed animals can be minimized in in vivo imaging studies because researchers do not have to dissect animals at each time point of the study. Moreover, in vivo imaging tests can enhance the preciseness of investigations because interindividual errors would be minimized by longitudinally observing same animals.

Considering these merits, the usefulness of in vivo imaging tests would be immeasurable. In this chapter, we introduce current in vivo imaging tests that are applicable to animal experiments such as computed tomography (CT), magnetic resonance imaging (MRI), nuclear medicine tests, ultrasonography (US) tests, and optical imaging tests. Recently, many kinds of imaging devices dedicated for small animal tests have been developed. The features of scanners for small animals are also mentioned. After that, we describe the usefulness of these in vivo imaging tests in researches of LN metastases [2].

6.2 Animal Models for Studies with Lymph Node Metastases

6.2.1 Types of Animal Models

Animal models that are used in experimental oncology studies are roughly classified into the following three groups: (1) transplantation models, (2) carcinogen-induced models, and (3) genetically modified models including transgenic models

Table 6.1 Classifications of preclinical animal models

Category	Characterization (description)	Advantages	Disadvantages
Transplantation models	1. The most commonly used animal models 2. Transplantation of cancer cell lines or xenografts into wild-type or immunocompetent inbred animals	1. Simple procedure and easy tumor monitoring 2. Easy-to-use (rapid assessment, reproducible and low cost)	1. Considered "poorly realistic" for multiple reasons 2. Genetically homogeneous tumor development lacks many features of spontaneously occurred tumors.
Carcinogen-induced models	1. Induced by carcinogens such as UV light and DNA-damaging agents such as DMBA and TPA	1. More realistic features such as diversity and high heterogeneity 2. Normal immune system	1. Long time to obtain 2. Difficulties in continuous tumor monitoring 3. Absence of defined genetic manipulation
Genetically modified model	1. Transgenic expression of oncogenes or the inactivation of tumor suppressor genes 2. Bring in important insights into the relationship between cancer and the immune system.	1. Accurately reflect features of human diseases 2. Yield useful insights into the interaction between malignant cells and immune effectors	1. Long time to obtain 2. Features of tumors depend on the strain of host animals. 3. Difficulties in continuous tumor monitoring 4. High cost

Modified with permission from Table 1 in Ref. [1]

[1]. Each model has both advantage and disadvantage and these are summarized in Table 6.1.

Since most commonly used in studies about LN metastases are transplantation models among them, we mainly describe this types of models in this chapter.

Transplantation models can be sub-classified from two kinds of viewpoints. In the light of the relationship between host and transplantation cells, these models can be classified into syngeneic ones and xenograft ones. In the light of transplantation sites, transplantation models can be classified into orthotropic ones and ectopic ones. The features of these models are summarized in Table 6.2.

Some animal models that are used for experiments of LN metastases are reported in mice, rats, swine, and so on. Among them, mouse models are most popular. Mouse models are generally easy to handle and there are many immunocompromised models.

Xenograft-orthotopic models and syngeneic-orthotopic models are common and some syngeneic-ectopic (mainly subcutaneous transplantation) models are also reported. Representative animal models with LN metastases are shown in Table 6.3.

When human tumor cells are examined, xenograft models whose hosts are (1) BALB/c $^{nu/nu}$ mice that are most popular nude mice, (2) severe combined immunodeficiency (SCID) ones, and (3) nonobese diabetic (NOD)/SCID ones are

Table 6.2 Classifications of tumor transplantation models

	Category	Advantages	Disadvantages
The original species	Synergic	1. Normal immune system in host animals 2. Easy-to-use (rapid assessment, reproducible and low cost)	Hard to evaluate human tumors
	Xenograft	1. Use tumor cells obtained from actual patients. Recently, patient-derived xenograft (PDX) models are actively investigated.	Expensive host animals
The transplantation sites	Orthotopic	Investigation of original features of tumor cells including tumor microenvironments would be expected.	1. High cost 2. Difficulties in tumor monitoring 3. Difficult to evaluate the tumor initiation. 4. Limited metastatic ability
	Ectopic	Transplantation site can be chosen according to the purpose of studies. The interval changes of size would be easy in subcutaneous models.	The features of tumors might be different from original ones.

Modified with permission from Ref. [3]

Table 6.3 Animal models with lymph node metastases

Mouse models					
Syngeneic-Orthotopic models					
Tumor type	Cell line	Host	Inoculation site	Lymph nodes of interest	Refs.
Colon cancer	CT26	BALB/c	Submucosal layer of the cecal wall	Mesenteric LNs	[4]
Pancreatic cancer	Pan02 6606PDA	C57BL/6	Head or tail of the pancreas	Mesenteric and peritoneal LNs	[5, 6]
Bladder tumor	MBT-2	C3H	Bladder epithelial layer	Iliac LN	[7]
Breast cancer	4T1	BALB/c	Mammary fat pad	Axillary and inguinal LNs	[8, 9]
Melanoma	B16 [F0, F1, F10]	C57BL/6	Subcutaneous	Inguinal LN	[10, 11]
Xenograft-Orthotopic models					
Gastric cancer	SGC-7901	BALB/c nu/nu	Implanted in the gastric wall (2 mm diameter pieces)	Mesenteric LNs	[12]
	OCUM-2MLN	BALB/c nude	The stomach wall of the antrum ($2 \times 10^6 - 1 \times 10^7$)	Regional LNs	[13]

Table 6.3 (continued)

	44As3, 58As1, 58As9 (Derived from HSC-44PE, HSC-58)	BALB/c nude	Implanted in the middle wall of the greater curvature of the stomach (2×10^6)	Regional LNs	[14]
Colorectal cancer	HT-29 HCT116	BALB/c nu/nu	Implanted in the cecal wall between the mucosa and the muscularis externa layers (2×10^6)	Peripancreatic, axillary and inguinal LNs	[15]
	HT-29 HCT116	CB17 SCID	1 mm^3-sized fragment implanted in the cecal wall	Regional LNs	[16]
	LS174T, HT-29	CB17 SCID	Techniques of transanal low-dose colonic mucosal electrocoagulation (1×10^6)	Mesenteric and retroperitoneal LNs	[17]
Esophageal cancer	PT1590	NMRI/nu	1 mm^3-sized fragment implanted in the abdominal esophagus	Mesenteric, coeliac, paraesophageal and axillary LN	[18]
Breast cancer	MDA-MB -231	BALB/c nu/nu	Mammary fat pad	Axillary and inguinal LN	[19]
Rat models					
Tumor type	Cell line	Host	Inoculation site	Lymph nodes of interest	Refs.
Liver hepatoma	AH130	Donryu rats	Cecum submucosa	Meso-cecum LNs	[20]
Hepatocarcinoma	He/De	Buffalo rat	Capsule of the left kidney	Parathymic LNs	[21]
Other animal models					
Animal	Cell line	Host	Inoculation site	Lymph nodes of interest	Refs.
Rabbit	VX2 squamous cell carcinoma	New Zealand white rabbits	Submucosal layer of the stomach	Intraperitoneal LN	[22]
Rabbit	VX2 squamous cell carcinoma	New Zealand white rabbits	The submucosa of the lateral wall of the pyriform sinus.	Parotid LN	[23]
Swine	(Melanoma)	Sinclair miniature swine	(Spontaneous)	Regional draining LNs	[24]
Swine	(Melanoma)	Sinclair miniature swine	(Spontaneous)	LN in the posterior neck	[25]

commonly used. Among xenograft models, orthotopic ones are recently getting popular because the interaction between tumor cells and stromal cells is attracting attention of researchers.

Cancer immunotherapies including immune checkpoint molecules such as programmed cell death-1 ligand-1 (PD-L1), programmed cell death-1 (PD-1), and cytotoxic T-lymphocyte antigen-4 (CTLA-4) are current topics. Since animal models used in researches in this field must have normal immune system, syngeneic models with normal immune system must be selected instead of immunocompromised xenograft models. A recent study reported that transplantation of human hematopoietic stem cells into NOG (NOD/Shi-*scid*, IL-2Rγ^{null}) [26] or NSG (NOD-*scid* IL2Rγ^{null}) [27] mice can simulate human immune system to some degree.

The optimal models should be selected considering the aim of researches and this is very important to investigate the pathogenesis [28].

6.2.2 The Production of Transplantation Model for Experiments of LN Metastases

When transplantation models with LN metastases are produced by injecting tumor cells in tissues, researchers must carefully inject tumor cells with minimal pressure. When cancer cells are injected in soft tissues of footpads of mice putting pressure, the pressure in tissues increases and gaps between endothelial cells of lymph channels are enlarged [29]. As a result, cancer cells can easily migrate into lymphatic vessels and move into popliteal LNs, which correspond to SNs of footpads, on nonphysiological lymphatic flow. Then, unexpected metastatic lesions can appear inside popliteal LNs.

Lymphatic flow is an important factor in experiments to identify SNs and evaluate the location of metastatic foci inside SNs [30]. When the results of experiments are sensitive to the conditions of lymphatic flow, tumor cells and/or SN-seeking probes should be slowly injected using injecting devices (Fig. 6.1).

6.3 Imaging Tests for Animal Models with Lymph Node Metastases

6.3.1 Computed Tomography (CT) Tests

In X-ray computed tomography tests, the object is irradiated from multiple directions, and X-ray signals that penetrated the object are acquired by X-ray detectors. The acquired X-ray signals are mathematically reconstructed and tomographic images of the object are obtained. CT images can provide minute anatomical information and this test is the most basic and important imaging test.

Recently, X-ray CT scanners dedicated for small animals are developed (Fig. 6.2).

Its spatial resolution is very excellent and it is usually less than 0.1 mm. But, the tissue contrast of CT images is not so good. As CT numbers of tumors and parenchymal organs are similar, it is not easy to distinguish tumors from normal

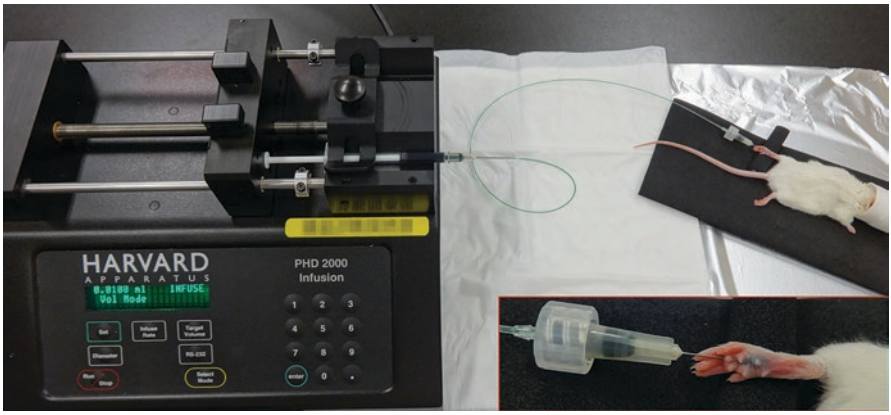

Fig. 6.1 Slow injection with constant speed by a syringe pump (Harvard Apparatus, Holliston, MA, USA)

Fig. 6.2 Preclinical CT imaging system (Latheta LCT-200; Hitachi, Tokyo, Japan)

parenchymal organs on CT images. Since CT numbers of fat and parenchymal organs are different, tumors can be depicted when they are surrounded by fat tissues. But, fat deposition between organs is not prominent in rodents and it is not easy to interpret CT images of small animals. LNs are usually depicted as small soft tissue nodules in fat tissues on CT images (Fig. 6.3).

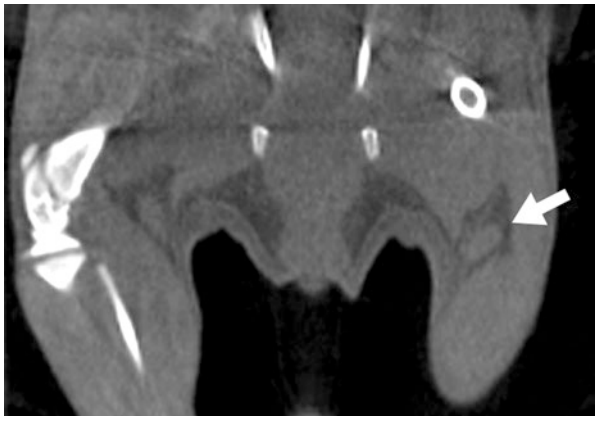

Fig. 6.3 A normal popliteal LN of a mouse in the CT image (arrow)

Contrast media including iodine compounds for small animal CT tests are now commercially available as clinical CT tests. Contrast media can contribute the diagnosis of tumors because tumors are often rich in vasculature.

6.3.2 Nuclear Medicine Tests

In nuclear medicine tests, radioactive compounds that emit gamma rays or X-rays are administered in living bodies and the biodistribution of administered agents are imaged by acquiring emitted photons by detectors, which is usually made of scintillators such as sodium iodine. But, recently, semiconductor detectors are also used.

Nuclear medicine tests are classified into two categories: (1) conventional nuclear medicine tests in which single photon emitters such as ^{99m}Tc and ^{111}In are used and (2) positron emission tomography (PET) in which positron emitters such as ^{18}F are used. Recently, dedicated scanners for small animal imaging are commercially available for both nuclear medicine tests.

In conventional nuclear medicine tests of small animal imaging, tomographic imaging called single photon emitted computed tomography (SPECT) is usually performed. The performance of SPECT scanner strongly depends on that of collimators. In clinical SPECT scanners, parallel-hole collimators are usually equipped to get good sensitivity. But, the spatial resolution of parallel-hole collimators is bad. Since the size of the object is much smaller than human bodies in small animal imaging, both excellent spatial resolution and good sensitivity, which are generally trade-off, are required in small animal imaging. To overcome this trade-off issue, unique multi-pinhole collimators are used in small animal SPECT scanners (Fig. 6.4).

Scanners with multi-pinhole collimators can show excellent spatial resolution as short as 1 mm and good sensitivity of approximately 0.1% for ^{99m}Tc [31].

In PET scanners, annihilation gamma rays produced by the collision of positron and regular electron are acquired by coincidence detectors. This detection system

Fig. 6.4 A multi-pinhole collimator for small animal SPECT imaging

enables to omit collimators from scanners and PET scanners show rather better sensitivity (>1%) than SPECT scanners.

Although both kinds of nuclear medicine tests can provide meaningful functional information of the object animals, locations where interesting reactions occur are often unclear because nuclear medicine tests can provide no anatomical information. To overcome this issue, combined scanners of nuclear medicine ones and morphological imaging ones are developed for animal imaging (Fig. 6.5).

When radiopharmaceuticals accumulate in LNs, the LNs are drawn as hot spots. SN mapping using radiocolloids is performed based on this concept. The details of this test are described in the latter section.

6.3.3 Magnetic Resonance Imaging (MRI) Tests

MRI is an imaging test in which signals induced by nuclear magnetic resonance (NMR) phenomena are visualized. When the objects are put in high magnetic fields and electric waves with special frequency are irradiated, tissue-specific signals are emitted based on NMR phenomena. MR images can be obtained by acquiring these NMR signals and mathematically reconstructing them. By changing the strength of magnetic fields and the patterns of irradiating electric waves, which is called pulse sequence, images with various kinds of tissue contrast are available. The most

Fig. 6.5 A SPECT/CT combined scanner (NanoSPECT/CT, Mediso, Budapest, Hungary)

important parameters to acquire images are repetition time (TR) and echo time (TE). By changing these two imaging parameters, various kinds of images are available. The representative images are T1-weighted image (T1WI) and T2-weighted image (T2WI).

Normal tissues show intermediate signals on both T1WIs and T2WIs (Fig. 6.6).

Compared to normal tissues, tumor lesions usually show lower signals on T1WIs and higher signals on T2WIs.

Contrast media including paramagnetic agents such as gadolinium and iron are used to enhance the contrast between tissues.

MRI tests can provide detailed anatomical information with good tissue contrast. Spatial resolution can reach less than 0.1 mm. Moreover, MRI tests can also present unique functional information about temperature, pH, and so on by modifying pulse sequences of electric waves.

Some scanners dedicated for small animal imaging are developed for MRI, too. As the diameter of the bore can be short for these animal imaging scanners, compact scanners with high magnetic fields can be manufactured (Fig. 6.7).

In MRI, image quality can be improved by using receiver coils that can be set near the target sites. When special receiver coils that fit bodies of small animals such as rodents are introduced, images of small animals with good quality can be obtained even when clinical scanners with large bores are used [32].

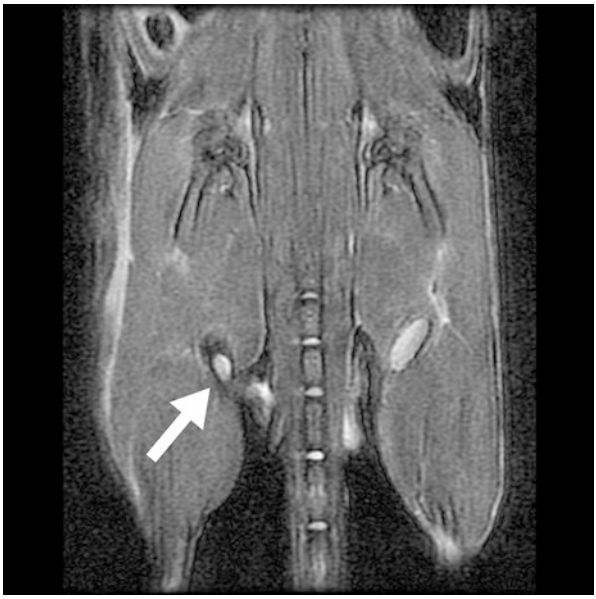

Fig. 6.6 A normal popliteal LN of a mouse on the T2WI MR image obtained by a 3.0T scanner (arrow)

Fig. 6.7 A preclinical 9.4T MR scanner (BioSpec, BRUKER, Etlingen, Germany)

6.3.4 Optical Imaging

Optical imaging is now attracting interests of researchers in the field of molecular imaging because optical imaging devices are usually more compact than other imaging devices such as CT scanners and MRI scanners and it is easy for researchers in biological fields to operate optical imaging devices (Fig. 6.8).

In optical imaging, signals from living bodies are acquired by detectors dedicated for light signals such as charge coupled device (CCD) detectors and complementary metal oxide semiconductor (CMOS) detectors. Optical agents are often administered to the animals before imaging. Previously, signals of only visual lights were observed. But, recently, optical technology has advanced and optical signals with wide range of wave lengths can be acquired. Especially, imaging of

Fig. 6.8 An in vivo optical imaging system (IVIS® Spectrum, PerkinElmer, Waltham, MA, USA)

near-infrared light signals, whose wave length is longer than 800 nm and which are invisible to human eyes, is actively investigated because little background signals are detected from living bodies in the range of wave length of near-infrared lights. That is why this range of wave length is called "biological windows." When optical imaging agents that emit fluorescent lights with this range of wave length are administered, the biodistribution of imaging agents can be depicted with good contrast to background areas of normal tissues.

Indocyanine green (ICG, Daiichi-Sankyo, Tokyo), which is a blue dye that is used for SN mapping, also emits near-infrared fluorescent signals. As this dye has already been used in routine clinical practice under the coverage of health insurance in Japan, near-infrared light imaging using this dye are investigated in many institutes (Fig. 6.9).

6.3.5 Ultrasonography (US)

US is an imaging test in which the behavior of high-frequency sound waves inside living bodies is observed. High-frequency sound waves produced by piezoelectric transducers are transmitted to the objects. Some sound waves in the objects are reflected from the layers between different tissues and some of these echoes are detected as signals. The obtained echo signals are reconstructed into images. As US imaging devices are usually compact and some devices are portable, US tests can be easily performed in regular experimental rooms (Fig. 6.10) [33].

The depth to which sound waves can reach depends on the frequency of sound waves and structure of the objects. Sound waves with high frequency can visualize the minute structure of tissues while they cannot reach deep areas. There is the trade-off between image resolution and observable depth. In small animal imaging, sound waves whose frequency was 10–50 MHz were used to visualize minute structure in small objects. Although the depth that can be observed would be limited to a few centimeters, LNs located in the superficial area can be clearly detected by US [34] (Fig. 6.11).

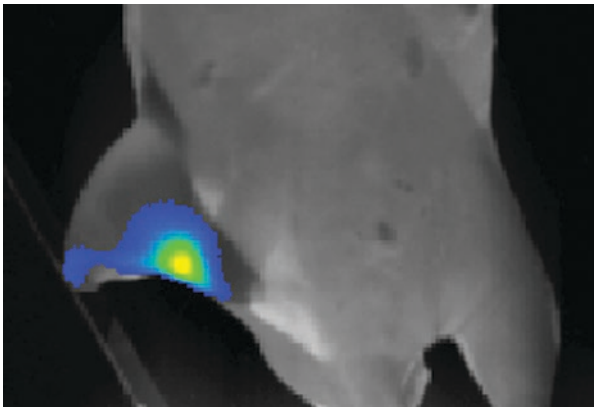

Fig. 6.9 A SN in the popliteal region of a mouse visualized by near-infrared fluorescent signal. The image was obtained after the subcutaneous injection of the ICG in the left footpad by an in vivo optical imaging system

Fig. 6.10 A high-frequency ultrasound imaging system (Vevo® 3100, FUJIFILM Visualsonics, Inc.; Toronto, Canada)

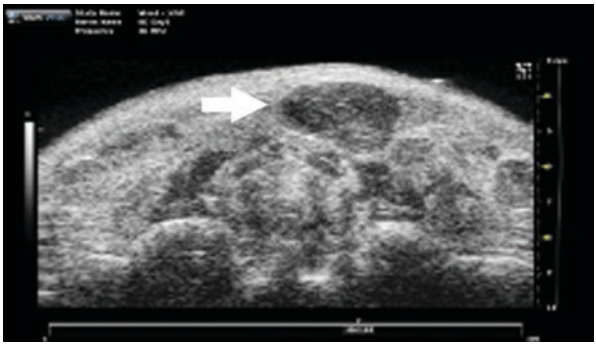

Fig. 6.11 A normal superficial cervical LN of a mouse in the ultrasound image (arrow). Reprinted with some modification with permission from Ref. [34]

There are some contrast media for US, too. Most of contrast media for US are microbubble agents made of phospholipids or carbohydrates. When these agents are administered and accumulated in the target tissues, echo signals on US images are enhanced by the increase of the reflection of sound waves.

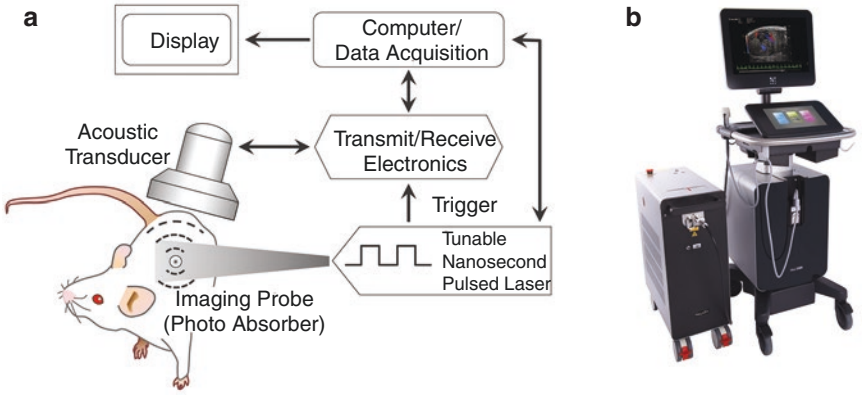

Fig. 6.12 Photoacoustic imaging (PAI) system. (**a**) Schematic diagram of PAI system. (**b**) The Vevo® LAZR Photoacoustic Imaging System (FUJIFILM Visualsonics, Inc.; Toronto, Canada)

6.3.6 Opt-acoustic (Photoacoustic) Imaging

Opt-acoustic or photoacoustic imaging is a new imaging modality although the mechanism of this imaging modality was first reported by Alexander Graham Bell, who is famous for the invention of telephone, in 1880 [35].

When light signals are delivered into the tissues, some energy of light signals is converted into heat and, finally, photoacoustic waves are induced. These phenomena are called photoacoustic effects and sound waves induced by these effects can be detected by US scanners [36] (Fig. 6.12).

According to the review article by James ML and Gambhir SS [33], opt-acoustic imaging tests have the following advantage compared with the conventional US tests: (1) the amount of imaging agent used for opt-acoustic imaging is picograms to micrograms, whereas US requires microgram to milligram amounts of imaging agent; and (2) US images contain speckles (noise) due to coherent addition of sound waves. In the case of "light in and sound out, opt-acoustic imaging" there is very minimal interference for the sound waves on their way out; therefore, the images are speckle free.

6.4 Direct Visualization of LN Metastases

6.4.1 Computed Tomography (CT)

When LNs are involved by metastatic lesions, the size of LNs increase and their shape changes to round sphere from flat ellipsoid according to the growth of metastatic lesions. CT tests can detect these morphological changes. Among them, the enlargement of the short axis of LNs can be usually the most important finding to diagnose LN metastasis. There are many reports about the size criteria on LN

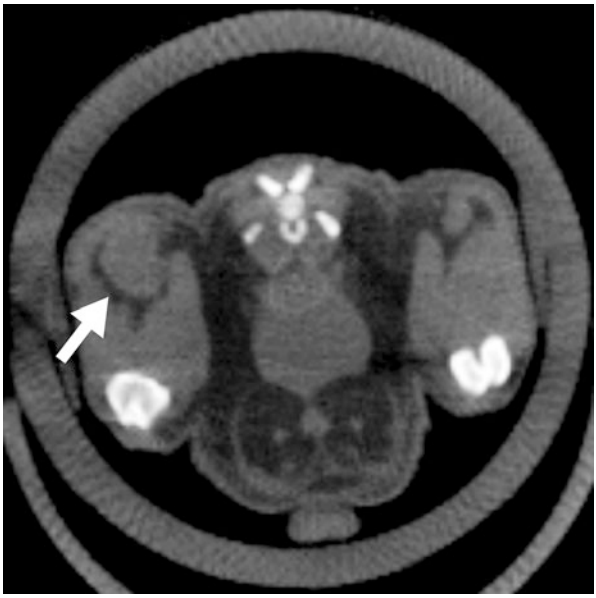

Fig. 6.13 A metastatic popliteal LN in the CT image (arrow), which is swollen compared to the contralateral one

metastases in human CT tests. For example, Dorfman, et al. reported that the normal upper limit of LN size in human upper abdomen would be 6–11 mm in human CT studies [37].

But, there are little reports about the size criteria on LN metastases in animal CT tests. As for animal studies, it would be useful to compare the size of affected LN with that of the LN on the opposite side (Fig. 6.13).

As described above, these morphological changes can occur when metastatic lesions in LNs grew to some size. It is difficult to detect early stage of metastases by CT tests.

When contrast media are administered, metastatic LNs are likely to be more strongly enhanced than normal LNs. This finding on CT tests with contrast media might improve the accuracy in the diagnosis of LN metastases. But, it is not easy to detect small LN metastases even by contrast-enhanced CT tests.

There are some other pitfalls in the diagnosis of LN metastasis by CT tests. One of the most important pitfalls is the enlargement of LNs due to inflammation. Inflamed LN can be also enlarged and round-shaped.

6.4.2 Nuclear Medicine Tests

In nuclear medicine tests, LN metastasis can be diagnosed by evaluating the functional information in LNs. The most popular nuclear medicine test to diagnose malignant tumors is ^{18}F-fluorodeoxyglucose (FDG) PET test. This test can evaluate the activity of glucose metabolism in lesions. Glucose metabolism in LNs is usually activated when LNs are involved by tumors. Therefore, metastatic LNs show high avidity to FDG and they are visualized as hot spots on FDG PET images [38](Fig. 6.14).

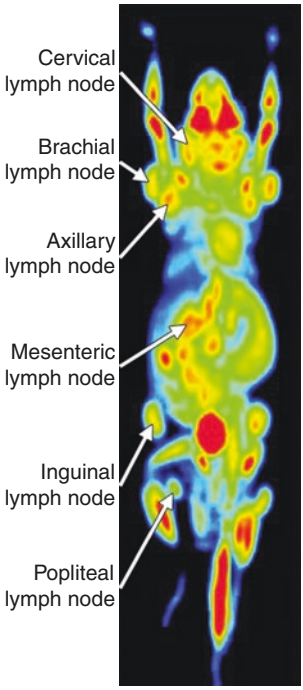

Fig. 6.14 LN metastases of plasma cell tumor-bearing mouse in ^{18}F-FDG-PET image. Reprinted with some modification with permission from Ref. [38]

FDG PET tests have the potential to detect metastatic LNs with normal size by the increased activity of glucose metabolism. But, it is impossible to detect small metastatic LNs even by FDG PET tests, too. Inflammatory lesions in LNs can also be false-positive findings in FDG PET tests because some kinds of cells inside inflamed LNs such as activated macrophages show high avidity to FDG.

The activation of glucose metabolism is a common finding in malignant lesions. As a finding more specific to lymph node metastasis, lymphangiogenesis in LNs, which is considered as an early sign of LN metastasis, is attracting attention of researchers. Lymphatic vessel endothelial hyaluronan receptor 1 (LYVE-1) is a lymphatic-specific epitope and it is expected to be a biomarker of lymphangiogenesis (Fig. 6.15). Mumprecht et al. [39] reported that immuno-PET using ^{124}I-labled LYVE-1 successfully detected early stage of LN metastasis in mouse experiments.

6.4.3 Magnetic Resonance Imaging (MRI) Tests

Metastatic LNs are imaged as enlarged LNs in MR tests as shown in CT ones. In addition to these morphological changes, MRI can provide more detailed information about interiors of metastatic LNs than CT. The most common MR images are T1WIs and T2WIs on spine echo sequences. Generally speaking, tumor lesions show lower signal on T1WI and higher signal on T2WI, compared with normal LNs. Complicated interiors of LNs including metastatic foci cause heterogeneous signal pattern on MR images (Fig. 6.16).

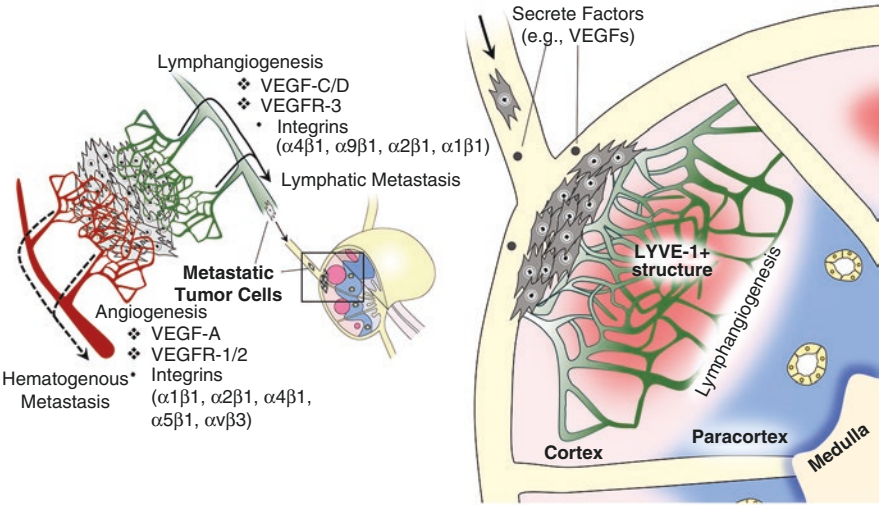

Fig. 6.15 The theory to visualize metastatic LNs by targeting lymphangiogenesis. The lymphatic vessels induced in SLN are composed of LYVE-1-positive lymphatic endothelia, which are expected to be the target of the anti-LYVE-1 antibody

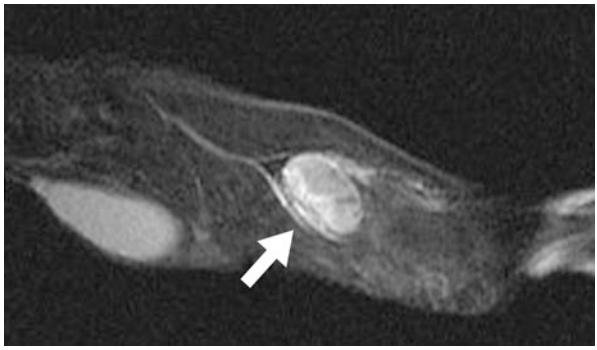

Fig. 6.16 A metastatic popliteal LN of a Balb/c mouse inoculated with Colon26 tumor cells in the T2W MR image (arrow)

Heterogeneous signal patterns can be more significant on MR images obtained by scanners with strong magnetic field such as 9.4T. Administration of contrast media including paramagnetic agents can also enhance the contrast between tumors and non-affected areas. Contrast media can shorten both T1 and T2 relaxation times. When the concentration of contrast media is low, T1 relaxation time is prominently shortened. On the contrary, when the concentration of contrast media is high, T2 relaxation time is strongly shortened. In the diagnosis of LN metastases, contrast-enhanced T1WIs with Gd-chelating agents are usually acquired utilizing the T1 shortening effect. Metastatic lesions in LNs are brightly depicted on these images.

Inflammatory changes and fat deposits in LNs can cause false-positive findings.

6.4.4 Optical Imaging

In optical imaging, optical signals can be detected from metastatic LNs when optical agents that show high affinity to tumor tissues are administered. Unfortunately, no good optical imaging agents to visualize wide variety of tumors like FDG in PET tests. One of the popular optical imaging methods to visualize metastatic LNs is to use tumor-seeking agents conjugated with IRDye 800 CW, a fluorescent dye that emits near-infrared lights with the wave length of 800 nm [40] (Fig. 6.17).

In animal experiments with transplantation models, bioluminescence imaging is also available to investigate LN metastases. When tumor cells with luciferase activity are implanted to animals, tumor lesions can emit luminescent lights. When these tumor cells metastasized to LNs, these LNs with metastatic lesions are also visualized by bioluminescence imaging system (Fig. 6.18).

6.4.5 Ultrasonography (US) and Opt-acoustic (Photoacoustic) Imaging

As ultrasonography is primarily a morphological imaging test, metastatic LNs are diagnosed based on the size and shape. Enlarged and round shaped LNs can be diagnosed as metastatic like CT and MRI tests although it is often difficult to distinguish inflamed LNs from metastatic ones. Generally speaking, the heterogeneity of interior signals would be more significant in metastatic LNs than inflamed ones. Some US devise can provide doppler images. On doppler images, perfusion of metastatic lesions is likely to be enhanced. In contrast-enhanced studies, metastatic LNs are often strongly enhanced.

Recently, opt-acoustic imaging, which is also called photoacoustic imaging, is used for the detection of metastatic lesions. When some agents that can enhance the photoacoustic effects are administered, metastatic lesions in LNs show strong signals. Zhang et al. [41] reported the possibility of ultrasound-guided photoacoustic imaging for the selective detection of EGFR-expressing breast cancer and lymph node metastases in the experiments using anti-EGFR antibody-conjugated gold nanorods (Fig. 6.19).

6.5 Nonclinical Imaging Studies for SN Mapping

Direct visualization of LN metastasis at early stage is not easy even when imaging scanners with high performance are used because LNs with early metastases is often as small as normal LNs.

SN biopsy is an alternative way to diagnose LN metastases at the early stage. This procedure has been already performed for patients with early stage of breast cancer and malignant melanoma in routine clinical practice. Accurate identification of SNs is essential to successfully perform SN biopsy. In the clinical situation, two kinds of

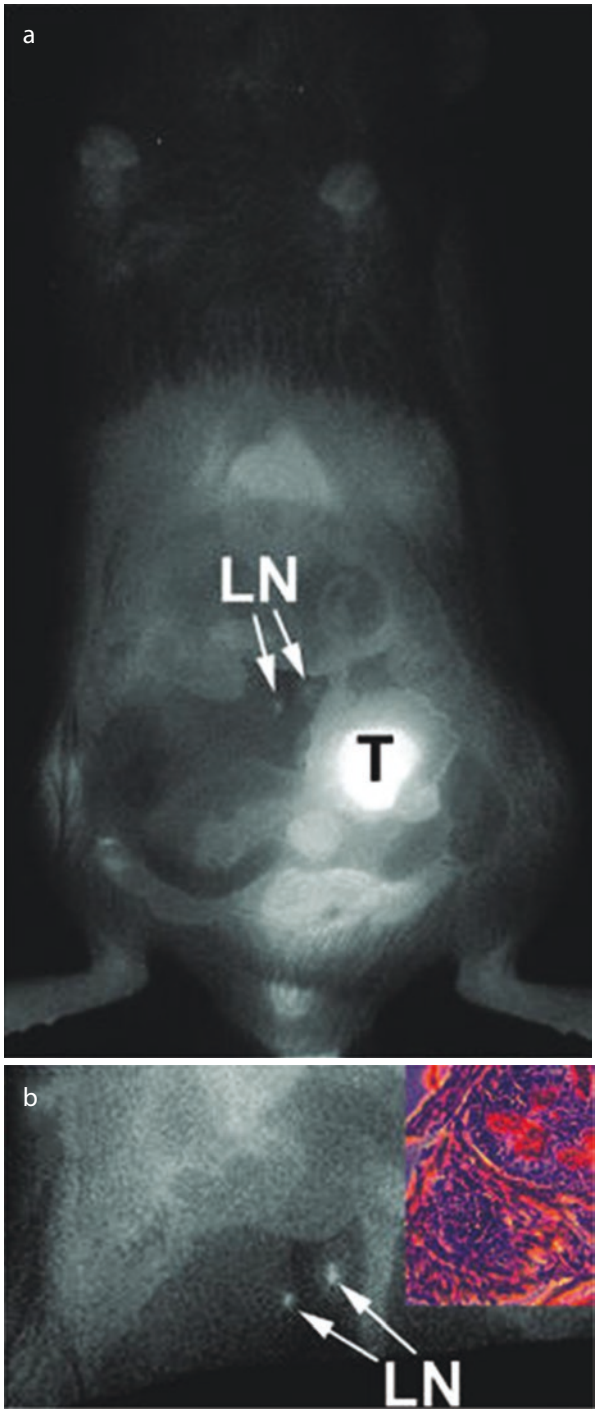

Fig. 6.17 Metastatic lesions including LN lesions in the mouse model visualized by the optical imaging using EGF conjugated with IRDye 800CW. Reprinted with some modification with permission from Ref. [40]

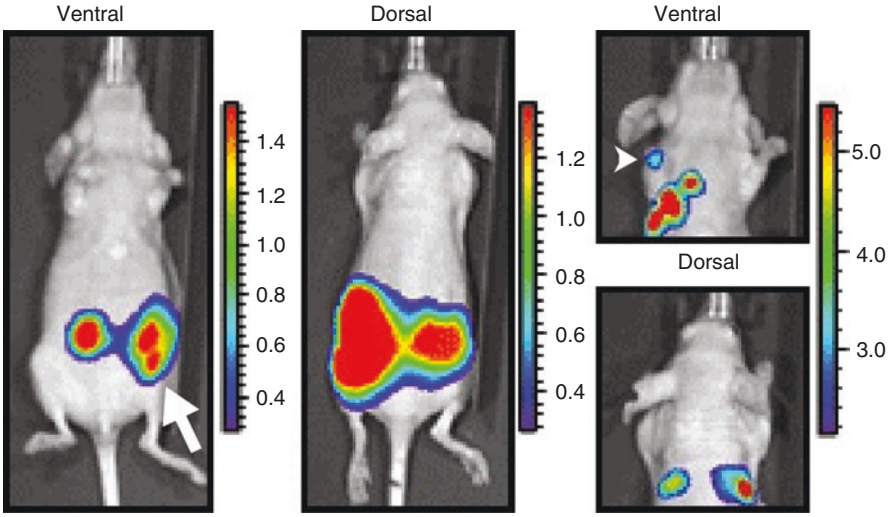

Fig. 6.18 An involved axillary LN (arrowhead) of an HT-29 orthotopic colorectal cancer (arrow) mouse model depicted by in vivo bioluminescence imaging. Reprinted with some modification with permission from Ref. [15]

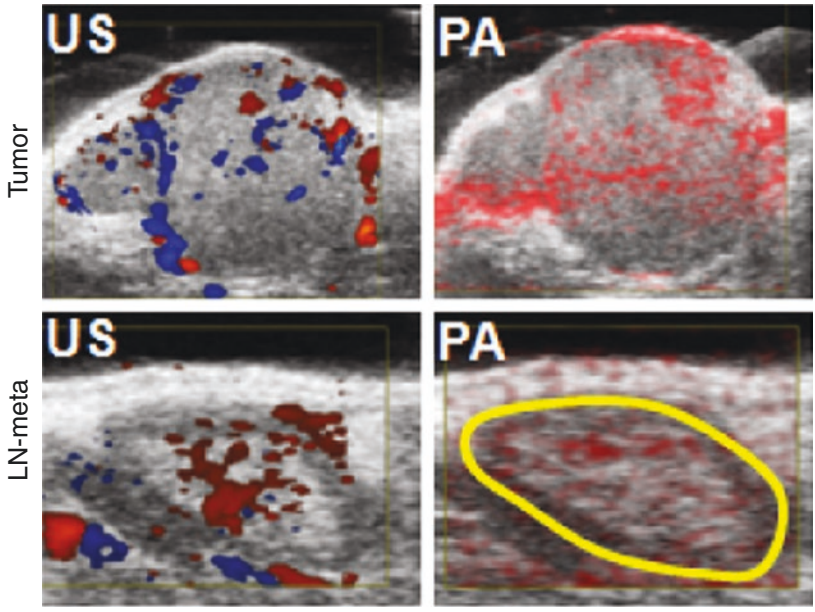

Fig. 6.19 The primary tumor and the metastatic LN in MDA-MB-231 orthotopic mouse xenograft model on the superimposed images of ultrasonography and acoustic imaging. Photoacoustic signal was enhanced by photo absorber (gold nanorods) conjugated antibodies. Reprinted with permission from Ref. [41]

lymphotropic agents are used for the detection of SNs: radiopharmaceuticals and optical imaging agents including blue dyes. In the preclinical investigation about SN mapping, these two kinds of new imaging agents are mainly under investigation.

6.5.1 Nonclinical Studies About Radiopharmaceuticals for SN Mapping

Most commonly used radiopharmaceuticals used in actual clinical SN mapping are radioactive colloids. In Japan, ^{99m}Tc-labeled phytate (FUJIFILM RI Pharma, Tokyo) and ^{99m}Tc-labeled tin colloids (Nihon Medi-physics, Nishinomiya) are covered by health insurance for SN mapping of breast cancer and malignant melanoma.

Regional LNs show high activity on SPECT images after ^{99m}Tc-labeled colloids are injected in animal models. For example, radiocolloids are injected in the mouse footpad, the popliteal LN shows high activity (Fig. 6.20).

These radioactive colloidal agents accumulate in SNs by phagocytosis of macrophages in SNs. Since molecular size of colloidal agents is large, most of injected colloidal agents stay at the injection site. This hinders the detection of SNs located near the injection site.

Therefore, new SN mapping agents with smaller molecular size are required. Although small molecules can easily move into lymphatic channels, they are likely to pass through SNs because they can be escaped from phagocytosis by macrophages. Therefore, SN seeking agents with small molecular size have to be trapped in SNs by some mechanisms. Mannose receptors on macrophages inside SNs can be good candidates to trap small molecular SN mapping agents. Vera et al. reported ^{99m}Tc-labeled tilmanocept that shows high affinity to these mannose receptors [42]. In Japan, Arano et al. [43] is also studying a new SN imaging agent that shows high affinity to mannose receptors on macrophages inside SNs. Nonclinical imaging tests are useful in the development of these new imaging agents. Arano's team demonstrated the clear visualization of SNs on SPECT tests in rat studies (Fig. 6.21).

These agents show good retention in SNs and they have potentials to clearly depict SNs located near the primary tumors since the molecular weight of these radioactive agents are small enough to wash out from the injection site.

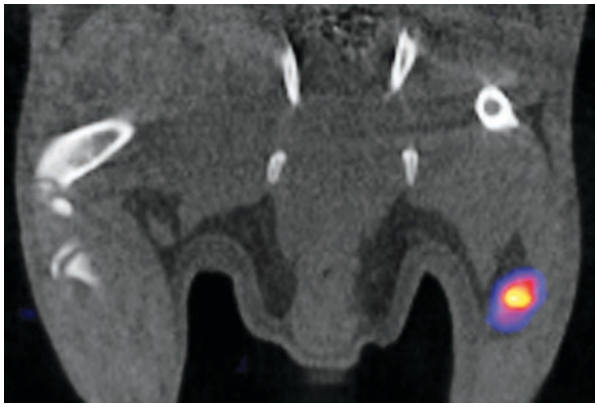

Fig. 6.20 A hot node in the popliteal region in ^{99m}Tc-labeled phytate SPECT/CT image. This hot node can be regarded as a SN of the left footpad lesion

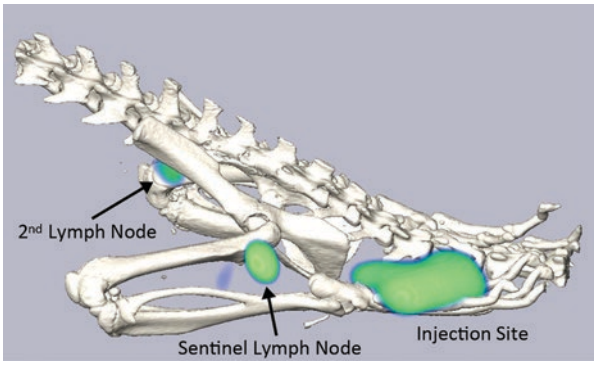

Fig. 6.21 The SN of a rat footpad visualized by the injection of ^{99m}Tc-labeled unique compounds with high affinity to mannose receptors on macrophages. By courtesy of Professor Yasushi Arano, Chiba University

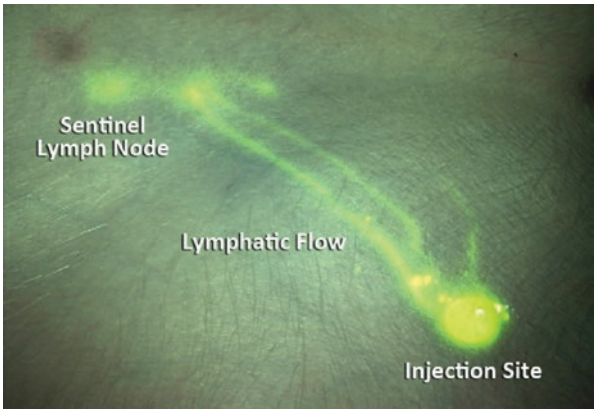

Fig. 6.22 The experimental SN mapping by quantum dots using a swine. Quantum dots can emit stronger fluorescent lights than that of ICG. By courtesy of Professor John V. Frangioni, Harvard Medical School

6.5.2 Nonclinical Studies About Optical Imaging Agents for SN Mapping

Optical methods are also important to identify SNs. Blue dyes are traditional optical imaging agents. In Japan, two kinds of blue dyes, ICG and Indigo carmine (Daiichi-Sankyo, Tokyo), are covered by health insurance for SN mapping of breast cancer and malignant melanoma.

As mentioned above, optical imaging with near-infrared lights is recently attracting interests of researchers. Since ICG emits near-infrared fluorescent lights in addition to blue visible lights, this dye is now used in SN biopsy under near-infrared light because optical imaging with near-infrared lights can visualize imaging agents with good contrast to low background signal.

As quantum dots can emit much stronger near-infrared fluorescent lights than ICG, they would be useful if they could be used in the clinical situation [44] (Fig. 6.22).

But, no quantum dots are approved for clinical use because of the toxicity issues due to heavy metals included in these agents.

Recently, optical imaging using near-infrared lights whose wave length is longer than 1000 nm (OTN-NIR lights) is spotlighted. An imaging scanner with InGaAs detectors and organic imaging dyes are developed [45, 46].

Since OTN-NIR lights can penetrate thicker soft tissues and observe deeper areas in the body, compared with conventional NIR lights, clinical application of SN mapping by optical imaging with these lights will be examined after this.

The clinical application of opt-acoustic imaging, another new imaging method, is also actively investigated [47].

6.5.3 Nonclinical Studies About Multi-modality Imaging for SN Mapping

In clinical SN mapping, it is reported that dual modality methods can yield the best performance, compared with radionuclides or optical agents alone.

Some dual modality imaging probes are reported in western countries. In Europe, the cocktails of ICG and ^{99m}Tc-labeled colloidal albumin are examined in mouse xenograft model [48].

Recently, Araki and our group [49] found that the cocktail of ICG and phytate showed good performance to detect SNs. When this cocktail was injected to mouse models, near-infrared fluorescence slowly appeared in SNs and this fluorescence continued for more than 1 day. This long fluorescent activity is suitable for the operation on head and neck regions. When phytate is labeled by ^{99m}Tc, the obtained radioactive ICG is expected to be useful to dual-modal detection of SNs. Since both of ICG and ^{99m}Tc-pytate are covered by health insurance in Japan, the clinical application of this unique cocktail would be feasible.

As for the evaluation of these dual-modality probes, fusion of two kinds of images is useful. Recently, as three-dimensional reconstruction method of optical images is proposed [50], information of optical images can be superimposed on tomographic scintigrams (Fig. 6.23).

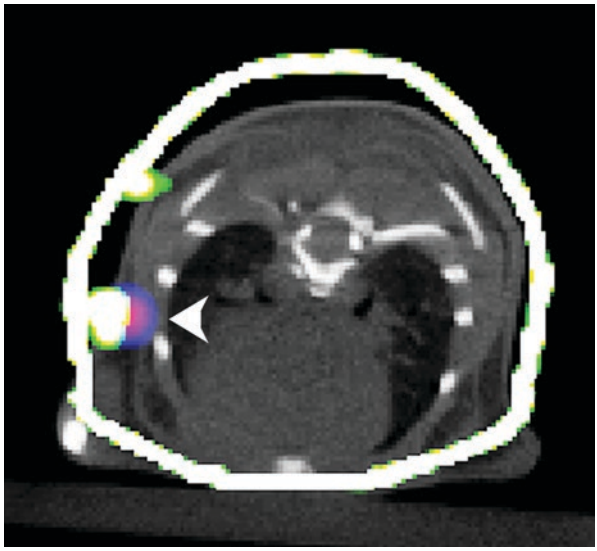

Fig. 6.23 The SN of a mouse forepaw (arrowhead) in optical and radionuclide fusion image. Three-dimensionally reconstructed optical images using ICG were superimposed on SPECT images with ^{99m}Tc-pytate after the injection of the cocktail of these two kinds of imaging agents

6.6 Indirect Visualization of Metastases in SNs

Although SN mapping is a useful method to detect LNs that are likely to have metastases, it is difficult to directly diagnose metastatic lesions only by SN mapping.

Since metastatic foci in SNs are usually small, most parts of interiors of SNs are occupied by non-tumor tissues. The evaluation of signals of these non-tumor tissues in SNs has a potential to detect metastatic lesions in SNs.

6.6.1 Visualization of Metastases in SNs by Negative Contrast Enhancement

Modifying signals of non-tumor tissues in SNs to enhance the contrast between metastatic foci and non-tumor areas can be alternative way to depict metastatic lesions in SNs. As described in the previous section, there are many macrophages in SNs and macrophages show strong phagocytic activity. When superparamagnetic iron oxide-based colloids are administered as contrast media of MRI, macrophages located in non-tumor areas in LNs phagocytose them and non-tumor areas are negatively enhanced, that is these areas show significant low signal, on T2*WI (When images are acquired using gradient echo sequences, T2*WIs were obtained instead of T2WIs).

Harisinghani et al. [51] reported small tumor lesions in LNs could be successfully diagnosed by this method in patients with prostatic cancer. Tatsumi et al. [52] reported that this strategy is also useful to diagnose LN metastases in gastric cancer.

But, some follow-up reports including our experimental study [53] revealed that inflammatory process or fat deposition could be false-positive findings (Fig. 6.24).

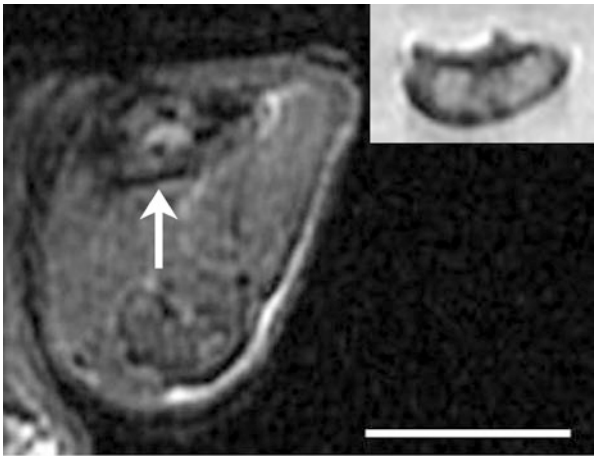

Fig. 6.24 An inflammatory swollen LN in the T2-star weighted MR image obtained after the injection of superparamagnetic iron oxide-based colloids. This non-tumor bearing LN looks like metastatic one. Reprinted with some modification with permission from Ref. [53]

6.6.2 Surrogate Imaging Based on Immune Response in Metastatic SNs

There are many immune cells in SNs besides macrophages and various kinds of immune reactions occur when SNs are involved by tumors. Although most researches have focused on the behavior of T cells, especially CD8+ T cells (CTL), B cells also react to metastatic lesions in SNs.

B cells are mainly located in superficial areas of LNs and these areas are called B-cell areas. When tumor antigens flow in LNs through afferent lymphatic channels, B cells interact with antigen-presenting cells and form follicles. Then, germinal centers appear in follicles.

We recently studied the interval changes of numbers of immune cells inside SNs by flow cytometry using C57BL/6 mice inoculated with B16 melanoma B cells and BALB/c mice with mouse breast cancer cells. Localization of these immune cells inside SNs was also longitudinally observed by immunohistochemistry.

Flow cytometry analyses revealed that, when compared to the control, the relative growth ratio of CD19-positive cells (B cells) increased more significantly than that of CD3-positive cells (T cells) according to the progression of metastases inside SNs. Immunohistochemical findings demonstrated the formation of germinal centers inside SNs was facilitated by advances of metastases (Fig. 6.25).

In the light of diagnostic imaging tests, more attention should be paid to cell groups that show more dramatic change in numbers according to the progress of metastases. We think that significant increase of the B cells and the formation of germinal centers inside SNs according to the progress of metastases would be good candidates for surrogate imaging biomarkers of metastases in SNs.

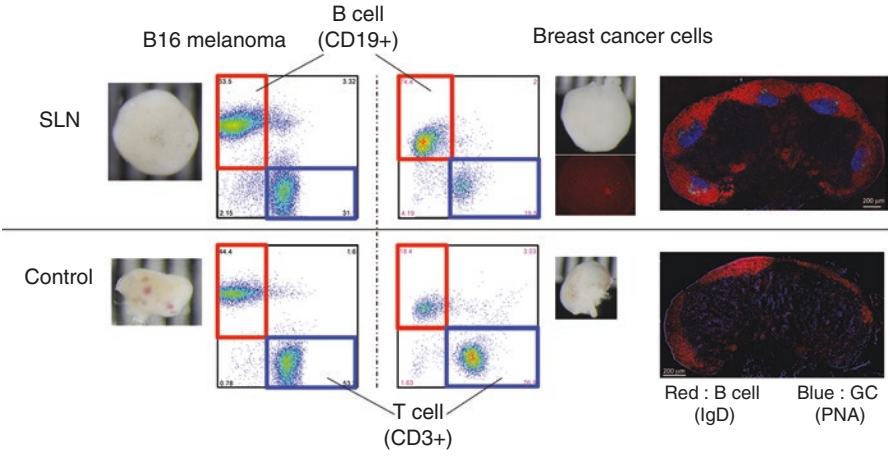

Fig. 6.25 Lymphocytes in the SN. The flow cytometry analyses showed that the B-cell (CD19+)/T-cell (CD3+) ratio in SNs increased compared to that in control nodes. Immunohistochemical analysis of SNs showed abundant germinal centers organized by lymphocytes with the expression of B-cell markers

Recently, Li et al. reported that ^{99m}Tc-labeled rituximab was useful to visualize SNs of patients with breast cancer [54]. Since rituximab is the monoclonal antibody drug that shows high affinity to CD20 antigen on B cells, it is considered that CD20-positive B cells increase in SNs of patients with breast cancer and these increased B cells are successfully detected by ^{99m}Tc-labeled rituximab on scintigrams.

As CD19 is an antigen that appears on B cells, like CD20, radioactive anti-CD19 antibodies have potential to evaluate the metastatic status of SNs. Since rituximab has been already approved as a drug to treat CD20-positive malignant lymphoma, anti-CD19 antibodies would be clinically applicable.

6.7 Summary and Key Points

In this chapter, we explained nonclinical imaging study to investigate LN metastases.

In the research of LN metastases, animal experiments are essential like other biomedical researches. The application of imaging tests is very useful because imaging tests can yield reliable and meaningful results at the sacrifice of minimal number of animals. But, the design of animal experiments must be carefully considered to obtain the fruitful results.

The followings are key points to achieve the aim of the study.

- The optimal animal models must be chosen considering the aim of researches although various kinds of animal models are now available.
- The most suitable imaging modality should be used although many different imaging scanners have been developed. Recently, combined scanners of different imaging modalities are getting popular such as PET/CT scanners. These combined scanners can provide more information that the simple summation of that is acquired from each scanner. Imaging devices dedicated for small animal imaging have been also developed, which show excellent spatial resolution and good sensitivity that are suitable for small animal imaging although these devices can image only small size of objects.
- Alternative imaging strategy should be considered in the detection of metastatic foci in LNs. Although direct visualization of metastatic lesions in LNs is ideal, small metastatic lesions in LNs are often difficult to visualize by current in vivo imaging technology. SN mapping is useful to identify LNs that are most likely to be invaded by tumors. The evaluation of signals of non-tumor areas in LNs would be a new strategy to diagnose small metastases in LNs because most parts of interiors of LNs are occupied by non-tumor tissues when metastatic lesions are small.

Since LN metastases are most important prognostic factors of gastrointestinal cancer, it is expected that accurate and reliable diagnostic criteria in in vivo diagnostic imaging tests will be established based on the valuable results induced by nonclinical animal imaging experiments.

References

1. Zitvogel L, Pitt JM, Daillere R, Smyth MJ, Kroemer G. Mouse models in oncoimmunology. Nat Rev Cancer. 2016;16(12):759–73. https://doi.org/10.1038/nrc.2016.91.
2. Lewis JS, Achilefu S, Garbow JR, Laforest R, Welch MJ. Small animal imaging: current technology and perspectives for oncological imaging. Eur J Cancer. 2002;38(16):2173–88. https://doi.org/10.1016/S0959-8049(02)00394-5.
3. Eckhardt BL, Francis PA, Parker BS, Anderson RL. Strategies for the discovery and development of therapies for metastatic breast cancer. Nat Rev Drug Discov. 2012;11(6):479–97. https://doi.org/10.1038/nrd2372.
4. Terracina KP, Aoyagi T, Huang W-C, Nagahashi M, Yamada A, Aoki K, et al. Development of a metastatic murine colon cancer model. J Surg Res. 2015;199(1):106–14. https://doi.org/10.1016/j.jss.2015.04.030.
5. Partecke LI, Sendler M, Kaeding A, Weiss FU, Mayerle J, Dummer A, et al. A syngeneic Orthotopic murine model of pancreatic adenocarcinoma in the C57/BL6 mouse using the Panc02 and 6606PDA cell lines. Eur Surg Res. 2011;47(2):98–107. https://doi.org/10.1159/000329413.
6. Jiang YJ, Lee CL, Wang Q, Zhou ZW, Yang F, Jin C, et al. Establishment of an orthotopic pancreatic cancer mouse model: cells suspended and injected in Matrigel. World J Gastroenterol. 2014;20(28):9476–85. https://doi.org/10.3748/wjg.v20.i28.9476.
7. Yang H, Kim C, Kim MJ, Schwendener RA, Alitalo K, Heston W, et al. Soluble vascular endothelial growth factor receptor-3 suppresses lymphangiogenesis and lymphatic metastasis in bladder cancer. Mol Cancer. 2011;10:36. https://doi.org/10.1186/1476-4598-10-36.
8. Aslakson CJ, Miller FR. Selective events in the metastatic process defined by analysis of the sequential dissemination of subpopulations of a mouse mammary-tumor. Cancer Res. 1992;52(6):1399–405.
9. Jeong HS, Jones D, Liao S, Wattson DA, Cui CH, Duda DG, et al. Investigation of the lack of angiogenesis in the formation of lymph node metastases. J Natl Cancer I. 2015;107(9):djv155. https://doi.org/10.1093/jnci/djv155.
10. Fidler IJ. Biological behavior of malignant melanoma cells correlated to their survival in vivo. Cancer Res. 1975;35(1):218–24.
11. Partridge SC, Kurland BF, Liu CL, Ho RJ, Ruddell A. Tumor-induced lymph node alterations detected by MRI lymphography using gadolinium nanoparticles. Sci Rep. 2015;5:15641. https://doi.org/10.1038/srep15641.
12. Zhu B, Lu L, Cai W, Yang X, Li C, Yang Z, et al. Kallikrein-binding protein inhibits growth of gastric carcinoma by reducing vascular endothelial growth factor production and angiogenesis. Mol Cancer Ther. 2007;6(12 Pt 1):3297–306. https://doi.org/10.1158/1535-7163.MCT-06-0798.
13. Fujihara T, Sawada T, Hirakawa K, Chung YS, Yashiro M, Inoue T, Sowa M. Establishment of lymph node metastatic model for human gastric cancer in nude mice and analysis of factors associated with metastasis. Clin Exp Metastasis. 1998;16(4):389–98.
14. Yanagihara K, Takigahira M, Tanaka H, Komatsu T, Fukumoto H, Koizumi F, et al. Development and biological analysis of peritoneal metastasis mouse models for human scirrhous stomach cancer. Cancer Sci. 2005;96(6):323–32. https://doi.org/10.1111/j.1349-7006.2005.00054.x.
15. Fernández Y, Foradada L, García-Aranda N, Mancilla S, Suárez-López L, Céspedes MV, Herance JR, Arango D, Mangues R, Schwartz S Jr, Abasolo I. Bioluminescent imaging of animal models for human colorectal cancer tumor growth and metastatic dissemination to clinically significant sites. J Mol Biol Mol Imaging. 2015;2:2.
16. Hackl C, Man S, Francia G, Milsom C, Xu P, Kerbel RS. Metronomic oral topotecan prolongs survival and reduces liver metastasis in improved preclinical orthotopic and adjuvant therapy colon cancer models. Gut. 2013;62(2):259–71. https://doi.org/10.1136/gutjnl-2011-301585.

17. Bhullar JS, Subhas G, Silberberg B, Tilak J, Andrus L, Decker M, et al. A novel nonoperative Orthotopic colorectal Cancer murine model using electrocoagulation. J Am Coll Surg. 2011;213(1):54–60. https://doi.org/10.1016/j.jamcollsurg.2011.02.022.
18. Gros SJ, Dohrmann T, Peldschus K, Schurr PG, Kaifi JT, Kalinina T, et al. Complementary use of fluorescence and magnetic resonance imaging of metastatic esophageal cancer in a novel orthotopic mouse model. Int J Cancer. 2010;126(11):2671–81. https://doi.org/10.1002/ijc.24980.
19. Le CP, Nowell CJ, Kim-Fuchs C, Botteri E, Hiller JG, Ismail H, et al. Chronic stress in mice remodels lymph vasculature to promote tumour cell dissemination. Nat Commun. 2016;7:10634. https://doi.org/10.1038/ncomms10634.
20. Nagata H, Arai T, Soejima Y, Suzuki H, Ishii H, Hibi T. Limited capability of regional lymph nodes to eradicate metastatic cancer cells. Cancer Res. 2004;64(22):8239–48. https://doi.org/10.1158/0008-5472.Can-04-1182.
21. Trencsenyi G, Marian T, Bako F, Emri M, Nagy G, Kertai P, et al. Metastatic hepatocarcinoma he/de tumor model in rat. J Cancer. 2014;5(7):548–58. https://doi.org/10.7150/jca.9315.
22. Tang L, Duan R, Zhong YJ, Firestone RA, Hong YP, Li JG, et al. Synthesis, identification and in vivo studies of tumor-targeting agent peptide doxorubicin (PDOX) to treat peritoneal carcinomatosis of gastric cancer with similar efficacy but reduced toxicity. Mol Cancer. 2014;13:44. https://doi.org/10.1186/1476-4598-13-44.
23. Shen N, Tan J, Wang P, Wang J, Shi Y, Lv W, et al. Indirect magnetic resonance imaging lymphography identifies lymph node metastasis in rabbit pyriform sinus VX2 carcinoma using ultra-small super-paramagnetic iron oxide. PLoS One. 2014;9(4):e94876. https://doi.org/10.1371/journal.pone.0094876.
24. Goldberg BB, Merton DA, Liu JB, Thakur M, Murphy GF, Needleman L, et al. Sentinel lymph nodes in a swine model with melanoma: contrast-enhanced lymphatic US. Radiology. 2004;230(3):727–34. https://doi.org/10.1148/radiol.2303021440.
25. Benezra M, Penate-Medina O, Zanzonico PB, Schaer D, Ow H, Burns A, et al. Multimodal silica nanoparticles are effective cancer-targeted probes in a model of human melanoma. J Clin Invest. 2011;121(7):2768–80. https://doi.org/10.1172/JCI45600.
26. Ito M, Hiramatsu H, Kobayashi K, Suzue K, Kawahata M, Hioki K, et al. NOD/SCID/gamma(null)(c) mouse: an excellent recipient mouse model for engraftment of human cells. Blood. 2002;100(9):3175–82. https://doi.org/10.1182/blood-2001-12-0207.
27. Shultz LD, Lyons BL, Burzenski LM, Gott B, Chen XH, Chaleff S, et al. Human lymphoid and myeloid cell development in NOD/LtSz-scid IL2R gamma(null) mice engrafted with mobilized human hemopoietic stem cells. J Immunol. 2005;174(10):6477–89.
28. de Jong M, Essers J, van Weerden WM. Imaging preclinical tumour models: improving translational power. Nat Rev Cancer. 2014;14(7):481–93. https://doi.org/10.1038/nrc3751.
29. Wiig H, Swartz MA. Interstitial fluid and lymph formation and transport: physiological regulation and roles in inflammation and cancer. Physiol Rev. 2012;92(3):1005–60. https://doi.org/10.1152/physrev.00037.2011.
30. Trevaskis NL, Kaminskas LM, Porter CJ. From sewer to saviour – targeting the lymphatic system to promote drug exposure and activity. Nat Rev Drug Discov. 2015;14(11):781–803. https://doi.org/10.1038/nrd4608.
31. Fujii H, Umeda IO, Kojima Y. Instruments for radiation measurement in life sciences (5). 'Development of imaging technology in life sciences'. 8. Small animal imaging using SPECT. Radioisotopes (Tokyo). 2008;57(3):219–32.
32. Mitsuda M, Yamaguchi M, Furuta T, Nabetani A, Hirayama A, Nozaki A, et al. Multiple-animal MR imaging using a 3T clinical scanner and multi-channel coil for volumetric analysis in a mouse tumor model. Magn Reson Med Sci. 2011;10(4):229–37.
33. James ML, Gambhir SS. A molecular imaging primer: modalities, imaging agents, and applications. Physiol Rev. 2012;92(2):897–965. https://doi.org/10.1152/physrev.00049.2010.
34. Walk EL, McLaughlin SL, Weed SA. High-frequency ultrasound imaging of mouse cervical lymph nodes. J Vis Exp. 2015;101:e52718. https://doi.org/10.3791/52718.

35. Bell AG. LXVIII. Upon the production of sound by radiant energy. London Edinburgh Dublin Philos Mag J Sci. 1881;11(71):510–28.
36. Mehrmohammadi M, Yoon SJ, Yeager D, Emelianov SY. Photoacoustic imaging for cancer detection and staging. Curr Mol Imaging. 2013;2(1):89–105. https://doi.org/10.2174/2211555211302010010.
37. Dorfman RE, Alpern MB, Gross BH, Sandler MA. Upper abdominal lymph-nodes – criteria for normal size determined with Ct. Radiology. 1991;180(2):319–22.
38. Duncan K, Rosean TR, Tompkins VS, Olivier A, Sompallae R, Zhan F, et al. (18)F-FDG-PET/CT imaging in an IL-6- and MYC-driven mouse model of human multiple myeloma affords objective evaluation of plasma cell tumor progression and therapeutic response to the proteasome inhibitor ixazomib. Blood Cancer J. 2013;3:e165. https://doi.org/10.1038/bcj.2013.61.
39. Mumprecht V, Honer M, Vigl B, Proulx ST, Trachsel E, Kaspar M, et al. In vivo imaging of inflammation- and tumor-induced lymph node lymphangiogenesis by immuno-positron emission tomography. Cancer Res. 2010;70(21):8842–51. https://doi.org/10.1158/0008-5472.Can-10-0896.
40. Kovar JL, Johnson MA, Volcheck WM, Chen J, Simpson MA. Hyaluronidase expression induces prostate tumor metastasis in an orthotopic mouse model. Am J Pathol. 2006;169(4):1415–26. https://doi.org/10.2353/ajpath.2006.060324.
41. Zhang MH, Kim HS, Jin TF, Yi A, Moon WK. Ultrasound-guided photoacoustic imaging for the selective detection of EGFR-expressing breast cancer and lymph node metastases. Biomed Opt Express. 2016;7(5):1920–31. https://doi.org/10.1364/Boe.7.001920.
42. Vera DR, Wallace AM, Hoh CK, Mattrey RF. A synthetic macromolecule for sentinel node detection: Tc-99m-DTPA-mannosyl-dextran. J Nucl Med. 2001;42(6):951–9.
43. Takagi K, Uehara T, Kaneko E, Nakayama M, Koizumi M, Endo K, et al. 99mTc-labeled mannosyl-neoglycoalbumin for sentinel lymph node identification. Nucl Med Biol. 2004;31(7):893–900. https://doi.org/10.1016/j.nucmedbio.2004.04.008.
44. Kim S, Lim YT, Soltesz EG, De Grand AM, Lee J, Nakayama A, et al. Near-infrared fluorescent type II quantum dots for sentinel lymph node mapping. Nat Biotechnol. 2004;22(1):93–7. https://doi.org/10.1038/nbt920.
45. Jaque D, Richard C, Viana B, Soga K, Liu X, García SJ. Inorganic nanoparticles for optical bioimaging. Adv Opt Photon. 2016;8(1):1. https://doi.org/10.1364/aop.8.000001.
46. Antaris AL, Chen H, Cheng K, Sun Y, Hong GS, Qu CR, et al. A small-molecule dye for NIR-II imaging. Nat Mater. 2016;15(2):235. https://doi.org/10.1038/Nmat4476.
47. Luke GP, Myers JN, Emelianov SY, Sokolov KV. Sentinel lymph node biopsy revisited: ultrasound-guided photoacoustic detection of micrometastases using molecularly targeted plasmonic nanosensors. Cancer Res. 2014;74(19):5397–408. https://doi.org/10.1158/0008-5472.Can-14-0796.
48. van Leeuwen AC, Buckle T, Bendle G, Vermeeren L, Olmos RV, van de Poel HG, et al. Tracer-cocktail injections for combined pre- and intraoperative multimodal imaging of lymph nodes in a spontaneous mouse prostate tumor model. J Biomed Opt. 2011;16(1):016004. https://doi.org/10.1117/1.3528027.
49. Araki K, Mizokami D, Tomifuji M, Yamashita T, Ohnuki K, Umeda IO, et al. Novel indocyanine green-phytate colloid technique for sentinel node detection in head and neck: mouse study. Otolaryngol Head Neck Surg. 2014;151(2):279–85. https://doi.org/10.1177/0194599814530409.
50. Okawa S, Ikehara T, Oda I, Yamada Y. Reconstruction of localized fluorescent target from multi-view continuous-wave surface images of small animal with lp sparsity regularization. Biomed Opt Express. 2014;5(6):1839–60. https://doi.org/10.1364/BOE.5.001839.
51. Harisinghani MG, Barentsz J, Hahn PF, Deserno WM, Tabatabaei S, van de Kaa CH, et al. Noninvasive detection of clinically occult lymph-node metastases in prostate cancer. New Engl J Med. 2003;348(25):2491–U5. https://doi.org/10.1056/NEJMoa022749.
52. Tatsumi Y, Tanigawa N, Nishimura H, Nomura E, Mabuchi H, Matsuki M, et al. Preoperative diagnosis of lymph node metastases in gastric cancer by magnetic resonance imaging with ferumoxtran-10. Gastric Cancer. 2006;9(2):120–8. https://doi.org/10.1007/s10120-006-0365-8.

53. Suzuki D, Yamaguchi M, Furuta T, Okuyama Y, Yoshikawa K, Fujii H. Central high signal in inflammatory swollen lymph nodes on SPIO-enhanced interstitial MR lymphograms: a mimic of lymph node metastasis. Magn Reson Med Sci. 2012;11(1):61–3.
54. Li N, Wang XJ, Lin BH, Zhu H, Liu C, Xu XB, et al. Clinical evaluation of Tc-99m-rituximab for sentinel lymph node mapping in breast cancer patients. J Nucl Med. 2016;57(8):1214–20. https://doi.org/10.2967/jnumed.115.160572.

In Vivo Imaging of Lymphatic Vessels and Lymph Nodes

7

Takeshi Imamura, Takashi Saitou, Sota Takanezawa, and Ryosuke Kawakami

Abstract

Intravital (*in vivo*) imaging of lymphatic vessels and lymph node is clinically necessary during diagnosis or treatment of many conditions and diseases, including lymphedema and cancer metastasis. Cancers are complex diseases, and the cancer microenvironment, including lymphatic vessels and blood vessels, play important roles throughout cancer development, from carcinogenesis to malignancy. Efforts aimed at elucidating the pathology of complex cancers and developing novel therapeutic agents for cancer treatment are limited by the exclusive use of in vitro analysis of conventional cultured cells and tissue sections. Therefore, it is necessary to analyze cancer cells and their microenvironments spatiotemporally *in vivo*.

To address this issue, *in vivo* imaging has attracted attention in cancer research. Multiple *in vivo* imaging technologies have been developed, including computed tomography (CT), positron emission tomography (PET), and magnetic resonance imaging (MRI), and these modalities already serve as powerful tools for the diagnosis of cancer. Optical imaging *in vivo* using biological light has not yet been applied clinically so much; however, it has superior spatiotemporal resolution, making it possible to perform real-time observation of microscopic structures such as blood and lymphatic system in living animals. In this chapter, we first review technologies for visualizing the blood and lymphatic system for clinical applications, and then describe the use of *in vivo* imaging technology in experimental analysis of cancer cell growth, angiogenesis, lymphangiogenesis, and lymph node metastasis, focusing in particular on the usefulness of *in vivo* optical imaging technology.

T. Imamura (✉) · T. Saitou · S. Takanezawa · R. Kawakami
Department of Molecular Medicine for Pathogenesis, Ehime University Graduate School of Medicine, Toon City, Japan

Translational Research Center, Ehime University Hospital, Toon City, Japan
e-mail: timamura-ind@umin.ac.jp

S. Natsugoe (ed.), *Lymph Node Metastasis in Gastrointestinal Cancer*,
https://doi.org/10.1007/978-981-10-4699-5_7

Keywords
In vivo imaging · Fluorescence imaging · Multiphoton laser excitation microscopy · Light-sheet illumination microscopy

7.1 Intravital (*In Vivo* Imaging of Lymphatic System for Clinical Applications

Lymph vessels, together with blood vessels, constitute the vascular system and function cooperatively to maintain body fluid homeostasis [1]. Blood vessels supply oxygen and nutrients to peripheral tissues and remove waste products, whereas lymphatic vessels maintain a closed circulatory system by absorbing interstitial fluid, proteins, lipids, cells, and other components that leak out of blood vessels and refluxing to the venous system [2]. In particular, the lymphatic vessels are responsible for maintaining proper tissue–fluid balance, and disruption of lymphatic function results in imbalance of body fluids and lymphedema. In addition, lymphatic vessels and lymph nodes organize the immune system, through which the lymph and immune cells traffic to establish and maintain immune responses, and absorb lipids in the gut. Therefore, disruption of the lymphatic system results in abnormal immune function. Moreover, because entry of metastatic cancer cells into the lymphatic system can result in lymph node metastases, the lymphatic system is also involved in cancer progression and metastasis. Thus, lymphatic vessels and lymph nodes are central to various pathological processes, and many techniques have been developed to allow visualization of their structure and function [3–5].

7.1.1 Lymphangiography

Conventional lymphangiography with administration of radiocontrast agent has long been the only method available for the detection of lymphatic vessels. This method was originally developed by Kinmonth (1952) as a surgical procedure guide, and has been modified and adapted for various diagnostic and experimental applications [6]. Although it can provide clinically useful information, lymphangiography is a very time-consuming procedure and is highly invasive [7–9].

7.1.2 Lymphoscintigraphy

Lymphoscintigraphy, a commonly used imaging modality in the clinic, involves injection of radioactive tracers such as technetium-99 m (^{99m}Tc) into the tissue [4, 9, 10]. Both 2D and 3D images of the lymphatic network can be obtained with a scintillation camera. However, because of the poor resolution of lymphoscintigraphy, it is difficult to clearly identify the locations of lymphatic vessels and lymph nodes using this technique. For these reasons, and in order to avoid exposure of the patient

and clinician to radioactive compounds, other methods have emerged to replace lymphoscintigraphy in the context of several applications.

7.1.3 Magnetic Resonance Imaging (MRI)

Magnetic resonance imaging (MRI) with contrast agents relies on variations in T1 or T2 relaxation times of protons in different tissue environments, and thus has relatively high contrast and good spatial resolution. This imaging modality is relatively noninvasive and can be used to detect physiological abnormalities associated with lymphatic dysfunction in breast cancer [11] and lymphedema [12]. However, because of the negative contrast of the detection method, small lesions can be missed in magnetic resonance lymphography (MRL). After the development and improvement of imaging contrast agents with high sensitivity and specificity, MRL may be a preferable approach for identifying pathologies in the lymphatic system.

7.1.4 Positron Emission Tomography (PET) and Computed Tomography (CT)

Among advanced imaging modalities for the lymphatic system, positron emission tomography (PET) takes advantage of uptake of ^{18}fluorodeoxyglucose into metabolically active cancer cells, which accumulate sufficient ^{18}F to image and can therefore be detected in lymph nodes even in low numbers [13]. On the other hand, the spatial resolution of PET is still low, and it must be combined with other imaging modalities such as computed tomography (CT) to clearly define microstructures and small numbers of cells [14]. However, the sensitivity and spatial resolution of PET/CT are controversial, and many reports have argued that this method is unreliable due to false positives from inflammatory conditions [15–17].

7.1.5 Other Modalities

Among various *in vivo* imaging modalities for the lymphatic system, traditional lymphangiography was initially adopted in the clinic for diagnosis of lymphatic disorders. Subsequently, several advanced *in vivo* imaging techniques, including MRI and PET/CT, have been applied to diagnosis and determining treatment effects in various lymphatic diseases. In addition to the aforementioned modalities, ultrasound and fluorescence imaging are also useful for detecting lymphatic vessels and lymph nodes. When lymph nodes are visualized by ultrasound, it is useful to administer microbubbles that are phagocytosed by macrophages [18]. Because precise staging of lymph node metastasis is essential for guiding therapeutic decisions and determining the prognosis of several types of cancers, multiple fluorescence imaging methods have been developed to identify sentinel lymph nodes. The most critical limitation of fluorescence imaging is the low penetration depth of light in tissue

due to absorption and scattering. To solve this problem, fluorescence imaging using indocyanine green (ICG) with near infrared (NIR) wavelength has been applied to lymph node detection. In particular, NIR fluorescence imaging using ICG has been adopted for the detection of sentinel lymph nodes and evaluation of treatment of lymphatic disorders [19–21].

7.2 *In Vivo* Imaging in Oncology and Lymphology

7.2.1 Importance of Blood Vessels, Lymphatic Vessels, and Lymph Nodes in Cancer Progression

Based on remarkable progress in medical technology, early cancer diagnosis and treatment have become more available in recent years, resulting in a decrease in the rate of death due to primary cancer. On the other hand, few treatments are available for recurrent and metastatic cancers, and most cancer patients die of these types of tumors. Accordingly, the greatest challenge facing cancer treatment today is overcoming recurrence and metastasis.

The mode of cancer metastasis is classified as hematogenous spread, lymphatic spread, hematogenous metastasis, lymphoid metastasis, or disseminated spread from routes. The key target for the treatment of recurrence and metastasis of cancer is the cancer microenvironment, including blood vessels, lymphatic vessels, and the immune system. Lymphatic metastasis is a particularly important factor in determining how to treat cancer, the scope of surgery, and prognosis.

7.2.2 Functions of Blood Vessels, Lymphatic Vessels, and Lymph Nodes in Cancer

Blood vessels and lymph vessels are formed in over the course of development, but also under pathological conditions such as inflammation and cancer. In particular, angiogenesis and lymphangiogenesis in cancer tissues are closely related to cancer malignancy. Cancer tissues contain not only cancer cells but also constituent factors such as fibroblasts, inflammatory cells, blood vessels, and lymph vessels; collectively, these components comprise the cancer microenvironment [22]. New blood vessels supply oxygen and nutrients to cancer tissues and support the growth of the primary tumor. In addition, both blood vessels and lymphatic vessels function as routes for cancer metastasis. Angiogenesis and lymphangiogenesis in cancer tissues are the result of extension of existing blood and lymph vessels [22].

In the case of angiogenesis, angiogenic factors such as vascular endothelial growth factor (VEGF)-A are secreted from cancer and stromal cells present in the tumor tissue. VEGF-A enhances the proliferation and movement of vascular endothelial cells from normal blood vessels around the cancer, resulting in formation of new blood vessels.

In the case of lymphangiogenesis, lymphangiogenic factors such as VEGF-C and D are secreted from cancer and inflammatory cells in tumor tissues, thereby enhancing the proliferation and movement of lymphatic endothelial cells in normal lymphatic vessels around the tumor, ultimately resulting in formation of new lymphatic vessels. It has become clear that the cancer microenvironment, including blood vessels and interstitials, has an important influence on the proliferation and metastasis of cancer cells. Therefore, in order to understand cancer comprehensively, it is necessary to perform both *in vitro* studies and *in vivo* spatiotemporal investigations of cancer cells and cancer microenvironments.

7.3 Advances in *In Vivo* Imaging of Lymph Vessels and Lymph Nodes

7.3.1 Various Modalities for *In Vivo* Imaging of Blood Vessels, Lymph Vessels, and Lymph Nodes

In vivo imaging is useful technique for noninvasive analysis of lymphatic vessels and lymph nodes *in vivo*. Although X-ray lymphangiography can generate clinically useful information, it is very time-consuming and highly invasive. As previously mentioned, recently, several advanced *in vivo* imaging techniques, including CT, PET, and MRI, have been applied in clinical practice to diagnosis and determination of treatment effects in various diseases, including cancer [23–25]. Using these advanced imaging modalities that are miniaturized, it has been used to detect blood vessels, lymphatic vessels, and lymph nodes involved in a wide variety of diseases, particularly in cancer [25, 26]. For example, because CT angiography and magnetic resonance angiography (MRA) have high spatial resolution, they are useful for analyzing blood vessel structures such as vascular networks. In addition, functional CT, dynamic contrast-enhanced MRI, PET using ^{15}O-labeled carbon oxide and water molecules, and single-photon emission CT (SPECT) can image the structure of blood vessels, as well as evaluate vascular functions such as blood flow and blood leakage [27–29]. It is also possible to image blood vessels by using ^{124}I-labeled VEGF or integrin avb3-binding peptide [30]. Ultrasound diagnostic methods are useful for conveniently and noninvasively imaging blood vessels, and it is possible to analyze the blood flow velocity of deep blood vessels in real time using color Doppler imaging, or to visualize microvessels with microbubbles coupled to antibodies [31, 32]. Moreover, imaging modalities previously applied to blood vessels have been used to detect lymphatic vessels and lymph nodes [25, 26].

As previously mentioned, refinements of CT and MRI have allowed these methods to progressively replace conventional X-ray lymphangiography in clinical lymph node imaging [25, 26]. The increased availability of functional imaging, especially through the use of FDG-PET, has greatly improved the accuracy of identification of lymph node metastases. However, due to the requirement of a cyclotron for preparing radioactive isotope probes, only a few facilities are capable of using

PET. MRI has the disadvantage of low sensitivity, whereas CT has the disadvantage of low spatial resolution. Although these modalities excel from the standpoint of penetration depth, their resolution and specificity are not sufficient to detect small lymphatic vessels or cancer cells at early phases of lymph node metastasis.

7.3.2 Necessity of *In Vivo* Optical Imaging in Oncology and Lymphology

Bioluminescence imaging and fluorescence imaging techniques, collectively referred to as optical imaging techniques, have already been developed for *in vitro* and ex vivo applications in molecular and cellular biology, including cancer research and lymphology [23–25]. Because optical imaging techniques are noninvasive, rapid, and convenient, there has been growing interest in applying these techniques to the study of complex biology and various disease processes, such as cancer, *in vivo*. In recent years, the development of new bioluminescence and fluorescent probes and further improvements in performance of equipment such as microscopes has enabled visualization of various biological phenomena, including cancer, using *in vivo* optical imaging technology. In addition, because *in vivo* optical imaging does not require special equipment or a large machine such as a cyclotron or MRI instrument, the clinician is not limited by availability of facilities in the research environment.

In vivo bioluminescence imaging has several advantages, including low background and high sensitivity, and can easily detect signals in the deep tissues of living animals; consequently, it is useful for research on cancer metastasis [23–25]. In *in vivo* bioluminescence imaging experiments, genetically manipulated cells that stably express firefly or *Renilla* luciferase protein produce bio-permeable luminescence after administration of substrates such as D-luciferin or coelenterazine, respectively. Recently, the development of ultra-sensitive charge-coupled device (CCD) cameras has made it possible to detect trace amounts of photons in deep tissues of living animals. In addition, the development of software for digitization of imaging data has enabled detection of photons emitted by cancer cells in living animals [33, 34].

By contrast, *in vivo* fluorescence imaging is convenient and economical because it does not require administration of substrates. Furthermore, *in vivo* fluorescence imaging is capable of multicolor imaging in three dimensions, in real time and at high spatial resolution. In addition, it is possible to devise fluorescent probes capable of imaging not only the structure, but also function. However, *in vivo* fluorescence imaging does have a disadvantage; namely, it is difficult to detect a signal in deep tissues because of the high background *in vivo* and the low sensitivity of the technique. One potential solution for these problems is NIR imaging, which uses probes with wavelengths in the NIR region [23–25]. Because such probes are less susceptible to absorption of hemoglobin and tissue scattering, NIR imaging can observe even deeper within the body, with low background and high sensitivity. In multiphoton excitation fluorescence microscopy with nonlinear optics, the

wavelength of the excitation light is twice as long as that used for conventional single-photon excitation, making it possible to observe deep tissue of living animals with less influence from tissue scattering and absorption by hemoglobin. Thus, *in vivo* fluorescence imaging is a very useful method.

Unfortunately, in contrast to X-ray CT, PET, and MRI, *in vivo* optical imaging has not yet been used clinically so much [23–25]. In particular, because bioluminescence imaging techniques require genetic introduction of luminescent enzymes such as luciferase, as well as administration of their substrates, they are difficult to apply clinically. It is also difficult to clinically apply fluorescence imaging techniques using genetically introduced fluorescent proteins. As an alternative, however, it is possible to adopt methods that use fluorescent dyes or do not require probes (non-staining imaging).

7.4 Application of *In Vivo* Fluorescence Imaging for Oncology and Lymphology

7.4.1 Principles of Fluorescence Imaging

In fluorescence imaging, fluorescent proteins or fluorescent dyes are excited with light, and the emitted fluorescence is detected and imaged. When a low-energy fluorescent molecule (ground state) is excited with light, it absorbs a photon and is converted to the high-energy state (excited state). The excited fluorescent molecule immediately returns to the ground state, and the energy released becomes fluorescence (Fig. 7.1a). Because part of the energy is lost before returning from the excited state to the ground state, the fluorescence is shifted to a longer wavelength (i.e., lower energy) relative to excitation light. Within the sample, all parts in the optical path are excited at the same time; thus, the image blurs due to light emission outside

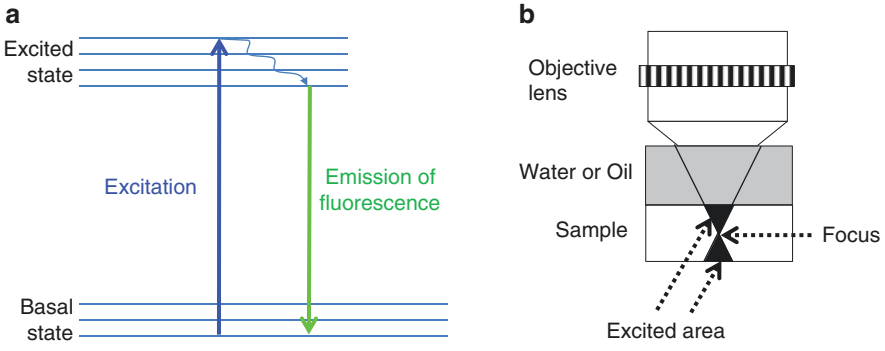

Fig. 7.1 Principle of single-photon excitation. (**a**) The principle of fluorescence imaging (single-photon excitation) is shown using a Jablonski diagram. Lower line: ground state; upper line: excited state; upward arrow: excitation light; downward arrow: fluorescence. (**b**) Excitation region in the sample at the time of fluorescence imaging (single-photon excitation). The hourglass-like area indicates the portion excited in the sample

the focal plane (Fig. 7.1b). In a confocal laser microscope, by disposing a pinhole having a circular opening in the confocal plane of the lens, the light from extensive background area (i.e., out of the focal plane in the Z-axis direction) is removed, and contrast is enhanced.

7.4.2 Visualization of the Cancer Cell Cycle by *In Vivo* Fluorescence Imaging

In fluorescence imaging, it is possible to visualize intracellular functions such as protein–protein interactions, transcriptional activity, and cell cycle progression. Fucci (fluorescent ubiquitination-based cell cycle indicator) is an advanced fluorescence imaging technique that visualizes cell cycle progression in real time [35]. Using Fucci, it is possible to analyze phenomena related to the cell cycle, including development, regeneration, and carcinogenesis, in living cells and animals. For example, the cell cycle of Fucci-expressing cancer cells transplanted into mice can be visualized in three dimensions (Fig. 7.2). Transgenic mice and zebra fish expressing Fucci have been generated and used in developmental biology, neuroscience, and cancer research [36–38].

7.4.3 Visualization of Tumor Angiogenesis by *In Vivo* Fluorescence Imaging

Tumor angiogenesis plays important roles in cancer proliferation, as well as during metastasis. Accordingly, angiogenesis inhibitors have anticancer activity. To develop angiogenesis inhibitors, it is necessary to evaluate angiogenesis *in vivo*. For this

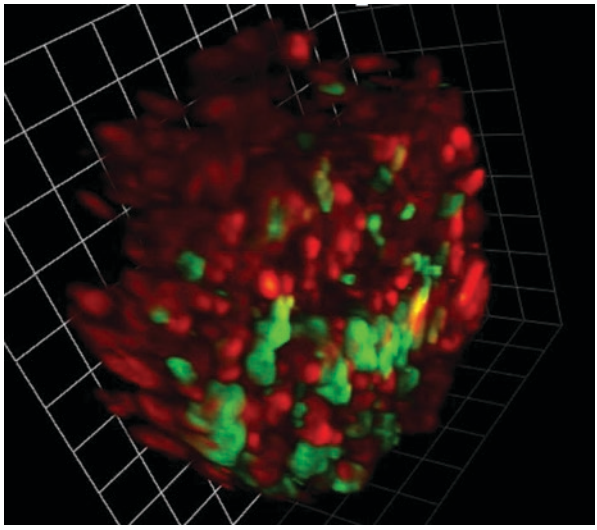

Fig. 7.2 *In vivo* 3D imaging of cell cycle of cancer cells. Fucci-MDA-D (Fucci-expressing, highly bone-metastatic, human breast cancer cells) were transplanted into the left ventricle of nude mice. When bone metastasis occurred 5 weeks later, skin incisions were made, and fluorescence imaging of metastatic foci in the femur was performed. Cells in G1 phase (red) and S/G2/M phase (green) were both present

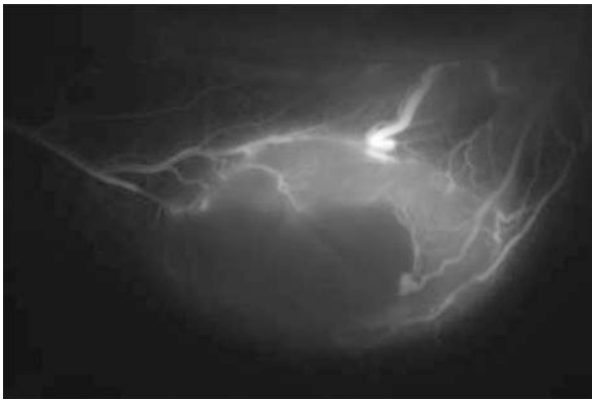

Fig. 7.3 *In vivo* imaging of tumor angiogenesis by ICG. HT1080 cells were transplanted subcutaneously into a nude mouse, and fluorescence imaging of newly generated blood vessels in the cancer was performed on an OV100 after administration of ICG

purpose, researchers often measure microvascular density (MVD) by immunohistochemical staining for CD34, a marker of vascular endothelial cells. However, in order to measure MVD, animals must be sacrificed for collection of tissue samples, and it is impossible to observe them sequentially. Because of individual differences among model animals, it is necessary to prepare large numbers of animals to achieve statistical power. Because *in vivo* fluorescence imaging can be analyzed over time in the same individual, the number of animals used in experiments can be reduced.

In this regard, it is useful to sequentially visualize tumor angiogenesis in tumor-bearing mice *in vivo* using a NIR fluorescence imaging probe. After nude mice transplanted with human fibrosarcoma cell line HT 1080 cells were treated with the NIR-wavelength fluorescent probe indocyanine green (ICG), which labels blood vessels, tumor angiogenesis was observed *in vivo* using the OV100 fluorescence imaging system (Olympus Corporation) (Fig. 7.3). Because ICG is a NIR fluorescent dye with an excitation wavelength of 774 nm and an emission wavelength of 805 nm, ICG imaging is highly bio-permeable and suitable for biological imaging. Tumor blood vessel analysis using an *in vivo* fluorescence imaging system can evaluate changes over time in the same individual, allowing highly reliable data to be obtained. In addition, because fewer animals are necessary for statistical analysis, this approach improves animal welfare.

7.4.4 Visualization of Lymphatic Vessels and Lymph Nodes by *In Vivo* Fluorescence Imaging

ICG is a dye widely used for tests of liver function and liver reserve capacity. As aforementioned, it has already been applied to clinical imaging, such as sentinel lymph node imaging in breast cancer [39–41]. In addition to tumor angiogenesis, discussed above, it is also possible to image lymphatic vessels and lymph nodes in living mice by administering ICG. For example, we injected ICG into the base of the tail of an immunodeficient BALB/c *nu/nu* mouse and performed noninvasive fluorescence imaging of the lymphatic vessels, sub-iliac lymph nodes, and proper

axillary lymph nodes (Fig. 7.4). Next, we attempted fluorescence imaging of cancer lymphangiogenesis in a living mouse harboring cancer cells. In this experiment, HT1080 human fibrosarcoma cells were transplanted subcutaneously into immunodeficient mice. Five weeks after transplantation, the NIR fluorescent probe AngioSense was administered to the cancer stroma, and the neo-lymphatic vessels and sentinel lymph nodes were fluorescently imaged (Fig. 7.5). *In vivo* fluorescence imaging using a NIR fluorescent probe for blood vessel can evaluate lymphangiogenesis over time in the same individual, reducing the number of experimental animals required for statistical analysis and easily generating highly accurate data.

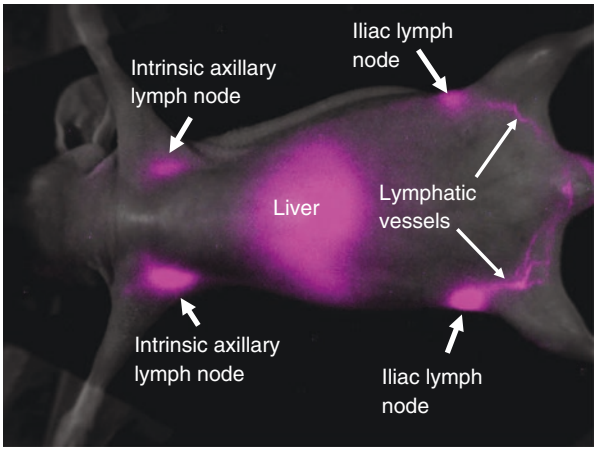

Fig. 7.4 *In vivo* imaging of lymphatic vessels and lymph nodes by ICG. Normal lymphatic vessels and lymph nodes of a nude mouse were fluorescently imaged on an OV100 after administration of ICG in the interstitium of the buttocks

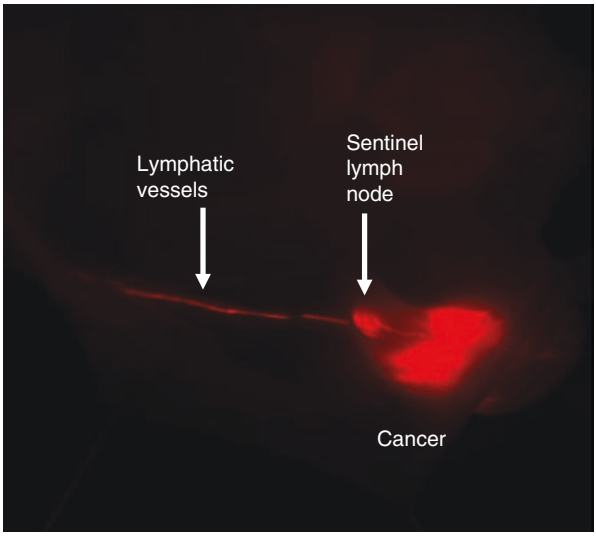

Fig. 7.5 *In vivo* imaging of lymphatic vessels and sentinel lymph nodes in a tumor-bearing mouse. HT1080 cells were transplanted subcutaneously into a nude mouse, and neonatal lymphatic vessels and sentinel lymph nodes were fluorescently imaged on an OV100 after administration of AngioSense to cancer stroma

7.5 Applications of Multiphoton Excitation Microscopy in Oncology and Lymphology

7.5.1 Principles of Multiphoton Excitation Microscopy

Multiphoton excited fluorescence microscopy is a promising method for deep-tissue fluorescence imaging in living animals [42, 43]. As mentioned above (Fig. 7.1a), in conventional single-photon absorption, a fluorescent molecule absorbs a photon that has an energy equal to the energy difference between its ground state and first excited state (Fig. 7.6a). By contrast, in multiphoton excitation fluorescence microscopy, a fluorescent molecule simultaneously absorbs two photons with approximately twice the wavelength and half the excitation energy of the single photon (Fig. 7.6). This two-photon excitation process is very rare, and occurs only at the focal point. The use of long-wavelength light for excitation decreases the influence of scattering, making it possible to image deep tissues *in vivo*. Moreover, because fluorescent molecules are only excited at the focal position, resolution is increased and phototoxicity is decreased.

Research using two-photon excitation microscopy was first developed in neuroscience, and subsequently applied in immunology. Imaging of cerebral neocortical pyramidal cells [44], dynamics of lymph node immune cells [45], and kinetics of bone marrow osteoclast precursor cells [46] has been reported in living animals. For example, using two-photon excitation fluorescence microscopy, it is possible to perform *in vivo* fluorescence imaging of pyramidal cells of the cerebral neocortex at a depth of about 1 mm from the brain surface (Fig. 7.7).

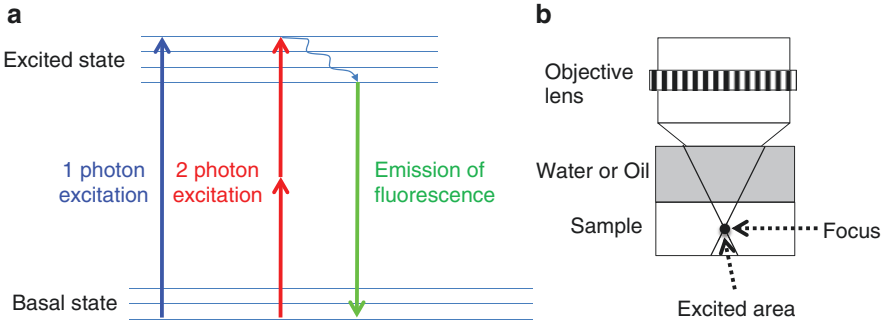

Fig. 7.6 Difference between single-photon excitation and two-photon excitation. (**a**) Comparison of the energy transitions of single-photon and two-photon excitation, shown as a Jablonski diagram. Lower line: ground state; upper line: excited state; upward arrow: excitation light; downward arrow: fluorescence. (**b**) Excitation region in the sample at the time of fluorescence imaging by two-photon excitation. The black circular area indicates the portion excited in the sample

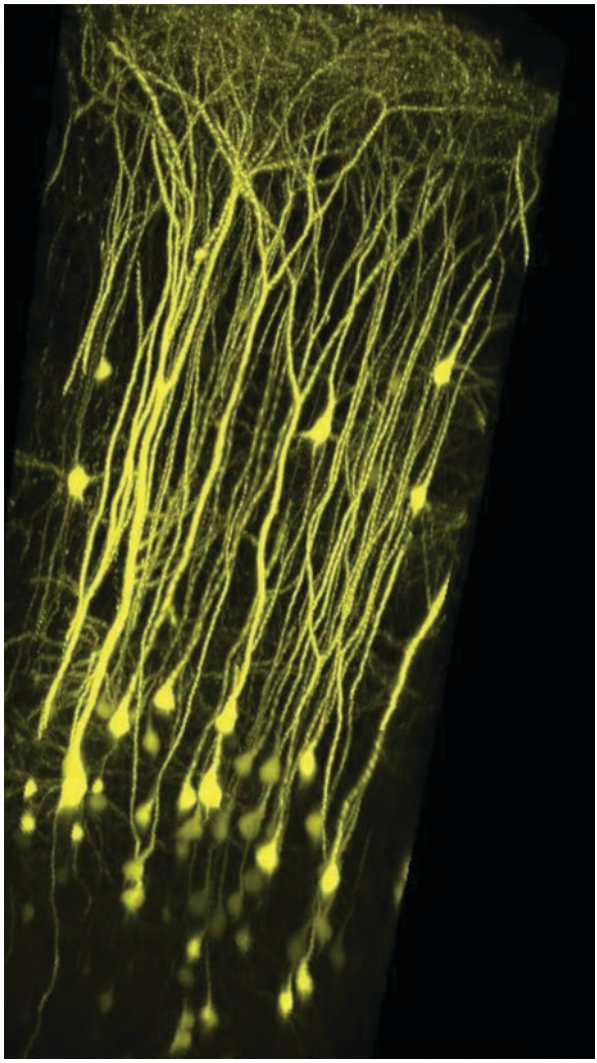

Fig. 7.7 *In vivo* 3D imaging of neural cells in mouse brain by multiphoton laser excitation microscopy. H-line transgenic mice expressing EYFP under the control of the Thy1 promoter were subjected to the open-skull method with cranial bone fenestration under anesthesia. Fluorescence imaging was performed with a two-photon excitation microscope, and cerebral neoplasm at a depth of 1 mm. Cortical pyramidal cells were constructed in 3D

7.5.2 *In Vivo* Imaging of Immune Cells in Lymph Node by Multiphoton Excitation Microscopy

In immunology, advances in fluorescence microscopy technology have enabled several strategies for visualizing the behavior and function of cells within intact lymphoid tissues in living animals [47–51]. Multiphoton laser excitation microscopy has been used to image the dynamic nature of lymphocytes, as well as the interactions between cells such as T cells and dendritic cells (DCs) in lymph nodes [50–55]. This imaging modality has been used not only in explanted lymph nodes incubated at 37 °C with oxygen-perfused medium [48, 53–55], but also in intravital microscopy of lymph nodes [50, 51].

7.5.3 *In Vivo* Imaging of Cancer and Lymph-Node Metastasis by Two-Photon Excitation Microscopy Using a Fluorescence-Conjugated Antibody

Two-photon excitation microscopy, originally developed in neuroscience and immunology, has been applied in various medical and biological fields, including cancer research. In cancer research, in order to apply *in vivo* fluorescence imaging to clinical settings, several groups have developed imaging protocols that use antibodies against tumor markers conjugated to fluorescent substances. For example, Koga et al. established a sensitive and highly specific imaging method using two-photon excitation microscopy in combination with a fluorophore-conjugated antibody against carcinoembryonic antigen (CEA), a marker of malignant cancer [56]. Specifically, CEA-expressing human cancer cells were subcutaneously transplanted into immunodeficient mice, and the cancer cells were imaged by two-photon excitation microscopy after administration of fluorescence-labeled anti-CEA antibody (Fig. 7.8). These results suggest that two-photon excitation microscopy, in conjunction with fluorophore-conjugated antibodies, could be widely adopted for detection of cancer-specific cell-surface molecules, both in cancer research and in clinical applications. In images of cancer tissue obtained by two-photon excitation microscopy, cancer cells are displayed in the same manner as in a stained image of a pathological section. A method that can diagnose without resection is referred to as "optical biopsy" [57].

To further test the usefulness of this combination of two-photon excitation microscopy and fluorophore-conjugated anti-CEA antibody in a more clinically relevant setting, Koga et al. used their method to detect lymph-node metastases.

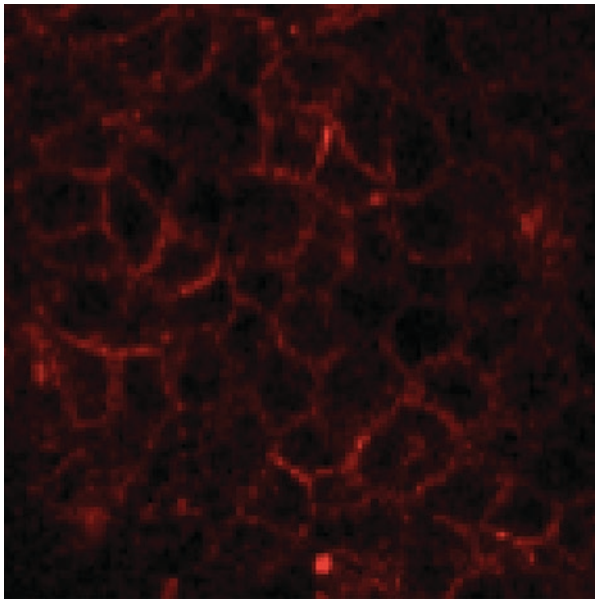

Fig. 7.8 *In vivo* imaging of cancer cells by multiphoton laser excitation microscopy with fluorophore-conjugated anti-CEA antibody. MKN45 human gastric cancer cells were transplanted subcutaneously into the dorsum of immunodeficient mice, Alexa Fluor 594-labeled anti-CEA antibody was injected via the tail vein 4 weeks after transplantation. Twenty-four hours later, mice were subjected to the skin flap method, and multiphoton excitation microscopic imaging was performed

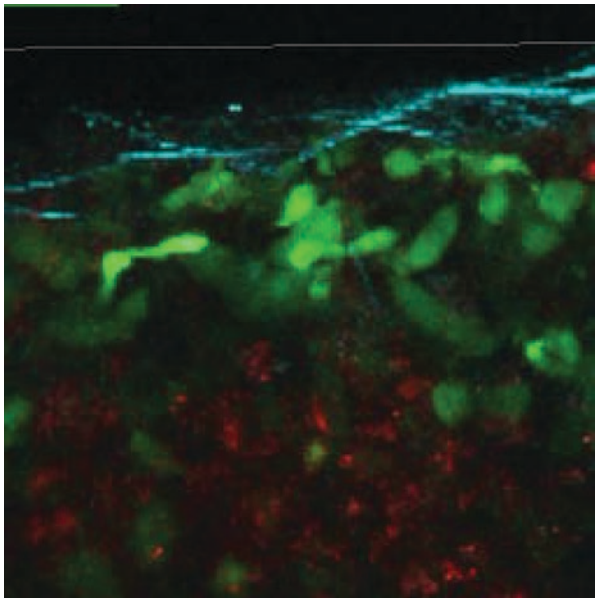

Fig. 7.9 *In vivo* imaging of lymph node metastasis by multiphoton laser excitation microscopy with fluorophore-conjugated anti-CEA antibody. A footpad spontaneous metastasis model consisting of HT1080-GFP-CEA cells in the popliteal lymph node was observed by two-photon excitation microscopy. Red, green, and blue indicate Alexa Fluor 594 fluorescence, GFP fluorescence, and second harmonic generation (SHG), respectively

In a footpad spontaneous metastasis model, they showed that it is possible to detect a small number of metastasized cancer cells in a lymph node (Fig. 7.9).

7.5.4 *In Vivo* Imaging of Lymph Ducts of Medaka Fish by Multiphoton Excitation Light-Sheet Illumination Microscopy

In light-sheet illumination microscopy, a sample is illuminated in a plane, and single-photon–excitation fluorescence images are captured with a camera in the direction perpendicular to the light sheet. Because image acquisition is relatively fast, resulting in reduction of phototoxicity, this method is potentially useful for observing biological specimens. In particular, light-sheet illumination microscopy system is the most suitable technique for observing embryos and small animals. In the past, in developmental biology, digital-scanned light-sheet microscopy (DSLM) and selective plane-illuminated microscopy (SPIM) were developed and applied to live-cell imaging [58]. However, light-sheet illumination microscopy cannot be effectively applied to high-scattering materials due to image blur resulting from thickening of the light sheet by scattered photons. Notably in this regard, multiphoton excitation light-sheet illumination microscopy with NIR excitation enables collection of high-contrast images [59].

Using multiphoton excitation light-sheet illumination microscopy, whole-body lymph ducts of medaka fish can be visualized *in vivo*. For this purpose, a transgenic

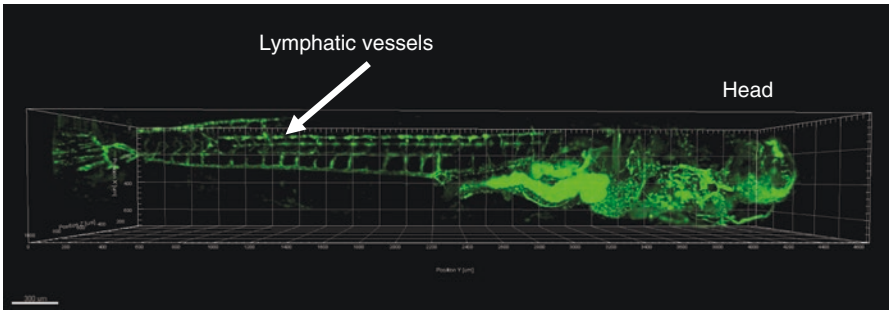

Fig. 7.10 *In vivo* 3D imaging of lymphatic vessels of medaka fish by multiphoton excitation light-sheet illumination microscopy. Lymphatic vessels in FLT4-EGFP transgenic medaka were visualized *in vivo* by multiphoton excitation light-sheet illumination microscopy

"see-through" medaka fish, in which the lymphatic vessels and some blood vessels are visible *in vivo*, was prepared by introduction of a transgene consisting of the medaka Feline McDonough Sarcoma (FMS)-like tyrosine kinase 4 (*FLT4*) promoter driving the expression of enhanced green fluorescent protein (EGFP) [60]. As shown in Fig. 7.10, lymphatic vessels and some blood vessels could be visualized *in vivo* in the transgenic fish. Because a see-through medaka line is transparent until adulthood, the model is useful for visualizing lymphatic vessels, not only in embryos and fry, but also in adult. Thus, this model will be useful for analyzing lymphatic development.

7.6 Conclusion and Perspectives

In this chapter, we reviewed technologies for visualizing the lymphatic system in the context of clinical applications, including lymphangiography, lymphoscintigraphy, MRI, PET, CT, ultrasound, and fluorescence imaging. *In vivo* imaging of the lymphatic system is clinically necessary during diagnosis or treatment of many conditions and diseases, including cancer metastasis. We then described the use of *in vivo* imaging technology in the experimental analysis of cancer and the lymphatic system, focusing in particular on the usefulness of *in vivo* optical imaging technology. It is difficult to observe deep tissues *in vivo* by fluorescence imaging due to the large number of endogenous fluorescent substances, such as water and hemoglobin, that either scatter light or emit autofluorescence. To solve this problem, several tools and methods have been developed including NIR fluorescence probes and two-photon excitation microscopy.

Acknowledgments There are many important papers in this field; for reasons of space, we have not been able to mention all of them. We apologize to those investigators whose papers could not be cited.

References

1. Yoshimatsu Y, Miyazaki H, Watabe T. Roles of signaling and transcriptional networks in pathological lymphangiogenesis. Adv Drug Deliv Rev. 2016;99:161–71. https://doi.org/10.1016/j.addr.2016.01.020.
2. Karpanen T, Alitalo K. Molecular biology and pathology of lymphangiogenesis. Annu Rev Pathol. 2008;3:367–97.
3. Rockson SG. Lymphatic investigation: from the endothelium to in vivo imaging. Lymphat Res Biol. 2003;1:99. https://doi.org/10.1089/153968503321642598.
4. Sevick-Muraca EM, Kwon S, Rasmussen JC. Emerging lymphatic imaging technologies for mouse and man. J Clin Invest. 2014;124:905–14. https://doi.org/10.1172/JCI71612.
5. Munn LL, Padera TP. Imaging the lymphatic system. Microvasc Res. 2014;96:55–63. https://doi.org/10.1016/j.mvr.2014.06.006.
6. Kinmonth JB. Lymphangiography in man; a method of outlining lymphatic trunks at operation. Clin Sci (Lond). 1952;11:13–20.
7. Halsell JT, Smith JR, Bentlage CR, Park OK, Humphreys JW Jr. Lymphatic drainage of the breast demonstrated by vital dye staining and radiography. Ann Surg. 1965;162:221–6.
8. Clement O, Luciani A. Imaging the lymphatic system: possibilities and clinical applications. Eur Radiol. 2004;14:1498–507.
9. Weissleder R, Thrall JH. The lymphatic system: diagnostic imaging studies. Radiology. 1989;172:315–7.
10. Wen Z, Tong G, Liu Y, Meeks JK, Ma D, Yang J. The lymphoscintigraphic manifestation of (99m)Tc-dextran lymphatic imaging in primary intestinal lymphangiectasia. Nucl Med Commun. 2014;35:493–500. https://doi.org/10.1097/MNM.0000000000000080.
11. Lu Q, Hua J, Kassir MM, Delproposto Z, Dai Y, Sun J, et al. Imaging lymphatic system in breast cancer patients with magnetic resonance lymphangiography. PLoS One. 2013;8:e69701. https://doi.org/10.1371/journal.pone.0069701.
12. Rane S, Donahue PM, Towse T, Ridner S, Chappell M, Jordi J, et al. Clinical feasibility of noninvasive visualization of lymphatic flow with principles of spin labeling MR imaging: implications for lymphedema assessment. Radiology. 2013;269:893–902. https://doi.org/10.1148/radiol.13120145.
13. Birim O, Kappetein AP, Stijnen T, Bogers AJ. Meta-analysis of positron emission tomographic and computed tomographic imaging in detecting mediastinal lymph node metastases in nonsmall cell lung cancer. Ann Thorac Surg. 2005;79:375–82.
14. Uchiyama S, Haruyama Y, Asada T, Hotokezaka M, Nagamachi S, Chijiiwa K. Role of the standardized uptake value of 18-fluorodeoxyglucose positron emission tomography-computed tomography in detecting the primary tumor and lymph node metastasis in colorectal cancers. Surg Today. 2012;42:956–61. https://doi.org/10.1007/s00595-012-0225-6.
15. Al-Sarraf N, Gately K, Lucey J, Wilson L, McGovern E, Young V. Lymph node staging by means of positron emission tomography is less accurate in non-small cell lung cancer patients with enlarged lymph nodes: analysis of 1,145 lymph nodes. Lung Cancer. 2008;60:62–8.
16. Cooper KL, Harnan S, Meng Y, Ward SE, Fitzgerald P, Papaioannou D, et al. Positron emission tomography (PET) for assessment of axillary lymph node status in early breast cancer: a systematic review and meta-analysis. Eur J Surg Oncol. 2011;37:187–98. https://doi.org/10.1016/j.ejso.2011.01.003.
17. Akbulut Z, Canda AE, Atmaca AF, Caglayan A, Asil E, Balbay MD. Is positron emission tomography reliable to predict post-chemotherapy retroperitoneal lymph node involvement in advanced germ cell tumors of the testis? Urol J. 2011;8:120–6.
18. Abe H, Schacht D, Kulkarni K, Shimauchi A, Yamaguchi K, Sennett CA, et al. Accuracy of axillary lymph node staging in breast cancer patients: an observer-performance study comparison of MRI and ultrasound. Acad Radiol. 2013;20:1399–404. https://doi.org/10.1016/j.acra.2013.08.003.

19. Rasmussen JC, Tan IC, Marshall MV, Fife CE, Sevick-Muraca EM. Lymphatic imaging in humans with near-infrared fluorescence. Curr Opin Biotechnol. 2009;20:74–82. https://doi.org/10.1016/j.copbio.2009.01.009.
20. Mieog JS, Troyan SL, Hutteman M, Donohoe KJ, van der Vorst JR, Stockdale A, et al. Toward optimization of imaging system and lymphatic tracer for near-infrared fluorescent sentinel lymph node mapping in breast cancer. Ann Surg Oncol. 2011;18:2483–91. https://doi.org/10.1245/s10434-011-1566-x.
21. Tan IC, Maus EA, Rasmussen JC, Marshall MV, Adams KE, Fife CE, et al. Assessment of lymphatic contractile function after manual lymphatic drainage using near-infrared fluorescence imaging. Arch Phys Med Rehabil. 2011;92:756–64. https://doi.org/10.1016/j.apmr.2010.12.027.
22. Stacker SA, Williams SP, Karnezis T, Shayan R, Fox SB, Achen MG. Lymphangiogenesis and lymphatic vessel remodelling in cancer. Nat Rev Cancer. 2014;14:159–72. https://doi.org/10.1038/nrc3677.
23. Massoud TF, Gambhir SS. Molecular imaging in living subjects: seeing fundamental biological processes in a new light. Genes Dev. 2003;17:545–80.
24. Weissleder R, Pittet MJ. Imaging in the era of molecular oncology. Nature. 2008;452:580–9.
25. Weissleder R, Nahrendorf M. Advancing biomedical imaging. Proc Natl Acad Sci U S A. 2015;112:14424–8.
26. Luciani A, Itti E, Rahmouni A, Meignan M, Clement O. Lymph node imaging: basic principles. Eur J Radiol. 2006;58:338–44.
27. Goh V, Padhani AR, Rasheed S. Functional imaging of colorectal cancer angiogenesis. Lancet Oncol. 2007;8:245–55.
28. Hylton N. Dynamic contrast-enhanced magnetic resonance imaging as an imaging biomarker. J Clin Oncol. 2006;24:3293–8.
29. Wells P, Jones T, Price P. Assessment of inter- and intrapatient variability in $C^{15}O_2$ positron emission tomography measurements of blood flow in patients with intra-abdominal cancer. Clin Cancer Res. 2003;9:6350–6.
30. Cai W, Chwn X. Multimodality molecular imaging of tumor angiogenesis. J Nucl Med. 2008;49:113S–28S.
31. Korpanty G, Carbon JG, Grayburn PA, Fleming JB, Brekken RA. Monitoring response to anticancer therapy by targeting microbubbles to tumor vasculature. Clin Cancer Res. 2007;13:323–30.
32. Willimann JK, Paulmurugan R, Chen K, Gheysens O, Rodriguez-Porcel M, Lutz AM, et al. US imaging of tumor angiogenesis with microbubbles targeted to vascular endothelial growth factor receptor type 2 in mice. Radiology. 2008;246:508–18.
33. Hara-Miyauchi C, Tsuji O, Hanyu A, Okada S, Yasuda A, Fukano T, et al. Bioluminescent system for dynamic imaging of cell and animal behavior. Biochem Biophys Res Commun. 2012;419:188–93.
34. Katsuno Y, Hanyu A, Kanda H, Ishikawa Y, Akiyama F, Iwase T, et al. Bone morphogenetic protein signaling enhances invasion and bone metastasis of breast cancer cells through Smad pathway. Oncogene. 2008;27:6322–33.
35. Sakaue-Sawano A, Kurokawa H, Morimura T, Hanyu A, Hama H, Osawa H, et al. Visualizing spatiotemporal dynamics of multicellular cell-cycle progression. Cell. 2008;132:487–98. https://doi.org/10.1016/j.cell.2007.12.033.
36. Dan S, Okamura M, Mukai Y, Yoshimi H, Inoue Y, Hanyu A, et al. ZSTK474, a specific phosphatidylinositol 3-kinase inhibitor, induces G1 arrest of the cell cycle in vivo. Eur J Cancer. 2012;48:936–43.
37. Sugiyama M, Saitou T, Kurokawa H, Sakaue-Sawano A, Imamura T, Miyawaki A, et al. Live imaging-based model selection reveals periodic regulation of the stochastic G1/S phase transition in vertebrate axial development. PLoS Comput Biol. 2014;10:e1003957.
38. Saitou T, Imamura T. Quantitative imaging with Fucci and mathematics to uncover temporal dynamics of cell cycle progression. Develop Growth Differ. 2016;58:6–15.

39. Ogata F, Azuma R, Kikuchi M, Koshima I, Morimoto Y. Novel lymphography using indocyanine green dye for near-infrared fluorescence labeling. Ann Plast Surg. 2007;58:652–5.
40. Kusano M, Tajima Y, Yamazaki K, Kato M, Watanabe M, Miwa M. Sentinel node mapping guided by indocyanine green fluorescence imaging: a new method for sentinel node navigation surgery in gastrointestinal cancer. Dig Surg. 2008;25:103–8. https://doi.org/10.1159/000121905.
41. Murawa D, Hirche C, Dresel S, Hünerbein M. Sentinel lymph node biopsy in breast cancer guided by indocyanine green fluorescence. Br J Surg. 2009;96:1289–94. https://doi.org/10.1002/bjs.6721.
42. Denk W, Strickler JH, Webb WW. Two-photon laser scanning fluorescence microscopy. Science. 1990;248:73–6.
43. Helmchen F, Denk W. Deep tissue two-photon microscopy. Nat Methods. 2005;2:932–40.
44. Theer P, Hasan MT, Denk W. Two-photon imaging to a depth of 1000 μm in living brains by use of a Ti:Al_2O_3 regenerative amplifier. Opt Lett. 2003;28:1022–4.
45. Germain RN, Miller MJ, Dustin ML, Nussenzweig MC. Dynamic imaging of the immune system: progress, pitfalls and promise. Nat Rev Immunol. 2006;6:497–507.
46. Ishii M, Egen JG, Klauschen F, et al. Sphingosine-1-phosphate mobilizes osteoclast precursors and regulates bone homeostasis. Nature. 2009;458:524–8.
47. Miller MJ, Wei SH, Parker I, Cahalan MD. Two-photon imaging of lymphocyte motility and antigen response in intact lymph node. Science. 2002;296:1869–73.
48. Stoll S, Delon J, Brotz TM, Germain RN. Dynamic imaging of T cell-dendritic cell interactions in lymph nodes. Science. 2002;296:1873–6.
49. Bousso P, Bhakta NR, Lewis RS, Robey E. Dynamics of thymocyte-stromal cell interactions visualized by two-photon microscopy. Science. 2002;296:1876–80.
50. Miller MJ, Wei SH, Cahalan MD, Parker I. Autonomous T cell trafficking examined in vivo with intravital two-photon microscopy. Proc Natl Acad Sci U S A. 2003;100:2604–9.
51. Mempel TR, Henrickson SE, Von Andrian UH. T-cell priming by dendritic cells in lymph nodes occurs in three distinct phases. Nature. 2004;427:154–9.
52. Cahalan MD, Parker I, Wei SH, Miller MJ. Two-photon tissue imaging: seeing the immune system in a fresh light. Nat Rev Immunol. 2002;2:872–80.
53. Bousso P, Robey E. Dynamics of CD8+ T cell priming by dendritic cells in intact lymph nodes. Nat Immunol. 2003;5:579–85.
54. Miller MJ, Hejazi AS, Wei SH, Cahalan MD, Parker I. T cell repertoire scanning is promoted by dynamic dendritic cell behavior and random T cell motility in the lymph node. Proc Natl Acad Sci U S A. 2004;101:998–1003.
55. Miller MJ, Safrina O, Parker I, Cahalan MD. Imaging the single cell dynamics of CD4+ T cell activation by dendritic cells in lymph nodes. J Exp Med. 2004;200:847–56.
56. Koga S, Oshima Y, Honkura N, Iimura T, Kameda K, Sato K, Yoshida M, et al. *In vivo* subcellular imaging of tumors in mouse models using a fluorophore-conjugated anti-carcinoembryonic antigen antibody in two-photon excitation microscopy. Cancer Sci. 2014;105:1299–306.
57. Wang TD, Van Dam J. Optical biopsy: a new frontier in endoscopic detection and diagnosis. Clin Gastroenterol Hepatol. 2004;2:744–53.
58. Huisken J, Swoger J, Del Bene F, Wittbrodt J, Stelzer EH. Optical sectioning deep inside live embryos by selective plane illumination microscopy. Science. 2004;305:1007–9.
59. Maruyama A, Oshima Y, Kajiura-Kobayashi H, Nonaka S, Imamura T, Naruse K. Wide field intravital imaging by two-photon-excitation digital-scanned light-sheet microscopy (2p-DSLM) with a high-pulse energy laser. Biomed Opt Express. 2014;5:3311–25.
60. Deguchi T, Fujimori KE, Kawasaki T, Maruyama K, Yuba S. *In vivo* visualization of the lymphatic vessels in pFLT4-EGFP transgenic medaka. Genesis. 2012;50:625–34.

Part II

Lymph Node Micrometastasis

Basic Aspect: Methodology

8

Shuhei Ito, Takaaki Masuda, Yosuke Kuroda, Hidetoshi Eguchi, and Koshi Mimori

Abstract

Initially, micrometastases in the regional lymph nodes (lymph node [LN] micrometastases; LNMs) were detected by immunohistochemical analysis of epithelial markers, and the prognostic significance of LNMs has been a major focus for many years. In addition, recent technological innovations have enabled us to detect LNMs more accurately, with some techniques even showing promising applications in the clinical setting. In this chapter, we will review the methodology to detect LNMs, as follows. First, we will discuss the histopathological method to detect LNMs including conventional hematoxylin and eosin (H&E) staining and immunohistochemical analysis. Next, we will describe methods for detection of cancer-associated mRNA and review quantitative reverse transcription polymerase chain reaction (qRT-PCR) and the reverse transcription loop-mediated isothermal amplification (RT-LAMP) method, which are currently being used in the clinical setting. Third, genetic or epigenetic techniques to detect LNMs will be discussed, and we will introduce methods to detect LNMs by cancer-specific events, such as mutations and methylation. Finally, we will describe future perspectives, such as potential discoveries related to LNMs, with a specific focus on the development of new strategies for detecting LNMs.

Keywords

Immunohistochemistry · mRNA expression · Mutation · Methylation Visualization · Malignant potential · Host factor

S. Ito · T. Masuda · Y. Kuroda · H. Eguchi · K. Mimori (✉)
Department of Surgery, Kyushu University Beppu Hospital, Beppu, Japan
e-mail: kmimori@beppu.kyushu-u.ac.jp

S. Natsugoe (ed.), *Lymph Node Metastasis in Gastrointestinal Cancer*,
https://doi.org/10.1007/978-981-10-4699-5_8

8.1 Pathology of LNMs

8.1.1 Hematoxylin and Eosin (H&E) Staining

The TNM classification defines micrometastasis (MM) as being between 0.2 cm and 0.2 mm at the greatest dimension [1]. Histopathological examination of regional LNs is usually carried out on a representative section of the node with H&E staining to ascertain whether metastasis is present. However, LNMs that cannot be detected by H&E staining have been reported to be present in some carcinomas. Therefore, specific antibodies to detect cancer cells may be required.

8.1.2 Examination of Serial Sections

Serial sectioning results in more accurate evaluation of the extent of LN metastasis [2]. Natsugoe et al. [3] reported that an initial routine examination confirmed metastasis in 19 LNs from 11 patients; however, when the LNs were reexamined in three additional sections, metastasis was newly detected in another 9 nodes from 8 patients. The overall incidence of LN metastasis in 57 patients with sm gastric cancer was 19.3% (11/57) by the initial routine examination, but was as high as 29.8% (17/57) following detailed reexamination. Therefore, it was necessary to determine how many slides per LN are needed to detect MM.

This method is simple but time consuming, and problems can arise in determining how many sections are sufficient for detection of LNMs. Noura et al. [4] advocated that examination of serial sections requires at least five sections because a survey of five LN sections led to a superb detection rate for MM (11.8% of LNs and 45.9% of patients) compared with that achieved using 1- or 2-slice sections (3.8% and 6.3% of LNs and 23.5% and 36.7% of patients, respectively).

8.1.3 Immunohistochemical Staining

According to previous reports, several antibodies, including anti-cytokeratin (CK) antibodies (AE1/AE3, CAM5.2, Ber-EP4, Lu-5, MNF116, 35βH11, O.N.352, KL1, and CK20), can be used for immunohistochemical staining. For accurate results, antibodies that can recognize multiple subtypes of CK should be used for immunohistochemistry (IHC), e.g., AE1/AE3 or CAM5.2 monoclonal antibodies.

CAM5.2 recognizes intracellular CK component numbers 8 and 18, which make up an intermediate fragment representing the intracellular network of the cytoskeleton; this component is expressed only in simple epithelium. Additionally, AE1/AE3 recognizes many CKs, including CK10, CK14, CK15, CK16, and CK19, which are recognized by AE1, and CK1, CK3, CK4, CK5, CK6, CK7, and CK8, which are recognized by AE3. Glandular cells contain CK7 and CK17 in epithelial cells and CK8 and CK18 in basal cells, whereas squamous cells contain CK1 and

CK10. Therefore, esophageal squamous cell carcinoma is positive for AE1/AE3 but negative for CAM5.2.

The procedure for IHC was described by Maehara et al. [5]. Sections were immunostained with monoclonal mouse antibodies against human CK (CAM5.2). Xylene was used to remove paraffin from the sections, and the sections were then progressively hydrated in decreasing concentrations of alcohol. The sections were covered with normal rabbit serum for 15 min to reduce nonspecific staining and then incubated with a primary antibody at room temperature for 1 h. In their report, 420 LNs from 34 patients with node-negative early gastric cancer (EGC) were examined after staining with the monoclonal antibody CAM5.2 directed against CK polypeptides expressed in all simple epithelium and all transformed cells derived from epithelial cells. Fifteen of 420 (3.6%) LNs and 8 of 34 (23.5%) patients harbored CK-positive cancer cells.

Similarly, Cai et al. [6] reported that LNMs were found in 17 of 69 patients (25%), with cancer-free nodes examined by H&E staining. Lee et al. [7] found scattered tumor cells in LNs that could not be detected by routine H&E staining. In patients with EGC, LNMs were found to be uncommon, with positivity detected in only 13 of 1018 LNs. However, 28 LNs contained micrometastases in patients with EGC. In all 28 LNs, only 1 or 2 scattered tumor cells were identified in the cortex and subcapsular sinus. This suggested that conventional H&E staining frequently failed to show LNMs in patients with EGC and that immunohistochemical staining for MM may be more useful.

In the case of colorectal cancer, Noura et al. [4] considered multiple sectioning and IHC. Because they surveyed five sections, LNMs were detected at a high rate (11.8% of LNs and 45.9% of patients) compared with those detected in 1- or 2-slice sections, and subsequent analysis was performed based on the results obtained through examination of the five sections. In total, 45 (45.9%) of 98 patients were found to harbor MMs in 11.8% of 878 LNs examined.

Because the presence of LNM is an increasingly important issue in sentinel node analysis, the diagnosis of node metastasis should be as accurate and fast as possible. IHC requires time; however, a rapid IHC technique using frozen sections was established [8]. This method, described below, could be applied to the intraoperative diagnosis of LN metastasis. First, LN samples were embedded in medium, frozen at −80 °C, cut, and mounted on glass slides. All frozen sections were then cut at five additional levels. The slides were placed in 100% acetone for 15-s and then air-dried. After a 15-s rinse in Tris-buffered saline (TBS), sections were incubated for 5 min at room temperature with the monoclonal antibody cocktail AE1/AE3, which is reactive with a broad spectrum of human CKs. After a 15-s rinse in TBS, the sections were incubated with peroxidase-labeled polymer conjugated to primary antibody for 10 min. After briefly rinsing once again in TBS, sections were incubated with the substrate chromogen for 5 min, counterstained with hematoxylin, and mounted with glycerin gelatin. The entire rapid immunostaining procedure required only 30 min to complete.

Matsumoto et al. [8] reported that histological examination with H&E staining revealed 36 metastatic nodes (17%) in 210 dissected nodes from 27 (34%) of

79 patients (47 esophageal squamous cell carcinoma and 32 gastric adenocarcinoma). Of 174 LNs diagnosed as not metastatic by H&E staining, LNMs were newly detected in 12 LNs (7%) from 10 patients by rapid immunostaining. Immunohistochemical examination therefore detected metastasis in a total of 48 (23%) of 210 dissected nodes, and the expression of CK by rapid IHC was similar to that for conventional IHC.

Recently, not only MMs but also isolated tumor cells (ITCs) have been assessed. To detect ITCs, combined techniques of serial sectioning and IHC staining are recommended. In one study, 1656 sections from 91 sentinel LNs of 15 patients were evaluated by a pathologist; MM was found in 1 case, and ITCs were found in 1 case. Overall, 2 out of 15 cases (13.3% of the patients) showed MM/ITCs by IHC staining. Thus, serial sectioning along with IHC was superior to serial sectioning and routine H&E staining. The combined techniques of serial sectioning and IHC staining could be used to reassess the 13.3% of patients with colon cancer who were found to be LN negative [9].

According to the above investigation, combining the methods of serial sectioning and IHC staining results in highly sensitive detection of LNMs in gastrointestinal cancer. Moreover, the specificity of cancer cell detection in LNs using antibodies for epithelial cells is a problem in clinical diagnosis. Cancer-specific single nucleotide variations or copy number variations in LNs will be applied in future clinical work. However, further studies of sentinel LNs are needed to overcome the limitations of these time-consuming, costly techniques.

8.2 Detection of Cancer-Associated mRNAs in LNMs

The accurate diagnosis of LN metastasis in patients with gastric cancer is critical for accurate staging and for planning additional treatments, such as postoperative adjuvant chemotherapy. The detection of LN metastases is commonly performed using conventional histological examinations, i.e., H&E staining of one section containing the largest dimension of the LN. However, LN metastases may be overlooked because of the random distribution of cancer cells throughout the LN. More accurate information about LN metastases can be obtained by conducting more detailed histological examinations of many slides. However, this is time-consuming and increases the workload of the surgeons and pathologists involved. Therefore, it would be more ideal to replace such histological examinations with a quicker, simpler approach.

Molecular biological approaches, such as reverse transcription polymerase chain reaction (RT-PCR) and immunohistochemical staining, have been developed for the detection of LNMs in patients with gastric cancer [10]. These methods should be more sensitive and are expected to become alternatives to conventional histological examination. In this section, we will focus on qRT-PCR and RT-LAMP, which is currently being used in the clinical setting in some countries. These methods allow analysis of whole LNs, avoidance of sampling bias, and objective quantification.

8.2.1 Markers

Target mRNA markers should be highly expressed by epithelial malignant cells with minimal expression in lymphoid tissue. Epithelial markers are usually used to detect LN metastasis because epithelial components are highly and constantly expressed in epithelial malignant cells and are not normally present in LNs. CKs, carcinoembryonic antigen (CEA), and squamous cell carcinoma-related antigen (SCC) are often used for the detection of LN metastasis in gastrointestinal cancers [11].

8.2.2 qRT-PCR

RT-PCR is a technique commonly used in molecular biology to detect mRNA expression. In RT-PCR, the mRNA template is first converted into complementary DNA (cDNA) using a reverse transcriptase. The cDNA is then used as a template for exponential amplification by PCR using thermal cycling, i.e., cycles of heating and cooling. qPCR is used to quantitatively measure the amplification of DNA by employing fluorescent dyes. Currently, there are four different fluorescent DNA probes available for the real-time detection of PCR products: SYBR Green, TaqMan, Molecular Beacons, and Scorpions. All of these probes allow the detection of PCR products by generating a fluorescent signal. While the SYBR Green dye emits its fluorescent signal simply by binding to the double-stranded DNA in solution, the TaqMan probes, Molecular Beacons, and Scorpions generate fluorescence dependent on Förster resonance energy transfer (FRET) coupling of the dye molecule and a quencher moiety to the oligonucleotide substrates [12].

Multiplex PCR refers to the use of PCR to amplify several different targets simultaneously to increase sensitivity and specificity [13]. This process amplifies cDNA in samples using multiple primers and a temperature-mediated DNA polymerase in a thermal cycler. This is also important when sample input is limited. The primer design for all primer pairs has to be optimized so that all primer pairs can work at the same annealing temperature during PCR.

Numerous studies have reported that RT-PCR can detect MM in a background of normal cells and has the potential to overcome the limitations of conventional histological examination. However, this method still has some restrictions with regard to its clinical applications in rapid, intraoperative analysis. Namely, qRT-PCR can be a labor-intensive and time-consuming process owing to the multistep processes of RNA isolation, RT, and PCR. Moreover, these procedures are prone to contamination and RNA degradation, resulting in possible false positives and false negatives, despite the recent technological improvements [14].

8.2.3 RT-LAMP

RT-LAMP is a new nucleic acid amplification method that, similar to RT-PCR, uses reverse transcriptase to generate cDNA from RNA. The target cDNA is then

amplified using DNA polymerase and a set of four specific primers that recognize a total of six distinct sequences on the target cDNA under isothermal conditions, providing high specificity, efficiency, and rapidity [15]. This method measures the time taken to exceed a predetermined threshold turbidity caused by magnesium pyrophosphate, a by-product of the amplification reaction. The one-step nucleic acid amplification (OSNA) assay (Sysmex, Kobe, Japan) is an automated system for rapid and quantitative detection of *CK19* mRNA using RT-LAMP [16]. This method is specifically advantageous because it can be carried out quickly in one step with a low false-positive rate [17]. Moreover, this method is very cost-effective because there is no need for the expensive thermocycling equipment that is necessary for PCR. The detailed procedures are described in the manufacture's protocol. RT-LAMP has been used to diagnose infectious diseases caused by bacteria or viruses [18].

A disadvantage of this method is the generation of the sequence-specific primers, except for primers targeting *CK19*. For each LAMP assay, primers must be specifically designed to be compatible with the target DNA. However, free software called Primer Explorer, developed by Fujitsu in Japan, is available to aid in the selection of these primers.

A comparison of pathological examination, qRT-PCR, and RT-LAMP for detecting LN metastasis is shown in Table 8.1. RT-LAMP (OSNA) is considered to be comparable to pathological examination in terms of the ability to detect LN metastasis and has been increasingly widely applied to the intraoperative investigation of sentinel LNs [19, 20]. In fact, for CK19, RT-LAMP serves as an alternative to pathological examination in patients with breast cancer in Japan [21]. Furthermore, this assay for CK19 in patients with gastric and colorectal cancer has been covered by

Table 8.1 Comparison of pathological examination, qRT-PCR, and RT-LAMP for detecting lymph node metastasis

	Pathological examination	qRT-PCR	RT-LAMP (OSNA)
Judge	Pathologist	Automated	Automated
Method	Morphology	Molecular biology	Molecular biology
Marker	HE staining	Multiplex	CK19
Target tissue	One section	Whole	Whole
Diagnosis			
Sensitivity/specificity	Depends on the pathologist	High, but false positive	High
Quantification	–	+	+
Objectivity	–	+	+
Time requirement	Cytology: 20 min, histology: 30 min	1–2 h	30 min
Protocol	Depends on the pathologist	Depends on the researcher	Standardized
Clinical application	+	–	+

the public health insurance of Japan since 2013. OSNA is expected to be assessed for clinical applications in gastrointestinal cancers in the future.

8.3 Detection of Genetic and Epigenetic Changes in LNMs

Meta-analyses have shown that MMs in regional LNs detected by immunohistochemical approaches or molecular techniques, such as RT-PCR, are significantly associated with poor prognosis in node-negative colorectal cancer based on the conventional histopathologic method [22]. According to the adenoma carcinoma sequence model for the evolution of colorectal cancer, mutations in *K-ras*, *APC*, and *TP53* are representative driver events indicating the clonal distinction of malignant cells. These mutations should potentially be useful and precise molecular markers of small numbers of colorectal cancer cells in LNs or distant organs [23].

8.3.1 Cancer-Specific Mutations in Driver Genes

Hayashi et al. have detected a small number of cancer cells by screening for *K-ras* and *p53* gene alterations using mutant allele-specific amplification (MASA) analysis in LNs negative for tumor cells by conventional histopathologic analysis [24]. In their study, 22 colorectal cancers were screened for *K-ras* and *p53* mutations. Fourteen cases were found to harbor genetic alterations; six of the primary tumors contained certain *K-ras* mutations, and nine contained *p53* mutations (mutations in both genes were found in one tumor). Four cases were positive by both histological and genetic diagnoses, three cases were negative by both histological and genetic diagnoses, and seven cases were negative by histology but positive by genetic diagnosis.

8.3.2 Cancer-Specific Methylation

In addition to genetic alterations, cancers also often exhibit silencing of tumor-suppressor genes due to hypermethylated promoters. Cancer-specific hypermethylation of normally unmethylated CpG islands in the promoter regions of many key cancer-related genes, including *p16*, *p15*, E-cadherin, and *VHL*, correlates with loss of transcription in human tumors [25]. Sanchez-Cespedes et al. examined both genetic (*K-ras* and *p53* gene mutations) and epigenetic (*p16* promoter hypermethylation) molecular markers in perihepatic LNs from patients with colorectal cancer with isolated liver metastases [26]. A sensitive oligonucleotide-mediated mismatch ligation assay was used to search for the presence of *K-ras* and *p53* mutations in occult disease in 68 of 80 LNs positive for these gene mutations from 21 patients with colorectal cancer. Promoter hypermethylation at the *p16* tumor-suppressor gene was examined in both liver lesions and LNs using methylation-specific PCR (MSP). Sixteen of the 21 (76%) liver metastases harbored either gene point

mutations or *p16* promoter hypermethylation. Twelve of the 68 LNs were positive for tumor cells by molecular evaluation and negative for tumor cells by histopathology and CK IHC, whereas none were positive for tumor cells by histopathology or negative for tumor cells.

Approaches for genetic alterations of malignant cells tend to be absolutely specific because they detect genetic abnormalities present only in the neoplastic DNA and not in the normal DNA. Therefore, genetic-based methods are more sensitive than conventional histology for detecting MM colorectal cancer cells. However, these genetic approaches are limited by the ability to detect specific genetic or epigenetic alterations in primary tumors. In the future, studies are needed to develop more accurate approaches to identification of a number of gastrointestinal cancers using next-generation sequencing of target sequences by selecting effective genetic alterations to detect LNMs.

8.4 Future Perspectives

To date, various biological techniques, such as IHC and RT-PCR, have been developed. However, several technical obstacles are interfering with the routine use of these methods in clinical practice. For example, these methods are not sufficiently accurate (i.e., may yield false positives and false negatives), are labor intensive, and are not cost-effective. Although major advancements in our knowledge of the molecular and cellular biology of new lymphatic vessels through lymphangiogenesis and the remodeling of existing lymphatics in cancer has been made in the past decade, we still need to improve our understanding of tumor metastasis to LNs in order to improve diagnostic approaches for detection of LNMs. In this section, we will review potential approaches for the detection of LNMs and discuss future perspectives with a specific focus on the development of new strategies for detecting LNMs.

8.4.1 Visualization of LNMs

Detection of tumor draining LNs, particularly first draining LNs (sentinel LNs), is frequently necessary during surgery in patients with breast cancers and melanomas and can be carried out using peritumoral tracer injection, such as dyes and radioisotopes. Imaging approaches that may allow cancer cells to be monitored in vivo are currently being developed.

Fluorescence-guided surgery has attracted the attention of many clinicians and is an area of intense research. To date, conventional imaging modalities, such as computed tomography and magnetic resonance imaging, cannot differentiate between adenopathy related to inflammation and that caused by deposition of cancer cells preoperatively. Moreover, the unaided human eye also cannot detect LNMs during surgery. Recently, a rapidly activatable, cancer-selective fluorescence imaging prove, γ-glutamyl hydroxymethyl rhodamine green (gGlu-HMRG), was developed [27]. This fluorescence-based technique relies on the fact that activation occurs by

rapid cleavage of glutamate by γ-glutamyltranspeptidase (GGT), which is not expressed in normal tissue, but is overexpressed on the membranes of cancer cells. This technique was initially applied to breast cancer. Breast cancers smaller than 1 mm in size were discriminated from normal mammary gland tissues, with high sensitivity (92%) and specificity (94%), within only 5 min after gGlu-HMRG administration [28]. In addition, in LNs of patients with breast cancer, this fluorescent method was also found to be useful for visualizing breast cancer cells with high sensitivity (97%), specificity (79%), and negative predictive value (99%) [29]. Since LNMs are defined as microscopic deposits of malignant cells with a largest dimension of 0.2–2 mm, this technique may theoretically be able to detect LNMs. This technique will not only reduce the manpower, cost, and labor requirements compared with those of intraoperative pathological analysis using frozen sections but will also offer the advantages of rapidity, safety, and convenience. Additionally, telomerase-dependent adenovirus (OBP-401), which expresses the *gfp* gene only in cancer cells, has been used successfully for complete resection of colon cancer liver metastasis in a mouse model [30]. This fluorescence virus-guided approach was also useful to detect circulating tumor cells (CTCs) in clinical blood samples from patients with gastric and colorectal cancer [31, 32].

Recently developed in vivo imaging approaches have the potential for clinical applications based on the visualization of tumor-induced changes, such as LN lymphangiogenesis and lymphatic flow through draining LNs instead of the tumor cells themselves [33]. LN lymphangiogenesis can be found in tumor-draining LNs prior to the actual onset of lymphatic metastasis, indicating the formation of a premetastatic niche, which is a favorable microenvironment at future sites of metastasis [34]. Lymphatic vessel endothelial hyaluronan receptor 1 (LYVE1) is a protein that has been used for identification of lymphatic vessels [35]. In a mouse model of melanoma, immune-positron emission tomography (I-PET) with a ^{124}I-radiolabeled anti-LYVE1 antibody was used to detect LN metastases that could not be detected by [^{18}F]fluorodeoxyglucose-PET, which is used to detect cancer metastases in clinical practice [36]. Moreover, near-infrared (IR) imaging of an intradermally injected liposomal formulation of ICG enabled quantification of lymphatic flow in a mouse model of melanoma [37]. Polyethylene glycol conjugates of bright near-IR dye, a class of much brighter near-IR dyes, were developed and enabled the visualization of tumor-draining lymphatic vessels [38]. Further studies are required to evaluate the usefulness of these direct and indirect visualization approaches of cancer cells in more detail.

8.4.2 Malignant Potential of Cancer Cells Forming LNMs: An Approach Based on Cancer Cells Properties

Cancer is a heterogeneous disease, and not all cancer cells possess the same phenotypes, including metastatic potential through LNs. Therefore, colonization of cancer cells is not definitely associated with physical dissemination based on the fact that not all multiple MMs in LNs have progressed to macroscopic metastatic tumors.

The biological signatures of cancer cells, such as the epithelial-to-mesenchymal transition (EMT) and cancer stemness, are considered part of the essential metastatic phenotype. Therefore, these properties would be a potential diagnostic marker of the malignant phenotype in LNMs.

The EMT is a biological process in which epithelial cells acquire a mesenchymal cell phenotype. In the primary tumor, cancer cells induce local dissemination through the EMT and invade into the lymphatic system. Transcriptional factors, such as Slug, Snail, Twist, and Zeb1, have been suggested to have a role in inducing the EMT. In intrahepatic cholangiocarcinoma, altered expression of ZEB1 is associated with LN metastasis [39]. In gastric cancer, C-C motif chemokine receptor 7 (CCR7) enhances the transforming growth factor (TGF)-β1-induced EMT and facilitates LN metastasis [40]. In colorectal cancer, non-coding RNAs (ncRNAs), particularly microRNAs (miRNAs), such as miR-92a and miR-187, are also involved in the EMT process [41, 42]. Thus, expression of these EMT-associated factors could be promising future diagnostic markers.

Cancer stem cells (CSCs) are thought to be responsible for tumor initiation, resistance to chemotherapy and radiation, invasive growth, metastasis, and tumor relapse in gastrointestinal cancers, such as esophageal, stomach, and colorectal cancers [43]. CSCs are capable of self-renewal, multipotency, tumorigenicity, and metastatic potential. If CSCs are the only subsets of cells capable of initiating new tumor growth, then CSCs must be involved in the metastatic process. For example, lymphatic vessels in metastatic tissues stimulate the metastasis of cancer cells that express CXC-chemokine receptor 4 (CXCR4) and the stem cell marker CD133 to target organs by secretion of stromal cell-derived factor-1 (SDF-1) [44]. Since gastrointestinal CSCs express unique surface markers, such as CD133, CD44, and aldehyde dehydrogenase-1 activity [43], these markers would be useful for detection of the malignant phenotype of cancer cells in LNMs.

8.4.3 Monitoring Changes in the Microenvironment Associated with LNMs: An Approach Based on Host Factors

Although the molecular mechanisms of tumor cell migration and metastasis to LNs are not fully characterized, the “seed and soil” hypothesis is now widely accepted. According to this hypothesis, metastasis is determined both by cancer cell characteristics and by the host microenvironment. Host cells, including macrophages, mesenchymal stem cells, and bone marrow-derived cells, have attracted much attention because they form a favorable microenvironment (“soil”), also called a premetastatic niche, for cancer cells [45].

Cancer cells are thought to use chemokine-mediated mechanisms during the process of LN metastasis of cancer cells. Isolated cancer cells from primary cancers are guided to the premetastatic niche by chemokines from the host cells. Various tumor models have shown that cancer cells expressing certain chemokine receptors show increased rates of LN metastasis in the presence of appropriate chemokines. For example, expression of CCR7 by cancer cells has been detected and found to be

associated with increased LN metastasis in gastric cancer and colorectal cancer [46, 47]. In our previous report, the FBXW7/NOTCH/CCL2 pathway was also shown to play an essential role in the regulation of the premetastatic niche [48]. Moreover, the CCL1 chemokine produced by LN lymphatic sinuses mediates the LN entry of CCR8-expressing melanoma cells, whereas the CCR8 blockade reduces LN metastasis [49]. Thus, chemokines have the potential to provide large amounts of biological information due to their essential roles in mediating tumor cell entry into LNs.

The lymphatic vasculature is essential for immune function. The immune surveillance theory proposed that cells are constantly monitored by the immune system, which is responsible for recognizing and eliminating the majority of cancer cells. However, cancer cells metastasize to LNs via lymphatic vessels. One reason is that lymphatic endothelial cells (LECs) express major histocompatibility complex (MHC) class I and MHC class II molecules and function as antigen-presenting cells to induce self-tolerance [50, 51]. In addition, lymphatic vessels may provide an immunoprotective microenvironment through chemokine secretion. CCL21 can shift the host immune response from immunogenic to tolerogenic, which can facilitate tumor progression [52]. Moreover, vascular endothelial growth factor (VEGF)-C and associated LN lymphangiogenesis have been shown to suppress antitumor immunity and drive disease progression and metastasis in a melanoma model [53].

Thus, detecting host-side markers, such as chemokine that induce LNMs and molecules that induce immune tolerance, may be useful for the prediction of LN metastasis as well as the detection of LNMs.

8.4.4 Miscellaneous Factors

Recently, exosomes, i.e., small membrane-enveloped vesicles containing functional biomolecules, such as protein, RNA, and DNA, have received attention in the field of intercellular communication. Tumor-derived exosomes may contribute to LN lymphangiogenesis as part of the premetastatic niche [54]. Exosomes are also expected to be useful biomarkers because they are remarkably stable.

A large number of transcripts in the human genome are ncRNAs, including miRNAs and long non-coding RNAs (lncRNAs). MiRNA are molecules of around 22 nucleotides in length that regulate target gene expression at the posttranscriptional level. Aberrant expression of miRNAs has been detected in various types of cancers and has been shown to promote or suppress metastasis [55, 56]. LncRNAs are defined as molecules greater than 200 nucleotides in length that are devoid of an apparent open reading frame. Aberrant expression of lncRNAs frequently occurs in gastrointestinal cancers and plays important roles in cancer metastasis [57].

Recent cancer genome-wide analyses revealed the presence of intratumor heterogeneity within individual tumors as well as intertumor heterogeneity among patients [58]. The existence of multiple clones in a single tumor mass presumably results in the development of drug resistance in tumors. In our recent study, we demonstrated the presence of intratumor heterogeneity in colorectal cancer by analyzing samples obtained from geographically separated regions of nine colorectal

tumors [59]. In two of nine cases, samples from liver metastasis were obtained, and metastatic lesions contained mutations in the same driver genes as those observed in the primary colorectal tumor. These findings suggested that metastatic lesions may include mutations in the same driver genes as those in the primary tumor. Therefore, mutations in driver genes in primary tumors may become markers to detect LNMs. Extensive characterization of the cancer genome in the primary tumor will identify which gene mutations in cancer cells are associated with patterns of gene expression that favor metastasis through the lymphatics. Furthermore, identification of genetic prerequisites required for metastatic properties in primary tumor cells may lead to early detection of LNMs. In the near future, molecular biological techniques, such as next-generation sequencing and single-cell analysis of primary tumor cells, will likely help to clarify the malignant potential of cancer cells in LNMs to develop metastatic lesions. Considering the treatment strategies for gastrointestinal cancers, we should be more careful in the diversities of metastatic tumors in LNs as well as heterogeneity of primary tumors.

8.4.5 Future Directions

Despite improvements in surgical techniques, general patient care, and systemic adjuvant therapies, most deaths from cancer result from metastasis. Since LNMs can be prognostic factors for patient survival, early detection of LNMs that have malignant potential could be used to determine the optimal therapeutic strategy, such as the choice of adjuvant therapies and the decision for regional LN dissection during surgery. In particular, when we perform minimally invasive surgery, such as sentinel LN navigation surgery, to maintain a balance between curability and quality of life, there is a great need for the identification of biomarkers to aid in the rapid and accurate diagnosis of LNMs. In the near future, genome-wide functional approaches that identify the genomic, transcriptional, and proteomic changes in cancer cells may be used to elucidate important signaling pathways that could be potential diagnostic targets. Ideally, reliable assays for detecting increased concentrations of targets in the blood should also be required to reduce invasiveness and improve simplicity. Ultimately, comprehensive assessments of detection methods and target genes as well as labor of medical staffs and cost-benefit analysis for medical economy are needed. Therefore, it is critical to improve our understanding of the characteristics of metastatic cells that will allow us to detect LNMs.

References

1. Sobin L, Gospodarowicz M, Wittekind C. TNM classification of malignant tumours. 7th ed. Hoboken, NJ: Wiley-Blackwell; 2009.
2. Isozaki H, Okajima K, Fujii K. Histological evaluation of lymph node metastasis on serial sectioning in gastric cancer with radical lymphadenectomy. Hepato-Gastroenterology. 1997;44:1133–6.

3. Natsugoe S, Aikou T, Shimada M, Yoshinaka H, Takao S, Shimazu H, et al. Occult lymph node metastasis in gastric cancer with submucosal invasion. Surg Today. 1994;24:870–5.
4. Noura S, Yamamoto H, Miyake Y, Kim B, Takayama O, Seshimo I, et al. Immunohistochemical assessment of localization and frequency of micrometastases in lymph nodes of colorectal cancer. Clin Cancer Res. 2002;8:759–67.
5. Maehara Y, Oshiro T, Endo K, Baba H, Oda S, Ichiyoshi Y, et al. Clinical significance of occult micrometastasis lymph nodes from patients with early gastric cancer who died of recurrence. Surgery. 1996;119:397–402.
6. Cai J, Ikeguchi M, Maeta M, Kaibara N. Micrometastasis in lymph nodes and microinvasion of the muscularis propria in primary lesions of submucosal gastric cancer. Surgery. 2000;127:32–9.
7. Lee E, Chae Y, Kim I, Choi J, Yeom B, Leong AS. Prognostic relevance of immunohistochemically detected lymph node micrometastasis in patients with gastric carcinoma. Cancer. 2002;94:2867–73.
8. Matsumoto M, Natsugoe S, Ishigami S, Uenosono Y, Takao S, Aikou T. Rapid immunohistochemical detection of lymph node micrometastasis during operation for upper gastrointestinal carcinoma. Br J Surg. 2003;90:563–6.
9. Sanei MH, Tabatabie SA, Hashemi SM, Cherei A, Mahzouni P, Sanei B. Comparing the efficacy of routine H&E staining and cytokeratin immunohistochemical staining in detection of micro-metastasis on serial sections of dye-mapped sentinel lymph nodes in colorectal carcinoma. Adv Biomed Res. 2016;5:13.
10. Kumagai K, Yamamoto N, Miyashiro I, Tomita Y, Katai H, Kushima R, et al. Multicenter study evaluating the clinical performance of the OSNA assay for the molecular detection of lymph node metastases in gastric cancer patients. Gastric Cancer. 2014;17:273–80.
11. Natsugoe S, Arigami T, Uenosono Y, Yanagita S, Nakajo A, Matsumoto M, et al. Lymph node micrometastasis in gastrointestinal tract cancer--a clinical aspect. Int J Clin Oncol. 2013;18:752–61.
12. Arya M, Shergill IS, Williamson M, Gommersall L, Arya N, Patel HR. Basic principles of real-time quantitative PCR. Expert Rev Mol Diagn. 2005;5:209–19.
13. Chamberlain JS, Gibbs RA, Ranier JE, Nguyen PN, Caskey CT. Deletion screening of the Duchenne muscular dystrophy locus via multiplex DNA amplification. Nucleic Acids Res. 1988;16:11141–56.
14. Keilholz U, Willhauck M, Rimoldi D, Brasseur F, Dummer W, Rass K, et al. Reliability of reverse transcription-polymerase chain reaction (RT-PCR)-based assays for the detection of circulating tumour cells: a quality-assurance initiative of the EORTC Melanoma Cooperative Group. Eur J Cancer. 1998;34:750–3.
15. Notomi T, Okayama H, Masubuchi H, Yonekawa T, Watanabe K, Amino N, et al. Loop-mediated isothermal amplification of DNA. Nucleic Acids Res. 2000;28:E63.
16. Tsujimoto M, Nakabayashi K, Yoshidome K, Kaneko T, Iwase T, Akiyama F, et al. One-step nucleic acid amplification for intraoperative detection of lymph node metastasis in breast cancer patients. Clin Cancer Res. 2007;13:4807–16.
17. Tamaki Y, Akiyama F, Iwase T, Kaneko T, Tsuda H, Sato K, et al. Molecular detection of lymph node metastases in breast cancer patients: results of a multicenter trial using the one-step nucleic acid amplification assay. Clin Cancer Res. 2009;15:2879–84.
18. Mori Y, Notomi T. Loop-mediated isothermal amplification (LAMP): a rapid, accurate, and cost-effective diagnostic method for infectious diseases. J Infect Chemother. 2009;15:62–9.
19. Snook KL, Layer GT, Jackson PA, de Vries CS, Shousha S, Sinnett HD, et al. Multicentre evaluation of intraoperative molecular analysis of sentinel lymph nodes in breast carcinoma. Br J Surg. 2011;98:527–35.
20. Cserni G. Intraoperative analysis of sentinel lymph nodes in breast cancer by one-step nucleic acid amplification. J Clin Pathol. 2012;65:193–9.
21. Tamaki Y. One-step nucleic acid amplification (OSNA): where do we go with it? Int J Clin Oncol. 2017;22(1):3–10.

22. Rahbari NN, Bork U, Motschall E, Thorlund K, Buchler MW, Koch M, et al. Molecular detection of tumor cells in regional lymph nodes is associated with disease recurrence and poor survival in node-negative colorectal cancer: a systematic review and meta-analysis. J Clin Oncol. 2012;30:60–70.
23. Losi L, Benhattar J, Costa J. Stability of K-ras mutations throughout the natural history of human colorectal cancer. Eur J Cancer. 1992;28A:1115–20.
24. Hayashi N, Arakawa H, Nagase H, Yanagisawa A, Kato Y, Ohta H, et al. Genetic diagnosis identifies occult lymph node metastases undetectable by the histopathological method. Cancer Res. 1994;54:3853–6.
25. Baylin SB, Herman JG, Graff JR, Vertino PM, Issa JP. Alterations in DNA methylation: a fundamental aspect of neoplasia. Adv Cancer Res. 1998;72:141–96.
26. Sanchez-Cespedes M, Esteller M, Hibi K, Cope FO, Westra WH, Piantadosi S, et al. Molecular detection of neoplastic cells in lymph nodes of metastatic colorectal cancer patients predicts recurrence. Clin Cancer Res. 1999;5:2450–4.
27. Urano Y, Sakabe M, Kosaka N, Ogawa M, Mitsunaga M, Asanuma D, et al. Rapid cancer detection by topically spraying a gamma-glutamyltranspeptidase-activated fluorescent probe. Sci Transl Med. 2011;3:110ra9.
28. Ueo H, Shinden Y, Tobo T, Gamachi A, Udo M, Komatsu H, et al. Rapid intraoperative visualization of breast lesions with gamma-glutamyl hydroxymethyl rhodamine green. Sci Rep. 2015;5:12080.
29. Shinden Y, Ueo H, Tobo T, Gamachi A, Utou M, Komatsu H, et al. Rapid diagnosis of lymph node metastasis in breast cancer using a new fluorescent method with gamma-glutamyl hydroxymethyl rhodamine green. Sci Rep. 2016;6:27525.
30. Yano S, Takehara K, Miwa S, Kishimoto H, Hiroshima Y, Murakami T, et al. Improved resection and outcome of colon-cancer liver metastasis with fluorescence-guided surgery using in situ GFP labeling with a telomerase-dependent adenovirus in an orthotopic mouse model. PLoS One. 2016;11:e0148760.
31. Shigeyasu K, Tazawa H, Hashimoto Y, Mori Y, Nishizaki M, Kishimoto H, et al. Fluorescence virus-guided capturing system of human colorectal circulating tumour cells for non-invasive companion diagnostics. Gut. 2015;64:627–35.
32. Ito H, Inoue H, Kimura S, Ohmori T, Ishikawa F, Gohda K, et al. Prognostic impact of the number of viable circulating cells with high telomerase activity in gastric cancer patients: a prospective study. Int J Oncol. 2014;45:227–34.
33. Karaman S, Detmar M. Mechanisms of lymphatic metastasis. J Clin Invest. 2014;124:922–8.
34. Hirakawa S, Kodama S, Kunstfeld R, Kajiya K, Brown LF, Detmar M. VEGF-A induces tumor and sentinel lymph node lymphangiogenesis and promotes lymphatic metastasis. J Exp Med. 2005;201:1089–99.
35. Banerji S, Ni J, Wang SX, Clasper S, Su J, Tammi R, et al. LYVE-1, a new homologue of the CD44 glycoprotein, is a lymph-specific receptor for hyaluronan. J Cell Biol. 1999;144:789–801.
36. Mumprecht V, Honer M, Vigl B, Proulx ST, Trachsel E, Kaspar M, et al. In vivo imaging of inflammation- and tumor-induced lymph node lymphangiogenesis by immuno-positron emission tomography. Cancer Res. 2010;70:8842–51.
37. Proulx ST, Luciani P, Derzsi S, Rinderknecht M, Mumprecht V, Leroux JC, et al. Quantitative imaging of lymphatic function with liposomal indocyanine green. Cancer Res. 2010;70:7053–62.
38. Proulx ST, Luciani P, Christiansen A, Karaman S, Blum KS, Rinderknecht M, et al. Use of a PEG-conjugated bright near-infrared dye for functional imaging of rerouting of tumor lymphatic drainage after sentinel lymph node metastasis. Biomaterials. 2013;34:5128–37.
39. Terashita K, Chuma M, Hatanaka Y, Hatanaka K, Mitsuhashi T, Yokoo H, et al. ZEB1 expression is associated with prognosis of intrahepatic cholangiocarcinoma. J Clin Pathol. 2016;69:593–9.
40. Ma H, Gao L, Li S, Qin J, Chen L, Liu X, et al. CCR7 enhances TGF-beta1-induced epithelial-mesenchymal transition and is associated with lymph node metastasis and poor overall survival in gastric cancer. Oncotarget. 2015;6:24348–60.

41. Zhang G, Zhou H, Xiao H, Liu Z, Tian H, Zhou T. MicroRNA-92a functions as an oncogene in colorectal cancer by targeting PTEN. Dig Dis Sci. 2014;59:98–107.
42. Zhang F, Luo Y, Shao Z, Xu L, Liu X, Niu Y, et al. MicroRNA-187, a downstream effector of TGFbeta pathway, suppresses Smad-mediated epithelial-mesenchymal transition in colorectal cancer. Cancer Lett. 2016;373:203–13.
43. Taniguchi H, Moriya C, Igarashi H, Saitoh A, Yamamoto H, Adachi Y, et al. Cancer stem cells in human gastrointestinal cancer. Cancer Sci. 2016;107:1556.
44. Kim M, Koh YJ, Kim KE, Koh BI, Nam DH, Alitalo K, et al. CXCR4 signaling regulates metastasis of chemoresistant melanoma cells by a lymphatic metastatic niche. Cancer Res. 2010;70:10411–21.
45. Masuda T, Hayashi N, Iguchi T, Ito S, Eguchi H, Mimori K. Clinical and biological significance of circulating tumor cells in cancer. Mol Oncol. 2016;10:408–17.
46. Mashino K, Sadanaga N, Yamaguchi H, Tanaka F, Ohta M, Shibuta K, et al. Expression of chemokine receptor CCR7 is associated with lymph node metastasis of gastric carcinoma. Cancer Res. 2002;62:2937–41.
47. Gunther K, Leier J, Henning G, Dimmler A, Weissbach R, Hohenberger W, et al. Prediction of lymph node metastasis in colorectal carcinoma by expression of chemokine receptor CCR7. Int J Cancer. 2005;116:726–33.
48. Yumimoto K, Akiyoshi S, Ueo H, Sagara Y, Onoyama I, Ueo H, et al. F-box protein FBXW7 inhibits cancer metastasis in a non-cell-autonomous manner. J Clin Invest. 2015;125:621–35.
49. Das S, Sarrou E, Podgrabinska S, Cassella M, Mungamuri SK, Feirt N, et al. Tumor cell entry into the lymph node is controlled by CCL1 chemokine expressed by lymph node lymphatic sinuses. J Exp Med. 2013;210:1509–28.
50. Tewalt EF, Cohen JN, Rouhani SJ, Engelhard VH. Lymphatic endothelial cells – key players in regulation of tolerance and immunity. Front Immunol. 2012;3:305.
51. Tewalt EF, Cohen JN, Rouhani SJ, Guidi CJ, Qiao H, Fahl SP, et al. Lymphatic endothelial cells induce tolerance via PD-L1 and lack of costimulation leading to high-level PD-1 expression on CD8 T cells. Blood. 2012;120:4772–82.
52. Shields JD, Kourtis IC, Tomei AA, Roberts JM, Swartz MA. Induction of lymphoidlike stroma and immune escape by tumors that express the chemokine CCL21. Science. 2010;328:749–52.
53. Lund AW, Duraes FV, Hirosue S, Raghavan VR, Nembrini C, Thomas SN, et al. VEGF-C promotes immune tolerance in B16 melanomas and cross-presentation of tumor antigen by lymph node lymphatics. Cell Rep. 2012;1:191–9.
54. Hood JL, San RS, Wickline SA. Exosomes released by melanoma cells prepare sentinel lymph nodes for tumor metastasis. Cancer Res. 2011;71:3792–801.
55. Ma L, Teruya-Feldstein J, Weinberg RA. Tumour invasion and metastasis initiated by microRNA-10b in breast cancer. Nature. 2007;449:682–8.
56. Tavazoie SF, Alarcon C, Oskarsson T, Padua D, Wang Q, Bos PD, et al. Endogenous human microRNAs that suppress breast cancer metastasis. Nature. 2008;451:147–52.
57. Zhang FF, Luo YH, Wang H, Zhao L. Metastasis-associated long noncoding RNAs in gastrointestinal cancer: implications for novel biomarkers and therapeutic targets. World J Gastroenterol. 2016;22:8735–49.
58. Burrell RA, McGranahan N, Bartek J, Swanton C. The causes and consequences of genetic heterogeneity in cancer evolution. Nature. 2013;501:338–45.
59. Uchi R, Takahashi Y, Niida A, Shimamura T, Hirata H, Sugimachi K, et al. Integrated multiregional analysis proposing a new model of colorectal cancer evolution. PLoS Genet. 2016;12:e1005778.

Clinical Aspect: Esophageal Cancer

9

Itaru Omoto, Yasuto Uchikado, Ken Sasaki,
Takaaki Arigami, and Shoji Natsugoe

Abstract

Lymph node micrometastasis (LNM), including isolated tumor cells (ITC), has recently been the focus of study for the development of a biological method to detect lymph node metastasis in various malignant neoplasms. The applicability of immunohistochemistry (IHC) and reverse transcription-polymerase chain reactions (RT-PCR) to the detection of LNM in esophageal cancer has already been reported. However, the clinical significance of LNM currently remains unclear in patients with esophageal cancer. The presence of LNM is clinically important in patients without nodal metastasis in a routine histological examination (pN0) because patients with pN0, but also with LNM already exhibit metastatic potential. Accurate evaluations need to be performed using the same antibody or primer as well as the same technique in a large number of patients. A rapid diagnosis of LNM using IHC and RT-PCR during surgery will be clinically useful. Minimally invasive treatments such as endoscopic submucosal dissection and laparoscopic surgery with individualized lymphadenectomy are now being increasingly performed in consideration of postsurgical quality of life (QOL). However, it is important to maintain the balance between QOL and curability when selecting surgical treatments for patients with esophageal cancer. We reviewed the clinical significance of LNM as an important strategic target in patients with esophageal cancer.

Keywords

Lymph node micrometastasis · Esophageal cancer · Minimally invasive surgery

I. Omoto (✉) · Y. Uchikado · K. Sasaki · T. Arigami · S. Natsugoe
Department of Digestive Surgery, Breast and Thyroid Surgery, Kagoshima University Graduate School of Medical and Dental Sciences, Kagoshima, Japan
e-mail: itaru@m3.kufm.kagoshima-u.ac.jp

S. Natsugoe (ed.), *Lymph Node Metastasis in Gastrointestinal Cancer*,
https://doi.org/10.1007/978-981-10-4699-5_9

9.1 Introduction

One of the characteristics of a malignant tumor is its ability to metastasize. If a tumor exhibits high malignant potential, metastasis is often detected in a wide range of areas. The prognosis of esophageal cancer is poor. It frequently metastasizes to any of a number of lymph nodes, including the cervical, mediastinal, and abdominal lymph nodes. Lymph node metastasis is one of the most important prognostic factors in patients with esophageal cancer [1, 2]. Even if complete lymph node dissection is performed in patients with early cancer, recurrent disease is sometimes encountered. Therefore, in Japan, radical lymph node dissection, such as extended three-field lymphadenectomy, is performed on patients with esophageal cancer. However, this type of surgical procedure in patients with esophageal cancer is associated with a higher incidence of postoperative complications and hospital mortality than surgical treatments for patients with other gastrointestinal tract cancers [3–5]. If it is possible to perform minimally invasive surgery to treat esophageal cancer, the mortality rate after surgery and postsurgical quality of life (QOL) may be improved. There are currently several therapeutic strategies in the clinical management of patients with early esophageal cancer. Regarding surgical treatments, minimally invasive surgery, such as endoscopic mucosal resection (EMR), endoscopic submucosal dissection (ESD), and blunt dissection, are selected and performed based on the stages and preoperative conditions of patients [6, 7]. In surgical procedures, the clinical efficacy of sentinel node navigation surgery (SNNS) has been investigated in patients preoperatively free of lymph node metastasis (cN0), and many investigators have reported that SNNS is applicable to patients who are preoperatively diagnosed with cT1 and cN0 esophageal cancer [8–10]. Since patients who undergo esophagectomy with standard lymphadenectomy have a promising prognosis, oncological curability needs to be secured in patients receiving less-invasive treatments, such as ESD and SNNS; disease recurrence following less-invasive treatments is undesirable. Accordingly, the precise assessment of the intraoperative lymph node status is extremely important in the strategic process when performing less-invasive treatments.

A histological examination for lymph node metastasis is typically performed using representative sections from the removed nodes. However, lymph node micrometastasis (LNM) may be identified in multiple sections of lymph nodes despite not being detected by a routine histological examination using hematoxylin and eosin (HE) staining. Even in early gastric cancer, lymph node metastasis was detected in 10.5% of patients when additional sections of nodes were examined [11]. However, these procedures are labor-intensive and not cost-effective in active clinical practice. To date, several investigators have demonstrated the clinical impact of LNM identified by immunohistochemistry (IHC) [12–14]. Furthermore, real-time reverse transcription-polymerase chain reactions (RT-PCR) have been reported to detect LNM better than IHC [15–17]. However, few studies have focused on SN mapping based on LNM assessed by RT-PCR in patients with esophageal cancer.

This review will focus on the clinical significance of LNM as an important therapeutic target in esophageal cancer, including recent advances.

9.2 Definition of LNM

Historically, several terms for very small metastatic foci have been used, including occult metastasis, harbored metastasis, tumor microinvolvement, and tumor deposits. Micrometastasis (MM) is currently defined according to the criteria of the tumor–node–metastasis (TNM) classification established by the International Union Against Cancer (UICC) in 2002 [18] and is completely differentiated from isolated tumor cells (ITC) by size [19]. ITC represent either single tumor cells or small clusters of cells measuring <0.2 mm at their greatest dimension and are commonly identified by IHC, but may also be confirmed by routine HE staining. Moreover, ITC do not basically demonstrate evidence of metastatic activity, such as proliferation or a stromal reaction, or the penetration of vascular or lymphatic sinus walls. Patients with ITC in the lymph nodes are staged as pN0 (i+). On the other hand, MM refers to tumor cell clusters measuring >0.2 mm, but <2.0 mm at the greatest dimension. Patients with MM in the lymph nodes are staged as pN1 (mi). Furthermore, patients with node positivity diagnosed by non-morphological findings using RT-PCR are staged as pN0 (mol+).

9.3 Detection of MM

Many researchers have reported several procedures for the detection of LNM in patients with esophageal cancer. The development of sensitive IHC techniques and RT-PCR has led to the detection of LNM that cannot be found in routine histological examinations. IHC as well as conventional HE staining has been clinically utilized as a standard tool for detecting LNM in esophageal cancer. Furthermore, due to advances in molecular biological techniques, RT-PCR is now available for the detection of LNM. Epithelial markers are commonly used to identify LNM in IHC. Cytokeratin (CK) is representative of epithelial markers. According to previous studies, CK AE1/AE3 and CAM5.2 monoclonal antibodies are often used for IHC [9, 13, 14, 20–28]. Each technique has specific advantages and disadvantages. Since IHC is relatively simple and has the capacity to morphologically identify a single tumor cell or small clusters of tumor cells in lymph nodes, it is a technique this is available in many institutions. Matsumoto et al. [29] established a rapid IHC procedure with the ability to diagnose LNM within 30 min, and this procedure has recently been applied to the detection of LNM during surgery for upper gastrointestinal tract cancer, including esophageal cancer. However, difficulties are associated with selecting a sufficient number of sections for the detection of LNM. Noura et al. [30], in a study on 98 patients with colorectal cancer, demonstrated that the diagnosis of LNM by immunostaining requires staining of at least five slices and therefore is expensive, and generates false-negatives.

On the other hand, RT-PCR offers an objective method for estimating LNM. In RT-PCR assays, several epithelial markers may be used to detect LNM in lymph nodes; however, one of the key issues is selecting what kind of marker is suitable for each carcinoma. CK, carcinoembryonic antigen (CEA), and squamous cell

carcinoma-related antigen (SCC) are typically used for the detection of LNM in esophageal cancer. CEA, CK, and Mucin 1 (MUC 1) are used as target markers of LNM [9, 31–34]. CEA is an epithelial-specific antigen that is expressed in most cancers as well as in normal gastrointestinal tissues [35]. The MUC1 gene is one of the specific markers of epithelial tissues that does not appear in normal lymph nodes [36, 37]. Epithelial markers are generally available for the detection of LNM because epithelial components are not normally present in the lymph nodes. Although this approach offers high sensitivity for detecting low numbers of occult cancer cells in lymph nodes, false-positive results are sometimes obtained as a result of contamination and the presence of pseudogenes. Moreover, false-negatives may be obtained due to the heterogeneous expression of a target marker. Therefore, a detailed assessment using a multiplex RT-PCR assay is currently recommended in order to decrease the rate of false-negative results [38].

In order for RT-PCR assays to be applied as an intraoperative diagnostic tool for the detection of LNM, they need to enable rapid analyses during surgery and retain high sensitivity and specificity. Yanagita et al. reported the clinical availability of another RT-PCR assay named the SmartCycler system as an intraoperative diagnostic tool for detecting LNM in patients with gastric cancer [39]. The reverse transcription of cDNA from target mRNA and the amplification of cDNA are automatically performed by one step in this system. Moreover, the SmartCycler system using a prototype kit may assess the expression of CEA and CK 19 mRNAs and complete the detection of lymph node metastasis within approximately 40 min. According to their study on 47 overt metastatic lymph nodes from 8 patients with advanced gastric cancer and 22 benign lymph nodes from patients without malignant tumors, the sensitivity of the multiplex assay using double markers was 100%. Since the further development of RT-PCR assays will continue in the future, this molecular system may be a promising tool for the intraoperative detection of LNM when performing minimally invasive surgery with personalized lymphadenectomy on patients with esophageal cancer.

9.4 Incidence of MM in Esophageal Cancer

Several studies have investigated LNM detected by IHC in esophageal cancer (Table 9.1) [9, 13, 14, 20–28, 40, 41]. Marked differences were noted in the number of patients and dissected lymph nodes, the depth of tumor invasion, antibodies used for IHC, and the number of node sections assessed by IHC. LNM is basically defined as the presence of a single or small clusters of esophageal tumor cells identified by IHC in pN0 lymph nodes assessed by HE staining [9, 14, 20, 21, 23, 25–27, 40]. The incidence of LNM ranged between 8.1 and 55.5% in all studies. Since the diagnosis of LNM was based on morphology, this discrepancy may be due to the estimations performed by each author. Shiozaki et al. [23] conducted a multi-institutional study and the results of LNM were compared between institutional researchers and pathologists. Among 164 patients with pN0, 51 patients were diagnosed as MM-positive by institutional evaluations, whereas pathologists only

Table 9.1 Immunohistochemical studies in patients with esophageal cancer

Prognostic significance	Yes	No	Yes	No	Yes	No	Yes	No	Yes	Yes	No	Yes	No	No
P	<0.05	–	0.002	0.91	<0.01	0.16	0.0188	–	0.0462	0.009	n.s.	0.002	–	–
5-year survival (positive vs. negative)	–	–	44.6 vs. 91.0%	78.0 vs. 75.0%	34.0 vs.72.0%	–	28.0 vs. 79.0%	–	20.0 vs. 70%	30.0 vs. 76.0%	35.7 vs. 61.1%	57.0 vs. 79.0%	–	–
No. of patients with micrometastasis (%)	13 (31.7)	20 (25.6)	39 (55.5)	20 (40.0)	47 (45.2)	14 (26.4)	11 (26.8)	12 (26.1)	25 (15.0)	3 (27.3)	7 (8.1)	7 (14.6)	8 (14.0)	7 (20.5)
Definition of micrometastasis	<0.5 mm	<2 mm	pN0 by HE staining	pN0 by HE staining	pN0 by HE staining	pN0 by HE staining	pN0 by HE staining	<5 cells	pN0 by HE staining	<10 cells	>0.2, <2 mm	pN0 by HE staining	pN0 by HE staining	pN0 by HE staining
Sections for IHC	Single	Multiple	Single	Single	Multiple	Single	Single	Multiple	Multiple	Multiple	Multiple	Multiple	Single	Multiple
Antibody	CK (AE1/AE3)	CK (AE1/AE3)	CK (AE1/AE3)	CK (AE1/AE3)	CK (AE1/AE3)	CK (AE1/AE3)	CK (AE1/AE3)	CK (AE1/AE3)	CK (AE1/AE3)	CK (AE1/AE3)	CK (Lu-5)	CK (AE1/AE3)	CK (AE1/AE3)	CK (AE1/AE3)
Method	IHC	IHC	IHC	IHC	IHC	IHC	IHC	IHC	IHC	IHC	IHC	IHC	IHC	IHC
Histological type	SCC	SCC, AC	SCC	SCC	SCC	SCC	SCC	SCC	SCC	SCC, AC	SCC, AC	SCC, AC	SCC, AC	SCC, AC
Depth of invasion	T1–3		T1–3	T1–4	T1–3	T1–3	T1–4	T1	T1–3	T1–3	T1–3	T1	T1–2	T1–4
Average no. of LNs	–	7.4	46.0	36.8	74.7	47.4	52.9	–	–	–	14.0	28.0	22.8	30.3
No. of patients	41	78	59	50	104	53	41	46	167	33	86	48	46	34
Study	Natsugoe et al. [13]	Glickan et al. [27]	Matsumoto et al. [14]	Sato et al. [26]	Komukai et al. [24]	Nakamura et al. [39]	Doki et al. [25]	Tanabe et al. [23]	Shiozaki et al. [22]	Koenig et al. [21]	Zingg et al. [40]	Prenzel et al. [20]	Hagihara et al. [9]	Kinjo et al. [19]
Years	1998	1999	2000	2001	2002	2002	2002	2003	2007	2009	2009	2012	2013	2014

identified 25 patients with MM-positive lymph nodes. Institutional positivity for MM was negated by these pathologists for the following reasons: (1) lack of nuclei in CK-positive cells; (2) location of stained cells outside the lymph node structure; or (3) stained cells with morphologically different appearances from cancer cells or epithelial cells. If the evaluation of LNM detected by IHC differs between each institution, the results from different studies will also naturally be different. Therefore, common criteria for identifying LNM using IHC are necessary. Even patients with mucosal and submucosal tumors have 10% or more LNM in pN0 esophageal cancer [21, 24]. Tanabe et al. [24], in a study on 46 node-negative patients with pT1 tumors, such as mucosal and submucosal tumors, reported a high incidence (26.1%) of LNM by IHC using a CK AE1/AE3 antibody. Furthermore, patients with deeper tumor invasion showed a slightly higher incidence of LNM than those with pT1 tumors in pN0 esophageal cancer. Matsumoto et al. [14] showed that LNM was identified by IHC in 1 (4.3%) out of 23 node-negative patients with pT1 tumors, but in 32 (88.9%) out of 36 node-negative patients with pT2 or pT3 tumors. Similarly, Sato et al. [27] detected LNM by IHC in 13 (54.1%) out of 24 node-negative patients with pT2-pT4a tumors.

Table 9.2 summarizes studies on LNM assessed by RT-PCR in patients with pN0 esophageal cancer. According to these studies, simplex or multiplex RT-PCR assays using target molecular markers were performed for the detection of LNM in patients with esophageal cancer [9, 31–34]. Hagihara et al. compared the incidence of LNM between IHC and RT-PCR assays in 1284 lymph nodes obtained from 50 patients with pN0 esophageal cancer [9]. Lymph nodes were cut into two blocks at the plane of the largest dimension. Half of each lymph node was then used in an RT-PCR analysis of CEA and SCC mRNA and sections of the remaining halves were stained for IHC using CK AE1/AE3 mAb. LNM was identified in 4 out of 50 patients (8.0%) and in 19 out of 1284 nodes (1.5%) by IHC, whereas RT-PCR assays detected

Table 9.2 RT-PCR studies in patients with esophageal cancer

Prognostic significance	Yes	Yes	Yes	Yes	–
P	<0.0001	0.0023	0.004	0.0001	–
5-year survival (positive vs. negative)	–	–	18.8 vs. 47.6%	21.7 vs. 62.7%	–
No. of patients with micrometastasis (%)	11(36.7)	5 (14.7)	32 (34.4)	23 (28.1)	4 (8.7)
Markers	CEA	CK19, TACSTD-1	MUC1	MUC1	CEA, SCC
Method	RT-PCR	RT-PCR	RT-PCR	RT-PCR	RT-PCR
Histological type	SCC, AC	AC	SCC	SCC	SCC, AC
Depth of invasion	T1-T3	Tis-T3	T1-T3	T1-T3	T1-T2
Total no. of LNs	387	314	426	501	–
No. of patients	30	34	93	82	46
Study	Godfrey et al.	Xi et al.	Li et al.	Sun et al.	Hagihara et al.
Years	2001	2005	2007	2011	2013

LNM in 7 patients (14.0%) and 25 nodes (1.9%) [9]. Only 3 out of the 25 LNM were detected by RT-PCR [9]. On the other hand, only one LNM was detected by IHC alone [9]. These findings indicate that an RT-PCR assay is the most sensitive tool for detecting LNM in patients with esophageal cancer.

9.5 Clinical Significance of MM

A large number of studies have investigated the clinical impact of LNM in various malignant tumors, such as breast cancer, non-small cell lung cancer, gastric cancer, colorectal cancer, pancreatic cancer, and biliary cancer [42–49]. Although many investigators have also demonstrated the clinical significance of LNM in patients with esophageal cancer, it currently remains controversial [9, 13, 14, 20–28, 40, 41].

Shiozaki et al. [23], in a study on 164 esophageal cancer patients with pT1-3N0 tumors, reported that 51 out of 164 patients with pN0 were diagnosed as LNM-positive by institutional evaluations, and LNM based on an institutional diagnosis did not have a significant impact on survival. Based on diagnoses made by pathologists, LNM, including IHC-positive single cells and clusters, did not have a clinical impact on survival, whereas metastasis with clusters of IHC-positive cells only had a significant clinical impact on prognosis, with 5-year overall survival rates of 20% and 70%, respectively. They indicated a need to correlate MM-IHC-positive cells with the morphological aspects of stained cells and that only LNs with clusters of stained cells are prognostically significant in esophageal carcinoma. They suggested that patients with clusters of positive cells showed worse prognoses if they had pathologically positive lymph nodes, which suggests that cluster-type-positive cells in lymph nodes are a biological feature of malignant potential in esophageal carcinoma. Zingg et al. [41], in a study on 86 esophageal cancer patients (32 with squamous cell carcinoma and 54 with adenocarcinoma), reported that there was no significant difference in the frequency of LNM between adenocarcinoma and squamous cell carcinoma (11.3% vs. 3.1%, p = n.s.). In this study, the definition of LNM was as follows: intra-nodal tumor cell infiltrates measuring between 0.2 and 2 mm were classified as MM, while those measuring less than 0.2 mm were classified as ITC according to the proposition of Hermanek et al. [50]. Cytokeratin-positive material devoid of any evidence of vital nuclei was classified as “avital cytokeratin-positive material” (ACPM). They demonstrated that IHC-negative patients with squamous cell carcinoma showed significantly better overall survival ($p < 0.02$) and disease-free intervals ($p < 0.01$). No significant differences were observed in adenocarcinoma. They identified differences in biological behavior and outcomes, indicating that it is inappropriate to treat adenocarcinoma and squamous cell carcinoma as one entity. Kinjo et al. [20], in a study on 77 esophageal cancer patients with pT1-pT4 tumors, classified each esophageal tumor into 1 of 3 categories in accordance with the sixth edition of the Tumor–Node–Metastasis (TNM) Classification of Malignant Tumors, a cancer staging system developed by the International Union Against Cancer (UICC), based on the relationship between the initial tumor status and applicability of upfront R0 resection for esophageal cancer. In terms of tumor

categories, IHC-positive LNM was present in 12 (30%), 11 (52.4%), and 11 (68.8%) of 40, 21, and 16 Category 1, 2, and 3 patients, respectively. A significant difference in the frequency of IHC-positive LNM was observed among these three patient groups ($p = 0.019$). They also reported that 5-year survival rates in patients with or without LNM were 42.5% and 61.8%, respectively. However, the survival rates were not significantly different according to the presence or absence of micrometastasis by immunostaining, although the 5-year survival rate of 27 cases positive for both lymph node metastasis by HE staining and micrometastasis by immunostaining was 30.6%, significantly different from 65.1% in the remaining 50 cases. In addition, they identified simultaneous HE-positive lymph node metastasis and IHC-positive LNM and pT as independent prognostic predictors that correlated with survival. Matsumoto et al. [14] examined clinicopathological factors in 59 patients with T1-4 tumors without lymph node metastasis. They reported that the rate of recurrent disease was significantly higher in patients with than in those without LNM (94.1% vs. 40.5% respectively). LNM was immunohistochemically detected in all patients with lymph node recurrence. The 5-year survival rate was significantly lower in patients with than in those without LNM (91.0% vs. 44.6%, respectively). They demonstrated that the frequency of micrometastases increases in T2 and 3 tumors. It should be noted that such tumors are associated with micrometastasis, especially, lymph node recurrence. However, since 17 patients with LNM did not develop recurrence, these patients benefited from lymph node dissection. They concluded that the presence of LNM positively correlated with disease recurrence and poor outcomes. Extended lymphadenectomy and postoperative adjuvant therapy may be indicated for patients with esophageal SCC. Koenig et al. [22], in a study on 33 esophageal cancer patients (18 with squamous cell carcinoma and 15 with adenocarcinoma) with pT1-3N0 tumors, reported that 9 patients were diagnosed with IHC-positive LNM, and 5-year overall survival probability was 76% in patients without LNM, but was 30% in patients with LNM ($P = 0.009$, the Log-rank test). Further analyses revealed that 5-year overall survival probability in patients with nodal microinvolvement was similar to that of pN1 patients (the Log-rank test; $P = 0.875$). They also identified the LNM ratio as the most powerful predictive variable for overall survival in patients with esophageal carcinoma irrespective of the histological tumor type in a multivariate analysis. They concluded not only that the global presence or absence of nodal microinvolvement may serve as a tool for differentiating high-risk from low-risk patients, but also that the IHC ratio of affected lymph nodes to the total number of lymph nodes appears to enable improved risk stratification for esophageal cancer patients.

Hagihara et al. [9] focused on SNs in a study on 57 esophageal cancer patients with cT1-2N0 tumors. They reported that conventional HE staining detected histological lymph node metastasis in 7 out of 57 patients (12.3%). Lymph node metastasis, including MM, was identified in 11 patients (19.3%) by IHC. In the remaining 46 node-free patients assessed by HE staining and IHC, MM was identified in 4 patients (7.0%) by RT-PCR. They suggested the applicability of RT-PCR to the detection of a very small number of tumor cells within lymph nodes. Li et al. [31], in a study on 93 esophageal squamous cell carcinoma patients with pT1-3N0

tumors, detected MUC1 mRNA in 32 patients, which accounted for 34.4% of all 93 patients. Tumor relapse developed during the follow-up in 61 (65.6%) out of the 93 patients, 26 of whom had LNM while 35 did not. Patients with LNM had a significantly shorter disease-free interval than those without LNM (26 vs. 32 months). The 5-year survival rate of patients with LNM was significantly lower than that of those without LNM (18.8 vs. 47.6%). They also indicated that the T status and LNM were independent prognostic factors. They concluded that TNM staging needs to involve LNM, and improved staging may be expected with further information on LNM, whereby a subgroup of patients who may benefit greatly from adjuvant therapy may be identified.

Xi et al. [33], in a study on 34 esophageal adenocarcinoma patients with pTis-3N0 tumors, detected CK19/TACSTD-1 mRNA in the nodes of 5 patients. Quantitative RT-PCR (QRT-PCR)-positive patients had significantly worse disease-free survival than QRT-PCR-negative patients ($P = 0.0023$). The ongoing clinical trial of chemotherapy by the Eastern Cooperative Oncology Group demonstrated that chemotherapy is effective for patients with trace amounts of residual lesions, such as micrometastasis. Furthermore, a major benefit of more accurate staging may be the ability to identify low-risk, truly node-negative patients, thereby avoiding the potential morbidity of unnecessary chemotherapy for these patients. The RT-PCR method is more sensitive than IHC for detecting LNM because of the greater quantity of the sample available. However, several issues are still associated with RT-PCR examinations. Since these epithelial markers are not specific to cancer, the number of markers needed remains unclear. Furthermore, suitable primers have not yet been identified. If esophageal cancer-specific markers become available, the results of RT-PCR examinations will become more reliable.

9.6 Future Possibilities for MM

The existence of LNM indicates that metastasis from the primary tumor has already begun. According to the findings of this review, a high incidence of LNM > 10% exists in patients with pN0 esophageal cancer. It currently remains unclear whether all small tumor cells graft and grow in lymph nodes; however, the potential existence of LNM in patients with pN0 needs to be considered. In our study, LNM already exhibited proliferative activity, even in ITC [51]. If LNM exists in patients diagnosed as pN0, these patients need to be considered as pN1. Therefore, examinations of LNM are favorable for correct staging, particularly in pN0 patients. The detection of LNM, and subsequently improved patient staging, may have significant consequences for the treatment of esophageal cancer. Since prognoses differ significantly between patients with and without LNM according to several studies, adjuvant therapy appears to be necessary for patients with LNM. Due to the lack of systemic adjuvant therapy for esophageal cancer, any correct staging system currently lacks clinical significance for decision-making in individual patients and is only of prognostic importance. This may change as soon as advances are achieved in the field of new adjuvant chemotherapeutic and targeted therapy regimens.

Prospective randomized controlled studies need to be conducted in order to examine the effectiveness of adjuvant therapies in patients with LNM.

Surgical approaches and the extent of lymph node dissection may also be selected based on the lymph node status, with some surgeons advocating extensive lymph node dissection in node-positive patients. Furthermore, there is strong evidence that patients with extensive lymph node metastasis have a poor prognosis. Therefore, curative surgery may be difficult for such patients. These findings indicate that the revision of the TNM staging system is necessary. The examination of LNM in patients with pN0 assessed by routine HE staining may facilitate screening and validation of whether they are truly node-negative patients. The former subgroup may benefit from more extensive nodal dissection, whereas the latter group may achieve curative resection with less aggressive surgical resection.

An accurate intraoperative diagnosis of the lymph node status, including LNM, by molecular methods is necessary when performing minimally invasive surgery with individualized lymphadenectomy. For example, the supraclavicular lymph nodes are not dissected in patients negative for micrometastasis in the recurrent neural and cervical paraesophageal lymph nodes [52]. Currently, SNNS is performed for breast cancer and malignant melanoma [53, 54]. We investigated LNM in all dissected lymph nodes, including the SN, because SN mapping using IHC and RT- PCR yields good results in patients with esophageal and gastric cancer classified as clinical T1 and N0 [8, 55]. It is reasonable to apply less-invasive procedures than surgical treatments when intraoperative histological and molecular diagnoses reveal that SNs in cT1N0 patients are negative for metastasis. On the other hand, standard surgery with standard lymph node dissection is currently recommended for patients with SN metastasis verified by intraoperative diagnostic tools. Furthermore, ESD with thoracoscopic and laparoscopic SN dissection may serve as the ultimate esophageal-preserving surgery in the future to avoid lymph node recurrence in selected patients with extended indications for ESD. Thus, if SNNS based on the LNM status is clinically developed as a surgical treatment for patients with esophageal cancer, minimally invasive surgery with individualized lymphadenectomy may be safely performed in the near future and achieve good results for the balance between postsurgical QOL and curability. Future studies on the biological behavior of MM tumor cells will greatly contribute to the development of further treatments for patients with esophageal cancer.

In conclusion, LNM needs to be recognized as the first and important step in the path to lymphatic metastasis. Minimally invasive surgery may be safely performed in clinical situations with a correct diagnosis of LNM. New treatment strategies that apply the diagnosis of LNM are expected for esophageal cancer.

References

1. Robey-Cafferty SS, el-Naggar AK, Sahin AA, Bruner JM, Ro JY, Cleary KR. Prognostic factors in esophageal squamous carcinoma. A study of histologic features, blood group expression, and DNA ploidy. Am J Clin Pathol. 1991;95(6):844–9.

2. Roder JD, Busch R, Stein HJ, Fink U, Siewert JR. Ratio of invaded to removed lymph nodes as a predictor of survival in squamous cell carcinoma of the oesophagus. Br J Surg. 1994;81(3):410–3.
3. Dimick JB, Pronovost PJ, Cowan JA Jr, Lipsett PA, Stanley JC, Upchurch GR Jr. Variation in postoperative complication rates after high-risk surgery in the United States. Surgery. 2003;134(4):534–40. discussion 40-1
4. Birkmeyer JD, Siewers AE, Finlayson EV, Stukel TA, Lucas FL, Batista I, et al. Hospital volume and surgical mortality in the United States. N Engl J Med. 2002;346(15):1128–37.
5. Begg CB, Cramer LD, Hoskins WJ, Brennan MF. Impact of hospital volume on operative mortality for major cancer surgery. JAMA. 1998;280(20):1747–51.
6. Lambert R. Treatment of esophagogastric tumors. Endoscopy. 2003;35(2):118–26.
7. Tilanus HW, Hop WC, Langenhorst BL, van Lanschot JJ. Esophagectomy with or without thoracotomy. Is there any difference? J Thorac Cardiovasc Surg. 1993;105(5):898–903.
8. Uenosono Y, Arigami T, Yanagita S, Kozono T, Arima H, Hirata M, et al. Sentinel node navigation surgery is acceptable for clinical T1 and N0 esophageal cancer. Ann Surg Oncol. 2011;18(7):2003–9.
9. Hagihara T, Uenosono Y, Arigami T, Kozono T, Arima H, Yanagita S, et al. Assessment of sentinel node concept in esophageal cancer based on lymph node micrometastasis. Ann Surg Oncol. 2013;20(9):3031–7.
10. Takeuchi H, Kawakubo H, Takeda F, Omori T, Kitagawa Y. Sentinel node navigation surgery in early-stage esophageal cancer. Ann Thorac Cardiovasc Surg. 2012;18(4):306–13.
11. Natsugoe S, Aikou T, Shimada M, Yoshinaka H, Takao S, Shimazu H, et al. Occult lymph node metastasis in gastric cancer with submucosal invasion. Surg Today. 1994;24(10):870–5.
12. Izbicki JR, Hosch SB, Pichlmeier U, Rehders A, Busch C, Niendorf A, et al. Prognostic value of immunohistochemically identifiable tumor cells in lymph nodes of patients with completely resected esophageal cancer. N Engl J Med. 1997;337(17):1188–94.
13. Natsugoe S, Mueller J, Stein HJ, Feith M, Hofler H, Siewert JR. Micrometastasis and tumor cell microinvolvement of lymph nodes from esophageal squamous cell carcinoma: frequency, associated tumor characteristics, and impact on prognosis. Cancer. 1998;83(5):858–66.
14. Matsumoto M, Natsugoe S, Nakashima S, Sakamoto F, Okumura H, Sakita H, et al. Clinical significance of lymph node micrometastasis of pN0 esophageal squamous cell carcinoma. Cancer Lett. 2000;153(1–2):189–97.
15. Arigami T, Natsugoe S, Uenosono Y, Mataki Y, Ehi K, Higashi H, et al. Evaluation of sentinel node concept in gastric cancer based on lymph node micrometastasis determined by reverse transcription-polymerase chain reaction. Ann Surg. 2006;243(3):341–7.
16. Mori M, Mimori K, Inoue H, Barnard GF, Tsuji K, Nanbara S, et al. Detection of cancer micrometastases in lymph nodes by reverse transcriptase-polymerase chain reaction. Cancer Res. 1995;55(15):3417–20.
17. Raj GV, Moreno JG, Gomella LG. Utilization of polymerase chain reaction technology in the detection of solid tumors. Cancer. 1998;82(8):1419–42.
18. Sobin L, Wittekind C. TNM classification of malignant tumours. 6th ed. New York: Wiley; 2002. (International Union Against Cancer)
19. Sobin L, Wittenkind C. TNM classification of malignant tumors. 6th ed. New York: John Wiley-Liss; 2002.
20. Kinjo T, Shimoji H, Nagahama M, Karimata H, Yoshimi N, Nishimaki T. Prognostic significance of simultaneous presence of histological and immunohistochemical metastasis to lymph nodes in patients with esophageal cancer. Ann Thorac Cardiovasc Surg. 2014;20(6):951–60.
21. Prenzel KL, Holscher AH, Drebber U, Agavonova M, Gutschow CA, Bollschweiler E. Prognostic impact of nodal micrometastasis in early esophageal cancer. Eur J Surg Oncol. 2012;38(4):314–8.
22. Koenig AM, Prenzel KL, Bogoevski D, Yekebas EF, Bubenheim M, Faithova L, et al. Strong impact of micrometastatic tumor cell load in patients with esophageal carcinoma. Ann Surg Oncol. 2009;16(2):454–62.

23. Shiozaki H, Fujiwara Y, Hirai T. Clinical significance of immunohistochemically detected lymph node micrometastasis in patients with histologically node-negative esophagealcarcinoma: a multi-institutional study. Esophagus. 2007;4:35–9.
24. Tanabe T, Nishimaki T, Watanabe H, Ajioka Y, Akazawa K, Komukai S, et al. Immunohistochemically detected micrometastasis in lymph nodes from superficial esophageal squamous cell carcinoma. J Surg Oncol. 2003;82(3):153–9.
25. Komukai S, Nishimaki T, Suzuki T, Kanda T, Kuwabara S, Hatakeyama K. Significance of immunohistochemical nodal micrometastasis as a prognostic indicator in potentially curable oesophageal carcinoma. Br J Surg. 2002;89(2):213–9.
26. Doki Y, Ishikawa O, Mano M, Hiratsuka M, Sasaki Y, Kameyama M, et al. Cytokeratin deposits in lymph nodes show distinct clinical significance from lymph node micrometastasis in human esophageal cancers. J Surg Res. 2002;107(1):75–81.
27. Sato F, Shimada Y, Li Z, Watanabe G, Maeda M, Imamura M. Lymph node micrometastasis and prognosis in patients with oesophageal squamous cell carcinoma. Br J Surg. 2001;88(3):426–32.
28. Glickman JN, Torres C, Wang HH, Turner JR, Shahsafaei A, Richards WG, et al. The prognostic significance of lymph node micrometastasis in patients with esophageal carcinoma. Cancer. 1999;85(4):769–78.
29. Matsumoto M, Natsugoe S, Ishigami S, Uenosono Y, Takao S, Aikou T. Rapid immunohistochemical detection of lymph node micrometastasis during operation for upper gastrointestinal carcinoma. Br J Surg. 2003;90(5):563–6.
30. Noura S, Yamamoto H, Miyake Y, Kim B, Takayama O, Seshimo I, et al. Immunohistochemical assessment of localization and frequency of micrometastases in lymph nodes of colorectal cancer. Clin Cancer Res. 2002;8(3):759–67.
31. Li SH, Wang Z, Liu XY, Liu FY, Sun ZY, Xue H. Lymph node micrometastasis: a predictor of early tumor relapse after complete resection of histologically node-negative esophageal cancer. Surg Today. 2007;37(12):1047–52.
32. Godfrey TE, Raja S, Finkelstein SD, Gooding WE, Kelly LA, Luketich JD. Prognostic value of quantitative reverse transcription-polymerase chain reaction in lymph node-negative esophageal cancer patients. Clin Cancer Res. 2001;7(12):4041–8.
33. Xi L, Luketich JD, Raja S, Gooding WE, Litle VR, Coello MC, et al. Molecular staging of lymph nodes from patients with esophageal adenocarcinoma. Clin Cancer Res. 2005;11(3):1099–109.
34. Sun ZG, Wang Z, Liu XY, Liu FY. Mucin 1 and vascular endothelial growth factor C expression correlates with lymph node metastatic recurrence in patients with N0 esophageal cancer after Ivor-Lewis esophagectomy. World J Surg. 2011;35(1):70–7.
35. Gerhard M, Juhl H, Kalthoff H, Schreiber HW, Wagener C, Neumaier M. Specific detection of carcinoembryonic antigen-expressing tumor cells in bone marrow aspirates by polymerase chain reaction. J Clin Oncol. 1994;12(4):725–9.
36. Song ZB, Gao SS, Yi XN, Li YJ, Wang QM, Zhuang ZH, et al. Expression of MUC1 in esophageal squamous-cell carcinoma and its relationship with prognosis of patients from Linzhou city, a high incidence area of northern China. World J Gastroenterol. 2003;9(3):404–7.
37. Wang Z, Yin H. Diagnosis of occult metastasis to mediastinal lymph nodes in patients with NSCLC: detection of MUC1 mRNA by reverse transcriptase-polymerase chain reaction (RT-PCR). Zhongguo Fei Ai Za Zhi. 2002;5(3):191–3.
38. Kuo CT, Hoon DS, Takeuchi H, Turner R, Wang HJ, Morton DL, et al. Prediction of disease outcome in melanoma patients by molecular analysis of paraffin-embedded sentinel lymph nodes. J Clin Oncol. 2003;21(19):3566–72.
39. Yanagita S, Natsugoe S, Uenosono Y, Arigami T, Funasako Y, Hirata M, et al. The utility of rapid diagnosis of lymph node metastasis in gastric cancer using a multiplex real-time reverse transcription polymerase chain reaction assay. Oncology. 2009;77(3–4):205–11.
40. Nakamura T, Ide H, Eguchi R, Hayashi K, Ota M, Takasaki K. Clinical implications of lymph node micrometastasis in patients with histologically node-negative (pN0) esophageal carcinoma. J Surg Oncol. 2002;79(4):224–9.

41. Zingg U, Montani M, Busch M, Metzger U, Went P, Oertli D. Prognostic influence of immunohistochemically detected lymph node micrometastasis and histological subtype in pN0 oesophageal cancer. Eur J Surg Oncol. 2009;35(6):593–9.
42. Cai J, Ikeguchi M, Maeta M, Kaibara N. Micrometastasis in lymph nodes and microinvasion of the muscularis propria in primary lesions of submucosal gastric cancer. Surgery. 2000;127(1):32–9.
43. Maehara Y, Oshiro T, Endo K, Baba H, Oda S, Ichiyoshi Y, et al. Clinical significance of occult micrometastasis lymph nodes from patients with early gastric cancer who died of recurrence. Surgery. 1996;119(4):397–402.
44. Harrison LE, Choe JK, Goldstein M, Meridian A, Kim SH, Clarke K. Prognostic significance of immunohistochemical micrometastases in node negative gastric cancer patients. J Surg Oncol. 2000;73(3):153–7.
45. Nakajo A, Natsugoe S, Ishigami S, Matsumoto M, Nakashima S, Hokita S, et al. Detection and prediction of micrometastasis in the lymph nodes of patients with pN0 gastric cancer. Ann Surg Oncol. 2001;8(2):158–62.
46. Schoenfeld A, Luqmani Y, Smith D, O'Reilly S, Shousha S, Sinnett HD, et al. Detection of breast cancer micrometastases in axillary lymph nodes by using polymerase chain reaction. Cancer Res. 1994;54(11):2986–90.
47. Gu CD, Osaki T, Oyama T, Inoue M, Kodate M, Dobashi K, et al. Detection of micrometastatic tumor cells in pN0 lymph nodes of patients with completely resected nonsmall cell lung cancer: impact on recurrence and survival. Ann Surg. 2002;235(1):133–9.
48. Niedergethmann M, Rexin M, Hildenbrand R, Knob S, Sturm JW, Richter A, et al. Prognostic implications of routine, immunohistochemical, and molecular staging in resectable pancreatic adenocarcinoma. Am J Surg Pathol. 2002;26(12):1578–87.
49. Sasaki E, Nagino M, Ebata T, Oda K, Arai T, Nishio H, et al. Immunohistochemically demonstrated lymph node micrometastasis and prognosis in patients with gallbladder carcinoma. Ann Surg. 2006;244(1):99–105.
50. Hermanek P, Hutter RV, Sobin LH, Wittekind C. International Union Against Cancer. Classification of isolated tumor cells and micrometastasis. Cancer. 1999;86(12):2668–73.
51. Yanagita S, Natsugoe S, Uenosono Y, Kozono T, Ehi K, Arigami T, et al. Sentinel node micrometastases have high proliferative potential in gastric cancer. J Surg Res. 2008;145(2):238–43.
52. Qubain SW, Natsugoe S, Matsumoto M, Nakashima S, Baba M, Takao S, et al. Micrometastases in the cervical lymph nodes in esophageal squamous cell carcinoma. Dis Esophagus. 2001;14(2):143–8.
53. Morton DL, Wen DR, Wong JH, Economou JS, Cagle LA, Storm FK, et al. Technical details of intraoperative lymphatic mapping for early stage melanoma. Arch Surg. 1992;127(4):392–9.
54. Giuliano AE, Kirgan DM, Guenther JM, Morton DL. Lymphatic mapping and sentinel lymphadenectomy for breast cancer. Ann Surg. 1994;220(3):391–8. discussion 8-401
55. Uenosono Y, Natsugoe S, Ehi K, Arigami T, Hokita S, Aikou T. Detection of sentinel nodes and micrometastases using radioisotope navigation and immunohistochemistry in patients with gastric cancer. Br J Surg. 2005;92(7):886–9.

Clinical Aspect: Gastric Cancer

10

Takaaki Arigami, Yoshikazu Uenosono, Shigehiro Yanagita, Sumiya Ishigami, and Shoji Natsugoe

Abstract

Recent advances in the development of molecular diagnostic tools have improved the detection of lymph node micrometastasis (LNM) in patients with gastric cancer. Isolated or micrometastatic tumor cells are also heterogeneously distributed in lymph nodes. Since the incidence of LNM in patients with early gastric cancer (pT1) ranges between 10% and 31.8%, even patients with early gastric cancer are at a high risk of developing LNM. Moreover, the incidence of LNM is slightly higher in patients with advanced gastric cancer than in those with early gastric cancer. A close relationship has been reported between LNM and lymphatic invasion in primary tumors. The clinical impact of LNM currently remains controversial in patients with gastric cancer. Therefore, it is clinically difficult to reach concrete conclusions regarding the prognostic significance of LNM. However, the rate of positivity for Ki-67 in LNM was previously reported to be between 92.0% and 94.2%. Consequently, tumor cells within LNM exhibit high proliferative activity. In clinical management, therapeutic strategies for LNM need to be planned in order to avoid lymph node recurrence. It is considered important to preserve the balance between quality of life and curability

T. Arigami (✉) · S. Natsugoe
Department of Digestive Surgery, Breast and Thyroid Surgery, Kagoshima University Graduate School of Medical and Dental Sciences, Kagoshima, Japan

Molecular Frontier Surgery, Kagoshima University Graduate School of Medical and Dental Sciences, Kagoshima, Japan
e-mail: arigami@m.kufm.kagoshima-u.ac.jp

Y. Uenosono
Molecular Frontier Surgery, Kagoshima University Graduate School of Medical and Dental Sciences, Kagoshima, Japan

S. Yanagita · S. Ishigami
Department of Digestive Surgery, Breast and Thyroid Surgery, Kagoshima University Graduate School of Medical and Dental Sciences, Kagoshima, Japan

S. Natsugoe (ed.), *Lymph Node Metastasis in Gastrointestinal Cancer*,
https://doi.org/10.1007/978-981-10-4699-5_10

when selecting minimally invasive surgery, such as sentinel node navigation _ surgery and endoscopic submucosal dissection, for patients with early gastric cancer. This chapter will focus on the clinical aspect of LNM in patients with gastric cancer.

Keywords
Lymph node micrometastasis · Isolated tumor cells · Lymphatic invasion Gastric cancer

10.1 Introduction

Lymph node metastasis is one of the most important prognostic factors for patients with gastric cancer [1, 2]. Accordingly, the Japanese Gastric Cancer Treatment Guidelines 2010 (ver. 3) recommends D2 lymph node dissection as a standard surgical approach to avoid lymph node recurrence in patients with gastric cancer [3]. However, lymph node recurrence occasionally develops in spite of a node-negative (pN0) diagnosis based on conventional histological hematoxylin-eosin (HE) staining. Several studies focused on lymph node micrometastasis (LNM) as a key causative factor for lymph node recurrence in patients with gastric cancer [4–6]. Difficulties are associated with evaluating the metastatic node status including LNM using preoperative imaging examinations such as ultrasonography, computed tomography, and positron emission tomography in preoperative assessments of patients with gastric cancer [7].

Endoscopic treatments, such as endoscopic mucosal resection (EMR) and endoscopic submucosal dissection (ESD), have been widely accepted for selected patients with early gastric cancer. Moreover, the Japanese Gastric Cancer Treatment Guidelines 2010 (ver. 3) recommends an expanded indication for ESD, the validity of which has been verified in clinical studies [3, 8]. Patients receiving endoscopic treatments have a good prognosis. Although the indication of additional surgery after non-curative endoscopic resection is reported in these guidelines [3], oncological curability without lymph node recurrence needs to be secured for patients receiving endoscopic treatments. Consequently, the precise evaluation of lymph node metastasis including LNM is very important for preventing disease recurrence in the clinical management of patients with gastric cancer. This chapter will focus on the clinical aspect of LNM in patients with gastric cancer.

10.2 Morphology and Distribution of LNM

Micrometastasis and isolated tumor cells (ITCs) are completely distinguished and defined based on the criteria of the tumor-node-metastasis (TNM) classification established by the International Union Against Cancer (UICC) in 2002 [9]. According to the TNM classification, the size of metastatic tumor cells within lymph nodes is an important indicator for discriminating between micrometastasis

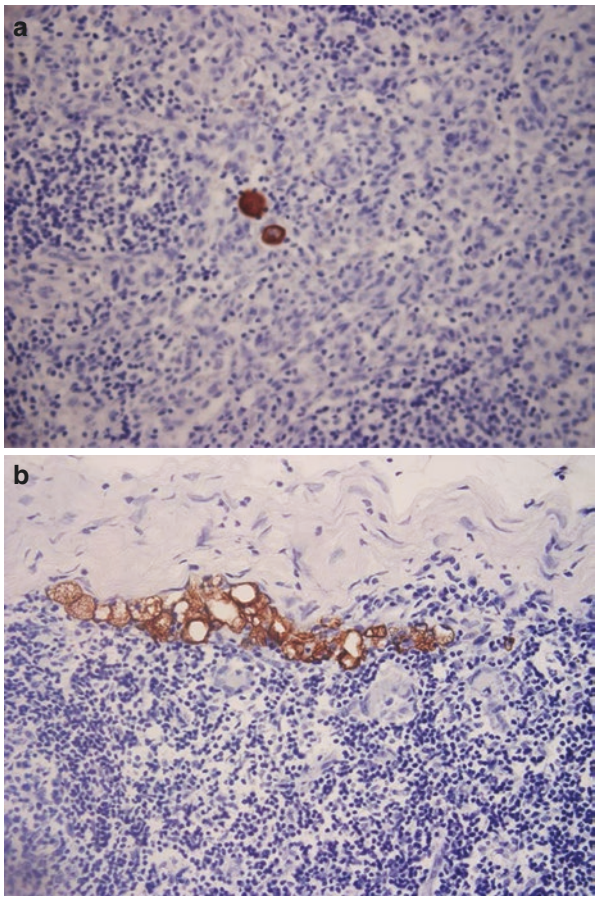

Fig. 10.1 Representative immunohistochemical staining for lymph node micrometastasis. (**a**) Isolated tumor cells. (**b**) Micrometastasis. Original magnification ×400

and ITCs [9]. ITCs are single tumor cells or small clusters of cells measuring ≤0.2 mm at their greatest dimension and are generally detected using immunohistochemistry (IHC) but may also be confirmed by conventional HE staining (Fig. 10.1a). On the other hand, micrometastasis refers to tumor cell clusters measuring between 0.2 mm and 2.0 mm at their greatest dimension (Fig. 10.1b). The criteria of the TNM classification have an impact on the clinical management of LNM in patients with various malignancies, including gastric cancer.

Yanagita et al. investigated the morphological distribution of isolated or micrometastatic tumor cells with IHC using AE1/AE3 monoclonal antibodies (mAb) in lymph nodes obtained from patients with gastric cancer [10]. The distribution of metastatic tumor cells within lymph nodes was classified into the following four groups: marginal sinus (MS), intermediate sinus (IS), parenchymal (PA), and diffuse (DF) types. The incidences of the MS, IS, PA, and DF types in 14 nodes with micrometastasis were 72%, 7%, 7%, and 14%, respectively. Moreover, the incidences of the MS, IS, PA, and DF types in 16 nodes with ITCs were 69%, 12%, 19%, and 0%, respectively. These findings indicated that more than 50% of micrometastasis and ITCs were initially trapped in the MS of lymph nodes.

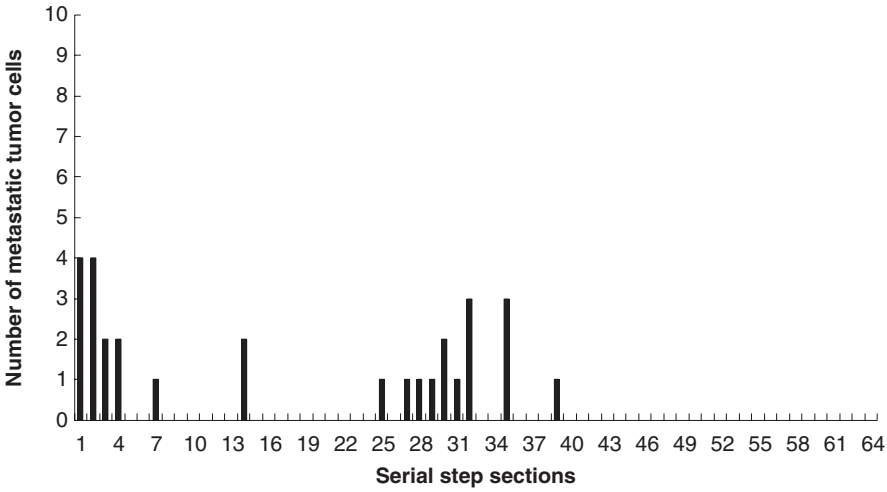

Fig. 10.2 Relationship between tumor cells and numbers of sections assessed by immunohistochemistry

Isozaki et al. examined 3449 lymph nodes dissected from 111 patients with gastric cancer and demonstrated the clinical significance of serial sectioning assessments for lymph node metastasis in dissected lymph nodes [11]. The findings of this study suggested the heterogeneous distribution of metastatic tumor cells in lymph nodes. We herein examined one lymph node diagnosed as pN0 by IHC in patients with gastric cancer. The paraffin-embedded tissues of lymph nodes were cut into 3-μm-thick sections. All serial step sections at 30-μm intervals were stained with IHC using AE1/AE3 mAb. Tumor cells were heterogeneously distributed in lymph nodes (Fig. 10.2). Consequently, further IHC assessments on serial sections may result in the highly sensitive detection of LNM in patients with gastric cancer. However, this processing based on serial sections is clinically laborious for the intraoperative diagnosis of LNM. In the near future, reverse transcription-polymerase chain reaction (RT-PCR) assays may be a promising tool to overcome this issue in the intraoperative diagnosis of LNM.

10.3 Incidence of LNM

Although many investigators have reported the incidence and clinical significance of LNM in patients with gastric cancer, few studies have assessed LNM based on the criteria of the TNM classification [4, 12–28]. According to most findings on LNM, LNM is basically defined as the existence of tumor cells identified by a molecular approach, such as IHC and RT-PCR, in pN0 lymph nodes by HE staining [4, 12–19, 22, 23, 25, 26].

Table 10.1 summarizes studies published between 1996 and 2015 on LNM assessed by IHC in patients with pN0 gastric cancer [4, 12–28]. Marked differences

Table 10.1 Immunohistochemical studies on gastric cancer patients with pN0 diagnosed by hematoxylin-eosin staining

Year	Author	Number of patients	Depth of tumor invasion	Antibody	Assessed sections	Definition of micrometastasis	Average number of assessed LNs	Number of patients with micrometastasis (%)	5-year survival rate (positive vs. negative)	*P*-value (Log-rank test)
1996	Maehara et al. [4]	34	T1	CK (CAM5.2)	–	pN0 by HE staining	12.4	8 (23.5)	–	<0.05
2008	Yanagita et al. [10]	69	T1b	CK (CAM5.2)	Single	pN0 by HE staining	25.0	17 (24.6)	82.0% vs. 100.0%	<0.01
1997	Isozaki et al. [11]	25	T1–T4	CK (CAM5.2)	–	pN0 by HE staining	9.0	9 (36.0)	35.0% vs. 66.0%	0.048
2000	Cai et al. [12]	107	T2–T3	CK (AE1/AE3)	Multiple	pN0 by HE staining	41.9	38 (35.5)	94.0% vs. 89.0%	0.86
2000	Harrison et al. [13]	139	T1	CK (MNF 116)	Multiple	pN0 by HE staining	10.7	24 (17.3)	87.0% vs. 88.0%	0.6564
2001	Fukagawa et al. [14]	67	T1–T3	CK (AE1/AE3)	Single	pN0 by HE staining	26.3	10 (14.9)	–	<0.05
2001	Morgagni et al. [15]	88	T1b	CK (35ßH11)	Single	pN0 by HE staining	25.8	28 (31.8)	92.9% vs. 95.0%	0.6836
2001	Nakajo et al. [16]	64	T2–T4a	CK (CAM5.2)	Multiple	pN0 by HE staining	31.9	20 (31.3)	66.0% vs. 95.0%	<0.01
2002	Choi et al. [17]	300	T1	CK (MNF 116)	Multiple	pN0 by HE staining	18.0	30 (10.0)	94.0% vs. 89.0%	0.7797
2002	Yasuda et al. [18]	120	T1	CK (AE1/AE3)	Multiple	≤0.2 mm	29.1	27 (22.5)	–	–
2003	Morgagni et al. [19]	308	T1–T4	CK (AE1/AE3)	–	≤0.2 mm	39.0	37 (12.0)	–	0.014
2006	Miyake et al. [20]	35	T1b–T2	CK (O.N.352)	Multiple	pN0 by HE staining	29.4	4 (11.0)	–	–

(continued)

Table 10.1 (continued)

Year	Author	Number of patients	Depth of tumor invasion	Antibody	Assessed sections	Definition of micrometastasis	Average number of assessed LNs	Number of patients with micrometastasis (%)	5-year survival rate (positive vs. negative)	*P*-value (Log-rank test)
2007	Yonemura et al. [21]	184	T1–T4a	CK (AE1/AE3)	–	pN0 by HE staining	27.1	31 (16.8)	58.5% vs. 91.8%	<0.001
2008	Ishii et al. [22]	90	T1	CK (AE1/AE3)	–	≤2 mm	39.2	9 (10.0)	100% vs. 100% (DSS)	–
2008	Kim et al. [23]	160	T1	CK (AE1/AE3)	–	pN0 by HE staining	10.4	34 (21.3)	55.9% vs. 92.9%	<0.001
2009	Kim et al. [24]	45	T1-T4	CK19	Multiple	pN0 by HE staining	7.8	15 (33.3)	63.6% vs. 95.6% (2-year survival)	0.011
2011	Cao et al. [25]	191	T1-T3	CK (AE1/AE3)	Multiple	>0.2 mm and ≤ 2 mm	22.0	54 (28.3)	27.8% vs. 87.1%	<0.001
2012	Ru et al. [26]	95	T1-T4	CK (KL1)	Single	≤2 mm	21.2	19 (20.0)	–	0.386

T1 invasion of the lamina propria or submucosa, *T2* invasion of the muscularis propria, *T3* invasion of the subserosa, *T4* penetration of the serosa without the invasion of adjacent structures (*T4a*) or the invasion of adjacent structures, *CK* cytokeratin, *pN0* node-negative, *HE* hematoxylin-eosin, *DSS* disease-specific survival

were noted in the characteristics of enrolled patients and antibodies used for IHC. Since cytokeratin (CK) is a representative marker for epithelial cells, CK CAM 5.2 or AE1/AE3 monoclonal antibodies (mAb) were used in 12 out of 18 studies (66.7%).

Maehara et al. initially reported that the incidence of LNM assessed by IHC using CAM 5.2 mAb was 23.5% in 34 patients with pT1N0 tumors [4]. Similarly, Morgagni et al. demonstrated the high incidence (10.0%) of LNM in 300 node-negative patients with pT1 tumors by IHC using MNF 116 mAb [19]. Choi et al. identified LNM by IHC using 35ßH11 mAb in 28 (31.8%) out of 88 patients with pT1bN0 tumors [17]. The incidence of LNM in patients with early gastric cancer (pT1) generally ranges between 10% and 31.8% [4, 12–28]. These findings suggest that even patients with early gastric cancer are at a high risk of developing LNM. On the other hand, Fukagawa et al. detected LNM by IHC using AE1/AE3 mAb in 38 (35.5%) out of 107 node-negative patients with pT2-pT3 advanced gastric cancer [14]. Yasuda et al. showed that the incidence of LNM in 64 node-negative patients with pT2-pT4a advanced gastric cancer examined by IHC using CAM 5.2 mAb was 31.3% [18]. These findings indicate that the incidence of LNM is slightly higher in patients with advanced gastric cancer than in those with early gastric cancer. According to Table 10.1, LNM was assessed in multiple sections for IHC in eight studies. Nakajo et al. reported that LNM was identified by IHC on a single section using AE1/AE3 mAb in 10 (14.9%) out of 67 patients with pT1-pT3N0 gastric cancer [16]. Wang et al., in a study on the same population with pT1-pT3N0 gastric cancer, showed that the incidence of LNM evaluated by IHC on multiple sections using AE1/AE3 mAb was 28.3% [27]. These findings demonstrate the clinical benefit of IHC based on multiple sections for detecting LNM in patients with gastric cancer.

Table 10.2 summarizes findings obtained for LNM examined by RT-PCR in patients with pN0 gastric cancer [29–34]. CK and carcinoembryonic antigen (CEA) are widely used as target markers for mRNA in order to detect LNM. Yanagita et al. demonstrated the clinical utility of a multiplex RT-PCR assay using several target markers in patients with gastric cancer [35].

The incidence of LNM assessed by RT-PCR assays ranges between 20% and 41.7% [29–34]. We compared sensitivity between IHC and RT-PCR assays to detect LNM in 1862 lymph nodes obtained from 80 patients with pN0 gastric cancer [31]. The incidences of LNM identified by IHC and RT-PCR were 11.3% (9/80) and 31.3% (25/80), respectively [31]. These findings indicate that the sensitivity of the RT-PCR assay for detecting LNM is higher than that of IHC.

10.4 Relationship Between Clinicopathological Factors and LNM

The presence or absence of macrometastasis identified by HE staining is closely associated with the depth of tumor invasion, tumor size, lymphatic invasion, and venous invasion [36, 37]. Yonemura et al. reported that LNM detected by IHC in

Table 10.2 RT-PCR studies on gastric cancer patients with pN0 diagnosed by hematoxylin-eosin staining

Year	Author	Number of patients	Depth of tumor invasion	Target markers	Total number of assessed LNs	Number of patients with micrometastasis (%)
2001	Okada et al. [27]	24	T1–T4a	CEA, CK 20, MAGE 3	335	10 (41.7)
2002	Matsumoto et al. [28]	50	T1–T4	CEA	312	14 (28.0)
2005	Arigami et al. [29]	80	T1–T3	CEA	1862	25 (31.3)
2006	Sonoda et al. [30]	33	T1	MUC 2, TFF 1	310	11 (33.3)
2007	Wu et al. [31]	10	–	CK 20	–	2 (20.0)
2013	Jagric et al. [32]	14	T1–T3	CEA, CK 20	–	4 (28.6)

T1 invasion of the lamina propria or submucosa, *T3* invasion of the subserosa, *T4* penetration of the serosa without the invasion of adjacent structures (*T4a*) or the invasion of adjacent structures

308 patients with pT1-pT4N0 gastric cancer correlated with lymphatic or venous invasion of the primary tumor site ($P < 0.001$ and $P = 0.018$, respectively) [21]. Similarly, Kim et al. showed that the presence or absence of LNM identified by IHC in 90 patients with pT1N0 gastric cancer correlated with lymphatic invasion, venous invasion, and larger primary tumors ($P = 0.012$, $P = 0.026$, and $P = 0.003$, respectively) [24]. We previously reported that LNM detected by RT-PCR assays correlated with the depth of tumor invasion and lymphatic invasion assessed by HE staining in 80 patients with pT1-pT3N0 gastric cancer ($P = 0.0042$ and $P = 0.015$, respectively) [31]. We also evaluated lymphatic invasion using D2-40 immunohistochemical staining in that study [31]. D2-40 is a specific lymphatic endothelial marker, and IHC using D2-40 mAb is the most sensitive tool for detecting lymphatic invasion in various malignancies including gastric cancer [38]. This study demonstrated that LNM correlated more closely with D2-40 than with HE staining ($P < 0.0001$ vs. $P = 0.015$) (Fig. 10.3a–c) [31]. These findings indicate the close relationship between LNM and the lymphatic invasion of primary tumors. Therefore, not only macrometastasis but also LNM exhibit the same oncologic properties in patients with gastric cancer. Consequently, it is important to precisely assess lymphatic invasion from the viewpoint of LNM in clinical management.

10.5 Prognostic Impact of LNM

Many investigators have demonstrated the prognostic impact of LNM identified by IHC in patients with gastric cancer [4, 12–28]. However, few studies have investigated the relationship between prognosis and LNM identified by RT-PCR assays.

Morgagni et al. showed that 5-year survival rates in 300 patients with pT1N0 gastric cancer with or without LNM were 94% and 89%, respectively [19]. Additionally, no significant differences were observed in 10-year survival rates between these groups [19]. These findings suggest the clinical ambiguity of LNM as a prognostic factor in patients with gastric cancer. They also reported that a host-related immune surveillance system has a powerful impact on LNM [19]. Fukagawa et al. demonstrated that 5-year survival rates in 107 patients with pT2N0 or pT3N0 gastric cancer with or without LNM were 94% and 89%, respectively, while 10-year survival rates were 79% and 74%, respectively [14]. Accordingly, they concluded that LNM did not have a prognostic impact in patients with pT2N0 or pT3N0 advanced gastric cancer undergoing standard gastrectomy with D2 lymphadenectomy [14]. These findings suggest that curative gastrectomy with D2 lymphadenectomy prevents disease recurrence associated with lymph node metastasis including micrometastasis in patients with pT2N0 or pT3N0 gastric cancer.

On the other hand, Yonemura et al., in a study of 308 patients with pT1-pT4N0 gastric cancer, reported that patients with ITCs had a significantly worse prognosis than those without ITCs ($P = 0.014$) [21]. Therefore, they demonstrated that even ITCs exhibit high proliferative activity for evolving into established lymph node metastasis [21]. Wang et al. reported that 5-year survival rates in 191 patients with pT1-pT3N0 gastric cancer with or without LNM were 27.8% and 87.1%,

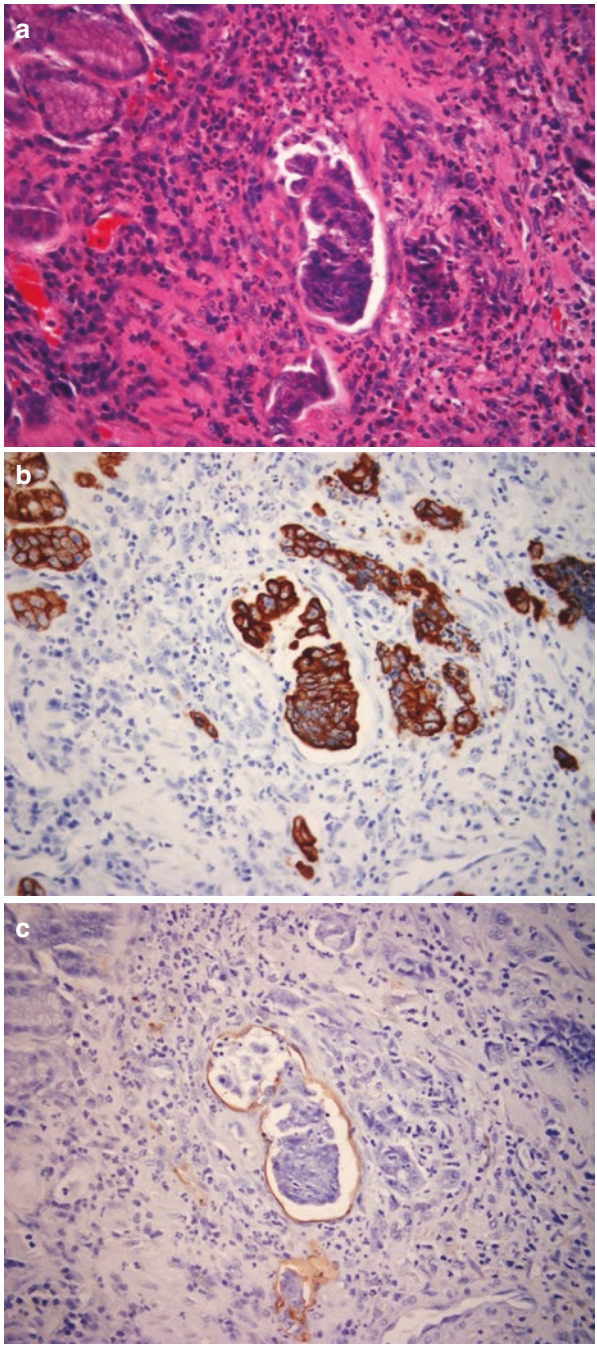

Fig. 10.3 Assessment of lymphatic invasion in a patient with lymph node micrometastasis. (**a**) Routine hematoxylin-eosin staining. (**b**) Cytokeratin (AE1/AE3) staining. (**c**) D2-40 staining. Original magnification ×400

respectively, and a multivariate analysis identified LNM as one of the independent prognostic factors ($P = 0.008$) [27]. Li et al., in a meta-analysis of 18 eligible studies, showed that patients with LNM were more likely to have a poor 5-year survival rate (HR: 2.81, 95% CI: 1.96–4.02) [39]. They concluded that a close relationship exists between the presence of LNM and an unfavorable surgical outcome in patients with pN0 gastric cancer [39]. Jo et al. suggested that lymphadenectomy with D1 + β or more is necessary for preventing disease recurrence by clearing LNM involving the N2 station defined by the Japanese classification of gastric carcinoma in patients with micrometastatic sentinel nodes [40].

10.6 Molecular Behavior of LNM

Few studies have assessed the molecular metastatic potential of isolated or micrometastatic tumor cells in gastric cancer. According to the criteria of the TNM classification established by UICC in 2002, ITCs do not demonstrate the ability to metastasize, such as proliferation, stromal reactions, and the penetration of vascular or lymphatic sinus walls [9]. However, recent molecular studies have indicated the malignant behaviors of LNM including ITCs in patients with gastric cancer [21, 41].

Yanagita et al. investigated the proliferative activity of ITCs and LNM by IHC using Ki-67 mAb [41]. They reported that the positivity rates of Ki-67 for ITCs and LNM were 29% and 92%, respectively [41]. Yonemura et al. also performed an IHC analysis and revealed that the positivity rates of Ki-67 for ITCs with a single cell and clusters of cells were 48.0% and 94.2%, respectively [21]. These two studies obtained similar findings for the proliferative activity of LNM and showed high positivity rates for Ki-67, even in ITCs [21, 41]. Therefore, these findings indicate that tumor cells within LNM have metastatic potential based on high proliferative activity.

We previously assessed the relationship between LNM and several molecular markers, such as the chemokine receptors CCR7 and CXCR4, as well as the vascular endothelial growth factors (VEGF)-C and VEGF-D in patients with gastric cancer [42, 43]. Immunohistochemical analyses demonstrated that CCR7 and CXCR4 expression in primary gastric tumors correlated with the lymph node status including LNMM ($P = 0.0092$ and $P = 0.0075$, respectively) [42]. This finding indicates that CCR7 and CXCR4 expressed by gastric tumor cells play a major role in the mechanisms underlying lymph node metastasis including LNM from primary tumor cells. We also examined the expression of VEGF-C and VEGF-D by IHC in 80 patients with pT1N0 gastric cancer [43]. The findings obtained showed that patients with the strong expression of VEGF-C and VEGF-D had a significantly higher incidence of LNM than those with their weak expression ($P = 0.039$ and $P = 0.021$, respectively) [43]. The VEGF family members VEGF-C and VEGF-D have been associated with the lymphatic spread of cancer cells [44, 45]. VEGFR-3, a receptor

for VEGF-C and VEGF-D, is specifically expressed in the cells of the lymphatic endothelium [46, 47]. Since these signals promote the multiplication, migration, and luminal formation of lymphatic vessels, the expression of VEGF-C and VEGF-D induces lymphangiogenesis in patients with malignant neoplasms. Accordingly, this study demonstrated that lymphangiogenesis via VEGF-C and VEGF-D was closely associated with the developmental process of lymph node metastasis including LNM in patients with gastric cancer.

It is clinically difficult to reach concrete conclusions regarding the clinical significance of LNM in patients with gastric cancer. However, basic research on the biological behavior of ITCs and prospective clinical studies on LNM may provide definitive evidence that will positively influence the clinical management of patients with gastric cancer.

10.7 Future Perspectives of LNM in Clinical Management

A focus has been placed on minimally invasive surgery with individualized lymphadenectomy in consideration of the postsurgical quality of life (QOL) of patients with early gastric cancer. Sentinel node navigation surgery (SNNS) is a representative approach for minimally invasive surgery [48, 49]. Since SNNS targets patients with early gastric cancer rather than those with advanced gastric cancer, lymph node recurrence may be completely avoided in postsurgical management. Therefore, we cannot ignore the existence of LNM due to its controversial significance when performing SNNS. Consequently, an intraoperative assessment of lymph node metastasis based on histological and molecular examinations will be helpful for securing the oncological curability of SNNS. We examined LNM in 61 patients with cT1-T2N0 gastric cancer receiving sentinel node mapping [50]. Sentinel nodes were identified in all patients (100%) [50]. The incidences of metastasis by HE and IHC were 8.2% (5/61) and 13.1% (8/61), respectively [50]. LNM undetectable by IHC was identified in 14 patients (23.0%) using RT-PCR assays [50]. These findings showed that the sentinel node concept is applicable to early gastric cancer, even when IHC and RT-PCR confirm the presence of LNM [50]. In the near future, laparoscopic partial or segmental gastrectomy with sentinel node basin dissection will be widely accepted in future perspectives for SNNS.

Further advances in the development of endoscopic devices have markedly contributed to the spread of endoscopic treatments for selected patients with early gastric cancer. Current endoscopic treatments, such as endoscopic mucosal resection (EMR) and endoscopic submucosal dissection (ESD), have been extensively performed on selected patients with early gastric cancer. Bok et al., in a study on 13 patients with cT1 ($\leq$3 cm) N0 early gastric cancer, reported that ESD with SNNS was a promising minimally invasive procedure that allows en bloc tumor resection to be achieved while assessing the pathological nodal status [51]. In the future, ESD with laparoscopic sentinel node basin dissection may be focused on as an ultimate stomach-preserving surgery for preventing lymph node recurrence in selected patients with the extended indication of ESD. If SNNS based on LNM is clinically

established in the near future, patients with early gastric cancer may safely receive less invasive treatments in consideration of the balance between postsurgical QOL and curability.

References

1. Kwon SJ, Kim GS. Prognostic significance of lymph node metastasis in advanced carcinoma of the stomach. Br J Surg. 1996;83:1600–3.
2. Nitti D, Marchet A, Olivieri M, Ambrosi A, Mencarelli R, Belluco C, Lise M. Ratio between metastatic and examined lymph nodes is an independent prognostic factor after D2 resection for gastric cancer: analysis of a large European monoinstitutional experience. Ann Surg Oncol. 2003;10:1077–85.
3. Japanese Gastric Cancer Association. Japanese gastric cancer treatment guidelines 2010 (ver. 3). Gastric Cancer. 2011;14:113–23. https://doi.org/10.1007/s10120-011-0042-4.
4. Maehara Y, Oshiro T, Endo K, Baba H, Oda S, Ichiyoshi Y, Kohnoe S, Sugimachi K. Clinical significance of occult micrometastasis lymph nodes from patients with early gastric cancer who died of recurrence. Surgery. 1996;119:397–402.
5. Siewert JR, Kestlmeier R, Busch R, Bottcher K, Roder JD, Muller J, Fellbaum C, Hofler H. Benefits of D2 lymph node dissection for patients with gastric cancer and pN0 and pN1 lymph node metastases. Br J Surg. 1996;83:1144–7.
6. Ishida K, Katsuyama T, Sugiyama A, Kawasaki S. Immunohistochemical evaluation of lymph node micrometastases from gastric carcinomas. Cancer. 1997;79:1069–76.
7. Sim SH, Kim YJ, Oh DY, Lee SH, Kim DW, Kang WJ, Im SA, Kim TY, Kim WH, Heo DS, Bang YJ. The role of PET/CT in detection of gastric cancer recurrence. BMC Cancer. 2009;9:73. https://doi.org/10.1186/1471-2407-9-73.
8. Yamaguchi N, Isomoto H, Fukuda E, Ikeda K, Nishiyama H, Akiyama M, Ozawa E, Ohnita K, Hayashi T, Nakao K, Kohno S, Shikuwa S. Clinical outcomes of endoscopic submucosal dissection for early gastric cancer by indication criteria. Digestion. 2009;80:173–81. https://doi.org/10.1159/000215388.
9. Sobin LH, Wittenkind CH. International union against cancer. TNM classification of malignant tumors. 6th ed. New York: John Wiley-Liss; 2002.
10. Yanagita S, Natsugoe S, Uenosono Y, Arima H, Kozono T, Ehi K, Arigami T, Higashi H, Aikou T. Morphological distribution of metastatic foci in sentinel lymph nodes with gastric cancer. Ann Surg Oncol. 2008;15:770–6.
11. Isozaki H, Okajima K, Fujii K. Histological evaluation of lymph node metastasis on serial sectioning in gastric cancer with radical lymphadenectomy. Hepatogastroenterology. 1997;44:1133–6.
12. Cai J, Ikeguchi M, Maeta M, Kaibara N. Micrometastasis in lymph nodes and microinvasion of the muscularis propria in primary lesions of submucosal gastric cancer. Surgery. 2000;127:32–9.
13. Harrison LE, Choe JK, Goldstein M, Meridian A, Kim SH, Clarke K. Prognostic significance of immunohistochemical micrometastases in node negative gastric cancer patients. J Surg Oncol. 2000;73:153–7.
14. Fukagawa T, Sasako M, Mann GB, Sano T, Katai H, Maruyama K, Nakanishi Y, Shimoda T. Immunohistochemically detected micrometastases of the lymph nodes in patients with gastric carcinoma. Cancer. 2001;92:753–60.
15. Morgagni P, Saragoni L, Folli S, Gaudio M, Scarpi E, Bazzocchi F, Marra GA, Vio A. Lymph node micrometastases in patients with early gastric cancer: experience with 139 patients. Ann Surg Oncol. 2001;8:170–4.
16. Nakajo A, Natsugoe S, Ishigami S, Matsumoto M, Nakashima S, Hokita S, Baba M, Takao S, Aikou T. Detection and prediction of micrometastasis in the lymph nodes of patients with pN0 gastric cancer. Ann Surg Oncol. 2001;8:158–62.

17. Choi HJ, Kim YK, Kim YH, Kim SS, Hong SH. Occurrence and prognostic implications of micrometastases in lymph nodes from patients with submucosal gastric carcinoma. Ann Surg Oncol. 2002;9:13–9.
18. Yasuda K, Adachi Y, Shiraishi N, Inomata M, Takeuchi H, Kitano S. Prognostic effect of lymph node micrometastasis in patients with histologically node-negative gastric cancer. Ann Surg Oncol. 2002;9:771–4.
19. Morgagni P, Saragoni L, Scarpi E, Zattini PS, Zaccaroni A, Morgagni D, Bazzocchi F. Lymph node micrometastases in early gastric cancer and their impact on prognosis. World J Surg. 2003;27:558–61.
20. Miyake K, Seshimo A, Kameoka S. Assessment of lymph node micrometastasis in early gastric cancer in relation to sentinel nodes. Gastric Cancer. 2006;9:197–202.
21. Yonemura Y, Endo Y, Hayashi I, Kawamura T, Yun HY, Bandou E. Proliferative activity of micrometastases in the lymph nodes of patients with gastric cancer. Br J Surg. 2007;94:731–6.
22. Ishii K, Kinami S, Funaki K, Fujita H, Ninomiya I, Fushida S, Fujimura T, Nishimura G, Kayahara M. Detection of sentinel and non-sentinel lymph node micrometastases by complete serial sectioning and immunohistochemical analysis for gastric cancer. J Exp Clin Cancer Res. 2008;27:7. https://doi.org/10.1186/1756-9966-27-7.
23. Kim JH, Park JM, Jung CW, Park SS, Kim SJ, Mok YJ, Kim CS, Chae YS, Bae JW. The significances of lymph node micrometastasis and its correlation with E-cadherin expression in pT1-T3N0 gastric adenocarcinoma. J Surg Oncol. 2008;97:125–30.
24. Kim JJ, Song KY, Hur H, Hur JI, Park SM, Park CH. Lymph node micrometastasis in node negative early gastric cancer. Eur J Surg Oncol. 2009;35:409–14. https://doi.org/10.1016/j.ejso.2008.05.004.
25. Cao L, Hu X, Zhang Y, Huang G. Adverse prognosis of clustered-cell versus single-cell micrometastases in pN0 early gastric cancer. J Surg Oncol. 2011;103:53–6. https://doi.org/10.1002/jso.21755.
26. Ru Y, Zhang L, Chen Q, Gao SG, Wang GP, Qu ZF, Shan TY, Qian N, Feng XS. Detection and clinical significance of lymph node micrometastasis in gastric cardia adenocarcinoma. J Int Med Res. 2012;40:293–9.
27. Wang J, Yu JC, Kang WM, Wang WZ, Liu YQ, Gu P. The predictive effect of cadherin-17 on lymph node micrometastasis in pN0 gastric cancer. Ann Surg Oncol. 2012;19:1529–34. https://doi.org/10.1245/s10434-011-2115-3.
28. Jeuck TL, Wittekind C. Gastric carcinoma: stage migration by immunohistochemically detected lymph node micrometastases. Gastric Cancer. 2015;18:100–8. https://doi.org/10.1007/s10120-014-0352-4.
29. Okada Y, Fujiwara Y, Yamamoto H, Sugita Y, Yasuda T, Doki Y, Tamura S, Yano M, Shiozaki H, Matsuura N, Monden M. Genetic detection of lymph node micrometastases in patients with gastric carcinoma by multiple-marker reverse transcriptase-polymerase chain reaction assay. Cancer. 2001;92:2056–64.
30. Matsumoto M, Natsugoe S, Ishigami S, Nakashima S, Nakajo A, Miyazono F, Hokita S, Takao S, Eizuru Y, Aikou T. Lymph node micrometastasis and lymphatic mapping determined by reverse transcriptase-polymerase chain reaction in pN0 gastric carcinoma. Surgery. 2002;131:630–5.
31. Arigami T, Natsugoe S, Uenosono Y, Arima H, Mataki Y, Ehi K, Yanagida S, Ishigami S, Hokita S, Aikou T. Lymphatic invasion using D2-40 monoclonal antibody and its relationship to lymph node micrometastasis in pN0 gastric cancer. Br J Cancer. 2005;93:688–93.
32. Sonoda H, Yamamoto K, Kushima R, Yamamoto H, Naitoh H, Okabe H, Tani T. Detection of lymph node micrometastasis in pN0 early gastric cancer: efficacy of duplex RT-PCR with MUC2 and TFF1 in mucosal cancer. Oncol Rep. 2006;16:411–6.
33. Wu ZY, Li JH, Zhan WH, He YL, Wan J. Effect of lymph node micrometastases on prognosis of gastric carcinoma. World J Gastroenterol. 2007;13:4122–5.
34. Jagric T, Potrc S, Ivanecz A, Horvat M, Plankl M, Mars T. Evaluation of focused sentinel lymph node RT-qPCR screening for micrometastases with the use of the Maruyama computer program. Eur Surg. 2013;45:270–6.

35. Yanagita S, Uenosono Y, Arigami T, Daisuke M, Okubo K, Kijima T, Arima H, Hirata M, Haraguchi N, Hagihara T, Nishizono Y, Ishigami S, Natsugoe S. The clinical usefulness of the intraoperative detection of sentinel lymph node metastases by a rapid RT-PCR system in patients with gastric cancer. Cancer. 2016;122:386–92. https://doi.org/10.1002/cncr.29740.
36. An JY, Baik YH, Choi MG, Noh JH, Sohn TS, Kim S. Predictive factors for lymph node metastasis in early gastric cancer with submucosal invasion: analysis of a single institutional experience. Ann Surg. 2007;246:749–53.
37. Tajima Y, Murakami M, Yamazaki K, Masuda Y, Aoki S, Kato M, Sato A, Goto S, Otsuka K, Kato T. Risk factors for lymph node metastasis from gastric cancers with submucosal invasion. Ann Surg Oncol. 2010;17:1597–604. https://doi.org/10.1245/s10434-010-0930-6.
38. Kalof AN, Cooper K. D2-40 immunohistochemistry – so far! Adv Anat Pathol. 2009;16:62–4. https://doi.org/10.1097/PAP.0b013e3181915e94.
39. Li Y, Du P, Zhou Y, Cheng Q, Chen D, Wang D, Sun T, Zhou J, Patel R. Lymph node micrometastases is a poor prognostic factor for patients in pN0 gastric cancer: a meta-analysis of observational studies. J Surg Res. 2014;191:413–22. https://doi.org/10.1016/j.jss.2014.05.088.
40. Jo MJ, Park JY, Song JS, Kook MC, Ryu KW, Cho SJ, Lee JH, Nam BH, Hong EK, Choi IJ, Kim YW. Biopathologic features and clinical significance of micrometastasis in the lymph node of early gastric cancer. World J Gastroenterol. 2015;21:667–74. https://doi.org/10.3748/wjg.v21.i2.667.
41. Yanagita S, Natsugoe S, Uenosono Y, Kozono T, Ehi K, Arigami T, Arima H, Ishigami S, Aikou T. Sentinel node micrometastases have high proliferative potential in gastric cancer. J Surg Res. 2008;145:238–43.
42. Arigami T, Natsugoe S, Uenosono Y, Yanagita S, Arima H, Hirata M, Ishigami S, Aikou T. CCR7 and CXCR4 expression predicts lymph node status including micrometastasis in gastric cancer. Int J Oncol. 2009;35:19–24.
43. Arigami T, Natsugoe S, Uenosono Y, Yanagita S, Ehi K, Arima H, Mataki Y, Nakajo A, Ishigami S, Aikou T. Vascular endothelial growth factor-C and -D expression correlates with lymph node micrometastasis in pN0 early gastric cancer. J Surg Oncol. 2009;99:148–53. https://doi.org/10.1002/jso.21228.
44. Yonemura Y, Endo Y, Fujita H, Fushida S, Ninomiya I, Bandou E, Taniguchi K, Miwa K, Ohoyama S, Sugiyama K, Sasaki T. Role of vascular endothelial growth factor C expression in the development of lymph node metastasis in gastric cancer. Clin Cancer Res. 1999;5:1823–9.
45. Onogawa S, Kitadai Y, Tanaka S, Kuwai T, Kimura S, Chayama K. Expression of VEGF-C and VEGF-D at the invasive edge correlates with lymph node metastasis and prognosis of patients with colorectal carcinoma. Cancer Sci. 2004;95:32–9.
46. Jeltsch M, Kaipainen A, Joukov V, Meng X, Lakso M, Rauvala H, Swartz M, Fukumura D, Jain RK, Alitalo K. Hyperplasia of lymphatic vessels in VEGF-C transgenic mice. Science. 1997;276:1423–5.
47. Achen MG, Jeltsch M, Kukk E, Mäkinen T, Vitali A, Wilks AF, Alitalo K, Stacker SA. Vascular endothelial growth factor D (VEGF-D) is a ligand for the tyrosine kinases VEGF receptor 2 (Flk1) and VEGF receptor 3 (Flt4). Proc Natl Acad Sci U S A. 1998;95:548–53.
48. Aikou T, Higashi H, Natsugoe S, Hokita S, Baba M, Tako S. Can sentinel node navigation surgery reduce the extent of lymph node dissection in gastric cancer? Ann Surg Oncol. 2001;8:90S–3S.
49. Kitagawa Y, Kitano S, Kubota T, Kumai K, Otani Y, Saikawa Y, Yoshida M, Kitajima M. Minimally invasive surgery for gastric cancer – toward a confluence of two major streams: a review. Gastric Cancer. 2005;8:103–10.
50. Arigami T, Natsugoe S, Uenosono Y, Mataki Y, Ehi K, Higashi H, Arima H, Yanagida S, Ishigami S, Hokita S, Aikou T. Evaluation of sentinel node concept in gastric cancer based on lymph node micrometastasis determined by reverse transcription-polymerase chain reaction. Ann Surg. 2006;243:341–7.
51. Bok GH, Kim YJ, Jin SY, Chun CG, Lee TH, Kim HG, Jeon SR, Cho JY. Endoscopic submucosal dissection with sentinel node navigation surgery for early gastric cancer. Endoscopy. 2012;44:953–6. https://doi.org/10.1055/s-0032-1310162.

Clinical Aspects: Colorectal Cancer

11

Hirofumi Yamamoto and Masaki Mori

Abstract

Colorectal cancer (CRC) is one of the most common cancers worldwide. Currently, postoperative adjuvant chemotherapy is recommended for node-positive stage III patients, but not for those who are node-negative, with stage II disease. However, a systematic meta-analysis revealed that the presence of micrometastases in regional lymph nodes (LNs) was associated with poor survival in 4087 patients with node-negative CRC. Unfortunately, the majority of studies used in that meta-analysis were performed retrospectively. In a prospective clinical trial, we revealed that the micrometastasis volume, as determined by qRT-PCR of carcinoembryonic antigen (CEA) mRNA, is a useful marker with which to stratify patients at risk of recurrence of stage II CRC. Furthermore, our quantitative data illustrated the concept that stage II CRC represents a transitional stage between localized (stage I) and a more expansive (stage III) disease. At the cellular level, the intermediary stage II disease involves CRC tumors that continuously "seed" micrometastases in LNs, which then increases the risk of tumor recurrence.

The one-step nucleic acid amplification (OSNA) assay is a novel and rapid technique with which to detect cytokeratin (CK) 19 mRNA using reverse transcription loop-mediated isothermal amplification (RT-LAMP). Using OSNA, a prospective study showed that rates of upstaging in 124 node-negative patients

H. Yamamoto (✉)
Department of Surgery, Gastroenterological Surgery, Graduate School of Medicine, Osaka University, Suita City, Osaka, Japan

Division of Health Sciences, Department of Molecular Pathology, Graduate School of Medicine, Osaka University, Suita City, Osaka, Japan
e-mail: hyamamoto@sahs.med.osaka-u.ac.jp

M. Mori
Department of Surgery, Gastroenterological Surgery, Graduate School of Medicine, Osaka University, Suita City, Osaka, Japan

S. Natsugoe (ed.), *Lymph Node Metastasis in Gastrointestinal Cancer*,
https://doi.org/10.1007/978-981-10-4699-5_11

(pN0) with pStages I, IIA, IIB, and IIC were 2.0%, 17.7%, 12.5%, and 25%, respectively. These findings suggest that OSNA may usefully substitute for RT-PCR of CEA mRNA owing to its ease of use and rapidity.

Keywords
Micrometastasis · CEA · CK19 · OSNA · Colorectal cancer

11.1 Introduction

Colorectal cancer (CRC) is one of the most common cancers worldwide. Disease prognosis depends on several risk factors related to patient background, their treatment, and tumor characteristics [1]. Of the latter, metastasis to regional lymph nodes (LNs) is known to be a crucial prognostic factor. This notion is codified in the tumor-node-metastasis (TNM) staging system of the Union for International Cancer Control (UICC) used to predict clinical outcomes. LN metastasis is also used to inform therapeutic decision-making [2, 3].

The MOSAIC (Multicenter International Study of Oxaliplatin/5-Fluorouracil (5-FU)/Leucovorin (LV) in the Adjuvant Treatment of Colon Cancer) study has demonstrated the benefit of adding oxaliplatin to infusional 5-FU and LV (FOLFOX versus FL) in node-positive stage III colon cancer patients having undergone a curative resection. On the other hand, no survival benefit was reported for node-negative stage II colon cancer patients [4]. Overall, postoperative adjuvant chemotherapy is currently recommended for node-positive stage III patients, diagnosed by histopathology, but not for node-negative stage II patients. However, it is plausible that a subgroup of at-risk (of recurrence) patients resides within the node-negative stage II group and that these patients may still benefit from postoperative adjuvant treatment [5, 6].

While the biology that underlies a high risk of recurrence is incompletely understood in terms of CRC, various risk factors are associated with this outcome. For example, the current American Society of Clinical Oncology (ASCO) guidelines define T4 primary disease, inadequately sampled nodes, a poorly differentiated histology, and perforation as high-risk factors for disease relapse in stage II CRC [7]. Moreover, according to the current European Society for Medical Oncology (ESMO) guidelines, adjuvant chemotherapy is recommended in stage II patients who have the following tumor characteristics: a pT4 tumor, fewer than 12 LNs sampled, a poorly differentiated tumor, lymph-vascular invasion, perineural invasion, tumor obstruction, or perforation [8]. However, the use of adjuvant therapy for these patients remains controversial as we lack robust evidence for any survival benefit. In this context, a retrospective study by O'Connor and colleagues demonstrated that while 75% of 24,847 stage II cancers exhibited one or more of these poor prognostic features (including perforation, T4 stage, poor histology, etc.), no survival benefit was obtained from postoperative adjuvant chemotherapy (irrespective of the presence of these poor prognostic factors) [9]. These findings question

the utility of these prognostic guides in predicting patient survival following adjuvant treatment.

Therefore novel, more robust clinical approaches are required that allow us to more accurately identify those stage II patients who may benefit from adjuvant chemotherapy.

11.2 A Genetic Diagnosis of Micrometastasis

Patients with CRCs clinically diagnosed as localized resectable tumors without LN involvement or distant metastases are generally considered to present a low risk for recurrence. Theoretically, these patients should be cured by surgical resection without the need for adjuvant chemotherapy. However, it was reported that about 30–40% of node-negative stage II patients subsequently develop recurrent disease despite their low tumor stage [10]. Tumor progression after curative resection of CRC is primarily driven by the dissemination of tumor cells to LNs, blood, and the bone marrow, with these tumor cells currently going undetected by standard clinical staging techniques [11]. Previous studies have suggested the presence of occult cancer metastasis (also designated as micrometastasis) in the LNs of CRC patients [5]. The detection of these micrometastases in stage II patients could therefore be of clinical use in stratifying a patient subgroup at an elevated risk of relapse.

Micrometastases ordinarily escape detection by conventional H&E-stained sections because so few cells are involved. Thus, a different approach is needed to detect these events. Ideally, the technique used should be accurate and easy to use in the clinical context. Candidate techniques include immunohistochemistry (IHC) or reverse transcription polymerase chain reaction (RT-PCR), with either technique shown to provide direct evidence of micrometastases in various studies of node-negative CRCs. Cytokeratin (CK), a specific marker of epithelial cells, has been widely used for the immunohistochemical examination of micrometastases in CRC [12–16]. IHC has identified micrometastatic cells at a frequency of 17–39% in histologically negative LNs. However, logistically, this method is limited by the time and effort required to examine sufficient sections to identify occult metastases in a lymph node. Alternatively, certain tumor-specific mRNAs, e.g., CK19, carcinoembryonic antigen (CEA), and CK20, have been successfully amplified by RT-PCR in patients with a variety of malignant tumors, including CRC [17–21]. However, although this genetic detection method is reported to demonstrate a high sensitivity [22, 23], issues with false positives can arise.

Ideally, it would be preferable to use both techniques (IHC and nucleic acid amplification), so as to accommodate for their individual weaknesses. Taking this approach, Miyake et al. examined 237 LNs from 11 CRC patients who underwent curative resection (stages I–III) by means of IHC for CK and then RT-PCR for the CEA and CK20 mRNAs. Conventional histological examination (H&E) was also used to evaluate the extent of micrometastasis in each case by constructing an anatomical map of the involved LNs [6]. This group reported that histological analyses identified 20 (of 237) LNs as positive for metastatic cells, all of which were

subsequently found to be positive by both IHC and RT-PCR. Of the 217 histologically negative LNs, 14 (6.5%) contained micrometastases by IHC on a single-slice examination, and 57 (26.2%) were positive for at least one of the two genetic markers (CEA and CK20) by RT-PCR. Anatomical mapping of the regional LNs for all patients indicated that micrometastases were dispersed not only at the pericolic LNs but also (often) at distant LNs. A clinical follow-up study showed that two patients developed disease recurrence within 1 year of their surgery and that both exhibited RT-PCR positive micrometastases in not less than 70% of the LNs examined. In addition, these patients had frequent micrometastases at distant LNs, i.e., those around the root or along the inferior mesenteric artery. These data suggested that a genetic diagnosis of micrometastasis using RT-PCR might therefore be of clinical use.

Rahbari et al. recently reported a systematic meta-analysis of micrometastases using the regional LNs of 4087 patients with node-negative CRC [24]. In their analysis of 39 studies, it was revealed that micrometastases in regional LNs were associated with poor values for overall survival (HR, 2.20; 95% CI: 1.43–3.40), disease-specific survival (HR, 3.37; 95% CI: 2.31–4.93), and disease-free survival (HR, 2.24; 95% CI: 1.57–3.20). Subgroup analyses also showed that molecular tumor cell detection was a significant independent prognostic factor. Although their designs were consistent, most of these studies were performed retrospectively. Prospective studies were therefore warranted in order to confirm the results of this meta-analysis.

11.3 A Novel One-Step Nucleic Acid Amplification (OSNA)-Based Molecular Technique for the Detection of LN Micrometastases

A histological diagnosis of postoperative LN metastasis is commonly made by microscopic examination of H&E-stained specimens using the largest cross-sectional area of the LN. Using this method, micrometastases are often overlooked because of their small size and localization. Despite the availability of the previously mentioned IHC and RT-PCR detection techniques, these have yet to be applied in clinical practice given that both are labor intensive and complex.

The OSNA assay is a new and rapid technique that employs the reverse transcription loop-mediated isothermal amplification of nucleic acids (RT-LAMP). Since this method can directly analyze the supernatant of a homogenized LN, without the need to purify mRNAs, it can be completed relatively quickly and easily. The utility of the OSNA assay has already been proven in breast cancer patients, for whom OSNA is used to diagnose axillary LN metastases, which saves these patients from having to undergo a second surgery for axillary clearance [25, 26].

In a multicenter clinical study in Japan, we used OSNA-based genetic diagnosis for LN micrometastases in CRC [27]. In this study, we evaluated the clinical significance of the OSNA assay in precisely diagnosing LN metastases in CRC patients using cytokeratin 19 (CK19) mRNA as a molecular marker. These data allowed us

to clarify the diagnostic power achieved by combining pathology with OSNA. The OSNA assay was performed on 121 LNs dissected from early-stage CRC patients (pStage 0 or I) or from patients with benign colorectal disease. This group was set to assess whether the OSNA assay would yield false-positive results for histologically negative LNs in which no metastatic cells could be detected following extensive (0.1-mm interval) histopathological examination. Moreover, 385 LNs were collected from 85 CRC patients (any stage) to examine whether the OSNA assay could match the performance of a 2-mm interval histopathological examination. Study results revealed that the accuracy of the OSNA assay was comparable to the 2-mm interval histological examination, rendering it more accurate than the more commonly performed pathological exam. Based on these findings, the OSNA molecular detection technique was approved as a novel diagnostic kit for LN micrometastasis in CRC by the Japanese Ministry of Health, Labor, and Welfare in 2013.

11.4 A Clinical Investigation of Micrometastases in LNs: Retrospective Studies

It is important to know the distribution of micrometastases in the regional LNs of CRC patients. Although several studies have shown the existence of micrometastases in the LNs of CRC patients, comparatively little is known as to their localization and frequency. This issue is important from the surgical perspective given that surgeons should appreciate the invasive potential of cancer cells during surgery, even when such cells are rare. In this context, Noura et al. assessed the localization and frequency of micrometastases using IHC with a pan-cytokeratin monoclonal antibody (AE1/AE3) in 878 LNs from 98 patients with CRC [28]. In this study, the anatomical position of LNs was defined as levels 1–3, according to their distance from the main tumor. This group showed that the frequency with which micrometastases could be identified increased as more 4-μm-thick LN sections were examined (using 1, 2, and 5 slices). When examining five LN slices, micrometastases were frequently and extensively present in 49.1, 35.7, and 53.3% of histologically LN-negative patients, LN-positive patients at level 1, and LN-positive patients at level 2, respectively. This group also assessed the prognostic value of detecting micrometastases in LN-negative patients and reported no significant impact. While these data indicated the high frequency with which micrometastasis could be detected in the LNs of CRC patients, they also ultimately revealed that IHC-based detection of micrometastases in LN-negative CRC patients was not helpful in predicting patient outcome.

To assess the possible clinical applications of micrometastasis detection, the previous discrepant findings between genetic diagnoses and IHC must be resolved. With this in mind, and because the majority of previous studies had used a single method rather than side-by-side comparisons of IHC and molecular analyses, Noura et al. examined the presence of micrometastases in pericolic LNs by means of IHC and molecular testing. IHC was with an anti-cytokeratin antibody, complemented with carcinoembryonic antigen (CEA)-specific RT-PCR with (the same) N0 CRC

patients who had undergone curative surgery and whose clinical outcomes were already known [22]. In this study, 64 CRC patients for whom good quality RNA was available (from paraffin-embedded LN specimens) were selected from 84 stage II patients. Micrometastases were detected in 19 (29.6%) of the 64 patients by RT-PCR and in 35 (54.7%) of the 64 patients by IHC. By RT-PCR analysis, those patients that manifested a positive band for CEA mRNA had a significantly worse prognosis than those who were RT-PCR negative with respect to both disease-free and overall survival ($P = 0.027$ and 0.015, respectively). However, in IHC analysis, the presence of micrometastases did not predict patient outcome, neither for disease-free nor overall survival. By multivariate Cox regression analysis, both micrometastases detected by RT-PCR and Crohn's-like lymphoid reactions were independent prognostic factors. These data strongly suggest that micrometastases in LNs detected by CEA-specific RT-PCR, but not by IHC, might be useful in predicting a high risk for relapse in stage II CRC patients. A prospective randomized controlled study was therefore needed to ascertain whether high-risk patients, as identified by RT-PCR, could benefit from adjuvant therapy.

11.5 The Clinical Impact of the Volume of Micrometastases in LNs: Prospective Multicenter Studies

The clinical benefit of OSNA in CRC is currently under investigation in several studies [27, 29, 30]. As mentioned previously, our clinical study based on 385 LNs demonstrated that the OSNA technique is comparable to a 2-mm interval histopathological examination in terms of its accuracy in detecting LN metastases [27]. Based on those findings, we performed a prospective analysis to examine LN metastases in patients with CRC ($n = 204$ cases), with an investigation of the migration of clinical stage when OSNA was used to complement the standard pathological examination [31]. In this study, it was demonstrated that the agreement between single-slice H&E examination and the OSNA assay was 95.7% (1842/1925 LNs). Moreover, sensitivity and specificity values for the OSNA assay were 86.2% (125/145) and 96.5% (1717/1780), respectively. Among 124 LN-negative patients (pN0), the respective upstaging rates of pStages I, IIA, IIB, and IIC were 2.0% (1/50), 17.7% (11/62), 12.5% (1/8), and 25% (1/4), respectively. Moreover, the OSNA-positive patients demonstrated a deeper invasion of the colonic wall and severe lymphatic invasion ($P = 0.048$ and $P = 0.004$, respectively). In terms of quantitative data, mRNA copies as identified by OSNA were found to increase in line with the number of involved LNs. For example, 1550 copies/lL were identified for pN0, 24,050 copies/lL for pN1, and 90,600 copies/lL for pN2. These findings indicate that the sum of CK19 mRNAs, as assessed by OSNA [which indicates the total tumor load (TTL)], displays a trend compatible to the current pathological diagnostic system. These findings also suggest the future possibility of developing a novel molecular staging technique using OSNA and metastasis volume (amount of CK19 mRNA), rather than the number of LN metastases. Further, the TTL values of the cases upstaged using the OSNA method from stage II to stage III largely overlapped

those found for stage III CRCs, suggesting that these upstaged patients were likely to be at a high risk of disease recurrence.

Currently, the prognostic value of molecular tumor cell detection in patients with LN-negative CRC has remained uncertain because of a paucity of relevant data from prospective studies [11, 32–34]. The National Comprehensive Cancer Network (NCCN) clinical practice guidelines in oncology (version 4, 2013) recommend that the detection of cancer cells by IHC, or the molecular detection of cancer cells in regional LNs, should be considered investigational. This recommendation comes with the caveat that the majority of evidence cited in this guideline is derived from retrospective studies. To address this issue, we conducted a prospective multicenter clinical trial to assess the utility of a prognostic marker for patients with LN-negative stage II CRC [35]. In this study, we employed the molecular detection of CEA mRNA by qRT-PCR, in addition to conventional qualitative RT-PCR (i.e., the so-called "a band" method), in order to establish a clinically appropriate threshold (i.e., cutoff) for a high risk of disease recurrence. A total of 296 patients with pathologic stage II CRC were eventually analyzed for their long-term prognosis. Multivariate Cox regression analyses revealed that a high micrometastasis volume (high MMV; $n = 95$) was an independent poor prognostic factor for 5-year disease-free survival (DFS; $P = 0.001$) and 5-year overall survival (OS; $P = 0.016$) (Fig. 11.1a, b). This prospective clinical trial clearly demonstrates that the MMV, as determined by qRT-PCR of CEA mRNA, is a useful marker in stratifying patients' risk of recurrence for stage II CRC. Furthermore, these data introduce the concept that stage II CRC represents a transition between localized stage I disease and expanding stage III disease, with CRC tumors continuously building their MMVs in LNs and therefore increasing the risk of tumor recurrence (Fig. 11.2).

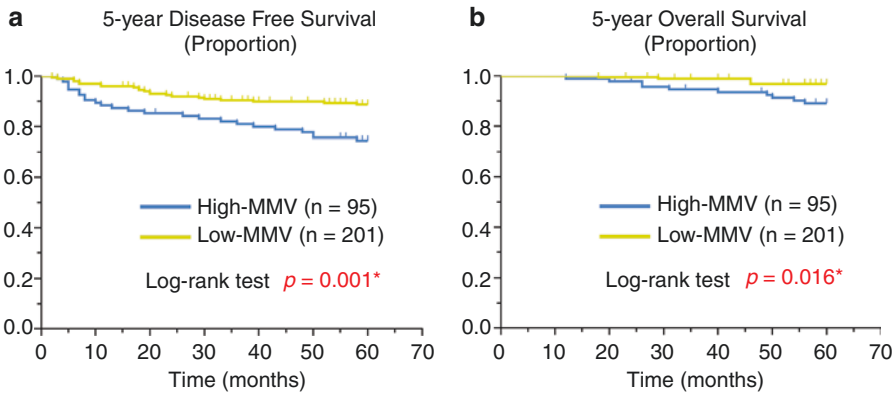

Fig. 11.1 Survival curves stratified by high and low MMV. Survival analyses indicated that the high MMV group had a significantly worse 5-year DFS (**a**) and 5-year OS (**b**) vs. the low MMV group (DFS high/low MMV: 74.7% vs. 88.6%, $P = 0.001$; OS high/low MMV: 89.5% vs. 95.5%, $P = 0.016$). There was no difference in the mean follow-up period for the high vs. low MMV groups ($P = 0.8471$; mean ± SD, 86.0 ± 25.8 vs. 79.9 ± 22.1 months). The median follow-up periods were 82.9 (12.6–133.2) months and 81.4 (5.3–124.9) months, respectively. DFS, disease-free survival; OS, overall survival

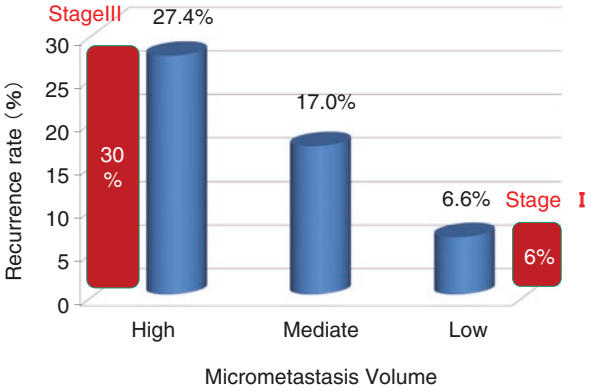

Fig. 11.2 This figure shows a positive correlation between elevated micrometastasis volumes and a higher 5-year recurrence rate in CRC. The 5-year recurrence rates for high micrometastasis volume patients largely overlapped with those of the stage III CRC patients

Although these findings are not sufficient to determine the efficacy of chemotherapy in high MMV patients, such a group may benefit from postoperative adjuvant chemotherapy. Indeed, LN metastasis in stage III CRC is a well-established predictive marker of survival benefit by chemotherapy [36, 37]. The current study also showed that MMV, as determined by qRT-PCR for CK19 mRNA, was of use in discerning high-risk stage II CRC patients in the same clinical setting [35]. In this context, OSNA may be able to substitute for CEA targeted RT-PCR owing to its ease of use and rapidity.

11.6 Future Perspectives

Micrometastases were originally defined as small occult metastases that are present not only in the LNs but also in the peripheral blood or bone marrow. Recent advances in immunocytochemical and molecular assays now allow us to detect circulating tumor cells (CTCs) in the peripheral blood and disseminated cells (DTCs), including epithelial cancer cells of various tumor origins that "home" to the bone marrow. The previous results provide direct evidence that tumor cell dissemination commences early in tumor development and progression. Tumor cells are frequently detected in the blood and bone marrow of cancer patients with no clinical or even pathological signs of metastasis. The detection of DTCs and CTCs constitutes important prognostic data that might help to tailor systemic therapies to individual needs [38]. Previously, Wikman et al. described the importance of various factors in controlling tumor cell dissemination in the bone marrow. These included angiogenic factors (HIF1alpha, VEGF), immunological factors (CD274, HLA class I antigen), phenotypic characteristics (Ki67, CD44+/CD24-, CK19+/MUC1-), oncogenes and metastasis suppressor gene activity (MUC, HER2, nm23-H1, KISS1), growth stimulatory factors (EGFR/uPAR, ERK, and the p38 pathways), and microenvironment epithelial-stromal cross talk (CXCL12) [39]. However, there has been no molecular study of the cancer cells that form micrometastases in the LNs of patients with CRC. We would speculate that recent innovative techniques might also reveal the significance of these cancer cells in LN micrometastases.

Recent and accumulating evidence suggests that a diversity of cancer cells, and therefore intra-tumor heterogeneity, exists within a micrometastasis. Until now, molecular datasets have been acquired using large numbers of cells. Consequently, these data represent an average of the molecular diversity within a population [40]. Recently, the focus has shifted to single-cell quantitative analyses (of various materials and nucleic acids) [41]. At present, it is possible to study the mRNAs in a single cell using several technical innovations. Brenner et al. have reported the use of massively parallel signature sequencing (MPSS) to analyze gene expression by sequencing a small amount of cDNA without a next-generation sequencer [42]. Islam et al. described single-cell tagged reverse transcription (STRT), a highly multiplexed method for single-cell RNA sequencing using the Illumina platform [43]. More recently, RNA sequencing (RNA-Seq) in breast cancer has revealed the varied molecular landscape of the breast transcriptome together with novel regulatory interactions [44, 45]. As a powerful next-generation sequencing technology, RNA-Seq can profile a full set of transcripts including mRNAs, small RNAs, and other non-coding RNAs, both qualitatively and quantitatively, to provide a snapshot of gene expression patterns and regulatory elements in a single cell, tissue, or organism. It can also identify novel isoforms and exons, allele-specific expression, mutations, and fusion transcripts [46].

Overall, these recent advances now make it possible to investigate novel biomarkers of LN micrometastases other than CEA or CK19. In the near future, a more precise and easier detection of LN micrometastases may allow us to improve clinical decision-making and to deliver tangible personalized medicines to patients with CRC.

References

1. Weitz J, Koch M, Debus J, Hohler T, Galle PR, Buchler MW. Colorectal cancer. Lancet. 2005;365(9454):153–65.
2. Nelson H, Petrelli N, Carlin A, Couture J, Fleshman J, Guillem J, et al. Guidelines 2000 for colon and rectal cancer surgery. J Natl Cancer Inst. 2001;93(8):583–96.
3. Sobin LH, Gospodarowicz MK, Wittekind C. UICC international union against cancer. In: TNM classification of malignant tumors. 7th ed. New York, NY: Wiley-Blackwell; 2009.
4. de Gramont ABC, Navarro M, et al. Oxaliplatin/5FU/LV in the adjuvant treatment of stage II and stage III colon cancer: efficacy results with a median follow-up of 4 years. J Clin Oncol. 2005;23:246s.
5. Weitz J, Kienle P, Magener A, Koch M, Schrodel A, Willeke F, et al. Detection of disseminated colorectal cancer cells in lymph nodes, blood and bone marrow. Clin Cancer Res. 1999;5(7):1830–6.
6. Miyake Y, Yamamoto H, Fujiwara Y, Ohue M, Sugita Y, Tomita N, et al. Extensive micrometastases to lymph nodes as a marker for rapid recurrence of colorectal cancer: a study of lymphatic mapping. Clin Cancer Res. 2001;7(5):1350–7.
7. Benson AB 3rd, Schrag D, Somerfield MR, Cohen AM, Figueredo AT, Flynn PJ, et al. American Society of Clinical Oncology recommendations on adjuvant chemotherapy for stage II colon cancer. J Clin Oncol. 2004;22(16):3408–19.
8. Labianca R, Nordlinger B, Beretta GD, Brouquet A, Cervantes A. Primary colon cancer: ESMO Clinical Practice Guidelines for diagnosis, adjuvant treatment and follow-up. Ann Oncol. 2010;21(Suppl 5):v70–7.

9. O'Connor ES, Greenblatt DY, LoConte NK, Gangnon RE, Liou JI, Heise CP, et al. Adjuvant chemotherapy for stage II colon cancer with poor prognostic features. J Clin Oncol. 2011;29(25):3381–8.
10. Deans GT, Parks TG, Rowlands BJ, Spence RA. Prognostic factors in colorectal cancer. Br J Surg. 1992;79(7):608–13.
11. Kronberg U, Lopez-Kostner F, Soto G, Zuniga A, Wistuba I, Miranda V, et al. Detection of lymphatic micrometastases in patients with stages I and II colorectal cancer: impact on five-year survival. Dis Colon Rectum. 2004;47(7):1151–7.
12. Cutait R, Alves VA, Lopes LC, Cutait DE, Borges JL, Singer J, et al. Restaging of colorectal cancer based on the identification of lymph node micrometastases through immunoperoxidase staining of CEA and cytokeratins. Dis Colon Rectum. 1991;34(10):917–20.
13. Greenson JK, Isenhart CE, Rice R, Mojzisik C, Houchens D, Martin EW Jr. Identification of occult micrometastases in pericolic lymph nodes of Duke's B colorectal cancer patients using monoclonal antibodies against cytokeratin and CC49. Correlation with long-term survival. Cancer. 1994;73(3):563–9.
14. Jeffers MD, O'Dowd GM, Mulcahy H, Stagg M, O'Donoghue DP, Toner M. The prognostic significance of immunohistochemically detected lymph node micrometastases in colorectal carcinoma. J Pathol. 1994;172(2):183–7.
15. Adell G, Boeryd B, Franlund B, Sjodahl R, Hakansson L. Occurrence and prognostic importance of micrometastases in regional lymph nodes in Dukes' B colorectal carcinoma: an immunohistochemical study. Eur J Surg. 1996;162(8):637–42.
16. Oberg A, Stenling R, Tavelin B, Lindmark G. Are lymph node micrometastases of any clinical significance in Dukes Stages A and B colorectal cancer? Dis Colon Rectum. 1998;41(10):1244–9.
17. Noguchi S, Hiratsuka M, Furukawa H, Aihara T, Kasugai T, Tamura S, et al. Detection of gastric cancer micrometastases in lymph nodes by amplification of keratin 19 mRNA with reverse transcriptase-polymerase chain reaction. Jpn J Cancer Res. 1996;87(6):650–4.
18. Noguchi S, Aihara T, Motomura K, Inaji H, Imaoka S, Koyama H. Detection of breast cancer micrometastases in axillary lymph nodes by means of reverse transcriptase-polymerase chain reaction. Comparison between MUC1 mRNA and keratin 19 mRNA amplification. Am J Pathol. 1996;148(2):649–56.
19. Matsumura M, Niwa Y, Kato N, Komatsu Y, Shiina S, Kawabe T, et al. Detection of alpha-fetoprotein mRNA, an indicator of hematogenous spreading hepatocellular carcinoma, in the circulation: a possible predictor of metastatic hepatocellular carcinoma. Hepatology. 1994;20(6):1418–25.
20. Mori M, Mimori K, Inoue H, Barnard GF, Tsuji K, Nanbara S, et al. Detection of cancer micrometastases in lymph nodes by reverse transcriptase-polymerase chain reaction. Cancer Res. 1995;55(15):3417–20.
21. Futamura M, Takagi Y, Koumura H, Kida H, Tanemura H, Shimokawa K, et al. Spread of colorectal cancer micrometastases in regional lymph nodes by reverse transcriptase-polymerase chain reactions for carcinoembryonic antigen and cytokeratin 20. J Surg Oncol. 1998;68(1):34–40.
22. Noura S, Yamamoto H, Ohnishi T, Masuda N, Matsumoto T, Takayama O, et al. Comparative detection of lymph node micrometastases of stage II colorectal cancer by reverse transcriptase polymerase chain reaction and immunohistochemistry. J Clin Oncol. 2002;20(20):4232–41.
23. Bilchik AJ, Hoon DS, Saha S, Turner RR, Wiese D, DiNome M, et al. Prognostic impact of micrometastases in colon cancer: interim results of a prospective multicenter trial. Ann Surg. 2007;246(4):568–75; discussion 75–7.
24. Rahbari NN, Bork U, Motschall E, Thorlund K, Buchler MW, Koch M, et al. Molecular detection of tumor cells in regional lymph nodes is associated with disease recurrence and poor survival in node-negative colorectal cancer: a systematic review and meta-analysis. J Clin Oncol. 2012;30(1):60–70.

25. Schem C, Maass N, Bauerschlag DO, Carstensen MH, Loning T, Roder C, et al. One-step nucleic acid amplification-a molecular method for the detection of lymph node metastases in breast cancer patients; results of the German study group. Virchows Arch. 2009;454(2):203–10.
26. Tamaki Y, Akiyama F, Iwase T, Kaneko T, Tsuda H, Sato K, et al. Molecular detection of lymph node metastases in breast cancer patients: results of a multicenter trial using the one-step nucleic acid amplification assay. Clin Cancer Res. 2009;15(8):2879–84.
27. Yamamoto H, Sekimoto M, Oya M, Yamamoto N, Konishi F, Sasaki J, et al. OSNA-based novel molecular testing for lymph node metastases in colorectal cancer patients: results from a multicenter clinical performance study in Japan. Ann Surg Oncol. 2011;18(7):1891–8.
28. Noura S, Yamamoto H, Miyake Y, Kim B, Takayama O, Seshimo I, et al. Immunohistochemical assessment of localization and frequency of micrometastases in lymph nodes of colorectal cancer. Clin Cancer Res. 2002;8(3):759–67.
29. Croner RS, Geppert CI, Bader FG, Nitsche U, Spath C, Rosenberg R, et al. Molecular staging of lymph node-negative colon carcinomas by one-step nucleic acid amplification (OSNA) results in upstaging of a quarter of patients in a prospective, European, multicentre study. Br J Cancer. 2014;110(10):2544–50.
30. Banerjee SM, Williams NR, Davidson TI, El Sheikh S, Tran-Dang M, Davison S, et al. The use of onestep nucleic acid amplification (OSNA) and tumour related factors in the treatment of axillary breast cancer: a predictive model. Eur J Surg Oncol. 2016;42(5):641–9.
31. Yamamoto H, Tomita N, Inomata M, Furuhata T, Miyake Y, Noura S, et al. OSNA-assisted molecular staging in colorectal cancer: a prospective multicenter trial in Japan. Ann Surg Oncol. 2016;23(2):391–6.
32. Waldman SA, Hyslop T, Schulz S, Barkun A, Nielsen K, Haaf J, et al. Association of GUCY2C expression in lymph nodes with time to recurrence and disease-free survival in pN0 colorectal cancer. JAMA. 2009;301(7):745–52.
33. Messerini L, Cianchi F, Cortesini C, Comin CE. Incidence and prognostic significance of occult tumor cells in lymph nodes from patients with stage IIA colorectal carcinoma. Hum Pathol. 2006;37(10):1259–67.
34. Koyanagi K, Bilchik AJ, Saha S, Turner RR, Wiese D, McCarter M, et al. Prognostic relevance of occult nodal micrometastases and circulating tumor cells in colorectal cancer in a prospective multicenter trial. Clin Cancer Res. 2008;14(22):7391–6.
35. Yamamoto H, Murata K, Fukunaga M, Ohnishi T, Noura S, Miyake Y, et al. Micrometastasis volume in lymph nodes determines disease recurrence rate of stage II colorectal cancer: a prospective multicenter trial. Clin Cancer Res. 2016;22(13):3201–8.
36. Andre T, Boni C, Mounedji-Boudiaf L, Navarro M, Tabernero J, Hickish T, et al. Oxaliplatin, fluorouracil, and leucovorin as adjuvant treatment for colon cancer. N Engl J Med. 2004;350(23):2343–51.
37. Andre T, Boni C, Navarro M, Tabernero J, Hickish T, Topham C, et al. Improved overall survival with oxaliplatin, fluorouracil, and leucovorin as adjuvant treatment in stage II or III colon cancer in the MOSAIC trial. J Clin Oncol. 2009;27(19):3109–16.
38. Alix-Panabieres C, Riethdorf S, Pantel K. Circulating tumor cells and bone marrow micrometastasis. Clin Cancer Res. 2008;14(16):5013–21.
39. Wikman H, Vessella R, Pantel K. Cancer micrometastasis and tumour dormancy. APMIS. 2008;116(7–8):754–70.
40. Mimori K, Shinden Y, Eguchi H, Sudo T, Sugimachi K. Biological and molecular aspects of lymph node metastasis in gastro-intestinal cancer. Int J Clin Oncol. 2013;18(5):762–5.
41. Cottingham K. The single-cell scene. Anal Chem. 2004;76(13):235a–8a.
42. Brenner S, Johnson M, Bridgham J, Golda G, Lloyd DH, Johnson D, et al. Gene expression analysis by massively parallel signature sequencing (MPSS) on microbead arrays. Nat Biotechnol. 2000;18(6):630–4.
43. Islam S, Kjallquist U, Moliner A, Zajac P, Fan JB, Lonnerberg P, et al. Characterization of the single-cell transcriptional landscape by highly multiplex RNA-seq. Genome Res. 2011;21(7):1160–7.

44. Horvath A, Pakala SB, Mudvari P, Reddy SD, Ohshiro K, Casimiro S, et al. Novel insights into breast cancer genetic variance through RNA sequencing. Sci Rep. 2013;3:2256.
45. Liang F, Qu H, Lin Q, Yang Y, Ruan X, Zhang B, et al. Molecular biomarkers screened by next-generation RNA sequencing for non-sentinel lymph node status prediction in breast cancer patients with metastatic sentinel lymph nodes. World J Surg Oncol. 2015;13:258.
46. Kaur H, Mao S, Shah S, Gorski DH, Krawetz SA, Sloane BF, et al. Next-generation sequencing: a powerful tool for the discovery of molecular markers in breast ductal carcinoma in situ. Expert Rev Mol Diagn. 2013;13(2):151–65.

Clinical Aspect: Chemo- and/or Radiation Therapy and Micrometastasis

12

Ken Sasaki and Shoji Natsugoe

Abstract

The significance of lymph node micrometastasis (LNM), including isolated tumor cells (ITCs), in gastrointestinal (GI) cancers has long been investigated and discussed. Due to advances in the development of diagnostic tools, the detection rate of LNM is increasing. However, the clinical significance of LNM in GI cancers remains controversial, much less than that for chemo- and/or radiation therapy and LNM. This chapter summarizes the present clinical aspects of chemo- and/or radiation therapy and LNM in GI cancers from a limited number of studies. Neoadjuvant therapy may reduce LNM in patients with esophageal cancer, and LNM has an equal negative impact on prognosis as in node-positive patients. In gastric cancer, chemotherapy has a marked effect on LNM in regional lymph nodes independent of whether the effects of chemotherapy are active against the primary tumor. In patients with colorectal cancer (CRC), neoadjuvant radiotherapy (NART) or neoadjuvant chemoradiotherapy (NACRT) may reduce LNM, and LNM after neoadjuvant therapy had a negative impact on the prognosis of node-negative cases. These findings suggest that neoadjuvant therapy effectively reduces LNM; however, the significance of LNM after neoadjuvant therapy on the prognosis of patients with GI cancer currently remains unclear.

Keywords

Lymph node micrometastasis · Isolated tumor cell · Gastrointestinal cancers Chemotherapy · Radiotherapy · Chemoradiotherapy

K. Sasaki (✉) · S. Natsugoe (✉)
Department of Digestive Surgery, Breast and Thyroid Surgery, Graduate School of Medical and Dental Sciences, Kagoshima University, Kagoshima, Japan
e-mail: k-sasaki@m.kufm.kagoshima-u.ac.jp; natsugoe@m2.kufm.kagoshima-u.ac.jp

S. Natsugoe (ed.), *Lymph Node Metastasis in Gastrointestinal Cancer*,
https://doi.org/10.1007/978-981-10-4699-5_12

12.1 Introduction

Lymph node metastasis is one of the most important prognostic factors in patients with gastrointestinal (GI) cancer including esophageal and gastric cancers as well as colorectal cancer (CRC) [1–8]. However, a pathological node-negative (pN0) state at resection confirmed by conventional histological hematoxylin-eosin (HE) staining does not guarantee long-term survival without recurrence. The existence of lymph node micrometastasis (LNM), including isolated tumor cells (ITCs), which are not detected by conventional HE staining, has been attracting attention as a candidate for recurrence and/or as a prognostic factor. The LNM status of GI cancer patients may be evaluated using immunohistochemistry (IHC) and a reverse transcription polymerase chain reaction (RT-PCR). Due to advances in the development of diagnostic tools, the detection rate of LNM is increasing. The significance of LNM in GI cancers has long been investigated and discussed but currently remains unclear. Perioperative treatments are widely used against various cancers. Neoadjuvant therapy potentially results in the downstaging/downsizing and elimination of LNM, which contributes to improved resectability and curability rates. On the other hand, adjuvant therapy is directed toward micrometastases existing at distant sites and outside of the surgical field and contributes to improvements in the prognosis of patients with GI cancers. However, since it is impossible to investigate the therapeutic effects of adjuvant therapy after surgery for LNM, clinical samples of LN and LNM are examined after neoadjuvant therapy in order to evaluate the influences of chemo- and/or radiation therapy on LNM. Limited information is available on the rates and effects of chemo- and/or radiation therapy in clinical samples of LNM, and the clinical aspects of chemo- and/or radiation therapy and LNM have not yet been evaluated or discussed. This chapter focuses on the clinical significance of LNM after chemo- and/or radiation therapy as well as the influences of chemo- and/or radiation therapy on LNM in carcinomas of the GI tract such as esophageal and gastric cancers as well as CRC.

12.2 Esophageal Cancer

Esophageal cancer is a difficult malignancy to treat, and lymph node metastasis has been identified as one of the most important prognostic factors in patients with esophageal cancer [1–3, 8]. A clinical aspect of LNM [9] and the possibility of the sentinel lymph node concept [10, 11] have been reported; however, the significance of LNM has not yet been elucidated in esophageal cancer. Even if complete tumor resection with lymphadenectomy is performed, the disease is already in an advanced stage beyond the scope of curative therapy by the time of surgery. Multiple randomized trials have established neoadjuvant therapy for the management of esophageal cancer patients based on improved survival rates over those achieved with upfront surgery. Neoadjuvant chemotherapy (NACT) or chemoradiotherapy (NACRT) has been shown to extend postoperative survival, and preoperative therapy followed by esophagectomy has become the standard treatment worldwide for patients with

resectable locally advanced esophageal or esophagogastric junctional carcinoma [12–19]. The potential benefits of neoadjuvant therapy are considered to be the downstaging/downsizing and elimination of LNM, which contribute to improved resectability and curability rates. Few studies have focused on the relationship between NACT and/or NACRT and LNM in esophageal cancer patients, with only six studies being reported to date [20–25]. Table 12.1 summarizes six studies on the relationship between neoadjuvant therapy and LNM in esophageal cancer patients. There were three studies on chemotherapy, two on chemoradiotherapy, and one on chemo- or chemoradiotherapy. The numbers of patients were relatively small, and patients with any disease stage were included. In Eastern countries, squamous cell carcinoma (SCC) was a major histological type, while SCC and adenocarcinoma are both included in Western countries. The CK antibody (AE1/AE3) was commonly used for IHC, except for one study that used CK8/CK18 (CAM 5.2). Single sections were used in two studies and multiple sections in four studies. Estimations of the therapeutic effects on LNM varied according to the authors. Three authors estimated LNM and cytokeratin-positive deposits without nuclei, while another two estimated reductions in LNM, and one author estimated LNM with or without stromal reactions. Cytokeratin-positive particles, named "cytokeratin deposits" (CDs), are frequently observed in lymph nodes by IHC staining for cytokeratin. CDs have been defined as hyalinized denucleated particles and are regarded as the cadavers of carcinoma cells. CDs are round and eosinophilic and do not include a nucleus in serial sections and have been observed more frequently in patients treated with NACT than in those without [25]. Matsuyama et al. [20] evaluated the presence of CD, other than immunohistochemical LNM, in 75 esophageal squamous cell carcinoma (ESCC) patients treated with NACT using cisplatin (CDDP), doxorubicin hydrochloride, and 5-fluorouracil (5-FU) in order to examine the influence of NACT on LNM. The anti-cytokeratin antibody cocktail, AE1/AE3, was used as the primary antibody. They reported that successful NACT converted cancer cells from immunohistochemical LNM to CD and improved the status of ESCC patients from systemic disease to regional disease, and the disappearance of immunohistochemical LNM and emergence of CD suggested the eradication of LNM by NACT in ESCC of the thoracic esophagus. Based on the above findings, they concluded that the clinical benefit of NACT was apparent for immunohistochemical LNM-negative and CD-positive patients. Lee et al. evaluated the histological effects of NACT using 5-FU/CDDP or nedaplatin or NACRT (40 Gy delivered in daily fractions of 2 Gy) on lymph node metastasis in ESCC by performing IHC using the anti-cytokeratin antibody cocktail, AE1/AE3. A total of 3061 lymph nodes were examined from 36 and 26 patients who received NACRT and NACT, respectively, followed by esophagectomy with lymphadenectomy. They also evaluated hyalinized cytokeratin particles (HCP); HCP were defined as cytokeratin deposits without cellular nuclei, similar to CD. Consistent with previous findings for CD, HCP were suggested to reflect a degenerative change in cancer cells in lymph nodes and may predict responses to neoadjuvant therapy [22]. One limitation of these studies is that they did not prove whether cytokeratin-positive particles, CD and HCP, are truly the cadavers of cancer cells. However, this hypothesis is strongly supported by the

Table 12.1 Studies on the relationship between neoadjuvant therapy and LNM in esophageal cancer patients

	Year	Study, ref. no.	No. of patients NAT (surgery alone)	Ave_ rage no. of LNMs	cStage	Histo-logical type	Method	Anti-body	Sections for IHC	Neo-adjuvant therapy	Regimen	Total dose of RT	Difference in no. of patients with LNM Surgery only vs. NAC	Definition of LNM	Estimation of effectiveness against LNM	Influence on LNM	*"Prog-nostic impact of LNM after NAC"
1	2002	Doki et al. [25]	11 (30)	52.9	cT3-4cN0	SCC	IHC	CK (AE1/AE3)	Multiple (5 sections)	CT	CDDP/adria-mycin/5-FU	–	N.S. (CD, significant)	IHM and CD	CD	Effective	Yes
2	2007	Matsuyama et al. [20]	75 (107)	84.8	cT2-3cN1	SCC	IHC	CK (AE1/AE3)	Multiple (5 sections)	CT	CDDP/doxo-rubicin/5-FU	–	Significant	IHM and CD	CD	Effective	Yes
3	2000	Natsugoe et al. [21]	20 (20)	49.5	cT1-4cN0-1cM0-1	SCC	IHC	CK (AE1/AE3)	Single	CT	CDDP/5-FU	–	N.S. (TCM, significant)	MM, tumor cells with a stromal reaction	TCM	Effective	–
4	2014	Lee et al. [22]	–	49.4	cT2-4cNx	SCC	IHC	CK (AE1/AE3)	Single	CT or CRT	5-FU/CDDP or nedaplatin	40 Gy	–	IHM and CD	CD	–	Yes
5	2007	Prenzel et al. [23]	–	24.4	cT2-4cNx	SCC and AC	IHC	CK (AE1/AE3)	Multiple (6 sections)	CRT	CDDP/5-FU	36 Gy	–	pN0 by HE staining	Reduction in LNM	–	–
6	2013	Wang et al. [24]	20 (20)	19.4	cT1-3cN1	AC	IHC	CK8/CK18 (CAM 5.2)	Multiple (4 sections)	CRT	Paclitaxel/carboplatin	41.4–45 Gy	Significant	pN0 by HE staining	Reduction in LNM	Effective	Yes

NAT neoadjuvant therapy, *IHM* immunohistochemical micrometastases, *CD* cytokeratin deposits, *MM* tumor cells with a stromal reaction, *TCM* tumor cells without a stromal reaction

following findings on cytokeratin-positive particles: their anatomic distribution was identical to LNM and pathological node metastases, associated with the pathological grade of the primary tumor, and reciprocally associated with LNM in its incidence and influence on prognosis [20, 22]. Furthermore, Matsuyama et al. proved the biological origin of cytokeratin-positive deposits using IHC, showing that they were positive for the epithelial marker E-cadherin and negative for the macrophage marker CD68 [25]. The presence of cytokeratin-positive deposits in lymph nodes has not been described in other histological types of GI cancers, except for ESCC. These findings suggest that cytokeratin-positive deposits are immunohistochemically specific to ESCC [25].

We evaluated LNM—LNM was defined as tumor cells in lymph nodes with a stromal reaction (granulation tissue or desmoplastic connective tissue) and/or tumor cell micro-involvement (TCM) and tumor cells in lymph nodes without a stromal reaction immunohistochemically using the anti-cytokeratin antibody cocktail, AE1/AE3, in 1052 lymph nodes from 20 ESCC patients treated with NACT using CDDP and 5-FU—and reported that the incidence of LNM and/or TCM in the chemotherapy group was similar to that in the surgical group of patients with ESCC. However, chemotherapy may be effective in patients with TCM alone before cancer cells form clusters with stromal reactions in lymph nodes. Patients with lymph node metastasis including LNM do not benefit from NACT, and LNM, but not TCM, is prognostically equivalent to lymph node metastasis and needs be examined using IHC in order to classify these cases correctly as pathological node-positive (pN1) in ESCC [21]. We also evaluated the usefulness of NACRT for ESCC and reported that fewer metastatic lymph nodes were present in the NACRT group than in the surgery only group [26]. Furthermore, we immunohistochemically evaluated LNM and/or TCM using the anti-cytokeratin antibody cocktail, AE1/AE3, in 663 lymph nodes from 20 ESCC patients treated with NACRT, a total radiation dose of 40 Gy and concurrent intravenous chemotherapy with CDDP and 5-FU. The extent of lymph node metastasis was slightly greater in the surgery group than in the NACRT group. However, the incidence of patients with LNM ± TCM and TCM alone was significantly higher in the surgery group than in the NACRT group. NACT may be effective for patients with TCM alone, whereas NACRT was effective for LNM and TCM. These findings indicate that NACRT is more effective for LNM than NACT in patients with node-positive ESCC [21]. The presence of pathological lymph node metastasis was identified as a prognostic predictor in the surgery alone and NACRT groups. Furthermore, assessments of the simultaneous presence of pathological lymph node metastasis and LNM may facilitate highly accurate predictions of survival in esophageal cancer patients undergoing esophagectomy, regardless of whether they have received NACRT. This finding was consistent with previously reported data from other studies [4]. Prenzel et al. investigated the influence of NACRT on LNM in 52 esophageal cancer patients (21 adenocarcinomas and 31 SCC) who received NACRT by performing IHC using the anti-cytokeratin antibody cocktail, AE1/AE3. Intravenous chemotherapy was performed using CDDP (20 mg/m^2/day, short-term infusion) and 5-FU (1000 mg/m^2/day, over 24 h) on days 1–5. Radiation was delivered in daily fractions of 1.8 Gy to a total dose of 36 Gy. They categorized the extent of

histomorphological regression of the primary tumor into a major (<10%) and minor response (>10% vital residual tumor cells) and evaluated 1186 lymph nodes that were diagnosed as negative for metastases in a routine histopathological analysis. In patients with a major histomorphological response following NACRT, the presence of LNM was significantly less than that in those with a minor response [23]. Wang et al. evaluated the influence of NACRT on LNM in 20 ypN0 esophageal adenocarcinoma (EAC) patients and ypN1 EAC patients who received NACRT followed by surgery by performing IHC for cytokeratin CK8/CK18 (CAM 5.2) and compared the impact of NACRT on LNM with 20 surgery-alone EAC patients. Radiation was delivered in daily fractions of 1.8 Gy to a total dose of 41.4–45 Gy. Concurrent intravenous chemotherapy was performed using paclitaxel (50 mg/m^2) and carboplatin (area under the curve = 2). They concluded that a 30% reduction in LNM was achieved with NACRT from that with surgery alone in ypN0 [24]. Based on the six studies that investigated neoadjuvant therapy and LNM in ESCC and EAC, neoadjuvant therapy appeared to reduce LNM and had an equal negative impact on prognosis to that in node-positive patients with esophageal cancer. If the evaluation of LNM detection and effectiveness of neoadjuvant therapy differ between each institution, the findings of different studies will naturally vary. Regarding prognostic impacts, three out of six studies reported that the effectiveness of neoadjuvant therapy against LNM reflects prognosis. The numbers of patients and nodes examined were not high. All studies included early and advanced carcinoma. Four studies included only SCC, one study examined SCC and adenocarcinoma, and one study only investigated adenocarcinoma. Common criteria are needed in order to accurately evaluate the effectiveness of neoadjuvant therapy for LNM.

12.3 Gastric Cancer

Lymph node metastasis is one of the significant prognostic factors for gastric cancer [5, 27]. Although the prognostic value of LNM remains controversial, its clinical impact is apparently strong in early and advanced gastric cancer [28]. Surgery in combination with adjuvant treatments is the globally accepted standard of care for locally advanced gastric cancer. However, approaches to adjuvant treatment vary among countries. In Asia, the standard adjuvant treatment for stage II or III gastric cancer is postoperative chemotherapy with the oral fluoropyrimidine derivative S-1 for 1 year or capecitabine plus oxaliplatin for 6 months after D2 surgery based on the findings of the ACTS-GC trial or CLASSIC trial [29, 30]. In the USA, surgery followed by NACRT is the standard protocol for T3 or greater and/or positive-node gastric cancer based on findings of the INT-0116 trial [31]. In the UK and some European countries, preoperative and postoperative chemotherapy with epirubicin, CDDP, and 5-FU is used based on evidence from the MAGIC trial [16]. Postoperative adjuvant chemotherapy is directed toward micrometastases that may exist as residual disease after surgery. Chemotherapy in the neoadjuvant setting may also be considered for the downstaging/downsizing and eradication of microscopic disease prior to surgery, which contributes to improved resectability and curability rates [32]. The detection rate of LNM is increasing due to advances in the development

of diagnostic tools, such as IHC and RT-PCR; however, the clinical significance of LNM in gastric cancer is still controversial, much less than that for chemo- and/or radiation therapy and LNM. Very few studies have focused on the relationship between chemotherapy and LNM in gastric cancer, and only three studies on LNM and chemotherapy have been reported to date. Becker et al. [33] evaluated 622 lymph nodes that were resected from ypN0 17 locally advanced gastric adenocarcinoma (GAC) patients who received NACT followed by gastrectomy by performing IHC for cytokeratin (AE1/AE3 and Ber-Ep4) and compared the impact of NACT on TCM in ypN0 62 surgery-alone GAC patients. Six patients (35%) and 25 out of 622 lymph nodes (4.0%) had TCM, whereas 93% of patients and 21.8% of lymph nodes had TCM in patients treated with surgery alone. In their previous study on lymph node micro-involvement in 100 GAC patients after primary surgery, the rates of TCM in lymph nodes were 90% and 97% in cases classified by routine histology as pN0 and pN1, respectively [34]. Furthermore, this study indicated that the degree of the pathological responses of primary tumors to NACT correlated with effects on tumor cells in regional lymph nodes [33]. Yokoyama et al. established an in vivo lymph node metastasis model using the green fluorescent protein (GFP)-transfected gastric cancer cell line, GCIY-EGFP, which metastasizes spontaneously to the inguinal lymph nodes when inoculated subcutaneously into the abdominal wall. They also demonstrated that ITCs in lymph nodes regressed spontaneously through natural killer cell-mediated antitumor activity following the resection of primary subcutaneous tumors, whereas micrometastasis in lymph nodes continued to proliferate and may be effectively eliminated by postoperative chemotherapy using this model [35]. Using the same model, Eguchi et al. evaluated the effects of perioperative chemotherapy against micrometastasis in gastric cancer. After the inoculation of GCIY-EGFP into the lower abdominal wall of nude mice, a preoperative treatment with S-1 and docetaxel or postoperative treatment with S-1 was performed in addition to the resection of primary tumors in order to assess the efficacy of chemotherapy on micrometastases, metastatic foci measuring 0.2–2 mm in diameter and ITCs, and metastatic foci measuring less than 0.2 mm, in the lymph nodes. NACT was effective against micrometastases and ITCs in the lymph nodes, despite chemotherapy not being active against primary tumors [36]. These findings indicated that chemotherapy has a marked effect on LNM in regional lymph nodes independent of whether the effects of chemotherapy are active against the primary tumor.

12.4 CRC

Regional lymph node metastasis is a reliable prognostic factor and is used for clinical decision-making [6, 7]. In Western countries, the standard treatment for patients with locally advanced rectal cancer is 5-FU-based NACRT followed by total mesorectal excision (TME) [37]. On the other hand, NACRT is still not a standard treatment in Japan. The Japanese guidelines for the treatment of CRC recommend upfront surgery followed by adjuvant chemotherapy [38]. In either case, the prognostic value of LNM in patients with node-negative CRC has remained unclear because of a lack of evidence from prospective studies. In a

meta-analysis by Rahbari et al., the relationship between the molecular detection of occult disease in regional lymph nodes and an increased risk of disease recurrence and poor survival in patients with node-negative CRC was reported, and the necessity for prospective studies was emphasized [39]. In another systematic review and meta-analysis, LNM had a worse prognosis than that for patients without occult tumor cells; however, ITC did not have predictive value in patients with stage I/II CRC [40]. Yamamoto et al. recently reported the findings of a prospective multicenter clinical trial in terms of the usefulness of the micrometastasis volume in lymph nodes in 315 patients with node-negative stage II CRC using the molecular detection of CEA mRNA by quantitative RT-PCR in addition to conventional qualitative RT-PCR [41]. However, few studies have focused on the relationship between NACT and/or NACRT and LNM in CRC; only three studies have been reported to date. Table 12.2 summarizes studies on the relationship between neoadjuvant therapy and LNM in CRC patients [42–44]. Kinoshita et al. examined the pathological effects of neoadjuvant radiotherapy (NART) on the intramural spread of tumors and risk factors for local recurrence, including tumor deposits, the budding growth of primary tumors, and LNM by performing IHC using the anti-cytokeratin antibody cocktail, AE1/AE3, for lower rectal cancer. Twenty-five stage-matched patients were enrolled, with 25 patients who received 50 Gy NART and 25 who did not. LNM was significantly smaller in patients who received NART than in those who did not. These findings suggested the beneficial effects of NART for LNM in lower rectal cancer [42]. Perez et al. examined 518 lymph nodes that were resected from 56 distal rectal cancer patients who received NACRT followed by radical surgery by performing IHC using the anti-cytokeratin antibody cocktail, AE1/AE3, and compared the impact of NACRT on LNM. Radiation was delivered in daily fractions of 1.8 Gy to a total dose of 50.4 Gy. Intravenous chemotherapy was performed using 5-FU (20 mg/m^2/day) and folinic acid (1000 mg/m^2/day, over 24 h) for 3 consecutive days on the first and last 3 days of radiation therapy. The detection rate of LNM was markedly low in patients treated with NACRT (7%), even in high-risk patients (T3 and T4 tumors); however, LNM was not associated with decreased overall or disease-free survival [43]. Sprenger et al. prospectively examined 2412 lymph nodes that were resected from 81 rectal adenocarcinoma patients who received NACRT followed by total mesorectal excision. Radiation was delivered in daily fractions of 1.8 Gy to a total dose of 50.4 Gy. Intravenous chemotherapy was performed using either the continuous infusion of 5-FU (1000 mg/m^2 on days 1–5 and 29–33) or a combined regime of 5-FU/oxaliplatin (5-FU, 250 mg/m^2 on days 1–14 and 22–35, and oxaliplatin, 50 mg/m^2 on days 1, 8, 22, and 29). Conventional HE staining was performed to detect lymph nodes metastases and revealed a markedly high incidence of mesorectal LNM (32.8%) after NACRT. They concluded that residual LNM did not impair disease-free survival or cancer-specific survival [44]. Based on the three studies that investigated neoadjuvant therapy and LNM in CRC, NART or NACRT exhibited the ability to reduce LNM. However, LNM after neoadjuvant therapy had a negative impact on the prognosis of patients with node-negative CRC.

Table 12.2 Studies on the relationship between neoadjuvant therapy and LNM in colorectal cancer patients

	Year	Study, ref. no.	No. of patients NAT (surgery alone)	Average no. of LNMs	cStage	Histological type	Method	Antibody	Sections for IHC	Neoadjuvant therapy	Regimen	Total dose of RT	No. of patients with LNM Surgery only vs. NAC (%)	Influence on LNM	Prognostic impact LNM after NAC
1	2004	Kinoshita et al. [42]	47 (94)	–	cT2-3cN0-1	AC	IHC	CK (AE1/AE3)	Single	RT	–	50 Gy	Significant	Effective	–
2	2005	Perez et al. [43]	56 (0)	9.6	ypT3-4N0M0	AC	IHC	CK (AE1/AE3)	Multiple (3 sections)	CRT	5-FU/leucovorin	50.4 Gy	–	Effective	No
3	2013	Sprenger et al. [44]	81 (0)	29.8	cT2-4cN0-1	AC	H.E.	–	Multiple (2 sections)	CRT	5-FU or 5-FU/oxaliplatin	50.4 Gy	–	Unknown	No

NAT neoadjuvant therapy

12.5 Future Perspectives of NACT and/or NACRT and LNM

According to the findings of our previous review, a high incidence of LNM ≥10% was found in patients with pN0 GI cancer [9]. In our study on gastric cancer, LNM already exhibited proliferative activity, even in ITCs [45]. If LNM is present in patients diagnosed with pN0, these patients need to be categorized as pN1. Prospective randomized controlled studies need to be conducted in order to examine the effectiveness of adjuvant therapies for patients with LNM. In conclusion, further studies on the biological behavior of LNM treated with NACT and/or NACRT are required in order to elucidate the efficacy of NACT and/or NACRT for LNM and may lead to a better understanding of LNM and the development of further treatments for patients with GI cancers.

References

1. Natsugoe S, Yoshinaka H, Shimada M, Sakamoto F, Morinaga T, Nakano S, et al. Number of lymph node metastases determined by presurgical ultrasound and endoscopic ultrasound is related to prognosis in patients with esophageal carcinoma. Ann Surg. 2001;234(5):613–8.
2. Okumura H, Uchikado Y, Matsumoto M, Owaki T, Kita Y, Omoto I, et al. Prognostic factors in esophageal squamous cell carcinoma patients treated with neoadjuvant chemoradiation therapy. Int J Clin Oncol. 2013;18(2):329–34.
3. Izbicki JR, Hosch SB, Pichlmeier U, Rehders A, Busch C, Niendorf A, et al. Prognostic value of immunohistochemically identifiable tumor cells in lymph nodes of patients with completely resected esophageal cancer. N Engl J Med. 1997;337(17):1188–94.
4. Kinjo T, Shimoji H, Nagahama M, Karimata H, Yoshimi N, Nishimaki T. Prognostic significance of simultaneous presence of histological and immunohistochemical metastasis to lymph nodes in patients with esophageal cancer. Ann Thorac Cardiovasc Surg. 2014;20(6):951–60.
5. Siewert JR, Bottcher K, Stein HJ, Roder JD. Relevant prognostic factors in gastric cancer: ten-year results of the German Gastric Cancer Study. Ann Surg. 1998;228(4):449–61.
6. Weitz J, Koch M, Debus J, Hohler T, Galle PR, Buchler MW. Colorectal cancer. Lancet. 2005;365(9454):153–65.
7. Nelson H, Petrelli N, Carlin A, Couture J, Fleshman J, Guillem J, et al. Guidelines 2000 for colon and rectal cancer surgery. J Natl Cancer Inst. 2001;93(8):583–96.
8. Akutsu Y, Matsubara H. The significance of lymph node status as a prognostic factor for esophageal cancer. Surg Today. 2011;41(9):1190–5.
9. Natsugoe S, Arigami T, Uenosono Y, Yanagita S, Nakajo A, Matsumoto M, et al. Lymph node micrometastasis in gastrointestinal tract cancer – a clinical aspect. Int J Clin Oncol. 2013;18(5):752–61.
10. Hagihara T, Uenosono Y, Arigami T, Kozono T, Arima H, Yanagita S, et al. Assessment of sentinel node concept in esophageal cancer based on lymph node micrometastasis. Ann Surg Oncol. 2013;20(9):3031–7.
11. Uenosono Y, Arigami T, Yanagita S, Kozono T, Arima H, Hirata M, et al. Sentinel node navigation surgery is acceptable for clinical T1 and N0 esophageal cancer. Ann Surg Oncol. 2011;18(7):2003–9.
12. Shapiro J, van Lanschot JJ, Hulshof MC, van Hagen P, van Berge Henegouwen MI, Wijnhoven BP, et al. Neoadjuvant chemoradiotherapy plus surgery versus surgery alone for oesophageal or junctional cancer (CROSS): long-term results of a randomised controlled trial. Lancet Oncol. 2015;16(9):1090–8.

13. Sjoquist KM, Burmeister BH, Smithers BM, Zalcberg JR, Simes RJ, Barbour A, et al. Survival after neoadjuvant chemotherapy or chemoradiotherapy for resectable oesophageal carcinoma: an updated meta-analysis. Lancet Oncol. 2011;12(7):681–92.
14. Ando N, Kato H, Igaki H, Shinoda M, Ozawa S, Shimizu H, et al. A randomized trial comparing postoperative adjuvant chemotherapy with cisplatin and 5-fluorouracil versus preoperative chemotherapy for localized advanced squamous cell carcinoma of the thoracic esophagus (JCOG9907). Ann Surg Oncol. 2012;19(1):68–74.
15. Urschel JD, Vasan H. A meta-analysis of randomized controlled trials that compared neoadjuvant chemoradiation and surgery to surgery alone for resectable esophageal cancer. Am J Surg. 2003;185(6):538–43.
16. Cunningham D, Allum WH, Stenning SP, Thompson JN, Van de Velde CJ, Nicolson M, et al. Perioperative chemotherapy versus surgery alone for resectable gastroesophageal cancer. N Engl J Med. 2006;355(1):11–20.
17. Stahl M, Stuschke M, Lehmann N, Meyer HJ, Walz MK, Seeber S, et al. Chemoradiation with and without surgery in patients with locally advanced squamous cell carcinoma of the esophagus. J Clin Oncol. 2005;23(10):2310–7.
18. Medical Research Council Oesophageal Cancer Working Group. Surgical resection with or without preoperative chemotherapy in oesophageal cancer: a randomised controlled trial. Lancet. 2002;359(9319):1727–33.
19. Al-Sukhni E, Gabriel E, Attwood K, Kukar M, Nurkin SJ, Hochwald SN. No survival difference with neoadjuvant chemoradiotherapy compared with chemotherapy in resectable esophageal and gastroesophageal junction adenocarcinoma: results from the national cancer data base. J Am Coll Surg. 2016;223(6):784–792.e1.
20. Matsuyama J, Doki Y, Yasuda T, Miyata H, Fujiwara Y, Takiguchi S, et al. The effect of neoadjuvant chemotherapy on lymph node micrometastases in squamous cell carcinomas of the thoracic esophagus. Surgery. 2007;141(5):570–80.
21. Natsugoe S, Matsumoto M, Nakashima S, Okumura H, Miyazono F, Kijima F, et al. Effect of neoadjuvant chemotherapy for lymph node micrometastasis and tumor cell microinvolvement in the patients with esophageal carcinoma. Cancer Lett. 2000;159(2):119–25.
22. Lee T, Tanaka H, Ohira M, Kubo N, Sakurai K, Toyokawa T, et al. Intranodal cytokeratin particles is a predictive marker of efficacy for neoadjuvant therapies in patients with squamous cell carcinoma of the esophagus. Hepato-Gastroenterology. 2014;61(133):1235–40.
23. Prenzel KL, Konig A, Schneider PM, Schnickmann C, Baldus SE, Schroder W, et al. Reduced incidence of nodal micrometastasis after major response to neoadjuvant chemoradiation in locally advanced esophageal cancer. Ann Surg Oncol. 2007;14(2):954–9.
24. Wang D, Smit JK, Zwaan E, Muijs CT, Groen H, Hollema H, et al. Neoadjuvant therapy reduces the incidence of nodal micrometastases in esophageal adenocarcinoma. Am J Surg. 2013;206(5):732–8.
25. Doki Y, Ishikawa O, Mano M, Hiratsuka M, Sasaki Y, Kameyama M, et al. Cytokeratin deposits in lymph nodes show distinct clinical significance from lymph node micrometastasis in human esophageal cancers. J Surg Res. 2002;107(1):75–81.
26. Natsugoe S, Okumura H, Matsumoto M, Uchikado Y, Setoyama T, Yokomakura N, et al. Randomized controlled study on preoperative chemoradiotherapy followed by surgery versus surgery alone for esophageal squamous cell cancer in a single institution. Dis Esophagus. 2006;19(6):468–72.
27. Nitti D, Marchet A, Olivieri M, Ambrosi A, Mencarelli R, Belluco C, et al. Ratio between metastatic and examined lymph nodes is an independent prognostic factor after D2 resection for gastric cancer: analysis of a large European monoinstitutional experience. Ann Surg Oncol. 2003;10(9):1077–85.
28. Lee CM, Park SS, Kim JH. Current status and scope of lymph node micrometastasis in gastric cancer. J Gastric Cancer. 2015;15(1):1–9.
29. Sasako M, Sakuramoto S, Katai H, Kinoshita T, Furukawa H, Yamaguchi T, et al. Five-year outcomes of a randomized phase III trial comparing adjuvant chemotherapy with S-1 versus surgery alone in stage II or III gastric cancer. J Clin Oncol. 2011;29(33):4387–93.

30. Bang YJ, Kim YW, Yang HK, Chung HC, Park YK, Lee KH, et al. Adjuvant capecitabine and oxaliplatin for gastric cancer after D2 gastrectomy (CLASSIC): a phase 3 open-label, randomised controlled trial. Lancet. 2012;379(9813):315–21.
31. Smalley SR, Benedetti JK, Haller DG, Hundahl SA, Estes NC, Ajani JA, et al. Updated analysis of SWOG-directed intergroup study 0116: a phase III trial of adjuvant radiochemotherapy versus observation after curative gastric cancer resection. J Clin Oncol. 2012;30(19):2327–33.
32. De Vita F, Giuliani F, Galizia G, Belli C, Aurilio G, Santabarbara G, et al. Neo-adjuvant and adjuvant chemotherapy of gastric cancer. Ann Oncol. 2007;18(Suppl 6):vi120–3.
33. Becker K, Fumagalli U, Mueller JD, Fink U, Siewert JR, Hofler H. Neoadjuvant chemotherapy for patients with locally advanced gastric carcinoma: effect on tumor cell microinvolvement of regional lymph nodes. Cancer. 1999;85(7):1484–9.
34. Siewert JR, Kestlmeier R, Busch R, Bottcher K, Roder JD, Muller J, et al. Benefits of D2 lymph node dissection for patients with gastric cancer and pN0 and pN1 lymph node metastases. Br J Surg. 1996;83(8):1144–7.
35. Yokoyama H, Nakanishi H, Kodera Y, Ikehara Y, Ohashi N, Ito Y, et al. Biological significance of isolated tumor cells and micrometastasis in lymph nodes evaluated using a green fluorescent protein-tagged human gastric cancer cell line. Clin Cancer Res. 2006;12(2):361–8.
36. Eguchi T, Kodera Y, Nakanishi H, Yokoyama H, Ohashi N, Ito Y, et al. The effect of chemotherapy against micrometastases and isolated tumor cells in lymph nodes: an in vivo study. In Vivo. 2008;22(6):707–12.
37. van Gijn W, Marijnen CA, Nagtegaal ID, Kranenbarg EM, Putter H, Wiggers T, et al. Preoperative radiotherapy combined with total mesorectal excision for resectable rectal cancer: 12-year follow-up of the multicentre, randomised controlled TME trial. Lancet Oncol. 2011;12(6):575–82.
38. Hida J, Okuno K, Tokoro T. Distal dissection in total mesorectal excision, and preoperative chemoradiotherapy and lateral lymph node dissection for rectal cancer. Surg Today. 2014;44(12):2227–42.
39. Rahbari NN, Bork U, Motschall E, Thorlund K, Buchler MW, Koch M, et al. Molecular detection of tumor cells in regional lymph nodes is associated with disease recurrence and poor survival in node-negative colorectal cancer: a systematic review and meta-analysis. J Clin Oncol. 2012;30(1):60–70.
40. Sloothaak DA, Sahami S, van der Zaag-Loonen HJ, van der Zaag ES, Tanis PJ, Bemelman WA, et al. The prognostic value of micrometastases and isolated tumour cells in histologically negative lymph nodes of patients with colorectal cancer: a systematic review and meta-analysis. Eur J Surg Oncol. 2014;40(3):263–9.
41. Yamamoto H, Murata K, Fukunaga M, Ohnishi T, Noura S, Miyake Y, et al. Micrometastasis volume in lymph nodes determines disease recurrence rate of stage II colorectal cancer: a prospective multicenter trial. Clin Cancer Res. 2016;22(13):3201–8.
42. Kinoshita H, Watanabe T, Yanagisawa A, Nagawa H, Kato Y, Muto T. Pathological changes of advanced lower-rectal cancer by preoperative radiotherapy. Hepato-Gastroenterology. 2004;51(59):1362–6.
43. Perez RO, Habr-Gama A, Nishida Arazawa ST, Rawet V, Coelho Siqueira SA, Kiss DR, et al. Lymph node micrometastasis in stage II distal rectal cancer following neoadjuvant chemoradiation therapy. Int J Color Dis. 2005;20(5):434–9.
44. Sprenger T, Rothe H, Becker H, Beissbarth T, Homayounfar K, Gauss K, et al. Lymph node metastases in rectal cancer after preoperative radiochemotherapy: impact of intramesorectal distribution and residual micrometastatic involvement. Am J Surg Pathol. 2013;37(8):1283–9.
45. Yanagita S, Natsugoe S, Uenosono Y, Kozono T, Ehi K, Arigami T, et al. Sentinel node micrometastases have high proliferative potential in gastric cancer. J Surg Res. 2008;145(2):238–43.

Esophageal Cancer

13

Yoshiaki Kajiyama, Natsumi Tomita,
and Takashi Hashimoto

Abstract

Lymph node metastasis has a great significance in the diagnosis and the treatment of esophageal cancer. Esophageal cancer shows more virulent characteristics comparing to gastric or colorectal cancer, and the lymph node dissection during esophageal cancer surgery has more important meaning than that of other gastrointestinal cancer surgeries. The frequency of lymph node metastasis in esophageal cancer is higher than any other gastrointestinal malignancies, and when the depth of tumor invasion is at the submucosal layer, the frequency of lymph node metastasis reaches up to 50%. The distribution of lymph node metastasis is also curious in esophageal cancer. The most frequent site of the metastasis is "along the recurrent laryngeal nerve," and the second most frequent site is the upper lesser curvature of the stomach; these two sites are far from the primary cancer. The size of the metastasis in the lymph nodes was small; 63% of the metastasis was less than 5 mm in diameter. The completely correct preoperative diagnosis for lymph node metastasis was achieved in only 62.7% of the cases. We usually perform a three-field lymph node dissection esophagectomy. From survival analysis, a lymph node dissection achieved its significance when the pathological number of lymph node metastasis was less than five. However, when the number of lymph node metastasis exceeded five, the procedure of lymph node metastasis would begin to lose its meaning. Then, we may say that the number of lymph node metastasis is a "predictor" AND a "governor."

Y. Kajiyama (✉) · N. Tomita · T. Hashimoto
Department of Esophageal and Gastroenterological Surgery, Juntendo University, Tokyo, Japan
e-mail: kaji@juntendo.ac.jp

S. Natsugoe (ed.), *Lymph Node Metastasis in Gastrointestinal Cancer*,
https://doi.org/10.1007/978-981-10-4699-5_13

Keywords
Depth of tumor invasion · Frequency of lymph node metastasis · Distribution of lymph node metastasis · Neck lymph node metastasis · Preoperative diagnosis of lymph node metastasis · Survival benefit of lymph node dissection

Lymph node metastasis has a great significance in the diagnosis and the treatment of esophageal cancer. Esophageal cancer shows more virulent characteristics comparing to gastric or colorectal cancer, and the lymph node dissection during esophageal cancer surgery has more important meaning than that of other gastrointestinal cancer surgeries. In this chapter, we describe the reality and clinical significance of lymph node metastasis in esophageal squamous cell carcinoma.

13.1 Frequency

13.1.1 Frequency of Lymph Node Metastasis in Esophageal Cancer

The frequency of lymph node metastasis in esophageal cancer is higher than that of other gastrointestinal cancers. In gastrointestinal cancers, it is well known that the frequency of lymph node metastasis depends on the depth of tumor invasion. As the tumor invades deeper, the frequency of lymph node metastasis rises. Here we compare the metastatic rate of lymph node in the same depth of tumor invasion between the esophagus and stomach in Fig. 13.1. When the tumor invaded up to the submucosal layer, the rate of lymph node metastasis was almost 50% in esophageal cancer and around 20% in gastric cancer. When the tumor invaded the proper muscle layer, the rate of lymph node metastasis was almost 70% in esophageal cancer and around

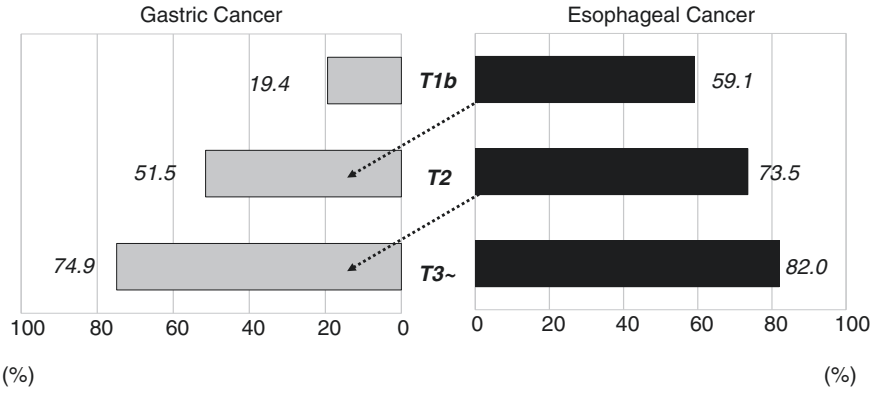

Fig. 13.1 Frequency of lymph node metastasis according to the tumor depth between esophageal and gastric cancer

Site	Mean No. of Dissect	Mean No. of Met.	Mean Positive Rate
Neck	43	0.8	*27.4*
Chest	38	1.8	*55.6*
Abd.	33	1.3	*41.0*
Total	*114*	*3.9*	*69.2*

Fig. 13.2 Our results of three-field lymph node dissection surgery. Mean number of dissected nodes, metastatic nodes, and mean positive rate of metastasis

50% in gastric cancer. From Fig. 13.1, we can realize that the rate of lymph node metastasis in esophageal cancer corresponded to that of gastric cancer with deeper tumor invasion. For example, the frequency of lymph node metastasis in submucosal esophageal cancer was around 50%, which was almost the same rate of gastric cancer with T2 tumor invasion. And the frequency of lymph node metastasis in T2 esophageal cancer was around 70%, which was almost the same rate of gastric cancer with T3 and deeper tumor invasion.

Figure 13.2 shows our results of 1470 cases with three-field (neck, mediastinal, and abdominal) lymph node dissection surgery. The mean number of the harvested lymph node was 114: 43 in the neck, 38 in the mediastinum, and 33 in the abdomen. The mean number of the metastatic lymph nodes was 3.9: 0.8 in the neck, 1.8 in the mediastinum, and 1.3 in the abdomen. Among the 1470 cases, did 69.2% of the patients have any lymph node metastasis? The positive rate of lymph node metastasis was 27.4% in the neck, 55.6% in the mediastinum, and 41.0% in the abdomen. In the thoracic esophageal cancer, we experience the lymph node metastasis from a neck to an abdominal region.

13.1.2 The Frequency of Lymph Node Metastasis in Superficial Esophageal Cancer

Superficial cancer is defined when the depth of tumor invasion is at the mucosal or submucosal layer. Mucosal esophageal cancer is expressed as “T1a” and submucosal esophageal cancer is expressed as “T1b” [1]. According to the “Japanese Classification of Esophageal Cancer” by Japan Esophageal Society [1], mucosal cancer is classified into three categories. These were M1, M2, and M3 mucosal cancers. The M1 cancer (T1a-EP) is carcinoma in situ (Tis). In the M2 cancer (T1a-LPM), a tumor invades lamina propria mucosae (LPM). In the M3 cancer (T1a-MM), a tumor invades muscularis mucosae (MM). In the M1 and M2 cancer, we have experienced no lymph node metastasis. However, when the tumor invades muscularis mucosae (MM), around 10% of the cases show lymph node metastasis. Then an endoscopic resection, such as endoscopic mucosal resection (EMR) or endoscopic submucosal dissection (ESD), is indicated for the M1 or M2 mucosal cancer. When the depth of tumor invasion proved to be M3 and deeper from pathologic examination after endoscopic resection, additional treatment such as chemoradiotherapy or surgery will be needed.

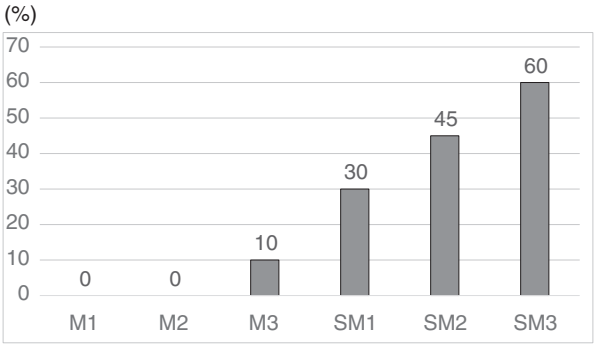

Fig. 13.3 Incidence rate of lymph node metastasis according to the subclassified superficial esophageal cancer

And "Japanese Classification of Esophageal Cancer" also classified submucosal cancer into three categories [1]. Those are T1b-SM1, T1b-SM2, and T1b-SM3. The definitions are as follows: T1b-SM1, tumor invades the upper third of the submucosal layer; T1b-SM2, tumor invades the middle third of the submucosal layer; and T1b-SM3, tumor invades the lower third of the submucosal layer. In the submucosal esophageal cancer, the frequency of lymph node metastasis was around 50%, and the detailed frequency of lymph node metastasis in SM1, SM2, and SM3 cancer was around 30%, 45%, and 60%, respectively. The incidence rate of lymph node metastasis according to the subclassified superficial esophageal cancer is summarized in Fig. 13.3.

From the standpoint of frequency of lymph node metastasis, we can conclude that surgical treatment should be considered when the depth of tumor invasion reaches the submucosal layer. As compared to gastric or colorectal cancer, submucosal esophageal cancer should be recognized as "almost advanced cancer" from high incidence rate of lymph node metastasis. In fact, from the "Japanese Classification of Esophageal Cancer," the definition of early esophageal cancer is limited only to "mucosal cancer" [1]. However, in gastric or colorectal cancer, early cancer is defined as mucosal or submucosal cancer. Esophageal cancer bears more malignant characteristics than gastric or colorectal cancer.

13.2 The Distribution

13.2.1 The Distribution of Lymph Node Metastasis in Esophageal Cancer

Figure 13.4 shows the rate of lymph node metastasis in three fields (neck, mediastinum, and abdomen) according to the tumor location (upper thoracic, middle thoracic, and lower thoracic). When the tumor is located in upper thoracic, more than 30% of the cases showed lymph node metastasis in the neck and the mediastinum. However, in 17% of the cases, we experienced lymph node metastasis in the abdomen. When the tumor was in the lower thoracic region, we experienced lymph node metastasis in the mediastinum in almost 50% of the cases and, in the abdomen, in

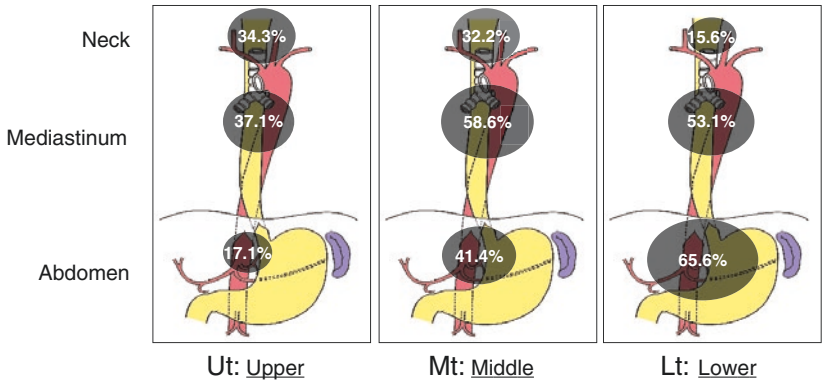

Fig. 13.4 Rate of lymph node metastasis in three fields (neck, mediastinum, and abdomen) according to tumor location

65% of the cases. However, neck lymph node metastasis was also observed in up to 15% of the cases. When the tumor location was in the middle thoracic, we experienced lymph node metastasis in the neck in 32% of the cases, in the mediastinum in 59% of the cases, and in the abdomen in 41% of the cases. From the incidence rate of lymph node metastasis, we need an abdominal lymph node dissection even when the tumor was in the upper thoracic, and we need a neck lymph node dissection when the tumor was in the lower thoracic region. Certainly, three-field lymph node dissection is indicated in the middle thoracic esophageal cancer. Then three-field lymph node dissection surgeries will be indicated for thoracic esophageal cancer irrespective of the tumor location.

In addition to the high incidence rate of lymph node metastasis, the distribution of lymph node metastasis in esophageal cancer is quite different from other gastrointestinal cancers. Generally, when the primary cancer metastasizes to lymph nodes, metastasis will usually occur at the near site of lymphatic drainage from the primary cancer. The distance between primary cancer and the first metastatic lymph node is usually short. However, in esophageal cancer, this regulation will never be adopted. Figure 13.5 shows the most and the second most frequent sites of lymph node metastases in thoracic esophageal cancer from the pathologic examinations of our 1470 cases with the three-field (neck, mediastinal, and abdominal) lymph node dissection surgery. The most frequent site of lymph node metastasis was "along the recurrent laryngeal nerve." In this region 34.4% of the cases showed lymph node metastasis; this corresponded to one-third of the examined patients. The second most frequent site of lymph node metastasis was around the upper lesser curvature of the stomach. In this area 24.6% of the cases showed lymph node metastasis; this corresponds to one-fourth of the examined patients. These two regions are very important from the point of lymph node dissection. The lymph node dissection around the stomach is a relatively simple and easy procedure for the esophageal surgeons. However, the lymph node dissection along the recurrent laryngeal nerve is a difficult procedure and will sometimes lead to the incidence of postoperative

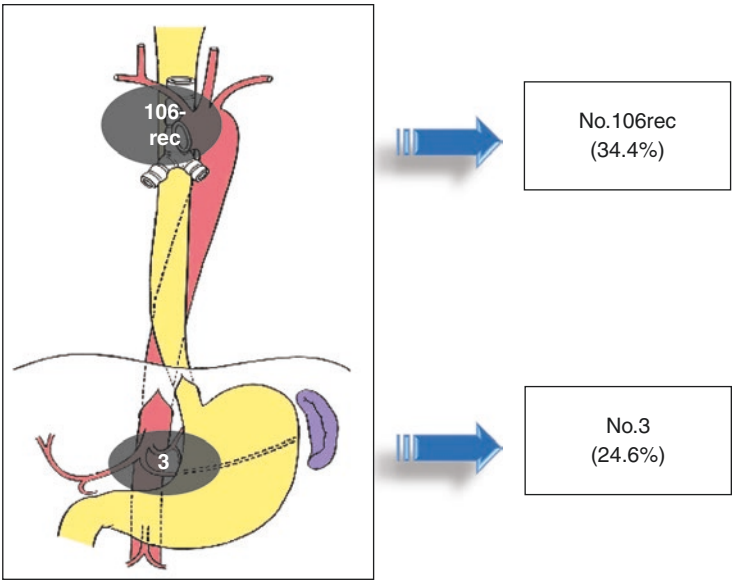

Fig. 13.5 The most and the second most frequent site of lymph node metastasis. (No.106rec, along the recurrent laryngeal nerve; No.3, along the lesser curvature of the upper stomach, from the Japanese classification of esophageal cancer)

recurrent laryngeal nerve palsy complication, especially in the left side. The lymph node dissection is the most important procedure in esophageal cancer surgery from the point of high incidence rate of lymph node metastasis and the difficulty of the procedure.

13.2.2 The Distribution of Lymph Node Metastasis in Superficial Esophageal Cancer

Was the tendency of distant distribution of lymph node metastasis observed in only advanced esophageal cancer or not? To verify the characteristics of the distribution of lymph node metastasis in superficial esophageal cancer, we examined 66 cases with the submucosal esophageal cancer. Figure 13.6a showed the rate of lymph node metastasis to the three fields in the submucosal esophageal cancer from the pathologic examination. Even in the submucosal esophageal cancer, lymph node metastasis was observed in the neck (16.7%), mediastinum (37.9%), and abdomen (25.8%) in a relatively high incidence rate. And the distribution of lymph node metastasis was not confined to the near area from the primary esophageal cancer. Figure 13.6b showed the detailed metastatic sites of lymph node metastasis in the submucosal esophageal cancer. Interestingly the most frequent site of lymph node metastasis was also "along the recurrent laryngeal nerve," and the second most frequent site of metastasis was "the upper lesser curvature of the stomach." Even in the

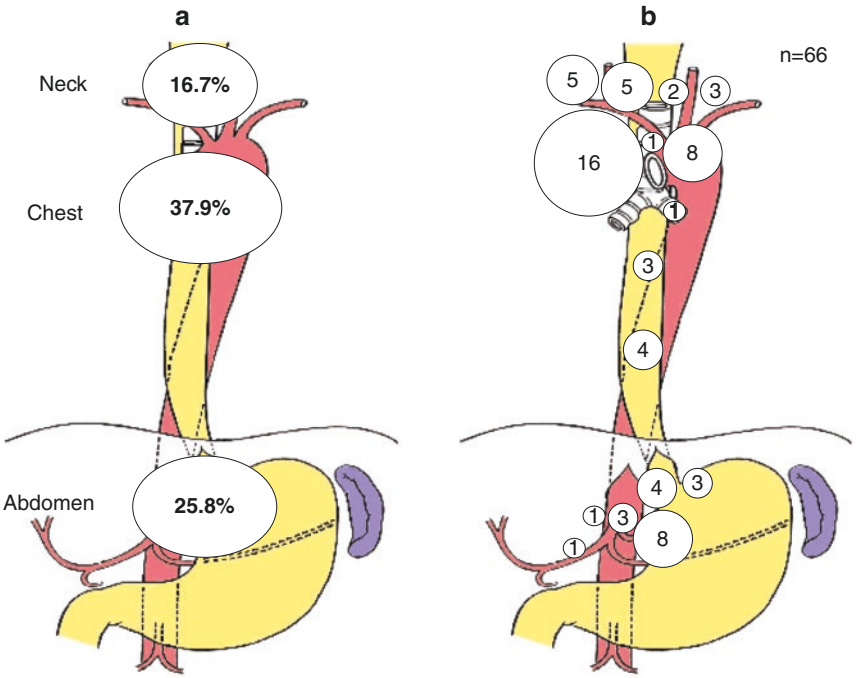

Fig. 13.6 (**a**) Rate of lymph node metastasis to three fields in submucosal esophageal cancer. (**b**) Detailed metastatic sites of lymph node metastasis in submucosal esophageal cancer

submucosal esophageal cancer, the characteristics of the frequent sites of lymph node metastasis were quite the same as the whole examined cases including advanced cases, which were already mentioned above. Again, the important sites of lymph node dissection were "along the recurrent laryngeal nerve" and "the upper lesser curvature of the stomach," irrespective of the depth of tumor invasion in esophageal cancer.

13.2.3 The Distribution of Lymph Node Metastasis in Esophageal Cancer with Only One Lymph Node Metastasis

Where is the first site of lymph node metastasis in esophageal cancer? Among the 16 cases with only one lymph node metastasis from postoperative pathologic examination, we retrospectively analyzed the first site of lymph node metastasis. From Fig. 13.7 the most frequent site of the first lymph node metastasis was again "along the recurrent laryngeal nerve," and the second most frequent site of the first lymph node metastasis was "along the upper lesser curvature of the stomach."

These two important sites, "along the recurrent laryngeal nerve" and "along the upper lesser curvature of the stomach," were frequent and early metastatic sites in esophageal cancer, which should be completely dissected during the operation.

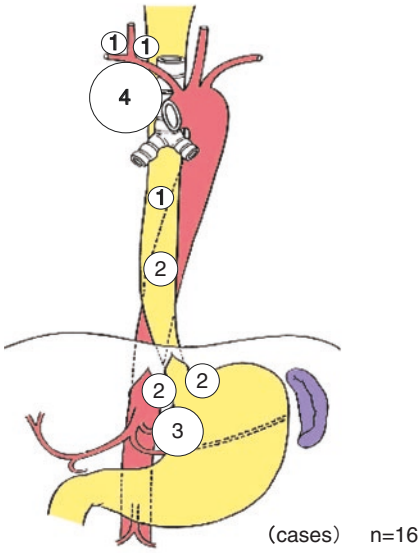

Fig. 13.7 Distribution of lymph node metastasis with only one lymph node metastasis

13.2.4 The Distribution of Lymph Node Metastasis in the Neck

Until 2014, we performed three-field (neck, mediastinal, and abdominal) lymph node dissection surgeries in 1470 cases with the thoracic esophageal cancer. From the pathologic examination of the dissected neck lymph nodes of these cases, the distribution of neck lymph node metastases was shown in Fig. 13.8. We subdivided the neck areas into nine compartments in both sides. For the thoracic esophageal cancer, we usually dissect five compartments (Fig. dotted areas; those are compartment "1," "2," "3," "5," and "6") in both sides. Compartments "4" and "7" are only dissected when the laryngectomy is performed, and compartments "8" and "9" are usually dissected for the pharyngeal or laryngeal cancer surgery. From Fig. 13.8, the most frequent site for lymph node metastasis in the thoracic esophageal cancer was "along the recurrent laryngeal nerve in the neck" (compartment "1" in Fig. 13.8), and the metastasis was observed in almost 17% of the cases. The second most frequent site for metastasis was the "medial side of the supraclavicular area" (compartment "2" in Fig. 13.8), and metastasis occurred in around 14% of the cases. Generally, the middle compartments and lateral compartments in Fig. 13.8 were quite less frequent metastatic areas than the most and the second most frequent metastatic areas "along the recurrent laryngeal nerve in the neck" (compartment "1" in Fig. 13.8) and "medial side of the supraclavicular area" (compartment "2" in Fig. 13.8). We can conclude that the important areas for the neck lymph node dissection are "along the recurrent laryngeal nerve in the neck" and "medial side of the supraclavicular area." In other compartments, lymph node metastasis usually occurs in pharyngeal or laryngeal cancer cases, and the frequency of lymph node metastasis was quite rare in the thoracic esophageal cancer.

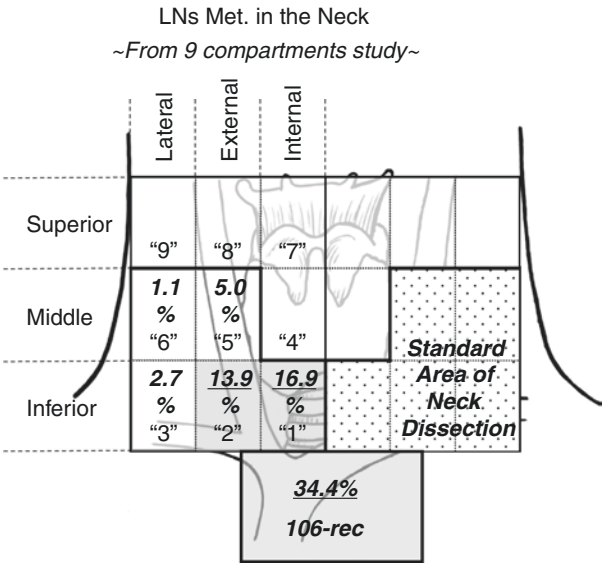

Fig. 13.8 Distribution of neck lymph node metastasis after subclassification of neck field

13.3 The Preoperative Diagnostic Rate for Lymph Node Metastasis

In esophageal cancer, it is sometimes quite difficult to diagnose lymph node metastases accurately prior to an operation as compared to other gastrointestinal malignancies. From our operative cases with clinically diagnosed as stage II/III, we compared diagnostic accuracy for lymph node metastasis between preoperative clinical diagnosis and postoperative pathologic results. The results were shown in Fig. 13.9. The preoperative diagnostic methods for lymph node metastasis were CT scan, neck and abdominal ultrasonography, and endoscopic ultrasonography for all cases. In those who were diagnosed "no lymph node metastasis" preoperatively, up to 62.5% of the cases proved to have more than one lymph node metastasis by postoperative pathologic examination. 62.5% of the cases were "false negative" for lymph node metastasis. In those who were diagnosed "positive for lymph node metastasis" preoperatively, 32.2% of the cases proved to have no lymph node metastasis by postoperative pathologic examination. These 32.2% of the cases were "false positive" for lymph node metastasis. And overall correct diagnostic rate for lymph node metastasis was accomplished in only 62.7% of the cases. From the standpoint of clinical practice, relatively high false-negative rate was a serious problem. Almost two-thirds of the cases, who had been diagnosed as "no lymph node metastasis"

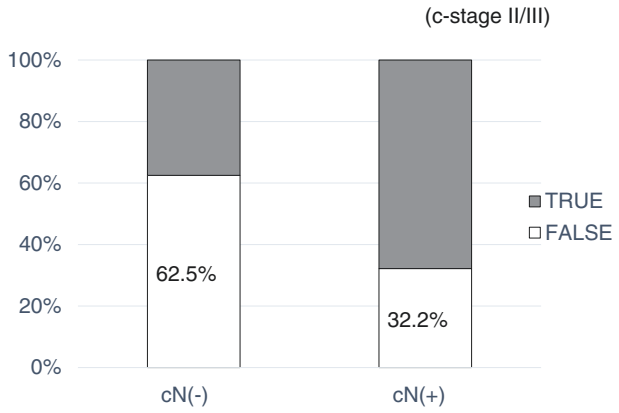

Fig. 13.9 Comparison between preoperative clinical diagnosis and postoperative pathologic diagnosis for lymph node metastasis

preoperatively, proved to have any lymph node metastasis postoperatively. We should not trust preoperative diagnosis for "no lymph node metastasis" with too much confidence. Even during the surgery, it is quite difficult to diagnose lymph node metastasis precisely by surgeon's eyes and hands. We must always realize the possibility and the potential of lymph node metastasis in the esophageal cancer operation.

13.4 The Size of Lymph Node Metastasis in Esophageal Cancer

Why was the correct preoperative diagnosis for lymph node metastasis in esophageal cancer so difficult? In 1999, we operated 92 cases of esophageal cancer and dissected 9254 lymph nodes in total [2]. Out of these nodes, 320 lymph nodes proved to be positive for metastasis by postoperative pathologic examination. We measured the actual size of the metastasis in these 320 metastatic lymph nodes under the microscope. The results are shown in Fig. 13.10. The most frequent size of the metastasis in lymph nodes was 2–3 mm in diameter. Surprisingly, 63% of the lymph nodes contained small metastases with under 5 mm in diameter. In only 13% of the lymph nodes, the size of the metastases was over 10 mm in diameter. Usually radiologists diagnose lymph node metastasis from its size when the size of the swollen lymph node is over 10 mm in diameter. However, we must recognize that small lymph node metastasis is very common in esophageal cancer, and sometimes it is very difficult to diagnose lymph node metastasis precisely prior to an operation. For this reason, quality control in lymph node dissection during the esophageal cancer surgery becomes very important, and esophageal surgeons must not leave lymph nodes behind even if the sizes of the lymph nodes are small. High quality in lymph node dissection will lead to a high survival rate. Figure 13.11 is an example of a small metastatic lymph node with 3 mm in diameter, which contained partly small

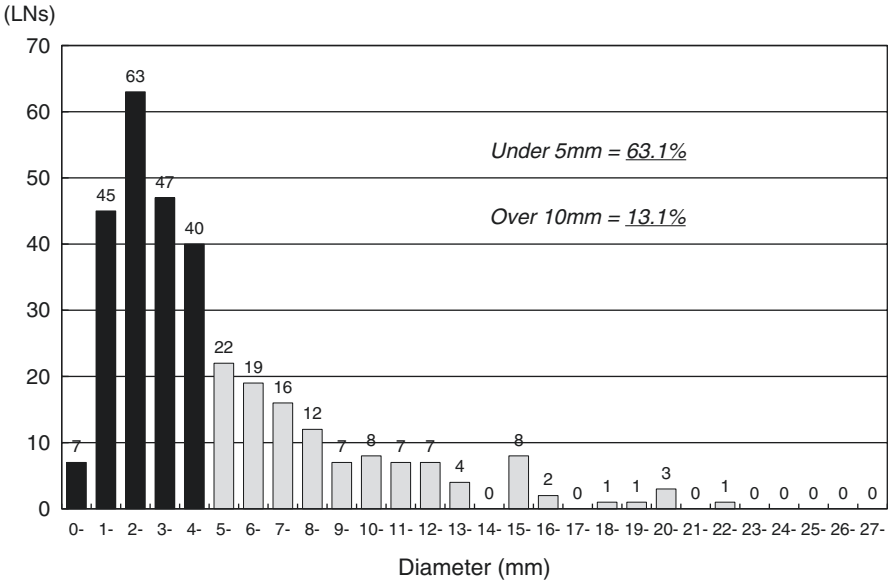

Fig. 13.10 Size (diameter) distribution of the metastasis in the lymph nodes

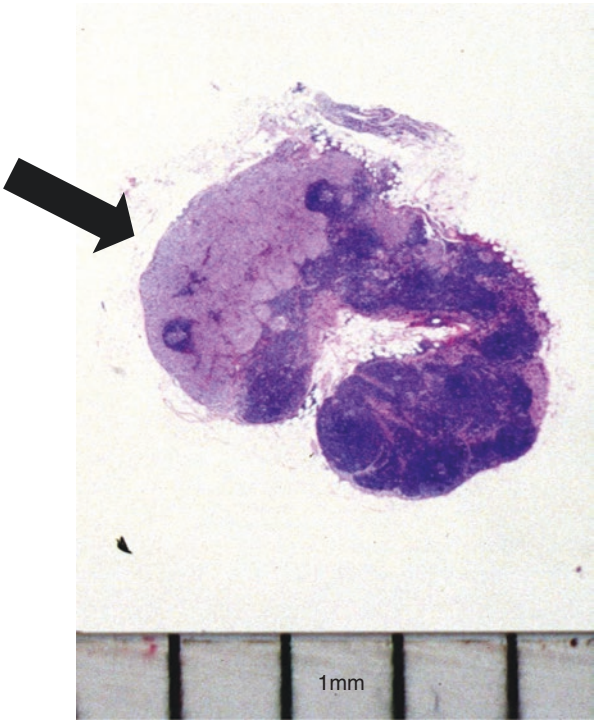

Fig. 13.11 An example of a small lymph node metastasis

metastasis (arrow) with 2 mm in diameter in the left side of the figure. Small lymph nodes with small metastases are common in esophageal cancer.

13.5 The Clinical and Biological Significance of the Number of Lymph Node Metastasis in Esophageal Cancer

The number of lymph node metastasis is widely recognized as one of the powerful prognostic factors in gastrointestinal malignancies. Esophageal cancer bears virulent characteristics, and here we analyze the unique meaning of the number of lymph node metastasis in esophageal cancer from the clinical and biological point of view.

13.5.1 The Prognostic Factors for Postoperative Esophageal Cancer Patients from Multivariate Analysis

We analyzed the prognostic factors for the 1470 patients who received esophagectomy with three-field lymph node dissection surgery in our department. The method of multivariate analysis was Cox regression analysis. The selected covariates for significant prognostic factors for overall survival were "age," "the number of lymph node metastasis," and "the presence of intramural metastasis" (Fig. 13.12). In a large-scale prognostic analysis, such as more than 1000 cases as ours, "age" is generally selected for significant prognosticator. Another most powerful prognostic factor from our analysis was "the number of lymph node metastasis" ($p = 0.0001$) with the relative risk of 1.05. We can conclude that the most significant prognostic factor for esophageal cancer patients following esophagectomy was "the number of lymph node metastasis."

13.5.2 Is "the Number of Lymph Node Metastasis" a "Predictor" or a "Governor"?

It has long been discussed whether "the number of lymph node metastasis" is a "governor" or a mere "predictor" for survival benefit. This proposition can be translated that "whether lymph node dissection in esophageal cancer surgery prolong the patient's survival or not." After we dissect around 1000 lymph nodes during

Fig. 13.12 Significant prognostic factors following esophagectomy with three-field lymph node dissection from multivariate regression study

~ Cox Regression Analysis ~

Covariates	p-value	Relative Risk
Age	0.0001	1.05
No. of LNs Met.	0.0001	1.05
Intramural Met.	0.018	2.03

esophageal cancer surgery, can we prolong the patient's survival or only predict survival rate from the number of metastatic lymph nodes without survival benefit?

From the above multivariate prognostic survival analysis with Cox regression for patients with esophageal cancer who received three-field lymph node dissection surgery, "the number of metastatic lymph nodes" was still selected for most significant prognostic factor. What does this mean? If we suppose the number of lymph node metastasis is a complete "governor," the survival of the patients should be benefited by the surgical lymph node dissection, and the survival rate of the patients between no lymph node metastasis and with metastases would be the same. Then the number of lymph node metastasis would not be selected for a significant prognostic factor theoretically. However, the number of lymph node metastasis after three-field lymph node dissection surgery was still selected for significant prognosticator. This means some limitations of lymph node dissection in esophageal cancer surgery for survival benefit and means that the number of lymph node metastasis is not a complete governor.

The next question is whether "the number of lymph node metastasis" is only a predictor or not. If we supposed that "the number of lymph node metastasis" is only a predictor, the survival benefit following lymph node dissection surgery would be denied.

We compared the mean survival time (MST) in patients with esophageal cancer who received three-field lymph node dissection surgery according to the number of lymph node metastasis from postoperative histopathological examination. The results of MST were shown in Fig. 13.13 (MST was expressed in months). When the patients bared no lymph node metastasis, MST was 76.8 months. And when the

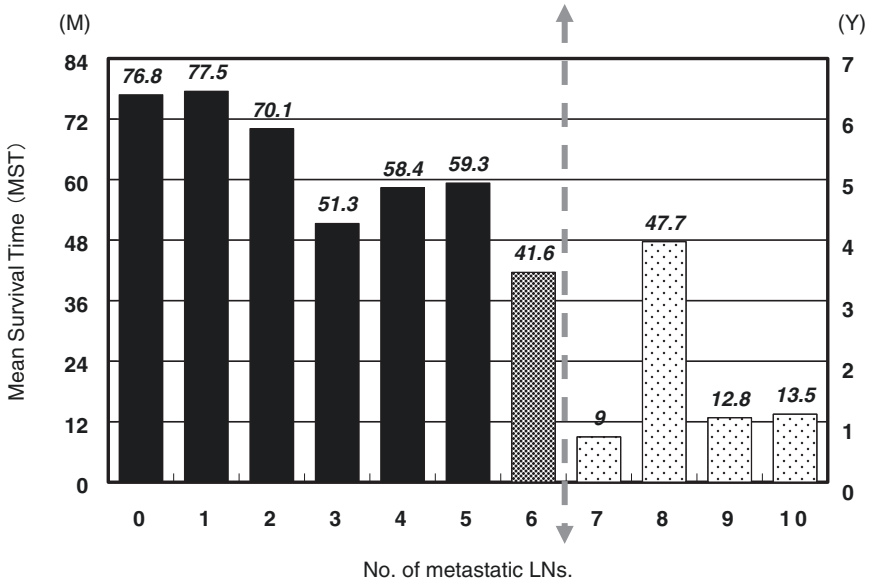

Fig. 13.13 Mean survival time following esophagectomy with three-field lymph node dissection according to the number of pathologic lymph node metastasis

number of lymph node metastasis was one, two, three, four, and five, the MST was 77.5, 70.1, 51.3, 58.4 and 59.3 months, respectively, and the MST reached almost up to 5 years (60 months). We can conclude that when the pathological number of lymph node metastasis was five or less, lymph node dissection had certain significance. However, the number of lymph node metastasis exceeded five, the MST declined keenly from 40 to 10 months (Fig. 13.13), and lymph node dissection procedure may lose its importance.

We can hypothesize that lymph node dissection procedure may be effective and meaningful when the pathological number of lymph node metastasis is five or less. Under this condition, "the number of lymph node metastasis" may be a "governor." However, when the number of lymph node metastasis surpasses five, "the number of lymph node metastasis" may become an only "predictor."

To confirm the above hypothesis, we investigated the overall survival rate in patients with c-stage II/III who received three-field lymph node dissection esophagectomy among three groups. Three groups were classified from the number of pathological lymph node metastasis: Group1, no pathological lymph node metastasis; Group2, the pathological number of lymph node metastasis was one to five; and Group3, the pathological lymph node metastasis was more than five.

The cumulative survival curve following esophagectomy was expressed in Fig. 13.14. When no pathological lymph node metastasis was observed, overall 5-year survival rate was 67.1%. When the number of lymph node metastasis was one to five, the 5-year survival rate was 60.5%, and there was no statistical difference in survival rate between Group 1 and Group 2 ($p = 0.31$). However, when the number of lymph node metastasis surpassed, the 5-year survival rate decreased to 24.8%. From the cumulative survival analysis, the "number of lymph node metastasis" was thought to be a "governor" when the number of lymph node metastasis was less than five and was thought to be an only "predictor," when the number of lymph node metastasis was more than five.

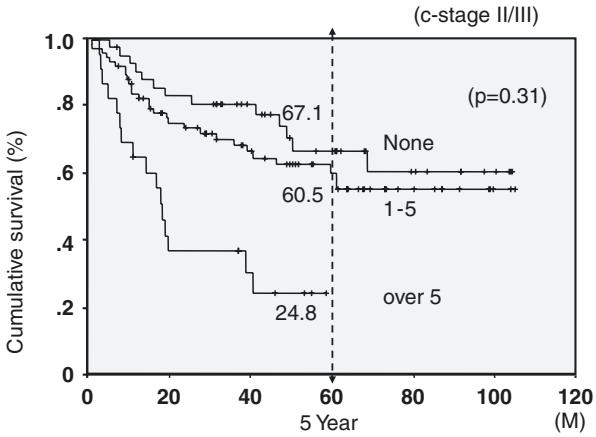

Fig. 13.14 Cumulative survival analysis among three groups. (No lymph node metastasis; No. of metastatic nodes, 1–5; No. of metastatic nodes, over 5)

We may answer the proposition "Is the number of lymph node metastasis a 'predictor' or a 'governor'?" The answer may be that the number of lymph node metastasis is a "predictor" AND a "governor."

References

1. Japan Esophageal Society. Japanese classification of esophageal cancer, 11th edition: part I. Esophagus. 2017;14:1–36. https://doi.org/10.1007/s10388-016-0551-7.
2. Kajiyama Y, Iwanuma Y, Tomita N, Amano T, Isayama F, Matsumoto T, Tsurumaru M. Size analysis of lymph node metastasis in esophageal cancer: diameter distribution and assessment of accuracy of preoperative diagnosis. Esophagus. 2006;3(4):189–95.

Part III

Lymph Node Metastasis: Clinical Significance

Gastric Cancer

14

Koshi Kumagai and Takeshi Sano

Abstract

Lymph node metastasis is the most important prognostic factor in potentially curable gastric cancer. Since 2010 the TNM classifications and the Japanese classification have been harmonized in terms of the N-category determined with the number of metastatic lymph nodes and of the stage grouping.

The D-number to describe the extent of lymph node dissection in gastrectomy is used to be defined in accordance with lymph node groups based on the primary tumor location. In the third edition of the Japanese guidelines published in 2010, the lymph node stations to be dissected in D1, D1+, and D2 were newly defined for total or distal gastrectomy regardless of the tumor location.

The 15-year follow-up of the Dutch trial demonstrated that the locoregional recurrence rate was significantly lower in patients treated with D2 than D1, showing a survival benefit. Today the D2 procedure has been recommended in most guidelines for patients with resectable advanced gastric cancer. There are debates on an optimal extent of lymph node dissection in esophagogastric junction cancer or cancer with duodenal invasion.

Keywords

Gastric cancer · Lymph node metastasis · Therapeutic value index · Classification Guidelines

K. Kumagai (✉) · T. Sano
Department of Gastroenterological Surgery, Cancer Institute Hospital, Japanese Foundation for Cancer Research, Tokyo, Japan
e-mail: koshi.kumagai@jfcr.or.jp

S. Natsugoe (ed.), *Lymph Node Metastasis in Gastrointestinal Cancer*,
https://doi.org/10.1007/978-981-10-4699-5_14

14.1 Prognostic Significance of Lymph Node Metastasis in Gastric Cancer

14.1.1 History of Gastric Cancer Staging System

The tumor-node-metastasis (TNM) classification has become the principal method for assessing the extent of malignant disease in most organs. The tumor stage generated by this system is a strong prognosticator that influences the treatment selection.

The extent of lymph node metastasis in gastric cancer used to be graded by anatomical location of the metastatic nodes both in the Japanese classifications (JC) by the Japanese Gastric Cancer Association (JGCA) and the TNM classification by the Union for International Cancer Control (UICC) and the American Joint Committee on Cancer (AJCC). In the fourth edition of the UICC/AJCC TNM classification [1], N1 signified metastasis in the perigastric nodes located within 3 cm from the border of the primary tumor; N2 were metastasis in the perigastric nodes more than 3 cm away from the border of the primary tumor or in the extra-perigastric nodes along the left gastric, hepatic, splenic, or celiac artery.

The JC had more complicated anatomical definitions. The lymph nodes around the stomach were first given "a station number" according to the anatomical location (Table 14.1 and Fig. 14.1) [2]. The nodes in the gastric drainage area were then grouped into three (Group 1–3) depending on the primary tumor location (Table 14.2). The grade of nodal metastasis (N1–N3) was defined based on these Group numbers 1–3: N1 signified metastasis in Group 1 but not in Group 2 or 3; N2 signified metastasis in Group 2 but not in Group 3, etc. The group numbers were also utilized to define the extent of lymphadenectomy (D1–D3) as will be described later. Although the definitions of groups were slightly modified in each edition, this basic rule had been consistent throughout the JC history until the major revision was made in the 14th edition [3] in 2010.

These anatomical definitions in the TNM and JC were not the same but roughly comparable, and in fact the treatment results reported from East and West were compared using the same terms "N" ignoring the differences between them. Then several studies suggested that the number, not the location, of metastatic nodes had strong prognostic power [4, 5], and in 1997, the TNM classification totally changed the N-category of gastric cancer from the anatomical system to the numerical one in its fifth edition [6]: N1, metastasis in 1–6 regional lymph nodes; N2, 7–15; and N3 more than 15. As the JGCA did not change their anatomical system, the N-category in the two classifications came to have incomparable, different meanings. This status continued until 2010 when the JGCA decided to adopt the numerical system. The TNM and JC were simultaneously revised (TNM 7th [7], and JC 14th [3]) introducing a new definition of N-category: N1, metastasis in 1–3 regional lymph nodes; N2, 3–6; and N3 more than 7. The JGCA abandoned the traditional anatomical system and instead proposed a new stage grouping based on the Japanese and Korean databases [8], which was adopted in the TNM. Thus the staging system of gastric cancer has been harmonized between East and West.

Table 14.1 Definitions of station numbers of the lymph nodes around the stomach (from Japanese classification of gastric carcinoma: third English edition [3])

No.	Definition
1	Right paracardial LNs, including those along the first branch of the ascending limb of the left gastric artery
2	Left paracardial LNs including those along the esophagocardiac branch of the left subphrenic artery
3a	Lesser curvature LNs along the branches of the left gastric artery
3b	Lesser curvature LNs along the second branch and distal part of the right gastric artery
4sa	Left greater curvature LNs along the short gastric arteries (perigastric area)
4sb	Left greater curvature LNs along the left gastroepiploic artery (perigastric area)
4d	Right greater curvature LNs along the second branch and distal part of the right gastroepiploic artery
5	Suprapyloric LNs along the first branch and proximal part of the right gastric artery
6	Infrapyloric LNs along the first branch and proximal part of the right gastroepiploic artery down to the confluence of the right gastroepiploic vein and the anterior superior pancreaticoduodenal vein
7	LNs along the trunk of left gastric artery between its root and the origin of its ascending branch
8a	Anterosuperior LNs along the common hepatic artery
8p	Posterior LNs along the common hepatic artery
9	Celiac artery LNs
10	Splenic hilar LNs including those adjacent to the splenic artery distal to the pancreatic tail and those on the roots of the short gastric arteries and those along the left gastroepiploic artery proximal to its first gastric branch
11p	Proximal splenic artery LNs from its origin to halfway between its origin and the pancreatic tail end
11d	Distal splenic artery LNs from halfway between its origin and the pancreatic tail end to the end of the pancreatic tail
12a	Hepatoduodenal ligament LNs along the proper hepatic artery, in the caudal half between the confluence of the right and left hepatic ducts and the upper border of the pancreas
12b	Hepatoduodenal ligament LNs along the bile duct, in the caudal half between the confluence of the right and left hepatic ducts and the upper border of the pancreas
12p	Hepatoduodenal ligament LNs along the portal vein in the caudal half between the confluence of the right and left hepatic ducts and the upper border of the pancreas
13	LNs on the posterior surface of the pancreatic head cranial to the duodenal papilla
14v	LNs along the superior mesenteric vein
15	LNs along the middle colic vessels
16a1	Para-aortic LNs in the diaphragmatic aortic hiatus
16a2	Para-aortic LNs between the upper margin of the origin of the celiac artery and the lower border of the left renal vein
16b1	Para-aortic LNs between the lower border of the left renal vein and the upper border of the origin of the inferior mesenteric artery
16b2	Para-aortic LNs between the upper border of the origin of the inferior mesenteric artery and the aortic bifurcation
17	LNs on the anterior surface of the pancreatic head deep to the pancreatic sheath
18	LNs along the inferior border of the pancreatic body

(continued)

Table 14.1 (continued)

No.	Definition
19	Infradiaphragmatic LNs predominantly along the left subphrenic artery
20	Paraesophageal LNs in the diaphragmatic esophageal hiatus
110	Paraesophageal LNs in the lower thorax
111	Supradiaphragmatic LNs separate from the esophagus
112	Posterior mediastinal LNs separate from the esophagus and the esophageal hiatus

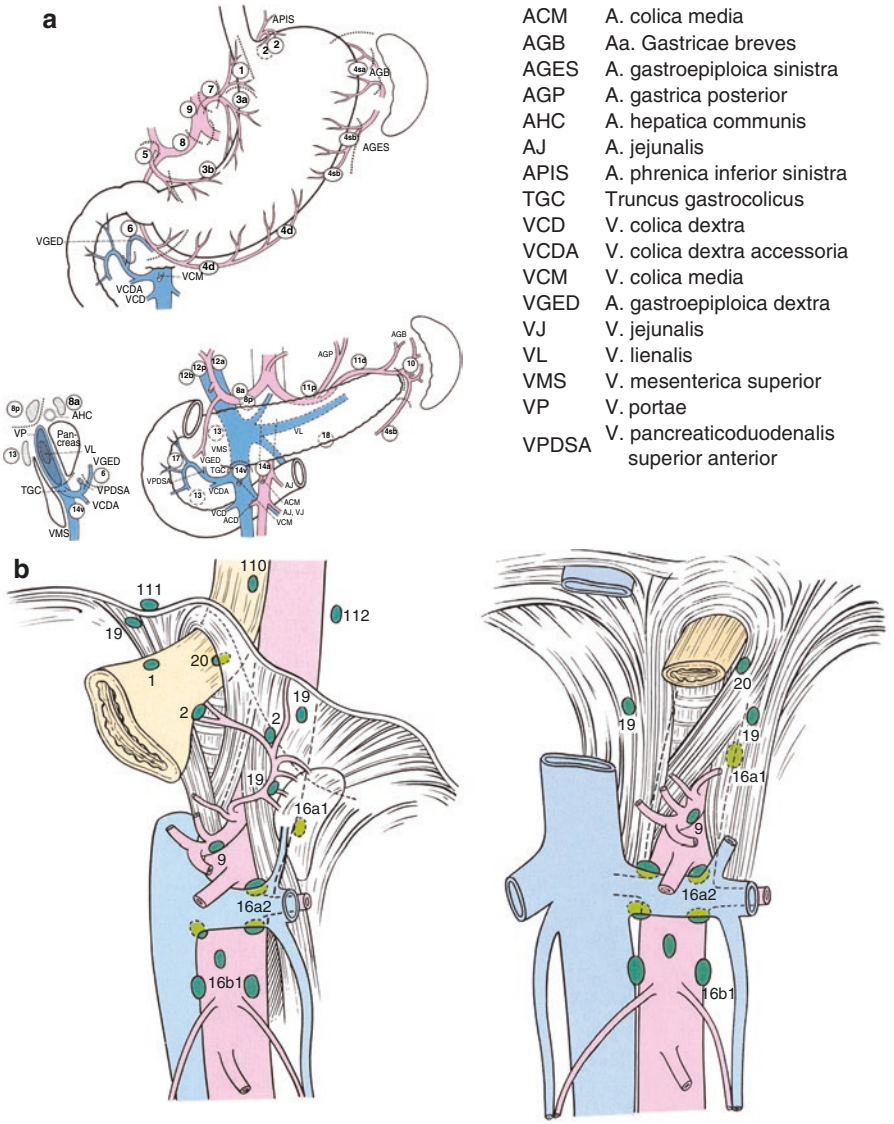

ACM	A. colica media
AGB	Aa. Gastricae breves
AGES	A. gastroepiploica sinistra
AGP	A. gastrica posterior
AHC	A. hepatica communis
AJ	A. jejunalis
APIS	A. phrenica inferior sinistra
TGC	Truncus gastrocolicus
VCD	V. colica dextra
VCDA	V. colica dextra accessoria
VCM	V. colica media
VGED	A. gastroepiploica dextra
VJ	V. jejunalis
VL	V. lienalis
VMS	V. mesenterica superior
VP	V. portae
VPDSA	V. pancreaticoduodenalis superior anterior

Fig. 14.1 Lymph node stations (**a**) Location of lymph node stations, (**b**) Location of lymph nodes in the esophageal hiatus and in the infradiaphragmatic and para-aortic regions [2]

Table 14.2 Lymph node grouping in the 13th edition of the Japanese classification

	LMU/MUL MLU/UML	LD/L	LM/M/ML	MU/UM	U	+E
No. 1	1	2	1	1	1	
No. 2	1	M	3	1	1	
No. 3	1	1	1	1	1	
No. 4sa	1	M	3	1	1	
No. 4sb	1	3	1	1	1	
No. 4d	1	1	1	1	2	
No. 5	1	1	1	1	3	
No. 6	1	1	1	1	3	
No. 7	2	2	2	2	2	
No. 8a	2	2	2	2	2	
No. 8b	3	3	3	3	3	
No. 9	2	2	2	2	2	
No. 10	2	M	3	2	2	
No. 11p	2	2	2	2	2	
No. 11d	2	M	3	2	2	
No. 12a	2	2	2	2	3	
No. 12bp	3	3	3	3	3	
No. 13	3	3	3	M	M	
No. 14v	2	2	3	3	M	
No. 14a	M	M	M	M	M	
No. 15	M	M	M	M	M	
No. 16a1	M	M	M	M	M	
No. 16a2, b1	3	3	3	3	3	
No. 16b2	M	M	M	M	M	
No. 17	M	M	M	M	M	
No. 18	M	M	M	M	M	
No. 19	3	M	M	3	3	2
No. 20	3	M	M	3	3	1
No. 110	M	M	M	M	M	3
No. 111	M	M	M	M	M	3
No. 112	M	M	M	M	M	3

14.1.2 Anatomical Definition of Regional Lymph Nodes

The number of lymph nodes included in the lymphatic drainage area largely varies among human organs, and the stomach has the most: a careful lymph node retrieval after total gastrectomy with D2 lymphadenectomy usually yields 40–60 nodes, sometimes up to 200 nodes [9]. Japanese surgeons have long believed that this dense network surrounding the stomach serves as a filter trapping cancer cells and keeping them localized. They regard lymph node metastasis as local disease that is still directly connected to the primary tumor, which is thus worth dissecting. The question is which nodes are considered as "regional" for the stomach.

Metastasis in the regional nodes is the determinant of N-category of the TNM classification, and metastasis in the non-regional nodes is classified as M1. In both JC and TNM, the perigastric lymph nodes (No. 1–6) and those along the main

branches of the celiac artery (left gastric, hepatic, and splenic arteries; No. 7–12) are defined as regional nodes. In addition, the para-aortic lymph nodes (PAN, No. 16) were classified as regional nodes until the 13th edition of JC. However, as survival benefit of PAN dissection was denied in a Japanese large-scale randomized controlled trial (JCOG9501) [10], they are now classified as non-regional nodes in the 14th edition of JC.

According to the UICC TNM system, if a tumor involves more than one site or subsite, the regional lymph nodes include those of all involved sites and subsites [11]. The JGCA decided to follow this rule. In gastric cancers invading the esophagus, the lymph nodes in the esophageal hiatus and lower mediastinum (no. 19, 20, 110, and 111) are regional lymph nodes. The retropancreatic nodes (No. 13) are not regional nodes of the stomach, but once a gastric cancer invades the duodenum, metastasis in No. 13 is not M1 but a regional nodal metastasis.

14.2 Surgical Management of Lymph Node Metastasis in Gastric Cancer

14.2.1 History of Lymphadenectomy

The first edition of JC was established in 1962, having two major purposes: first to provide common rules to record the disease for future registry and comparative studies and second to provide guidance for surgeons and pathologists. This showed a sharp contrast with the TNM classification that provides only classifications to record the disease without any proposal of treatment.

In the JC, therefore, the extent of lymphadenectomy was always the central subject. It used to be expressed with R-number such as R1 or R3 but was changed to the D-number in the 13th edition to avoid confusion with "R, residual disease" of the TNM classification. The D-number was linked to the group number of the lymph nodes determined according to the anatomical locations mentioned previously (Table 14.2). D1 signified complete dissection of the Group 1 nodes; D2, complete dissection of both Group 1 and 2 nodes, etc. Most randomized controlled trials (RCTs) of gastric cancer surgery including the Dutch [12], Medical Research Council (MRC) [13], and Taipei [14] were conducted using the 11th [15] or 12th edition of JC, in which surgeons obeyed the original definitions of D1 and D2. However, outside these trials, the terms "D1–3" were not always used with accuracy in the strict sense. It was generally and mistakenly believed outside Japan that the perigastric nodes (No. 1–6) were Group 1 and those along the celiac artery and its branches (No. 7–12) Group 2. The original definitions of N1–3 and D1–3 were not so simple. For example, the left paracardial lymph nodes (station No. 2) were classified as Group 1 in a tumor located in the upper third of the stomach, but as Group 3 in a middle or middle/lower tumor, and as M1 (distant metastasis) in a tumor confined to the lower third of the stomach.

This complicated definition of the nodal groups was established based on the results of detailed efficacy analysis on dissection of each lymph node station.

Sasako et al. proposed the concept of a "therapeutic value index" which is calculated by multiplying the incidence of metastasis in a lymph node station by the 5-year overall survival rate of the patients having metastasis in the station [16]. The nodal groups were defined based on the therapeutic value index for each primary tumor location in the 13th edition of JC (Table 14.2). Surgeons would have the best chance to remove the lymph nodes worth dissecting to cure patients as long as they perform D2 lymphadenectomy strictly obeying this table. However, the grouping was too complicated to be accurately understood worldwide. Moreover, the location of the primary tumor ("U," "M," "L," etc.), which is the basic determinant of nodal grouping, may not be universally categorized by surgeons or pathologists.

The anatomical lymph node groups were abandoned in the 14th edition of JC in 2010 and were replaced by the numerical N-category system in harmony with the seventh TNM as mentioned previously. Accordingly, the D-number lost its original meaning linked to the group numbers and had to be newly defined. This was realized in the third edition of the Japanese Gastric Cancer Treatment Guidelines [17] that was simultaneously published with the 14th JC. In this new D-number system, the extent of lymphadenectomy has been classified as D1, D1+, or D2, and the lymph node stations to be dissected in each D have been defined according not to the primary tumor location but to the type of surgery, i.e., total or distal gastrectomy (Fig. 14.2). D1 or D1+ are recommended for T1N0 disease and D2 for T2 to T4 disease. D3 is no longer defined because the rationale to recommend this super-extended surgery was lost by the negative results of the RCT [10]. In the guidelines, D1 and D1+ were also defined for proximal and pylorus-preserving gastrectomy but not D2 because these were function-preserving surgery recommended only for cT1N0 tumors (Fig. 14.3).

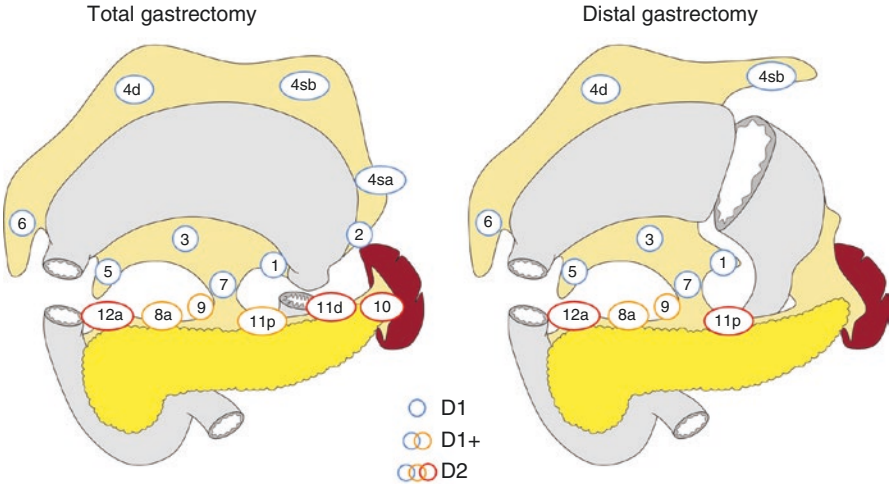

Fig. 14.2 Lymphadenectomy for standard surgery [40]

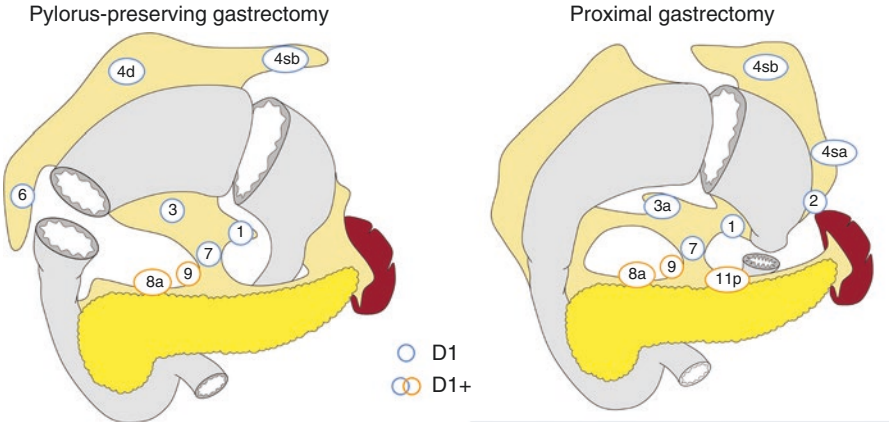

Fig. 14.3 Lymphadenectomy for function-preserving gastrectomy [40]

14.2.2 History of D2 Lymphadenectomy and Its Evidence

Following the first success of gastrectomy by Theodor Billroth in 1881, Jan Mikulicz-Radecki developed the concept of systematic lymphadenectomy for gastric cancer, which was inherited by his international apprentices. One of them was Hayari Miyake who brought the concept back to Japan, and it was further developed and refined by several pioneering surgeons including Tamaki Kajitani. He completed what we call D2 lymphadenectomy today, which was spread widely in Eastern Asia. In the West, the Mikulicz' concept was also expanded to as extensive as the Appleby's operation in which the celiac axis was dissected at the route, but then the extent of surgery was gradually reduced possibly under the influence of accumulated evidence in favor of conservative surgery in breast cancer.

In the 1990s, two RCTs were conducted in Europe to compare D1 and D2 lymphadenectomy for gastric cancer, and they both showed significantly higher operative morbidity and mortality in D2 than in D1 without any survival benefit by D2 [12, 13]. In these trials, the protocol was written based on the 11th JC [15], and the D2 procedure in principle included pancreatosplenectomy for proximal gastric tumors. This obviously caused increase in operative morbidity and mortality, offsetting the possible survival benefits by D2. It was clearly demonstrated that D2 lymphadenectomy in this style was technically complicated and required trained skills.

Although the trial results discouraged Western surgeons from performing D2 lymphadenectomy, some specialists in Europe showed its feasibility and safety [18, 19], especially by avoiding pancreatosplenectomy. Furthermore, additional analyses of the Dutch trial suggested survival advantage of extended lymphadenectomy, and finally, the 15-year follow-up showed significantly lower rates of locoregional recurrence and gastric-cancer-related death in D2 than in D1 [20].

In Asia, a single-institutional, small-scale RCT [14] to compare D1 and D2/D3 was conducted by specialized surgeons in Taipei (they used the 12th edition of JC

in which the definition of "D3" was almost identical to the D2 in the 13th edition; thus, it is expressed as "D2/D3" here). There was no operative death in this trial, and the D2/D3 group showed marginally but significantly longer survival than the D1 group. In Japan and Korea where D2 lymphadenectomy is safely performed and is believed superior to D1, no RCT has ever been planned.

With these results combined, the treatment guidelines today, both in the East and West, recommend D2 lymphadenectomy without splenectomy for curable, non-early gastric cancer, on condition in the West that it is performed by experienced surgeons in high-volume centers [21].

14.2.3 Splenectomy

When a gastric cancer directly invades the spleen or pancreas, splenectomy or pancreatosplenectomy is performed to achieve R0 resection. Even without such invasion, splenectomy has been performed in Japan, as a part of D2 in total gastrectomy, aiming at complete lymphadenectomy at the splenic hilum. Embryologically, the spleen develops in the dorsal mesogastrium and therefore naturally bears gastric draining lymph nodes in its hilar area. Indeed, 10–20% of proximal gastric cancers metastasize to the lymph nodes in this area, and complete dissection is technically difficult without splenectomy. On the other hand, splenectomy was shown to be associated with high postoperative morbidity and mortality in the European trials [12, 13] and thus is recommended to be avoided in routine practice [21]. A number of retrospective studies comparing splenectomy and spleen preservation showed no survival benefit of splenectomy [22, 23]. However, these studies were heavily biased in favor of spleen preservation in that splenectomy had been performed in patients with more advanced disease.

Several RCTs were conducted to evaluate splenectomy in total gastrectomy. Those in Chile [24] and Korea [25] were rather small scale (187 and 207 patients, respectively) and thus underpowered and inconclusive. There was another small-scale, Japanese old RCT [26] (79 patients), and a meta-analysis of these three trials [27] showed a slightly better 5-year survival with splenectomy, but the difference was not statistically significant.

A large-scale multi-institutional RCT (JCOG0110) was conducted in Japan [28]. Proximal gastric adenocarcinoma of T2-4/N0-2/M0 not invading the greater curvature of the upper gastric body was eligible. During the operation, surgeons confirmed that R0 resection was possible with negative lavage cytology, and 505 patients were randomly assigned to either splenectomy or spleen preservation. The primary endpoint was OS, and the trial was designed to confirm noninferiority of spleen preservation to splenectomy in OS. Splenectomy was associated with higher morbidity and larger blood loss, but the operation time was similar. The 5-year OS were 75.1% and 76.4% in the splenectomy and spleen preservation groups, respectively, and the noninferiority of spleen preservation was confirmed ($P = 0.025$). The study concluded that in total gastrectomy for proximal gastric cancer which does not invade the greater curvature, splenectomy should be avoided as it increases

operative morbidity without improving survival. However, the clinical question of whether splenectomy should be avoided for a tumor located at or limited to the greater curvature was not answered in the trial, because such patients were all excluded from the trial. Based on the results of this trial, the JGCA decided to remove No. 10 from the list of lymph nodes to be dissected in D2 total gastrectomy in the 15th edition of JC.

14.2.4 D2-Plus Lymphadenectomy for Advanced Gastric Cancer

Whether the lymphadenectomy beyond the standard D2 could add survival benefit is controversial. Two RCTs were conducted in Japan to answer these questions and were concluded.

The dissection of the para-aortic nodes (PAN) is used to be routinely performed in specialized centers in Japan, as PAN were regarded as the final part of the regional lymphatic drainage of the stomach. Although the PAN dissection was associated with increased operative morbidity, a considerable proportion of patients with positive metastasis in this area were reported to survive after systematic dissection [29, 30]. The Japan Clinical Oncology Group (JCOG) conducted a large-scale RCT (JCOG9501) [10] to show its survival benefit over D2. A total of 523 patients with subserosa or deeper gastric cancer without apparent PAN involvement were enrolled. After confirming operative curability including negative peritoneal cytology, the patient was intraoperatively allocated to either D2 or D2 + PAN dissection by central randomization. No adjuvant chemotherapy was given. Although the operative morbidity rate was slightly higher in D2 + PAN dissection, the mortality was equally low (0.8% each). Contrary to surgeons' expectations, the survival curves of the two groups were completely overlapped showing no benefit of prophylactic PAN dissection.

In this trial, some paradoxical results were obtained in the subset analyses. It had been repeatedly demonstrated in retrospective studies that the deeper the tumor invasion, the higher the PAN involvement. Nevertheless, in this JCOG9501 trial, in patients with pathologically deep invasive tumor or those with positive nodal metastases (i.e., high possibility of PAN metastasis), D2 alone showed significantly better survival than D2 + PAN dissection, whereas in those with pT1/T2 tumors or those without histological nodal metastasis (thus low possibility of PAN metastasis), D2 + PAN dissection showed significantly better survival than D2 alone. There is no convincing explanation for these paradoxical results, but it should be noted that D2 + PAN dissection did worse particularly in those for whom surgeons had expected its benefit.

Another RCT to evaluate extended lymphadenectomy beyond D2 was JCOG9502 that compared two different approaches to gastric cancer invading the esophagus [31]. Left thoracoabdominal approach was known to facilitate sufficient lower mediastinal lymphadenectomy and local tumor control around the cardia. Patients with gastric cancer invading the esophagus less than 3 cm were preoperatively allocated to either abdominal trans-hiatal approach (AT) or left thoracoabdominal

approach (LT). Total gastrectomy with D2-plus left upper para-aortic nodal dissection was performed in both groups. Lower mediastinal dissection was added in the LT group. The trial was terminated in the interim analysis because the invasive LT approach showed rather inferior survival and was quite unlikely to be finally superior to AT.

These two RCTs had a huge impact on the trend toward expansion of lymphadenectomy attempted by brave and aggressive surgeons who believed "the more extensive the surgery, the better the survival." Consequently, today, D2 lymphadenectomy, not less, not more, stays standard for curable non-early gastric cancer in Japan.

14.2.5 Multidisciplinary Approach to Extensive Lymph Node Metastasis

Prognosis of patients with extensive lymph node metastasis (ELM) from gastric cancer is poor even after macroscopic R0 resection. In expectation that downstaging by preoperative intensive chemotherapy may improve surgical outcomes, JCOG conducted a series of phase II trials to develop multidisciplinary therapy for such patients. They defined resectable ELM as either bulky nodal metastasis larger than 3 cm in diameter along the celiac artery or its branches ("bulky N2") or PAN metastasis confined to No.16a2/b1 regions [32]. In these trials, staging laparoscopy was mandatory to confirm absence of peritoneal metastasis (P0/CY0). Following two or three courses of neoadjuvant chemotherapy (NAC), gastrectomy with D2 + PAN dissection was performed.

As NAC regimen they first chose CPT-11 and cisplatin (JCOG0001) [32]. The study was terminated when 55 patients were enrolled (the projected sample size was 60) because three treatment-related deaths were reported. Although the 3-year survival rate (27%) exceeded prespecified threshold, the pathological response rate was lower (15%) than expected (Table 14.3). Then, S-1 + cisplatin was selected as NAC for the same target (JCOG0405) [33]. The toxicity was mild, and the pathological response was high including a case of complete response. The 3- and 5-year survival rates (59% and 53%, respectively) were far higher than the expected rates.

Table 14.3 Neoadjuvant chemotherapy studies for extensive lymph node metastasis

Trial	JCOG0001	JCOG0405	JCOG1002
Regimen	CPT-11+CDDP	S-1+CDDP	S-1+CDDP+DTX
No. of patients	55	53	53
Primary endpoint	3-year OS	R0 resection rate	Response rate
Response rate	54%	63%	58%
Histological response ≥ Grade 1b	15%	51%	50%
R0 resection rate	66%	82%	85%
TRD	3 (5.5%)	0	0
3-year survival	27%	59%	62%

CDDP cisplatin, *DTX* docetaxel, *TRD* treatment-related death
Histological response grade: by Japanese classification for gastric carcinoma

Then, docetaxel was added to S-1 + cisplatin aiming at better response and survival (JCOG1002) [34], but this toxic regimen did not exceed the results of JCOG0405 in terms of response rate and survival.

Based on these results, D2-plus PAN dissection after S-1 + cisplatin is regarded as the tentative standard treatment for potentially curable gastric cancer patients with ELM. Further evaluations are needed as to whether PAN dissection is mandatory in such patients especially after good clinical response to NAC. In addition, more effective regimens with less toxicity are awaited.

14.2.6 Esophagogastric Junction Cancer

Tumors arising in the esophagogastric junction (EGJ) have been known to have distinct clinicopathological features. In 1973, Nishi proposed that the area between 2 cm above and 2 cm below the EGJ should be called "EGJ zone" and that carcinomas arising in this zone, irrespective of histological type, should be called "EGJ cancer" [35]. In 1996, Siewert proposed a concept of "adenocarcinoma of the EGJ" classifying adenocarcinomas arising between 5 cm above and 5 cm below the EGJ into three types according to the location of its epicenter as follows [36]: type I, adenocarcinoma of the distal esophagus which usually arises from an area with specialized intestinal metaplasia of the esophagus (i.e., Barrett's esophagus) and which may infiltrate the EGJ from above; type II, true cardia carcinoma arising from the cardiac epithelium or short segments with intestinal metaplasia at the EGJ, between 1 cm above and 2 cm below the EGJ, this entity is also often referred to as "junctional carcinoma"; and type III, subcardial gastric carcinoma which infiltrates the EGJ and distal esophagus from below. There has been an alarming rise in the incidence and prevalence of adenocarcinoma at the EGJ in the Western countries. However, the optimal surgical approach to adenocarcinoma of EGJ, especially Siewert type II tumors, has not been established.

High metastatic rates from EGJ cancer to the abdominal lymph nodes have been reported regardless of the histological type or the invasion length toward the stomach. No. 1, 2, 3, and 7 nodes are frequently involved in up to 50%. No. 9 and 11p nodes are also involved in 10–20%. On the other hand, No. 4sb, 4d, 5, 6, and 10 lymph nodes were rarely involved, and their metastatic rates are reported to be less than 5% [37, 38].

There are few reports on the incidence of metastasis to mediastinal or paraaortic nodes around the left renal vein (No. 16a2 lat) from EGJ cancer. The JGCA and Japan Esophageal Society conducted a nationwide retrospective surveillance of EGJ cancer smaller than 4 cm in diameter, and the data of 3177 patients treated between 2001 and 2010 were collected from 273 institutions [39]. An algorithm in Fig. 14.4 has been proposed in the JGCA guidelines ver. 4 for lymphadenectomy for such tumors [40]. Following this, a prospective multi-institutional study is active in Japan (UMIN000013205) to determine the metastatic rates of the lymph nodes both in the mediastinum and the abdomen including No.16a2-lat from EGJ cancer. The optimal extent of lymphadenectomy will be proposed after conclusion of this study.

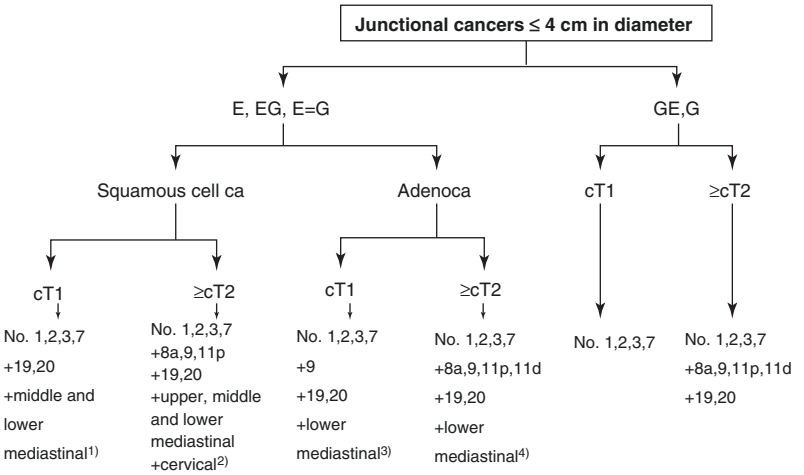

1) Clinical relevance of dissecting the upper mediastinal lymph nodes is unclear since the incidence of metastasis is low.
2) Cervical lymph nodes are infrequently dissected and clinical relevance of dissecting these nodes is unknown. However, it is noteworthy that there are long-term survivors among those with histologically confirmed metastases among the cervical nodes.
3) For the E=G category, lower mediastinal nodes and hiatal nodes were rarely dissected, and the incidence of metastasis among those who underwent resection was low.
4) Cervical, upper mediastinal and middle mediastinal nodes are rarely dissected for this category, and data to discuss on the clinical relevance of dissecting these nodes are lacking.

Fig. 14.4 Algorithm showing the tentative standard in the extent of lymphadenectomy for junctional cancer based on the tumor location, histology and T-categories [40]

14.2.7 Gastric Cancer with Duodenal Invasion

Gastric cancer located in the antrum sometimes invades the duodenum. The regional lymph nodes of the duodenum listed by the UICC include the pyloric, hepatic, and superior mesenteric lymph nodes, whereas those by AJCC include the hepatic, pancreaticoduodenal, infrapyloric, gastroduodenal, pyloric, and pericholedochal lymph nodes. The No. 13 (retropancreatic) nodes are anatomically close to the pylorus and often bear metastasis from tumors invading the duodenum [41]. The JGCA guidelines [40] state that D2-plus No. 13 lymphadenectomy could be an option in curative gastrectomy for such tumors. No. 12a should be dissected in a standard D2 gastrectomy, while No. 12b or 12p are regarded beyond D2 according to the guidelines. Neither previous studies nor the JGCA guidelines discuss the significance of a D2-plus dissection including No. 12b and No. 12p, although the higher incidence of "No.12 nodes" involvement has been reported [42]. Future study is required to clarify the significance of D2-plus gastrectomy.

Lymph nodes along the superior mesenteric vein (No. 14v) are not included in a D2 gastrectomy in the JGCA guidelines, but it is mentioned that D2-plus No. 14v dissection may be beneficial in tumors with apparent metastasis to the No. 6 nodes. For tumors in the distal stomach involving the duodenum, which frequently metastasize to No. 6 nodes, No. 14v dissection could also be an option.

14.3 Summary

Lymph node metastasis in gastric cancer has long been investigated as potentially curable local metastasis. Evidence has accumulated based on meticulous registry and clinical trials, and today D2 lymphadenectomy is considered to be the standard procedure recommended for non-early resectable gastric cancer. Further evidence of lymph node metastasis and the value of its dissection are needed in EGJ cancer. Combination with new chemotherapy will improve patients' survival, and the optimal extent of lymphadenectomy may change according to the effects of preoperative therapy.

References

1. Hermanek P, Sobin LH. International union against cancer: TNM classification of malignant tumours. 4th fully revised ed. Berlin: Springer-Verlag; 1987.
2. Japanese Gastric Cancer Association. Japanese classification of gastric carcinoma: 2nd English edition. Gastric Cancer. 1998;1:10–24.
3. Japanese Gastric Cancer Association. Japanese classification of gastric carcinoma: 3rd English edition. Gastric Cancer. 2011;14(2):101–12.
4. Ichikura T, Tomimatsu S, Okusa Y, Uefuji K, Tamakuma S. Comparison of the prognostic significance between the number of metastatic lymph nodes and nodal stage based on their location in patients with gastric cancer. J Clin Oncol. 1993;11(10):1894–900.
5. Wu CW, Hsieh MC, Lo SS, et al. Relation of number of positive lymph nodes to the prognosis of patients with primary gastric adenocarcinoma. Gut. 1996;38(4):525–7.
6. Sobin LH, Fleming ID. TNM Classification of Malignant tumors, fifth edition (1997). Union Internationale Contre le Cancer and the American Joint Committee on Cancer. Cancer. 1997;80(9):1803–4.
7. Sobin LH, Gospodarowicz MK, Wittekind C. TNM classification of malignant tumours. 7th ed. Oxford: Blackwell Publishing Ltd; 2010.
8. Washington K. 7th edition of the AJCC cancer staging manual: stomach. Ann Surg Oncol. 2010;17:3077–9.
9. Sano T, Sasako M, Yamamoto S, et al. Gastric cancer surgery: morbidity and mortality results from a prospective randomized controlled trial comparing D2 and extended para-aortic lymphadenectomy—Japan Clinical Oncology Group study 9501. J Clin Oncol. 2004;22(14):2767–73.
10. Sasako M, Sano T, Yamamoto S, et al. D2 lymphadenectomy alone or with para-aortic nodal dissection for gastric cancer. N Engl J Med. 2008;359(5):453–62.
11. Wittekind CH, Compton CC, Brierley J, Sobin LH. The TNM clinical and pathological classifications. In: TNM supplement. A commentary on uniform use. Oxford: Wiley-Blackwell; 2012. p. 7.
12. Bonenkamp JJ, Songun I, Hermans J, Sasako M, Welvaart K, Plukker JT, et al. Randomised comparison of morbidity after D1 and D2 dissection for gastric cancer in 996 Dutch patients. Lancet. 1995;345(8952):745–8.
13. Cuschieri A, Fayers P, Fielding J, Craven J, Bancewicz J, Joypaul V, et al. Postoperative morbidity and mortality after D1 and D2 resections for gastric cancer: preliminary results of the MRC randomised controlled surgical trial. The Surgical Cooperative Group. Lancet. 1996;347(9007):995–9.
14. Wu CW, Hsiung CA, Lo SS, Hsieh MC, Chen JH, Li AF, et al. Nodal dissection for patients with gastric cancer: a randomised controlled trial. Lancet Oncol. 2006;7(4):309–15.
15. Kajitani T. The general rules for the gastric cancer study in surgery and pathology. Part I. Clinical classification. Jpn J Surg. 1981;11(2):127–39.

16. Sasako M, McCulloch P, Kinoshita T, Maruyama K. New method to evaluate the therapeutic value of lymph node dissection for gastric cancer. Br J Surg. 1995;82(3):346–51.
17. Japanese Gastric Cancer Association. Japanese gastric cancer treatment guidelines 2010 (ver. 3). Gastric Cancer. 2011;14(2):113–23.
18. Sue-Ling HM, Johnston D, Martin IG, et al. Gastric cancer: a curable disease in Britain. Br Med J. 1993;307:591–6.
19. Degiuli M, Sasako M, Ponti A, et al. Morbidity and mortality in the Italian Gastric Cancer Study Group randomized clinical trial of D1 versus D2 resection for gastric cancer. Br J Surg. 2010;97(5):643–9.
20. Songun I, Putter H, Kranenbarg EM, Sasako M, van de Velde CJ. Surgical treatment of gastric cancer: 15-year follow-up results of the randomised nationwide Dutch D1D2 trial. Lancet Oncol. 2010;11(5):439–49.
21. Smyth EC, Verheij M, Allum W, Cunningham D, Cervantes A, Arnold D. Gastric cancer: ESMO Clinical Practice Guidelines for diagnosis, treatment and follow-up. Ann Oncol. 2016;27(suppl 5):v38–49.
22. Griffith JP, Sue-Ling HM, Martin I, Dixon MF, McMahon MJ, Axon AT, et al. Preservation of the spleen improves survival after radical surgery for gastric cancer. Gut. 1995;36(5):684–90.
23. Wanebo HJ, Kennedy BJ, Winchester DP, Stewart AK, Fremgen AM. Role of splenectomy in gastric cancer surgery: adverse effect of elective splenectomy on long term survival. J Am Coll Surg. 1997;185(2):177–84.
24. Csendes A, Burdiles P, Rojas J, Braghetto I, Diaz JC, Maluenda F. A prospective randomized study comparing D2 total gastrectomy versus D2 total gastrectomy plus splenectomy in 187 patients with gastric carcinoma. Surgery. 2002;131(4):401–7.
25. Yu W, Choi GS, Chung HY. Randomized clinical trial of splenectomy versus splenic preservation in patients with proximal gastric cancer. Br J Surg. 2006;93(5):559–63.
26. Toge T, Kameda A, Kuroi K, Seto Y, Yamada H, Hattori T. The role of the spleen in immunosuppression and the effects of splenectomy on prognosis in gastric cancer patients. Nihon Geka Gakkai Zasshi. 1985;86(9):1120–3.
27. Yang K, Chen XZ, Hu JK, et al. Effectiveness and safety of splenectomy for gastric carcinoma: a meta-analysis. World J Gastroenterol. 2009;15:5352–9.
28. Sano T, Sasako M, Mizusawa J, Yamamoto S, Katai H, Yoshikawa T, et al. Randomized controlled trial to evaluate splenectomy in Total gastrectomy for proximal gastric carcinoma. Ann Surg. 2017;265(2):277–83.
29. Kitamura M, Arai K, Iwasaki Y. Clinicopathological studies and problems on para-aortic lymph node dissection: D4 dissection. Nippon Geka Gakkai Zasshi. 1996;97:302–7.
30. Isozaki H, Okajima K, Fujii K, et al. Effectiveness of paraaortic lymph node dissection for advanced gastric cancer. Hepato-Gastroenterology. 1999;46:549–54.
31. Sasako M, Sano T, Yamamoto S, Sairenji M, Arai K, Kinoshita T, et al. Left thoracoabdominal approach versus abdominal-transhiatal approach for gastric cancer of the cardia or subcardia: a randomised controlled trial. Lancet Oncol. 2006;7(8):644–51.
32. Yoshikawa T, Sasako M, Yamamoto S, et al. Phase II study of neoadjuvant chemotherapy and extended surgery for locally advanced gastric cancer. Br J Surg. 2009;96(9):1015–22.
33. Tsuburaya A, Mizusawa J, Tanaka Y, et al. Neoadjuvant chemotherapy with S-1 and cisplatin followed by D2 gastrectomy with para-aortic lymph node dissection for gastric cancer with extensive lymph node metastasis. Br J Surg. 2014;101(6):653–60.
34. Ito S, Sano T, Mizusawa J, et al. A phase II study of preoperative chemotherapy with docetaxel, cisplatin, and S-1 followed by gastrectomy with D2 plus para-aortic lymph node dissection for gastric cancer with extensive lymph node metastasis: JCOG1002. Gastric Cancer. 2017;20(2):322–31.
35. Nishi M, Kaji S, Akune T, et al. Cardia cancer: a proposal of esophagogastric junction cancer. Geka Shinryo. 1973;15:1328–38. (in Japanese)
36. Siewert JR, Stein HJ. Carcinoma of the cardia: carcinoma of the gastroesophageal junction—classification, pathology and extent of resection. Dis Esophagus. 1996;9:173–82.

37. Fujitani K, Miyashiro I, Mikata S, Tamura S, Imamura H, Hara J, et al. Pattern of abdominal nodal spread and optimal abdominal lymphadenectomy for advanced Siewert type II adenocarcinoma of the cardia: results of a multicenter study. Gastric Cancer. 2013;16(3):301–8.
38. Mine S, Sano T, Hiki N, Yamada K, Nunobe S, Yamaguchi T. Lymphadenectomy around the left renal vein in Siewert type II adenocarcinoma of the oesophagogastric junction. Br J Surg. 2013;100(2):261–6.
39. Yamashita H, Seto Y, Sano T, et al. Results of a nation-wide retrospective study of lymphadenectomy for esophagogastric junction carcinoma. Gastric Cancer. 2017;20(Supple 1):S69–83.
40. Japanese Gastric Cancer Association. Japanese gastric cancer treatment guidelines 2014 (ver. 4). Gastric Cancer. 2017;20:1–19.
41. Tokunaga M, Ohyama S, Hiki N, Fukunaga T, Inoue H, Yamada K, et al. Therapeutic value of lymph node dissection in advanced gastric cancer with macroscopic duodenum invasion: is the posterior pancreatic head lymph node dissection beneficial? Ann Surg Oncol. 2009;16(5):1241–6.
42. Kakeji Y, Korenaga D, Baba H, Watanabe A, Tsujitani S, Maehara Y, et al. Surgical treatment of patients with gastric carcinoma and duodenal invasion. J Surg Oncol. 1995;59(4):215–9.

Colorectal Cancer

15

Kazushige Kawai, Kensuke Otani, Manabu Kaneko, Koji Murono, Kazuhito Sasaki, and Toshiaki Watanabe

Abstract

The location of the lymph nodes and the extent of their removal for an optimal response have been much discussed in the history of surgery, and considerable research in this field is still being conducted today. If lesions are removed with too wide margins, unnecessary complications can occur with no additional survival benefit. In contrast, incomplete lymph node dissection might leave residual cancer cells, which could cause disease recurrence in lymph nodes or local sites. For this perspective, the significance of performing complete mesocolic excision for colon cancer and total mesorectal excision for rectal cancer has been focused in recent years. Central vascular ligation has also been considered to be important in the lymph node dissection for colorectal cancer.

In this chapter, we describe the latest trends in the treatment for lymph node metastasis from colorectal cancer under four headings: (1) metastasis to mesenteric lymph nodes, (2) metastasis to lateral pelvic lymph nodes from rectal cancer, (3) metastasis to other distant lymph nodes, and (4) lymph node metastasis from T1 cancer.

Keywords

Complete mesocolic excision · Total mesorectal excision · Central vascular ligation · Lateral lymph node dissection

K. Kawai (✉) · K. Otani · M. Kaneko · K. Murono · K. Sasaki · T. Watanabe
Department of Surgical Oncology, The University of Tokyo, Tokyo, Japan
e-mail: kz-kawai@mvd.biglobe.ne.jp

S. Natsugoe (ed.), *Lymph Node Metastasis in Gastrointestinal Cancer*,
https://doi.org/10.1007/978-981-10-4699-5_15

15.1 Introduction

The presence or absence of lymph node metastasis from colorectal cancer is an important factor affecting patient prognosis, which is also the case with lymph node metastasis from other cancers; the cancer stage varies depending on different factors related to lymph node metastasis. In Japan, systematic lymph node dissection is well-established and is an important concept in surgical treatment. Meanwhile, in Europe and the USA, as reported by Cady et al. [1], lymph node metastasis is an important prognostic factor, and lymph node dissection is performed for local control and staging rather than treatment.

For a long time, the Japanese Classification of Colorectal Carcinoma (hereinafter referred to as the "Japanese classification") has classified metastatic lymph nodes according to their distance from tumors or their positional relationship with dominant blood vessels; this information has been used to determine the N factor. However, the TNM classification by the Union for International Cancer Control (UICC), which is commonly used worldwide, determines the N factor using the number of metastatic lymph nodes. To ensure consistency, the Japanese classification also introduced the number of lymph node metastases into its guidelines in the seventh edition, published in 2008.

The TNM classification (seventh edition) by the UICC categorizes the N factor as N0, N1a, N1b, N1c, N2a, and N2b, according to the number of metastases to the regional lymph nodes (Table 15.1). The Japanese classification (eighth edition) categorizes N0, N1, and N2 according to the number of metastases to the intestinal and intermediate lymph nodes, which is consistent with the TNM classification. The Japanese criteria also specify that the condition for N3 is main lymph node metastasis, and that of low rectal cancer is lateral lymph node metastases, emphasizing the importance of main lymph node dissection in surgery and defining N3 as an

Table 15.1 Differences in the definition of N staging between the Japanese Society for Cancer of the Colon and Rectum (JSCCR) classification and TNM classification

JSCCR	TNM
N1 Three or less metastases to lymph nodes that are located along the marginal artery and adjacent to the colon	N1a Metastasis in one regional lymph node N1b Metastasis in two to three regional lymph nodes N1c Tumor deposit(s) in the subserosa, mesentery, or nonperitonealized pericolic or perirectal tissues without regional nodal metastasis
N2 Four or more metastases to lymph nodes that are located along the marginal artery and adjacent to the colon	N2a Metastasis in four to six regional lymph nodes N2b Metastasis in seven or more regional lymph nodes
N3 Metastasis to lymph nodes that are located around the superior or inferior mesenteric vessels and/or metastasis to lateral lymph nodes from rectal cancer	

index to perform dissection (Table 15.1). The cancer staging of Japanese criteria is simpler than that of TNM. In stage M0 cancer, the stage is IIIa in cases of N1 cancer and IIIb in cases of N2 cancer.

In the treatment of lymph node metastasis from colorectal cancer, not only the presence and the number of metastases but also the presence and the number of surgically removed lymph nodes are regarded as the prognostic indices [2–5]. This can be explained by lymph node micrometastases that cannot be detected through standard pathological examination with hematoxylin and eosin staining [6–8]. It has also been reported that the metastatic lymph node ratio (LNR), which is calculated by dividing the number of metastatic lymph nodes by the total number of removed lymph nodes, has a higher correlation with prognosis than the N factor, which is defined by the number of metastatic lymph nodes [9–13]. These reports indicate the importance of lymph node dissection in surgical treatment.

The colonic lymph flows from the intestinal lymph nodes around the colon toward the intermediate lymph nodes and then on to the lymph nodes at the root of the dominant blood vessels; colon cancer usually metastasizes to the lymph nodes in this order. In addition to the tumor metastases that are regularly encountered in the lymph node, extranodal tumor metastases (EX) are sometimes observed within the mesentery of the colon. If the EX are not vessel or nerve invasive lesions, tumor nodules are not detected (ND), and then the lesions should be treated as the metastatic lymph nodes, as described in the eighth edition of the existing Japanese classification.

In Japan, lymph node dissection, along with high tie of the dominant blood vessels and resection of the mesocolon, has been the standard treatment for colon cancer. Furthermore, since Hohenberger et al. [14] suggested the use of complete mesocolic excision (CME) and central ligation in 2009, which were previously only used as the standard surgical procedures in Japan, these procedures have become widespread in Europe and the USA. The length of colon excision determines the range of lymph node dissection in the longitudinal direction, and a length of 10 cm has been used as the standard in colon excision, as described in the Japanese classification. However, a shorter length could still be potentially satisfactory, and the optimum length is currently being discussed.

The study of lymph node metastasis from rectal cancer that has attracted the most attention in recent years is the JCOG0212 study [15]; the study results were reported by Fujita et al. in the 2016 meeting of the American Society of Clinical Oncology (ASCO). The authors examined the significance of prophylactic lateral dissection in advanced low rectal cancer, and their results did not show noninferiority of mesorectal excision alone compared with mesorectal excision with lateral lymph node dissection for 5-year relapse-free survival, which was the primary end point. Both methods had nearly identical results for 5-year relapse-free survival, 73.3% in the group receiving mesorectal excision alone compared with 73.4% in the group receiving mesorectal excision with lateral lymph node dissection. The local relapse rate in the group with mesorectal excision alone was 12.6%, and that in the group with the addition of lateral lymph node dissection was 7.4% ($p = 0.024$), indicating the relapse rate in the group with additional lateral lymph node dissection

was significantly lower. Further analytical results are expected to be reported in the future; however, a full discussion is necessary to better understand the results and the future direction of treatment.

The clinical significance of lymph node metastasis from colorectal cancer is that the presence or extent of metastasis strongly affects the prognosis. Although there would be no objections to the thorough excision of the lymph nodes that are likely to be metastatic, attention must be paid to the effectiveness of prophylactic dissection and any associated postoperative functional disorder, particularly when lateral lymph node dissection is performed for rectal cancer. In this chapter, in addition to the introduction to the latest findings, the significance of the following items is explained in detail: (1) metastasis to mesenteric lymph nodes, (2) lateral metastasis, (3) distant metastasis, and (4) lymph node metastasis from T1 cancer.

15.2 Metastasis to Mesenteric Lymph Nodes

The frequency of metastasis to mesenteric lymph nodes from colorectal cancer is 42.9%, and surgical resection of mesenteric lymph nodes without an excess or deficit is important [16].

15.2.1 Lymph Node Dissection for Colon Cancer

As recommended in the Japanese classification, in Japan, regional lymph node dissection is performed according to the invasion depth of the tumor and the presence of lymph node metastasis [16]. Meanwhile, in Europe and the USA, it is recommended to perform dissection of at least 12 lymph nodes as well as identification of the lymph node at the origin of the feeding vessels. However, in Japan, there have been no such criteria defining the regional lymph nodes and thereby obtaining the definitive dissection range.

In the UK, West et al. examined 399 colon cancer samples obtained during surgery, in which the degree of mesocolon dissection was classified into four grades (A–D) and the prognosis of the patients was compared [17]. Their results showed that the dissections performed were not beyond the extent to which the colon wall on the mesenteric side was exposed (grade A) in approximately a quarter of the cases and that the survival rate in cases with stage III cancer was poor.

The significance of performing CME and central vascular ligation (CVL) has been reported [14, 18]; in these procedures, the mesocolon covered by the visceral fascia is identified and detached from the retroperitoneum, which prevents the mesocolon from being torn. The feeding vessels are also separated at their roots, indicating that the mesocolon and lymph nodes are resected without leaving residual disease. These methods are similar to D3 dissection performed in Japan [19]. Kotake et al. conducted a study of 10,098 patients with T3 or T4 depth of invasion who underwent radical resection. A total of 6580 patients who underwent D3 dissection were compared with 3518 patients who underwent D2 dissection. Patients

who underwent D3 dissection had significantly better outcomes. The results confirm the importance of the excision of feeding vessels at the disease origin [20].

When the intestinal tract is excised, it is appropriate to secure a length of 5 cm from the tumor, according to the National Comprehensive Cancer Network (NCCN) [21]. In contrast, Japanese guidelines require that excision be performed at a distance of 10 cm from cancers on the oral or anal side [16]. However, since lymph node metastasis away from the feeding vessels has also been reported, additional care should be taken. Park et al. reported that the most frequent site of lymph node metastasis from cecal cancer is in the region of the ileocolic artery; however, 10% of the metastases are also found in the feeding region of the right colic artery, which requires attention when performing ileocecal resection for cecal cancer [22]. In addition, even tumors near the hepatic flexure region had metastasized to the lymph nodes fed by the ileocolic artery in some cases, although this was observed at a low rate of 1.4%; thus, right hemicolectomy should be considered in the treatment of such tumors. Since approximately 10% of the lymph node metastases to the right colic artery are derived from the transverse colon cancer near the hepatic flexure region, the excision range of the intestinal tract should be carefully considered.

15.2.2 Lymph Node Dissection for Rectal Cancer

The survival rate of those who undergo rectal cancer surgery is worse than that of those who undergo colon cancer surgery [16]. A higher incidence of local recurrence in post-rectal than in post-colon cancer surgery patients contributes to the poor treatment outcome. It is therefore critical to reduce the incidence of local recurrence in the surgical treatment of rectal cancer. In conventional surgery that had previously been performed in Europe and the USA, rectal excision was conducted with blunt dissection of the region surrounding the rectum, and a high incidence of local recurrence, approximately 20%, was reported. Heald et al. showed that a causative factor of local recurrence in post-rectal cancer surgery patients was the existence of residual cancer micrometastases in the mesorectum on the anal side, that is, micrometastases that originated from tumors that were not excised during anterior resection.

Cancer invasion (distal tumor spread [DTS]) in the mesorectum is an important factor in local recurrence. In order to remove it, total mesorectal excision (TME) to completely excise the mesorectum is crucial, as stated by Heald [23, 24]. Scott analyzed the resected specimen of rectal cancer and reported that invasions in the mesorectum were noted in 25% of cases [25] at locations 1–3 cm away from the tumors in the direction of the anus. The combination of TME and preoperative adjuvant chemotherapy and radiotherapy is widely performed in Europe and the USA, and its benefit in reducing local recurrence has been shown in numerous studies [26, 27].

TME involves complete resection of the mesorectum when rectal cancer has spread to the anal side. In the treatment of low rectal cancer, complete excision of the mesorectum to the region immediately above the anal tube is required. However, in the treatment of rectal cancer with higher lesions, particularly in that of high

rectal cancer, it is not considered necessary to extend the excision of the mesorectum to the anal tube. Besides, completely excising and anastomosing the mesorectum in the treatment of high rectal cancer could lead to poor blood circulation in the rectal wall and increase the risk of suture failure. In these cases, excision of the mesorectum from the tumor to a point on the anal side (2–4 cm) is adequate, with no need to completely excise the mesorectum to the area immediately above the anal tube. This procedure, in which the mesorectum is completely excised with the length from the tumor to a point some distance away on the anal side, is referred to as tumor-specific mesorectal excision (TMSE) and is different from TME [28]. However, in the treatment of low rectal cancer, both TME and TMSE actually follow almost the same procedure.

Before lymph node dissection, it is necessary to determine the dissection range of the intestinal tract. The NCCN guidelines recommend that mesorectal excision be performed with a resection margin of 4–5 cm from the anal margin. In rectal cancers that develop at sites less than 5 cm away from the anal verge (AV), a resection margin of 1–2 cm is allowed, but the confirmation of negative resection margins by intraoperative rapid diagnosis is required [21]. In Japan, it is recommended to secure the following resection margins on the anal side in the treatment of rectal cancers: 3 cm in excision of the intestinal tract and the mesorectum in the case of upper rectal cancer and 2 cm in the case of lower rectal cancer [16].

Regarding the removal of lesions on the proximal side, the lymph nodes around the root of the inferior mesenteric artery (IMA) that feeds the cancer must be excised. In excising the IMA, the following two methods can be used: the first method is referred to as the high tie, in which the IMA is cut at a point near the aorta, a site proximal to the bifurcation of the left colic artery, and the second method is referred to as the low tie, in which the IMA is cut at a site distal to the origin of the left colic artery (Fig. 15.1) [29]. Since a low tie preserves the left colic artery, there is better blood flow compared with cases that underwent a high tie. However, Rutegard et al. reported that among 818 cases that underwent a high tie, suture failure was noted in 81 cases (9.9%). This rate was comparable to the 108 patients (9.8%) who had suture failure among 1101 patients who underwent a low tie [30]. Low tie is potentially insufficient in dissection because the IMA is not cut at the root; however, by dissecting the lymph nodes around the IMA root while the blood vessels are preserved, D3 lymph node dissection is possible. D3 lymph node dissection associated with a low tie requires a longer surgical time, but is not considered any different from a high tie in terms of treatment outcomes, including complications [31]. When there are concerns about blood flow at the anastomotic site, a low tie can be used to manage the blood vessels.

15.2.3 Significance of Lymph Node Metastasis that Remains After Radiotherapy

In the treatment of locally advanced rectal cancer, preoperative chemoradiotherapy (CRT) is often performed to reduce local recurrence. In cases where lymph node

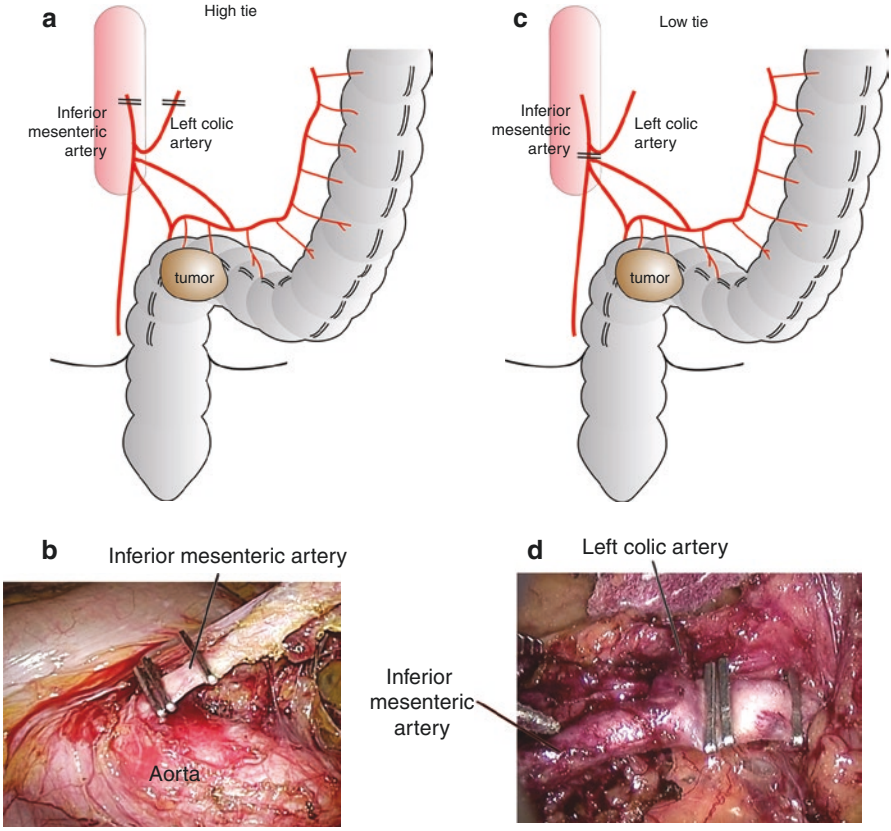

Fig. 15.1 Two types of lymph node dissection around the root of the inferior mesenteric artery (IMA). "High tie" means dissection of the IMA at the root (**a**, **b**), and "low tie" means dissection of the superior rectal artery after the first blanching of the IMA with dissection of lymph nodes around the root of the IMA (**c**, **d**)

metastases are seen before CRT, those metastases can disappear after CRT. According to Fernandez et al., in cases in which no lymph node metastases were found in the resected specimen, about half of the lymph nodes showed signs that metastases had been present before CRT, in terms of fibrosis or mucus production under pathological assessment of resected specimen [32].

In addition, dissection of 12 or more lymph nodes is important in standard surgery for colorectal cancer; however, the number of lymph nodes that need to be removed is lower after CRT [33, 34]. Since some reports also stated that the number of lymph nodes removed is not related to the prognosis in cases treated with CRT [35, 36], the necessary number of lymph nodes to be removed is controversial.

Surgical removal, including lymph node dissection, is generally performed after tumor shrinkage using CRT, although some medical institutions suggest a "wait and see" approach [37, 38]. Unlike standard methods, surgery associated with lymph node dissection is not performed for patients with a clinical complete response

(cCR); instead, they are first followed up or receive only local excision and then are carefully followed up. This method achieved a favorable outcome with a 5-year survival rate of 91%; however, among the 28 patients who had local recurrence, 2 were not able to undergo salvage surgery [39].

Sprenger et al. reported residual lymph node metastases in 25% of cases that responded to CRT and achieved ypT1/T2, and even in cases with achieved ypT0, although they were small in number. Therefore, in such patients, local excision with follow-up observation allowed the cancer to remain [40]. If lymph node metastasis was identified before surgery, the risk of residual disease would be reduced. However, accurate preoperative diagnosis of metastasis to the mesorectal lymph nodes is difficult even with magnetic resonance imaging (MRI) [41]; thus, caution is needed in performing follow-up observation with local excision in cases that respond to pretreatment.

15.3 Metastasis to Lateral Pelvic Lymph Nodes

The systematic resection of rectal cancer began with a report by Miles in 1908 on abdominoperineal resection of the rectum [42]. The lymph flows outside the rectal wall along the arteries. The main feeding vessels of the rectum are the superior rectal artery, middle rectal artery, and inferior rectal artery, and these arteries form many anastomoses both inside and outside the rectal tube. Thus, the blood vessels running along these arteries also form many anastomoses and allow for the organization of the lymph vessel network. The pathways of lymphatic flow of the rectal segment are broadly categorized into the ascending, lateral, and descending lymph vessels (Fig. 15.2) [43].

The currently accepted explanation of lateral lymph flow is given in the study by Senba et al. on rectal lymph flow using a fetal model [44]. Based on these studies, dissection was performed after considering the rectal lymph flow. In addition, in the USA, the expanded dissection of lymph nodes, including those along the lateral lymph flow, came into use in the 1950s. However, Stearns et al. reported, in 1959, that although expanded dissection improved the survival rate, it also increased the incidence of bleeding, complications, and adverse events. Since then, the effectiveness of lateral dissection has been unclear, and it remains so in both Europe and the USA [45].

The recurrence rate of rectal cancer is higher than that of colon cancer, and one of the known factors is the high local recurrence rate after surgery for rectal cancer [46]. In order to address the issue of local recurrences after rectal surgery, the concept of TME was suggested by Heald et al. in 1982 [23]. They proposed to remove the rectum and mesorectum without destroying the rectum-specific fascia. In the late 1980s, first in a Swedish trial and then in large-scale randomized comparative trials, significantly reduced local recurrence rates were reported in the groups that received preoperative radiotherapy compared with those that received surgery alone [26]. A Dutch trial also reported that preoperative irradiation significantly improved local recurrence rates and showed increased effectiveness when used in

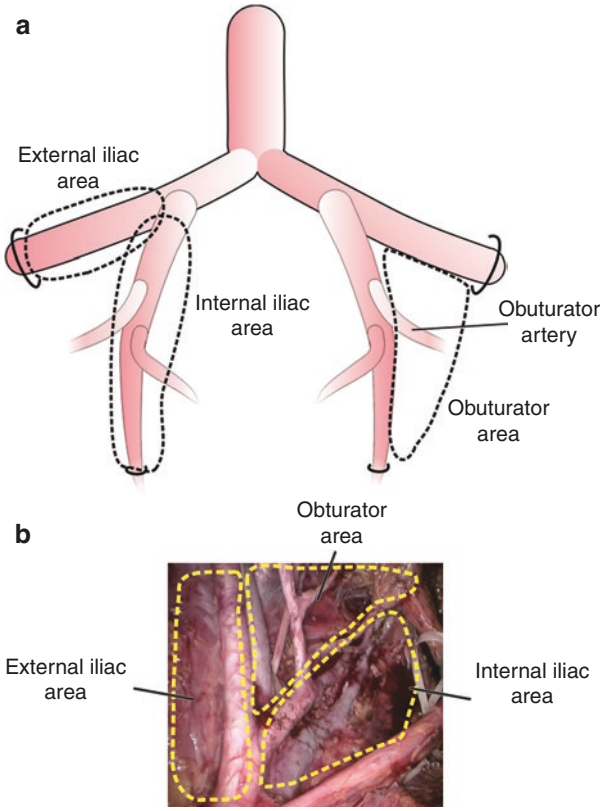

Fig. 15.2 Lateral lymph node dissection. (**a**) Schema of lateral pelvic lymph nodes. Nodes in the internal iliac area are classified as the regional lymph nodes of rectal cancer in the TNM classification, and those in the internal iliac and obturator area are classified as regional in the JSCCR classification. (**b**) Laparoscopic view after dissection of the lateral pelvic lymph nodes (left side)

combination with TME [47]. In recent years, long-term irradiation has been in widespread use because it is more effective at tumor shrinkage than short-term irradiation and can be expected to improve the anus preservation rate. CRT, i.e., combined radiation therapy and chemotherapy based on fluorouracil, is the current standard treatment method.

In Japan, reports in the 1970s showed that lateral lymph node dissection significantly improved survival rates and reduced local recurrence rates [48, 49]. Nerve-preserving lateral lymph node dissection was also developed thereafter, and the effectiveness of this procedure was supported by successive reports; this led to a unique treatment policy in our country, which is different from the policy in Europe and the USA. Specifically, the standard procedure for advanced low rectal cancer is TME or tumor-specific mesorectal excision, to which lateral lymph node dissection can be added.

The guidelines by the following institutions are widely known: the NCCN in the USA, the National Institute for Health and Clinical Excellence (NICE) in the UK,

and the European Society for Medical Oncology (ESMO) in Europe. Every guideline employs the TNM classification of the UICC or the American Joint Committee on Cancer (AJCC) as staging criteria but deals with the lateral lymph nodes in a manner different from the guidelines in Japan [50]. In the Japanese guidelines, the internal iliac lymph nodes, and obturator lymph nodes, are described as the regional lymph nodes of rectal cancer; however, the lesions in the external and common iliac lymph nodes are described as distant metastases that are classified as M1 [51, 52].

According to data on lateral dissection in Japan, patients with obvious lateral lymph node metastasis undergo lateral dissection (therapeutic dissection), which results in a 5-year survival rate of 40% [53]. The efficacy of dissection in patients with lateral lymph node metastasis has also been reported by Akiyoshi et al. [54]. They conducted a retrospective analysis of survival rates with the data from 5789 patients who underwent lateral dissection. In that study, patients with lateral lymph node metastasis were divided into two groups, those with metastasis to the internal iliac lymph nodes and those with metastasis to other lateral lymph nodes, and their prognoses were analyzed. Metastasis to the internal iliac lymph nodes was noted in 7.1% of patients, and that to the lateral lymph nodes was found in 4.2%. The 5-year cumulative survival rate in patients with internal iliac lymph node metastasis was 45%, and the rate in those with lateral lymph node metastasis was 29%, significantly better outcomes than the rate of 24% seen in the cases of stage IV cancer. Based on these results, the authors of the study concluded that lateral lymph node metastasis does not have the same clinical significance as distant metastasis but should instead be regarded as regional lymph node metastasis.

Meanwhile, the circumstances are different when lateral dissection is performed in cases with no obvious lateral lymph node metastasis (prophylactic dissection). To investigate these cases, the JCOG0212 study was conducted by the Japan Clinical Oncology Group (JCOG) Colorectal Cancer Study Group. This was a randomized comparative study to investigate mesorectal excision (ME) alone compared with ME combined with lateral dissection in cases of stage II and III cancers located below the peritoneal reflection. The results showed that the rate of lateral lymph node metastasis in the group undergoing lateral dissection was 7.4%. Compared with the group undergoing ME, the group undergoing lateral dissection had a significantly longer surgical time (360 min vs. 254 min, $p < 0.0001$) and a larger amount of intraoperative bleeding (576 mL vs. 337 mL, $p < 0.0001$) [15]. The frequency of postoperative complications of grade 3/4 was 21.7% in the group with lateral dissection and 16.0% in the group with ME alone, with no significant difference ($p = 0.07$). No differences were noted between the groups in the incidence of sexual dysfunction (79% vs. 68%), early postoperative urinary disorder (59% vs. 58%), or late postoperative urinary disorder (7% vs. 5%). Reports on the long-term outcomes are urgently needed. Ishihara et al. divided 1238 cases with T2–T4 N0 rectal cancers into two groups according to the presence or absence of lateral dissection with matched data. They reported that in the analysis of cancer-specific survival (CSS), an improvement of CSS with lateral dissection was noted in women [55].

In Japan, there are guidelines for the treatment of colorectal cancer [16] in addition to the Japanese classification [56] for staging. The application of lateral

dissection is described as rectal cancers with an inferior border located beyond the peritoneal reflection reaching the anal area and with invasion through the proper muscular layer. Because the lateral lymph nodes are classified as regional lymph nodes in Japan, the aim is to control the disease using systematic dissection, similar to the upper lymph nodes.

The guidelines also include a description of preoperative CRT, in which preoperative CRT is performed to increase the local control rate and improve the survival rate in rectal cancer, as well as to improve the preservation rate of the anal sphincter muscle and the rate of curative surgery. No clear conclusion has been drawn about whether preoperative CRT allows for the omission of lateral dissection. However, Nagawa et al. conducted a small-scale randomized controlled trial (RCT) and reported that a comparison of preoperative CRT cases divided into a group with TME and a group with TME and lateral dissection resulted in a significantly increased incidence of dysfunction, with no increased oncological improvement in the group that underwent lateral dissection [57]. It has been more than 50 years since the first report on the lateral lymph flow of the rectum and lateral dissection. The approach for lateral dissection in the treatment of advanced low rectal cancer is different between Western countries and Japan, including multidisciplinary therapy focusing on preoperative CRT or surgical treatment with lateral dissection in the center. A solution is required to determine how multidisciplinary therapy should be combined with lateral dissection, along with further improvements in treatment outcomes.

15.4 Metastasis to Other Lymph Nodes

Approximately 20% of patients with colorectal cancer already have metastasis when they are diagnosed [58]. Because of recent advancements in systemic chemotherapy, the survival time of patients with stage IV colorectal cancer has been extended. Furthermore, patients with lung or liver metastasis undergo resection as first-line treatment if R0 resection is possible [16]. Colorectal cancer with metastasis to non-regional lymph nodes has been categorized as stage IV [59, 60]; however, resection for these cases has demonstrated no obvious beneficial treatment effects so far [16]. This section describes metastasis to the para-aortic lymph nodes from colorectal cancer and metastasis to the inguinal lymph nodes from rectal cancer.

Among colorectal cancers, when considering colon cancer, the blood and lymph vessel networks are relatively simple. On the other hand, when considering rectal cancer, the following lymph flows exist: the flow in the vertical direction along the IMA to the para aorta; the flow in the lateral direction into the internal iliac artery; and, in the case of lesions near the anal tube, the flow from around the anal tube through the subcutaneous perineal region into the superficial inguinal lymph nodes [61, 62]. In Japan, the current standard site of dissection is the roots of the feeding vessels in terms of the effectiveness of dissection and the preservation of function, except for lateral lymph node metastasis from advanced low rectal cancer [16]. The major guidelines in Europe and the USA generally recommend to cut the blood and

lymph vessels at the roots of the feeding vessels [21, 63], and none recommend performing lymph node dissection at more proximal sites.

In the current guidelines used in Japan and other countries, the para-aortic lymph nodes in colorectal cancer and the inguinal lymph node in rectal cancer are considered non-regional lymph nodes, and the significance of their dissection is not described in detail. Metastases found in these non-regional lymph nodes are thought to indicate a poor prognosis [61, 64], and referral for systemic chemotherapy is the standard of care. However, in recent years, where multidisciplinary therapy has come to be performed, the usefulness of surgical removal has been reported in the treatment of isolated non-regional lymph node metastases that are not associated with other organ metastases.

15.4.1 Para-aortic Lymph Nodes

The frequency of para-aortic lymph node metastasis from colorectal cancer is 1–2% [65]. According to the results of research conducted in the 1980s and 1990s, there is no improvement in survival rate after para-aortic lymph node dissection, and the procedure is highly invasive. Under normal circumstances, no prophylactic para-aortic lymph node dissection is performed today [66, 67]. However, after 2000, several studies have reported favorable results [65, 68–70].

In a study conducted on patients who underwent surgical removal of synchronous para-aortic lymph node metastases that were not associated with other organ metastases, in every case, the dissection range was defined as that from below the renal vein to the bilateral iliac vessels [71–74]. No cases of operative mortality were reported, and postoperative complications (urinary disorder, ileus, wound infection, and suture failure) occurred in 7.8–15% of cases [72, 74]. Preoperative adjuvant chemotherapy was administered to 19–25% of the patients [71, 73, 74]. The 5-year overall survival rate was 22.7–33.9%, and the 5-year disease-free survival rate was 17.6–26.5% [71, 72]. The number of para-aortic lymph node metastases was a significant prognostic factor for overall survival [73, 74].

A study was conducted on patients undergoing surgical removal of metachronous para-aortic lymph node metastases that were not associated with other organ metastases; the results of the study showed that the median disease-free interval was 14–23 months [69, 70]. No deaths resulting from surgery were reported, and 28–33% of patients experienced postoperative complications. Preoperative adjuvant chemotherapy was administered to 20% of the patients [69]. Comparisons between the patients undergoing surgical removal, chemotherapy, and CRT showed significantly improved overall survival in those who underwent surgical removal [69, 70]. The overall survival of the patients undergoing resection was 34–40 months, and that of the patients not undergoing resection was 3–14 months. After curative surgery for para-aortic lymph node metastases, 56–80% of the patients experienced another recurrence. Favorable prognostic factors included a long disease-free interval, a tumor diameter of less than 5 cm, para-aortic lymph node metastases located below the renal vein, a well-differentiated primary colorectal tumor, and R0 resection [69, 70].

Another study on cases of CRT for metachronous para-aortic lymph node metastases resulted in a median disease-free survival of 13–30 months [75–77]. The occurrence of significant adverse events was rare. The evaluation of efficacy according to the response evaluation criteria in solid tumors (RECIST) [78] showed that a complete response (CR) was achieved in 43–100% of the patients, a partial response (PR) in 27–57%, and stable disease (SD) in 13%. The median overall survival was 37–41 months. After CRT, 60–68% of the patients developed another recurrence. The favorable prognostic factors included a long disease-free interval, a good response to treatment, and a small gross tumor volume.

The volume of the evidence is limited, and the majority of previous studies were retrospective studies with a small number of participants. However, it has been reported that among patients with para-aortic lymph node metastases, and in comparison with patients who received no resection, those receiving R0 resection were found to have a significantly better prognosis [68–70], with the incidence of postoperative complications within an acceptable range. Meanwhile, with a high postoperative recurrence rate, the prognosis of patients with para-aortic lymph node metastases is unfavorable, and thus, chemotherapy after para-aortic lymph node metastases dissection is essential. Depending on the general condition of the patient, CRT for para-aortic lymph node metastases could be a useful treatment option. Improved selection of candidates for para-aortic lymph node metastasis dissection is a subject for future research.

15.4.2 Inguinal Lymph Nodes

Inguinal lymph node metastasis from colorectal cancer is rare [61]. The development of inguinal lymph node metastases is thought to occur either because the primary tumor interrupts the vertical lymphatic channels, resulting in retrograde metastasis, or because a metastasis develops from recurrent lesions within the pelvis or in the perineal regions [43]. Inguinal lymph node metastasis usually occurs in association with other metastases, such as distant metastasis to the liver or lung or recurrent metastasis within the pelvis, and is indicative of severe systemic disease, as well as being associated with a poor prognosis [61]. However, some reports have suggested that isolated inguinal lymph node metastasis that is not associated with other organ metastases should be considered separately [61, 79, 80]. Although these results were from case series with a small number of patients, the patients had relatively favorable prognoses after dissection of the isolated inguinal lymph node metastasis.

In the anal area below the dentate line, lymph flow originates around the anal tube and passes through the subcutaneous perineal region into the superficial inguinal lymph nodes [61, 62]. When patients with lesions close to the dentate line are treated, the inguinal lymph nodes can be regarded as local lymph nodes instead of non-regional lymph nodes, in the same manner as the treatment of those with anal cancer [79]. In contrast, other studies have reported that, even if the lesion is isolated, the prognosis of patients with inguinal lymph node metastases was unfavorable [81]. In a retrospective study of 863 patients with rectal cancer, metachronous

isolated inguinal lymph node metastases were seen in 5 patients, and they all had poor prognoses with a mean survival of 14.8 months. However, all of the patients had para-rectal lymph node metastases, and this was thought to be responsible for the unfavorable prognosis [79].

Insufficient evidence is available to support the surgical removal of isolated inguinal lymph node metastases from rectal cancer that are not associated with other distant metastases; thus, the issue must be studied in the future.

15.5 Lymph Node Metastasis from T1 Colorectal Cancer

As a therapeutic measure for early-stage colorectal cancer, endoscopic resection has come into widespread use because of the improved safety resulting from advancements in the technique and its less invasive characteristics. Complete resection of tumors is endoscopically possible; however, concern remains about the possibility of residual lymph node metastasis. If lesions are associated with lymph node metastasis, removal of the intestinal tract with lymph node dissection is required. This situation is considerably different from that where treatment can be completed with endoscopic resection, in terms of the degree of surgical invasion or problems with postoperative dysfunction. Therefore, it is critical to determine whether the lesion could be associated with lymph node metastasis, and if it is, what degree of risk is involved in the condition.

Digestive Endoscopy published two reviews in 2016 about T1 colorectal cancers that were resected endoscopically [1, 2]. According to these reviews, the frequency of lymph node metastasis in Tis cancers was 0%, while that of T1 cancers was 6.8–17.8%. These articles also included an analysis of the risk factors for lymph node metastasis, and accumulation of such literature-based evidence has allowed relevant guidelines to be prepared in each country and region.

According to the definition used in the Japanese guidelines for the treatment of colorectal cancer [3], there is almost no risk of lymph node metastasis [4] in patients with the following clinical findings: intramucosal cancer, pTis cancer, submucosal cancer invading the submucosal layer to a depth of less than 1000 μm, and pT1a cancer. Endoscopic resection is performed for patients who have these conditions as well as a tumor that is of a size and location suitable for the procedure. Surgical resection is thus performed for cancers that have an invasion depth of 1000 μm or more. When cancer cells are detected in the vertical margin of a resected specimen collected during endoscopic resection, surgical removal of the intestinal tract is also performed. The risk factors for regional lymph node metastasis from pT1 cancer are reported as follows: deep invasion into the submucosal layer [4], histologically poorly differentiated adenocarcinoma, signet ring cell cancer, mucinous cancer [5], presence of a differentiated area or mucinous nodule at the invasive front, tumor budding, and vascular invasion [5, 6]. Therefore, in patients diagnosed with pT1 cancers using endoscopic resection and pathological analysis, removal of the intestinal tract together with lymph node dissection should be considered, if any of the following factors are found: (1) sm invasion depth ≥ 1000 μm; (2) vascular invasion; (3) histologically poorly differentiated adenocarcinoma, signet ring cell

cancer, or mucinous cancer; and (4) tumor budding at the invasive front (budding grade 2/3). However, the rate of lymph node metastasis was 12.5% in the cases with sm invasion depth of 1000 μm or more, and no metastases were noted in nearly 90% of cases. Thus, instead of consistently performing additional resection in all of these cases, the procedure should be fully discussed on an individual basis.

In the definition provided by the ESMO guidelines [7], surgical removal of the intestinal tract should be considered if a resected colorectal polyp has the following risk factors: pathological findings of cancer with sm invasion (pT1), vascular invasion, histologic grade 3, level 4 invasion (beyond the intestinal wall at the base of the polyp into the sm layers), and resection margin positivity.

The NCCN guidelines (ver. 2.2016) recommend colon resection associated with regional lymph node dissection when a malignant colonic polyp or a polyp with cancer (pT1) invading the sm layers fits the following criteria: assessment of the specimens obtained from piecemeal resection or the resection margin is impossible or unfavorable histologic characteristics are noted (including any of the characteristics of grade 3 or 4, vascular invasion positivity, or resection margin positivity) (https://www.nccn.org/professionals/physician_gls/pdf/colon.pdf). The guidelines also recommend transperitoneal rectal resection when a malignant rectal polyp fits the following criteria: assessment of the specimens obtained from piecemeal resection or the resection margin is inconclusive or unfavorable histologic characteristics are noted (polyps of more than 3 cm, histologic grade 3, vascular invasion positivity, resection margin positivity, or sm 3 invasion) (https://www.nccn.org/professionals/physician_gls/pdf/rectal.pdf).

Criteria for additional resection including resection margin positivity, histological type, and vascular invasion positivity are common among the different guidelines. However, invasion depth and tumor budding are adopted only by the Japanese guidelines, which are unique to our country. A multivariate analysis by Debove et al. included 73 patients who underwent TME for rectal cancer with submucosal invasion and showed that submucosal invasion was a risk factor for lymph node metastasis. Only vascular invasion and severe budding were independent risk factors. The results of this study suggest that the risk factors for lymph node metastasis might need to be classified differently for cases of colon and rectal cancers. A report by Nakadoi et al. also stated that the frequency of lymph node metastasis was as low as 1.2% in cases of T1 colorectal cancer that were not associated with risk factors such as histological types, vascular invasion, and tumor budding. They added that the low frequency of lymph node metastasis was not related to submucosal invasion depth, and it has been suggested that submucosal invasion depth should be excluded from the risk factors. As described above, new evidence has been reported, and the existing guidelines need to be continuously modified on the basis of emerging evidence.

15.6 Summary

Distant metastases to the liver or lung are not treated using prophylactic dissection; they are considered for surgical removal only after confirming the presence of metastases. In the case of lymph node metastasis, regardless of whether metastasis

is present, the regional lymph nodes are systematically removed. The location of the lymph nodes and the extent of their removal for an optimal response have been much discussed in the history of surgery, and considerable research in this field is still being conducted today. If lesions are removed with too wide margins, unnecessary complications can occur with no additional survival benefit. In contrast, incomplete lymph node dissection might leave residual cancer cells, which could cause disease recurrence in lymph nodes or local sites. Along with progress in imaging modalities, such as high-resolution MRI, computed tomography (CT), and positron emission tomography (PET), the accuracy of diagnosing the stage of cancer progression and detecting the presence of lesions in lymph nodes has been improved. It is critical that these methods are fully utilized so that surgeons can perform necessary and sufficient lymph node dissection for a true definitive cure of cancer.

References

1. Cady B. Lymph node metastases. Indicators, but not governors of survival. Arch Surg. 1984;119:1067–72.
2. Chang GJ, Rodriguez-Bigas MA, Skibber JM, Moyer VA. Lymph node evaluation and survival after curative resection of colon cancer: systematic review. J Natl Cancer Inst. 2007;99:433–41.
3. Tepper JE, O'Connell MJ, Niedzwiecki D, Hollis D, Compton C, Benson AB 3rd, Cummings B, Gunderson L, Macdonald JS, Mayer RJ. Impact of number of nodes retrieved on outcome in patients with rectal cancer. J Clin Oncol. 2001;19:157–63.
4. Kanemitsu Y, Komori K, Ishiguro S, Watanabe T, Sugihara K. The relationship of lymph node evaluation and colorectal cancer survival after curative resection: a multi-institutional study. Ann Surg Oncol. 2012;19:2169–77.
5. Kotake K, Honjo S, Sugihara K, Hashiguchi Y, Kato T, Kodaira S, Muto T, Koyama Y. Number of lymph nodes retrieved is an important determinant of survival of patients with stage II and stage III colorectal cancer. Jpn J Clin Oncol. 2012;42:29–35.
6. Greenson JK, Isenhart CE, Rice R, Mojzisik C, Houchens D, Martin EW Jr. Identification of occult micrometastases in pericolic lymph nodes of Duke's B colorectal cancer patients using monoclonal antibodies against cytokeratin and CC49. Correlation with long-term survival. Cancer. 1994;73:563–9.
7. Jeffers MD, O'Dowd GM, Mulcahy H, Stagg M, O'Donoghue DP, Toner M. The prognostic significance of immunohistochemically detected lymph node micrometastases in colorectal carcinoma. J Pathol. 1994;172:183–7.
8. Rosenberg R, Hoos A, Mueller J, Baier P, Stricker D, Werner M, Nekarda H, Siewert JR. Prognostic significance of cytokeratin-20 reverse transcriptase polymerase chain reaction in lymph nodes of node-negative colorectal cancer patients. J Clin Oncol. 2002;20:1049–55.
9. Peschaud F, Benoist S, Julie C, Beauchet A, Penna C, Rougier P, Nordlinger B. The ratio of metastatic to examined lymph nodes is a powerful independent prognostic factor in rectal cancer. Ann Surg. 2008;248:1067–73.
10. Ceelen W, Van Nieuwenhove Y, Pattyn P. Prognostic value of the lymph node ratio in stage III colorectal cancer: a systematic review. Ann Surg Oncol. 2010;17:2847–55.
11. Lu YJ, Lin PC, Lin CC, Wang HS, Yang SH, Jiang JK, Lan YT, Lin TC, Liang WY, Chen WS, Lin JK, Chang SC. The impact of the lymph node ratio is greater than traditional lymph node status in stage III colorectal cancer patients. World J Surg. 2013;37:1927–33.
12. Ozawa T, Ishihara S, Nishikawa T, Tanaka T, Tanaka J, Kiyomatsu T, Hata K, Kawai K, Nozawa H, Kanazawa T, Kazama S, Yamaguchi H, Sunami E, Kitayama J, Watanabe T. Prognostic significance of the lymph node ratio in stage IV colorectal cancer patients who have undergone curative resection. Ann Surg Oncol. 2015;22:1513–9.

13. Zhang MR, Xie TH, Chi JL, Li Y, Yang L, Yu YY, Sun XF, Zhou ZG. Prognostic role of the lymph node ratio in node positive colorectal cancer: a meta-analysis. Oncotarget. 2016;7:72898–907.
14. Hohenberger W, Weber K, Matzel K, Papadopoulos T, Merkel S. Standardized surgery for colonic cancer: complete mesocolic excision and central ligation—technical notes and outcome. Colorectal Dis. 2009;11:354–64. discussion 364–355
15. Fujita S, Akasu T, Mizusawa J, Saito N, Kinugasa Y, Kanemitsu Y, Ohue M, Fujii S, Shiozawa M, Yamaguchi T, Moriya Y. Postoperative morbidity and mortality after mesorectal excision with and without lateral lymph node dissection for clinical stage II or stage III lower rectal cancer (JCOG0212): results from a multicentre, randomised controlled, non-inferiority trial. Lancet Oncol. 2012;13:616–21.
16. Watanabe T, Itabashi M, Shimada Y, Tanaka S, Ito Y, Ajioka Y, Hamaguchi T, Hyodo I, Igarashi M, Ishida H, Ishihara S, Ishiguro M, Kanemitsu Y, Kokudo N, Muro K, Ochiai A, Oguchi M, Ohkura Y, Saito Y, Sakai Y, Ueno H, Yoshino T, Boku N, Fujimori T, Koinuma N, Morita T, Nishimura G, Sakata Y, Takahashi K, Tsuruta O, Yamaguchi T, Yoshida M, Yamaguchi N, Kotake K, Sugihara K. Japanese Society for Cancer of the Colon and Rectum (JSCCR) Guidelines 2014 for treatment of colorectal cancer. Int J Clin Oncol. 2015;20:207–39.
17. West NP, Morris EJ, Rotimi O, Cairns A, Finan PJ, Quirke P. Pathology grading of colon cancer surgical resection and its association with survival: a retrospective observational study. Lancet Oncol. 2008;9:857–65.
18. West NP, Hohenberger W, Weber K, Perrakis A, Finan PJ, Quirke P. Complete mesocolic excision with central vascular ligation produces an oncologically superior specimen compared with standard surgery for carcinoma of the colon. J Clin Oncol. 2010;28:272–8.
19. Paquette IM, Madoff RD, Sigurdson ER, Chang GJ. Impact of proximal vascular ligation on survival of patients with colon cancer. Ann Surg Oncol. 2018;25:38–45.
20. Kotake K, Mizuguchi T, Moritani K, Wada O, Ozawa H, Oki I, Sugihara K. Impact of D3 lymph node dissection on survival for patients with T3 and T4 colon cancer. Int J Color Dis. 2014;29:847–52.
21. Nelson H, Petrelli N, Carlin A, Couture J, Fleshman J, Guillem J, Miedema B, Ota D, Sargent D. Guidelines 2000 for colon and rectal cancer surgery. J Natl Cancer Inst. 2001;93:583–96.
22. Park IJ, Choi GS, Kang BM, Lim KH, Jun SH. Lymph node metastasis patterns in right-sided colon cancers: is segmental resection of these tumors oncologically safe? Ann Surg Oncol. 2009;16:1501–6.
23. Heald RJ, Husband EM, Ryall RD. The mesorectum in rectal cancer surgery—the clue to pelvic recurrence? Br J Surg. 1982;69:613–6.
24. Heald RJ, Ryall RD. Recurrence and survival after total mesorectal excision for rectal cancer. Lancet. 1986;1:1479–82.
25. Scott N, Jackson P, al-Jaberi T, Dixon MF, Quirke P, Finan PJ. Total mesorectal excision and local recurrence: a study of tumour spread in the mesorectum distal to rectal cancer. Br J Surg. 1995;82:1031–3.
26. Swedish Rectal Cancer Trial, Cedermark B, Dahlberg M, Glimelius B, Påhlman L, Rutqvist LE, Wilking N. Improved survival with preoperative radiotherapy in resectable rectal cancer. N Engl J Med. 1997;336:980–7.
27. Kapiteijn E, Kranenbarg EK, Steup WH, Taat CW, Rutten HJ, Wiggers T, van Krieken JH, Hermans J, Leer JW, van de Velde CJ. Total mesorectal excision (TME) with or without preoperative radiotherapy in the treatment of primary rectal cancer. Prospective randomised trial with standard operative and histopathological techniques. Dutch ColoRectal Cancer Group. Eur J Surg. 1999;165:410–20.
28. Lowry AC, Simmang CL, Boulos P, Farmer KC, Finan PJ, Hyman N, Killingback M, Lubowski DZ, Moore R, Penfold C, Savoca P, Stitz R, Tjandra JJ. Consensus statement of definitions for anorectal physiology and rectal cancer: report of the Tripartite Consensus Conference on Definitions for Anorectal Physiology and Rectal Cancer, Washington, D.C., May 1, 1999. Dis Colon Rectum. 2001;44:915–9.

29. Corder AP, Karanjia ND, Williams JD, Heald RJ. Flush aortic tie versus selective preservation of the ascending left colic artery in low anterior resection for rectal carcinoma. Br J Surg. 1992;79:680–2.
30. Rutegard M, Hemmingsson O, Matthiessen P, Rutegard J. High tie in anterior resection for rectal cancer confers no increased risk of anastomotic leakage. Br J Surg. 2012;99:127–32.
31. Kobayashi M, Okamoto K, Namikawa T, Okabayashi T, Araki K. Laparoscopic lymph node dissection around the inferior mesenteric artery for cancer in the lower sigmoid colon and rectum: is D3 lymph node dissection with preservation of the left colic artery feasible? Surg Endosc. 2006;20:563–9.
32. Fernandez-Acenero MJ, Granja M, Sastre J, Garcia-Paredes B, Estrada L. Prognostic significance of tumor regression in lymph nodes after neoadjuvant therapy for rectal carcinoma. Virchows Arch. 2016;468:425–30.
33. Okada K, Sadahiro S, Suzuki T, Tanaka A, Okamura H, Kamijo A. Effect of chemoradiotherapy (CRT) for rectal cancer on the lymph nodes (LNs): exploration of the number of retrieved LNs, number of metastatic LNs, and the size of LNs. J Clin Oncol. 2012;30:651.
34. Hall MD, Schultheiss TE, Smith DD, Fakih MG, Kim J, Wong JY, Chen YJ. Impact of total lymph node count on staging and survival after neoadjuvant chemoradiation therapy for rectal cancer. Ann Surg Oncol. 2015;22(Suppl 3):S580–7.
35. Damin DC, Rosito MA, Contu PC, Tarta C, Ferreira PR, Kliemann LM, Schwartsmann G. Lymph node retrieval after preoperative chemoradiotherapy for rectal cancer. J Gastrointest Surg. 2012;16:1573–80.
36. Ishihara S, Fukushima Y, Akahane T, Horiuchi A, Shimada R, Nakamura K, Aoyagi Y, Hayama T, Yamada H, Nozawa K, Matsuda K, Hashiguchi Y, Watanabe T. Number of lymph nodes in rectal cancer is correlated with response to preoperative chemoradiotherapy but is not associated with patient survival. Hepato-Gastroenterology. 2014;61:1000–7.
37. Habr-Gama A, Perez RO, Proscurshim I, Campos FG, Nadalin W, Kiss D, Gama-Rodrigues J. Patterns of failure and survival for nonoperative treatment of stage c0 distal rectal cancer following neoadjuvant chemoradiation therapy. J Gastrointest Surg. 2006;10:1319–28. discussion 1328–1319
38. Li J, Liu H, Yin J, Liu S, Hu J, Du F, Yuan J, Lv B, Fan J, Leng S, Zhang X. Wait-and-see or radical surgery for rectal cancer patients with a clinical complete response after neoadjuvant chemoradiotherapy: a cohort study. Oncotarget. 2015;6:42354–61.
39. Habr-Gama A, Gama-Rodrigues J, Sao Juliao GP, Proscurshim I, Sabbagh C, Lynn PB, Perez RO. Local recurrence after complete clinical response and watch and wait in rectal cancer after neoadjuvant chemoradiation: impact of salvage therapy on local disease control. Int J Radiat Oncol Biol Phys. 2014;88:822–8.
40. Sprenger T, Rothe H, Conradi LC, Beissbarth T, Kauffels A, Kitz J, Homayounfar K, Wolff H, Strobel P, Ghadimi M, Wittekind C, Sauer R, Rodel C, Liersch T. Stage-dependent frequency of lymph node metastases in patients with rectal carcinoma after preoperative chemoradiation: results from the CAO/ARO/AIO-94 trial and from a comparative prospective evaluation with extensive pathological workup. Dis Colon Rectum. 2016;59:377–85.
41. Ogawa S, Hida J, Ike H, Kinugasa T, Ota M, Shinto E, Itabashi M, Okamoto T, Sugihara K. The important risk factor for lateral pelvic lymph node metastasis of lower rectal cancer is node-positive status on magnetic resonance imaging: study of the Lymph Node Committee of Japanese Society for Cancer of the Colon and Rectum. Int J Color Dis. 2016;31:1719–28.
42. WE M. A method of performing abdominoperineal excision for carcinoma of the rectum and of the terminal portion of the pelvic colon. Lancet. 1908;2:1812–3.
43. Grinnell RS. The lymphatic and venous spread of carcinoma of the rectum. Ann Surg. 1942;116:200–16.
44. Senba Y. An anatomical study of the lymphatic system of the rectum. J Fukuoka Med Coll. 1927;20:1213–68.
45. Stearns MW Jr, Deddish MR. Five-year results of abdominopelvic lymph node dissection for carcinoma of the rectum. Dis Colon Rectum. 1959;2:169–72.

46. Kobayashi H, Mochizuki H, Sugihara K, Morita T, Kotake K, Teramoto T, Kameoka S, Saito Y, Takahashi K, Hase K, Oya M, Maeda K, Hirai T, Kameyama M, Shirouzu K, Muto T. Characteristics of recurrence and surveillance tools after curative resection for colorectal cancer: a multicenter study. Surgery. 2007;141:67–75.
47. Kapiteijn E, Marijnen CA, Nagtegaal ID, Putter H, Steup WH, Wiggers T, Rutten HJ, Pahlman L, Glimelius B, van Krieken JH, Leer JW, van de Velde CJ, Dutch Colorectal Cancer Group. Preoperative radiotherapy combined with total mesorectal excision for resectable rectal cancer. N Engl J Med. 2001;345:638–46.
48. Hojo K. Extended wide lymphadenectomy and preservation of pelvic autonomic nerves in the rectal cancer surgery. G Chir. 1989;10:149–53.
49. Hojo K, Koyama Y. The effectiveness of wide anatomical resection and radical lymphadenectomy for patients with rectal cancer. Jpn J Surg. 1982;12:111–6.
50. Edge SB, Compton CC. The American Joint Committee on Cancer: the 7th edition of the AJCC cancer staging manual and the future of TNM. Ann Surg Oncol. 2010;17:1471–4.
51. Engstrom PF, Arnoletti JP, Benson AB 3rd, Chen YJ, Choti MA, Cooper HS, Covey A, Dilawari RA, Early DS, Enzinger PC, Fakih MG, Fleshman J Jr, Fuchs C, Grem JL, Kiel K, Knol JA, Leong LA, Lin E, Mulcahy MF, Rao S, Ryan DP, Saltz L, Shibata D, Skibber JM, Sofocleous C, Thomas J, Venook AP, Willett C, National Comprehensive Cancer Network. NCCN Clinical Practice Guidelines in Oncology: rectal cancer. J Natl Compr Canc Netw. 2009;7:838–81.
52. Glimelius B, Tiret E, Cervantes A, Arnold D, E.G.W. Group. Rectal cancer: ESMO Clinical Practice Guidelines for diagnosis, treatment and follow-up. Ann Oncol. 2013;24(Suppl 6):vi81–8.
53. Sugihara K, Kobayashi H, Kato T, Mori T, Mochizuki H, Kameoka S, Shirouzu K, Muto T. Indication and benefit of pelvic sidewall dissection for rectal cancer. Dis Colon Rectum. 2006;49:1663–72.
54. Akiyoshi T, Watanabe T, Miyata S, Kotake K, Muto T, Sugihara K, Japanese Society for Cancer of the Colon and Rectum. Results of a Japanese nationwide multi-institutional study on lateral pelvic lymph node metastasis in low rectal cancer: is it regional or distant disease? Ann Surg. 2012;255:1129–34.
55. Ishihara S, Kanemitsu Y, Murono K, Otani K, Yasuda K, Nishikawa T, Tanaka T, Tanaka J, Kiyomatsu T, Kawai K, Hata K, Nozawa H, Kazama S, Yamaguchi H, Sunami E, Sugihara K, Watanabe T. Oncological benefit of lateral pelvic lymph node dissection for rectal cancer treated without preoperative chemoradiotherapy: a multicenter retrospective study using propensity score analysis. Int J Color Dis. 2016;31:1315–21.
56. Rectum JSfCotCa, editor. Japanese classification of colorectal carcinoma. English ed. Tokyo: Kanehara; 2013.
57. Nagawa H, Muto T, Sunouchi K, Higuchi Y, Tsurita G, Watanabe T, Sawada T. Randomized, controlled trial of lateral node dissection vs. nerve-preserving resection in patients with rectal cancer after preoperative radiotherapy. Dis Colon Rectum. 2001;44:1274–80.
58. Siegel R, Desantis C, Jemal A. Colorectal cancer statistics, 2014. CA Cancer J Clin. 2014;64:104–17.
59. Japanese Society for Cancer of the Colon and Rectum. Japanese classification of colorectal carcinoma. 2nd English ed. Tokyo: Kanehara & Co. Ltd; 2009.
60. Sobin LH, Gospodarowicz MK, Wittekind C, International Union against Cancer. TNM classification of malignant tumours. 7th ed. Chichester: Wiley-Blackwell; 2010.
61. Graham RA, Hohn DC. Management of inguinal lymph node metastases from adenocarcinoma of the rectum. Dis Colon Rectum. 1990;33:212–6.
62. Bebenek M, Wojnar A. Infralevator lymphatic drainage of low-rectal cancers: preliminary results. Ann Surg Oncol. 2009;16:887–92.
63. Labianca R, Nordlinger B, Beretta GD, Brouquet A, Cervantes A, E.G.W. Group. Primary colon cancer: ESMO Clinical Practice Guidelines for diagnosis, adjuvant treatment and follow-up. Ann Oncol. 2010;21(Suppl 5):v70–7.
64. Hojo K, Koyama Y, Moriya Y. Lymphatic spread and its prognostic value in patients with rectal cancer. Am J Surg. 1982;144:350–4.

65. Gagnière J, Dupré A, Chabaud S, Peyrat P, Meeus P, Rivoire M. Retroperitoneal nodal metastases from colorectal cancer: curable metastases with radical retroperitoneal lymphadenectomy in selected patients. Eur J Surg Oncol. 2015;41:731–7.
66. Glass RE, Ritchie JK, Thompson HR, Mann CV. The results of surgical treatment of cancer of the rectum by radical resection and extended abdomino-iliac lymphadenectomy. Br J Surg. 1985;72:599–601.
67. Leggeri A, Roseano M, Balani A, Turoldo A. Liumboaortic and iliac lymphadenectomy: what is the role today? Dis Colon Rectum. 1994;37:S54–61.
68. Choi PW, Kim HC, Kim AY, Jung SH, Yu CS, Kim JC. Extensive lymphadenectomy in colorectal cancer with isolated para-aortic lymph node metastasis below the level of renal vessels. J Surg Oncol. 2010;101:66–71.
69. Shibata D, Paty PB, Guillem JG, Wong WD, Cohen AM. Surgical management of isolated retroperitoneal recurrences of colorectal carcinoma. Dis Colon Rectum. 2002;45:795–801.
70. Min BS, Kim NK, Sohn SK, Cho CH, Lee KY, Baik SH. Isolated paraaortic lymph-node recurrence after the curative resection of colorectal carcinoma. J Surg Oncol. 2008;97:136–40.
71. Min BS, Kim JS, Kim NK, Lim JS, Lee KY, Cho CH, Sohn SK. Extended lymph node dissection for rectal cancer with radiologically diagnosed extramesenteric lymph node metastasis. Ann Surg Oncol. 2009;16:3271–8.
72. Bae SU, Han YD, Cho MS, Hur H, Min BS, Baik SH, Lee KY, Kim NK. Oncologic outcomes of colon cancer patients with extraregional lymph node metastasis: comparison of isolated paraaortic lymph node metastasis with resectable liver metastasis. Ann Surg Oncol. 2016;23:1562–8.
73. Ogura A, Akiyoshi T, Takatsu Y, Nagata J, Nagasaki T, Konishi T, Fujimoto Y, Nagayama S, Fukunaga Y, Ueno M. The significance of extended lymphadenectomy for colorectal cancer with isolated synchronous extraregional lymph node metastasis. Asian J Surg. 2017;40:254–61.
74. Song SH, Park SY, Park JS, Kim HJ, Yang CS, Choi GS. Laparoscopic para-aortic lymph node dissection for patients with primary colorectal cancer and clinically suspected para-aortic lymph nodes. Ann Surg Treat Res. 2016;90:29–35.
75. Kim MS, Cho CK, Yang KM, Lee DH, Moon SM, Shin YJ. Stereotactic body radiotherapy for isolated paraaortic lymph node recurrence from colorectal cancer. World J Gastroenterol. 2009;15:6091–5.
76. Yeo SG, Kim DY, Kim TH, Jung KH, Hong YS, Kim SY, Park JW, Choi HS, Oh JH. Curative chemoradiotherapy for isolated retroperitoneal lymph node recurrence of colorectal cancer. Radiother Oncol. 2010;97:307–11.
77. Lee J, Chang JS, Shin SJ, Lim JS, Keum KC, Kim NK, Ahn JB, Kim TI, Koom WS. Incorporation of radiotherapy in the multidisciplinary treatment of isolated retroperitoneal lymph node recurrence from colorectal cancer. Ann Surg Oncol. 2015;22:1520–6.
78. Eisenhauer EA, Therasse P, Bogaerts J, Schwartz LH, Sargent D, Ford R, Dancey J, Arbuck S, Gwyther S, Mooney M, Rubinstein L, Shankar L, Dodd L, Kaplan R, Lacombe D, Verweij J. New response evaluation criteria in solid tumours: revised RECIST guideline (version 1.1). Eur J Cancer. 2009;45:228–47.
79. Bardia A, Greeno E, Miller R, Alberts S, Dozois E, Haddock M, Limburg P. Is a solitary inguinal lymph node metastasis from adenocarcinoma of the rectum really a metastasis? Color Dis. 2010;12:312–5.
80. Adachi T, Hinoi T, Egi H, Ohdan H. Surgical treatment for isolated inguinal lymph node metastasis in lower rectal adenocarcinoma patients improves outcome. Int J Color Dis. 2013;28:1675–80.
81. Tocchi A, Lepre L, Costa G, Liotta G, Mazzoni G, Agostini N, Miccini M. Rectal cancer and inguinal metastases: prognostic role and therapeutic indications. Dis Colon Rectum. 1999;42:1464–6.

Part IV

Sentinel Node Navigation Surgery

Methodology: Dye and Isotope Method

16

Shinichi Kinami and Takeo Kosaka

Abstract

Sentinel node (SN) biopsy has been attempted for digestive tract cancers, including esophageal, gastric, colon, and rectal cancers. Among these cancers, tailor-made surgical procedures guided by SN navigation have been planned for gastric cancer, while ultrastaging by SN biopsy is conducted for colon cancer. SN biopsy is a complex multistep surgical technique. This technique requires a suitable limitation of the indication, the selection of an adequate tracer, a proper tracer injection method, the objective detection of tracer uptake by the nodes, a reliable biopsy technique for the nodes that showed tracer uptake, and the precise detection of nodal metastasis. The selection of an adequate tracer for SN mapping has been an important issue. The advantages of dye methods are low cost, tractable, no radioactivity, and the direct visualization of the lymphatic canals and primary lymphatic drainage areas. The disadvantages of dye method are lack of objectivity, difficulty for digitizing, and quick washing out and deterioration. The advantages of radioactive imaging (RI) methods are high detection ability, objectivity, ease of digitizing, and possibility of easily distinguishing SN from secondary nodes. The disadvantages of the RI method are high cost, difficulty in handling, exposure to radioactivity, difficulty in detection of lymphatic vessels and lymphatic basin, and shine-through effect in the surgical field. Therefore, combination mapping of the dye method and the RI method is recommended because of its synergistic effect. Surgeons can detect both primary lymphatic canals visually and the SN objectively.

Keywords

Sentinel node · Gastric cancer · Combination mapping

S. Kinami (✉) · T. Kosaka
Department of Surgical Oncology, Kanazawa Medical University, Ishikawa, Japan
e-mail: kinami@kanazawa-med.ac.jp

S. Natsugoe (ed.), *Lymph Node Metastasis in Gastrointestinal Cancer*,
https://doi.org/10.1007/978-981-10-4699-5_16

16.1 Introduction

In the era of molecular targeting therapy for cancer, the importance of lymph node metastasis remains the same. The degree of the lymph node metastasis is still the most important prognostic factor. Micrometastasis of the regional lymph nodes is also an important prognostic factor in various cancers. At present, the most rational strategy for estimation of the presence of micrometastasis is narrowing the nodal choice to the sentinel nodes (SN).

An SN is defined as the node that directly receives lymphatic drainage from a primary tumor [1]. Therefore, the SN is thought to be the first node that is caught in the lymph node micrometastasis. The detection and biopsy of SN are thought to be very important in various cancers.

The SN biopsy is a complex multistep surgical technique [2]. This technique requires a suitable limitation of the indication, the selection of an adequate tracer, a proper tracer injection method, the objective detection of tracer uptake by the nodes, a reliable biopsy technique for the nodes that show tracer uptake, and the precise detection (micrometastasis level) of nodal metastasis. These six features are essential to establish the accurate result of SN biopsy.

In this section, we present an overview of the dye and isotope method, which are most commonly used for SN biopsy.

16.2 The Aim of SN Biopsy for Gastrointestinal Cancer

SN biopsy has been considered to have two main roles in various cancers: ultrastaging and guidance of lymph node dissection omission. In malignant melanoma management, SN biopsy is primarily used for ultrastaging [1]. It is mainly used to guide lymph node dissection omission in breast cancer surgery [3].

For gastrointestinal cancer, SN biopsy has been attempted for digestive tract cancers, including esophageal [4], gastric [5], colon [6], and rectal cancer [7]. Esophagogastric junction cancer [8], gastric stump cancer, and duodenal cancer are also candidates for SN biopsy. Among these digestive tract cancers, customized surgical procedures guided by SN navigation have been planned for gastric cancer [5, 9–13], and ultrastaging by SN biopsy is conducted for colon cancer [6, 14, 15]. As for esophageal cancer, the omission of neck dissection and the guidance for the planning of the irradiation field are attempted by SN navigation and ultrastaging [16, 17]. The omission of lateral pelvic nodal dissection guided by SN biopsy is attempted in rectal cancer surgery [18]. In esophagogastric junction cancer and gastric stump cancer, SN biopsy is applied for the investigation of lymphatic flow in establishing adequate lymph node dissection.

Gastric cancer, along with other cancers, is well investigated by many researchers trying to determine the validity of the SN concept [5, 9–13]. As it is important to avoid postgastrectomy symptoms, such research is essential. The standard curative procedure for early gastric cancers out of indication for endoscopic resection is gastrectomy with lymph node dissection. However, patients undergoing standard

gastrectomy with lymph node dissection experience postgastrectomy symptoms [19], which often pose life-long problems for patients. Thus, lymph node dissection should be avoided to preserve the stomach, avoid postgastrectomy symptoms, and improve postoperative quality of life. Many prospective studies have successfully demonstrated the utility of SN biopsy in gastric cancer [5, 9–13]. The SNNS study [20], a large-scale multicenter prospective study, provided evidence for the validity of the SN concept in gastric cancer. In this study, the sensitivity and specificity of SN biopsy were 93% and 99%, respectively.

SN biopsy for hepatic-pancreatic-biliary tract cancers, than for digestive tract cancers, has been less studied. The reason for the limited studies in this area is the technical difficulty of the tracer injection procedure.

16.3 Patient Selection

Careful selection of patients is very important to obtain successful results for SN biopsy. There are two important points that determine if a case is suitable for SN biopsy.

The first point is selecting the clinically node-negative cases. The main role of SN biopsy is the diagnosis of microscopic node-positive cases. Therefore, a suitable case for SN biopsy is thought to be one diagnosed as node-negative clinically otherwise having microscopic nodal metastasis. As for gastrointestinal cancers, the indication of SN biopsy would be out of indication for endoscopic mucosal resection (or endoscopic submucosal dissection) and no obvious nodal metastasis (cN0 case).

The second point is considering the characteristics of tracers. The SN needs to be detectable by the injected tracer. Therefore, the indication of SN biopsy for gastrointestinal cancer should be limited to the adequate size and depth of invasion in consideration of the characteristics of tracers. It is desirable that the size of the tumor should be limited to within 4–5 cm in diameter, which is within the spreading limits of the tracer. It is also desirable that the indication should be restricted to submucosal cancer, because lymphatic vessels are most developed in the submucosa.

16.4 Selection of Adequate Dye Tracer

In detection of the SN, it is common to use tracers that flow from the injection site surrounding the primary tumor to the SN through the primary drainage lymphatic canals. The selection of an adequate tracer for SN mapping has been an important issue. The ideal tracer is thought to have the following characteristics: no toxicity, no allergic reaction, low radioactivity, strong selectivity to the lymphatic systems, rapid and easy flow out from the injection site, easy to visualize the lymphatic canals, good permeating and strong accumulation in SN, and little flow out from the SN to secondary nodes. However, such an ideal tracer is not yet in existence.

There are many types of tracers available for SN biopsy, and they are classified into categories according to the type of material. They include dye tracers, radioactive colloid tracers, other small particle tracers (superparamagnetic iron oxide [21], fluoresbrite microspheres [22], nanocrystal beads [23], etc.), X-ray contrast mediums [24], and functional tracers (99mTc tilmanocept [25], etc.).

Dye methods have been most commonly used for SN biopsy in various cancer surgeries. One of the advantages of dye methods is the visualization of the lymphatic canals and primary lymphatic drainage areas directly. Surgeons can distinguish SN from secondary nodes by tracing the dyed lymphatic canals. The other advantages of dye are low cost, easy to obtain, tractable, and no radioactivity. The disadvantages of the dye method include lack of objectivity, difficulty in digitizing, quick washout and deterioration, unusual allergic reactions, and, at times, difficulty in nodal detection at the fatty patient. As dye tracers are not particles, they are easily washed out from the SN to secondary nodes, to more distant nodes, and finally to the terminal nodes. The strength of dying reduces quickly, and the detection of SN becomes gradually more difficult. Based on these characteristics of the dye material, the dye method is suitable in early gastric cancer because regional lymph nodes in gastric cancer are mainly confined to the perigastric and suprapancreatic areas, where detection of dyed lymph nodes and lymphatic canals is easy, given the thin fat layer [5, 26]. Figure 16.1 represents an intraoperative picture of SN biopsy for early gastric cancer. In contrast, dye methods are not suitable for esophageal and rectal cancers, because these cancers are buried deep in the fat of the mediastinum or retroperitoneum, and it is difficult to trace all dyed lymphatic vessels.

The frequently used dye tracers are sulphan blue (Patent Blue Violet®), isosulfan blue (Lymphazurin®), indocyanine green (ICG), charcoal, and indigo carmine.

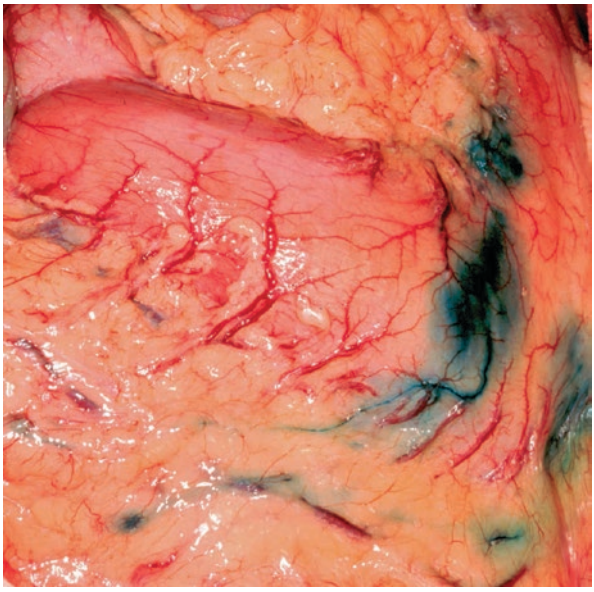

Fig. 16.1 Dye method of SN biopsy for early gastric cancer using 2% Patent Blue Violet

Blue dye is the standard dye color for SN biopsy. The representative blue dye is isosulfan blue or sulphan blue. Blue dye presents good blue-contrasted lymphatic images against the yellow peritoneal fat [5, 26]. In contrast to blue dye, the strength of dying and contrast against fat are weak with the use of ICG.

16.5 Selection of Adequate Radioactive Imaging Tracer

Radioactive imaging (RI) colloid tracers are also common in SN biopsy for gastrointestinal cancers. One of the advantages of the RI method is the high detection ability of the SN. The surgeon can detect the SN even with a small amount of radioactive colloid by using the high-sensitivity gamma probe. The SN located under a deep fat layer or hidden behind another organ can also be detected. By using lymphoscintigraphy, an SN located far from the primary lesion can be detected. Another advantage is the ability to withstand time deterioration of tracer uptake. This peculiarity works in favor of the time-consuming surgical procedures, such as for esophageal cancer, rectal cancer, and laparoscopic surgery. The other advantages are as follows: rare allergic reactions, objectivity, ease of digitizing, and possibility of easily distinguishing SN from secondary nodes. The disadvantages of the RI method include the following: high cost, difficulty in handling, exposure to radioactivity, no visual detection, difficulty in detection of lymphatic vessels and lymphatic basin, and shine-through effect in the surgical field. Considering these factors, the RI method is suitable for esophageal cancer and rectal cancer because the SNs of these cancers are buried deep in the fat or located far from the primary lesion. SN biopsy with the aim of ultrastaging is also suitable for RI method. In contrast, it seems to be difficult in conducting the omission of lymph node dissection by using RI method only, because of the lack of visualization of lymphatic basin and shine-through effect at the surgical field.

The type of RI colloid is an important issue. The frequently used RI colloid tracers include the following: tin colloid [13, 20], phytate [26], human serum albumin colloid [27], sulfur colloid [28], and rhenium colloid [29]. All these colloids were not developed for SN biopsy but have been applied in practical use for SN biopsy. The sizes of particles of these colloids are 50–1000 nm. For SN biopsy, the particle size of colloid is thought to be important [30, 31]. If the size is small, the RI colloid would flow out easily from the injection site and have good permeation into the SN while easily flowing out from the SN to the secondary node. If the size is large, RI colloid would accumulate strongly in SN and little will flow out to secondary nodes, while also little will flow out from injection site, and the amount of RI colloid in SN would be little.

In this issue, the author introduces here our data for RI mapping for early gastric cancer.

The localization of the intranodal RI colloid was not precisely known. Previous researchers suspected that the colloid was phagocyted as a foreign body by intranodal macrophages or trapped at peripheral sinuses. We succeeded in visualization of the intranodal location of radioactive colloid in the SN using high-resolution

autoradiography. A frozen section of hot node was made and exposed to the BAS-TR2025 imaging plate (Fujifilm, Tokyo, Japan) for 24 h. The intranodal radioactive distribution images were drawn using a BAS-5000 IP reader (Fujifilm) (condition: G 65536 R 25 L5 S30000). The radioactive image was composed of hematoxylin and eosin picture to get the RI colloid distribution image. The representative image was shown in Fig. 16.2. The colloid was thought to be initially trapped in the cortex near the peripheral sinus of the node.

Therefore, we planned to compare tin colloid and phytate, which are two major colloids for SN biopsy for gastric cancer, from the viewpoint of the intranodal distribution. One hundred and eight hot nodes from 18 gastric cancer patients detected using 99mTc-tin colloid and 115 nodes from 15 patients using 99mTc-phytate were analyzed. All of these patients underwent SN biopsy using the standard combination mapping. RI colloids were injected as RI tracer to the four points of submucosal layer surrounding the primary tumor endoscopically the day before surgery.

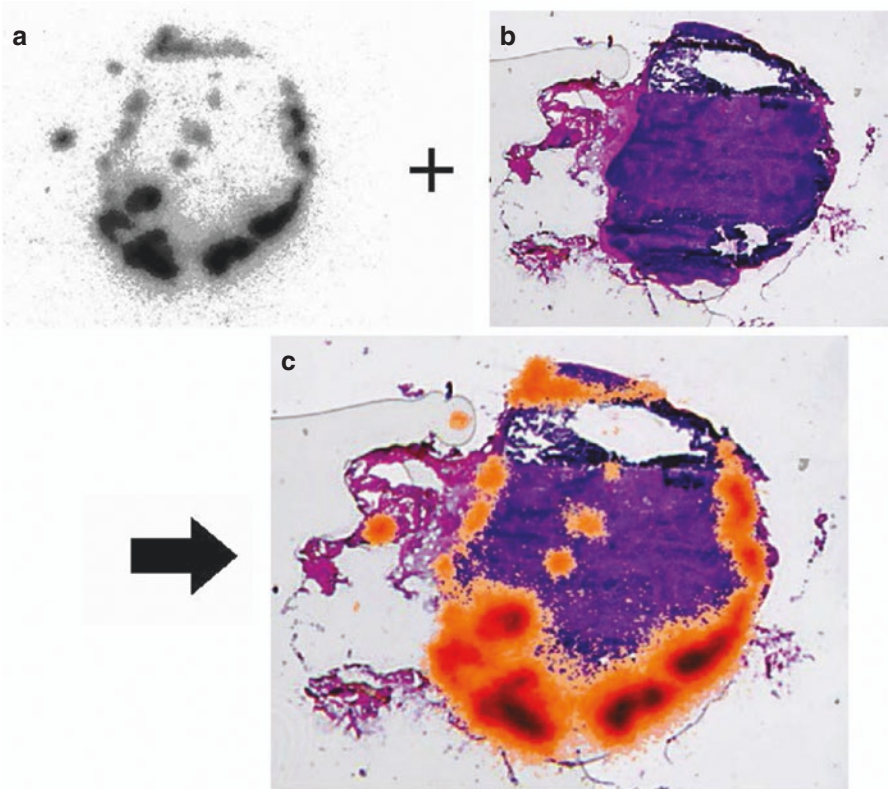

Fig. 16.2 The intranodal radioactive distribution image of SN. (**a**) The picture of the intranodal location of radioactive colloid in the frozen section of SN using high-resolution autoradiography. (**b**) The picture of the same slice of frozen section stained by hematoxylin and eosin. (**c**) The intranodal radioactive distribution image was obtained in composing (**a**) and (**b**). The colloid was thought to be initially trapped in the cortex near the peripheral sinus of the node

The composed intranodal radioactive distribution images were obtained from these hot nodes.

The images were classified into four categories: radioactivity accumulated in part of the periphery of the section (type A), radioactivity surrounding the periphery of the section (type B), radioactivity distributed from part of the periphery to the hilus of the section (type C), and radioactivity occupying the whole area of the section (type D). Figure 16.3 showed these images.

The intranodal distribution images were obtained from 81% of tin group and 78% of phytate group. The median 10-s RI counts obtained using a gamma probe were 153 in the tin group and 306 in the phytate group, and there was no significant difference (Fig. 16.4). Table 16.1 shows the ratio of the types of distribution. In the tin group, type A was common and type C was only 7%. Type C was 21% in the phytate group, and there was a significant difference. Though the amount of RI colloid was almost equal, the pattern of intranodal localization was different between the two colloids; tin colloid was mainly trapped in the outer cortex, while phytate tended to flow to the medulla easily. These data would show that the colloid was thought to be trapped first in the cortex near peripheral sinus of SN; however, in cases in which a large volume of colloid flows from the primary injection site, larger-sized colloid like tin colloid might spread to the peripheral sinus of the node; in contrast, smaller-sized colloid like phytate might readily flow from the periphery to the medullary sinus and also trapped medulla (Fig. 16.5).

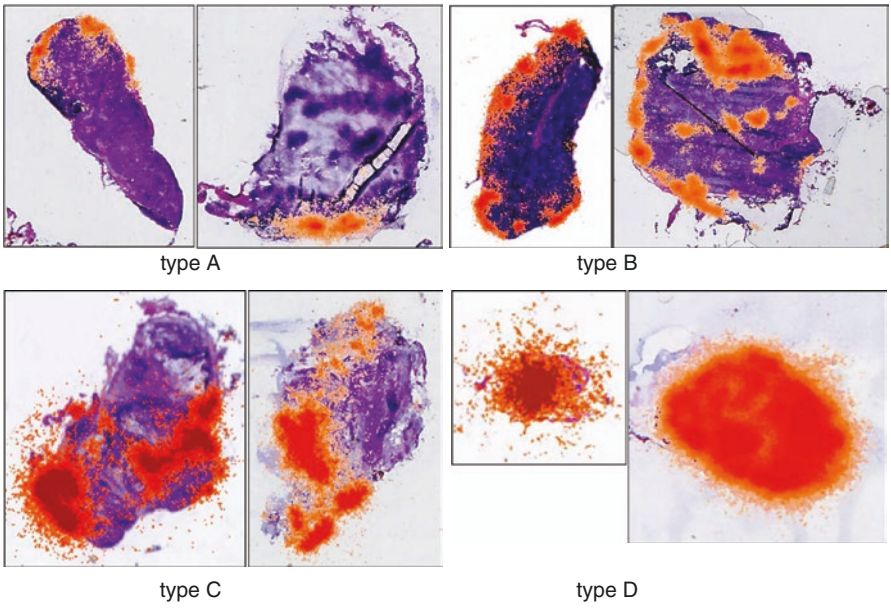

Fig. 16.3 The categories of the intranodal radioactive distribution image. Type A: radioactivity accumulated in part of the periphery of the section. Type B: radioactivity surrounding the periphery of the section. Type C: radioactivity distributed from part of the periphery to the hilus of the section. Type D: radioactivity occupying the whole area of the section

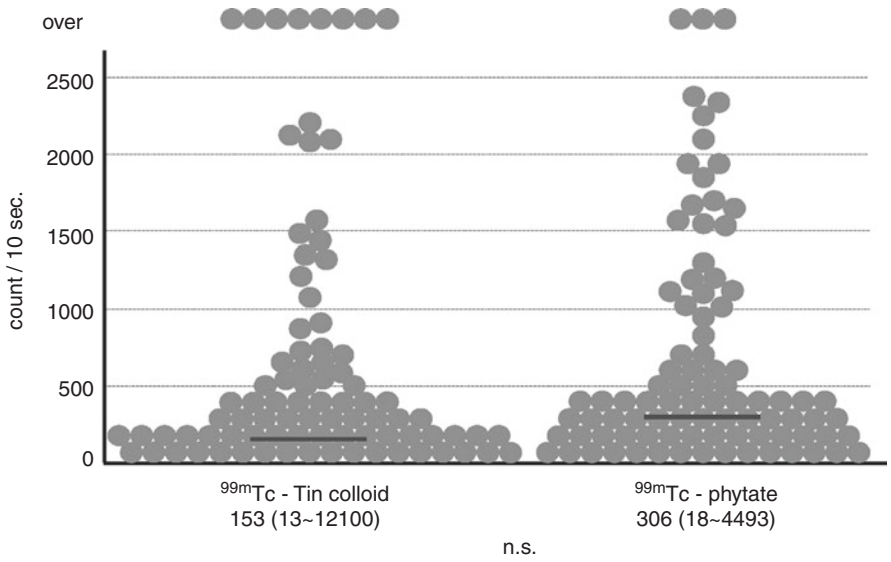

Fig. 16.4 The comparison of the median 10-s RI counts obtained using a gamma probe between two groups. There was no significant difference

Table 16.1 The comparison of the types of intranodal radioactive distribution of SN between tin colloid group and phytate group

	^{99m}Tc-tin colloid	^{99m}Tc-phytate	
Failure to obtain IP image	21	25	
Success to obtain IP image	77	90	n.s.
Type A	55	45	
Type B	10	8	
Type C	6	19	
Type D	16	18	$p < 0.05$

In these nodes, there were two nodes involving metastasis and six nodes involving isolated tumor cells (ITC). The types of metastasis of two metastatic nodes were both large nodular type, and intranodal activity could be successfully visualized in one node. The type of the distribution pattern was type D, radioactivity, occupying the whole area of the section; therefore, the metastatic foci were within the radioactivity area. Similarly, there were five nodes successfully visualized by radioactivity of six nodes involving ITC, and all ITCs were located within the radioactivity area regardless of the type of radioactive distribution pattern (Table 16.2).

From these data, 99mTc-tin colloid would be a standard RI tracer for SN biopsy of gastrointestinal cancer.

As stated previously, the dye method has some disadvantages, such as quick washout and deterioration and, at times, difficultly in nodal detection in fatty patients. Additionally, the RI method also has some weak points, such as difficulty in detection of lymphatic vessels and lymphatic basin and shine-through effect in the surgical field. Therefore, combination mapping of the dye method and the RI method is recommended in various cancer surgeries. Combination mapping is thought to be

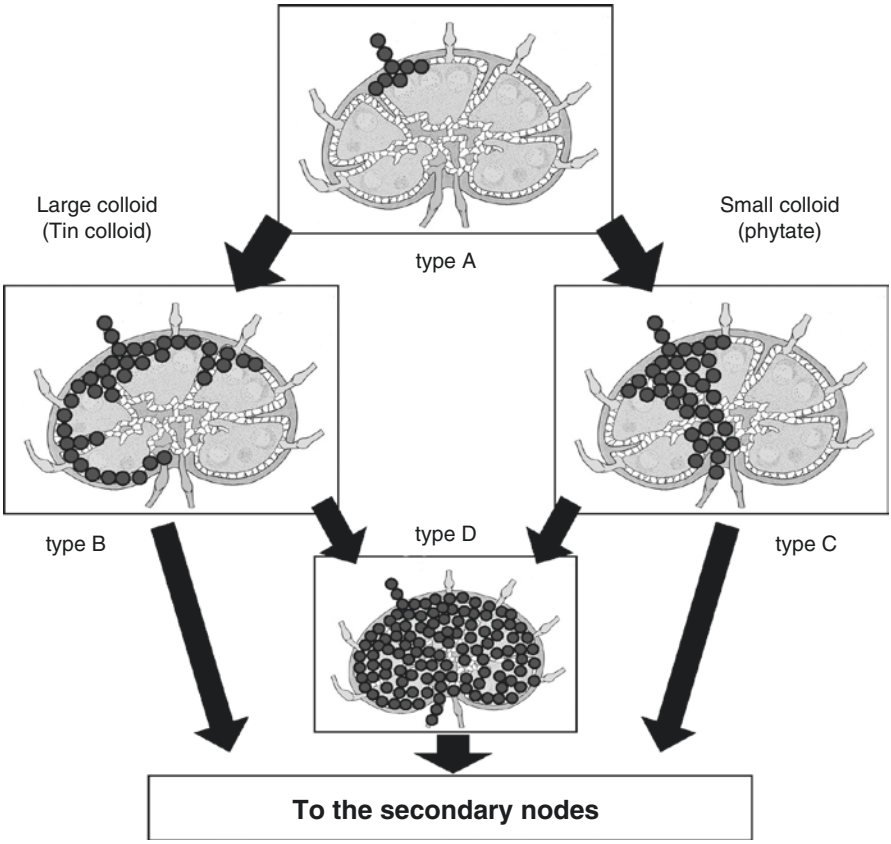

Fig. 16.5 The relationship between each type of the intranodal radioactive distribution in progress of flow of RI colloid. The particle size of colloid is thought to be important. Tin colloid was mainly trapped in the outer cortex, while phytate tended to flow to the medulla easily

Table 16.2 The relationship between the metastatic area and the intranodal radioactive distribution in SN involved metastasis or ITC

No.	Type of colloid	RI counts	Long axis of node (mm)	Type of metastasis	Type of distribution	Intranodal metastatic lesion
1	Tin	85	37	Large nodule	D	Inside radioactive area
2	Phytate	69	9	Large nodule	–	
3	Tin	86	8	ITC	A	Inside radioactive area
4	Tin	281	5	ITC	B	Inside radioactive area
5	Tin	643	6	ITC	B	Inside radioactive area
6	Tin	118	7	ITC	D	Inside radioactive area
7	Phytate	14	14	ITC	–	
8	Phytate	555	5	ITC	A	Inside radioactive area

superior to single tracer mapping because of its synergistic effect [32]. Surgeons can detect both primary lymphatic canals visually and the SN objectively.

16.6 Proper Tracer Injection Method

The method for tracer injection is important as well as the choice of tracer. For breast cancer, there are three methods of tracer injection: peritumoral, subdermal, and subareolar. Similarly, for gastrointestinal cancers, there are two injection methods: endoscopic submucosal injection into four points surrounding the tumor and intraoperative subserosal injection into the behind of tumor. In practice, the subserosal injection is difficult for esophageal and rectal cancers, but is otherwise easy for surgeons in cases of gastric or colon cancer surgeries. Nevertheless, the de facto standard procedure of tracer injection is now the endoscopic submucosal injection, without regard to the type of tracers or the location of the tumor. Many studies have provided recommendations regarding the tracer injection method for SN biopsy in gastric cancer. In a meta-analysis of SN biopsy for gastric cancer by Wang et al., the submucosal injection method was found to be associated with a higher SN identification rate and sensitivity [33]. In the successful SNNS study by Kitagawa et al., endoscopic submucosal injection was adopted [20].

16.7 Objective Detection and Reliable Biopsy Technique for SN

If the aim of SN biopsy is ultrastaging, it is easy to detect and harvest SNs with the RI method, because the surgical procedure is the same as the ordinary procedure and the timing of SN detection is sufficient after harvesting all dissected nodes. It does not require intraoperative biopsy and omitting the extent of lymph node dissection. In contrast, if the aim of SN biopsy is the guidance of lymph node dissection omission, the difficulty of SN biopsy rises, because objective detection and precise biopsy technique are required. For example, in breast cancer, SNs are usually hidden deep in the axillary fat, and it is difficult to search for the nodes showing tracer uptake through a small incision. Therefore, it is necessary to have a thorough learning phase to establish the accurate result of SN biopsy for breast cancer surgery [34]. With regard to gastrointestinal cancer surgery, precise completion of SN biopsy for guidance of lymph node dissection omission is more important than for breast cancer, because reoperation for additional nodal dissection is rarely performed for gastrointestinal cancers [2].

As for gastric cancer, these issues could be resolved by the adaptation of proper biopsy technique for SN biopsy. That is the lymphatic basin dissection [26]. The lymphatic basin is defined as the lymphatic zone divided by the stream of the dyed lymphatic canals in dye mapping; the proximal border is the fatty tissue attached to the stomach wall, and the distal border is the front of the blue node furthest from the stomach [26]. The lymphatic basins are thought to be the primary lymphatic drainage areas in each patient, and patients with gastric cancer often have two or three basins. All SNs exist within the lymphatic basin. Lymphatic basin dissection is a selective

lymphadenectomy to dissect lymphatic basins en bloc, collecting lymph nodes and lymphatic vessels stained with dye. Lymphatic basin dissection is considered a standard SN biopsy technique for gastric cancer, unlike for other cancers. SNs are retrieved after lymphatic basin dissection and subjected to intraoperative pathological analysis. Lymphatic basin dissection is superior to the ordinary pickup method, not only for minimizing the rate of missed SNs but also in terms of oncological safety as it complements intraoperative pathological diagnosis by serving as a backup dissection. Kinami et al. reported that there were no recurrent cases, including two false-negative cases in 190 patients diagnosed as node-negative by SN biopsy intraoperatively and treated by function-preserving gastrectomy with lymphatic basin dissection [26].

16.8 Precise Detection of Nodal Metastasis

The most important issue in performing SN biopsy for gastrointestinal cancer is the intraoperative diagnosis of nodal metastasis. Nodal diagnosis demands precise detection up to a micrometastasis level, especially if the aim of SN biopsy is guidance of lymph node dissection omission. The clinical diagnosis of nodal metastasis is ordinarily performed by examining the nodes with the largest dimension in one plane by frozen section with rapid hematoxylin-eosin staining. However, this type of rapid diagnosis can potentially result in misdiagnosis.

Two large-scale, nationwide, multicenter prospective studies were conducted to establish the usefulness of SN biopsy in gastric cancer: the JCOG0302 study [35] and the SNNS study [20]. Unfortunately, the JCOG0302 trial was terminated because of the high proportion of false-negative results obtained from intraoperative histological examinations. This failure demonstrated that the combination of pickup method for SN biopsy in gastric cancer and intraoperative histological examination using a single plane is not suitable for clinical applications. However, the SNNS study provided proof of the SN concept in gastric cancer, where the sensitivity and specificity of SN biopsy were 93% and 99%, respectively. Metastasis was diagnosed using permanent sections; therefore, the intraoperative diagnostic ability of SN biopsy for nodal metastasis did not influence the results of this study. Indeed, the sensitivity of intraoperative frozen section diagnosis was 79%. The occurrence of false-negative results is a serious issue. To solve this issue and establish oncological safety, molecular methods to diagnose nodal metastasis, such as reverse transcriptase-polymerase chain reaction and one-step nucleic acid amplification assay, should be developed for clinical use [36, 37]. Please refer to other chapters of this book.

16.9 About the Leaning Phase for SN Biopsy in Gastrointestinal Cancer

The SN biopsy is a complex, multistep, surgical technique. It is well known that there exists a learning phase for SN biopsy. For breast cancer, it takes about 40 cases to establish correct technique for SN biopsy [34]. Similarly, it has been proposed that 30 cases are required for adequate for learning for SN biopsy of gastric cancer

[20]. The results of the JCOG0302 trial were influenced by intraoperative SN detection techniques and demonstrated that a learning curve exists in conducting SN biopsies. In contrast, the learning curve issues did not influence the results of the SNNS study, because the hospitals that participated in the study were highly skilled in SN biopsy, with over 30 procedures performed at each institution.

16.10 The Aspect of New Techniques for SN Biopsy

In recent years, ICG fluorescence mapping—a new alternative dye method of SN biopsy—has been developed. ICG is a widely used diagnostic reagent that is clinically approved for use in the assessment of hepatic function and cardiac output. ICG was formerly used as a dye tracer for gastric cancer. However, ICG is generally less visible than blue dye because of its weaker contrast against the background adipose tissue. Conversely, ICG emits maximal fluorescence at a wavelength of 840 nm when it binds to plasma proteins. ICG fluorescence imaging was developed after the recent invention of the camera system known as the photodynamic eye (PDE; Hamamatsu Photonics Co. Ltd., Hamamatsu, Shizuoka, Japan). Kusano et al. demonstrated the high sensitivity of this ICG fluorescence imaging system for SN mapping in gastric cancer [38]. The advantages of ICG fluorescence imaging are as follows: lower frequency of allergic reactions than that with blue dye, ability to detect bright nodes under thick adipose tissue, obvious visualization, easier detection of bright nodes and lymphatic canals than with the naked eye, very high sensitivity to detect minute concentrations of ICG, and signal stability [39–41]. Signal stability is the most important advantage of ICG fluorescence imaging over dye and radioisotope-guided methods [41].

At present, laparoscopic gastrectomy is the most commonly used approach for early gastric cancers in Japan, though laparoscopic gastrectomy merely replicates standard gastrectomy. It is difficult to perform function-preserving curative gastrectomy using the laparoscopic approach, because of the difficulty of SN mapping laparoscopically. In the SNNS study, combination mapping with technetium-99m tin colloid and isosulfan blue was used and has been adopted as a temporary standard. However, blue dye deteriorates quickly, and radioactive colloids exhibit a shine-through effect during gamma probe detection of hot nodes in the surgical field. These limitations increase the difficulty in performing laparoscopic SN biopsy by impairing lymphatic basin visualization and hot node detection [2]. However, if ICG fluorescence mapping for early gastric cancer becomes feasible, laparoscopic function-preserving curative gastrectomy would be a good alternative to the commonly used D1+ gastrectomy for patients with node-negative gastric cancer [2, 39–41]. Fortunately, several ICG fluorescence imaging systems have been developed and are available, including the IMAGE 1 HD system by Karl Storz, the IRI system by Olympus, the ICG fluorescent laparoscope by Senko Optical, and the PINPOINT system by Novadaq. The use of these systems would allow avoidance of the upper abdomen incision and promote widespread proliferation of ICG fluorescence imaging and function-preserving curative gastrectomy. However, there are

disadvantages of ICG fluorescence imaging, which include the subjectivity of SN evaluation and potential secondary node contamination because of the high sensitivity of the PDE system [2]. Further investigation is needed to overcome this limitation of ICG fluorescence imaging.

New fluorescence agents have already been developed that have both fluorescence and colloid particle characteristics [42–46]. These new agents would only detect fluorescent SNs and not secondary nodes and, therefore, would be the most potentially useful for conducting laparoscopic SN biopsy in gastric cancer. Furthermore, they may potentially be used alone as a standard tracer instead of in combination with other SN mapping tracers.

16.11 Recommended Procedures

Finally, the typical mapping procedures of SN biopsy for gastric cancer surgery are introduced. Table 16.3 is the combination mapping using 99mTc-tin colloid and 1% isosulfan blue—the standard SN mapping procedure for early gastric cancer. This method was adopted by the SNNS study [20]. In Japan, kit formulation of 99mTc-tin colloid was commercially available by Nippon Medi-physics Co. Ltd. The standard technique also adopted Lymphazurin® as dye tracer intraoperatively. In the SNNS study, intraoperative SN biopsy was not required; therefore, the lymphatic basin dissection method for detecting and harvesting SN is recommended.

Table 16.3 The standard combination mapping for early gastric cancer using 99mTc-tin colloid and 1% isosulfan blue

Indications	• confirmed clinical T1N0M0 or T2N0M0 adenocarcinoma of the stomach (UICC TNM classification, sixth edition) • Single primary lesions below 4 cm • Without previous treatment, including endoscopic mucosal resection or endoscopic submucosal dissection
RI mapping	• The day before surgery • Endoscopic submucosal injection • 20 mL of technetium 99m tin colloid solution (0.5 mL × 4 points; total 150 MBq; 0.3 mCi at the time of surgery) was injected in four quadrants of the submucosal layer of the primary lesion by using an endoscopic puncture needle
Dye mapping	• Intraoperatively • After the gastrocolic ligament was divided to visualize all possible directions of lymphatic flow from the stomach • Lymphazurin® was injected via intraoperative endoscopy in exactly the same manner as the preoperative injection of the radioactive tracer
SN biopsy	• Blue nodes were defined as the nodes dyed blue within 15 min • Simultaneously, a handheld gamma probe was used to locate the radioactive SN. Lymph nodes with radioactivity over ten times of background activity were defined as hot nodes • All hot and/or blue nodes were identified as the SNs

Table 16.4 The ICG fluorescence SN mapping procedure for gastric cancer, suitable for laparoscopic surgery

Indications	• Histologically confirmed clinical type 0 (superficial-type) adenocarcinoma of the stomach (Japanese classification of gastric carcinoma, 14th edition) • Single primary lesions less than 5 cm in diameter • No distant metastasis (cM0) nor evident nodal metastasis (cN0) • Out of indication of endoscopic mucosal resection or endoscopic submucosal dissection
ICG mapping	• The day before surgery • Endoscopic submucosal injection • Prepare ×100 ICG solution (50 μg/mL) • Each 0.5 mL of ×100 ICG solution was injected in four quadrants of the submucosal layer of the primary lesion by using an endoscopic puncture needle
SN biopsy	• PDE or PDE neo was used • For laparoscope-assisted surgery cases, the stomach and perigastric lymph nodes were pulled up and exposed from a 4–6 cm median upper abdominal incision, and ICG fluorescence in the lymphatic vessels and lymph nodes was detected with the PDE or PDE neo • Bright nodes were defined as clearly fluorescent nodes • All bright nodes were identified as the SNs • Patients received function-preserving gastrectomy with lymphatic basin dissection • Following resection, the bright nodes were detected and harvested at the surgical field and sent for pathological diagnosis of the intraoperative frozen section • For bright nodes without metastasis, the surgical team continued the reconstruction and finished the procedure. For cases with nodal metastasis, the surgery was converted to a standard D2 gastrectomy

In addition, the ICG fluorescence SN mapping procedure for gastric cancer is introduced in Table 16.4 as the alternative but suitable for laparoscopic surgery. The process of establishing this optimal setting was publicized in detail [2]. The sensitivity and accuracy of ICG fluorescence imaging were reported to be 90.1% and 98.6%, respectively. It should be noted that this optimal setting was regulated according to the extra-high sensitivity of the PDE system. It may be necessary to reexamine the proper concentration of ICG if other detection devices are to be used.

References

1. Morton DL, Wen DR, Wong JH, Economou JS, et al. Technical details of intraoperative lymphatic mapping for early stage melanoma. Arch Surg. 1992;127:392–9.
2. Kinami S, Oonishi T, Fujita J, Tomita Y, Funaki H, Fujita H, et al. Optimal settings and accuracy of indocyanine green fluorescence imaging for sentinel node biopsy in early gastric cancer. Oncol Lett. 2016;11:4055–62.
3. Giuliano AE, Haigh PI, Brennan MB, Hansen NM, Kelley MC, Ye W, et al. Prospective observational study of sentinel lymphadenectomy without further axillary dissection in patients with sentinel node-negative breast cancer. J Clin Oncol. 2000;18:2553–9.

4. Takeuchi H, Saikawa Y, Oyama T, Kitagawa Y. Clinical application of sentinel node navigation surgery for esophageal cancer. Kyobu Geka. 2009;62:749–53.
5. Miwa K, Kinami S, Taniguchi K, Fushida S, Fujimura T, Nonomura A. Mapping sentinel nodes in patients with early-stage gastric carcinoma. Br J Surg. 2003;90:178–82.
6. Saha S, Bilchik A, Wiese D, Espinosa M, Badin J, Ganatra BK, et al. Ultrastaging of colorectal cancer by sentinel lymph node mapping technique—a multicenter trial. Ann Surg Oncol. 2001;8:94S–8S.
7. Hladík P, Vizd'a J, Hadzi Nikolov D, Dvorák J, Voboril Z. Radio-guided sentinel node detection during the surgical treatment of rectal cancer. Nucl Med Commun. 2005;26:977–82.
8. Matsuda T, Takeuchi H, Tsuwano S, Nakahara T, Mukai M, Kitagawa Y. Sentinel node mapping in adenocarcinoma of the esophagogastric junction. World J Surg. 2014;38:2337–44.
9. Miwa K. Sentinel node concept and its application for cancer surgery. Nihon Geka Gakkai Zasshi. 2000;101:307–10.
10. Hiratsuka M, Miyashiro I, Ishikawa O, Furukawa H, Motomura K, Ohigashi H, et al. Application of sentinel node biopsy to gastric cancer surgery. Surgery. 2001;129:335–40.
11. Carlini M, Carboni F, Petric M, Santoro R, Guadagni F, Marandino F, et al. Sentinel node in gastric cancer surgery. J Exp Clin Cancer Res. 2002;21:469–73.
12. Ichikura T, Morita D, Uchida T, Okura E, Majima T, Ogawa T, et al. Sentinel node concept in gastric carcinoma. World J Surg. 2002;26:318–22.
13. Kitagawa Y, Fujii H, Mukai M, Kubota T, Otani Y, Kitajima M. Radio-guided sentinel node detection for gastric cancer. Br J Surg. 2002;89:604–8.
14. Saha S, Sirop S, Korant A, Nalluri S, Machek OL, Desai D, et al. Detection of aberrant drainage after sentinel lymph node mapping and its impact on staging and change of operation in colon cancer. J Clin Oncol. 2011;29:500.
15. Saha S, Sirop S, Korant A, Chakravarty B, Krishnaiah N, Wiese D, et al. The number of lymph node metastases as a prognostic indicator of disease-specific survival in the era of sentinel lymph node mapping in colon cancer. J Clin Oncol. 2009;20:27.
16. Kaburagi T, Takeuchi H, Oyama T, Nakamura R, Takahashi T, Wada N, et al. Radiotherapy, including sentinel lymph node, to superficial cancer of esophagus. J Clin Oncol. 2011;29:126.
17. Dabbagh Kakhki VR, Bagheri R, Tehranian S, Shojaei P, Gholami H, et al. Accuracy of sentinel node biopsy in esophageal carcinoma: a systematic review and meta-analysis of the pertinent literature. Surg Today. 2014;44:607–19.
18. Kawahara H, Watanabe K, Enomoto H, Tomoda M, Akiba T, Yanaga K. Sentinel node navigation surgery for lower rectal cancer. Anticancer Res. 2015;35:3489–93.
19. Eagon JC, Miedema BW, Kelly KA. Postgastrectomy syndromes. Surg Clin North Am. 1992;72:445–65.
20. Kitagawa Y, Takeuchi H, Takagi Y, Natsugoe S, Terashima M, Murakami N, et al. Sentinel node mapping for gastric cancer: a prospective multicenter trial in Japan. J Clin Oncol. 2013;31:3704–10.
21. Nakagawa T, Minamiya Y, Katayose Y, Saito H, Taguchi K, Imano H, et al. A novel method for sentinel lymph node mapping using magnetite in patients with non-small cell lung cancer. J Thorac Cardiovasc Surg. 2003;126:563–7.
22. Ueno H, Hihara J, Shimizu K, Osaki A, Yamashita Y, Yoshida K, et al. Experimental study on fluorescent microspheres as a tracer for sentinel node detection. Anticancer Res. 2005;25:821–5.
23. Kim S, Lim YT, Soltesz EG, De Grand AM, Lee J, Nakayama A, et al. Near-infrared fluorescent type II quantum dots for sentinel lymph node mapping. Nat Biotechnol. 2004;22:93–7.
24. Suga K, Ogasawara N, Okada M, Matsunaga N. Interstitial CT lymphography-guided localization of breast sentinel lymph node: preliminary results. Surgery. 2003;133:170–9.
25. Wallace AM, Hoh CK, Vera DR, Darrah DD, Schulteis G. Lymphoseek: a molecular radiopharmaceutical for sentinel node detection. Ann Surg Oncol. 2003;10:531–8.
26. Kinami S, Fujimura T, Ojima E, Fushida S, Ojima T, Funaki H, et al. PTD classification: proposal for a new classification of gastric cancer location based on physiological lymphatic flow. Int J Clin Oncol. 2008;13:320–9.

27. Bedrosian I, Scheff AM, Mick R, Callans LS, Bucky LP, Spitz FR, et al. 99mTc-human serum albumin: an effective radiotracer for identifying sentinel lymph nodes in melanoma. J Nucl Med. 1999;40:1143–8.
28. Zulfikaroglu B, Koc M, Ozmen MM, Kucuk NO, Ozalp N, Aras G. Intraoperative lymphatic mapping and sentinel lymph node biopsy using radioactive tracer in gastric cancer. Surgery. 2005;138:899–904.
29. Watanabe T, Kimijima I, Ohtake T, Tsuchiya A, Shishido F, Takenoshita S. Sentinel node biopsy with technetium-99m colloidal rhenium sulphide in patients with breast cancer. Br J Surg. 2001;88:704–7.
30. Uenosono Y, Natsugoe S, Higashi H, Ehi K, Miyazono F, Ishigami S, et al. Evaluation of colloid size for sentinel nodes detection using radioisotope in early gastric cancer. Cancer Lett. 2003;200:19–24.
31. Higashi H, Natsugoe S, Uenosono Y, Ehi K, Arigami T, Nakabeppu Y, et al. Particle size of tin and phytate colloid in sentinel node identification. J Surg Res. 2004;121:1–4.
32. Hayashi H, Ochiai T, Mori M, Karube T, Suzuki T, Gunji Y, et al. Sentinel lymph node mapping for gastric cancer using a dual procedure with dye- and gamma probe-guided techniques. J Am Coll Surg. 2003;196:68–74.
33. Wang Z, Dong ZY, Chen JQ, Liu JL. Diagnostic value of sentinel lymph node biopsy in gastric cancer: a meta-analysis. Ann Surg Oncol. 2012;19:1541–50.
34. Clarke D, Newcombe RG, Mansel RE. The learning curve in sentinel node biopsy: the ALMANAC experience. Ann Surg Oncol. 2004;11:211S–5S.
35. Miyashiro I, Hiratsuka M, Sasako M, Sano T, Mizusawa J, Nakamura K, et al. High false-negative proportion of intraoperative histological examination as a serious problem for clinical application of sentinel node biopsy for early gastric cancer: final results of the Japan Clinical Oncology Group multicenter trial JCOG0302. Gastric Cancer. 2014;17:316–23.
36. Takeuchi H, Ueda M, Oyama T, Shimizu Y, Kitagawa Y. Molecular diagnosis and translymphatic chemotherapy targeting sentinel lymph nodes of patients with early gastrointestinal cancers. Digestion. 2010;82:187–91.
37. Yaguchi Y, Sugasawa H, Tsujimoto H, Takata H, Nakabayashi K, Ichikura T, et al. One-step nucleic acid amplification (OSNA) for the application of sentinel node concept in gastric cancer. Ann Surg Oncol. 2011;18:2289–96.
38. Kusano M, Tajima Y, Yamazaki K, Kato M, Watanabe M, Miwa M. Sentinel node mapping guided by indocyanine green fluorescence imaging: a new method for sentinel node navigation surgery in gastrointestinal cancer. Dig Surg. 2008;25:103–8.
39. Miyashiro I, Miyoshi N, Hiratsuka M, Kishi K, Yamada T, Ohue M, et al. Detection of sentinel node in gastric cancer surgery by indocyanine green fluorescence imaging: comparison with infrared imaging. Ann Surg Oncol. 2008;15:1640–3.
40. Yoshida M, Kubota K, Kuroda J, Ohta K, Nakamura T, Saito J, et al. Indocyanine green injection for detecting sentinel nodes using color fluorescence camera in the laparoscopy-assisted gastrectomy. J Gastroenterol Hepatol. 2012;27(Suppl 3):29–33.
41. Tajima Y, Yamazaki K, Masuda Y, Kato M, Yasuda D, Aoki T, et al. Sentinel node mapping guided by indocyanine green fluorescence imaging in gastric cancer. Ann Surg. 2009;249:58–62.
42. Brouwer OR, Buckle T, Vermeeren L, Klop WM, Balm AJ, van der Poel HG, et al. Comparing the hybrid fluorescent-radioactive tracer indocyanine green-99mTc-nanocolloid with 99mTc-nanocolloid for sentinel node identification: a validation study using lymphoscintigraphy and SPECT/CT. J Nucl Med. 2012;53:1034–40.
43. Frontado LM, Brouwer OR, van den Berg NS, Mathéron HM, Vidal-Sicart S, van Leeuwen FW, et al. Added value of the hybrid tracer indocyanine green-99mTc-nanocolloid for sentinel node biopsy in a series of patients with different lymphatic drainage patterns. Rev Esp Med Nucl Imagen Mol. 2013;32:227–33.
44. Heuveling DA, Visser GW, de Groot M, de Boer JF, Baclayon M, et al. Nanocolloidal albumin-IRDye 800CW: a near-infrared fluorescent tracer with optimal retention in the sentinel lymph node. Eur J Nucl Med Mol Imaging. 2012;39:1161–8.

45. Kong SH, Noh YW, Suh YS, Park HS, Lee HJ, Kang KW, et al. Evaluation of the novel near-infrared fluorescence tracers pullulan polymer nanogel and indocyanine green/γ-glutamic acid complex for sentinel lymph node navigation surgery in large animal models. Gastric Cancer. 2015;18:55–64.
46. Toyota T, Fujito H, Suganami A, Ouchi T, Ooishi A, Aoki A, et al. Near-infrared-fluorescence imaging of lymph nodes by using liposomally formulated indocyanine green derivatives. Bioorg Med Chem. 2014;22:721–7.

Methodology: CT Lymphography

17

CT Lymphography for Superficial Esophageal Cancer

Akira Tangoku, Takahiro Yoshida, Hiroaki Toba, Hirokazu Takechi, Masakazu Okumua, Takeshi Nishino, Seiya Inoue, Misako Nakagawa, Masami Morimoto, Toru Sawada, Mariko Aoyama, Naoki Miyamoto, Kohei Nishioka, Keisuke Fujimoto, and Hiromitsu Takizawa

Abstract

Sentinel lymph node (SLN) navigation surgery became the routine clinical procedure in breast cancer (BC) surgery. SLN navigation has also been introduced to gastrointestinal cancer but still remains controversial for esophageal cancer, because the lymphatic network spread widely from the abdomen to the neck compared with gastric and colon cancer. We developed SLN navigation surgery using multidetector (MD) computed tomography lymphography (CTLG) with a water-soluble iodine tracer injection in BC, which predict not only the precise number and location of the SLNs but also the existence of lymph node metastasis surrounding detailed anatomy, during a screening CT for metastasis.

During the surgery, indocyanine green (ICG) solution was injected around the tumor. SLNs were identified using ICG fluorescence imaging (IGFI) navigated by preoperative CTLG. Lymphatic vessels and SLNs were clearly visualized, and SLNs were identified and sampled using IGFI referring to CTLG, resulting in successful SLN navigation.

The results that micrometastases were existed only in the SLNs which were detected by CTLG navigation authorize the reliability of this method.

Keywords

Sentinel lymph node (SLN) · Navigation surgery · CT lymphography · Superficial esophageal cancer · Minimal invasive surgery

A. Tangoku (✉) · T. Yoshida · H. Toba · H. Takechi · M. Okumua · T. Nishino · S. Inoue
M. Nakagawa · M. Morimoto · T. Sawada · M. Aoyama · N. Miyamoto · K. Nishioka
K. Fujimoto · H. Takizawa
Department of Thoracic, Endocrine Surgery and Oncology, Institute of Biomedical Sciences, Tokushima University Graduate School, Tokushima, Japan
e-mail: tangoku@tokushima-u.ac.jp

S. Natsugoe (ed.), *Lymph Node Metastasis in Gastrointestinal Cancer*,
https://doi.org/10.1007/978-981-10-4699-5_17

17.1 Introduction

Lymph node (LN) metastasis is very common and widely spread from not only in the mediastinum but also in the abdomen to the neck transversally and longitudinally even in superficial esophageal cancer.

And the number of affected lymph nodes is the most important prognostic factor [1]. Therefore, three-field radical lymphadenectomy has improved the prognosis of esophageal cancer [1–3].

Sentinel lymph node navigation surgery has been introduced in melanoma [4] and breast cancer (BC) and became a routine clinical procedure [5, 6].

SLN navigation surgery was also introduced in gastrointestinal tract cancer, especially in gastric cancer [7] and colon cancer [8].

However SLN detection was thought to be difficult in esophageal cancer surgery due to the following specific characteristics. The esophagus has a multi-directional lymphatic flow. The lymphatic flows from the primary lesion spread widely and show random patterns of LN metastasis from the cervix to abdominal areas. Actually, anatomical skip metastases to the second or third compartment of regional LNs were found in 50–60% of esophageal cancer. Lymph node metastasis is common even in the case of superficial cancer. Based on these clinical observations, extended radical esophagectomy with three-field LN dissection has become recognized as a standard procedure in Japan, even for clinically node-negative cases [1–3].

The SLN identification was made by blue dye [5] and gamma probe using a radioisotope [6], and combination of those techniques has been recommended for correct SLN detection in the guideline [9].

Blue dye method can be used only during operation and cannot visualize LN well in the mediastinum because of anthracnosis.

Preoperative lymphoscintigraphy using a radioisotope cannot show detailed anatomical information, but this information can be shown when using SPECT/CT [10].

Shine-through phenomenon interferes the detection of small SLN besides the primary tumor on a radio-scintigraphy, and SLN of the distant area cannot be detected with dye.

We developed a three-dimensional (3D) computed tomography lymphography (CTLG) technique with commercially available iodine medium and adopted to preoperative evaluation of BC to detect SLN before surgery [11, 12]. CTLG visualized the correct number and position of SLNs and afferent and efferent lymphatic vessels connected to SLNs in 3D anatomy. This CTLG was introduced to superficial esophageal cancer and successfully showed the SLNs [13–15].

17.2 Methods

17.2.1 Endoscopic Medium Injection

Iopamidol (Iopamiron 370; Nihon Schering, Osaka, Japan) is a commercially available water-soluble monometric iodine CT contrast medium for intravenous use, with a molecular weight of 777.09 Da, and the solute has an iodine concentration of

370 mg/mL and an osmolality of 780 mOsm/kg, <3 times the osmolality of physiological saline (~300 mOsm/kg), viscosity of 9.1 mPa/s, and pH of 6.5–7.5. Iopamidol was injected endoscopically into the four submucosal regions around the tumor tissues at high pressure with a 23-gauge needle. The injection was performed until swelling was confirmed with every 0.5-mL administration.

17.2.2 3D CTLG

CTLG was performed using a multidetector row helical CT scanner (Siemens Volume Zoom; Siemens-Asahi Medical Technologies Ltd., Tokyo, Japan). Each patient was placed in the supine position on the cradle, and 5 min later, multidetector row CT was performed using 1 mm slices, enabling direct visualization of lymphatic drainage pathways from primary tumor sites. Tracing the lymphatic flows, the LNs taking up iopamidol were defined as SLNs by a monitoring camera. Three-dimensional images were then constructed to clarify where the SLNs exist in comparison to the detailed anatomy of the surrounding structures [13–15].

17.2.3 SLN Biopsy During Surgery

Intraoperative SLN biopsy with ICG fluorescence imaging (IGFI) was performed in all patients who received the CTLG. ICG binds to plasma proteins, and protein-bound ICG emits light with a peak wavelength of about 830 nm when illuminated by near-infrared light [16, 17]. Lymphatic vessels toward the SLN were detected with an endoscopic fluorescence imaging system (Infrared Endoscopic Camera System; Olympus, Tokyo, Japan) and fluorescent image (HyperEye Medical System, Mizuho, Japan). The light source was a light-emitting diode that emitted light at a wavelength of 760 nm, and the detector was a charge-coupled device (CCD) camera with a cut filter used to filter out light with wavelengths below 820 nm. ICG binds to plasma proteins, and protein-bound ICG emits light with a peak wavelength of about 830 nm when illuminated by near-infrared light. Fluorescence signals were transmitted to a digital video processor displayed on a TV monitor in real time. This method has already been applied in clinical studies of esophageal and gastric cancer [18–21].

17.2.4 SLN Sampling and Backup Dissection

Esophagectomy was performed by a thoracoscopic-assisted approach. The esophagus was exposed, and 0.5 mL of ICG solution (Diagnogreen 0.5%; Daiichi Pharmaceutical, Tokyo, Japan) was injected in two regions around the tumor in a direction from the adventitia into the submucosa using a 25-gauge butterfly needle. The lymphatic vessels and SLNs emitting fluorescence were then visualized clearly in vivo, and the esophagus and fluorescing LNs were dissected. These dissected LNs and surrounding adipose tissues were removed together, placed on the

experimental table, and observed again using the photodynamic eye. LNs that were confirmed to fluoresce were diagnosed as SLNs on the basis of the CTLG findings.

This study was authorized by the Institutional Review Board of the Tokushima University Hospital. Before entry into the study, each patient was informed about the investigational nature of the study, and a written informed consent which was approved by the institutional review board was obtained.

17.2.5 Results

CTLG was safely performed in 20 patients with thoracic superficial esophageal cancer (all squamous cell carcinoma) and 12 patients with esophagogastric junction cancer (4 squamous cell carcinoma and 8 adenocarcinoma) in a short time without any complications. Lymphatic drainage routes were identified in all patients, corresponding to the SLNs detected by CTLG and IGF in all patients. LN metastasis was pathologically confirmed in five patients; four of five metastatic nodes were involved in the SLNs that had been detected by CTLG and IGFI. Among these four patients, a small metastatic lesion was observed in three patients. Only one false-negative finding was found in five metastatic nodes.

Three-dimensional images were then constructed to clarify where the SLNs exist in comparison to the detailed anatomy of the surrounding structures [13–15]. The most widely used 3D imaging techniques to date were maximum intensity projection (MIP) (left two) and shaded surface display (SSD) (right one). The lymphatic routes from the tumor occupied the upper middle thoracic esophagus connected to right recurrent nerve nodes (#106recR). Figure 17.1 shows the ascending lymphatic routes (white arrows) and two SLNs (#106recR) (gray arrows) with detailed anatomy of the surrounding structures. Pathology proved a micrometastasis is involved in one of two SLNs.

Lymphatic network spread widely in the mediastinum, toward the neck and the abdomen. The lymphatic routes from the primary tumor showed ascending and descending exist together. Bronchial node (#107) and paragastric node (#2) are the SLN in this case. Micrometastasis existed in the paragastric node (Fig. 17.2).

Small SLN (arrow) besides the primary tumor which cannot be detected using radioisotope because of shine-through phenomenon was detected.

This paraesophageal node showed mottled pattern (scattered defects were observed); it proved to be metastatic node (Fig. 17.3).

In one patient with IIc-like esophagogastric junction tumor, CTLG showed the descending lymphatic routes connected to the paragastric nodes (#1 and #3) (Fig. 17.4a). During surgery, SLNs were sampled by retrieving with ICG fluorescent images using infrared camera system. They could be also checked on the back table (Fig. 17.4b). Histopathology proved micrometastasis exists in #3 node with IHC (cytokeratin CAM5.2) (Fig. 17.4b).

In one patient, an unusual lymphatic route and left supraclavicular node (#104L) were enhanced by CTLG, and an enlarged round right recurrent nerve node

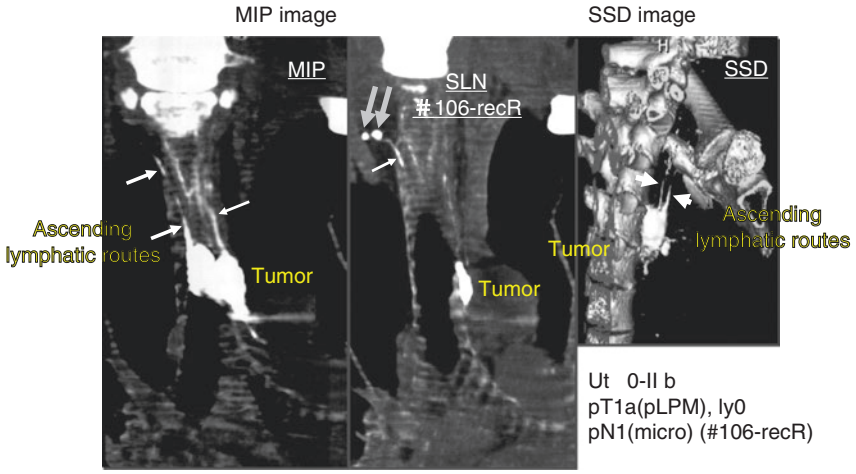

Fig. 17.1 Three-dimensional (3D) CT lymphography. Five minutes after endoscopic injection of iodine medium (iopamidol) into the four submucosae around the tumor, CT scan was performed using 1 mm slices, enabling direct visualization of lymphatic drainage pathways from primary tumor sites. Tracing the lymphatic flows, the LNs taking up iopamidol were defined as SLNs by a monitoring camera. Three-dimensional images were then constructed to clarify where the SLNs (arrow) and afferent lymphatic vessels exist in comparison to the detailed anatomy of the surrounding structures [13–15]. The most widely used 3D imaging techniques to date were maximum intensity projection (MIP) (left two) and shaded surface display (SSD) (right one). The lymphatic routes from the tumor occupied the upper middle thoracic esophagus connected to right recurrent nerve nodes (#106recR). The figure shows the ascending lymphatic routes (white arrows) and two SLNs (#106recR) (gray arrows) with detailed anatomy of the surrounding structures. Pathology proved a micrometastasis is involved in one of the two SLNs

(#106recR) 10 mm diameter was not enhanced on lymphography but enhanced on dynamic CT that was performed 5 min after CTLG with intravenous iopamidol injection. This enlarged node was recognized as metastatic node preoperatively. The true SLN was occupied by metastatic tumor tissue, and another detoured route with LN was visualized. Pathologic examination proved that macroscopic metastases were recognized in two of five dissected #106recR nodes while no metastasis in #104L (Fig. 17.5).

17.3 Discussion

CTLG is a safe technique allowing SLN navigation for breast [11, 12], esophageal [13–15], and lung [22, 23] malignancies, with favorable results.

SLNs were detected preoperatively on CT scan with a commercially available water-soluble iodine contrast medium. This procedure is easy and inexpensive, requiring only a short time during routine CT to evaluate distant metastases, thus resulting in successful SLN navigation while saving time and cost.

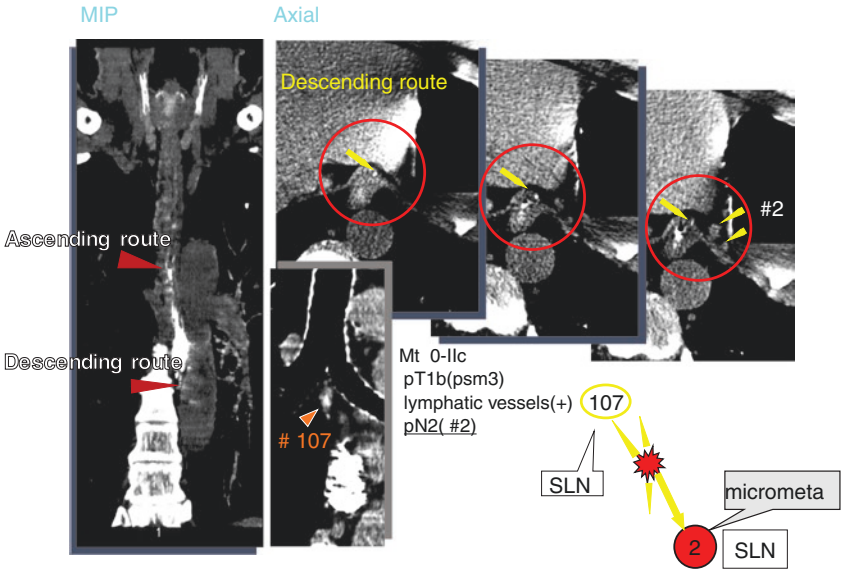

Fig. 17.2 Multi-directional lymphatic routes and multiple SLNs. Lymphatic network spread widely in the mediastinum, toward the neck and the abdomen. The lymphatic routes from the primary tumor showed ascending and descending exist together. Bronchial node (#107) and paragastric node (#2) are the SLN in this case. Micrometastasis existed in the paragastric node

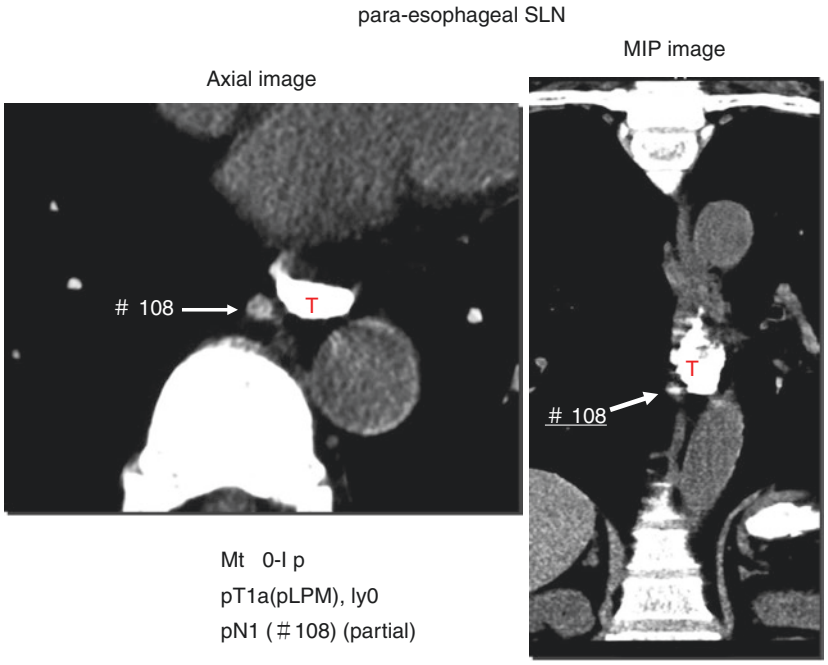

Fig. 17.3 SLN close to primary tumor can be visualized with its stain pattern. Small SLN (arrow) besides the primary tumor which cannot be detected because of shine-through phenomenon using radioisotope was detected. This paraesophageal node showed mottled pattern (scattered defects were observed), proved to be metastatic node

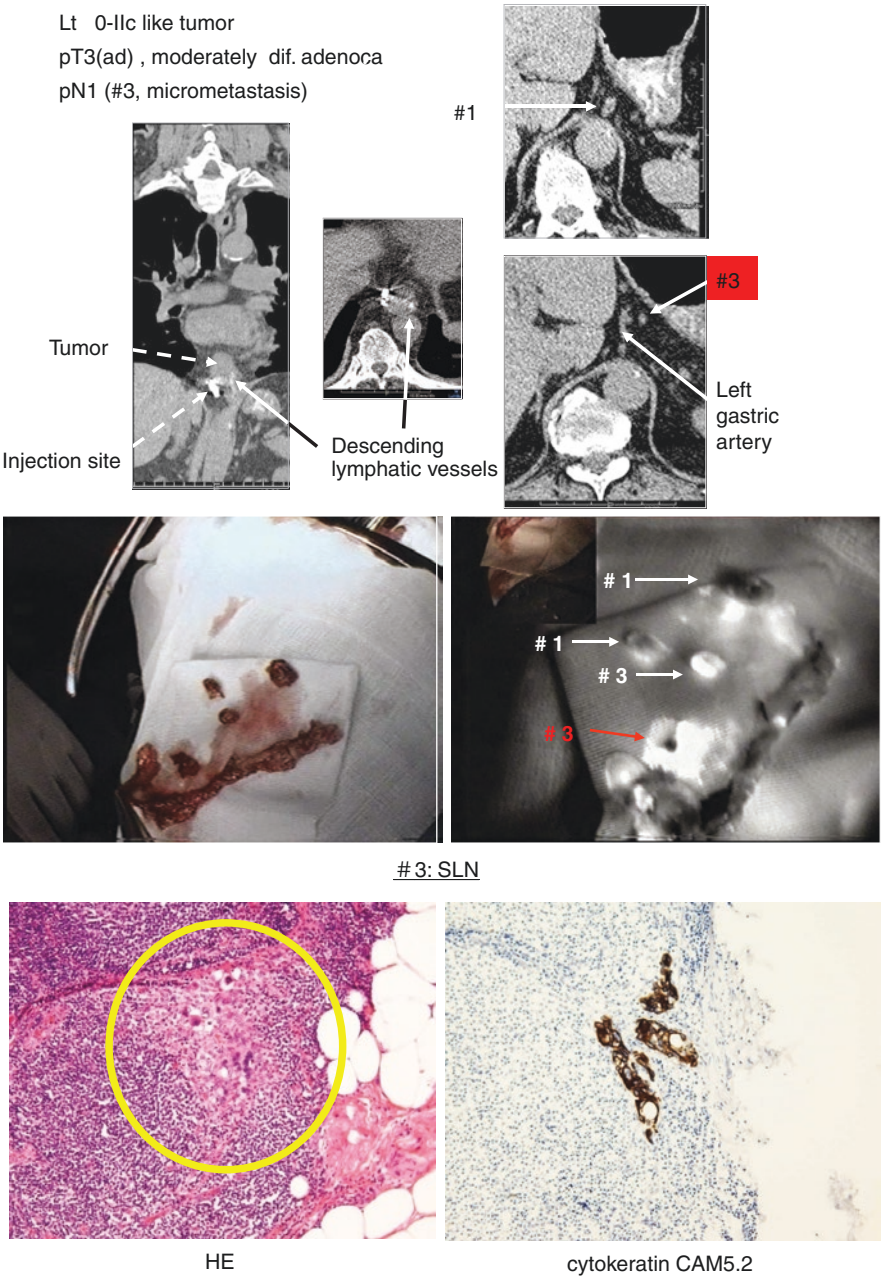

Fig. 17.4 (**a**) CTLG of EC junction tumor. In one patient with IIc-like esophagogastric junction tumor, CTLG showed the descending lymphatic routes connected to the paragastric nodes (#1 and #3). (**b**) SLN sampling retrieved ICG based on CTLG. During surgery, SLNs were sampled by retrieving with ICG fluorescent images using infrared camera system. Histopathology proved micrometastasis exist in #3 node with IHC (cytokeratin CAM5.2). Pathology: #1 SLN, 0/3; **#3 SLN, 1/2**; #105, 0/0; #106pre, 0/1; #106recR, 0/2; #107, 0/6; #108, 0/1; #108, 0/3; #109, 0/3; #1 non-SN, 0/2; #3 non-SN, 0/12; #7, 0/2

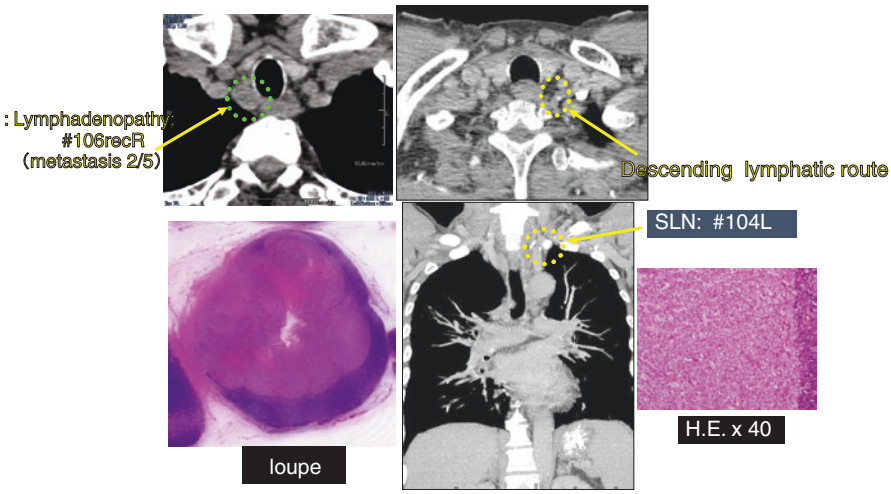

Fig. 17.5 CTLG visualized image of metastatic node and detour route to false SLN. In one patient, an unusual lymphatic route and left supraclavicular node (#104L) were enhanced by CTLG, and an enlarged round right recurrent nerve node (#106recR) 10 mm diameter was not enhanced on lymphography but enhanced on dynamic CT that was performed 5 min after CTLG with intravenous iopamidol injection. This enlarged node was recognized as metastatic node preoperatively. The true SLN was occupied by metastatic tumor tissue, and another detoured route with LN was visualized. Pathologic examination proved that macroscopic metastases were recognized in two of the five dissected #106recR nodes while no metastasis in #104L

Pathologic examination proved successful provability of SLN mapping with CTLG (Figs. 17.1, 17.2, 17.3, 17.4, and 17.5). CTLG covers a weak point of lymphoscintigraphy because of no shine-through phenomenon. The SLN neighboring the primary tumor is visualized clearly (Fig. 17.3).

A number of stocked data from the patients have proved the accurate percentage of LN metastases and prognosis after surgery according to the tumor extent. An accurate diagnosis of tumor invasion and LN metastasis is a key for the choice of an appropriate treatment. But those are very difficult; especially preoperative lymph node metastasis is decided by size and shape of the lymph node. It is well known that LN metastasis is found often in very small-sized LN [24].

Development of the endoscope, MDCT, magnetic resonance imaging system (MRI), and 18F-fluoro-2-deoxy-D-glucose positron emission tomography (^{18}F-FDG-PET) has obtained the accurate diagnosis about tumor extent of esophageal cancer. Patients who were diagnosed by endoscopy and biopsy with no evidence of distant metastatic disease on CT and FDG-PET were referred for EUS for locoregional staging. The results of N staging with CT, FDG-PET, and EUS were compared with surgical pathology or EUS-FNA cytology [24, 25]. Overall accuracy for N staging was 69% for CT, 56% for FDG-PET, and 81% for EUS [26]. Several investigators have reported that PET/CT scan has limited sensitivity in detecting subclinical nodal metastasis, such as micrometastasis in esophageal cancer [27–30].

The combination of CT plus EUS appears to be accurate for locoregional staging in esophageal cancer [26]. EUS is also the most accurate technique for preoperative locogional staging of esophageal carcinoma, once CT and/or the FDG-PET scan has excluded the presence of distant metastasis. EUS-guided fine needle aspiration (EUS-FNA) might help improve diagnostic accuracy in esophageal cancer LN staging, and the therapeutic decision might be derived from such a practice [24].

At present, SN biopsy is believed to detect micrometastasis more accurately and cost-effectively than other imaging procedures in patients with cN0 early esophageal cancer [25, 31].

Many reports have indicated that immunohistochemical nodal micrometastasis is a significant prognostic indicator in patients with cN0 esophageal cancer [32–34].

SLN mapping in esophageal cancer is obviously more invasive than other imaging techniques; nodal micrometastasis in SLN that may affect survival of the patient cannot be ignored [25]. Our results showed many SLNs involved micrometastasis only in SLNs which have been detected with CTLG. The results authorize the reliability of this procedure.

CTLG visualized SLNs with afferent lymphatic route clearly in 3D image; therefore lymph node metastasis can be diagnosed preoperatively according to the following criteria: an appearance of afferent lymph vessel obstruction due to tumor embolism and occupied lymph nodes. The tumor occupation resulted in stagnation, dilation, and detour of the lymph vessels and defect of the lymph node staining. Partial staining (crab claw-shaped stain, shadow defect, and mottled stain pattern) of the SLNs, and stagnation, dilation, and detour pattern of the afferent lymphatic routes are suspicious signs of lymph node metastasis [35, 36].

The afferent lymph vessel and SLN were completely visualized in two right recurrent nerve nodes (Figs. 17.1, 17.2, 17.4, and 17.5). Lymph vessel was smooth and completely stained as shown in the figures. Metastatic nodes (true SLN) were not stained as shown in Fig. 17.5. The lymph flow was detoured to another route, and another LN adjacent to true SLN was stained like SLN. Those nodes would diagnose the false negative in histopathology if using the conventional methods like blue dye and gamma probe.

17.4 Conclusions

CTLG visualized the precise number and position of SLNs in 3D anatomy preoperatively during CT scan screening for distant metastasis. SLN biopsy can detect micrometastasis in SLNs and would make super staging. Existence of many SLNs sampled under navigation with CTLG involved micrometastasis. Macrometastasis is also detected by CTLG with the information of obstructed afferent lymphatic routes and shadow defects due to tumor occupation. These results showed that CTLG would be a new preoperative strategy for precise information on staging of esophageal cancer.

References

1. Fujita H. The history of lymphadenectomy for esophageal cancer and the future prospects for esophageal cancer surgery. Surg Today. 2015;45:140–9.
2. Akiyama H, Tsurumaru M, Udagawa H, Kajiyama Y. Radical lymph node dissection for cancer of the thoracic esophagus. Ann Surg. 1994;220:364–73.
3. Ando N, Ozawa S, Kitagawa Y, Shinozawa Y, Kitajima M. Improvement in the results of surgical treatment of advanced squamous esophageal carcinoma during 15 consecutive years. Ann Surg. 2000;232:225–32.
4. Morton DL, Wen DR, Wong JH, Economou JS, Cagle LA, Storm FK, et al. Technical details of intraoperative lymphatic mapping for early stage melanoma. Arch Surg. 1992;127:392–9.
5. Giuliano AE, Kirgan DM, Guenther JM, Morton DL. Lymphatic mapping and sentinel lymphadenectomy for breast cancer. Ann Surg. 1994;220:391–8. discussion 398–401
6. Krag D, Weaver D, Ashikaga T, Moffat F, Klimberg VS, Shriver C, et al. The sentinel node in breast cancer—a multicenter validation study. N Engl J Med. 1998;339:941–6.
7. Kitagawa Y, Fujii H, Mukai M, Mukai M, Nakahara T, Kubo A, Kitajima M. Radio-guided sentinel node detection for gastric cancer. Br J Surg. 2002;89:604–8.
8. Bilchik AJ, Saha S, Wiese D, Stonecypher JA, Wood TF, Sostrin S, et al. Molecular staging of early colon cancer on the basis of sentinel node analysis: a multicenter phase II trial. J Clin Oncol. 2001;19:1128–36.
9. Veronesi U, Paganelli G, Galimberti V, Viale G, Zurrida S, Bedoni M, et al. Sentinel-node biopsy to avoid axillary dissection in breast cancer with clinically negative lymph-nodes. Lancet. 1997;349:1864–7.
10. Vermeeren L, van der Ploeg IM, Olmos RA, Meinhardt W, Klop WM, Kroon BB, Nieweg OE. SPECT/CT for preoperative sentinel node localization. J Surg Oncol. 2010;101:184–90.
11. Suga K, Yuan Y, Okada M, Matsunaga N, Tangoku A, Yamamoto S, Oka M, et al. Breast sentinel lymph node mapping at CT lymphography with iopamidol: preliminary experience. Radiology. 2004;230:543–52.
12. Tangoku A, Yamamoto S, Suga K, Ueda Y, Nagashima M, Hida T, Sato K, Sakamoto K, Oka M, et al. Sentinel lymph node biopsy using computed tomography-lymphography in patients with breast cancer. Surgery. 2004;135:258–65.
13. Suga K, Shimizu K, Kawakami Y, Tangoku A, Zaki M, Matsunaga N, Oka M. Lymphatic drainage from esophagogastric tract: feasibility of endoscopic CT lymphography for direct visualization of pathways. Radiology. 2005;237(3):952–60.
14. Hayashi H, Tangoku A, Suga K, Shimizu K, Ueda K, Yoshino S, Abe T, Sato T, et al. CT lymphography-navigated sentinel lymph node biopsy in patients with superficial esophageal cancer. Surgery. 2006;139(2):224–35.
15. Yuasa Y, Seike J, Yoshida T, Takechi H, Yamai H, Yamamoto Y, et al. Sentinel lymph node biopsy using intraoperative indocyanine green fluorescence imaging navigated with preoperative CT lymphography for superficial esophageal cancer. Ann Surg Oncol. 2012;19:486–93.
16. Landsman ML, Kwant G, Mook GA, Zijlstra WG. Light-absorbing properties, stability, and spectral stabilization of indo-cyanine green. J Appl Physiol. 1976;40:575–83.
17. Mordon S, Devoisselle JM, Soulie-Begu S, Desmettre T. Indocyanine green: physicochemical factors affecting its fluorescence in vivo. Microvasc Res. 1998;55:146–52.18.
18. Parungo CP, Ohnishi S, Kim SW, Kim S, Laurence RG, Soltesz EG, et al. Intraoperative identification of esophageal sentinel lymph nodes with near-infrared fluorescence imaging. J Thorac Cardiovasc Surg. 2005;129:844–50.
19. Tajima Y, Yamazaki K, Masuda Y, Kato M, Yasuda D, Aoki T, et al. Sentinel node mapping guided by indocyanine green fluorescence imaging in gastric cancer. Ann Surg. 2009;249:58–62.
20. Miyashiro I, Miyoshi N, Hiratsuka M, Kishi K, Yamada T, Ohue M, et al. Detection of sentinel node in gastric cancer surgery by indocyanine green fluorescence imaging: comparison with infrared imaging. Ann Surg Oncol. 2008;15:1640–3.

21. Oguma J, Ozawa S, Kazuno A, Yamasaki Y, Ninomiya Y, Yoshida M. Sentinel node navigation surgery with indocyanine green fluorescence-guided method for metachronous early gastric carcinoma arising from reconstructed gastric tube after esophagectomy. Gen Thorac Cardiovasc Surg. 2016;64(5):298–301.
22. Ueda K, Suga K, Kaneda Y, Li TS, Ueda K, Hamano K. Pre-operative imaging of the lung sentinel lymphatic basin with computed tomographic lymphography: a preliminary study. Ann Thorac Surg. 2004;77:1033–7.
23. Takizawa H, Kondo K, Toba H, Kajiura K, Ali AHK, Sakiyama S, Tangoku A. Computed tomography lymphography by transbronchial injection of iopamidol to identify sentinel nodes in preoperative patients with non-small cell lung cancer: A pilot study. J Thorac Cardiovasc Surg. 2012;144(1):94–9.
24. Tangoku A, Yamamoto Y, Furukita Y, Goto M. The new era of staging as a key for an appropriate treatment for esophageal cancer. Ann Thorac Cardiovasc Surg. 2012;18(3):190–9.
25. Takeuchi H, Kawakubo H, Takeda F, Omori T, Kitagawa Y. Sentinel node navigation surgery in early-stage esophageal cancer. Ann Thorac Cardiovasc Surg. 2012;18:306–13.
26. Vazquez-Sequeiros E, Foruny-Olcina JR. Linear EUS: the clinical impact of N staging in esophageal carcinoma. Minerva Med. 2007;98:313–9.
27. Bruzzi JF, Munden RF, Truong MT, Marom EM, Sabloff BS, Gladish GW, et al. PET/CT of esophageal cancer: its role in clinical management. Radiographics. 2007;27:1635–52.
28. van Vliet EP, Heijenbrok-Kal MH, Hunink MG, Kuipers EJ, Siersema PD, et al. Staging investigations for oesophageal cancer: a metaanalysis. Br J Cancer. 2008;98:547–57.
29. Kato H, Kimura H, Nakajima M, Sakai M, Sano A, Tanaka N, et al. The additional value of integrated PET/CT over PET in initial lymph node staging of esophageal cancer. Oncol Rep. 2008;20:857–62.
30. Shimizu S, Hosokawa M, Itoh K, Fujita M, Takahashi H, Shirato H, et al. Can hybrid FDG-PET/CT detect subclinical lymph node metastasis of esophageal cancer appropriately and contribute to radiation treatment planning? A comparison of image-based and pathological findings. Int J Clin Oncol. 2009;14:421–5.
31. Zhang J, Chen H, Luketich JD. Sentinel lymph node biopsy in esophageal cancer: has its time come? Ann Surg. 2010;252:413–4. author reply 415
32. Komukai S, Nishimaki T, Suzuki T, Kanda T, Kuwabara S, Hatakeyama K, et al. Significance of immunohistochemical nodal micrometastasis as a prognostic indicator in potentially curable oesophageal carcinoma. Br J Surg. 2002;89:213–9.
33. Li SH, Wang Z, Liu XY, Liu FY, Sun ZY, Xue H, et al. Lymph node micrometastasis: a predictor of early tumor relapse after complete resection of histologically node-negative esophageal cancer. Surg Today. 2007;37:1047–52.
34. Koenig AM, Prenzel KL, Bogoevski D, Yekebas EF, Bubenheim M, Faithova L, et al. Strong impact of micrometastatic tumor cell load in patients with esophageal carcinoma. Ann Surg Oncol. 2009;16:454–62.
35. Mokhtar M, Tadokoro Y, Nakagawa M, Morimoto M, Takechi H, Kondo K, Tangoku A. Triple assessment of sentinel lymph node metastasis in early breast cancer using preoperative CTLG, intraoperative fluorescence navigation and OSNA. Breast Cancer. 2016;23(2):202–10.
36. Nakagawa M, Morimoto M, Takechi H, Tadokoro Y, Tangoku A. Preoperative diagnosis of sentinel lymph node (SLN) metastasis using 3D CT lymphography (CTLG). Breast Cancer. 2016;23(3):519–24.

Clinical Aspect: Esophageal Cancer

18

Yoshikazu Uenosono, Takaaki Arigami, Shigehiro Yanagita, Itaru Omoto, Ken Sasaki, Yasuto Uchikado, and Shoji Natsugoe

Abstract

If the sentinel node (SN) concept is established for esophageal cancer, SN navigation surgery will be clinically useful. The following personalized treatments will also be possible: reducing the extent of lymphadenectomy in upper mediastinal and cervical regions, targeting radiotherapy for SN, and SN sampling with endoscopic therapy. Since difficulties are associated with using the dye method for the detection of SN due to complex lymphatic flow in the esophagus and anthracosis in the lymph nodes, the radioisotope method is available for esophageal cancer. When SN navigation surgery is introduced in the clinical field, an accurate diagnosis is essential for nodal metastasis, including micrometastasis. Only a few studies have been published on the SN concept for esophageal cancer, and clinical evidence is currently not available. In our experience, the SN concept is applicable to patients with cT1 and cN0 esophageal cancer; however, the role of SN navigation surgery for clinical T2 or more remains unclear. Multicenter trials are needed in the near future in order to establish standard personalized therapy.

Y. Uenosono (✉)
Molecular Frontier Surgery, Kagoshima University Graduate School of Medical and Dental Sciences, Kagoshima, Japan
e-mail: uenosono@m3.kufm.kagoshima-u.ac.jp

T. Arigami · S. Natsugoe
Molecular Frontier Surgery, Kagoshima University Graduate School of Medical and Dental Sciences, Kagoshima, Japan

Department of Digestive Surgery, Breast and Thyroid Surgery, Kagoshima University Graduate School of Medical and Dental Sciences, Kagoshima, Japan

S. Yanagita · I. Omoto · K. Sasaki · Y. Uchikado
Department of Digestive Surgery, Breast and Thyroid Surgery, Kagoshima University Graduate School of Medical and Dental Sciences, Kagoshima, Japan

S. Natsugoe (ed.), *Lymph Node Metastasis in Gastrointestinal Cancer*,
https://doi.org/10.1007/978-981-10-4699-5_18

Keywords
Sentinel node · Esophageal cancer · Lymph node metastasis · Micrometastasis · Minimally invasive surgery

18.1 Introduction

Esophageal cancer has one of the greatest malignant potentials among gastrointestinal cancers and frequently metastasizes to the lymph nodes, such as the cervical or abdominal lymph nodes, which are distant from the primary tumor. Since the sites of lymph node metastases are extensively distributed, difficulties are associated with focusing on the removal of specific lymph nodes, even in superficial esophageal cancer [1]. Therefore, radical lymph node dissection such as extended three-field lymphadenectomy has been widely accepted as a treatment for esophageal cancer [2, 3]. Furthermore, esophageal cancer surgery is one of the most invasive types of digestive surgery [4, 5]. To date, endoscopic submucosal dissection (ESD) and minimally invasive surgery with thoracoscopy and laparoscopy are performed for early-stage disease. If minimally invasive surgery is possible for patients with esophageal cancer, the mortality rate after surgery and postsurgical quality of life will be improved.

The sentinel node (SN) concept of lymph node metastasis has been established for melanoma and breast cancer. Recent studies have attempted to verify this concept for gastrointestinal cancer. If this concept is established for esophageal cancer, it will be possible to safely reduce the extent of lymphadenectomy. This chapter will focus on the clinical aspect of SN navigation surgery for patients with esophageal cancer.

18.2 The SN Concept

The SN concept was initially advocated by Morton et al. for patients with melanoma [6]. According to the definition of this concept, SN is the first lymph node that receives lymphatic flow from the primary tumor, and lymph node micrometastasis occurs from this SN; however, this node is not necessarily the nearest lymph node to the primary tumor site. The SN concept has been clinically applied to melanoma and breast cancer for minimally invasive surgery. A large number of studies have demonstrated the utility of the SN concept for patients with early-stage gastric cancer. In 2013, the findings of a prospective multicenter trial on SN navigation surgery were reported by a Japanese group [7]. Three hundred and ninety-seven patients were enrolled in this study. The detection rate, sensitivity, and accuracy were 97.5%, 93%, and 99%, respectively, and there were only four false-negative cases. Accordingly, the clinical application of SN navigation surgery for gastric cancer may be possible.

Several studies demonstrated the utility of the SN concept for patients with esophageal cancer (Table 18.1) [8–18]. Kitagawa et al. initially indicated its potential in 2000 [8]. They demonstrated SN mapping using a radioisotope (RI) method

Table 18.1 Results of studies evaluating sentinel node mapping in patients with esophageal cancer

Author	Year	T factor	Histological type	Tracer	No. of pts.	Detection rate (%)	Sensitivity (%)	Accuracy (%)
Kitagawa [8]	2000	cT1-3	SCC	RI	27	93	88	92
Kato [9]	2003	pT1-4	SCC	RI	25	92	87	91
Yasuda [10]	2003	pT1-3	NA	RI	23	100	75	87
Burian [16]	2004	pT1-3	Adeno	Blue dye	20	85	–	88
Lamb [11]	2005	NA	Adeno	RI	57	100	95	96
Takeuchi [12]	2009	cT1-2	SCC + adeno	RI	75	95	88	94
Thompson [13]	2011	pT1a-3	SCC + adeno	RI	16	88	100	100
Kim [14]	2011	cT1-4	SCC	RI	23	91	100	100
Uenosono [15]	2011	cT1-3 + CRT	SCC + adeno	RI	134	90	63	80
Yuasa [17]	2012	cT1	NA	CTLG + ICG	20	100	75	95
Hachey [18]	2016	pT1-3	Adeno	ICG (HSA)	10	60	NA	NA

SCC squamous cell carcinoma, *Adeno* adenocarcinoma, *RI* radioisotope, *CTLG* computed tomographic lymphography, *ICG* indocyanine green, *HAS* human serum albumin, *NA* not available

in 27 patients with esophageal cancer, with detection and accuracy rates of 88% and 92%, respectively. Although identification and accuracy rates were reported to be 90–100% and 78–100%, respectively, most studies included advanced stages, and the number of patients was small. Many studies have indicated the usefulness of the SN concept for adenocarcinoma, mainly Barrett's esophageal cancer (BEC) of the esophagus in Western countries and squamous cell carcinoma in Eastern countries. Burian et al. reported detection and accuracy rates of 90% and 85% for BEC, respectively [16]. The incidence of adenocarcinoma of the esophagogastric junction (AEG) has recently increased, and this finding has been already described in several reports in SN [19, 20].

18.3 Identification of SN

RI and/or dye methods are the two main procedures used to detect SN in breast cancer, melanoma, and gastric cancer. In these cancers, the dye method is advantageous because it allows for the visualization of the lymph nodes and lymphatics themselves, which are stained blue. Since the esophagus exists in the posterior mediastinum, it is difficult to identify lymph nodes with blue dye until the mediastinal pleura is opened. Furthermore, in many patients with esophageal cancer, mediastinal lymph nodes are black due to anthracosis. Therefore, the RI-guided method is useful for the detection of SN in esophageal cancer, while the dye method alone may not be suitable.

SN is currently detected using the infrared fluorescence imaging method, with indocyanine green as a tracer. Kubota et al. described the infrared fluorescence imaging method using the HyperEye Medical System in esophageal cancer surgery [21]. A laparoscopic near-infrared imaging system was recently developed by Novadaq [18]. Fluorescence imaging is clearer than absorbance imaging. On the other hand, Yuasa et al. reported the utility of preoperative computed tomographic lymphography (CTLG) with fluorescence imaging [17]. They found that CTLG clearly visualized the relationship between SLN and lymphatic routes by detecting obstructions in the lymph vessels and tumor replacement and may be used to diagnose lymph node metastasis. Lymph flow from tumors was visualized on a 3D CT image with the surrounding anatomy during preoperative routine CT examinations for tumor infiltration and metastasis.

We used the RI method with 99m Technetium-Tin colloid as a tracer (Fig. 18.1). One day prior to surgery (approximately 18 h), 3mCi 99m Technetium-Tin colloid (Nihon Medi-physics, Nishinomiya, Japan) is injected endoscopically into the esophageal submucosa at four sites (0.5 mL each) near a tumor using a 23-gauge needle.

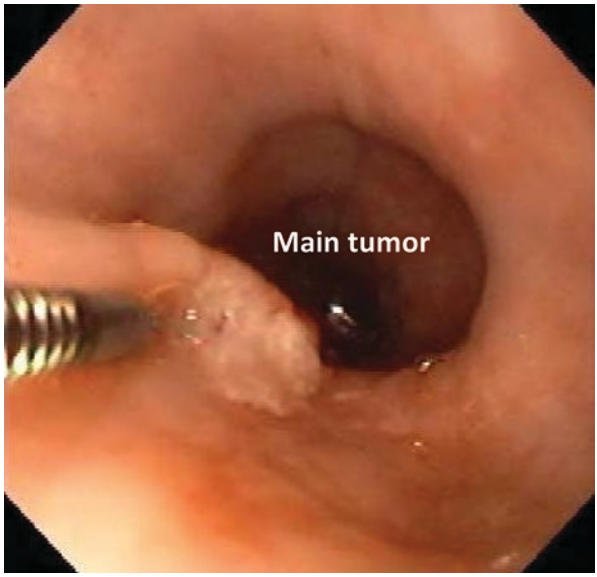

Fig. 18.1 One day prior to surgery, 99m Technetium-Tin colloid was injected endoscopically into the esophageal submucosa at four sites around the tumor

18.4 Clinical Utility of Lymphoscintigraphy for Esophageal Cancer

Lymphoscintigraphy is performed using planar images (E-CAM Nuclear Gamma Camera: TOSHIBA, Japan) from the anterior, and right and left lateral views are obtained 2 h after the radioisotope injection. Lymphoscintigraphy for esophageal cancer is particularly useful because it has the ability to identify SN distant from the injection site, such as the cervical, upper mediastinal, or abdominal nodes (Fig. 18.2). We identify these SNs by performing lymphoscintigraphy before surgery and then verify our findings using a direct measure of the RI count during surgery. Image processing by single-photon emission computed tomography (SPECT) is useful for depicting SN in the vicinity of the RI injection site, and we can identify the positional relation between main lesions and SNs, three-dimensionally (Fig. 18.3a, b). Tsai et al. demonstrated the utility of hybrid SPECT/CT imaging and concluded that the preoperative identification of SN with hybrid SPECT/CT imaging after the endoscopic injection of a radiocolloid has potential for SN mapping in esophageal cancer [22]. Cooperation with radiologists is important for SPECT and the analysis of lymphoscintigraphy. However, some SN around RI injection sites cannot be identified during surgery due to the "shine-through" phenomenon.

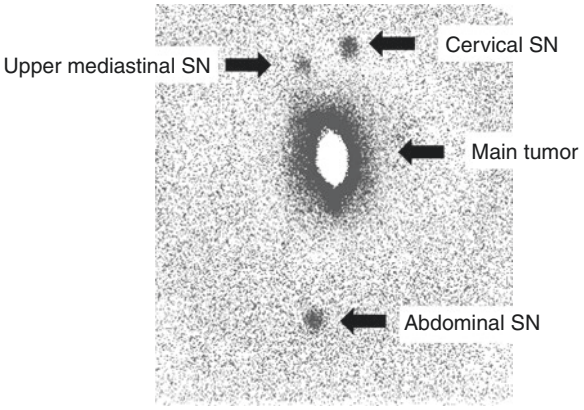

Fig. 18.2 Lymphoscintigraphy: SNs distant from the injection site, such as the cervical, upper mediastinal, or abdominal nodes, were detected by lymphoscintigraphy in this case

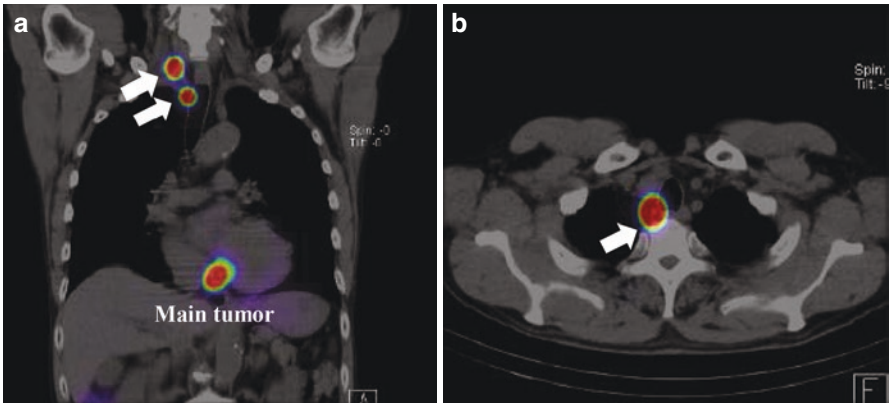

Fig. 18.3 Image processing by single-photon emission computed tomography (SPECT) is useful to three-dimensionally identify the positional relation between main lesions and SNs. (**a**) Right recurrent nerve and cervical paraesophageal lymph nodes as SNs are found in the coronal view (arrow). (**b**) The right recurrent nerve lymph node as SN is found in the transverse view (arrow)

18.5 Intraoperative Identification and Biopsy of SN

Most SNs are intraoperatively identified using a gamma probe such as Navigator GPS (Dilon Diagnostics, USA). During surgery, the uptake of RI by each lymph node is measured with a gamma probe. Cervical SN is identified from the surface of a body using a gamma probe, and sampling by a small incision is possible. Mediastinal SN is identified under thoracoscopy or a small incision (Fig. 18.4a, b). SN is carefully searched for using a gamma probe because some SNs around the RI injection sites cannot be identified during surgery due to the "shine-through" phenomenon. Abdominal SNs are identified under laparoscopy (Fig. 18.4c). Some SNs are identified after checking with the gamma probe. It is important to dissect

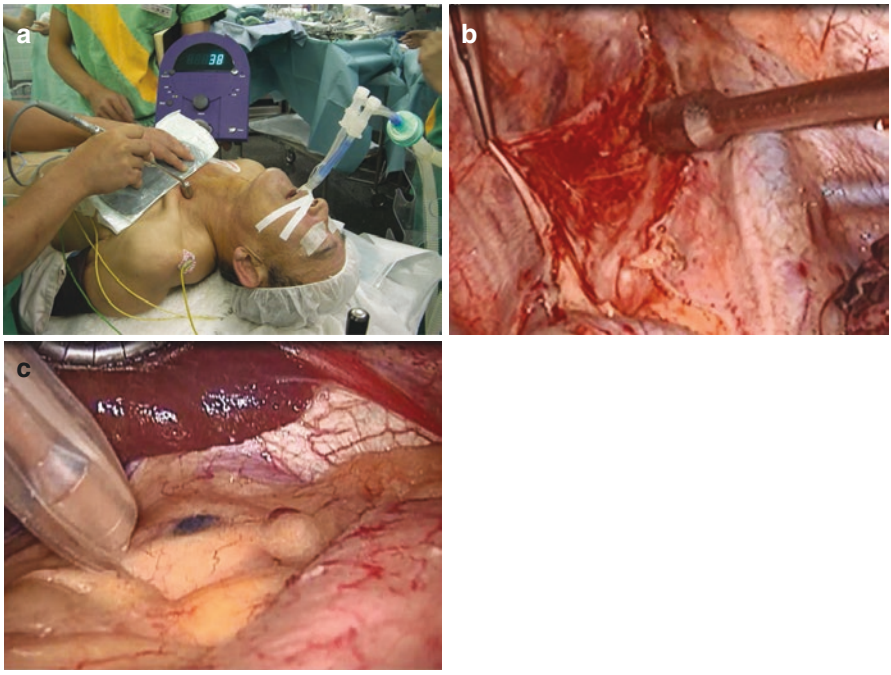

Fig. 18.4 Intraoperative identification and biopsy of SN. (**a**) Cervical SNs are identified from the surface of a body using the gamma probe. (**b**) Upper mediastinal SNs are identified under thoracoscopy. (**c**) Abdominal SNs are identified under laparoscopy

peripheral connective and adipose tissues in order to avoid injuring the capsule of SN because micrometastases are often detected in the marginal sinus under the lymph node capsule.

After the dissection of SN, the absence of residual radioactivity in the cervix, mediastinum, and abdomen is confirmed intraoperatively using a gamma probe. When counts for individual lymph nodes are fivefold greater than background levels, the lymph node is identified as a "hot node" or SN by our criteria.

18.6 SN Mapping

The findings of SN mapping have been reported by several single institutes; however, less than 50 patients were enrolled in the majority of these studies. Takeuchi et al. reported the findings of SN mapping in 75 consecutive patients who were preoperatively diagnosed with T1N0M0 or T2N0M0 primary esophageal cancer [12]. 99m Technetium-tin colloid was used as the tracer, and SNs were successfully identified in 71 (95%) out of 75 patients. The mean number of SN identified per case was 4.7. Twenty-nine (88%) out of 33 cases with lymph node metastasis showed positive SLN. Diagnostic accuracy based on the SLN status was 94% (67/71). The

distribution of SLN identified spread from the cervical to abdominal areas. Lamb et al. reported the findings of SN mapping in 57 patients, although 17 patients with gastric cancer were included [11]. 99m Technetium nanocolloid was used as the tracer, and SNs were detected by a handheld gamma probe. SNs were identified in all patients; the mean number of SNs identified per case was 2.0, and the accuracy rate was 96%. Nagaraja et al. reported the findings of a meta-analysis of 23 relevant studies between 2002 and 2011 [23]. They found that the overall detection rate was 93%, sensitivity 87%, negative predictive value 77%, and accuracy 88%.

A feasibility study on SN mapping was performed on 134 patients with esophageal cancer who underwent esophagectomy with lymphadenectomy at Kagoshima University Hospital [15]. RI uptake in all dissected lymph nodes was measured after esophagectomy with standard lymphadenectomy.

Nineteen tumors were located in the upper third of the esophagus, 73 in the middle third, and 42 in the lower third. The depth of tumor invasion was clinically diagnosed before surgery based on gastrointestinal endoscopy, double contrast gastrography, and endoscopic ultrasonography. Based on the TNM classification, cT1 tumors were detected in 60 patients, cT2 in 31, and cT3 in 32. Apart from these patients, neoadjuvant chemoradiation therapy (CRT) was administered to 11 patients. Esophagectomy by right thoracotomy was performed on 93 patients, left thoracotomy on 14, and blunt dissection with lymphadenectomy on 27. The total number of dissected lymph nodes was 4483, and the number of resected nodes per patient ranged between 6 and 108, with a median of 30.5 nodes.

SNs were identified in 120 out of 134 cases by measuring all dissected lymph nodes using Navigator GPS. The detection rates of SN were 93.3% (56/60) in cT1, 100% (31/31) in cT2, and 87.5% (28/32) in cT3. SNs were only identified in five CRT patients, preoperatively, and the detection rate was 45.5%.

SNs were detected in 45 (40.2%) out of 112 patients by presurgical lymphoscintigraphy.

The mean number of SNs detected by lymphoscintigraphy was 1.4 (range, 1–3).

The sensitivity and accuracy of SN mapping were 91.7% and 98.2%, respectively, in cT1 patients. Although the false-negative case did not have metastasis or micrometastasis in SN, this case was clinically diagnosed as N1 because a metastatic node was preoperatively detected by endoscopic ultrasonography. This metastatic lymph node was almost completely occupied by cancer cells. However, the sensitivity and accuracy of SN mapping were 66.7% and 80.6% in cT2 patients and 54.2% and 60.7% in cT3 patients, respectively (Table 18.2). Accordingly, the SN concept is acceptable for clinical application to cT1 and N0 esophageal cancer only

Table 18.2 Our results for sentinel node mapping in each clinical T factor

	cT1	cT2	cT3	CRT
Sensitivity	91.7%(11/12)	66.7%(12/18)	54.2%(13/24)	0%(0/3)
False negative	8.3%(1/12)	33.3%(6/18)	45.8%(11/24)	100%(3/3)
NPV	97.8%(44/45)	68.4%(13/19)	26.7%(4/15)	40.0%(2/5)
Accuracy	98.2%(55/56)	80.6%(25/31)	60.7%(17/28)	40.0%(2/5)

NPV negative predictive value

based on our results. Furthermore, sensitivity was 0 and the accuracy of SN mapping was 40.0% in CRT patients. SN navigation surgery is not applicable to patients who have received neoadjuvant therapy.

18.7 Indication of SN Navigation Surgery for Esophageal Cancer

It is important to assess the indication of clinical applications based on the SN concept. Previous studies reported that SN biopsy is not feasible for advanced esophageal cancer [24]. Patients with overt lymph node metastasis by preoperative imaging means need to be excluded from SN navigation surgery. We investigated whether RI uptake reflects the ratio of the metastatic areas of SN in esophageal and gastric cancer, with the aim of decreasing the false-negative rate in the identification of SN. Our findings showed

that RI uptake was not detectable in lymph nodes with a >60% metastatic area [25]. Therefore, we consider the SN concept to be applicable to patients with cT1 and cN0 esophageal cancer.

18.8 Micrometastasis in SN

The accurate diagnosis of SN during surgery is important for the clinical application of SN navigation surgery. An intraoperative diagnosis of lymph node metastasis including micrometastasis is essential for performing SN navigation surgery because the clinical significance of lymph node micrometastasis is still controversial in patients with esophageal cancer. To date, several studies have demonstrated the clinical impact of lymph node micrometastasis identified by immunohistochemistry (IHC). Furthermore, it has been reported that a real-time reverse transcription-polymerase chain reaction (RT-PCR) detects lymph node micrometastasis more accurately than IHC. Due to advances in the field of genetics, the presence of micrometastasis in a lymph node may also be assessed; however, the clinical significance of this metastasis remains controversial in esophageal cancer. We previously reported that isolated tumor cells exhibited proliferative activity by CK and Ki-67 double staining using IHC [26]. We consider it important to test for lymph node micrometastasis even if lymph node metastases are negative in routine histological examinations.

We previously investigated the adequacy of the SN concept based on lymph node micrometastasis assessed by IHC and RT-PCR in patients with esophageal cancer [27]. SNs were mapped in 57 patients with cT1-T2 and cN0 esophageal cancer. The incidences of node positivity identified by HE and IHC were 12.3% (7/57) and 19.3% (11/57), respectively. RT-PCR detected micrometastasis in 4 out of 46 patients without nodal metastasis assessed by HE staining and IHC. Non-SN metastases were not found in 42 patients without micrometastasis identified by IHC and RT-PCR of SN. Accuracy and false-negative rates were 100% (57/57) and 0%

(0/42), respectively. The SN concept may be acceptable for patients with cT1-T2 and cN0 esophageal cancer, even in the presence of micrometastasis identified by IHC and RT-PCR.

18.9 Future Perspectives of Clinical Applications Based on the SN Concept

If the SN concept is established for esophageal cancer, SN navigation surgery will be clinically useful. The following personalized treatments will be possible: reducing the extent of lymphadenectomy in the upper mediastinal and cervical regions, targeting radiotherapy for SN, and SN sampling with endoscopic therapy.

The lymph nodes around the recurrent laryngeal nerve are frequent metastatic sites of esophageal cancer; however, upper mediastinal lymph node dissection is associated with the risk of recurrent laryngeal nerve paralysis [28]. If SN was not identified in upper mediastinal and cervical regions, and all SNs are confirmed to be pathologically negative in patients with cT1N0 middle/lower thoracic esophageal cancer and AEG, cervical lymph node dissection may be omitted.

Although chemoradiotherapy is a standard treatment, the design of radiation fields is still controversial [29]. Takeuchi et al. are conducting an ongoing study involving concurrent chemoradiotherapy for patients with cT1N0M0 esophageal cancer with minimized radiation fields that contain SN identified by lymphoscintigraphy in order to achieve the local control of subclinical metastasis in SN [30].

ESD is the standard treatment for clinical T1a superficial esophageal cancer. However, patients with clinical T1b superficial esophageal cancer undergo esophagectomy with lymph node dissection. If the tumor is completely removed by ESD and all SNs are confirmed to be pathologically negative, it may be unnecessary to perform esophagectomy and lymph node dissection. A combination of ESD and SN biopsy will be a new approach for cT1N0 esophageal cancer.

18.10 Conclusions

Several studies and our experience of SN mapping indicate relatively good outcomes. Multicenter trials are needed in the near future in order to establish standard personalized therapy, and some issues still need to be resolved such as the tracer to use, the diagnosis of SN including micrometastasis, and a concrete method for clinical application. SN navigation surgery may become the standard of care for esophageal cancer in the near future, particularly in the setting of minimally invasive surgery.

The SN concept is presently applicable to patients with cT1 and cN0 esophageal cancer; however, the role of SN navigation surgery for clinical T2 or more remains tentative.

References

1. Akutsu Y, Kato K, Igaki H, Ito Y, Nozaki I, Daiko H, Yano M, Udagawa H, Nakagawa S, Takagi M, et al. The prevalence of overall and initial lymph node metastases in clinical T1N0 thoracic esophageal cancer: from the results of JCOG0502, a prospective multicenter study. Ann Surg. 2016;264(6):1009–15.
2. Lerut T, Nafteux P, Moons J, Coosemans W, Decker G, De Leyn P, Van Raemdonck D, Ectors N. Three-field lymphadenectomy for carcinoma of the esophagus and gastroesophageal junction in 174 R0 resections: impact on staging, disease-free survival, and outcome: a plea for adaptation of TNM classification in upper-half esophageal carcinoma. Ann Surg. 2004;240(6):962–72. discussion 972–964
3. Igaki H, Tachimori Y, Kato H. Improved survival for patients with upper and/or middle mediastinal lymph node metastasis of squamous cell carcinoma of the lower thoracic esophagus treated with 3-field dissection. Ann Surg. 2004;239(4):483–90.
4. Natsugoe S, Matsumoto M, Okumura H, Uchikado Y, Setoyama T, Sasaki K, Sakurai T, Omoto I, Owaki T, Shinchi H, et al. Clinical course and outcome after esophagectomy with three-field lymphadenectomy in esophageal cancer. Langenbeck's Arch Surg. 2010;395(4):341–6.
5. Dimick JB, Pronovost PJ, Cowan JA Jr, Lipsett PA, Stanley JC, Upchurch GR Jr. Variation in postoperative complication rates after high-risk surgery in the United States. Surgery. 2003;134(4):534–40. discussion 540–531
6. Morton DL, Wen DR, Wong JH, Economou JS, Cagle LA, Storm FK, Foshag LJ, Cochran AJ. Technical details of intraoperative lymphatic mapping for early stage melanoma. Arch Surg. 1992;127(4):392–9.
7. Kitagawa Y, Takeuchi H, Takagi Y, Natsugoe S, Terashima M, Murakami N, Fujimura T, Tsujimoto H, Hayashi H, Yoshimizu N, et al. Sentinel node mapping for gastric cancer: a prospective multicenter trial in Japan. J Clin Oncol. 2013;31(29):3704–10.
8. Kitagawa Y, Fujii H, Mukai M, Kubota T, Ando N, Watanabe M, Ohgami M, Otani Y, Ozawa S, Hasegawa H, et al. The role of the sentinel lymph node in gastrointestinal cancer. Surg Clin North Am. 2000;80(6):1799–809.
9. Kato H, Miyazaki T, Nakajima M, Takita J, Sohda M, Fukai Y, Masuda N, Fukuchi M, Manda R, Ojima H, et al. Sentinel lymph nodes with technetium-99m colloidal rhenium sulfide in patients with esophageal carcinoma. Cancer. 2003;98(5):932–9.
10. Yasuda S, Shimada H, Chino O, Tanaka H, Kenmochi T, Takechi M, Nabeshima K, Okamoto Y, Kato Y, Kijima H, et al. Sentinel lymph node detection with Tc-99m tin colloids in patients with esophagogastric cancer. Jpn J Clin Oncol. 2003;33(2):68–72.
11. Lamb PJ, Griffin SM, Burt AD, Lloyd J, Karat D, Hayes N. Sentinel node biopsy to evaluate the metastatic dissemination of oesophageal adenocarcinoma. Br J Surg. 2005;92(1):60–7.
12. Takeuchi H, Fujii H, Ando N, Ozawa S, Saikawa Y, Suda K, Oyama T, Mukai M, Nakahara T, Kubo A, et al. Validation study of radio-guided sentinel lymph node navigation in esophageal cancer. Ann Surg. 2009;249(5):757–63.
13. Thompson SK, Bartholomeusz D, Devitt PG, Lamb PJ, Ruszkiewicz AR, Jamieson GG. Feasibility study of sentinel lymph node biopsy in esophageal cancer with conservative lymphadenectomy. Surg Endosc. 2011;25(3):817–25.
14. Kim HK, Kim S, Park JJ, Jeong JM, Mok YJ, Choi YH. Sentinel node identification using technetium-99m neomannosyl human serum albumin in esophageal cancer. Ann Thorac Surg. 2011;91(5):1517–22.
15. Uenosono Y, Arigami T, Yanagita S, Kozono T, Arima H, Hirata M, Kita Y, Uchikado Y, Okumura H, Matsumoto M, et al. Sentinel node navigation surgery is acceptable for clinical T1 and N0 esophageal cancer. Ann Surg Oncol. 2011;18(7):2003–9.
16. Burian M, Stein HJ, Sendler A, Piert M, Nahrig J, Feith M, Siewert JR. Sentinel node detection in Barrett's and cardia cancer. Ann Surg Oncol. 2004;11(3 Suppl):255S–8S.
17. Yuasa Y, Seike J, Yoshida T, Takechi H, Yamai H, Yamamoto Y, Furukita Y, Goto M, Minato T, Nishino T, et al. Sentinel lymph node biopsy using intraoperative indocyanine green

fluorescence imaging navigated with preoperative CT lymphography for superficial esophageal cancer. Ann Surg Oncol. 2012;19(2):486–93.
18. Hachey KJ, Gilmore DM, Armstrong KW, Harris SE, Hornick JL, Colson YL, Wee JO. Safety and feasibility of near-infrared image-guided lymphatic mapping of regional lymph nodes in esophageal cancer. J Thorac Cardiovasc Surg. 2016;152(2):546–54.
19. Matsuda T, Takeuchi H, Tsuwano S, Nakahara T, Mukai M, Kitagawa Y. Sentinel node mapping in adenocarcinoma of the esophagogastric junction. World J Surg. 2014;38(9):2337–44.
20. Grotenhuis BA, Wijnhoven BP, van Marion R, van Dekken H, Hop WC, Tilanus HW, van Lanschot JJ, van Eijck CH. The sentinel node concept in adenocarcinomas of the distal esophagus and gastroesophageal junction. J Thorac Cardiovasc Surg. 2009;138(3):608–12.
21. Kubota K, Yoshida M, Kuroda J, Okada A, Ohta K, Kitajima M. Application of the HyperEye Medical System for esophageal cancer surgery: a preliminary report. Surg Today. 2013;43(2):215–20.
22. Tsai JA, Celebioglu F, Lindblad M, Lorinc E, Nilsson M, Olsson A, Lundell L, Axelsson R. Hybrid SPECT/CT imaging of sentinel nodes in esophageal cancer: first results. Acta Radiol. 2013;54(4):369–73.
23. Nagaraja V, Eslick GD, Cox MR. Sentinel lymph node in oesophageal cancer-a systematic review and meta-analysis. J Gastrointest Oncol. 2014;5(2):127–41.
24. Boone J, Hobbelink MG, Schipper ME, Vleggaar FP, Borel Rinkes IH, de Haas RJ, Ruurda JP, van Hillegersberg R. Sentinel node biopsy during thoracolaparoscopic esophagectomy for advanced esophageal cancer. World J Surg Oncol. 2016;14:117.
25. Arima H, Natsugoe S, Uenosono Y, Arigami T, Ehi K, Yanagita S, Higashi H, Ishigami S, Hokita S, Aikou T. Area of nodal metastasis and radioisotope uptake in sentinel nodes of upper gastrointestinal cancer. J Surg Res. 2006;135(2):250–4.
26. Yanagita S, Natsugoe S, Uenosono Y, Kozono T, Ehi K, Arigami T, Arima H, Ishigami S, Aikou T. Sentinel node micrometastases have high proliferative potential in gastric cancer. J Surg Res. 2008;145(2):238–43.
27. Hagihara T, Uenosono Y, Arigami T, Kozono T, Arima H, Yanagita S, Hirata M, Ehi K, Okumura H, Matsumoto M, et al. Assessment of sentinel node concept in esophageal cancer based on lymph node micrometastasis. Ann Surg Oncol. 2013;20(9):3031–7.
28. Sato Y, Kosugi S, Aizawa N, Ishikawa T, Kano Y, Ichikawa H, Hanyu T, Hirashima K, Bamba T, Wakai T. Risk factors and clinical outcomes of recurrent laryngeal nerve paralysis after esophagectomy for thoracic esophageal carcinoma. World J Surg. 2016;40(1):129–36.
29. Kato H, Sato A, Fukuda H, Kagami Y, Udagawa H, Togo A, Ando N, Tanaka O, Shinoda M, Yamana H, et al. A phase II trial of chemoradiotherapy for stage I esophageal squamous cell carcinoma: Japan Clinical Oncology Group Study (JCOG9708). Jpn J Clin Oncol. 2009;39(10):638–43.
30. Takeuchi H, Kawakubo H, Nakamura R, Fukuda K, Takahashi T, Wada N, Kitagawa Y. Clinical significance of sentinel node positivity in patients with superficial esophageal cancer. World J Surg. 2015;39(12):2941–7.

Clinical Aspect: Gastric Cancer

19

Hiroya Takeuchi and Yuko Kitagawa

Abstract

Recent meta-analyses and a prospective multicenter trial of sentinel node (SN) mapping for early gastric cancer have shown acceptable SN detection rates and accuracy of determination of lymph node status. A dual-tracer method that employs radioactive colloids and blue dyes is currently considered the most reliable method for the stable detection of SNs for early-stage gastric cancer. However the new technologies such as indocyanine green infrared or fluorescence imaging and molecular detection of occult tumor cells in SN may revolutionize the SN mapping procedures in gastric cancer. For early gastric cancer, the establishment of individualized, minimally invasive gastrectomy based on SN concept can retain the patients' quality of life. The combination of non-exposed endoscopic wall-inversion surgery with SN mapping and lymphatic basin dissection is expected to become a promising, ideal minimally invasive, function-preserving surgery to cure patients with cN0 early gastric cancer.

Keywords

Sentinel nodes · Gastric cancer · Laparoscopic · Non-exposed endoscopic wall-inversion surgery

H. Takeuchi (✉)
Department of Surgery, Hamamatsu University School of Medicine, Shizuoka, Japan
e-mail: takeuchi@hama-med.ac.jp

Y. Kitagawa
Department of Surgery, Keio University School of Medicine, Tokyo, Japan

S. Natsugoe (ed.), *Lymph Node Metastasis in Gastrointestinal Cancer*,
https://doi.org/10.1007/978-981-10-4699-5_19

19.1 Introduction

In Japan, early-stage gastric cancer (cT1) is found in many asymptomatic patients due to recent advances in endoscopic diagnosis, and the population with this condition currently reaches in excess of 50% in major institutions [1]. Endoscopic submucosal dissection (ESD) has already been accepted as the most minimally invasive procedures for the resection of early gastric cancer [1]. Laparoscopic gastrectomy represents an important intermediate option between ESD and open surgery for patients with gastric cancer [2]. The technique of laparoscopic gastrectomy has shifted from partial resection to more radical procedures such as laparoscopy-assisted distal gastrectomy (LADG) with D2 lymphadenectomy, which is comparable to conventional open distal gastrectomy and can be performed in clinical practices [3, 4].

Many patients with early gastric cancer are currently treated with advanced laparoscopic gastrectomy procedures, such as LADG and laparoscopy-assisted total gastrectomy (LATG) with standard lymph node dissection in Asian countries [1–4]. LADG and LATG contribute to both better esthetics and early postoperative recovery [5]. However, patients' quality of life (QOL) is mainly affected by late-phase complications including dumping syndrome and body weight loss resulting from oral intake disturbance due to large extent of gastric resection. Therefore, both minimal invasiveness for early-phase recovery by laparoscopic surgery and additional late-phase function-preserving gastrectomy should be carefully considered in patients indicated for these procedures.

Function-preserving gastrectomy such as partial gastrectomy, segmental gastrectomy, and proximal gastrectomy with limited lymph node dissection is known to improve postoperative late-phase function. However, a certain incidence of skip metastasis in the second or third compartment of regional lymph nodes remains an obstacle to the wider application of these procedures. To overcome these issues, the concept of sentinel node (SN) mapping may become a novel diagnostic tool for the identification of clinically undetectable lymph node metastasis in early gastric cancer.

SNs are defined as the first draining lymph nodes from the primary tumor site [6, 7], and they are thought to be the first possible site of micrometastasis along the route of lymphatic drainage from the primary lesion. The pathological status of SNs can theoretically predict the status of all regional lymph nodes. If SNs are recognizable and negative for cancer metastasis, unnecessary radical lymph node dissection could be avoided. SN navigation surgery is defined as a novel, minimally invasive surgery based on SN mapping and the SN-targeted diagnosis of nodal metastasis. SN navigation surgery can prevent unnecessary lymph node dissection, thus preventing the associated complications and improving the patient's QOL.

SN mapping and biopsy were firstly applied to melanoma and breast cancer patients and were subsequently extended to patients with many other solid tumors [7–9]. The clinical application of SN mapping for early gastric cancer has been controversial for years. However, single institutional results, including a recent multicenter trial of SN mapping for early gastric cancer, are considered acceptable in terms of the SN detection rate and accuracy of determination of lymph node status [10, 11]. On the basis of these results, we are developing a novel, minimally invasive function-preserving gastrectomy technique combined with SN mapping.

19.2 Laparoscopic SN Mapping Procedures for Gastric Cancer

A dual-tracer method that utilizes radioactive colloids and blue or green dyes is currently considered the most reliable method for the stable detection of SNs in patients with early gastric cancer [10, 11]. An accumulation of radioactive colloids facilitates the identification of SNs even in resected specimens by using a handheld gamma probe, and the blue dye is effective for intraoperative visualization of lymphatic flow, even during laparoscopic surgery. Technetium-99m tin colloid, technetium-99m sulfur colloid, and technetium-99m antimony sulfur colloid are preferentially used as radioactive tracers. Isosulfan blue and indocyanine green (ICG) are the currently preferred choices as dye tracers.

In our institution, patients with clinical T1 tumors, primary lesions less than 4 cm in diameter, and clinical N0 gastric cancer undergo SN mapping and biopsy [10, 11]. In our procedures, 2.0 mL (150 MBq) of technetium-99m tin colloid solution is injected the day before surgery into four quadrants of the submucosal layer of the primary tumor site using an endoscopic puncture needle. Endoscopic injections to the submucosal layer facilitate accurate tracer injection rather than laparoscopic injection from the seromuscular site of the gastric wall. Technetium-99m tin colloid with relatively large particle size accumulates in the SNs after local administration.

The blue or green dyes are injected into four quadrants of the submucosal layer of the primary site using an endoscopic puncture needle at the beginning of surgery. Blue lymphatic vessels and blue-stained nodes can be identified by laparoscopy within 15 min after the injection of the blue or green dyes. Simultaneously, a handheld gamma probe is used to locate the radioactive SN. Intraoperative gamma probing is feasible in laparoscopic gastrectomy using a special gamma detector introducible from trocar ports [10, 11].

For intraoperative SN sampling, the pickup method is well established for the detection of melanoma and breast cancer. However, it is recommended that the clinical application of intraoperative SN sampling for gastric cancer should include sentinel lymphatic basin dissection, which is a sort of focused lymph node dissection involving hot and blue nodes [10, 11]. The gastric lymphatic basins were considered to be divided in the following five directions along the main arteries: left gastric artery area, right gastric artery area, left gastroepiploic artery area, right gastroepiploic artery area, and posterior gastric artery area [12].

ICG is known to have excitation and fluoresce wavelengths in the near-infrared range [13]. Till date, some investigators have used infrared ray electronic endoscopy (IREE) to demonstrate the clinical utility of intraoperative ICG infrared imaging as a new tracer for laparoscopic SN mapping [13, 14]. IREE might be a useful tool to improve visualization of ICG-stained lymphatic vessels and SNs even in the fat tissues. More recently, ICG fluorescence imaging has been developed as another promising novel technique for SN mapping [15, 16]. SN could be clearly visualized by ICG fluorescence imaging compared to the naked eye. Further studies would be needed to evaluate the clinical efficacy of ICG infrared or fluorescence imaging and

to compare those with radio-guided methods in prospective studies. However these new technologies might revolutionize the SN mapping procedures in early gastric cancer.

19.3 Results of SN Mapping in Gastric Cancer

To date, more than 100 single institutional studies have demonstrated acceptable outcomes of SN mapping for early gastric cancer in terms of the SN detection rate (90–100%) and accuracy (85–100%) of determination of lymph node status; these outcomes are comparable to those of SN mapping for melanoma and breast cancer [11]. A recent large-scale meta-analysis, which included 38 relevant SN mapping studies with 2128 gastric cancer patients, demonstrated that the SN detection rate and accuracy of prediction of lymph node metastasis based on SN status were 94% and 92%, respectively [17]. They concluded that the SN concept is technically feasible for gastric cancer, especially patients with early T stage (T1), with the use of combined tracers and submucosal injection methods during the SN biopsy procedures.

Our group in Japan had conducted a multicenter prospective trial (UMIN ID: 000000476) of SN mapping using a dual-tracer method with a radioactive colloid and blue dye [10]. In the trial, SN mapping was performed between 2004 and 2008 for 397 patients with early gastric cancer at 12 comprehensive hospitals, including our institution. Eligibility criteria were that patients had cT1N0M0 or cT2N0M0 single tumor with diameter of primary lesion less than 4 cm, without any previous treatments. As results, the SN detection rate was 98% and the accuracy of determination of metastatic status was 99% [10]. The results of that clinical trial are expected to provide us with perspectives on the future of SN navigation surgery for early gastric cancer.

19.4 Clinical Significance of Micrometastasis in SN in Early Gastric Cancer

Accurate detection of nodal metastasis including micrometastasis during and after surgery is indispensable for clinical application of SN navigation surgery [18, 19]. Hematoxylin and eosin (H&E) and immunohistochemical (IHC) staining have been commonly used, in combination with serial sectioning of frozen and paraffin-embedded specimens, for the detection of micrometastatic disease in the SN [18, 20]. The application of IHC has markedly improved the sensitivity of micrometastatic disease detection in the SN beyond the capability of routine H&E staining alone [20]. The antibodies against tumor markers of interest must be highly specific and sensitive for detection of tumor cells and virtually nonreactive to the adjacent non-tumor cells in the SN. The most commonly used IHC target for gastric cancer are the cytokeratins (CK), which are ubiquitously expressed as intermediate filaments in normal eukaryotic epithelial cells [18, 20]. However, the risk of false-positive and false-negative results with the use of individual anti-CK antibodies and antibody cocktails has been described [21].

Moreover, there is another problem regarding the histopathological diagnosis of lymph node metastases including micrometastases [19]. Although lymph nodes are three-dimensional structures, histological and IHC investigations are usually performed on planar slices. Metastatic foci located in the center of lymph nodes may result in a correct positive identification. However, when they are not located in the hilus of the lymph node, the results might be deemed negative [19]. Isozaki et al. reported that serial sectioning of lymph nodes for H&E staining results in a more accurate evaluation of the extent of lymph nodes metastases in gastric cancer patients [22]. Morita et al. also examined occult metastasis using IHC in the 5-μm-thick serial step sections at 85 μm intervals of whole formalin-fixed paraffin-embedded tissues of all resected SN [23]. As results, occult metastasis in SN was detected by serial section examination in 2 (4.4%) of 46 patients with pN0. In general, however, the serial sectioning is clinically time- and labor-consuming. Limitations of histopathological diagnosis of micrometastasis using frozen sections for intraoperative pathology also have to be considered for clinical application of SN biopsy [24]. The quality of preservation of tissues and cell morphology in frozen sections is generally inferior to that in paraffin-embedded permanent specimens, especially for the diagnosis of isolated tumor cells or micrometastasis of undifferentiated types of gastric cancer cells. More rapid and comprehensive diagnostic methods are desired for the accurate diagnosis of lymph node metastases, especially for detecting micrometastases in the SN.

The molecular detection of tumor cells using RNA or DNA markers with various polymerase chain reaction (PCR) techniques has evolved exponentially in the last decade [18, 25]. The primary approach of molecular detection of tumor cells has been focused on the mRNA of tumor markers using reverse transcription (RT)-PCR assay. Detection of metastatic tumor cells has been clearly demonstrated in LN, organs, and body fluids. Using RT-PCR, it is now possible to reliably detect one to ten tumor cells within a background of 10^6–10^7 normal cells [25]. The high sensitivity of the RT-PCR assay, compared with H&E and IHC, allows the detection of the occult tumor cells among the lymphoid cells in whole SN. However, molecular-based techniques require the stringent optimization of sample processing, reagents, molecular targets, RT and PCR reactions, and PCR cDNA product detection assays [18]. Meticulous attention to techniques must be adhered to, throughout all stages of the assay, in order to ensure accurate results and prevent false-positive and false-negative results.

Quantitative RT-PCR assay is now being used more extensively to not only identify the presence of target mRNA but also to quantify the number of mRNA copies from tumor-associated genes [18]. Quantitative RT-PCR analysis permits the rapid molecular analysis of multiple mRNA targets expressed in tumor cells, and these results can then be correlated to clinical outcomes in order to study the relationship between gene expression levels and outcome. Real-time RT-PCR assay, which enables rapid analysis, is currently being attempted for intraoperative molecular diagnosis.

Arigami et al. [26] reported that 13 of 53 (25%) gastric cancer patients with histopathologically negative SNs were upstaged by the RT-PCR assay. They concluded that the SN concept was applicable to patients with cT1N0 gastric cancer, even after including the molecular diagnosis of micrometastasis. Molecular assessment of SNs

may be a variable tool to complement histological examination for gastrointestinal cancers. We also established a highly sensitive real-time RT-PCR system to detect the mRNA of cytokeratin (CK) 19, CK20, and carcinoembryonic antigen [27]. The results showed that 28 of 103 (27%) patients had negative histopathological but positive RT-PCR findings. This system generated results within 80 min, which might be available for intraoperative diagnosis.

Further improvements of the assay including one-step nucleic acid amplification (OSNA) assay may allow the PCR-based intraoperative diagnosis to be applicable to gastric cancer surgeries [28]. However, the clinical impact of micrometastasis or isolated tumor cells (ITCs) detected by histopathology and molecular analysis in SNs of patients with early gastric cancer remains controversial [29–31]. Ishigami et al. [29] reported that patients with micrometastasis detected by IHC using anti-CK antibodies had a significantly poorer survival rate than those without micrometastasis. On the other hand, another group showed that the presence of ITC in the lymph nodes did not affect the prognosis of gastric cancer patients who have undergone gastrectomy with D2 lymph node dissection [30]. However, Yanagita et al. [31] reported that not only gastric cancer cells in macrometastasis but also micrometastasis and even some of ITCs in the SNs may have the proliferative activity. We need to accumulate sufficient data to validate the accuracy of the molecular diagnosis and assess the clinical significance of molecular micrometastasis in SNs of patients with early gastric cancer. Until then, molecular-based intraoperative diagnosis might play a supplementary role in the clinical application of SN mapping and biopsy for gastric cancer.

19.5 Clinical Application of Laparoscopic SN Navigation Surgery in Early Gastric Cancer

The distribution of sentinel lymphatic basins and the pathological status of SNs would be useful in deciding on the minimized extent of gastric resection and in avoiding the universal application of distal or total gastrectomy with D2 dissection. Appropriate indications for laparoscopic surgeries such as partial (wedge) resection, segmental gastrectomy, pylorus-preserving gastrectomy, and laparoscopy-assisted proximal gastrectomy (LAPG) for cT1N0 gastric cancer could be individually determined on the basis of SN status (Figs. 19.1 and 19.2) [32–34]. Earlier recovery after surgery and preservation of QOL in the late phase can be achieved by laparoscopic limited gastrectomy with SN navigation. Our study group in Japan has currently been conducting the multicenter prospective trial (UMIN ID: 000014401) which will evaluate the function-preserving gastrectomy with SN mapping in terms of long-term survival and patients' QOL as the next step. A Korean group has also been conducting the multicenter prospective phase III trial to elucidate the oncologic safety including long-term survival of laparoscopic stomach-preserving surgery with sentinel lymphatic basin dissection compared to a standard laparoscopic gastrectomy [35].

A combination of laparoscopic SN biopsy and endoscopic mucosal resection (EMR)/endoscopic submucosal dissection (ESD) for early gastric cancer is another attractive option as a novel, whole stomach-preserved, minimally invasive approach. If all SNs are pathologically negative for cancer metastasis, theoretically, EMR/

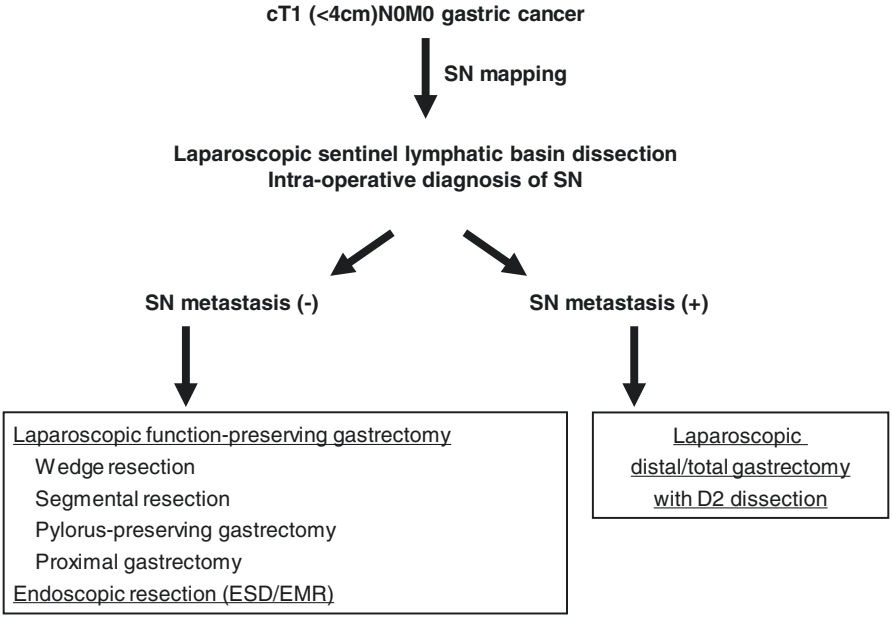

Fig. 19.1 Individualized function-preserving approaches for cT1N0M0 gastric cancer based on sentinel node mapping. *ESD* endoscopic submucosal dissection, *EMR* endoscopic mucosal resection

ESD instead of gastrectomy may be sufficient for the curative resection of cT1 gastric cancer beyond the ESD criteria (Fig. 19.2d) [34, 36]. However, further studies are required to verify the safety and effectiveness of combined treatments involving laparoscopic SN biopsy and EMR/ESD.

Nowadays, LADG and LAPG are frequently applied to the patients with early gastric cancer according to the results of pathological assessment of primary tumor resected by EMR/ESD in clinical practices. To date, it has not been clarified whether the SN mapping is feasible even after EMR/ESD. One of the most important issues is whether lymphatic flow from the primary tumor to the original SNs might change after EMR/ESD. In our preliminary study, however, at least the sentinel lymphatic basin is not markedly affected by previous EMR/ESD [34, 36]. Modified gastrectomy according to SN distribution and metastatic status might be feasible even for the patients who underwent EMR/ESD prior to surgery.

19.6 Non-exposed Endoscopic Wall-Inversion Surgery Plus SN Mapping

In current function-preserving surgeries such as laparoscopic local resection or segmental gastrectomy, the approach of gastrectomy is only from the outside of the stomach, in which the demarcation line of the tumor cannot be visualized at the phase of resection. Therefore, the surgeons cannot avoid a wider resection of the

stomach than is desired to prevent a positive surgical margin. The recent appearance of a new technique, referred to as non-exposed endoscopic wall-inversion surgery (NEWS), is a technique of full-thickness partial resection, which can minimize the extent of gastric resection using endoscopic and laparoscopic surgery without transluminal access mainly designed to treat gastric cancer. We have been accumulating cases of NEWS with SN biopsy for early gastric cancer with the risk of lymph node metastasis in the clinical trial [37, 38].

In brief, after placing mucosal markings, ICG was injected endoscopically into the submucosa around the lesion to examine SNs (Figs. 19.2e and 19.3) [37]. The SN basin including hot or stained SNs was dissected, and an intraoperative pathological diagnosis confirmed that no metastasis had occurred. Subsequently, NEWS was performed for the primary lesion. Serosal markings were placed laparoscopically, submucosal injection was added endoscopically, and circumferential seromuscular incision and suturing were performed laparoscopically, with the lesion inverted toward the inside of the stomach. Finally, the circumferential mucosal incision was performed endoscopically, and the lesion was retrieved perorally (Fig. 19.3).

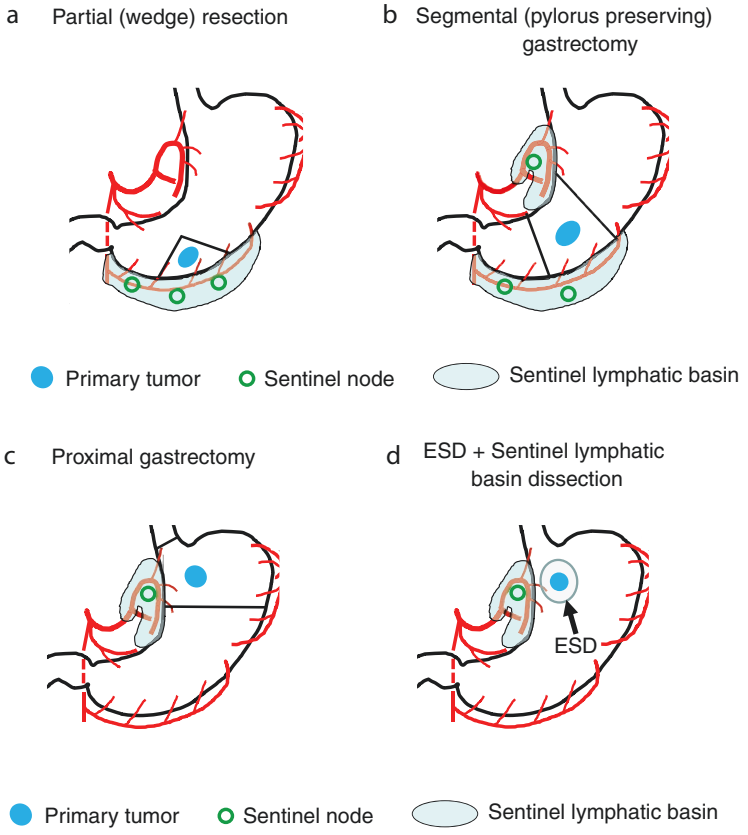

Fig. 19.2 Laparoscopic function-preserving gastrectomy with sentinel lymphatic basin dissection. (**a**) Partial (wedge) resection, (**b**) segmental (pylorus-preserving) gastrectomy, (**c**) proximal gastrectomy, (**d**) sentinel lymphatic basin dissection plus ESD, (**e**) non-exposed endoscopic wall-inversion surgery (NEWS) with SN mapping and sentinel lymphatic basin dissection

Fig. 19.2 (continued)

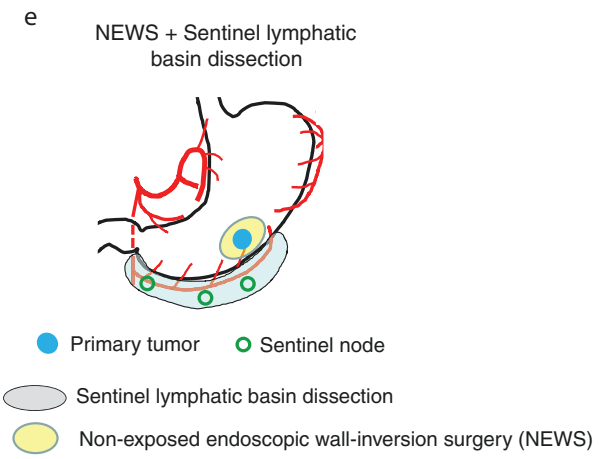

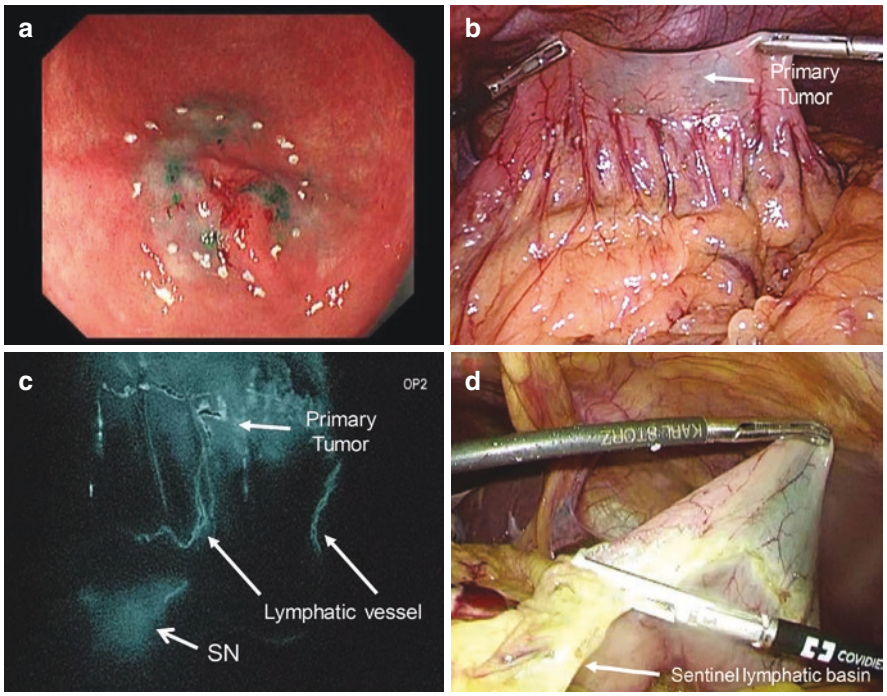

Fig. 19.3 Non-exposed endoscopic wall-inversion surgery (NEWS) with SN biopsy and sentinel lymphatic basin dissection. (**a**) Indocyanine green (ICG) was endoscopically injected to the gastric submucosal layer surrounding the primary tumor. (**b**) Laparoscopic observation of ICG with normal light. (**c**) Observation of ICG with infrared ray electronic endoscopy. Infrared ray electronic endoscopy can visualize SNs and lymphatics clearly. (**d**) Resection of sentinel lymphatic basin. (**e**) Laparoscopic circumferential seromuscular incision. (**f**, **g**) Laparoscopic seromuscular suturing and inversion of the primary lesion

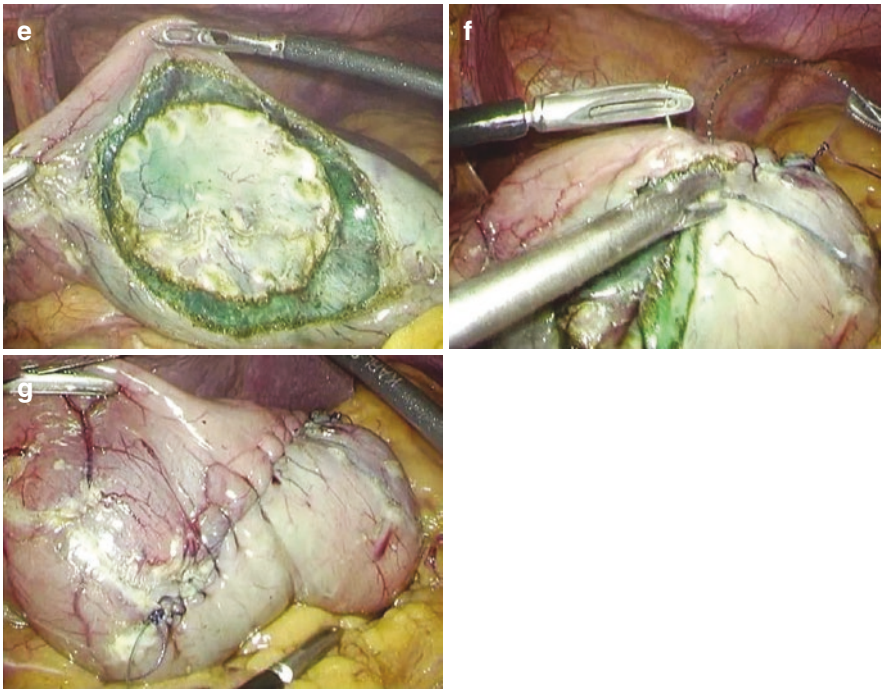

Fig. 19.3 (continued)

The NEWS combined with the SN biopsy can minimize not only the area of lymphadenectomy but also the extent of gastric resection as partial gastrectomy for patients with SN negative for metastasis [36]. Furthermore, NEWS does not need intentional perforation, which enables us to apply this technique to cancers without a risk of iatrogenic dissemination. The combination of NEWS with SN biopsy is expected to become a promising, ideal minimally invasive, function-preserving surgery to cure cases of cN0 early gastric cancer.

19.7 Conclusion

For early-stage gastric cancer, for which a better prognosis can be achieved through conventional surgical approaches, the establishment of individualized, minimally invasive treatments that may retain the patients' QOL should be the next surgical challenge. Although further studies are needed for careful validation, function-preserving gastrectomy based on SN navigation could be a promising strategy to achieve this goal.

References

1. Sano T, Hollowood K. Early gastric cancer: diagnosis and less invasive treatments. Scand J Surg. 2006;95:249–55.
2. Kitano S, Iso Y, Moriyama M, Sugimachi K. Laparoscopy-assisted Billroth I gastrectomy. Surg Laparosc Endosc. 1994;4:146–8.
3. Adachi Y, Shiraishi N, Shiromizu A, Shiromizu A, Bandoh T, Aramaki M, Kitano S. Laparoscopy-assisted Billroth I gastrectomy compared with conventional open gastrectomy. Arch Surg. 2000;135:806–10.
4. Shinohara T, Kanaya S, Taniguchi K, Fujita T, Yanaga K, Uyama I. Laparoscopic total gastrectomy with D2 lymph node dissection for gastric cancer. Arch Surg. 2009;144:1138–42.
5. Kim YW, Baik YH, Yun YH, Nam BH, Kim DH, Choi IJ, Bae JM. Improved quality of life outcomes after laparoscopy-assisted distal gastrectomy for early gastric cancer: results of a prospective randomized clinical trial. Ann Surg. 2008;248:721–7.
6. Kitagawa Y, Fujii H, Mukai M, Kubota T, Ando N, et al. The role of the sentinel lymph node in gastrointestinal cancer. Surg Clin North Am. 2000;80:1799–809.
7. Morton DL, Wen DR, Wong JH, et al. Technical details of intraoperative lymphatic mapping for early stage melanoma. Arch Surg. 1992;127:392–9.
8. Giuliano AE, Kirgan DM, Guenther JM, Morton DL. Lymphatic mapping and sentinel lymphadenectomy for breast cancer. Ann Surg. 1994;220:391–401.
9. Bilchik AJ, Saha S, Wiese D, et al. Molecular staging of early colon cancer on the basis of sentinel node analysis: a multicenter phase II trial. J Clin Oncol. 2001;19:1128–36.
10. Kitagawa Y, Takeuchi H, Takagi Y, Natsugoe S, Terashima M, Murakami N, Fujimura T, Tsujimoto H, Hayashi H, Yoshimizu N, Takagane A, Mohri Y, Nabshima K, Uenosono Y, Kinami S, Sakamoto J, Morita S, Aikou T, Miwa K, Kitajima M. Sentinel node mapping for gastric cancer: a prospective multicenter trial in Japan. J Clin Oncol. 2013;31:3704–10.
11. Takeuchi H, Kitagawa Y. New sentinel node mapping technologies for early gastric cancer. Ann Surg Oncol. 2013;20:522–32.
12. Kinami S, Fujimura T, Ojima E, Fushida S, Ojima T, Funaki H, Fujita H, Takamura H, Ninomiya I, Nishimura G, Kayahara M, Ohta T, Yoh Z. PTD classification: proposal for a new classification of gastric cancer location based on physiological lymphatic flow. Int J Clin Oncol. 2008;13:320–9.
13. Tajima Y, Murakami M, Yamazaki K, Masuda Y, Kato M, Sato A, Goto S, Otsuka K, Kato T, Kusano M. Sentinel node mapping guided by indocyanine green fluorescence imaging during laparoscopic surgery in gastric cancer. Ann Surg Oncol. 2010;17:1787–93.
14. Ishikawa K, Yasuda K, Shiromizu T, Etoh T, Shiraishi N, Kitano S. Laparoscopic sentinel node navigation achieved by infrared ray electronic endoscopy system in patients with gastric cancer. Surg Endosc. 2007;21:1131–4.
15. Nimura H, Narimiya N, Mitsumori N, Yamazaki Y, Yanaga K, Urashima M. Infrared ray electronic endoscopy combined with indocyanine green injection for detection of sentinel nodes of patients with gastric cancer. Br J Surg. 2004;91:575–9.
16. Miyashiro I, Miyoshi N, Hiratsuka M, Kishi K, Yamada T, Ohue M, Ohigashi H, Yano M, Ishikawa O, Imaoka S. Detection of sentinel node in gastric cancer surgery by indocyanine green fluorescence imaging: comparison with infrared imaging. Ann Surg Oncol. 2008;15:1640–3.
17. Wang Z, Dong ZY, Chen JQ, Liu JL. Diagnostic value of sentinel lymph node biopsy in gastric cancer: a meta-analysis. Ann Surg Oncol. 2012;19:1541–50.
18. Takeuchi H, Kitajima M, Kitagawa Y. Sentinel lymph node as a target of molecular diagnosis of lymphatic micrometastasis and local immunoresponse to malignant cells. Cancer Sci. 2008;99:441–50.

19. Yanagita S, Natsugoe S, Uenosono Y, et al. Detection of micrometastases in sentinel node navigation surgery for gastric cancer. Surg Oncol. 2008;17:203–10.
20. Matsuda J, Kitagawa Y, Fujii H, et al. Significance of metastasis detected by molecular techniques in sentinel nodes of patients with gastrointestinal cancer. Ann Surg Oncol. 2004;11:250–4.
21. Xu X, Roberts SA, Pasha TL, Zhang PJ. Undesirable cytokeratin immunoreactivity of native nonepithelial cells in sentinel lymph nodes from patients with breast carcinoma. Arch Pathol Lab Med. 2000;124:1310–3.
22. Isozaki H, Okajima K, Fujii K. Histological evaluation of lymph node metastasis on serial sectioning in gastric cancer with radical lymphadenectomy. Hepato-Gastroenterology. 1997;44:1133–6.
23. Morita D, Tsuda H, Ichikura T, et al. Analysis of sentinel node involvement in gastric cancer. Clin Gastroenterol Heapatol. 2007;5:1046–52.
24. Cochran AJ, Robert A, Wen DR et al. Accurate evaluation of nodal tissues for the presence of tumor is central to the sentinel node approach. Selective sentinel lymphadenectomy for human solid cancer. Cancer treatment and research. Springer: New York; 2005.
25. Pantel K, Cote RJ, Fodstad O. Detection and clinical importance of micrometastatic disease. J Natl Cancer Inst. 1999;91:1113–24.
26. Arigami T, Natsugoe S, Uenosono Y, et al. Evaluation of sentinel node concept in gastric cancer based on lymph node micrometastasis determined by reverse transcription-polymerase chain reaction. Ann Surg. 2006;243:341–7.
27. Shimizu Y, Takeuchi H, Sakakura Y, et al. Molecular detection of sentinel node micrometastases in patients with clinical N0 gastric carcinoma with real-time multiplex reverse transcription-polymerase chain reaction assay. Ann Surg Oncol. 2012;19:469–77.
28. Kumagai K, Yamamoto N, Miyashiro I, et al. Multicenter study evaluating the clinical performance of the OSNA assay for the molecular detection of lymph node metastases in gastric cancer patients. Gastric Cancer. 2014;17:273–80.
29. Ishigami S, Natsugoe S, Tokuda K, et al. Clinical impact of micrometastasis of the lymph node in gastric cancer. Am Surg. 2003;69:573–7.
30. Fukagawa T, Sasako M, Ito S, et al. The prognostic significance of isolated tumor cells in the lymph nodes of gastric cancer patients. Gastric Cancer. 2010;13:191–6.
31. Yanagita S, Natsugoe S, Uenosono Y, et al. Sentinel node micrometastases have high proliferative potential in gastric cancer. J Surg Res. 2008;145:238–43.
32. Takeuchi H, Saikawa Y, Kitagawa Y. Laparoscopic sentinel node navigation surgery for early gastric cancer. Asian J Endosc Surg. 2009;2:13–7.
33. Takeuchi H, Oyama T, Kamiya S, Nakamura R, Takahashi T, Wada N, Saikawa Y, Kitagawa Y. Laparoscopy-assisted proximal gastrectomy with sentinel node mapping for early gastric cancer. World J Surg. 2011;35:2463–71.
34. Takeuchi H, Kitagawa Y. Sentinel node navigation surgery in patients with early gastric cancer. Dig Surg. 2013;30:104–11.
35. Park JY, Kim YW, Ryu KW, Nam BH, Lee YJ, Jeong SH, Park JH, Hur H, Han SU, Min JS, An JY, Hyung WJ, Cho GS, Jeong GA, Jeong O, Park YK, Jung MR, Yoon HM, Eom BW. Assessment of laparoscopic stomach preserving surgery with sentinel basin dissection versus standard gastrectomy with lymphadenectomy in early gastric cancer—a multicenter randomized phase III clinical trial (SENORITA trial) protocol. BMC Cancer. 2016;16:340.
36. Mayanagi S, Takeuchi H, Kamiya S, Niihara M, Nakamura R, Takahashi T, Wada N, Kawakubo H, Saikawa Y, Omori T, Nakahara T, Mukai M, Kitagawa Y. Suitability of sentinel node mapping as an index of metastasis in early gastric cancer following endoscopic resection. Ann Surg Oncol. 2014;21:2987–93.
37. Goto O, Takeuchi H, Kawakubo H, Sasaki M, Matsuda T, Matsuda S, Kigasawa Y, Kadota Y, Fujimoto A, Ochiai Y, Horii J, Uraoka T, Kitagawa Y, Yahagi N. First case of non-exposed endoscopic wall-inversion surgery with sentinel node basin dissection for early gastric cancer. Gastric Cancer. 2015;18:440–5.
38. Takeuchi H, Kitagawa Y. Sentinel lymph node biopsy in gastric cancer. Cancer J. 2015;21:21–4.